EMERGING INFECTIOUS DISEASES®

U.S. CENTERS FOR DISEASE CONTROL AND PREVENTION

Bacterial Infections and Their Treatment

June 2026

Johannes [Jan] Vermeer (1632–1675), *The Geographer*, 1668–1669. Oil on canvas. 53 cm × 46.5 cm (20.9 in × 18.3 in). Städel Museum, Frankfurt am Main, Germany.

Pages 839–1038

EMERGING INFECTIOUS DISEASES

A Peer-Reviewed Journal Tracking and Analyzing Disease Trends

Emerging Infectious Diseases is published monthly by the Centers for Disease Control and Prevention, 1600 Clifton Rd NE, Mailstop H16-2, Atlanta, GA 30329-4018, USA. Telephone 404-639-1960; email eideditor@cdc.gov

EMERGING INFECTIOUS DISEASES®

Bacterial Infections and Their Treatment — June 2026

On the Cover

Johannes [Jan] Vermeer (1632–1675), *The Geographer*, 1668–1669. Oil on canvas. 53 cm × 46.5 cm (20.9 in × 18.3 in). Städel Museum, Frankfurt am Main, Germany.

About the Cover p. 1033

Perspective

Synopses

Medscape EDUCATION ACTIVITY

Research

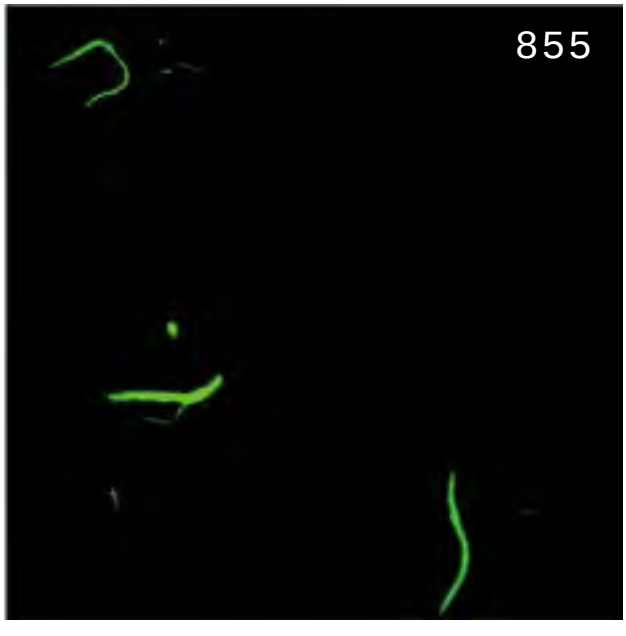

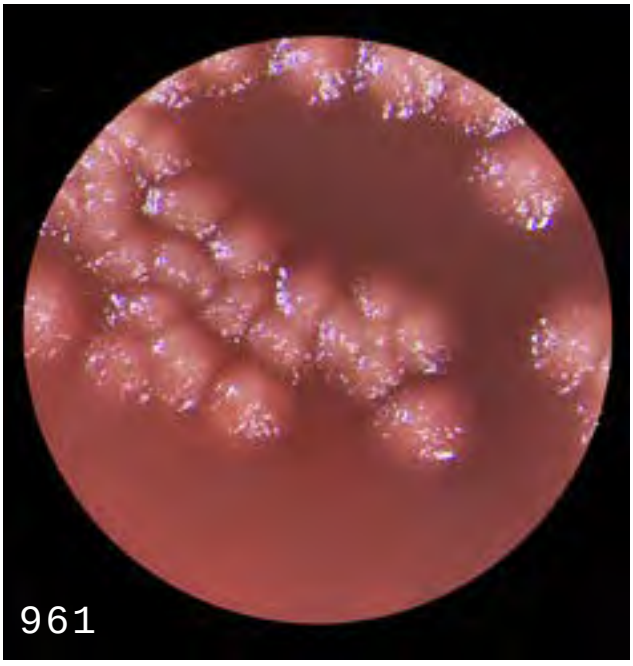

EMERGING INFECTIOUS DISEASES®

June 2025

Dispatches

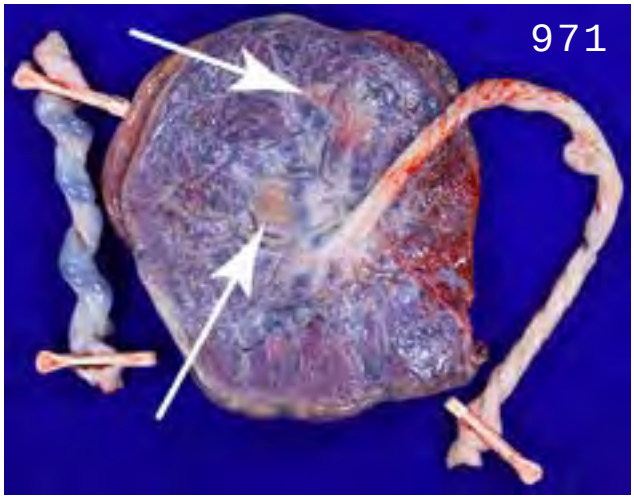

Commentary

Photo Quiz

Research Letters

EMERGING INFECTIOUS DISEASES®
June 2025

EIN Letter

Books and Media

About the Cover

Etymologia

Correction

EMERGING INFECTIOUS DISEASES®

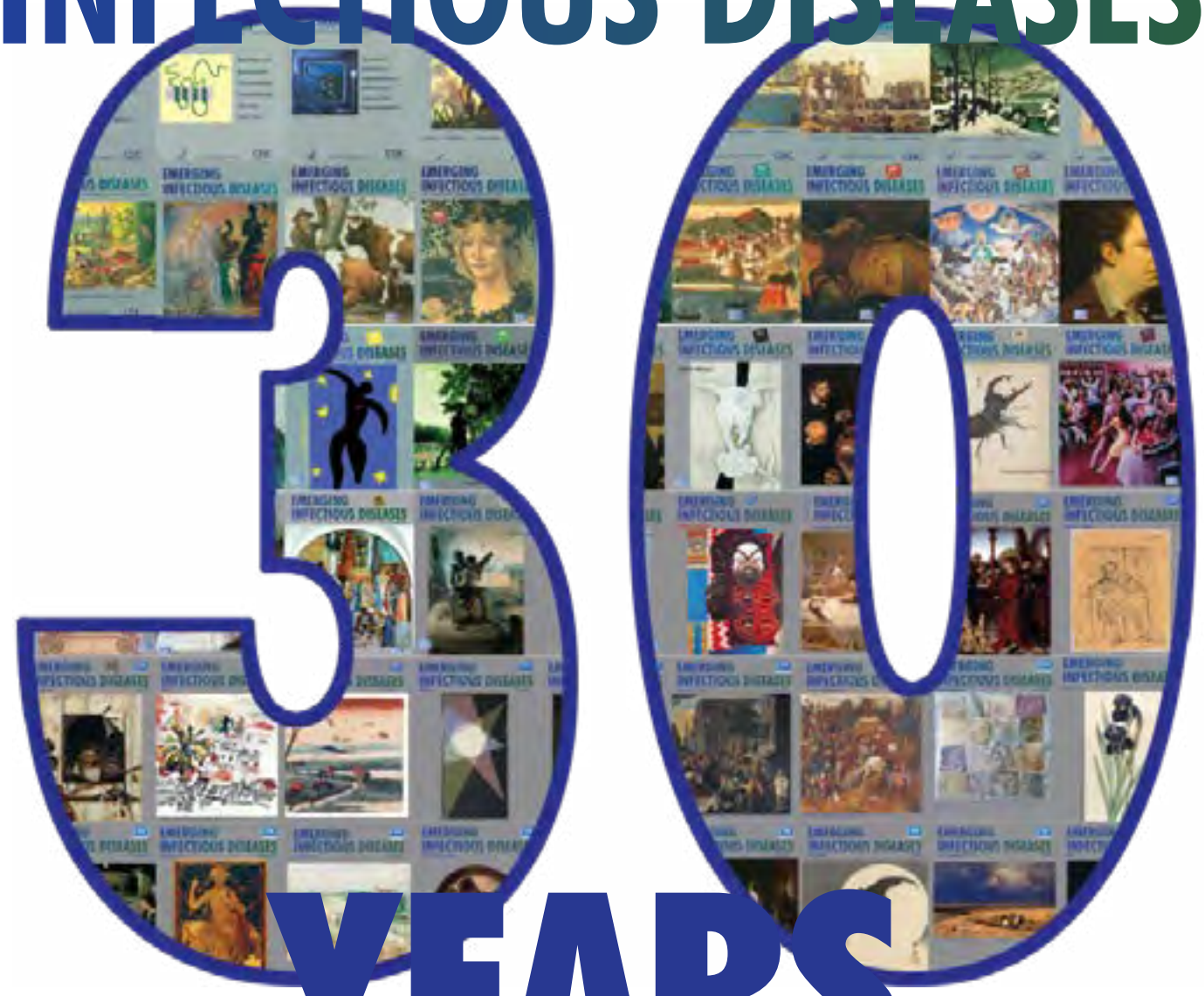

30 YEARS

Presenting the ongoing challenges that emerging microbial threats pose to global health

Limitations of Global Surveillance for *Neisseria gonorrhoeae* Antimicrobial Resistance

Sebastiaan J. van Hal, Helen Fifer, Monica M. Lahra

Neisseria gonorrhoeae bacteria cause ≈82 million infections annually worldwide. As antimicrobial resistance (AMR) accelerates, the actual prevalence of antimicrobial-resistant infections remains obscured because of fragmented, heterogeneous, and often absent surveillance systems. The efficacy of ceftriaxone, widely used as first-line therapy, is increasingly threatened by the expansion of strains harboring the mosaic *penA* 60.001 allele, first documented in 2015 and now recognized globally as the dominant determinant of AMR. Our systematic search of the published literature identified 212 such isolates; nearly half were detected after 2022 in England and Australia, and epidemiologic data frequently linked acquisition of infection to the Asia-Pacific region. The substantially higher case numbers reported in those countries reflect the strength of their gonococcal AMR surveillance systems and more timely public data sharing. Our findings suggest that underreporting of the actual prevalence of ceftriaxone resistance is likely and that the opportunity for action is limited.

Neisseria gonorrhoeae bacteria are a priority pathogen for the World Health Organization (WHO) and cause an estimated 82 million new infections annually worldwide. Optimal disease control strategies remain unclear in light of increasing reports of antimicrobial resistance (AMR) and very limited global surveillance. A systematic review of surveillance systems for monitoring gonococcal AMR from 2022 found no evidence of a current surveillance system for gonorrhea in 148 countries, and only 6 countries (Australia, England, Wales, Scotland, Canada, and New Zealand) had gonococcal surveillance systems that were comprehensive and national. Those systems include all culture-based diagnoses of antimicrobial-susceptible gonorrhea infections and cover >50% of jurisdictions in their respective countries (*1*).

Historically, *N. gonorrhoeae* bacteria have developed resistance to every first-line therapeutic agent (*2*), including ceftriaxone, the current first-line treatment; newer agents such as gepotidacin and zoliflodacin show promise as alternatives. However, the longevity of the newer agents remains uncertain, particularly in settings where circulating *N. gonorrhoeae* isolates harbor the *parC* D86N mutation, 1 of 2 observed mutations required to develop resistance to the newer agents (*3*). In 2015, the emergence and subsequent spread of the ceftriaxone-resistant *N. gonorrhoeae* FC428 clone (i.e., strains harboring the ceftriaxone-resistance determinant) heralded the beginning of an era of increasing uncertainty regarding future antimicrobial drug management strategies (*4*,*5*). More than a decade later, the mosaic *penA* allele 60.001 persists as the prevailing determinant of ceftriaxone resistance (*6*).

We searched the published literature in June 2025 to identify reports of ceftriaxone-resistant *N. gonorrhoeae* bacteria harboring the *penA* 60.001 allele with linked genomic sequence data, to gain a contemporary understanding of AMR. We limited the search to isolates carrying *penA* 60.001 because other resistance-associated alleles, including the emerging *penA* 237.001 allele, remain relatively rare (*7*), whereas *penA* 60.001 has been consistently detected through routine surveillance across diverse settings. Although ceftriaxone-resistant *N. gonorrhoeae* has been reported by Canada, Japan, China, and WHO programs, the corresponding MICs and genomic sequencing data were not available (*8*–*12*).

We collated a total of 440 ceftriaxone-resistant isolates and defined resistance as an MIC ≥0.25 mg/L, regardless of the original susceptibility testing method used. Of the 440 isolates, 296 (67.3%) harbored the *penA* 60.001 allele, and genomic data were available for 212 (48.2%) isolates. Fifty percent (106/212) of all

Author affiliations: Royal Prince Alfred Hospital, Sydney, New South Wales, Australia (S.J. van Hal); University of Sydney, Sydney (S.J. van Hal); United Kingdom Health Security Agency, London, UK (H. Fifer); Prince of Wales Hospital, Randwick, New South Wales, Australia (M.M. Lahra); University of New South Wales, Sydney (M.M. Lahra)

DOI: https://doi.org/10.3201/eid3206.260378

cases of ceftriaxone-resistant *N. gonorrhoeae* infection had been reported since 2022; 48% (51/106) of those were detected in England (n = 19) and Australia (n = 32). The remaining cases were detected in the Asia-Pacific region (n = 49), other countries in Europe (n = 4), and North America (n = 2) (*7*,*13*–*18*).

We constructed a phylogenetic tree, as previously described (*6*), following a mapping approach that used reference strain FA1090 (GenBank accession NC_002964.2) and masked recombination by using Gubbins version 2.12 (*19*). The phylogenetic analysis confirmed that the *penA* 60.001 allele associated with ceftriaxone resistance is predominantly in the Asia-Pacific region and that most cases detected elsewhere were linked to contact or travel in that region (Figure). The analysis also indicated that ceftriaxone resistance continues to evolve and has only a minority of recent isolates still clustering within the original FC428 clone. This trend of resistance evolution within multiple different clonal backbones signals an expanding and growing problem that is unlikely to be contained, portending serious challenges for therapy.

Of note, most gonococcal infections are diagnosed by using molecular testing, and culture rates vary substantially across countries. Nevertheless, outside of the Asia-Pacific region, most reported cases of ceftriaxone-resistant *N. gonorrhoeae* infection are reported from England and Australia. One plausible explanation for the higher detection rates in those countries is the strength and coverage of their surveillance systems and the close integration of culture-based testing and antimicrobial susceptibility testing.

Gonococcal AMR in England and Wales is monitored through the Gonococcal Resistance to Antimicrobials Surveillance Programme, a sentinel surveillance system covering ≈2% of total yearly gonorrhea diagnoses (*20*). In addition, all cases of gonorrhea, regardless of infection site, have a sample taken for culture, and all ceftriaxone-resistant isolates in England are referred to the national Sexually Transmitted Infections Reference Laboratory for confirmation and follow-up (*21*). The number of ceftriaxone-resistant infections is reported on a quarterly basis. In Australia, culture is similarly recommended when feasible, and isolates are forwarded to the relevant jurisdictional *Neisseria* reference laboratories for antimicrobial susceptibility testing and follow-up. Australia's jurisdictional *Neisseria* reference laboratories form a network, the National *Neisseria* Network, which is supported by the federal government and is responsible for the national surveillance system. National AMR surveillance data, derived from ≈24% of total annual cases, are publicly reported.

In contrast, even in countries with established surveillance systems, the low number of detected resistant isolates may primarily reflect underascertainment, resulting from the limited scope of culture-based surveillance, which typically tests or reports only a small fraction of cases through sentinel programs mainly targeting symptomatic men. Such restricted sampling might also explain why WHO-associated surveillance initiatives, including the Enhanced Gonococcal Antimicrobial Surveillance Programme in South-East Asia, have not detected higher rates of ceftriaxone resistance to date, except in Cambodia and Vietnam (*9*,*22*). Similarly, actual prevalence of antimicrobial-resistant *N. gonorrhoeae* infections in China remains unclear because accessible publications are largely regional and describe heterogeneous sampling strategies, limiting national-level interpretation (*8*,*23*). Alternatively, the routine public reporting of gonococcal AMR in China, especially when linked to genomic analyses, remains uncommon. As a result, antimicrobial-resistant cases may be identified locally but not reported widely.

Relying on the identification of treatment failure as an alternative signal of resistance is subject to many limitations. Only a small number of treatment failures have been reported globally, and those that have are almost exclusively in high-income countries, reflecting surveillance bias and underreporting. Detection of treatment failure is further complicated by inconsistent definitions of treatment failure, variability in treatment regimens, limited follow-up, and restricted access to culture-based diagnostics. As a result, AMR surveillance and treatment failure reporting probably underestimate the actual prevalence of ceftriaxone-resistant infections (*24*).

Therefore, for myriad reasons, the actual prevalence of gonococcal AMR is underestimated, which has prompted calls to expand AMR surveillance systems (*10*). However, such expansion is not always feasible, given social and political barriers, constraints in funding and laboratory capacity, and logistical challenges of scaling culture-based and antimicrobial susceptibility testing. In the absence of comprehensive global surveillance, data from England and Australia act as a canary in the coal mine, providing early warning of sentinel events. Furthermore, those datasets represent the best available evidence and should be used to model actual AMR prevalence and help guide international policy and intervention strategies.

The trajectory of *N. gonorrhoeae* AMR expansion is such that the window of opportunity for effective intervention is rapidly closing. Even with limited available global gonococcal AMR surveillance

data, ceftriaxone resistance is high in some parts of the Asia-Pacific region; recent reports indicate resistance estimates of ≥20% (when applying an MIC >0.25 mg/L threshold) in some settings (*7*,*8*,*25*). The surveillance systems in England and Australia are signaling that ceftriaxone-resistant *N. gonorrhoeae* are transmitting globally and are originating from countries that report no ceftriaxone resistance. Furthermore, resistant isolates remain undetected in countries without comprehensive surveillance, meaning that the global gonococcal AMR prevalence exceeds current assumptions.

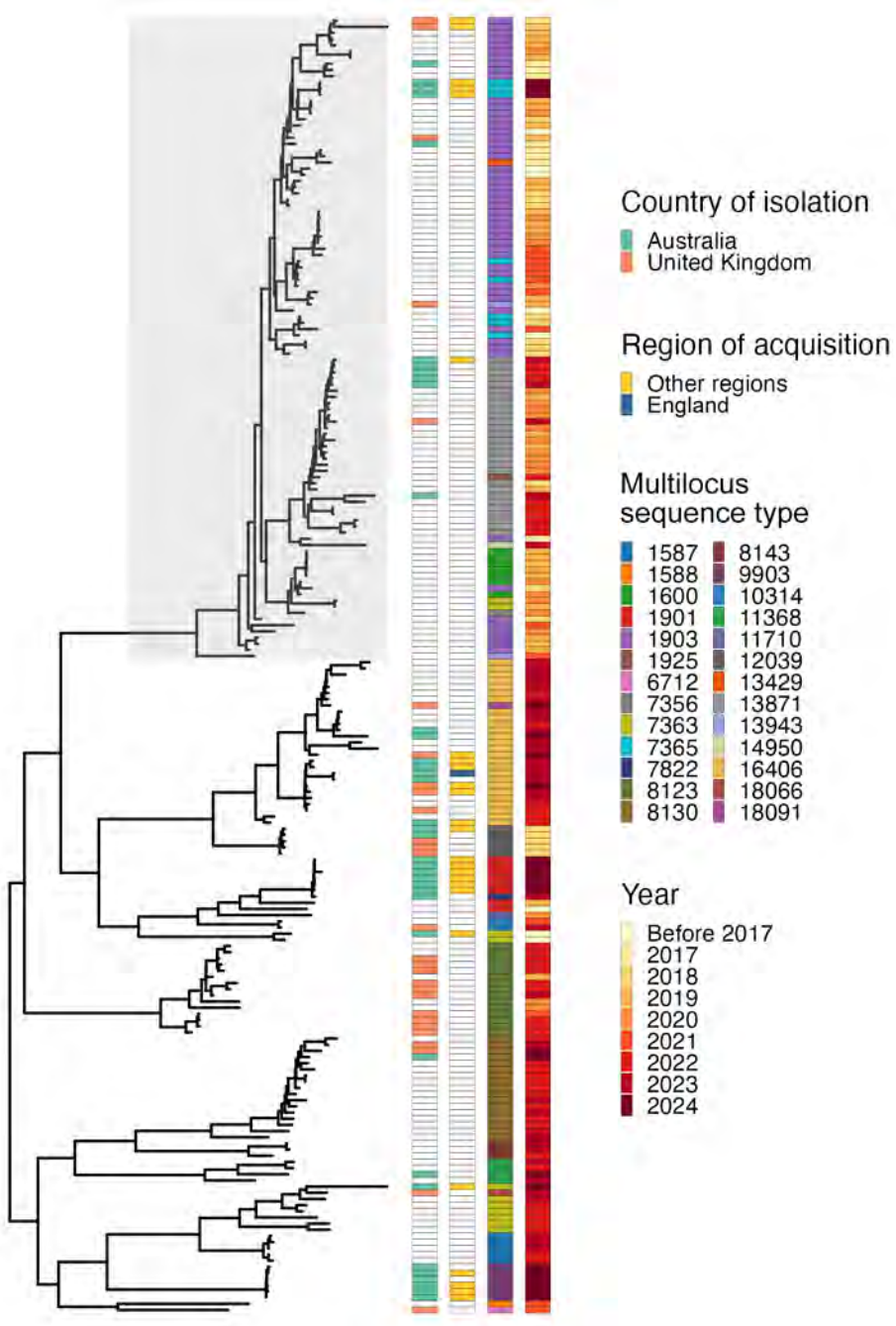

Figure. Maximum-likelihood phylogenetic tree of 212 ceftriaxone-resistant *Neisseria gonorrhoeae* isolates harboring *penA* 60.001 allele. Gray shading indicates original FC428 clone that emerged in 2015 in Japan and shows most new isolates clustering away from this clone. Columns at right shows isolates detected in England and Australia, reported regions where infections were acquired in Asia (countries include Cambodia, China, Indonesia, Japan, Thailand, Singapore, and Vietnam), multilocus sequence type, and year of isolation. Sequence types and isolate years demonstrate variation over time and genomic diversity.

The WHO Collaborating Center for Sexually Transmitted Infections and Antimicrobial Resistance, New South Wales Health Pathology, is the jurisdictional *Neisseria* Reference Laboratory responsible for gonococcal AMR surveillance, and the coordinating laboratory for the Australian Gonococcal Surveillance Programme, supported by the Government of Australia's Department of Health and Aged Care.

H.F. has received funding to attend a GSK Advisory Board meeting.

About the Author

Dr. van Hal is an infectious diseases physician and clinical microbiologist at the Royal Prince Alfred Hospital Sydney in Australia. His primary research interests include antimicrobial resistance, *Neisseria* infections, and pathogen genomics.

References

1. Medland NA, Zhang Y, Gunaratnam P, Lewis DA, Donovan B, Whiley DM, et al. Surveillance systems to monitor antimicrobial resistance in *Neisseria gonorrhoeae*: a global, systematic review, 1 January 2012 to 27 September 2020. Euro Surveill. 2022;27:2100917. https://doi.org/10.2807/1560-7917.ES.2022.27.18.2100917
2. Fifer H, Johnson A. The continuing evolution of antibiotic resistance in *Neisseria gonorrhoeae*: past, present and future threats to effective treatment. J Antimicrob Chemother. 2025;80:1213–9. https://doi.org/10.1093/jac/dkaf109
3. Mukherjee A, Blomqvist SOP, Helekal D, Das AA, Palace SG, Grad YH. Genetic background modulates zoliflodacin and gepotidacin cross-resistance and fitness in *Neisseria gonorrhoeae*. J Infect Dis. 2026;jiag174. https://doi.org/10.1093/infdis/jiag174
4. van der Veen S. Global transmission of the *penA* allele 60.001–containing high-level ceftriaxone-resistant gonococcal FC428 clone and antimicrobial therapy of associated cases: a review. Infect Microbes Dis. 2023;5:13–20. https://doi.org/10.1097/IM9.0000000000000113
5. Lee K, Nakayama SI, Osawa K, Yoshida H, Arakawa S, Furubayashi KI, et al. Clonal expansion and spread of the ceftriaxone-resistant *Neisseria gonorrhoeae* strain FC428, identified in Japan in 2015, and closely related isolates. J Antimicrob Chemother. 2019;74:1812–9. https://doi.org/10.1093/jac/dkz129
6. van Hal SJ, Sherry N, Coombs G, Mowlaboccus S, Whiley DM, Lahra MM. Emergence of an extensively drug-resistant *Neisseria gonorrhoeae* clone. Lancet Infect Dis. 2024;24:e547–8. https://doi.org/10.1016/S1473-3099(24)00486-9
7. Laumen JGE, Hieu VN, Nhung PH, Vandelannoote K, Nguyen TT, Nguyen TT, et al. High prevalence of ceftriaxone-resistant *Neisseria gonorrhoeae* in Hanoi, Vietnam, 2023–2024. J Infect Dis. 2025;232:e73–7. https://doi.org/10.1093/infdis/jiaf071
8. Zhu X, Xi Y, Gong X, Chen S. Ceftriaxone-resistant gonorrhea—China, 2022. MMWR Morb Mortal Wkly Rep. 2024;73:255–9. https://doi.org/10.15585/mmwr.mm7312a2
9. Lan PT, Nguyen HT, Golparian D, Thuy Van NT, Maatouk I, Unemo M, et al.; EGASP-Vietnam WGS Study Group. The WHO Enhanced Gonococcal Antimicrobial Surveillance Programme (EGASP) identifies high levels of ceftriaxone resistance across Vietnam, 2023. Lancet Reg Health West Pac. 2024;48:101125. https://doi.org/10.1016/j.lanwpc.2024.101125
10. Unemo M, Lahra MM, Cole MJ, Marcano Zamora D, Jacobsson S, Galarza P, et al. WHO global gonococcal antimicrobial surveillance programmes, 2019–22: a retrospective observational study. Lancet Microbe. 2025;6:101181. https://doi.org/10.1016/j.lanmic.2025.101181
11. Shimuta K, Ohama Y, Yoshida A, Nakayama SI, Ohnishi M, Kawahata T, et al.; Antibiotic-Resistant Gonorrhea Study Group. Emergence of a ceftriaxone-resistant *Neisseria gonorrhoeae* strain harbouring *penA*-60.001 in a novel genetic background (MLST 9903) in Japan, 2018–2024. Sex Transm Infect. 2025;sextrans-2025-056694. https://doi.org/10.1136/sextrans-2025-056694
12. Walsh TM, Plitt SS, Dingle TC, Charlton CL. Surveillance of antimicrobial resistance in *Neisseria gonorrhoeae* in Alberta from 2016–2022. Antibiotics (Basel). 2025;14:1119. https://doi.org/10.3390/antibiotics14111119
13. Lahra MM, van Hal S, Hogan TR. Australian Gonococcal Surveillance Programme annual report, 2023. Commun Dis Intell (2018). 2025;49:1–16
14. Fifer H, Doumith M, Rubinstein L, Mitchell L, Wallis M, Singh S, et al. Ceftriaxone-resistant *Neisseria gonorrhoeae* detected in England, 2015–24: an observational analysis. J Antimicrob Chemother. 2024;79:3332–9. https://doi.org/10.1093/jac/dkae369
15. Maubaret C, Caméléna F, Mrimèche M, Braille A, Liberge M, Mainardis M, et al. Two cases of extensively drug-resistant (XDR) *Neisseria gonorrhoeae* infection combining ceftriaxone-resistance and high-level azithromycin resistance, France, November 2022 and May 2023. Euro Surveill. 2023;28:2300456. https://doi.org/10.2807/1560-7917.ES.2023.28.37.2300456
16. Pleininger S, Indra A, Golparian D, Heger F, Schindler S, Jacobsson S, et al. Extensively drug-resistant (XDR) *Neisseria gonorrhoeae* causing possible gonorrhoea treatment failure with ceftriaxone plus azithromycin in Austria, April 2022. Euro Surveill. 2022;27:2200455. https://doi.org/10.2807/1560-7917.ES.2022.27.24.2200455
17. Jolley KA, Maiden MC. BIGSdb: Scalable analysis of bacterial genome variation at the population level. BMC Bioinformatics. 2010;11:595. https://doi.org/10.1186/1471-2105-11-595
18. Sánchez-Busó L, Yeats CA, Taylor B, Goater RJ, Underwood A, Abudahab K, et al. A community-driven resource for genomic epidemiology and antimicrobial resistance prediction of *Neisseria gonorrhoeae* at Pathogenwatch. Genome Med. 2021;13:61. https://doi.org/10.1186/s13073-021-00858-2
19. Croucher NJ, Page AJ, Connor TR, Delaney AJ, Keane JA, Bentley SD, et al. Rapid phylogenetic analysis of large samples of recombinant bacterial whole genome sequences using Gubbins. Nucleic Acids Res. 2015;43:e15. https://doi.org/10.1093/nar/gku1196
20. United Kingdom Health Security Agency. GRASP report: data to September 2025. 2025 Nov [cited 2026 Apr 20]. https://www.gov.uk/government/publications/gonococcal-resistance-to-antimicrobials-surveillance-programme-grasp-report/grasp-report-data-to-september-2025
21. Fifer H, Ismail MA, Soni S, Nwaosu U, Sadiq ST, Milligan A, et al. British Association of Sexual Health and HIV UK national guideline for the management of infection with *Neisseria gonorrhoeae*, 2025. Int J STD AIDS. 2025;36:826–40. https://doi.org/10.1177/09564624251345195

22. Ouk V, Pham CD, Wi T, van Hal SJ, Lahra MM; EGASP Cambodia Working Group. The Enhanced Gonococcal Surveillance Programme, Cambodia. Lancet Infect Dis. 2023;23:e332–3. https://doi.org/10.1016/S1473-3099(23)00479-6
23. Lin X, Chen W, Yu Y, Lan Y, Xie Q, Liao Y, et al. Emergence and genomic characterization of *Neisseria gonorrhoeae* isolates with high levels of ceftriaxone and azithromycin resistance in Guangdong, China, from 2016 to 2019. Microbiol Spectr. 2022;10:e0157022. https://doi.org/10.1128/spectrum.01570-22
24. Fagan L, Alexander S, Fifer H. The invisible tide of *Neisseria gonorrhoeae* treatment failures: a review and commentary. Clin Infect Dis. 2026;81(Supplement_5):S223–30. https://doi.org/10.1093/cid/ciaf532
25. Ouk V, Say HL, Virak M, Deng S, Frankson R, McDonald R, et al.; EGASP Cambodia Working Group. World Health Organization Enhanced Gonococcal Antimicrobial Surveillance Programme, Cambodia, 2023. Emerg Infect Dis. 2024;30:1493–5. https://doi.org/10.3201/eid3007.240354

Address for correspondence: Sebastiaan J. van Hal, Department of Infectious Diseases and Microbiology, NSW Health Pathology, Royal Prince Alfred Hospital, Sydney, NSW 2050, Australia; email: sebastiaan.vanhal@health.nsw.gov.au

Cerebrospinal Fluid Findings among Patients with Anaplasmosis and Central Nervous Involvement, Minnesota and Wisconsin, USA

Igor Dumic,[1] Charles W. Nordstrom,[1] Marie Schulz, Sagar B. Dugani, John Fox, Ronin Joshua Cosiquien, Tatjana Gavrancic, Margaret Paulson, Cristian Madrid, Wendelyn Bosch

Medscape CME Activity

In support of improving patient care, this activity has been planned and implemented by Medscape, LLC and Emerging Infectious Diseases. Medscape, LLC is jointly accredited with commendation by the Accreditation Council for Continuing Medical Education (ACCME), the Accreditation Council for Pharmacy Education (ACPE), and the American Nurses Credentialing Center (ANCC), to provide continuing education for the healthcare team.

Medscape, LLC designates this Journal-based CME activity for a maximum of 1.00 ***AMA PRA Category 1 Credit(s)™***. Physicians should claim only the credit commensurate with the extent of their participation in the activity.

Successful completion of this CME activity, which includes participation in the evaluation component, enables the participant to earn up to 1.0 MOC points in the American Board of Internal Medicine's (ABIM) Maintenance of Certification (MOC) program. Participants will earn MOC points equivalent to the amount of CME credits claimed for the activity. It is the CME activity provider's responsibility to submit participant completion information to ACCME for the purpose of granting ABIM MOC credit.

All other clinicians completing this activity will be issued a certificate of participation. To participate in this journal CME activity: (1) review the learning objectives and author disclosures; (2) study the education content; (3) take the post-test with a 75% minimum passing score and complete the evaluation at: https://www.medscape.org/qna/processor/ 77502?showStand Alone=true&isAspenArticle=true&src=prt_jcme_eid_mscpedu and (4) view/print certificate. For CME questions, see page 1037.

NOTE: It is the policy of Medscape Education to avoid the mention of brand names or specific manufacturers in accredited educational activities. However, trade and manufacturer names in this activity are provided in an effort to provide clarity. The use of brand or manufacturer names should not be viewed as an endorsement by Medscape of any specific product or manufacturer.

Release date: June 2, 2026; Expiration date: June 2, 2027

Learning Objectives

Upon completion of this activity, participants will be able to:

- Describe the epidemiology and clinical presentation of anaplasmosis.
- Distinguish the most common clinical presentation of anaplasmosis.
- Assess CSF findings in cases of anaplasmosis
- Evaluate outcomes of treatment of anaplasmosis

CME Editor

Amy J. Guinn, BA, MA, Technical Writer/Editor, Emerging Infectious Diseases. *Disclosure: Amy J. Guinn, BA, MA, has no relevant financial relationships.*

CME Author

Charles P. Vega, MD, Health Sciences Clinical Professor of Family Medicine, University of California, Irvine School of Medicine, Irvine, California. *Disclosure: Charles P. Vega, MD, has the following relevant financial relationships: consultant or advisor for: Boehringer Ingelheim; Exact Sciences; GlaxoSmithKline.*

Authors

Igor Dumic, MD; Charles W. Nordstrom, MD; Marie Schulz, BS; Sagar B. Dugani, MD, PhD; John Fox, MS; Ronin Joshua Cosiguien, BS; Tatjana Gavrancic, MD; Margaret Paulson, DO; Cristian Madrid, MD; Wendelyn Bosch, MD.

[1]These first authors contributed equally to this article.

Anaplasmosis, an emerging tickborne zoonosis, infrequently involves the central nervous system, and cerebrospinal fluid (CSF) profiles of anaplasmosis remain poorly characterized. We conducted a multisite retrospective study of patients hospitalized with anaplasmosis during November 1, 2014–November 29, 2024, in Minnesota and Wisconsin, USA, a hyperendemic region. Included patients had anaplasmosis confirmed by PCR on blood samples, exhibited neurologic symptoms, and had lumbar puncture procedures. Ten hospitalized patients met inclusion criteria, 6 with meningitis, 3 with meningoencephalitis, and 1 with encephalitis. CSF findings were within reference ranges for 5 patients; 4 patients demonstrated mild lymphocytic pleocytosis, but glucose and protein levels were within reference ranges. One patient underwent a traumatic lumbar puncture resulting in neutrophilic pleocytosis. CSF abnormalities did not correlate with neurologic severity, suggesting a cytokine-mediated process rather than direct central nervous system infection. All patients rapidly improved with doxycycline, highlighting the need for early recognition and empiric therapy for anaplasmosis.

Anaplasmosis is an emerging tickborne zoonosis that has substantially increased in incidence during the past 2 decades. That rise is attributed to improved diagnostic testing, heightened clinician awareness, and climate-related factors, mirroring trends observed with other vectorborne diseases that depend on vector survival for transmission (*1*–*6*). Anaplasmosis exhibits a wide spectrum of clinical manifestations, and common symptoms include fever, chills, rigors, headache, malaise, and myalgia. Laboratory abnormalities frequently include leukopenia, thrombocytopenia, and elevated transaminases (*1*–*6*). Patients with altered mental status, immunosuppression, advanced age, or multiple underlying conditions are at increased risk for hospitalization (*1*,*5*).

Although rare, neurologic manifestations of anaplasmosis can include encephalitis, meningitis, meningoencephalitis, focal paralysis, and stroke (*6*–*10*). Case reports describing patients with central nervous system (CNS) symptoms document variable cerebrospinal fluid (CSF) findings. In some instances, CSF profiles are within reference ranges, whereas other cases demonstrate variable pleocytosis, proteinorachia, or glycorrhachia (*8*–*16*).

Most data describing CSF profiles in CNS anaplasmosis have been limited to individual case reports (*8*–*16*), and retrospective studies or case series have not systematically evaluated CSF findings in patients primarily exhibiting CNS manifestations. Thus, we sought to characterize the CSF findings of patients hospitalized with anaplasmosis who exhibited predominantly CNS symptoms and underwent lumbar puncture (LP) and CSF analysis in an anaplasmosis hyperendemic region in Minnesota and Wisconsin, USA.

Methods

We conducted a retrospective chart review of adult patients with diagnosed *Anaplasma phagocytophilum* infection (International Classification of Diseases, 9th Revision, codes A77.49 or A79.82) who were admitted to Mayo Clinic Rochester or Mayo Clinic Health System sites in Minnesota and Wisconsin during November 1, 2014–November 29, 2024. The study was approved by the Mayo Clinic Institutional Review Board (approval no. 18-007901).

We manually reviewed a total of 101 patient charts. We included patients ≥18 years of age if they had a positive *A. phagocytophilum* PCR performed on EDTA-anticoagulated whole blood and predominantly had CNS symptoms when care was sought that prompted LP and CSF analysis.

We performed molecular detection by using the automated MagNA Pure 96 system (Roche Diagnostics, https://www.roche.com) for DNA extraction, followed by amplification of a conserved region of the *gro*EL heat shock protein operon gene. We identified organisms via melting curve analysis by using the LightCycler 480 Instrument II (Roche Diagnostics). That assay uses fluorescence resonance energy transfer probes to detect and differentiate *A. phagocytophilum*, *Ehrlichia chaffeensis*, *E. muris eauclairensis*, and *E. ewingii/canis* (*1*).

All patients underwent standard CSF testing including a meningitis/encephalitis panel per institutional protocol. We defined CNS symptoms as severe headache, confusion or altered mental status, central focal neurologic deficits, or signs of meningitis (including neck stiffness, photophobia, or positive meningeal signs).

Results

Of 101 hospitalized patients with anaplasmosis diagnoses, 10 (10%) met inclusion criteria. Among those,

Author affiliations: Mayo Clinic College of Medicine and Science, Rochester, Minnesota, USA (I. Dumic, C.W. Nordstrom, T. Gavrancic, M. Paulson, C. Madrid, W. Bosch); Mayo Clinic Health System, Eau Claire, Wisconsin, USA (I. Dumic, C.W. Nordstrom, M. Paulson, C. Madrid); Medical College of Wisconsin–Central Wisconsin, Wausau, Wisconsin, USA (M. Schulz, J. Fox); Mayo Clinic, Rochester (S.B. Dugani); University of Minnesota Twin Cities, Minneapolis, Minnesota, USA (R.J. Cosiquien); Mayo Clinic, Jacksonville, Florida, USA (T. Gavrancic, W. Bosch)

DOI: https://doi.org/10.3201/eid3206.260240

2 patients were immunocompromised and 4 required intensive care unit (ICU) admission. Six patients had clinical features consistent with meningitis, 3 with meningoencephalitis, and 1 with encephalitis (Table 1). All 10 patients underwent extensive infectious evaluation for alternative bacterial, viral, endemic fungal, and tickborne etiologies (Appendix Table, https://wwwnc.cdc.gov/EID/article/32/6/26-0240-App1.pdf), including testing for other *Ixodes scapularis* tick–transmitted pathogens. All of those results were negative, thereby excluding co-infection.

In all cases, LP was performed before initiation of doxycycline therapy. Five (50%) patient samples demonstrated pleocytosis, and the other 5 had CSF cell counts within reference ranges. Of the 5 patients with pleocytosis, 4 had mild lymphocytic pleocytosis (5–50 cells/μL [reference range 0–5 cells/μL]) and 1 had neutrophilic pleocytosis attributable to traumatic LP. CSF protein and glucose levels were within reference ranges in all patients except for patient 8, who had a traumatic LP.

Patient 1

A 75-year-old immunocompetent man was admitted with fever, headache, photophobia, chills, left-sided hemiparesis, and urinary retention. Laboratory evaluation revealed leukopenia, thrombocytopenia, and hyponatremia. Brain magnetic resonance imaging showed no evidence of acute infarction. After LP, empiric intravenous doxycycline was initiated, and complete neurologic and systemic improvement occurred within 72 hours. After 3 days, he was discharged to home to complete a 4-week course of doxycycline.

Patient 2

A 65-year-old immunocompetent woman was admitted with severe neck and facial pain localized to the frontal and maxillary sinuses, with suspected involvement of the bilateral V1 (ophthalmic division) and V2 (maxillary division) dermatomes. Associated signs and symptoms included headache, photophobia, blurred vision, fever (temperature 103°F), nausea, and vomiting. Symptoms began ≈2 weeks after sustaining a tick bite. Initial outpatient treatment with amoxicillin/clavulanate for presumed sinusitis was ineffective, and at admission she was febrile, tachycardic, and hypotensive, meeting sepsis criteria and requiring ICU admission. After LP and CSF collection, empiric broad-spectrum antimicrobial therapy, including doxycycline, was initiated. Clinical improvement occurred within 48 hours, and she achieved complete recovery after 2 weeks of therapy.

Patient 3

A 74-year-old immunocompetent woman was admitted for a 1-week history of intermittent headaches, photophobia, and abnormal involuntary movements characterized by akathisia and choreiform activity. On the day of admission, fever and chills developed. Laboratory evaluation revealed mild hyponatremia with an unremarkable complete blood count. After LP, empiric therapy with doxycycline and ceftriaxone was initiated. She demonstrated marked clinical improvement after the second dose and was discharged to complete a 10-day course of doxycycline. She reported residual fatigue and cognitive slowing for ≈3 months but ultimately achieved full recovery.

Patient 4

A 57-year-old immunosuppressed man with ulcerative colitis receiving prednisone therapy (20 mg/d) was admitted with 4 days of myalgias, arthralgias, chills, sweats, and fever, followed by onset of left

Table 1. Characteristics and cerebrospinal fluid findings among patients with anaplasmosis and central nervous system involvement, Minnesota and Wisconsin, USA*

Patient no.	Age, y/sex	Immune status	Neurologic manifestation	Sepsis	ICU admission	Cerebrospinal fluid results				
						Color	Leukocyte count†	Leukocyte type (%)	Protein, mg/dL‡	Glucose, mg/dL§
1	75/M	IC	Left hemiparesis, meningitis	N	N	Clear	5	Lymphocyte (40)	48	56
2	65/F	IC	Meningitis	Y	Y	Clear	1	Lymphocyte (78)	33	81
3	74/F	IC	Meningitis, akathisia	N	N	Clear	1	Lymphocyte (83)	33	67
4	57/M	IS	Meningitis	N	N	Clear	0	NA	31	61
5	57/M	IS	Meningitis	Y	Y	Clear	50	Lymphocyte (78)	40	58
6	67/F	IC	Meningitis	N	N	Clear	1	Lymphocyte (72)	34	66
7	60/M	IC	Meningoencephalitis	N	N	Clear	15	Lymphocyte (43); neutrophils (30)	27	53
8	60/F	IC	Meningoencephalitis	Y	Y	Bloody	198	Neutrophils (71)	18	60
9	70/F	IC	Meningoencephalitis	N	N	Clear	1	Lymphocyte (72)	33	80
10	70/M	IC	Encephalitis	Y	Y	Clear	10	Lymphocyte (50)	189	43

*IC, immunocompetent; ICU, intensive care unit; IS, immunosuppressed; NA, not applicable.
†Reference range 0.
‡Reference range <50 mg/dL.
§Reference range 36–101 mg/dL.

parietal headache. Physical examination revealed nuchal rigidity with a negative Brudzinski sign. Laboratory studies demonstrated neutropenia, thrombocytopenia, transaminitis, and elevated C-reactive protein. After CSF collection, intravenous doxycycline was initiated, resulting in complete symptom resolution within 2 days. He was discharged home to complete a 2-week course of doxycycline therapy.

Patient 5

A 57-year-old immunosuppressed man with primary sclerosing cholangitis and gallbladder carcinoma undergoing chemotherapy was admitted with a 9-day history of headache exacerbated by light and unresponsive to over-the-counter analgesics. Associated symptoms included nausea, vomiting, photophobia, fever, chills, and neck stiffness. Head CT demonstrated no acute abnormalities. On examination, he was febrile and tachycardic, with positive Kernig and Brudzinski signs. He met sepsis criteria and required ICU admission. After LP and CSF collection, empiric broad-spectrum antimicrobial therapy, including doxycycline, was initiated. He defervesced within 48 hours of doxycycline initiation and achieved complete recovery after a 2-week course of doxycycline therapy.

Patient 6

A 67-year-old woman was assessed for 1 day of frontal headache and fever. Initial head CT was unremarkable, and transient symptom improvement after treatment with droperidol and diphenhydramine prompted discharge. She returned the next day with worsening headache, photophobia, neck stiffness, and recurrent fever. Laboratory evaluation demonstrated pancytopenia, hyponatremia, and elevated aminotransferases. She reported extensive outdoor exposure with multiple tick bites. LP was performed and empiric doxycycline and ceftriaxone therapy initiated. She demonstrated rapid clinical improvement within 48 hours and was discharged home to complete a 10-day course of doxycycline.

Patient 7

A 60-year-old man had influenza-like illness develop several weeks after removing an engorged tick from his lower abdomen. Symptoms included fatigue, neck pain, headache, chills, and persistent fevers refractory to over-the-counter medications. At admission, he was febrile, confused, and tachycardic. After LP, empiric doxycycline therapy was initiated. His symptoms improved within 24 hours and resolved completely by the end of a 2-week course of doxycycline therapy.

Patient 8

A 60-year-old woman was assessed for a 1-week history of fever, severe diffuse headache radiating to the neck, photophobia, dizziness, and confusion. At admission, she was febrile and tachycardic, with pancytopenia, meeting sepsis criteria and requiring ICU admission. CSF analysis was consistent with a traumatic LP and demonstrated marked neutrophilic pleocytosis, low protein, and glucose within reference levels. Empiric broad-spectrum antimicrobial therapy was initiated, including intravenous doxycycline (initial dose of 200 mg). She completed a 2-week course of doxycycline and had a full clinical recovery.

Patient 9

A 70-year-old woman was admitted with a 3-week history of rigors, shaking chills, diaphoresis, nausea, malaise, myalgias, and intermittent fevers after a tick bite. She subsequently had photophobia, neck stiffness, headache, and progressive somnolence develop. CSF analysis showed clear fluid with no pleocytosis and protein and glycose levels within reference ranges. She improved within 48 hours of the start of intravenous doxycycline and achieved complete recovery by day 10.

Patient 10

A 70-year-old man with type 2 diabetes and hypertension was assessed with acute-onset confusion and inability to engage in meaningful conversation. He reported a mild frontal headache without associated photophobia, phonophobia, nausea, vomiting, or neck stiffness. On examination he was febrile and tachycardic. Laboratory studies demonstrated thrombocytopenia and leukopenia. CSF analysis demonstrated mild lymphocytic pleocytosis with proteinorachia and glucose within reference levels. He met sepsis criteria and required ICU admission. Despite empiric broad-spectrum antimicrobial therapy, fevers persisted, and encephalopathy worsened. After initiation of intravenous doxycycline (initial dose 200 mg), he defervesced within 24 hours, and his encephalopathy resolved within 72 hours. He completed a 3-week course of doxycycline therapy and recovered.

Discussion

Among the 10 patients described in this study, 6 had clinical features consistent with meningitis, 3 with meningoencephalitis, and 1 with encephalitis. Notable neurologic findings included akathisia and left hemiparesis in 2 patients who also exhibited meningitic symptoms. Two patients were immunocompromised, and 4 required ICU admission. All patients

demonstrated clinical improvement within 24–72 hours of initiating doxycycline therapy and achieved full recovery. Total duration of doxycycline therapy ranged from 10 to 28 days; most patients received 10–14 days of doxycycline therapy.

CSF profiles were variable and differed substantially from those typically observed in bacterial meningitis or meningoencephalitis (Table 1). One patient with severe meningitic symptoms requiring ICU-level care had CSF findings within reference ranges. Another patient experienced a traumatic LP resulting in neutrophilic pleocytosis and low protein levels. Because traumatic LP more commonly leads to elevated CSF protein concentrations, the low protein observed in this case was unexpected and might reflect laboratory measurement variability without clear clinical significance. In all remaining patients, mild lymphocytic pleocytosis was observed with protein and glucose levels within reference ranges. Total CSF cell counts generally were 0–50 cells/μL.

Those findings suggest that CNS symptom severity does not correlate with the degree of CSF pleocytosis or inflammation. Neurologic manifestations of anaplasmosis therefore might be mediated by systemic inflammatory responses rather than direct CNS invasion. Although human data are lacking, a canine study of meningoencephalomyelitis with concurrent anaplasmosis failed to detect pathogen nucleic acid in brain tissue or CSF, supporting the hypothesis that direct CNS invasion is unlikely (*17*). That interpretation is further supported by the limited penetration of doxycycline across the blood–brain barrier, suggesting that clinical improvement likely results from attenuation of systemic and neuroinflammatory processes rather than direct antimicrobial activity within the CNS. Doxycycline penetrates the blood–brain barrier at ≈15%–30% of serum levels. However, CNS penetration increases when inflammation is present. Penetration might be higher in cases of *Anaplasma* meningitis (*18*), but the rapid symptomatic improvement noted after doxycycline administration suggests that the primary benefit of the drug likely stems from attenuation of systemic processes rather than direct CNS activity.

The hyperinflammatory potential of anaplasmosis is further evidenced by its association with secondary hemophagocytic lymphohistiocytosis and markedly elevated serum ferritin levels during acute infection (*19*). In our study, 2 patients with sepsis who required ICU admission and in whom anaplasmosis was suspected at admission received an initial 200-mg intravenous dose of doxycycline to increase CNS concentrations because of its limited penetration across the blood–brain barrier. However, that practice is not recommended by current guidelines (*20*), and whether it provides clinical benefit remains unclear. Patient 1 initially had stroke-like symptoms, including hemiparesis and urinary retention, in addition to symptoms of meningitis. Although neuroimaging in this patient was unrevealing and symptoms resolved with doxycycline therapy, anaplasmosis-associated stroke has been reported in other cases and is thought to result from endothelial injury (*8*,*15*,*21*,*22*).

As observed previously, our findings suggest that CNS manifestations of anaplasmosis are common but seldom reported (*7*). Although encephalitis has been described as a relatively frequent CNS manifestation (*23*), many reported cases lacked CSF evaluation, raising the possibility of encephalopathy rather than true encephalitis. As of April 2025, only 1 prior case from our institution had documented encephalitis supported by CSF findings with rapid response to doxycycline therapy (*13*). Further studies are needed to elucidate the pathophysiologic mechanisms underlying CNS involvement in anaplasmosis.

Diagnosis of anaplasmosis relies on clinical evaluation within an appropriate epidemiologic context. Most patients exhibit fever, pancytopenia (particularly thrombocytopenia), elevated transaminases, and gastrointestinal symptoms (*5*). In endemic regions, recognition of that clinical constellation often prompts empiric doxycycline therapy, resulting in rapid symptom resolution. In all our cohort patients, CNS symptoms improved within 24–72 hours of initiating doxycycline. We hypothesize that many patients improve before LP can be performed, which might explain the relatively low frequency of CSF evaluation in anaplasmosis.

Although bacterial culture remains the most sensitive diagnostic modality for anaplasmosis (*24*), routine clinical use is impractical because specialized cell culture systems are needed and the incubation period can be up to 4 weeks (*24*). Consequently, blood-based molecular diagnostic tests commonly are used (*25*). Serologic testing is frequently negative early in the course of disease and cannot reliably exclude acute infection (*24*,*25*). We identified only 1 reported case in which *Anaplasma* spp. nucleic acid was detected in CSF (*26*).

Approximately 30% of patients with anaplasmosis require hospitalization with encephalopathy identified as a risk factor (*1*). In our cohort, 4 patients with CNS symptoms required ICU admission; however, all were clinically stable for transfer to a general medical ward within 48 hours, and only 1 required vasopressor support. ICU admission remains uncommon in

Table 2. Characteristics of patients with anaplasmosis from published case-reports used to investigate cerebrospinal fluid findings among patients with anaplasmosis and central nervous system involvement, Minnesota and Wisconsin, USA*

Reference no.	Age, y/sex	Immune status	Neurologic presentation	ICU admission	Cerebrospinal fluid†			
					Leukocyte count	Leukocyte type (%)	Protein, mg/dL	Glucose, mg/dL
(*8*)	65/F	IS	Stroke, encephalitis	Y	**7**	Lymphocyte (78)	28	**136**
(*9*)	70/F	IC	Syncope, meningoencephalitis	NR	**10**	Lymphocyte (50); neutrophils (50)	34	57.7
(*10*)	62/M	IC	Encephalitis	Y	**10**	Lymphocyte (50)	Within reference range	Within reference range
(*11*)	80/F	IC	Trigeminal neuralgia, fever, headache	N	0	NA	20	65
(*12*)	62/M	IC	OMA, saccades, encephalitis	NR	**160**	Lymphocyte (NR)	**243**	NR
(*13*)	33/M	IC	Meningitis	NR	**4**	Lymphocyte (85)	**52**	64
(*14*)	64/F	NR	Meningoencephalitis	NR	**6**	Lymphocyte (92)	38	60
(*15*)	70/F	NR	Encephalopathy, lacunar infarct	NR	0	NA	34.7	**130.2**
(*16*)	41/M	NR	Encephalitis, seizure	NR	**4**	NR	36	71

*Bold font indicates values above reference ranges. IC, immunocompetent; ICU, intensive care unit; IS, immunosuppressed; NA, not applicable; NR, not reported; OMA, opsoclonus-myoclonus-ataxia.
†Protein and glucose values were categorized as high according to reference ranges provided in the respective reports, when available. In adults, protein levels should be <50 mg/dL and glucose ranges from 36–101 mg/dL (2.0–5.6 mmol/L).

anaplasmosis, as demonstrated in a multicenter study in France (*27*). The higher ICU admission rate in our cohort might reflect recognition that anaplasmosis in Europe is generally a milder disease than in the United States (*28*). Genetic differences between *Anaplasma* spp. from North America and Europe might partially explain those clinical variations (*28*). Differences in strain pathogenicity, reporting practices, and underdiagnosis also might contribute to the observed disparity (*28*).

Our literature search identified 9 reported cases of anaplasmosis with CNS manifestations in which patients underwent LP and CSF examination (Table 2). Four of those patients had clinical signs and symptoms of encephalitis, 2 of meningoencephalitis, and 1 of meningitis. The other 2 patients who underwent LP had headache and CSF findings within reference ranges; they ultimately had trigeminal neuralgia and stroke diagnosed in addition to anaplasmosis. One patient with encephalitis also had concomitant ischemic stroke. Other rare neurologic manifestations, including opsoclonus-myoclonus-ataxia syndrome and hypometric saccades, have been described (*12*). Most (7/9) of the patients had CSF protein and glucose levels within reference ranges, and all 9 reported case-patients demonstrated lymphocytic pleocytosis, except for 1 patient with meningoencephalitis who had an equal percentage of neutrophils and lymphocytes in the CSF (Table 2). Although not routinely performed, metagenomic next-generation sequencing can detect *Anaplasma* spp. bacteria in CSF in select cases of meningitis or encephalitis (*26*,*29*).

In conclusion, patients with anaplasmosis who develop meningitis, encephalitis, or meningoencephalitis typically demonstrate minimal CSF abnormalities, characterized by absent or mild pleocytosis with protein and glucose levels within reference ranges. LP and CSF analysis might be of limited use for managing anaplasmosis-associated CNS symptoms and might be more valuable for excluding alternative infectious etiologies that can also cause neurologic symptoms after a tick bite, particularly neuroborreliosis, ehrlichiosis, and Powassan virus infection.

S.B.D. was supported by the National Institutes of Health/National Institute on Minority Health and Health Disparities (grant no. K23 MD016230). The funder had no role in study design, or data analysis and interpretation; in writing the manuscript; nor in the decision to submit the manuscript for publication. The findings and conclusions do not necessarily represent the views of the funder.

About the Author

Dr. Dumic is an associate professor of medicine at the Mayo Clinic College of Medicine and academic hospitalist in Eau Claire, Wisconsin, USA. His primary research interests include zoonosis, particularly tickborne infections.

References

1. Katragadda S, Yetmar ZA, Chesdachai S, Fida M, Pritt BS, Challener DW, et al. Trends in anaplasmosis over the past decade: a review of clinical features, laboratory data, and outcomes. Clin Infect Dis. 2026;82:539–47. https://doi.org/10.1093/cid/ciaf171
2. Biggs HM, Behravesh CB, Bradley KK, et al. Diagnosis and management of tickborne rickettsial diseases: Rocky Mountain spotted fever and other spotted fever group rickettsioses, ehrlichioses, and anaplasmosis—United States. MMWR Recomm Rep. 2016;65:1–44. https://doi.org/10.15585/mmwr.rr6502a1

3. Ingram D, Joseph B, Hawkins S, Spain J. Anaplasmosis in Pennsylvania: clinical features, diagnosis, and outcomes of patients diagnosed with *Anaplasma phagocytophilum* infection at Hershey Medical Center from 2008 to 2021. Open Forum Infect Dis. 2023;10:ofad193. https://doi.org/10.1093/ofid/ofad193
4. MacQueen D, Centellas F. Human granulocytic anaplasmosis. Infect Dis Clin North Am. 2022;36:639–54. https://doi.org/10.1016/j.idc.2022.02.008
5. Dumic I, Jevtic D, Veselinovic M, Nordstrom CW, Jovanovic M, Mogulla V, et al. Human granulocytic anaplasmosis—a systematic review of published cases. Microorganisms. 2022;10:1433. https://doi.org/10.3390/microorganisms10071433
6. Schudel S, Gygax L, Kositz C, Kuenzli E, Neumayr A. Human granulocytotropic anaplasmosis—a systematic review and analysis of the literature. PLoS Negl Trop Dis. 2024;18:e0012313. https://doi.org/10.1371/journal.pntd.0012313
7. Moniuszko-Malinowska A, Dunaj J, Andersson MO, Chmielewski T, Czupryna P, Groth M, et al. Anaplasmosis in Poland—analysis of 120 patients. Ticks Tick Borne Dis. 2021;12:101763. https://doi.org/10.1016/j.ttbdis.2021.101763
8. Guru S, Mahar M, Guru N, Parent L. Neurologic manifestation of anaplasmosis: a case report. Cureus. 2025;17:e77877. https://doi.org/10.7759/cureus.77877
9. Sohani Z, Zhao N, Weiss K, Knecht H. Anaplasmosis encephalitis and infection of non-myeloid bone marrow precursors. BMJ Case Rep. 2023;16:e254603. https://doi.org/10.1136/bcr-2023-254603
10. Cosiquien RJS, Stojiljkovic N, Nordstrom CW, Amadi E, Lutwick L, Dumic I. *Anaplasma phagocytophilum* encephalitis: a case report and literature review of neurologic manifestations of anaplasmosis. Infect Dis Rep. 2023;15:354–9. https://doi.org/10.3390/idr15040035
11. LeDonne MJ, Ahmed SA, Keeney SM, Nadworny H. Trigeminal neuralgia as the principal manifestation of anaplasmosis: a case report. Cureus. 2022;14:e21668. https://doi.org/10.7759/cureus.21668
12. Merati M, Rucker JC, McKeon A, Frucht SJ, Hu J, Balcer LJ, et al. A case of opsoclonus-myoclonus-ataxia with neuronal intermediate filament IgG detected in cerebrospinal fluid. J Neuroophthalmol. 2022;42:278–81. https://doi.org/10.1097/WNO.0000000000001599
13. Khera KD, Southerland DM, Miller NE, Garrison GM. A case of anaplasmosis during a warm Minnesota fall. J Prim Care Community Health. 2021;12:21501327211005895. https://doi.org/10.1177/21501327211005895
14. Mullholand JB, Tolman N, De Obaldia A, Hennrikus E. Central nervous system involvement of anaplasmosis. BMJ Case Rep. 2021;14:e243665. https://doi.org/10.1136/bcr-2021-243665
15. Kim SW, Kim CM, Kim DM, Yun NR. Manifestation of anaplasmosis as cerebral infarction: a case report. BMC Infect Dis. 2018;18:409. https://doi.org/10.1186/s12879-018-3321-4
16. Young NP, Klein CJ. Encephalopathy with seizures having PCR–positive *Anaplasma phagocytophilum* and *Ehrlichia chaffeensis*. Eur J Neurol. 2007;14:e3–4. https://doi.org/10.1111/j.1468-1331.2006.01582.x
17. Barber RM, Li Q, Diniz PP, Porter BF, Breitschwerdt EB, Claiborne MK, et al. Evaluation of brain tissue or cerebrospinal fluid with broadly reactive polymerase chain reaction for *Ehrlichia*, *Anaplasma*, spotted fever group *Rickettsia*, *Bartonella*, and *Borrelia* species in canine neurological diseases (109 cases). J Vet Intern Med. 2010;24:372–8. https://doi.org/10.1111/j.1939-1676.2009.0466.x
18. Nau R, Sörgel F, Eiffert H. Penetration of drugs through the blood-cerebrospinal fluid/blood-brain barrier for treatment of central nervous system infections. Clin Microbiol Rev. 2010;23:858–83. https://doi.org/10.1128/CMR.00007-10
19. Jevtic D, da Silva MD, Haylock AB, Nordstrom CW, Oluic S, Pantic N, et al. Hemophagocytic lymphohistiocytosis (HLH) in patients with tick-borne illness: a scoping review of 98 cases. Infect Dis Rep. 2024;16:154–69. https://doi.org/10.3390/idr16020012
20. Wormser GP, Dattwyler RJ, Shapiro ED, Halperin JJ, Steere AC, Klempner MS, et al. The clinical assessment, treatment, and prevention of Lyme disease, human granulocytic anaplasmosis, and babesiosis: clinical practice guidelines by the Infectious Diseases Society of America. Clin Infect Dis. 2006;43:1089–134. https://doi.org/10.1086/508667
21. García-Baena C, Cárdenas MF, Ramón JF. Cerebral haemorrhage as a clinical manifestation of human ehrlichiosis. BMJ Case Rep. 2017;2017:bcr2016219054. https://doi.org/10.1136/bcr-2016-219054
22. Eldaour Y, Hariri R, Yassin M. Severe anaplasmosis presenting as possible CVA: case report and 3-year *Anaplasma* infection diagnosis data is based on PCR testing and serology. IDCases. 2021;24:e01073. https://doi.org/10.1016/j.idcr.2021.e01073
23. Kositz C, Gygax L, Schudel S, Kuenzli E, Neumayr A. Comparison of the epidemiological and clinical fingerprints of human granulocytotropic anaplasmosis and human monocytotropic ehrlichiosis in the United States. PLoS One. 2025;20:e0334957. https://doi.org/10.1371/journal.pone.0334957
24. Aguero-Rosenfeld ME, Zentmaier L, Liveris D, Visintainer P, Schwartz I, Dumler JS, et al. Culture and other direct detection methods to diagnose human granulocytic anaplasmosis. Am J Clin Pathol. 2025;163:313–9. https://doi.org/10.1093/ajcp/aqae126
25. Wormser GP, Zentmaier L, Liveris D, Schwartz I, Schneider L, Aguero-Rosenfeld ME. Antibodies to *Anaplasma phagocytophilum* in patients with human granulocytic anaplasmosis confirmed by both polymerase chain reaction and culture. Am J Med. 2025;138:669–72. https://doi.org/10.1016/j.amjmed.2024.11.025
26. Lee FS, Chu FK, Tackley M, Wu AD, Atri A, Wessels MR. Human granulocytic ehrlichiosis presenting as facial diplegia in a 42-year-old woman. Clin Infect Dis. 2000;31:1288–91. https://doi.org/10.1086/317466
27. Gerber V, Lemmet T, Bonijoly T, Hoellinger B, Pachart A, Woerly A, et al. Retrospective multicenter study of human granulocytic anaplasmosis, France, 2012–2024. Emerg Infect Dis. 2025;31:2225–32. https://doi.org/10.3201/eid3112.250946
28. Matei IA, Estrada-Peña A, Cutler SJ, Vayssier-Taussat M, Varela-Castro L, Potkonjak A, et al. A review on the eco-epidemiology and clinical management of human granulocytic anaplasmosis and its agent in Europe. Parasit Vectors. 2019;12:599. https://doi.org/10.1186/s13071-019-3852-6
29. Piantadosi A, Mukerji SS, Ye S, Leone MJ, Freimark LM, Park D, et al. Enhanced virus detection and metagenomic sequencing in patients with meningitis and encephalitis. MBio. 2021;12:e0114321. https://doi.org/10.1128/mBio.01143-21

Address for correspondence: Igor Dumic, Mayo Clinic College of Medicine, 1221 Whipple St, Eau Claire, WI 54703, USA; email: dumic.igor@mayo.edu

Emergence of *Klebsiella pneumoniae* Carbapenemase–Producing *K. pneumoniae* with Penicillin-Binding Protein 3 Insertions,Taiwan, 2021

Tengfei Long, Arianne Lovey, Lillie Sanborn, Yanan Zhao, Zackery P. Bulman, Yi-Tsung Lin, Liang Chen

Carbapenem-resistant Enterobacterales (CRE) are a major global health threat with limited treatment options. Aztreonam/avibactam is a promising therapy against metallo-β-lactamase (MBL)–producing and other CRE, but emerging resistance threatens its effectiveness. Insertions in penicillin-binding protein 3 (PBP3), which are well described in *Escherichia coli*, are linked to reduced aztreonam/avibactam susceptibility but remain poorly characterized in *Klebsiella pneumoniae*. We report clinical *K. pneumoniae* carbapenemase–producing *K. pneumoniae* sequence type 11 isolates carrying a novel PBP3 YRIT insertion, conferring reduced susceptibility to aztreonam/avibactam and ceftazidime/avibactam. Functional and genetic studies suggest that the PBP3 insertion impairs β-lactam binding and, in combination with bla_{KPC-2} and other β-lactamases, contributes to reduced susceptibility. Those findings demonstrate the emergence of a PBP3 insertion in a high-risk *K. pneumoniae* clone, underscoring the expansion of this resistance mechanism and the critical need for genomic surveillance and novel therapeutics to identify and treat such infections.

Carbapenem-resistant Enterobacterales (CRE) have emerged as one of the most urgent antimicrobial resistance threats worldwide (*1*). Infections caused by CRE are associated with prolonged hospitalization, limited therapeutic options, and substantial mortality rates. Among CRE, strains producing metallo-β-lactamase (MBL) are of particular concern because MBL enzymes hydrolyze most β-lactams (except for aztreonam), including carbapenems, and are not inhibited by available β-lactamase inhibitors, such as clavulanate, tazobactam, avibactam, relebactam, and vaborbactam. The global spread of MBL-producing Enterobacterales, particularly New Dehli metallo-β-lactamase (NDM)–producing strains, poses a formidable challenge for clinicians and public health systems. Of note, a recent study documented a 461% increase in the age-adjusted incidence of NDM-producing CRE in the United States during 2019–2023 (*2*).

Aztreonam/avibactam is a promising therapeutic option for infections caused by MBL-producing organisms (*3*). Aztreonam is intrinsically stable to hydrolysis by MBLs, and avibactam provides inhibition to coproduced serine β-lactamases, such as extended-spectrum β-lactamase (ESBL) and *Klebsiella pneumoniae* carbapenemase (KPC). The aztreonam/avibactam drug combination overcomes common combined resistance mechanisms in MBL-producers and other CRE, addressing a major therapeutic gap.

Nevertheless, emerging resistance mechanisms threaten the durability of aztreonam/avibactam. One concerning development is the insertion of motifs containing 4 amino acids, most commonly YRIK or YRIN (*4*), into penicillin-binding protein 3 (PBP3). PBP3 is a target of aztreonam and other β-lactam antibiotics, including ceftazidime, cefepime, and cefiderocol (*4*–*7*). Those PBP3 insertions are thought to alter

Author affiliations: School of Pharmacy and Pharmaceutical Sciences, University at Buffalo, Buffalo, New York, USA (T. Long, A. Lovey, L. Sanborn, Y. Zhao, L. Chen); Retzky College of Pharmacy, University of Illinois Chicago, Chicago, Illinois, USA (Z.P. Bulman); Centre for Infection Control and Division of Infectious Diseases, Department of Medicine, Taipei Veterans General Hospital, Taipei, Taiwan (Y.-T. Lin); Institute of Emergency and Critical Care Medicine, National Yang Ming Chiao Tung University, Taipei (Y.-T. Lin)

DOI: https://doi.org/10.3201/eid3206.260478

access to the transpeptidase pocket, thereby reducing the activity of PBP3-targeting agents. On their own, PBP3 insertions confer only modest increases in MICs to aztreonam/avibactam and ceftazidime/avibactam (*5*,*6*,*8*,*9*). However, those mutations frequently occur alongside additional β-lactamases (e.g., bla_{NDM} and bla_{CMY}) and other resistance determinants (e.g., *cirA* mutation) (*10*–*12*). Combined, those mechanisms can drive near pan–β-lactam resistance, which can have serious clinical consequences, including treatment failure and patient death (*11*,*12*).

PBP3 insertions predominantly have been described in *Escherichia coli* (*4*); however, the occurrence and clinical significance of PBP3 insertions in *K. pneumoniae*, another multidrug-resistant pathogen and leading cause of healthcare-associated infections, remain poorly understood. A few amino acid substitutions in PBP3 of *K. pneumoniae* have been implicated in increased resistance to aztreonam/avibactam, ceftazidime/avibactam, or ceftibuten/avibactam (*13*–*15*). However, to our knowledge, PBP3 insertions in clinical cases of *K. pneumoniae* have not yet been described in the literature, and the interplay between the PBP3 alterations and β-lactamases warrants further investigation. In this study, we describe 2 clinical cases in Taipei, Taiwan, involving KPC-producing *K. pneumoniae* isolates carrying PBP3 insertions.

Cases and Methods

Case 1

The first case occurred in a woman in her mid-70s with a history of heart failure and hypertension who was admitted to a tertiary-care hospital in Taipei for gastrointestinal bleeding in mid-April 2021. She initially received ciprofloxacin for pyuria on the basis of a prior urine culture that had yielded *E. coli*. During that admission, she had acute osteomyelitis of the right great toe diagnosed and underwent sequestrectomy on hospitalization day 14. Cultures from that specimen grew *Enterococcus faecalis* and *Streptococcus constellatus*, and she was treated with moxifloxacin. On hospitalization day 24, a new urinary tract infection developed, and urine culture grew carbapenem-resistant *K. pneumoniae* (isolate no. LC1490). Ceftazidime/avibactam therapy was initiated but was switched to amikacin after susceptibility testing confirmed reduced susceptibility to ceftazidime/avibactam (MIC 8 μg/mL) (Table). After a 7-day course of amikacin, the patient recovered and was discharged. In mid-to-late June 2022, she was readmitted for a right intertrochanteric hip fracture and underwent open reduction and internal fixation. Postoperatively, respiratory failure and shock developed, requiring admission to the intensive care unit. She was treated sequentially

Table. Antimicrobial susceptibility of isolates from a study of emergence of *Klebsiella pneumoniae* carbapenemase-producing *K. pneumoniae* with PBP3 insertions, Taiwan, 2021*

Strain	*bla* plasmids	MIC, μg/mL†								
		IMP	MEM	CAZ	ATM	CAZ/AVI	ATM/AVI	IMP/REL	MEM/VBR	CFDC
LC1489	bla_{KPC-2}, bla_{SHV-11}, bla_{TEM-1}, bla_{DHA-1}	**128**	**>128**	**>128**	**>128**	8	**8**	0.5	2	0.5
LC1490	bla_{KPC-2}, bla_{SHV-11}, bla_{TEM-1}, bla_{DHA-1}	**128**	**>128**	**>128**	**>128**	8	**8**	0.25	1	0.5
LC1491	bla_{SHV-11}, bla_{KPC-2}	**128**	**>128**	**>128**	**>128**	4	1	0.5	2	0.25
ΔpKPC										
LC1489	bla_{SHV-11}, bla_{TEM-1}, bla_{DHA-1}	**2**	**2**	**>128**	**16**	4	2	0.25	0.25	0.06
LC1490	bla_{SHV-11}, bla_{TEM-1}, bla_{DHA-1}	**2**	**2**	**>128**	**32**	4	4	0.25	0.25	0.06
LC1491	bla_{SHV-11}	0.25	1	4	2	1	1	0.5	0.25	0.06
LC1491 derivative‡										
LC2124, KPC-21a	bla_{SHV-11}, bla_{KPC-21}	**32**	**>128**	**>128**	**>128**	**32**	**>128**	**2**	4	1
LC2125, KPC-21b	bla_{SHV-11}, bla_{KPC-21}	**32**	**>128**	**>128**	**>128**	**16**	**>128**	**2**	4	0.5
LC2126, KPC-21c	bla_{SHV-11}, bla_{KPC-21}	**32**	**>128**	**>128**	**>128**	**32**	**>128**	**2**	4	1
ΔpKPC-pUC-NDM§										
LC1489	bla_{NDM-1}, bla_{SHV-11}, bla_{TEM-1}, bla_{DHA-1}	**>128**	**>128**	**>128**	**64**	**>128**	4	**>128**	**>128**	**32**
LC1490	bla_{NDM-1}, bla_{SHV-11}, bla_{TEM-1}, bla_{DHA-1}	**>128**	**>128**	**>128**	**64**	**>128**	4	**>128**	**>128**	**32**
LC1491	bla_{NDM-1}, bla_{SHV-11}	**>128**	**>128**	**>128**	4	**>128**	1	**>128**	**>128**	**32**

*All isolates had PBP3 insertion YRIT, OmpK35 with a premature stop codon at amino acid position 63, and OmpK36 with a glycine–aspartate insertion at amino acid position 134 GD. Bold indicates nonsusceptibility. ΔpKPC, bla_{KPC-2} plasmid-cured mutants; ATM, aztreonam; ATM/AVI, aztreonam/avibactam; CAZ, ceftazidime; CAZ/AVI, ceftazidime/avibactam; CFDC, cefiderocol; IMP, imipenem; IMP/REL, imipenem/relebactam; KPC, *Klebsiella pneumoniae* carbapenemase; MEM, meropenem; MEM/VBR, meropenem/vaborbactam; NDM, New Dehli metallo-β-lactamase; PBP3, penicillin-binding protein 3.
†Susceptibility determined on the basis of Clinical and Laboratory Standards Institute 2025 breakpoints (*16*), except for ATM/AVI, for which we used EUCAST breakpoint (>4 μg/mL).
‡Selected KPC-21 mutant strains obtained through an in vitro selection experiment.
§bla_{KPC-2} plasmid-cured mutants carrying a pUC-bla_{NDM-1} vector.

with piperacillin/tazobactam and ceftriaxone, with clinical improvement. However, on hospitalization day 18, a sputum culture yielded carbapenem-resistant *K. pneumoniae* (isolate no. LC1491). She received ceftazidime/avibactam for 9 days and recovered.

Case 2

The second case occurred in a man in his mid-90s, who was admitted to the same hospital as in case 1 for weakness and turbid urine in late April 2021. His medical history included ischemic stroke with bedbound status and chronic urinary retention managed with a long-term indwelling catheter. Three months before admission, urosepsis caused by multidrug-resistant *E. coli* was diagnosed and treated sequentially with cefepime, meropenem, ceftazidime, and levofloxacin. He was discharged 3 weeks before the late April 2021 admission. Culture of urine collected at admission revealed carbapenem-resistant *K. pneumoniae* (isolate no. LC1489). He was started on ceftazidime/avibactam for urinary tract infection, but susceptibility testing revealed reduced ceftazidime/avibactam susceptibility (MIC 8 μg/mL) (Table). Treatment was then switched to fosfomycin monotherapy for 7 days, and he recovered and was discharged.

Methods

We performed antimicrobial susceptibility testing of bacterial isolates by broth microdilution, according to Clinical and Laboratory Standards Institute guidelines (*16*). We assessed cefiderocol susceptibility by using iron-depleted Mueller-Hinton media. We performed whole-genome sequencing on a NovaSeq platform (Illumina, https://www.illumina.com) and performed genome assembly, quality control, and identification of multilocus sequence type (ST), capsule (K locus [KL]) and O-antigen locus, resistance genes, and porin mutations, as previously described (*17*,*18*). To assess clonal relatedness among isolates, we used Snippy version 4.6 (https://github.com/tseemann/snippy) to perform core single-nucleotide polymorphism (SNP) analysis, filtering repetitive and recombination regions, as previously described (*17*). As the reference for core SNP analysis, we used the genome of a completely closed ST11 *K. pneumoniae* strain, 2020N17-130, from Taiwan (GenBank accession no. CP129835). That strain is genetically close to isolates from the 2 cases (LC1489–91) but has a wild-type PBP3.

To evaluate the functional contribution of resistance determinants, we cured the bla_{KPC-2} plasmid by using our previously established pCasCure plasmid curing system (*19*), then performed susceptibility testing of cured derivatives. To identify resistance evolution, we conducted multistep in vitro selection experiments under aztreonam/avibactam treatment by using our previously published method (*20*) and performed whole-genome sequencing of resistant mutants to define the underlying genetic changes. We used confocal microscopy of live/dead staining to characterize morphologic changes in *K. pneumoniae* carrying wild-type PBP3 and PBP3 insertions (*21*). In addition, we cloned bla_{NDM-1} into a pUC vector and introduced clones into bla_{KPC-2}–cured strains to assess its effect on antimicrobial susceptibility profiles.

The Institutional Review Board of Taipei Veterans General Hospital provided ethics approval for the clinical data collection of both patients (approval no. 2024-01-004BC); the requirement for informed consent was waived. We deposited raw sequence data into National Center for Biotechnology Information (https://www.ncbi.nlm.nih.gov/bioproject; BioProject no. PRJNA1308160).

Results

Susceptibility testing showed that the 3 patient strains (LC1489–91) were resistant to imipenem and meropenem and displayed reduced susceptibility to ceftazidime/avibactam (MIC 4–8 μg/mL) and aztreonam/avibactam (MIC 1–8 μg/mL) but remained susceptible to imipenem/relebactam, meropenem/vaborbactam, and cefiderocol (Table). We next conducted conventional PCR and Sanger sequencing to examine whether the reduced ceftazidime/avibactam and aztreonam/avibactam susceptibility was caused by KPC variants (e.g., D179Y) or MBLs. Sequencing results revealed that bla_{KPC-2} was the only carbapenemase gene in each of the 3 isolates. The absence of KPC variants or MBLs suggested that other mechanisms caused the reduced susceptibility to ceftazidime/avibactam and aztreonam/avibactam.

Genomic analysis revealed that all 3 isolates belonged to the high-risk ST11 clone and harbored KL47 and O-antigen locus type 13. Core SNP analysis showed that the isolates differed by an average of 10 (range 8–12) SNPs, indicating a high degree of clonality. All 3 isolates carried the β-lactamase genes bla_{KPC-2}, bla_{TEM-1}, and bla_{SHV-11}. The outer membrane protein OmpK35 contained a premature stop codon at amino acid position 63, and the OmpK36 protein had a glycine-aspartate insertion at position 134. Isolates LC1489 and LC1490 carried an additional plasmid-borne AmpC gene, bla_{DHA-1} (Table). We suspect that the OmpK defects, combined with different β-lactamases, could partially contribute to the reduced aztreonam/avibactam and ceftazidime/avibactam susceptibility

observed in the isolates, which is consistent with findings reported in previous studies (*20*,*22*).

Of note, further mining revealed that all 3 strains contained a 4–amino acid insertion, YRIT, after residue 333 (positions 334–7) in FtsI (PBP3) (Figure 1). Amino acid insertions in PBP3, particularly the tetrapeptides YRIN or YRIK at the same position (aa 334–7), frequently have been reported in *E. coli* and are associated with reduced susceptibility to aztreonam, cefepime, ceftazidime, and cefiderocol, all of which primarily target PBP3. However, a comparable PBP3 YRIX tetrapeptide insertion has not previously been reported in *K. pneumoniae*. We hypothesized that this PBP3 insertion contributed to the reduced aztreonam/avibactam and ceftazidime/avibactam susceptibility observed in those strains. Confocal laser scanning microscopy analysis showed that when treated with aztreonam (≈1/2 MICs for 6 hours), the wild-type PBP3 became elongated and filamentous (Figure 2, panel A), a typical feature of PBP3 inhibition, whereas the PBP3 with insertion mutations remained unchanged (Figure 2, panel B), suggesting that those mutations confer resistance by preventing β-lactam from effectively binding to PBP3.

Of note, on the basis of available data from *E. coli* (*23*), PBP3 tetrapeptide insertions alone are not usually sufficient to confer β-lactam resistance. Those insertions often co-occur with β-lactamases like NDM or CMY, leading to elevated resistance to aztreonam/avibactam and other β-lactams, whereas we detected KPC-2 in our 3 strains.

To assess the effects of KPC on aztreonam/avibactam susceptibility, we precisely removed the KPC plasmid, then performed susceptibility testing. Curing bla_{KPC-2} markedly reduced the imipenem and meropenem MICs, rendering the strains susceptible to carbapenems. However, the bla_{KPC-2}–cured LC1489 and LC1490 strains remained resistant to aztreonam and ceftazidime because of bla_{DHA-1}. By contrast, the bla_{KPC-2}–cured LC1491 strain, which lacked bla_{DHA-1}, showed an >32-fold reduction in MICs for imipenem, meropenem, aztreonam, and ceftazidime. Curing bla_{KPC-2} also resulted in a 2- to 4-fold decrease in the MICs of novel β-lactam/β-lactamase inhibitor combinations, including aztreonam/avibactam, ceftazidime/avibactam, meropenem/vaborbactam, and cefiderocol.

Mutations in the bla_{KPC} gene, particularly those located in the Ω-loop, are known to cause resistance to ceftazidime/avibactam, arising through both in vitro selection and in vivo evolution. To determine whether high-level aztreonam/avibactam resistance could be obtained through bla_{KPC} mutation, we conducted an in vitro selection experiment to evaluate whether the PBP3 YRIT insertion strain could develop high-level resistance, following a previously published protocol (*20*). We chose strain LC1491 for that experiment because it carried only the bla_{KPC-2} carbapenemase gene and the chromosome-bearing bla_{SHV-11}. After multistep selection for aztreonam/avibactam resistance, the LC1491 strain had a MIC >128 μg/mL (Table).

To elucidate the underlying resistance mechanism, we isolated 3 resistant colonies from LC1491 (LC2124–26) and performed next-generation sequencing by using the NovaSeq platform (Illumina). Core-genome analysis revealed that the 3 mutants were nearly identical to the parental LC1491 strain, differing by <2 SNPs. Of note, all 3 resistant derivatives harbored a bla_{KPC-21} variant, which contained a single-nucleotide substitution (T→A at position 310) resulting in an amino acid change from tryptophan to arginine at Ambler position 105 (Trp105Arg, W105R). That variant corresponds to KPC-21, which was previously identified in a clinical *E. coli* ST131 isolate (*24*) and, in a recent in vitro selection study, was shown to confer resistance to aztreonam/avibactam in *E. coli* when combined with a PBP3 insertion (*25*).

To assess the effects of bla_{NDM-1} on the antimicrobial susceptibility profile of PBP3 insertions *K. pneumoniae*,

```
                  301       310        320        330        337        347        357
                   ....|....| ....|....| ....|....| ....|....| ....|....| ....|....|
WP_000642213(Ec) DVFEPGSTVK PMVVMTALQR GVVRENSVLN TVP----YRI NGHEIKDVAR YSELTLTGVL
AWF10252.1(Ec)   DVFEPGSTVK PMVVMTALQR GVVRENSVLN TIPYRIKYRI NGHEIKDVAR YSELTLTGVL
UWB59055.1(Ec)   DVFEPGSTVK PMVVMTALQR GVVRENSVLN TIPYRINYRI NGHEIKDVAR YSKLTLTGVL
YP_005225104(Kp) DVFEPGSTVK PMVVMTALQR GIVNENTVLN TVP----YRI NGHEIKDVAR YSELTLTGVL
LC1489(Kp)       DVFEPGSTVK PMVVMTALQR GIVNENTVLN TVPYRITYRI NGHEIKDVAR YSELTLTGVL
LC1490(Kp)       DVFEPGSTVK PMVVMTALQR GIVNENTVLN TVPYRITYRI NGHEIKDVAR YSELTLTGVL
LC1491(Kp)       DVFEPGSTVK PMVVMTALQR GIVNENTVLN TVPYRITYRI NGHEIKDVAR YSELTLTGVL
```

Figure 1. Penicillin-binding protein 3 (PBP3) amino acid alignment of *Klebsiella pneumoniae* carbapenemase–producing *K. pneumoniae* with PBP3 insertions, Taiwan, 2021. Representative *Escherichia coli* genomes with wild-type PBP3 (GenBank accession no. WP_000642213) and YRIK (accession no. AWF10252) and YRIN (accession no. YP_005225104) insertions are shown, as is *K. pneumoniae* genome without insertions. LC1489–91 are patient-derived *K. pneumoniae* genomes with PBP3 YRIT insertions from this study. Ec, *E. coli*; Kp, *K. pneumoniae*.

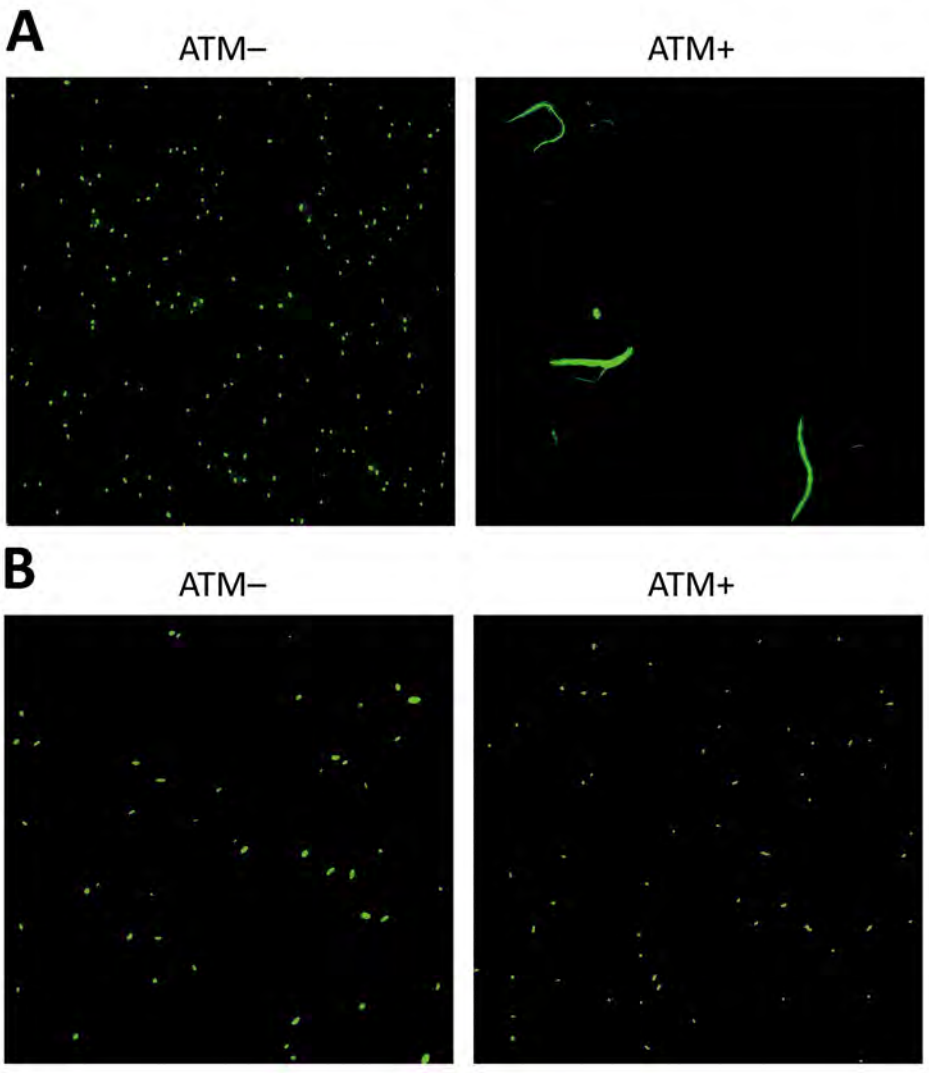

Figure 2. Confocal laser scanning microscopy of *Klebsiella pneumoniae* carbapenemase (KPC)–producing *K. pneumoniae* with penicillin-binding protein 3 (PBP3) insertions with and without ATM treatment, Taiwan, 2021. Isolates on the left (ATM–) were not treated with aztreonam and isolates on the right (ATM+) were treated with 64 μg/mL ATM for 6 hours. A) KPC-producing *K. pneumoniae* with wild-type PBP3 showing elongated and filamentous PBP3 in ATM+, a typical feature of PBP3 inhibition. Isolate used (isolate no. LC6990) was collected from the same hospital as patient isolate in this study (B) and had similar sequence type 11, K locus 47, KPC-2–producing background, and aztreonam MIC (>128 μg/mL). B) KPC-producing *K. pneumoniae* with PBP3 insertion mutations from isolate LC1491 from this study. Note that ATM+ does not show PBP3 inhibition (filamentation) under the conditions of this experiment. Images were acquired using a 63× objective. ATM, aztreonam.

we cloned bla_{NDM-1} into a pUC vector (pUC-bla_{NDM-1}) and introduced it into bla_{KPC}-cured LC1489, LC1490, and LC1491. The results showed that acquisition of bla_{NDM-1} led to high-level resistance to nearly all tested β-lactams and β-lactam/β-lactamase inhibitor combinations. Aztreonam/avibactam remained the most active agent against the 3 strains, with MICs of 4 μg/mL in pUC-bla_{NDM-1}–harboring LC1489 and LC1490 (both co-harboring bla_{DHA-1}) and of 1 μg/mL in pUC-bla_{NDM-1}–harboring LC1491. In addition, cefiderocol activity was substantially reduced in the bla_{NDM-1} constructs, with MICs increasing to 32 μg/mL.

Conclusions

Taken together, findings from this study identified the emergence of *K. pneumoniae* ST11 strains carrying a novel 4–amino acid YRIT insertion in PBP3, which was associated with reduced susceptibility to both aztreonam/avibactam and ceftazidime/avibactam. Although PBP3 insertions have been more commonly described in *E. coli*, detection in *K. pneumoniae* suggests the possibility for dissemination of this resistance mechanism across species. Of note, *K. pneumoniae* ST11 is a high-risk clone capable of acquiring diverse resistance and virulence plasmids and spreading efficiently (*26*–*28*). Our findings uncover a previously unrecognized mechanism contributing to β-lactam resistance in *K. pneumoniae* and underscore the urgent need for continued genomic surveillance, development of novel therapeutics, and reinforced infection control measures to identify, treat, and prevent such infections.

Research reported in this publication was supported in part by the National Institute of Allergy and Infectious Diseases of the National Institutes of Health (award nos. R21AI190454, R01AI182297, and R01AI173064). The content is solely the responsibility of the authors and does not necessarily represent the official views of the National Institutes of Health.

About the Author

Dr. Long is a postdoctoral researcher in the Chen Lab at the School of Pharmacy and Pharmaceutical Sciences, University at Buffalo, Buffalo, New York. His research interests focus on the molecular mechanisms of antimicrobial resistance and the development of novel therapeutics.

Reference

1. Sati H, Carrara E, Savoldi A, Hansen P, Garlasco J, Campagnaro E, et al.; WHO Bacterial Priority Pathogens List Advisory Group. The WHO bacterial priority pathogens list 2024: a prioritisation study to guide research, development, and public health strategies against antimicrobial resistance. Lancet Infect Dis. 2025;25:1033–43. https://doi.org/10.1016/S1473-3099(25)00118-5
2. Rankin DA, Stahl A, Sabour S, Khan MA, Armstrong T, Huang JY, et al. Changes in carbapenemase-producing carbapenem-resistant Enterobacterales, 2019 to 2023. Ann Intern Med. 2025;178:1818–21. https://doi.org/10.7326/ANNALS-25-02404
3. Tamma PD, Heil EL, Justo JA, Mathers AJ, Satlin MJ, Bonomo RA. Infectious Diseases Society of America 2024 guidance on the treatment of antimicrobial-resistant gram-negative infections. Clin Infect Dis. 2024;8:ciae403. https://doi.org/10.1093/cid/ciae403
4. Long H, Zhao F, Feng Y, Zong Z. Global emergence of *Escherichia coli* with PBP3 insertions. J Antimicrob Chemother. 2025;80:178–81. https://doi.org/10.1093/jac/dkae393
5. Le Terrier C, Nordmann P, Buchs C, Poirel L. Effect of modification of penicillin-binding protein 3 on susceptibility to ceftazidime-avibactam, imipenem-relebactam, meropenem-vaborbactam, aztreonam-avibactam, cefepime-taniborbactam, and cefiderocol of *Escherichia coli* strains producing broad-spectrum β-lactamases. Antimicrob Agents Chemother. 2024;68:e0154823. https://doi.org/10.1128/aac.01548-23
6. Sato T, Ito A, Ishioka Y, Matsumoto S, Rokushima M, Kazmierczak KM, et al. *Escherichia coli* strains possessing a four amino acid YRIN insertion in PBP3 identified as part of the SIDERO-WT-2014 surveillance study. JAC Antimicrob Resist. 2020;2:dlaa081. https://doi.org/10.1093/jacamr/dlaa081
7. Alm RA, Johnstone MR, Lahiri SD. Characterization of *Escherichia coli* NDM isolates with decreased susceptibility to aztreonam/avibactam: role of a novel insertion in PBP3. J Antimicrob Chemother. 2015;70:1420–8. https://doi.org/10.1093/jac/dku568
8. Wang Q, Jin L, Sun S, Yin Y, Wang R, Chen F, et al. Occurrence of high levels of cefiderocol resistance in carbapenem-resistant *Escherichia coli* before its approval in China: a report from China CRE-Network. Microbiol Spectr. 2022;10:e0267021. https://doi.org/10.1128/spectrum.02670-21
9. Helsens N, Sadek M, Le Terrier C, Poirel L, Nordmann P. Reduced susceptibility to aztreonam-avibactam conferred by acquired AmpC-type β-lactamases in PBP3-modified *Escherichia coli*. Eur J Clin Microbiol Infect Dis. 2024;2:6. https://doi.org/10.1007/s10096-024-04769-z
10. Fabrizio C, Valzano F, Giuliano S, Morelli E, Serio D, Buccoliero GB, et al. Optimizing target inactivation to treat multidrug-resistant *Escherichia coli* with NDM and PBP3 mutations: "going the extra mile." Antimicrob Agents Chemother. 2026;20:e0088725. https://doi.org/10.1128/aac.00887-25
11. Senchyna F, Murugesan K, Rotunno W, Nadimpalli SS, Deresinski S, Banaei N. Sequential treatment failure with aztreonam-ceftazidime-avibactam followed by cefiderocol due to preexisting and acquired mechanisms in a New Delhi metallo-β-lactamase–producing *Escherichia coli* causing fatal bloodstream infection. Clin Infect Dis. 2024;78:1425–8. https://doi.org/10.1093/cid/ciad759
12. Simner PJ, Bergman Y, Conzemius R, Jacobs E, Tekle T, Beisken S, et al. An NDM-producing *Escherichia coli* clinical isolate exhibiting resistance to cefiderocol and the combination of ceftazidime-avibactam and aztreonam: another step toward pan–β-lactam resistance. Open Forum Infect Dis. 2023;10:ofad276. https://doi.org/10.1093/ofid/ofad276
13. Guo Y, Liu N, Lin Z, Ba X, Zhuo C, Li F, et al. Mutations in porin LamB contribute to ceftazidime-avibactam resistance in KPC-producing *Klebsiella pneumoniae*. Emerg Microbes Infect. 2021;10:2042–51. https://doi.org/10.1080/22221751.2021.1984182
14. Mushtaq S, Vickers A, Doumith M, Garello P, Woodford N, Livermore DM. Frequencies and mechanisms of mutational resistance to ceftibuten/avibactam in Enterobacterales. J Antimicrob Chemother. 2025;80:645–56. https://doi.org/10.1093/jac/dkae452
15. Pasteran F, Manuel De Mendieta J, Pujato N, Dotta G, González LJ, Rizzo M, et al. From genomics to treatment: overcoming pan–drug-resistant *Klebsiella pneumoniae* in clinical settings. Front Pharmacol. 2025;16:1570278. https://doi.org/10.3389/fphar.2025.1570278
16. Clinical and Laboratory Standards Institute. Performance standards for antimicrobial susceptibility testing; thirty-fifth informational supplement (M100-S35). Wayne (PA): The Institute; 2025.
17. van Duin D, Arias CA, Komarow L, Chen L, Hanson BM, Weston G, et al.; Multi-Drug Resistant Organism Network Investigators. Molecular and clinical epidemiology of carbapenem-resistant Enterobacterales in the USA (CRACKLE-2): a prospective cohort study. Lancet Infect Dis. 2020;20:731–41. https://doi.org/10.1016/S1473-3099(19)30755-8
18. Wang M, Earley M, Chen L, Hanson BM, Yu Y, Liu Z, et al.; Multi-Drug Resistant Organism Network Investigators. Clinical outcomes and bacterial characteristics of carbapenem-resistant *Klebsiella pneumoniae* complex among patients from different global regions (CRACKLE-2): a prospective, multicentre, cohort study. Lancet Infect Dis. 2022;22:401–12. https://doi.org/10.1016/S1473-3099(21)00399-6
19. Hao M, He Y, Zhang H, Liao XP, Liu YH, Sun J, et al. CRISPR-Cas9–mediated carbapenemase gene and plasmid curing in carbapenem-resistant *Enterobacteriaceae*. Antimicrob Agents Chemother. 2020;64:e00843-20. https://doi.org/10.1128/AAC.00843-20
20. Niu S, Wei J, Zou C, Chavda KD, Lv J, Zhang H, et al. In vitro selection of aztreonam/avibactam resistance in dual-carbapenemase-producing *Klebsiella pneumoniae*. J Antimicrob Chemother. 2020;75:559–65. https://doi.org/10.1093/jac/dkz468
21. Lang Y, Shah NR, Tao X, Reeve SM, Zhou J, Moya B, et al. Combating multidrug-resistant bacteria by integrating a novel target site penetration and receptor binding assay platform into translational modeling. Clin Pharmacol Ther. 2021;109:1000–20. https://doi.org/10.1002/cpt.2205

22. Mendes RE, Doyle TB, Streit JM, Arhin FF, Sader HS, Castanheira M. Investigation of mechanisms responsible for decreased susceptibility of aztreonam/avibactam activity in clinical isolates of Enterobacterales collected in Europe, Asia and Latin America in 2019. J Antimicrob Chemother. 2021;76:2833–8. https://doi.org/10.1093/jac/dkab279
23. Ma K, Feng Y, McNally A, Zong Z. Struggle to survive: the choir of target alteration, hydrolyzing enzyme, and plasmid expression as a novel aztreonam-avibactam resistance mechanism. mSystems. 2020;5:e00821-20. https://doi.org/10.1128/mSystems.00821-20
24. Manageiro V, Romão R, Moura IB, Sampaio DA, Vieira L, Ferreira E, et al.; Network EuSCAPE-Portugal. Molecular epidemiology and risk factors of carbapenemase-producing *Enterobacteriaceae* isolates in Portuguese hospitals: results from European Survey on Carbapenemase-Producing *Enterobacteriaceae* (EuSCAPE). Front Microbiol. 2018;9:2834. https://doi.org/10.3389/fmicb.2018.02834
25. Ma K, Feng Y, Zong Z. Aztreonam-avibactam may not replace ceftazidime/avibactam: the case of KPC-21 carbapenemase and penicillin-binding protein 3 with four extra amino acids. Int J Antimicrob Agents. 2022;60:106642. https://doi.org/10.1016/j.ijantimicag.2022.106642
26. Dong N, Yang X, Chan EW, Zhang R, Chen S. *Klebsiella* species: taxonomy, hypervirulence and multidrug resistance. EBioMedicine. 2022;79:103998. https://doi.org/10.1016/j.ebiom.2022.103998
27. Yang X, Dong N, Chan EW, Zhang R, Chen S. Carbapenem resistance–encoding and virulence-encoding conjugative plasmids in *Klebsiella pneumoniae*. Trends Microbiol. 2021;29:65–83. https://doi.org/10.1016/j.tim.2020.04.012
28. Yang Y, Qin J, Hu Y, Wang J, Feng Y, Zong Z. Carbapenem-resistant *Klebsiella pneumoniae* of sequence type 11: a scoping review. J Infect Dis. 2026;233(Supplement_1):S72–80. https://doi.org/10.1093/infdis/jiaf635

Address for correspondence: Liang Chen, School of Pharmacy and Pharmaceutical Sciences, University at Buffalo, 360 Hayes Rd, Buffalo, NY 14214, USA; email: liangch@buffalo.edu; or Yi-Tsung Lin, Taipei Veterans General Hospital, No. 201, Sec. 2, Shih-Pai Rd, Taipei 11217, Taiwan; email: ytlin8@vghtpe.gov.tw

etymologia

New Delhi metallo-β-lactamase 1
[nū del'ē mə-tal'ō bāt'ə lak'tə-mās wuhn]

Surajit Chakraborty

New Delhi metallo-β-lactamase 1 (NDM-1) is an Ambler class B β-lactamase enzyme named after the capital of India, New Delhi. This class of enzymes requires Zn2+ ions for activity, hence metallo-β-lactamase. The transmissible genetic element–associated bla_{NDM-1} encodes NDM-1, which confers resistance to all β-lactam antibiotics except monobactams. The gene was first identified and reported in 2009 from a urinary tract infection–causing carbapenem-resistant *Klebsiella pneumoniae* isolate. Reportedly, the bla_{NDM-1}–harboring *K. pneumoniae* strain (linked to sequence type 14) was isolated from an India-born patient in Sweden who acquired a urinary tract infection while visiting New Delhi.

NDM's eponymous association with New Delhi sparked anguish among authorities in India, who saw the terminology as a means to tarnish the country's growing medical tourism industry. Some suggested changing the term to PCM (plasmid-encoding carbapenem-resistant metallo-β-lactamase). However, the sporadic concerns regarding nomenclature were never formally addressed, and the term NDM-1 eventually gained universal acceptance within the scientific community. By the end of 2025, >63 distinct NDM variants had been reported worldwide and sequentially designated NDM-1 through NDM-63.

Sources

1. Boncompagni SR, Antonelli A, Casciato B, Pieralli F, Vila AJ, Moreno DM, et al. NDM-63: a novel NDM metallo-β-lactamase variant in the L3 loop, from a *Klebsiella pneumoniae* clinical isolate. Antimicrob Agents Chemother. 2026;70:e0128625. https://doi.org/10.1128/aac.01286-25
2 Kumarasamy KK, Toleman MA, Walsh TR, Bagaria J, Butt F, Balakrishnan R, et al. Emergence of a new antibiotic resistance mechanism in India, Pakistan, and the UK: a molecular, biological, and epidemiological study. Lancet Infect Dis. 2010;10:597–602. https://doi.org/10.1016/S1473-3099(10)70143-2
3. Mohapatra PR. Metallo-β-lactamase 1—why blame New Delhi & India? Indian J Med Res. 2013;137:213–5.
4. Singh AR. Science, names giving and names calling: change NDM-1 to PCM. Mens Sana Monogr. 2011;9:294–319. https://doi.org/10.4103/0973-1229.77446
5. Yong D, Toleman MA, Giske CG, Cho HS, Sundman K, Lee K, et al. Characterization of a new metallo-β-lactamase gene, bla_{NDM-1}, and a novel erythromycin esterase gene carried on a unique genetic structure in *Klebsiella pneumoniae* sequence type 14 from India. Antimicrob Agents Chemother. 2009;53:5046–54. https://doi.org/10.1128/AAC.00774-09

Address for correspondence: Surajit Chakraborty, Department of Microbiology, All India Institute of Medical Sciences (AIIMS), Bathinda-151001, Punjab, India; email: surajitchakraborty285@gmail.com

Author affiliation: All India Institute of Medical Sciences, Bathinda, India

DOI: https://doi.org/10.3201/eid3206.241434

Group A *Streptococcus* Disease Outbreak Associated with Large Congregate Shelter, Chicago, Illinois, USA, October 2023–January 2024

Karrie-Ann Toews,[1] Lauren Tietje, Anne Meyers, Marco Ciaccio, Stephanie Gretsch, Alyse Kittner, Kendall Anderson, Matthew Bertagna, Elizabeth S. Davis, Stockton Mayer, Rebecca M. Singer, Margaret Mary Butler, Diana Arce-Garza, Thomas D. Huggett, Ryan Fabrizius, Jennifer Levy, Stephanie Black, Sopio Chochua, Christopher J. Gregory, Michelle Funk[1]

Chicago Department of Public Health identified 3 pediatric patients hospitalized with group A *Streptococcus* (GAS) disease during October 26–November 3, 2023, in a large congregate family migrant shelter in Chicago, Illinois, USA. One patient had invasive GAS infection; 2 had peritonsillar abscesses requiring drainage. Despite infection control measures, GAS pharyngitis cases continued through November 13. Chicago Department of Public Health coordinated clinical partners to perform rapid antigen detection testing and throat cultures for residents and staff with pharyngitis symptoms. During November 20, 2023–January 3, 2024, a total of 428 symptomatic persons were evaluated; 166 tested positive for GAS. Among persons with GAS pharyngitis, median age was 12 years (range 0–45 years); 54.2% were women and girls. Common symptoms included sore throat (87.3%) and fever (63.3%). One pediatric resident death caused by invasive GAS was confirmed postmortem. This response highlights outbreak challenges in large congregate shelters housing children.

From late 2022 through 2023, multiple countries marked increases in group A *Streptococcus* (GAS) infections, including less severe illnesses and invasive infections, especially in children <10 years of age (*1*,*2*). Invasive GAS (iGAS) infections increased in 10 US states during 2013–2022 and surged in the United States and Europe during 2022–2023 (*3*,*4*). GAS colonization is more common in children, in whom asymptomatic throat carriage ranges from 5% to 15% (*5*). Persons experiencing homelessness (PEH) have a higher risk for iGAS disease compared with the general population (*6*,*7*). Outbreaks of invasive and noninvasive GAS infections in PEH have been described predominantly in adults and have been linked to alcohol or injection drug use and wounds or other skin breakdown (*7*–*10*). Clusters of GAS infections in shelter settings have been characterized by whole-genome sequencing and have required rapid response activities to mitigate transmission (*8*,*10*). However, the transmission of GAS infections within homeless shelters is poorly understood, particularly in shelters that house children.

During August 31, 2022, through December 31, 2024, more than 50,000 migrant new arrivals, predominantly from Venezuela, traveled to Chicago, Illinois, USA, and the city of Chicago opened 27 shelters to house them (*11*). Shelters housed either families with children <18 years of age or single adults; for single adults, men and women were housed in sex-specific areas of the same building. Shelters ranged from hotel-based facilities with 1–2 families per room to warehouses with large open rooms housing hundreds of persons.

Author affiliations: Chicago Department of Public Health, Chicago, Illinois, USA (K.-A. Toews, L. Tietje, A. Meyers, M. Ciaccio, S. Gretsch, A. Kittner, K. Anderson, M. Bertagna, J. Levy, S. Black, M. Funk); Centers for Disease Control and Prevention, Atlanta, Georgia, USA (K.-A. Toews, S. Chochua, C.J. Gregory); Rush University Medical Center, Chicago (E.S. Davis, M.M. Butler); University of Illinois Chicago, Chicago (S. Mayer, R.M. Singer, D. Arce-Garza); Lawndale Christian Health Center, Chicago (T.D. Huggett, R. Fabrizius)

DOI: https://doi.org/10.3201/eid3205.250726

[1]These authors contributed equally to this article.

We describe the public health response to a GAS disease outbreak in a large, congregate new arrival shelter (shelter A) with a rapidly expanding census of ≈1,300–1,700 residents during October 26, 2023–January 3, 2024. Approximately 50% of the population housed at shelter A was <18 years of age.

Methods

iGAS infections are a reportable condition in Illinois and are defined as isolation of GAS from a normally sterile body site (e.g., blood or cerebrospinal fluid) or from a wound culture accompanied by necrotizing fasciitis or streptococcal toxic shock syndrome. Chicago Department of Public Health (CDPH) investigates all laboratory and provider-reported cases of iGAS disease in the city of Chicago. Investigations include identifying the clinical manifestations of infection, evaluating potential risk factors, and providing prevention and control guidance for cases that occur in a congregate or healthcare setting. Noninvasive GAS infections are those with clinically compatible illness and detection of GAS from a nonsterile site (e.g., throat or wound) and are not reportable in Illinois. The Illinois Department of Public Health defines an outbreak of GAS disease as either ≥2 epidemiologically linked iGAS disease cases or ≥1 iGAS disease case and ≥1 noninvasive GAS disease case that are epidemiologically linked within a 4-month period. We defined suspected cases in this outbreak as illness in persons at shelter A with symptoms consistent with pharyngitis that did not involve laboratory testing.

CDPH provides guidance and technical support to shelter facilities in infection prevention and control, outbreak response, disease reporting, behavioral health, maternal neonatal and child health, and healthcare navigation, and collaborates with healthcare providers serving this population. During August 2022–December 2024, healthcare for immigrant populations was provided predominantly by a health clinic associated with a large, publicly funded healthcare system. CDPH also funds shelter-based service teams that provide onsite clinical care at the shelters.

During the week beginning November 6, 2023, three cases of GAS infection requiring hospitalization were reported in residents of shelter A, who had symptom onset dates ranging from October 23 to November 3. One case was invasive, and 2 cases required surgical drainage of peritonsillar abscesses. All 3 cases were in children (<18 years of age); 2 cases were in children <5 years of age. Shelter A opened to house new arrivals approximately 3 weeks before the identification of the initial case. At that time, living quarters within the shelter were 3 large open congregate rooms on the first floor with multiple shared bathrooms and 2 large congregate eating spaces. Shelter A's capacity expanded from 3 large rooms for congregate living in November 8, 2023, to 8 congregate rooms in January 3, 2024 (housing ≈1,300–1,700 persons total). Data on admissions to and exits from the shelter are unavailable because admissions and exits during that period were fluid. CDPH conducted a site visit at shelter A on November 7 to identify spaces for isolation, introduce provider reporting, and implement an infection prevention assessment tool, which collected information on resident population, infection control practices, environmental cleaning, clinical partners, protocols for resident illness, isolation and exclusion policies, and disease reporting. On November 13, a CDPH-funded primary care team visited the shelter and evaluated ill persons. During November 3–13, CDPH identified additional residents of shelter A with suspected GAS pharyngitis. Beginning November 20, CDPH implemented enhanced case-finding and treatment for residents and staff.

Because resources for facilitywide screening and treatment were not available, CDPH collaborated with clinical partners to assess symptomatic residents and staff, conduct GAS testing, and provide treatment. Before the testing event, shelter managers distributed CDPH-developed Spanish-language handouts regarding GAS pharyngitis symptoms and the importance of testing and treatment, so that persons with sore throat or other compatible symptoms would seek care. During testing events, shelter managers and contracted clinical partners visited each room in shelter A to recruit residents for screening of symptoms consistent with GAS pharyngitis and refer symptomatic residents for onsite testing (*12*). Providers collected demographic information, sleeping location within the shelter, and symptoms; assessed symptomatic persons for signs of clinical instability; and, if needed, arranged emergency medical service transport. If patients were clinically stable, providers evaluated patients and performed a streptococcal rapid antigen detection test (RADT) to enable immediate diagnosis and treatment and collected a second swab specimen for culture. Because antimicrobial susceptibility testing results for 1 of the initial 3 hospitalized case-patients was pansusceptible, we administered azithromycin to persons testing positive on RADT (a regimen based on Centers for Disease Control and Prevention [CDC] guidance (*13*) and selected because of its short course and availability of liquid formulation for pediatric dosing), and we advised these patients to wear a face mask. Persons subsequently testing positive by culture received antibiotics if they could be located

after culture results were received. We recommended that persons testing negative on RADT receive additional clinical evaluation. If clinical suspicion of streptococcal pharyngitis remained high, especially in the context of close contacts testing positive on RADT, we administered antibiotics empirically. The CDC National Center for Immunization and Respiratory Diseases Division of Bacterial Diseases Streptococcus Laboratory and CDPH's locally contracted laboratory provided culture results. Provider teams visited shelter A for testing and treatment 3 times weekly for the first week and then decreased to once per week as resources allowed. The last testing and treatment event occurred on January 3, 2024, because the number of symptomatic persons seeking screening and the percentage testing positive declined and resources were prioritized to address an active varicella outbreak among residents of shelter A.

We sent bacterial cultures from the first testing event to the CDC Streptococcus Laboratory for strain characterization. The laboratory performed whole-genome sequencing (WGS) and single-nucleotide polymorphism (SNP) analyses to determine *emm* types and antimicrobial susceptibility and to verify temporal relatedness of the isolates. A commercial laboratory performed subsequent bacterial cultures, which were not available for WGS. We used results from WGS for surveillance purposes only and did not use them for diagnosis, treatment, assessment of patient health, or case management.

CDPH's activities were reviewed by the CDPH Institutional Review Board chair. The activities were determined to not constitute research and to be exempt from internal review board review.

Results

Surveillance, Outbreak Detection, Outbreak Response

During November 20, 2023–January 3, 2024, we tested a total of 428 persons (425 residents and 3 staff) for GAS at shelter A. Among persons tested, 260 (60.7%) tested negative, 166 (38.8%) tested positive, and 2 (0.5%) had missing test results (Figure 1). Of those who tested positive, we identified 114 (68.7%) through RADT and 52 (31.3%) through culture only (Table). We screened 25 symptomatic persons during >1 testing event, 2 (8%) of whom tested positive on subsequent testing. We identified cases among persons in all 8 rooms of the shelter, but we found most cases (109 [65.1%]) among persons in 2 rooms where the initial case-patients requiring hospitalization were housed (rooms A and B). Persons tested positive persons were predominantly women and girls (90 [54.2%]). Median age of persons testing positive was 12 years (range 0–45 years); 93 (56.0%) persons were in the 0–17-year age category. One child who previously tested negative during screening had disseminated iGAS diagnosed by a medical examiner outside of CDPH testing efforts.

We prescribed antibiotics to 144 (86.7%) persons testing positive and 73 (28.1%) symptomatic close contacts testing negative. Among persons testing positive through RADT, we treated 112 (98.2%) with antibiotics. Of the 52 who tested positive only through culture, 32 (61.5%) could be located and treated with azithromycin. We did not consider use of intramuscular benzathine G plus rifampin as a single dose because of limits on resources and operational capacity.

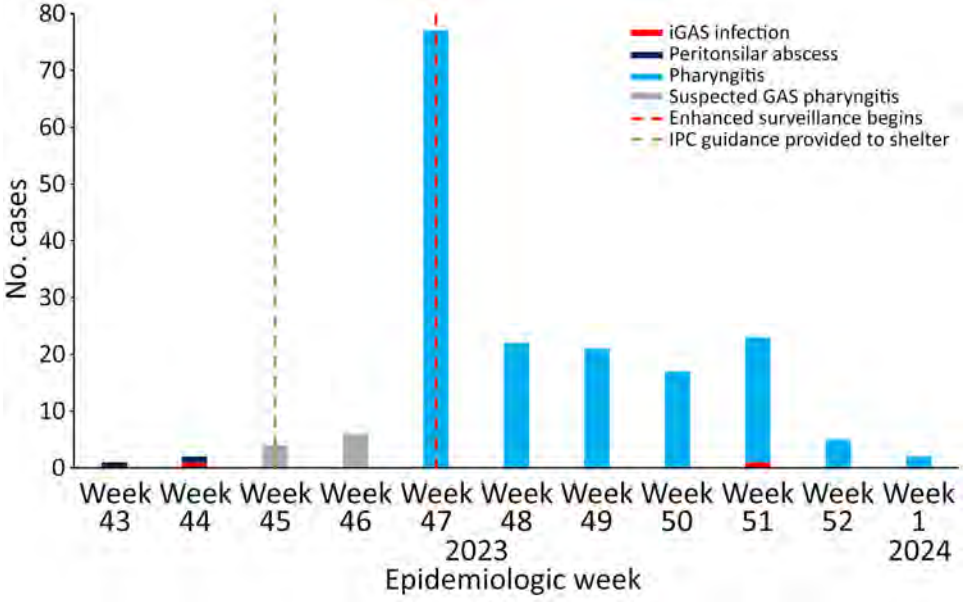

Figure 1. Epidemiologic curve for GAS *cases* in shelter A, by year and epidemiologic week, Chicago, Illinois, USA, October 25, 2023–January 3, 2024. Vertical dashed lines indicate key response activities. Suspect cases were identified clinically, without rapid or laboratory testing. Suspect cases identified clinically without rapid or laboratory testing. GAS, group A *Streptococcus*; iGAS, invasive GAS; IPC, infection prevention and control.

Table. Characteristics of 426 persons screened for *group A Streptococcus* during point prevalence survey screening in large congregate shelter, Chicago, Illinois, USA, November 20, 2023–January 3, 2024*

Characteristic	Identified through RADT, no. (%)	Identified through culture, no. (%)	Negative, no. (%)
Total	114 (100)	52 (100)	260 (100)
Resident	114 (100)	51 (98.1)	258 (99.2)
Staff	0 (0)	1 (1.9)	2 (0.8)
Sex			
M	54 (47.4)	21 (40.4)	108 (41.5)
F	60 (52.6)	30 (57.7)	152 (58.5)
Not reported	0	1 (1.9)	0
Age group, y			
0–17	61 (53.5)	32 (61.5)	135 (51.9)
18–29	27 (23.7)	14 (26.9)	57 (21.9)
30–39	22 (19.3)	6 (11.5)	52 (20.0)
40–49	4 (3.5)	0	13 (5.0)
50–59	0	0	2 (0.8)
≥60	0	0	1 (0.4)
Unknown	0	0	0
Room			
A	42 (36.8)	21 (40.4)	87 (33.5)
B	31 (27.2)	14 (26.9)	81 (31.2)
C	3 (2.6)	3 (5.8)	6 (2.3)
D	10 (8.8)	5 (9.6)	26 (10.0)
E	13 (11.4)	3 (5.8)	25 (9.6)
F	5 (4.4)	0	7 (2.7)
G	2 (1.8)	0	7 (2.7)
H	1 (0.9)	3 (5.8)	1 (0.4)
Unknown or unverified	7 (6.1)	1 (1.9)	18 (6.9)
NA	0	2 (3.8)	2 (0.8)
Symptoms			
Fever	76 (66.7)	29 (55.8)	162 (62.3)
Sore throat	102 (89.5)	43 (82.7)	212 (81.5)
Headache	72 (63.2)	26 (50.0)	146 (56.2)
Nausea	29 (25.4)	17 (32.7)	93 (35.8)
Vomiting	21 (18.4)	11 (21.2)	55 (21.2)
Abdominal pain	25 (21.9)	17 (32.7)	71 (27.3)
Difficulty breathing	35 (30.7)	21 (40.4)	108 (41.5)
Antibiotics prescribed	112 (98.2)	32 (61.5)	73 (28.1)

*Two cases had indeterminate results and are not included in this table. NA, not available; RADT, rapid antigen detection test.

During the outbreak, we conducted screening 13 times. On each testing day, 9–58 persons were tested (mean 33 persons). Screening positivity peaked on November 20, 2023, when 36 (78.3%) of 46 persons screened tested positive. The second-highest screening positivity occurred on December 27, 2023, when 5 (56.0%) of 9 persons screened tested positive (Figure 2). Because of rapid turnover, CDPH had no reliable mechanism to determine daily shelter census. We restricted GAS screening to those with clinically compatible symptoms. Close contacts of clinically compatible persons also were subject to screening at the discretion of the treating clinician. We observed no identifiable pattern to positivity during the screening period, and the number of persons screened varied because of the capacity of the testing teams.

Infection Control Assessment

After the November 5 infection control assessment, CDPH recommended that shelter A managers add signage for residents promoting hand hygiene and cough etiquette. Other recommendations were to ensure daily cleaning of bathrooms, coordinate transport of residents with respiratory illness to a contracted healthcare provider, retain onsite rapid COVID-19 and influenza testing capacity, and implement disease reporting.

Laboratory Testing

Of 48 cultures sent for typing, 14 (29.2%) were *emm*1.0, 19 (39.6%) were *emm*12, and 15 (31.3%) were *emm*75. We detected all 3 *emm* types in rooms A and B. In total, sequencing identified 6 different GAS sublineages (2 *emm*1, 3 *emm*12, and 1 *emm*75). WGS analysis identified 2 different clusters of *emm*1 isolates; cluster 1 consisted of 5 isolates with 0–2 SNP differences, and cluster 2 consisted of 8 isolates with 0–7 SNP differences. Two isolates available from the initial 3 case-patients were *emm*1 that were genetically indistinguishable and pan-susceptible.

Clinical Characteristics

Common symptoms among those persons in whom GAS pharyngitis was diagnosed were sore throat

(87.3%), fever (63.3%), and headache (59.0%). Among persons testing negative on RADT, we noted similar commonly reported symptoms, including sore throat (81.5%), fever (62.3%), and headache (56.2%). Among iGAS case-patients, the person with the invasive case during the initial cluster had otitis interna and infected mastoid air cells. The other case-patient with invasive disease was deceased on arrival to the emergency department, and testing demonstrated COVID-19 and adenovirus co-infection postmortem. The decedent child had GAS isolated from blood, cerebrospinal fluid, liver, and spleen; cause of death was determined by the medical examiner to be GAS sepsis. No additional peritonsillar abscesses or hospitalizations attributable to GAS after CDPH's response were reported.

Discussion

We describe a GAS disease outbreak in a new-arrival shelter in Chicago. Unlike outbreaks in traditional homeless shelters, which generally house an older population with wounds serving as a key risk factor (*5*,*6*,*8*,*9*), new arrival shelters may have a younger population with fewer underlying conditions, and clinical risk factors for infection may include co-infection with routine pediatric illnesses. New arrival shelter populations in Chicago were more dynamic than the traditional homeless shelter population because census spikes and housing demand were tied closely to the volume of new arrivals, and such populations may require tailored communication approaches because of language differences.

In more well-documented settings like healthcare facilities, outbreaks of GAS disease often are approached aggressively with testing and treatment of all potentially exposed persons (*14*,*15*). In response to another GAS disease outbreak among adults experiencing homelessness in Alaska, CDC's Arctic Investigations Program distributed treatment at sites frequently used by the population (e.g., shelters, soup kitchens, and supportive housing units) (*8*). The large and transient population in shelter A made neither of those approaches feasible. At the time of the outbreak, shelter A's census increased by ≈400 residents within a month's time, and lack of admission and exit tracking contributed to the challenge of quantifying this dynamic population. That rapid growth, coupled with limited public health resources, impeded deployment of shelterwide testing and treatment and necessitated targeted interventions. Because facilitywide screening or treatment was not feasible, we conducted testing of symptomatic persons at shelter A, aiming resources at persons more likely to spread infection among the shelter population.

Quick access to testing and treatment (including treatment of persons testing negative who had GAS-positive close contacts) onsite probably reduced the magnitude of spread. Because available laboratory data showed pansusceptibility, per CDC's guidelines on antibiotic regimens for carriage eradication in a long-term care facility (*13*), we selected azithromycin because of its shorter 5-day course and availability of pediatric liquid formulation for ease of administration. We used contracted clinical partners, experienced in working with transient populations, to enable rapid and repeated assessment and testing of shelter A residents during a nearly 2-month period. Use of streptococcal RADT, in conjunction with throat cultures, enabled immediate treatment of persons testing positive. Throat cultures were still critical diagnostic tools given that 12.4% of persons tested were found to be GAS culture positive while testing negative on RADT. Of note, persons testing GAS positive through culture alone were less likely

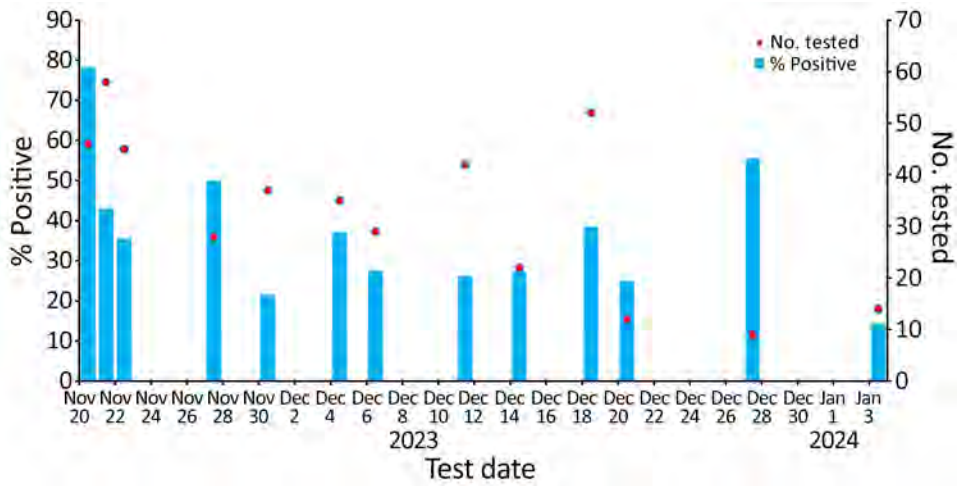

Figure 2. Group A *Streptococcus* percentage positivity on point prevalence screening dates and number of persons tested per day in shelter A, Chicago Illinois, USA, November 20, 2023–January 3, 2024.

to receive antibiotics because the large and rapidly changing population in shelter A made it challenging to relocate persons after their initial contact with the medical team. This situation led to ≥20 symptomatic persons who did not receive treatment and could potentially continue to spread disease to others in the shelter.

Despite intensive clinical assessment, we were not able to prevent a pediatric death caused by iGAS. The decedent child had been tested for GAS infection because of symptom onset (including fever, sore throat, headache, nausea, and vomiting) 13 days before their sudden death occurred and had tested negative for GAS by RADT and culture. We administered no antibiotics for this patient. Circulating viruses probably contributed to the child's death, given that infection with COVID-19 and adenovirus also were identified postmortem. That tragic outcome highlights the need for reevaluation and retesting of persistently symptomatic persons after a negative GAS test result, which is supported by the identification of 2 pharyngitis cases among the 25 persons tested >1 time. In addition, we could not assess the role of a language difference on health communication with this population in the context of this response. During a subsequent measles outbreak in a Chicago new arrival shelter, CDPH used a similar response infrastructure but also contracted community health workers to provide vaccine messaging. Those CDPH-contracted community health workers operated as part of the response architecture to provide culturally proficient vaccine messaging and validate resident comprehension. Our efforts substantially decreased the likelihood of a large measles outbreak in Chicago, and we hypothesize that similar messaging strategies may have led more shelter A residents with symptoms to seek care at our testing events during the iGAS response (*16*).

Although only a portion of isolates were able to be *emm* typed, we identified 3 *emm* types, suggesting multiple introductions of GAS to the shelter population as shelter A quickly expanded capacity. Further, multiple highly related isolates suggest transmission within the shelter. Adoption of routine entry screening or periodic screening in shelters could improve future outbreak response, contingent on available resources. Of note, the number of buses transporting new arrivals to Chicago tripled in number during this timeframe, and 27 shelters were opened.

The close aggregation of transient populations promotes transmission of viral illness (*17*), and the subsequent breakdown of skin from rash or respiratory epithelium from upper respiratory infections increases the risk for bacterial superinfections (*18*). We identified 1 co-infection with GAS and varicella rash in shelter A in January 2024, outside of the response period. Vaccine-preventable viral co-infections such as COVID-19 and varicella in a potentially vaccine-naive population may be contributing factors to GAS disease severity, hospitalization, and death. Varicella is not on the childhood vaccination schedule for many countries in South America and is not included on the childhood immunization list for Venezuela (*19*), which accounted for 88% of new arrivals arriving to Chicago during this period. Varicella infections frequently have been identified in new arrival shelter populations (*20*), resulting in multiple shelters in Chicago experiencing outbreaks. Shelter A was one of the most affected, having a large varicella outbreak beginning in January 2023. As GAS disease declined, public health resources were shifted to address that response as immunization teams were mobilized to prevent additional illness.

This outbreak highlights challenges with sheltering a highly dynamic population in a large, congregate space with a rapid increase in primary care needs. Although considerable pressure existed to house large numbers of new arrivals at the time, early containment of ill persons in an isolation space might have reduced transmission, overall disease prevalence, and hospitalization. Challenges included a daily dynamic shelter census, limited healthcare personnel resources, and limited ability to quantify symptomatic persons in an emergency shelter space not compatible with mass prophylaxis. Our response underscores the importance of access to healthcare and infection control resources in congregate shelter settings. CDPH's partnership with vulnerable population response teams with regular onsite symptom assessment, testing, and treatment in a culturally proficient manner, including the use of residents' language of choice, was instrumental in enabling a swift, well-coordinated, and prolonged response. WGS results provide evidence of multiple related transmission events in shelter A, underscoring transmission dynamics and the need for infection control measures in a congregate setting. Our findings augment previous experience that suggests the need for repeated assessment of continually symptomatic persons and communication recommending that those persons return for reevaluation may be critical in circumstances where whole facility screening is not feasible.

Acknowledgments

We thank shelter A staff for their support during this response, Massimo Pacilli, members of the CDC Streptococcal Laboratory, members of the Chicago

Department of Health Rapid Response Team at Rush University Medical Center and University of Illinois Chicago, collaborators at Lawndale Christian Health Center, Cook County Health, the Chicago Department of Family and Social Services, and the Cook County Chief Medical Examiner.

This project was supported in part by cooperative agreement NU50CK000556 from the Centers for Disease Control and Prevention.

About the Author

Ms. Toews is an epidemiologist with a focus on emerging infectious diseases and is a CDC Career Epidemiology Field Officer embedded in the Public Health Emergency Preparedness and Communicable Disease Programs at the Chicago Department of Public Health, where she currently manages invasive GAS surveillance and response activities.

References

1. Centers for Disease Control and Prevention. Increase in invasive group A strep infections, 2022–2023. 2023 Feb 2 [cited 2025 Apr 25]. https://archive.cdc.gov/#/details?url=https://www.cdc.gov/groupastrep/igas-infections-investigation.html
2. World Health Organization. Increased incidence of scarlet fever and invasive group A streptococcus infection—multi-country. 2022 Dec 15 [2025 Apr 25]. https://www.who.int/emergencies/disease-outbreak-news/item/2022-DON429
3. Bagcchi S. Surge of invasive group A streptococcus disease. Lancet Infect Dis. 2023;23:284. https://doi.org/10.1016/S1473-3099(23)00043-9
4. Gregory CJ, Okaro JO, Reingold A, Chai S, Herlihy R, Petit S, et al. Invasive group A streptococcal infections in 10 US states. JAMA. 2025;333:1498–507. https://doi.org/10.1001/jama.2025.0910
5. Shaikh N, Leonard E, Martin JM. Prevalence of streptococcal pharyngitis and streptococcal carriage in children: a meta-analysis. Pediatrics. 2010;126:e557–64. https://doi.org/10.1542/peds.2009-2648
6. Mosites E, Zulz T, Bruden D, Nolen L, Frick A, Castrodale L, et al. Risk for invasive streptococcal infections among adults experiencing homelessness, Anchorage, Alaska, USA, 2002–2015. Emerg Infect Dis. 2019;25:1911–8. https://doi.org/10.3201/eid2510.181408
7. Dohoo C, Stuart R, Finkelstein M, Bradley K, Gournis E. Risk factors associated with group A *Streptococcus* acquisition in a large, urban homeless shelter outbreak. Can J Public Health. 2020;111:117–24. https://doi.org/10.17269/s41997-019-00258-5
8. Mosites E, Frick A, Gounder P, Castrodale L, Li Y, Rudolph K, et al. Outbreak of invasive infections from subtype *emm*26.3 group A *Streptococcus* among homeless adults—Anchorage, Alaska, 2016–2017. Clin Infect Dis. 2018;66:1068–74. https://doi.org/10.1093/cid/cix921
9. Valenciano SJ, Onukwube J, Spiller MW, Thomas A, Como-Sabetti K, Schaffner W, et al. Invasive group A streptococcal infections among people who inject drugs and people experiencing homelessness in the United States, 2010–2017. Clin Infect Dis. 2021;73:e3718–26. https://doi.org/10.1093/cid/ciaa787
10. Adebanjo T, Mosites E, Van Beneden CA, Onukwube J, Blum M, Harper M, et al. Risk factors for group A *Streptococcus* colonization during an outbreak among people experiencing homelessness in Anchorage, Alaska, 2017. Clin Infect Dis. 2018;67:1784–7. https://doi.org/10.1093/cid/ciy429
11. City of Chicago. New arrivals situational awareness dashboard. 2024 Dec 18 [cited 2025 May 1]. https://www.chicago.gov/city/en/sites/texas-new-arrivals/home/Dashboard.html
12. Davis E, Mayer S, Pacilli M. Academic medical center–public health partnerships for outbreak response—collaborating with underresourced communities. N Engl J Med. 2024;391:679–81. https://doi.org/10.1056/NEJMp2407283
13. Centers for Disease Control and Prevention. Clinical guidance for group A streptococcal pharyngitis. 2025 Nov 18 [cited 2025 Apr 25]. https://www.cdc.gov/group-a-strep/hcp/clinical-guidance/strep-throat.html
14. Dooling KL, Crist MB, Nguyen DB, Bass J, Lorentzson L, Toews KA, et al. Investigation of a prolonged group A streptococcal outbreak among residents of a skilled nursing facility, Georgia, 2009–2012. Clin Infect Dis. 2013;57:1562–7. https://doi.org/10.1093/cid/cit558
15. Smith A, Li A, Tolomeo O, Tyrrell GJ, Jamieson F, Fisman D. Mass antibiotic treatment for group A Streptococcus outbreaks in two long-term care facilities. Emerg Infect Dis. 2003;9:1260–5. https://doi.org/10.3201/eid0910.030130
16. Gressick K, Nham A, Filardo TD, Anderson K, Black SR, Boss K, et al.; Chicago Department of Public Health Measles Response Team. Measles outbreak associated with a migrant shelter—Chicago, Illinois, February–May 2024. MMWR Morb Mortal Wkly Rep. 2024;73:424–9. https://doi.org/10.15585/mmwr.mm7319a1
17. Tietje L, Ghinai I, Cooper A, Tung EL, Borah B, Funk M, et al. Interventions to mitigate the impact of COVID-19 among people experiencing sheltered homelessness: Chicago, Illinois, March 1, 2020–May 11, 2023. Am J Public Health. 2024;114:S590–8. https://doi.org/10.2105/AJPH.2024.307801
18. Herrera AL, Huber VC, Chaussee MS. The association between invasive group A streptococcal diseases and viral respiratory tract infections. Front Microbiol. 2016;7:342. https://doi.org/10.3389/fmicb.2016.00342
19. World Health Organization. Introduction of varicella vaccine. 2025 [cited 2025 May 5]. https://immunizationdata.who.int/global/wiise-detail-page/introduction-of-varicella-vaccine?ISO_3_CODE=&CODE=Latin%20America%20and%20the%20Caribbean&YEAR=
20. Graham KA, Arciuolo RJ, Matalka O, Isaac BM, Jean A, Majid N, et al. Varicella outbreak among recent arrivals to New York City, 2022–2024. MMWR Morb Mortal Wkly Rep. 2024;73:478–83. https://doi.org/10.15585/mmwr.mm7321a1

Address for correspondence: Michelle Funk, Chicago Department of Public Health, 1340 South Damen Ave, Ste 400, Chicago, IL 60608, USA: email: michelle.funk@cityofchicago.org

Public Health Response to Toxigenic Respiratory Diphtheria Outbreaks at Correctional Facility, South Africa, 2023–2025

Maria Jose, Nectarios Papavarnavas, Arifa Parker, Charlene Lawrence, Janine Bezuidenhout, Levani Naidoo, Yolanda Cottee, Kathryn Grammer, Wentzel Dowling, Jocelyn Moyes, Anne von Gottberg, Mignon du Plessis, Hassan Mahomed

Since 2023, there have been 3 outbreaks of toxigenic respiratory diphtheria at a correctional facility in Cape Town, South Africa. The first outbreak in October 2023 included 1 fatal case and 8 asymptomatic carriers testing positive for *Corynebacterium diphtheriae*. In December 2024, the second outbreak resulted in 1 case and 12 asymptomatic carriers. A third outbreak in February 2025, occurring 6 weeks after the second, resulted in 1 case and 14 asymptomatic carriers among inmates and staff. Contact tracing, antimicrobial prophylaxis, and vaccination campaigns were conducted with each outbreak. We outline public health responses to the 3 outbreaks and highlight key barriers and enablers for effective control in a highly mobile, densely populated correctional setting. Effective outbreak response in correctional facilities requires intersectoral collaboration and the development of adult vaccination guidelines for staff and inmates to prevent future vaccine-preventable disease outbreaks.

Correctional service facilities are high-risk environments for the spread of infectious diseases because of overcrowded conditions, poor hygiene, reduced access to sanitation and healthcare, and lack of personal protective equipment for both inmates and staff (*1*). Although progress has been made in addressing tuberculosis and HIV among inmates, recent infectious disease outbreaks in correctional facilities, such as COVID-19 and leptospirosis, have been reported in South Africa (*2*,*3*).

Diphtheria, a category 1 notifiable medical condition in South Africa, is caused by toxin-producing strains of *Corynebacterium diphtheriae* and is known to be highly contagious and potentially fatal if not treated appropriately (*4*). The case-fatality rate for untreated, unvaccinated cases of respiratory toxigenic diphtheria has been estimated at 29%; asphyxia and endocarditis are the most frequent causes of death (*5*). Humans are the main reservoir; bacteria directly colonize the nasopharynx and spread via droplets from sneezing and coughing (*4*). Diphtheria can manifest as respiratory or cutaneous symptoms. Respiratory symptoms include low-grade fever, sore throat, and pseudomembranous pharyngitis with enlarged anterior cervical lymph nodes (bull neck). Systemic complications arising from toxin-induced tissue necrosis include myocarditis, neuropathy, nephropathy, and death (*6*). Fatalities among probable and confirmed symptomatic respiratory diphtheria cases in South Africa during January 2024–June 2025 were 12 (20%) of 60 cases (*7*). Although other countries with low vaccine coverage (Nigeria, Niger, Guinea, and Algeria) are currently experiencing diphtheria outbreaks, it is unlikely that the cases in South Africa are imported; the respiratory strains identified in South Africa to date appear to be unique to the country (*8*).

The Expanded Program for Immunisation schedule in South Africa recommends diphtheria-containing vaccine administration at 6, 10, and 14 weeks of age as the primary series, with boosters at 18 months,

Author affiliations: Western Cape Department of Health and Wellness, Cape Town, South Africa (M. Jose, N. Papavarnavas, A. Parker, C. Lawrence, J. Bezuidenhout, L. Naidoo, Y. Cottee, H. Mahomed); University of Cape Town, Cape Town (M. Jose, N. Papavarnavas, W. Dowling); Stellenbosch University, Cape Town (A. Parker, K. Grammer, H. Mahomed); National Health Laboratory Service at Groote Schuur Hospital, Cape Town (W. Dowling); National Institute for Communicable Diseases, Johannesburg, South Africa (J. Moyes, A. von Gottberg, M. du Plessis); University of the Witwatersrand, Johannesburg (A. von Gottberg, M. du Plessis)

DOI: https://doi.org/10.3201/eid3206.251957

6 years, and 12 years (*9*). Children <2 years of age receive diphtheria vaccination as part of the hexavalent vaccine (diphtheria, tetanus, pertussis, poliomyelitis, *Hemophilus influenzae* b, and hepatitis B). The vaccine antigen for *C. diphtheriae* is toxoid, generating antitoxin immunity. Vaccination coverage >90% is required to achieve adequate herd immunity (*5*). Booster doses at 6 and 12 years of age were given as a tetanus/diphtheria vaccine (Td); as of April 2024, the acellular pertussis vaccine (Tdap) vaccination for pregnant women became policy (*9*).

Literature on outbreak response in correctional facilities in low- and middle-income settings is limited. We describe the public health response to 3 consecutive outbreaks of toxigenic *C. diphtheriae* in a Cape Town, South Africa, correctional facility, prepared in accordance with the Canada Communicable Disease Report Outbreak reporting guide (*10*). The University of the Witwatersrand, Human Research Ethics Committee to the South Africa National Institute for Communicable Diseases, granted ethics approval (certificate no. M210752, formerly M160667) for essential communicable disease surveillance and outbreak investigation activities.

Methods

We used the NICD and Notifiable Medical Condition definitions as a reference guide for identifying cases and contacts (*4*). We defined a confirmed case as any person meeting the clinical criteria for ≥1 of the clinical forms of diphtheria and laboratory confirmation of the organism and toxin production. We defined a probable case as illness in any person meeting the clinical criteria for classic respiratory diphtheria and with an epidemiologic link to a confirmed case but for whom no diphtheria testing was performed, or illness in any person meeting the clinical criteria for classic respiratory diphtheria and laboratory confirmation of the organism but for which toxin production has not been confirmed. We defined an asymptomatic carrier as a person with laboratory confirmation of the organism and toxin production but no symptoms. We defined a close contact as a person with exposure to the case or known carrier in the preceding 10 days in a household-type setting or directly exposed to respiratory secretions or large-particle droplets without appropriate personal protective equipment (PPE) or exposure to an uncovered wound of a cutaneous case without appropriate PPE. We defined close contact in a healthcare setting as a person who came into contact with the patient without wearing a fluid-repellent mask who was within 2 meters of the patient and exposed for ≥15 minutes. In a prison setting, sharing the same cell would be considered close contact.

Outbreak Context

The correctional facility where the outbreaks occurred is managed by the Department of Correctional Services (DCS) and had an average number of 6,500 inmates and 1,287 staff during the period of documented outbreaks. The outbreaks occurred in the awaiting-trial section, which usually houses 1,200 inmates and 240 staff at any given time. Those awaiting trial usually have numerous contacts from court procedures and meetings with lawyers and family. Approximately 100 new and returning detainees are brought to the facility daily. The awaiting-trial section has 3 floors with 5–6 cells in use on each floor. One cell may house 60–70 detainees at a time with shared bunk beds and a sink and toilet in each.

With each confirmed outbreak (Figure), Western Cape Department of Health and Wellness (WCDHW) conducted contact tracing with symptom screening and nasopharyngeal and oropharyngeal swab testing. As a precaution, we placed detainee close contacts in group isolation and sorted them into cohorts on the basis of their symptom status initially, then reorganized cohorts after results identified confirmed cases. We offered all contacts a course of azithromycin, vaccinated them, and observed them for symptoms while awaiting their laboratory results.

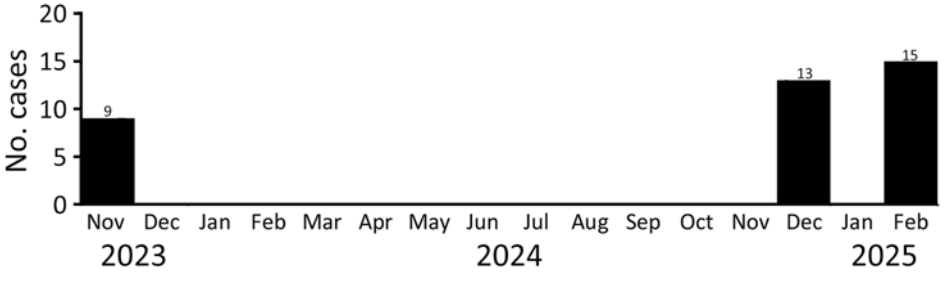

Figure. Epidemiologic curve for 3 outbreaks of toxigenic diphtheria at a correctional facility, Cape Town, South Africa, October 2023–February 2025. The outbreaks comprised 37 cases. Outbreak 1 control measures: extended vaccination campaign to staff and inmates, deep cleaning of affected section, no visitors to affected section of facility, and postponed court dates. Outbreak 2 control measure: an extended vaccine campaign to detainees in affected section of facility. Outbreak 3 control measures: extended vaccination campaign amongst detainees and staff, deep cleaning of facility, and personal protective equipment issued to visitors.

Laboratory Methods

We cultured clinical specimens at the National Health Laboratory Service Medical Microbiology Laboratory at the local academic hospital before sending them to the national reference laboratory at NICD for confirmation and additional characterization. We immediately conducted PCR on swab specimens and positive cultures to detect the *C. diphtheriae rpoB* gene and the *tox* gene (*11*). We conducted additional species identification for cultures by matrix-assisted laser desorption/ionization time-of-flight mass spectrometry and confirmed toxin production by modified Elek test (*12*). We performed whole-genome sequencing on *C. diphtheriae* isolates to determine sequence type using the 7-locus multilocus sequence type (ST) scheme (*8*). We submitted assembled genomes to the *Corynebacterium diphtheriae* complex BIGSdb public database (https://bigsdb.pasteur.fr/diphtheria) for ST assignment and core genome multilocus ST phylogeny.

Results

Outbreak 1: October–November 2023

The initial diphtheria outbreak began on October 22, 2023. The index patient was a young male detainee awaiting trial who had been in the correctional facility for several months. He was admitted to the hospital on October 28 for fever, swollen neck, shortness of breath, difficulty swallowing, sore throat, and a pseudomembrane. Assessment revealed that he had renal and cardiac complications as well. He received diphtheria antitoxin (DAT) at the central hospital. He died from complications on November 5, 2023.

The case was notified to the Western Cape Department of Health and Wellness (WCDHW) provincial Communicable Diseases Control office on October 28, 2023, activating the public health outbreak response. WCDHW collaborated with DCS, NICD, National Health Laboratory Service, emergency medical services (EMS), the City of Cape Town Municipality City Health Directorate, infectious disease experts, and infection prevention and control staff. Weekly meetings ensured timely communication and kept all stakeholders up to date. Despite initial uncertainty regarding which entity would support each aspect of outbreak response, such as contact tracing and provision of vaccinations, continued engagement clarified areas of overlap.

We identified 76 close contacts of the index patient; they were DCS staff and healthcare staff who had been in close contact with him and inmates that had shared a holding area with him. We screened those contacts, provided them with postexposure vaccination and the necessary antimicrobial prophylaxis, and isolated those whose test results were pending. We had not documented how long contacts were held in a common area with the index patient at the time of the outbreak response, although that information would have been helpful to understand the extent of that exposure.

Of the 55 inmates classified as close contacts, the 8 that tested positive were assigned a separate cohort from the 47 who tested negative. Eleven inmates reported nonspecific respiratory symptoms (Table). All court dates for the inmates in the affected section were postponed. DCS staff members who were close contacts were swabbed and provided with prophylaxis and vaccine; they were placed on special paid leave and advised to isolate themselves at home until laboratory results were available within 7 days and to

Table. Characteristics of 3 diphtheria outbreaks at a correctional facility, Cape Town, South Africa, October 2023–February 2025*

Characteristic	Outbreak 1, Nov 2023	Outbreak 2, Dec 2024	Outbreak 3, Feb 2025
Diphtheria contacts			
Inmate	55 (72.3)	53 (82.8)	60 (100)
Household	0	10 (15.6)	0
DCS staff	15 (19.7)	0	0
HCW	6 (7.9)	1 (1.6)	0
Total	76 (100)	64 (100)	60 (100)
Screening positivity of contacts, %	11	19	22
Contacts received postexposure prophylaxis vaccination	76 (100)	61 (95.3)	60 (100)
Contacts received postexposure prophylaxis antibiotics	76 (100)	61 (95.3)	60 (100)
Contacts with symptoms	22 (28.9)	0	0
Diphtheria cases in inmates and staff			
Symptomatic case-patients that did not receive DAT	0	0	1 (6.7)
Symptomatic case-patients that received DAT	1 (11.1)†	1 (7.7)	0
Asymptomatic carriers	8 (88.9)	12 (92.3)	14 (93.3)
Total	9 (100)	13 (100)	15 (100)
Diphtheria vaccinations			
Inmates	481 (79.6)	240 (94.1)	44 (55.0)
DCS staff	123 (20.4)	15 (5.9)	36 (45.0)
Total	604 (100)	255 (100)	80 (100)

*Values are no. (%) except as indicated. DCS, Department of Correctional Services staff; HCW, healthcare workers.
†Died.

wear a surgical mask when in contact with household members. A doctor from the outbreak response team was in telephone contact with DCS staff daily during their home isolation to assess symptoms and provide support.

Of the 14 correctional services staff contacts, 11 reported mild, nonspecific respiratory symptoms without pseudomembrane or bull neck, and all tested negative by culture and PCR for *C. diphtheriae*. Additional contacts exposed during the index patient's transport between hospitals included 1 carer, 1 DCS warden, 2 patients (not from the correctional facility), 2 EMS staff, and 4 healthcare workers at the hospital. All were swabbed, vaccinated, and given antimicrobial prophylaxis; all remained asymptomatic. EMS and healthcare workers used PPE during exposure. In accordance with guidelines, those contacts were not isolated but asked to seek healthcare if symptoms started.

By November 13, 2023, a total of 8 (11%) of the contacts tested positive for toxigenic *C. diphtheriae*; they were all inmates and were isolated together. Two of those were experiencing mild nonspecific respiratory symptoms without a pseudomembrane, and the rest were asymptomatic carriers. Sequenced isolates were ST906, a novel lineage not previously described outside of South Africa or the Western Cape.

WCDHW and DCS instituted a vaccination campaign providing Td boosters during November 6–15, 2023. In that week, a total of 604 persons were vaccinated: 123 (51%) of 240 DCS staff (both wardens and healthcare staff at the facility) and 481 (40%) 1,200 inmates (Table). During the vaccination campaign, DCS staff and inmates received health education about diphtheria, its symptoms, risks, and the purpose and possible side effects of vaccination. Some declined the vaccine because of fears of side effects or doubts about its effectiveness. Although transmission risk via fomites is low, DCS staff conducted environmental cleaning, including disinfection of holding cells, laundry, and cutlery affected during the outbreak.

Outbreak 2: December 2024–January 2025

A second outbreak at the same correctional facility started on December 9, 2024, when the index patient, a young man, experienced symptoms of a sore throat while still at the facility. He was released on December 11 after 9 months of incarceration. On the same day, he sought care at a community-based general practitioner with a sore throat, a typical pseudomembrane, and anterior cervical lymphadenopathy suggestive of the characteristic bull neck. He was admitted to the local tertiary hospital for antimicrobial drugs and timely administration of DAT and made a full recovery. Toxigenic *C. diphtheriae* was subsequently confirmed by culture, Elek testing, and PCR; all sequenced isolates were ST906.

Although the index case was identified on December 11, there was a delay in verifying the correctional facility from which he had recently been released. By December 16, his correctional facility close contacts had been swabbed, started on prophylactic drugs, and isolated. By December 24 their laboratory results were available, identifying 12 additional asymptomatic carriers among the inmates (Table). We identified a total of 64 close contacts from the index patient's DCS inmates and household contacts; all were asymptomatic, received drugs and were swabbed and vaccinated (Table). WCDHW and DCS strengthened communication through regular situational reports and meetings, and media queries were directed to the relevant departmental spokesperson for a coordinated response. A broader health education and vaccination campaign was conducted.

Outbreak 3: February 2025

The third diphtheria outbreak at the facility occurred on February 10, 2025, six weeks after the second outbreak, and was classified as new because of the 1.4-day median incubation of *C. diphtheriae* (range 1–10 days) (*5*). The index patient was a detainee awaiting trial, a young man who had been a close contact of the index patient in outbreak 2 and had declined vaccination at that time. He experienced a sore throat and pseudomembrane on February 10, received DAT, and was confirmed culture positive for toxigenic *C. diphtheriae* on February 16. He recovered fully and returned to the awaiting-trials section.

Prompt contact tracing efforts at the correctional facility during February 13–15 identified 60 asymptomatic detainee close contacts who were immediately isolated together pending results. No household or DCS staff contacts were identified. Contacts were swabbed, provided with antimicrobial drugs, and vaccinated (Table). Initially, 7 (12%) contacts were culture positive; an additional 6 (10%) cases were positive by PCR only. Those 13 cases constituted 22% of contacts; they were isolated together while completing the course of prophylactic treatment and remained asymptomatic throughout the period. Sequenced isolates were all of ST906.

High-resolution core genome phylogeny of ST906 genomes from all 3 outbreaks revealed 2 distinct clusters within the facility (data not shown). The first cluster included genomes from the first outbreak in November–December 2023, whereas the second

cluster included genomes from the December 2024–January 2025 and February 2025 outbreaks. The second cluster also included ST906 genomes from sporadic cases and community clusters reported during the same period.

A 2-day campaign was conducted among correctional services staff, providing health education on diphtheria infection prevention and control practices. Among the 70 on-duty DCS staff, 37 (53%) were tested and vaccinated and 20 (29%) accepted antimicrobial prophylaxis only. In total 57/70 (81%) of on-duty staff received prophylaxis, vaccination, or a combination. That wider screening approach identified an additional 2 positive asymptomatic carriers, 2/37 (5%) of DCS staff tested, who were advised to self-isolate while completing treatment. Although facemasks, hand sanitizer, and latex gloves are normally available to DCS staff, the provision of those to visitors to the facility was instituted during outbreak 3.

Discussion

We report recurrent outbreaks of toxigenic diphtheria that occurred in a correctional facility, requiring intersectoral public health responses that address asymptomatic carriage and waning childhood vaccine–derived immunity. Our analysis describes the public health response to 3 outbreaks of toxigenic *C. diphtheriae* that resulted in a total of 37 cases (3 symptomatic cases and 34 asymptomatic carriers) across both detainee and DCS staff populations and 1 death of an inmate from the awaiting-trials section of a correctional facility. Despite prompt outbreak response, the overcrowding and closed setting led to a substantial number of close contacts in each instance.

Each outbreak was caused by the same sequence type, which was first detected in the Western Cape Province in 2023 both at this facility and among sporadic cases in the community. ST906 appears to be localized in the province as of February 2025 and has not been reported from any other geographic region in South Africa. Both the first and second outbreaks at the facility were caused by new transmission events from the community, whereas the third reported outbreak appears to have been caused by ongoing circulation of the strain within the facility possibly introduced during the second outbreak. We will clarify the sources more precisely in a separate report.

Multiple infectious diseases spread rapidly in prison settings; a systematic review of infectious disease outbreaks across 7 countries found outbreaks of tuberculosis, influenza, measles, mumps, varicella, adenovirus, and SARS-CoV-2 (*1*). Containment of outbreaks is limited by the large number of close contacts and high degree of movement of the awaiting-trial detainees and staff (*1*). Traditional outbreak response tools, isolation and quarantine, are challenging to implement and contribute to delays in court processes (*1*). Approaches relevant to the carceral setting include opt-out testing, empirical vaccination, and requiring full immunization of staff as keys to preventing outbreaks (*13*).

During the second outbreak, infectious disease specialists shortened the deisolation protocol for laboratory-confirmed cases from 14 days to 7 days, if clinical response was good and repeat swabs on days 3–6 were culture negative. That change was made on the basis of evidence of faster time-to-clearance by antimicrobial therapy (4–6 days) (*5*).

Vaccine coverage among 6-year-olds and 12-year-olds in Western Cape is <50%, contributing to the outbreaks in the community and closed settings such as prisons (*14*,*15*). Optimizing coverage in those age groups could reduce risk for diphtheria among young adults.

Outbreak challenges included coordination, contact tracing, and vaccine hesitancy. Security concerns required close collaboration between WCDHW district officials and DCS to protect detainees and staff. A key lesson was the importance of leveraging COVID-19 outbreak response institutional knowledge and relationships, alongside intersectoral collaboration, to enable timely contact tracing, symptom screening, testing, prophylaxis, and vaccination. Ongoing engagement was key in clarifying overlapping responsibilities between stakeholders.

Tracing released detainees, off-duty staff, and unidentifiable court contacts was difficult. We identified no DCS staff as contacts during outbreak 2, possibly because of vaccination in outbreak 1, consistent use of PPE, and a desire to maintain minimum staffing levels during the festive season for continuity of essential services. A limitation of our study was incomplete information on the number of DCS staff and court contacts exposed in each outbreak, which could have affected the estimates of vaccination coverage among staff at the facility.

The presence of asymptomatic carriers makes declaration of the end of a diphtheria outbreak challenging; some asymptomatic carriers can be colonized for up to 18.5 days, which could result in ongoing transmission (*5*). Epidemiologic surveillance can be conducted in prisons by screening inmates and staff for infectious disease as a way to proactively identify asymptomatic cases, although the cost of setting up such programs and providing vaccination needs to be weighed against possible low uptake (*1*). More local

research is needed to understand the drivers of low vaccine uptake specifically in correctional facility detainees and staff in a bid to improve vaccine acceptance in future vaccination campaigns.

Globally, diphtheria outbreaks have been documented in community settings as well as refugee centers; mass vaccination efforts have been required to contain such outbreaks (*16*). A suggested alternative approach is mass antimicrobial prophylaxis; modeling studies estimate this approach to be sufficient to contain outbreaks (*5*). Although it is a relatively simple intervention and may be considered if a future outbreak occurs, the cost, feasibility, and benefit of that approach in the correctional facility with a highly mobile awaiting-trial population would need to be considered, along with the risk of antimicrobial resistance. We did not consider that approach appropriate for the subset of prisoners awaiting trial.

By formulating locally relevant clinical guidelines for healthcare workers on antitoxin eligibility, referral pathways, and isolation and deisolation protocols, infectious disease specialists supported the broader outbreak response. Kendig et al. emphasized the vital role of strengthening infection prevention and control practice in prison settings by training staff and inmates on handwashing, ensuring adequate sanitation facilities, and having appropriate outbreak response policies (*17*). The global supply shortage of DAT needed to manage diphtheria cases has also been highlighted during outbreaks, and international health bodies are encouraged to advocate for manufacturers to increase timely access to those medications.

As South Africa rolls out Tdap vaccines, which are more expensive than Td vaccines, the cost of mass vaccination efforts increases (*18*). An estimated 27% of diphtheria outbreaks could be contained by achieving full vaccination coverage alone, whereas simultaneously treating symptomatic cases promptly with antimicrobial drugs would contain 70% of outbreaks (*5*).

Immunization against diphtheria is 97% effective, but immunity wanes after ≈10 years; 30%–60% of adults become susceptible to infection again because the toxoid nature of the vaccine enables bacteria to colonize vaccinated persons without symptoms (*5*). Diphtheria-containing booster vaccination for adults is available in many countries at 10-year intervals, although there is no policy guide for that in South Africa (*19*). Although health education talks supported improved vaccine uptake in the diphtheria outbreaks, we note an increase since the COVID-19 pandemic in literature that documents the challenges of vaccination access and a rise in vaccine hesitancy among the public (*20*). That trend has specific implications for those who live and work in prison settings, where rebuilding trust and credibility in vaccines is necessary to address rising vaccine hesitancy (*21*,*22*).

Outbreaks could be caused by a combination of factors, including asymptomatic carriage, waning childhood-vaccine–derived immunity and insufficient herd immunity within communities. We have described the challenges to effective outbreak response occurring in correctional facilities. We recommend several actions for tackling diphtheria and other infectious diseases: strengthen the implementation of current childhood vaccination programs to improve immunity to vaccine-preventable diseases, adopt communication strategies to combat vaccine misinformation and create awareness about diphtheria and other vaccine-preventable conditions, and develop adult vaccination guidelines that address high-risk congregate settings. Such public health interventions are required to mitigate the risk for future vaccine-preventable disease outbreaks, particularly in closed environments like correctional facilities.

Acknowledgments

We thank the correctional services staff and hospital and substructure healthcare workers and laboratory staff who participated in the outbreak response. We also thank the colleagues at the National Health Laboratory Service and National Institute for Communicable Diseases whose technical expertise supported outbreak response efforts: Anne von Gottberg, Linda de Gouveia, Cheryl Cohen, Sibongile Walaza, and Phindi Zwane.

About the Author

Dr. Jose is a public health registrar based at the University of Cape Town and Western Cape Department of Health and Wellness. Her primary research interest is vaccine-preventable diseases.

References

1. Beaudry G, Zhong S, Whiting D, Javid B, Frater J, Fazel S. Managing outbreaks of highly contagious diseases in prisons: a systematic review. BMJ Glob Health. 2020;5:e003201. https://doi.org/10.1136/bmjgh-2020-003201
2. Oladimeji O, Atiba BP, Mbokazi J, Hyera FLM. The homeless, inmates and refugees in Africa in the face of COVID-19 outbreak. Open Public Health J. 2020;13:306–8. https://doi.org/10.2174/1874944502013010306
3. Essa A, Patel K. Al Jazeera. Thousands evacuated from rat-infested S Africa prison. 20 September 2015 [cited 2024 Jan 3]. https://www.aljazeera.com/news/2015/9/20/thousands-evacuated-from-rat-infested-s-africa-prison
4. National Institute of Communicable Disease. May 2025. Diphtheria: NICD recommendations for diagnosis, management and public health response [cited 2025 Aug 18].

https://www.nicd.ac.za/wp-content/uploads/2025/07/Diphtheria_NICD_Guidelines_02072025_Finalv1.pdf
5. Truelove SA, Keegan LT, Moss WJ, Chaisson LH, Macher E, Azman AS, et al. Clinical and epidemiological aspects of diphtheria: a systematic review and pooled analysis. Clin Infect Dis. 2020;71:89–97. https://doi.org/10.1093/cid/ciz808
6. Sharma NC, Efstratiou A, Mokrousov I, Mutreja A, Das B, Ramamurthy T. Diphtheria. Nat Rev Dis Primers. 2019;5:81. https://doi.org/10.1038/s41572-019-0131-y
7. Center for Respiratory Disease and Meningitis, National Institute for Communicable Diseases. Diphtheria situational report (week 18 of 2025). Situational report on toxigenic *Corynebacterium diphtheriae* disease in South Africa, 2024–2025. 2025 [cited 2025 Nov 20]. https://www.nicd.ac.za/wp-content/uploads/2025/05/Diphtheria-Situational-Report_2025_18_final.pdf
8. du Plessis M, Mikhari R, de Gouveia L, Duma N, Lovelock T, Lawrence C, et al. *Corynebacterium diphtheriae* infections, South Africa, 2015–2023. Emerg Infect Dis. 2025;31:417–26. https://doi.org/10.3201/eid3103.241211
9. Medicines Information Centre. Recommended catch-up immunisation schedule. 2024 [cited 2025 May 23]. https://mic.uct.ac.za/sites/default/files/media/documents/mic_uct_ac_za/2157/Catch-up%20Immunisation.pdf
10. Public Health Agency of Canada. Outbreak reporting guide. Canada Communicable Disease Report. 2015;41:73–5. https://doi.org/10.14745/ccdr.v41i04a02
11. Williams MM, Waller JL, Aneke JS, Weigand MR, Diaz MH, Bowden KE, et al. Detection and characterization of diphtheria toxin gene-bearing *Corynebacterium* species through a new real-time PCR assay. J Clin Microbiol. 2020;58:e00639-20. https://doi.org/10.1128/JCM.00639-20
12. Engler KH, Glushkevich T, Mazurova IK, George RC, Efstratiou A. A modified Elek test for detection of toxigenic corynebacteria in the diagnostic laboratory. J Clin Microbiol. 1997;35:495–8. https://doi.org/10.1128/jcm.35.2.495-498.1997
13. Junghans C, Heffernan C, Valli A, Gibson K. Mass vaccination response to a measles outbreak is not always possible. Lessons from a London prison. Epidemiol Infect. 2018;146:1689–91. https://doi.org/10.1017/S0950268818001991
14. Corrigall J, Coetzee D, Cameron N. Is the Western Cape at risk of an outbreak of preventable childhood diseases? Lessons from an evaluation of routine immunisation coverage. S Afr Med J. 2008;98:41–5. https://doi.org/10.10520/EJC69117
15. Blose N, Amponsah-Dacosta E, Kagina BM, Muloiwa R. Descriptive analysis of routine childhood immunisation timeliness in the Western Cape, South Africa. Vaccine X. 2021;10:100130. https://doi.org/10.1016/j.jvacx.2021.100130
16. Matsuyama R, Akhmetzhanov AR, Endo A, Lee H, Yamaguchi T, Tsuzuki S, et al. Uncertainty and sensitivity analysis of the basic reproduction number of diphtheria: a case study of a Rohingya refugee camp in Bangladesh, November–December 2017. PeerJ. 2018;6:e4583. https://doi.org/10.7717/peerj.4583
17. Kendig NE, Bur S, Zaslavsky J. Infection prevention and control in correctional settings. Emerg Infect Dis. 2024;30(Suppl 1):S88–93. https://doi.org/10.3201/eid3013.230705
18. UNICEF. Adolescent and adult tetanus-containing vaccines: market and supply update. 2023 [cited 2025 Nov 20]. https://www.unicef.org/supply/market-notes-and-updates
19. European Centre for Disease Prevention and Control. Vaccine scheduler [cited 2025 May 23]. https://vaccine-schedule.ecdc.europa.eu
20. Bangalee A, Bangalee V. Fake news and fallacies: exploring vaccine hesitancy in South Africa. S Afr Fam Pract. 2021;63:e1–3. https://doi.org/10.4102/safp.v63i1.5345
21. Ismail N, Tavoschi L, Moazen B, Roselló A, Plugge E. COVID-19 vaccine for people who live and work in prisons worldwide: A scoping review. PLoS One. 2022;17:e0267070. https://doi.org/10.1371/journal.pone.0267070
22. Greberman E, Kerrison EMT, Chalfin A, Hyatt JM. Understanding vaccine hesitancy in U.S. prisons: perspectives from a statewide survey of incarcerated people. Vaccines (Basel). 2024;12:600. https://doi.org/10.3390/vaccines12060600

Address for correspondence: Maria Jose, Groote Schuur Hospital, Anzio Rd, Observatory, Cape Town 7925, South Africa; email: maria.jose@uct.ac.za

Outcomes of Hospitalized and Critically Ill Adults with Murine Typhus, Galveston, Texas, USA, 2019–2023

Matthew Pickich, Puneet Singh, Efstathia Polychronopoulou, Shawn P. Nishi, Lucas S. Blanton, Alexander G. Duarte

Murine typhus is a reemerging infectious disease with the potential for severe manifestations. We conducted a retrospective study to examine severe illness in those hospitalized with murine typhus in Galveston, Texas. We identified 149 cases, of which 119 (79.8%) were hospitalized and 33 (28%) required admission to the intensive care unit (ICU). ICU patients were older than non-ICU patients (54.9 vs. 47.2 years; p<0.02). Thrombocytopenia was more severe in the ICU group (101×10^3 μ/L) compared to the non-ICU group (137×10^3 μ/L) (p<0.01). The median time from healthcare contact in the emergency department to initiation of appropriate antibiotics was similar for the ICU group (1 day) and non-ICU group (2 days) (p = 0.26). Two deaths (1.7%) in the ICU group were attributed to multiorgan failure and hemophagocytic lymphohistiocytosis. In murine typhus–endemic regions, early recognition and prompt treatment is imperative to mitigate adverse outcomes.

Murine typhus, also known as endemic or flea-borne typhus, is caused by *Rickettsia typhi*, an obligately intracellular gram-negative organism transmitted to humans by fleas that infest rats and opossums (*1*). Murine typhus has a global distribution, and in the United States, it is endemic to South Texas, Hawaii, and southern California (*2*–*4*). Furthermore, despite its near eradication in the United States during the 1940s, murine typhus has resurged in southeastern Texas and California (*5*–*7*). Murine typhus manifests as an undifferentiated febrile illness often accompanied by headache, myalgias, nausea, and malaise. It is frequently described as a mild illness. However, severe manifestations with organ dysfunction have been reported. Those include acute kidney injury, meningoencephalitis, myocarditis, respiratory failure, and septic shock (*8*–*13*). As a consequence, persons with organ dysfunction might require treatment in the intensive care unit (ICU), especially when appropriate antimicrobial therapy is delayed or not administered (*7*,*14*). A systematic review of murine typhus infections occurring around the world among children and adults in diverse healthcare systems described organ failure and hospitalization that ranged from 2% to 86% and ICU admission in 5.9% (*15*). However, characteristics of hospitalized and critically ill patients and their outcomes after antimicrobial treatment were not well defined. We examined the clinical characteristics, treatment, and outcomes of hospitalized adults with murine typhus with organ failure leading to ICU admission in Galveston, Texas, USA.

Author affiliation: University of Texas Medical Branch, Galveston, Texas, USA

DOI: https://doi.org/10.3201/eid3206.251015

Methods

Data and Cohort

We conducted a retrospective review of microbiology laboratory records at the University of Texas Medical Branch (UTMB; Galveston, TX, USA) to identify adults with typhus group rickettsiae indirect immunofluorescence assay (IFA) IgM or IgG titers of ≥1:128 treated during April 14, 2019–October 15, 2023. We selected those dates to include the start of available IFA data and electronic health records across our healthcare system. Although PCR amplification of *Rickettsia* spp. is a very specific testing method, clinical sensitivity of PCR from blood specimens is suboptimal and influenced by the assay, disease severity, and timing of sample collection relative to stage of illness (*16*). Amplification of cell-free DNA by next-generation sequencing also shows promise in the amplification of *R. typhi* DNA from plasma (*17*,*18*), but its cost and

current turnaround time are limitations. We included symptomatic patients ≥18 years of age with an emergency department (ED) encounter and IFA results reactive for typhus group rickettsiae. We excluded patients <18 years of age, persons hospitalized 30 days before or after laboratory testing for rickettsioses, and incarcerated persons. We collected data from the electronic health record to determine demographics, symptoms, laboratory and radiographic results, time to diagnostic testing, antimicrobial treatment, clinical disposition, and outcomes. The Institutional Review Board at UTMB approved this study (IRB approval no. 23-0313).

Case Definitions

We used the definitions used by the Flea-borne Typhus Case Definition/Case Classification of the Texas Department of State Health Services (*19*). In addition, we used the case classification described by the Centers for Disease Control and Prevention to categorize patients with probable or confirmed murine typhus (*20*). We defined clinical evidence as an acute febrile illness lasting <30 days with ≥2 of the following symptoms: headache, myalgia, rash, nausea/vomiting, thrombocytopenia, or elevated aspartate transaminase and alanine transaminase. Persons with probable murine typhus had clinical disease and supportive laboratory findings that consisted of IFA for *R. typhi* antigen taken within 60 days of illness with levels of IgG ≥1:128 or IgM ≥1:256. Persons with confirmed murine typhus had a clinically compatible illness and laboratory-confirmed results, which consisted of a 4-fold increase in *R. typhi* IgG titers by IFA between serum samples collected during the acute and convalescent phases of illness.

Data Collection

We collected information on patient demographics, comorbidities, laboratory results, and radiographic imaging findings. An investigator (M.P.) performed all chart reviews, and a second investigator (P.S.) reviewed 60% of the charts to confirm accuracy and reliability of the abstracted data. We calculated the Charlson Comorbidity Index for each patient on the basis of clinical diagnoses (International Classification for Diseases, 10th Revision) before or on the day of IFA laboratory testing. We collected information regarding the time to laboratory diagnosis, the time from ED admission to antibiotic administration during hospitalization or within 30 days of ED encounter and admitting diagnosis leading to hospitalization. For critically ill patients, we collected data regarding source of admission to the ICU, vasopressor administration, invasive or noninvasive ventilation use, and continuous renal replacement therapy. In addition, we collected data on doxycycline and azithromycin administration during the inpatient stay or within 30 days of discharge. Both of those agents were selected for their in vitro activity to *R. typhi* (*21*). Although azithromycin is believed to be inferior to doxycycline for the treatment of murine typhus (*22*), it is sometimes used as an alternative agent (*23*) and is frequently used as part of empiric treatment for community-acquired pneumonia, a diagnosis of many persons entering the ICU.

Data Analysis

We present patient demographic and clinical characteristics as means ±SD or frequencies and percentages. We compared patient characteristics, laboratory results, and time from initial contact at UTMB to appropriate antimicrobial administration between persons admitted to the inpatient ward (noncritical care) and the ICU (critical care) using a *t*-test or nonparametric test for continuous variables as appropriate and the χ^2 test for categorical variables. We conducted all analyses using SAS 9.4 (SAS Institute Inc., https://www.sas.com).

Results

During April 14, 2019–October 15, 2023, we identified 149 adults in aggregate with signs/symptoms of fever, malaise, weakness, nausea, vomiting, abdominal pain, diarrhea, or some combination of those associated with typhus group rickettsial serology that met the definition for either probable or confirmed infection. Of those 149 adults, 119 (79.8%) were hospitalized; the mean age was 49.3 ±16.6 years. Men represented 50.4% and women represented 49.6% of patients (Table 1). The most frequent comorbidities for hospitalized patients were obesity, diabetes, and chronic kidney disease. In the hospitalized patient group, 95 (79.8%) were classified as probable murine typhus on the basis of symptoms and IgG titers of ≥1:128 or IgM titers of ≥1:256. Twenty-four (20.1%) were classified as confirmed on the basis of symptoms and a 4-fold increase in IgG-specific titer (Table 2). Among the hospitalized group, 33 (27.7%) patients were admitted to the ICU because of hemodynamic instability, respiratory failure, delirium, or acute kidney injury. Among those critically ill patients, 27 were determined to have probable murine typhus and 6 were confirmed to have murine typhus.

The group admitted to the ICU was older and had a higher percentage of male patients than the non-ICU group. However, comorbidities did not

Table 1. Characteristics of hospitalized patients in study of outcomes of hospitalized and critically ill adults with murine typhus, Galveston, Texas, USA, 2019–2023*

Characteristic	All hospitalized patients, n = 119	Non-ICU, n = 86	ICU, n = 33	p value
Mean age, y (SD)	49.3 (16.6)	47.2 (16.4)	54.9 (15.9)	0.022
Sex				0.074
M	60 (50.4)	39 (45.35)	21 (63.6)	
F	59 (49.6)	47 (54.65)	12 (36.4)	
Race				
White	115 (96.6)	82 (95.35)	33 (100)	0.208
Non-white	4 (3.4)	4 (4.65)	0 (0)	
Ethnicity				0.258
Hispanic	43 (36.1)	32 (37.2)	11 (33.3)	
Not Hispanic	75 (63.1)	54 (62.8)	21 (63.6)	
Unknown	1 (0.8)	0 (0)	1 (3)	
Mean Charlson Comorbidity Index (SD)	1.05 (1.4)	0.98 (1.4)	1.24 (1.4)	0.247
Comorbidities				
Alcohol abuse	6 (5.0)	4 (4.7)	4 (12.1)	0.145
Renal disease	10 (8.4)	7 (8.1)	3 (9.1)	0.867
Diabetes	19 (16.0)	14 (16.3)	5 (15.1)	0.881
Cerebrovascular disease	7 (5.9)	4 (4.6)	3 (9.1)	0.357
Obesity	33 (27.7)	23 (26.7)	10 (30.3)	0.698
Most common diagnoses at time of admission (%)				
		Typhus (17.5); fever (39.5)	Fever (15.2); sepsis (33.3)	
		Sepsis (8); typhus (17.5)	Acute kidney failure (3); fever (15.2)	
		Pneumonia (4.7); sepsis (8)	Acute respiratory failure with hypoxia (3); acute kidney failure (3)	
		Altered mental status (2.3); pneumonia (4.7)	Dehydration (3); acute respiratory failure with hypoxia (3)	
		Altered mental status (2.3)	Dehydration (3)	

*Values are no. (%) except as indicated. ICU, intensive care unit.

differ significantly between the groups (Table 1). Frequent laboratory findings for hospitalized patients were elevated aspartate transaminase, alanine transaminase, and alkaline phosphatase (Table 3), but no significant difference in those initial values was noted between groups. At the time of hospital admission, impaired renal function was present in 27% (9/33) of the critically ill group, but no difference was observed in the median creatinine values of 0.99 mg/dL for the critically ill group and 0.87 mg/dL for the non-ICU group (p = 0.06) (Table 3). Leukocytosis with a leukocyte count of 12.0 ± 6.0 10^3 cells/μL was noted more often in the ICU group than in the non-ICU group (Table 3). In addition, a greater degree of thrombocytopenia (median platelet count of 97 ± 59 10^3/μL), hypoalbuminemia (median value of 3.2 ± 0.6 g/dL), and elevated procalcitonin (median value of 3.8 ± 4.3 ng/mL) was noted in the ICU group. As for initial chest radiographs, the ICU group was noted to have nonspecific parenchymal infiltrates and pleural effusions, but no significant differences between groups were noted.

The mean ±SD time to receiving serologic results was similar for the critically ill and non-ICU groups: 4.4 ±4.4 days for the critically ill group and 3.6 ±5.8 days for the non-ICU group (p = 0.06). Diagnostic testing and drug administration were performed on the same date. All patients but 1 were treated exclusively with doxycycline, and the timing of antimicrobial therapy was similar between groups (1.6

Table 2. Initial murine typhus immunofluorescence titers and confirmed versus probable cases in study of outcomes of hospitalized and critically ill adults with murine typhus, Galveston, Texas, USA, 2019–2023*

Category	Initial titers	Confirmed (%)	Probable (%)
IgM	1:256	4	24
	1:512	1	9
	1:1,024	11	57
IgG	1:128	2	11
	1:256	1	21
	1:512	2	8
	1:1,024	14	24
ICU		6 (18.2)	27 (81.8)
Non-ICU		18 (20.9)	68 (79.1)
Total		24 (20.1)	95 (79.8)

Table 3. Laboratory values and radiographic findings of hospitalized adults with murine typhus, Galveston, Texas, USA, 2019–2023*

Test	No. patients tested	Non-ICU patients, n = 86	ICU patients, n = 33	Reference range	p value
Alanine aminotransferase, U/L	112	111 (68–166)	95 (70–140)	5–35	0.34
Aspartate aminotransferase, U/L	118	143 (96–216)	153 (96–224)	13–40	0.71
Alkaline phosphatase, U/L	118	140 (84–216)	137 (90–207)	34–122	0.68
Creatinine, mg/dL	119	0.87 (0.69–1.04)	0.99 (0.81–2.21)	0.5–1.4	0.06
Leukocytes, × 10^3 cells/μL	119	7.8 (5.9–10.6)	10.8 (7.1–15.5)	4.3–11.1	0.005
Hemoglobin, g/dL	119	12.9 (11.7–14.3)	12.2 (11.3–13.6)	12.2–16.4	0.26
Platelets, × 10^3/μL	119	117 (79–162)	97 (45–151)	135–351	0.01
Neutrophils, × 10^3 cells/μL	117	6.0 (4.3–8.0)	8.3 (6.1–11.9)	1.99–6.95	0.002
Lymphocytes, × 10^3 cells/μL	117	1.2 (0.84–1.96)	0.85 (0.56–1.51)	1.09–3.23 L	0.04
Monocytes, × 10^3 cells/μL	117	0.36 (0.26–0.56)	0.38 (0.29–0.72)	0.36–1.02	0.40
Serum albumin, g/dL	118	3.5 (3.2–3.8)	3.2 (2.9–3. 5)	3.5–5 L	0.024
Serum sodium, mmol/L	119	131 (129–134)	128 (137–130)	135–145	0.022
Procalcitonin, ng/mL	44	1.1 (0.4–2.5)	3.8 (0.9–7.4)	<0.07	0.045
Chest radiograph findings, no. (%)					0.10
Clear lung fields		52 (64.2)	14 (43.8)		
Opacities/infiltrates		27 (33.3)	15 (46.8)		
Effusion		2 (2.5)	3 (9.4)		

*Values are median (interquartile range) except as indicated. ICU, intensive care unit.

±1.3 days for critically ill patients and 2.2 ±2.1 days for non-ICU patients) (p = 0.26) (Table 4). Most patients were directly admitted from the ED to the ICU, and their deteriorating clinical course resulted in the initiation of mechanical ventilation in 5 patients and renal replacement therapy in 2 patients (Table 3). In the critically ill group, hemodynamic instability resulted in intravenous fluid resuscitation followed by vasopressor initiation in 9 patients. Hospital length-of-stay was significantly greater for the critically ill group than for the non-ICU group: 9.3 ±8.4 days for the critically ill group and 4.8 ±2.2 days for the non-ICU group (p<0.001) (Table 4).

Two deaths occurred in the critically ill group, 1 caused by septic shock and 1 by multiorgan failure associated with hemophagocytic lymphohistiocytosis. Among the 2 deaths, 1 patient was a 66-year-old man who was admitted with shock, renal failure, and disseminated intravascular coagulation. He died within 24 hours after a cardiac arrest and exhibited laboratory features of myocarditis. The second patient, a 69-year-old man with daily alcohol consumption, was admitted with pancytopenia, ferritinemia, and elevated serum transaminase that raised concern for hemophagocytic lymphohistiocytosis, which was confirmed by bone marrow biopsy. Despite administration of doxycycline on hospital day 4 and corticosteroid therapy for hemophagocytic lymphohistiocytosis on hospital day 6, he died of septic shock and respiratory failure on day 9 of hospital admission.

Discussion

Although murine typhus is often considered a mild illness (*24*,*25*), we identified 119 adults hospitalized for symptoms associated with murine typhus, and 28% exhibited organ failure manifesting as hemodynamic instability, acute respiratory failure, or acute kidney injury that resulted in ICU admission.

Table 4. Comparison of treatment and outcomes of patients in study of outcomes of hospitalized and critically ill adults with murine typhus, Galveston, Texas, USA, 2019–2023*

Treatment or outcome	Non-ICU, n = 86	ICU, n = 33	p value
Mean time to diagnosis, d (SD)	3.6 (5.8)	4.1 (4.4)	0.063
Median time to diagnosis, d (IQR)	2 (1–3)	3 (1–4)	0.061
Mean time to antibiotic, d (SD)	1.6 (1.3)	2.2 (2.1)	0.264
Median time to antibiotic, d (IQR)	1 (1–2)	2 (1–3)	0.262
Doxycycline			0.145
Yes, no. (%)	82 (95.35)	29 (87.9)	
Median doxycycline inpatient duration, d (IQR)	4 (2–5)	5 (4–7)	<0.001
Azithromycin			0.127
Yes, no. (%)	11 (12.8)	8 (24.2)	
Median azithromycin inpatient duration, d (IQR)	3 (2–4)	2 (2–3)	0.489
Vasopressors, no. (%)			<0.001
Yes	5 (5.8)	12 (36.4)	
CRRT, no. (%)			0.021
Yes	0	2 (6)	
Ventilation, no. (%)			<0.001
Yes	0	5 (15.2)	
Mean hospital LOS, d (SD)	4.8 (2.2)	9.3 (8.4)	<0.001
Median hospital LOS, d (IQR)	4 (3–6)	7 (5–9)	<0.001

*CRRT, continuous renal replacement therapy; IQR, interquartile ratio; LOS, length of stay.

Furthermore, patients with organ dysfunction admitted to the ICU were older than those not admitted to the ICU and did not have recognized immunocompromised conditions. Of note, all but 1 of the hospitalized patients were prescribed tetracycline therapy during their hospital stay, and only 1 patient received macrolide therapy. Those findings highlight the illness and complications associated with this infectious disease, as well as the challenges associated with real-time diagnosis.

Murine typhus characteristically manifests as acute febrile illness with nonspecific symptoms that can mimic those of other infectious diseases, leading to misdiagnosis and a delay in the administration of effective antimicrobial therapy. As a consequence, delays in diagnosis or treatment in elderly or immunocompromised persons can lead to complications manifesting as organ dysfunction. A systematic review of worldwide published case series reported complications in 26.1% of patients, although the authors acknowledged a reporting bias that might overestimate certain findings (*15*). Those authors described complications that primarily involved the pulmonary system as pneumonia or radiographic pulmonary infiltrates, which was noted in 128 patients and developed into acute respiratory failure in 5 persons. Other complications in order of occurrence were central nervous system involvement, acute kidney injury, and, less commonly, shock. The authors proposed that geographic variation with respect to healthcare delivery accounted for differences in the severity of illness but were unable to identify risk factors associated with organ failure. Case series of murine typhus in Texas, a recognized endemic region, have reported complications leading to hospitalization and critical care services related to acute neuropsychiatric, renal, and pulmonary involvement (*26*–*29*). A 2008 study reported hospitalization for 23 of 33 persons with murine typhus and ICU admission for 9 persons (27%) (*26*), whereas another study reviewing medical records from 2013 to 2016 described complications in 18 of 54 adults (33%), 13 of whom required ICU admission (*27*). Similarly, we identified that 28% of hospitalized persons required ICU admission; 9 (27%) required vasopressors for shock, 5 (15%) had acute respiratory failure requiring mechanical ventilation, and 2 (6%) were started on renal replacement therapy for acute kidney injury. Therefore, severe complications related to murine typhus leading to hospitalization could occur in >1 of 4 patients, manifesting as single and multiorgan failure.

Individual risk factors associated with murine typhus and organ dysfunction have been described as increasing age, alcohol abuse, and glucose 6-phosphate dehydrogenase deficiency (*8*,*28*,*29*). Although laboratory findings associated with murine typhus include elevations in hepatic transaminases, leukocytosis, hypoalbuminemia, thrombocytopenia, and hyponatremia, published data concerning laboratory findings associated with organ failure from severe murine typhus are limited (*8*,*15*). In this study, we found greater reductions in platelet count in the critically ill group than in the noncritical group at the time of initial healthcare contact. In addition, impaired renal function was more commonly observed in the critically ill group, and the mechanism for this failure has been attributed to prerenal and immune-mediated causes (*30*). Delays in appropriate antimicrobial therapy have been proposed as another risk factor for complications associated with murine typhus infection (*8*,*14*,*31*). Antimicrobial therapy resolves symptoms by halting bacterial replication (*32*), thus mitigating further endothelial damage and allowing time for host-defense mechanisms to mount an effective response (*33*). However, recovery without antimicrobial therapy has been reported, although the factors associated with that phenomenon are unclear and might relate to the quantity of inoculum, individual comorbidities, and host immune response (*15*,*27*). In this study, we identified a similar time from admission to initiation of antibiotics for both groups that suggest host-related immune response might account for the progression from mild illness to organ dysfunction to multiorgan failure. However, we are unable to accurately account for the length of time from initial symptom onset to admission, and some persons might have delayed seeking medical attention, thereby prolonging the duration of infection and encouraging the subsequent development of organ failure.

Diagnostic laboratory testing relies on serologic testing because of the similarity of murine typhus symptoms with other acute febrile illnesses, which can pose dilemmas for clinicians. In addition, although a history of flea exposure is relevant, that information is infrequently obtained and reported in <25% of patients (*15*). Serologic testing is usually conducted using IFA to detect IgG and IgM reactive to typhus group rickettsiae (commercial assays use whole-cell *R. typhi* antigen), but diagnostic limitations are associated with this approach. Furthermore, real-time reverse transcription PCR amplification of ribosomal RNA targets for *R. typhi* shows promise as a more sensitive test, but it is not yet available commercially (*17*). In addition, reactive antibodies are seldom present at detectable levels during the first few

days to week of illness; therefore, acute- and convalescent-phase testing are required to soundly establish a diagnosis through seroconversion or a 4-fold increase in antibody titer. Another limitation concerns reliance on reference laboratories to perform IFA testing that can delay the test results. As a consequence, a confident laboratory diagnosis of murine typhus is retrospective in nature (*34*).

The absence of real-time testing for murine typhus can affect healthcare costs. A 2023 study examined healthcare resource utilization for persons with murine typhus and compared them to age-matched controls with influenza, which is often diagnosed with rapid point-of-care testing (*35*). Patients with influenza underwent a less expensive assessment (mean $817/patient) than did patients infected with murine typhus (mean $16,760/patient). In addition, the article reported substantially more healthcare encounters for patients with murine typhus than for patients with influenza. Thus, inability to identify and distinguish murine typhus from other febrile infections resulted in higher costs.

Although we did not examine healthcare costs, we found the mean time to diagnosis in hospitalized (noncritical) patients to be 3.6 days compared with 4.4 days in critically ill patients. Furthermore, time to initial healthcare contact and the initiation of appropriate antibiotics did not vary significantly between groups. An explanation for these findings is likely related to the early use of tetracycline-based therapy for acute febrile illnesses by clinicians, as well as infectious disease consultants who advocate for early diagnostic testing and prompt initiation of tetracycline therapy for symptomatic hospitalized patients with suspected murine typhus (*36*).

Murine typhus is associated with a low mortality rate; earlier reports have described a case-fatality rate of 0.4% and a case-fatality rate of up to 4% for hospitalized patients (*8*,*28*,*37*). In addition, a systematic review assessing mortality among 239 untreated patients with murine typhus also reported a low case-fatality rate of 0.4% (*14*). In this study, we found an associated mortality rate of 1.7% for hospitalized patients. Upon further investigation into the causes of death, hemophagocytic lymphohistiocytosis was diagnosed in 1 patient with confirmed murine typhus; despite 5 days of intravenous doxycycline and initiation of corticosteroid therapy, the patient died. Hemophagocytic lymphohistiocytosis has been described as a rare complication associated with murine typhus and is characterized by an exaggerated immune response with increased proliferation and activation of histiocytes (*38*,*39*). The development of critical illness and severe multiorgan dysfunction should prompt investigation into rickettsial infection–associated hemophagocytic lymphohistiocytosis (*40*–*42*).

The strengths of this study include the number of persons residing in an endemic area for whom clinical data were available, which enabled examination of numerous factors associated with murine typhus. The first limitation of this study is its retrospective nature, which might introduce bias. Second, our study only examined symptomatic patients seeking medical attention and might underreport the extent of disease in the community. Another limitation concerns the discrepancy between the number of confirmed infections and the number of probable infections. This discrepancy is attributable to the limitations of serologic testing; convalescent testing is seldom performed after discharge. Studies have shown a demonstrable seroprevalence of typhus group antibodies in the communities of Galveston County. Typhus group antibodies were found to be present in 1.2% of Galveston County residents in 2013 and 7.8% of residents in 2021 (*43*,*44*). Although that might raise doubt regarding the reliability of probable cases, a separate study describing the reemergence of typhus group rickettsiosis in the Galveston area indicated similarity in the signs and symptoms of confirmed and probable cases (*5*). Another limitation was the lack of clinical information regarding symptom duration before ED admission, which might have contributed to illness progression for older persons. In addition, our study did not examine for the presence of infection from spotted fever group rickettsiae. Antibodies stimulated by typhus group rickettsiae can also cross-react with spotted fever group antigen, albeit usually at titers that are at least 4-fold less than those against homologous antigen (*45*). Unless there is a history of tick bite or travel to an area with a greater abundance of ticks, spotted fever group antibodies are usually not routinely checked in conjunction with typhus group rickettsial serology at UTMB. Serum samples from Galveston residents reactive to *R. typhi* do not react with the immunodominant spotted fever group-specific outer membrane protein A (OmpA) by Western blot analysis (*43*). Although undiagnosed spotted fever group disease in our cohort is a possibility and a limitation of this study, typhus group rickettsiosis is likely the predominant cause of rickettsial illness in Galveston. The duration of onset of illness to initiation of antibiotics for our study was 1–2 days after contact at UTMB, which could be considered a limitation given that the median duration from onset of illness to initiation of doxycycline was documented to be 9 days in a previous Galveston study of cases

during 2012–2016) (*46*) and 10 days in a study that examined murine typhus throughout Texas (cases during 1980–1987) (*8*). An analysis of patients admitted to a hospital close to the southern Texas–Mexico border revealed that the median time to initiate doxycycline from initial point of healthcare contact was 5 days (*27*). Although our study did not calculate the time from symptom onset to initiation of doxycycline, over time, at our institution, recognition of murine typhus seems to have led to relatively swift empiric administration of doxycycline. Finally, this study lacks data regarding antimicrobial therapy before patients sought care at the ED.

In conclusion, in symptomatic hospitalized adults with murine typhus in the Galveston, Texas, area, severe organ dysfunction manifested as shock, acute kidney injury, and acute respiratory failure in 28% of patients. Among hospitalized patients with elevated hepatic transaminases and thrombocytopenia, empiric tetracycline therapy was initiated within 1–2 days of ED admission. Risk factors associated with organ dysfunction in adults were increased age and thrombocytopenia at time of initial healthcare contact. Clinicians in endemic areas must recognize murine typhus as a potentially severe illness and institute prompt, empirical therapy with doxycycline when a case is suspected.

About the Author

Dr. Pickich is a senior pulmonary and critical care fellow at the University of Texas Medical Branch in Galveston, Texas. He is actively engaged in research affecting clinical decision-making and quality and process improvement.

References

1. Blanton LS. The rickettsioses: a practical update. Infect Dis Clin North Am. 2019;33:213–29. https://doi.org/10.1016/j.idc.2018.10.010
2. Taylor JP, Betz TG, Rawlings JA. Epidemiology of murine typhus in Texas. 1980 through 1984. JAMA. 1986;255:2173–6. https://doi.org/10.1001/jama.1986.03370160071029
3. Eremeeva ME, Warashina WR, Sturgeon MM, Buchholz AE, Olmsted GK, Park SY, et al. *Rickettsia typhi* and *R. felis* in rat fleas (*Xenopsylla cheopis*), Oahu, Hawaii. Emerg Infect Dis. 2008;14:1613–5. https://doi.org/10.3201/eid1410.080571
4. Maina AN, Fogarty C, Krueger L, Macaluso KR, Odhiambo A, Nguyen K, et al. Rickettsial infections among *Ctenocephalides felis* and host animals during a flea-borne rickettsioses outbreak in Orange County, California. PLoS One. 2016;11:e0160604. https://doi.org/10.1371/journal.pone.0160604
5. Ruiz K, Valcin R, Keiser P, Blanton LS. Rise in murine typhus in Galveston County, Texas, USA, 2018. Emerg Infect Dis. 2020;26:1044–6. https://doi.org/10.3201/eid2605.191505
6. Pratt HD. The changing picture of murine typhus in the United States. Ann N Y Acad Sci. 1958;70:516–27. https://doi.org/10.1111/j.1749-6632.1958.tb35408.x
7. Snellgrove AN, Goddard J. Murine typhus: a re-emerging rickettsial zoonotic disease. J Vector Ecol. 2024;50:1–13. https://doi.org/10.52707/1081-1710-50.1-1
8. Dumler JS, Taylor JP, Walker DH. Clinical and laboratory features of murine typhus in south Texas, 1980 through 1987. JAMA. 1991;266:1365–70. https://doi.org/10.1001/jama.1991.03470100057033
9. Blanton LS. Murine typhus: a review of a reemerging flea-borne rickettsiosis with potential for neurologic manifestations and sequalae. Infect Dis Rep. 2023;15:700–16. https://doi.org/10.3390/idr15060063
10. Toy D, Vo C, Kwan WC, Shavelle DM. Fulminant myocarditis secondary to murine typhus mimicking acute coronary syndrome. J Cardiol Cases. 2021;24:99–101. https://doi.org/10.1016/j.jccase.2021.02.007
11. van der Vaart TW, van Thiel PP, Juffermans NP, van Vugt M, Geerlings SE, Grobusch MP, et al. Severe murine typhus with pulmonary system involvement. Emerg Infect Dis. 2014;20:1375–7. https://doi.org/10.3201/eid2008.131421
12. Tran LT, Helms JL, Sierra-Hoffman M, Stevens ML, Deliz-Aguirre R, Castro-Lainez MT, et al. *Rickettsia typhi* infection presenting as severe ARDS. IDCases. 2019;18:e00645. https://doi.org/10.1016/j.idcr.2019.e00645
13. Alarcón J, Sanosyan A, Contreras ZA, Ngo VP, Carpenter A, Hacker JK, et al. Fleaborne typhus–associated deaths—Los Angeles County, California, 2022. MMWR Morb Mortal Wkly Rep. 2023;72:838–43. https://doi.org/10.15585/mmwr.mm7231a1
14. Doppler JF, Newton PN. A systematic review of the untreated mortality of murine typhus. PLoS Negl Trop Dis. 2020;14:e0008641. https://doi.org/10.1371/journal.pntd.0008641
15. Tsioutis C, Zafeiri M, Avramopoulos A, Prousali E, Miligkos M, Karageorgos SA. Clinical and laboratory characteristics, epidemiology, and outcomes of murine typhus: a systematic review. Acta Trop. 2017;166:16–24. https://doi.org/10.1016/j.actatropica.2016.10.018
16. Paris DH, Dumler JS. State of the art of diagnosis of rickettsial diseases: the use of blood specimens for diagnosis of scrub typhus, spotted fever group rickettsiosis, and murine typhus. Curr Opin Infect Dis. 2016;29:433–9. https://doi.org/10.1097/QCO.0000000000000298
18. Blanton LS, Paddock CD. Murine typhus—a horse in zebra's clothing. Am J Med. 2025;138:1487–9.
19. Texas Department of State Health Services. Epi case criteria guide 2022 [cited 2021 Nov 1]. https://www.dshs.state.tx.us/sites/default/files/IDCU/investigation/epi-case-criteria-guide/2022-Epi-Case-Criteria-Guide.pdf
20. Centers for Disease Control and Prevention. Clinical overview of flea-borne typhus [cited 2021 Apr 18]. https://www.cdc.gov/typhus/hcp/clinical-overview/clinical-overview-of-murine-typhus.html
21. Keysary A, Itzhaki A, Rubinstein E, Oron C, Keren G. The in-vitro anti-rickettsial activity of macrolides. J Antimicrob Chemother. 1996;38:727–31. https://doi.org/10.1093/jac/38.4.727
22. Newton PN, Keolouangkhot V, Lee SJ, Choumlivong K, Sisouphone S, Choumlivong K, et al. A prospective, open-label, randomized trial of doxycycline versus azithromycin for the treatment of uncomplicated murine typhus. Clin Infect Dis. 2019;68:738–47. https://doi.org/10.1093/cid/ciy563
23. Dumler JS. Clinical disease: current treatment and new challenges. In: Palmer GH, Azad AF, editors. Intracellular pathogens II: rickettsiales. Washington: ASM Press; 2012. p. 1–39.

24. Stuart BM, Pullen RL. Endemic (murine) typhus fever: clinical observations of 180 cases. Ann Intern Med. 1945;23:17. https://doi.org/10.7326/0003-4819-23-4-520
25. Miller ES, Beeson PB. Murine typhus fever. Medicine (Baltimore). 1946;25:1–15. https://doi.org/10.1097/00005792-194602000-00001
26. Adjemian J, Parks S, McElroy K, Campbell J, Eremeeva ME, Nicholson WL, et al. Murine typhus in Austin, Texas, USA, 2008. Emerg Infect Dis. 2010;16:412–7. https://doi.org/10.3201/eid1603.091028
27. Afzal Z, Kallumadanda S, Wang F, Hemmige V, Musher D. Acute febrile illness and complications due to murine typhus, Texas, USA. Emerg Infect Dis. 2017;23:1268–73. https://doi.org/10.3201/eid2308.161861
28. Pieracci EG, Evert N, Drexler NA, Mayes B, Vilcins I, Huang P, et al. Fatal flea-borne typhus in Texas: a retrospective case series, 1985–2015. Am J Trop Med Hyg. 2017;96:1088–93. https://doi.org/10.4269/ajtmh.16-0465
29. Elyassi AR, Rowshan HH. Perioperative management of the glucose-6-phosphate dehydrogenase deficient patient: a review of literature. Anesth Prog. 2009;56:86–91. https://doi.org/10.2344/0003-3006-56.3.86
30. Blanton LS, Berman MA, Afrouzian M. Case report: renal failure due to focal segmental glomerulosclerosis in a patient with murine typhus. Am J Trop Med Hyg. 2020;103:1017–9. https://doi.org/10.4269/ajtmh.20-0116
31. Chandramohan D, Awobajo M, Fisher O, Dayton CL, Anstead GM. Flea-borne typhus causing hemophagocytic lymphohistiocytosis: an autopsy case. Infect Dis Rep. 2023;15:132–41. https://doi.org/10.3390/idr15010014
32. Botelho-Nevers E, Socolovschi C, Raoult D, Parola P. Treatment of *Rickettsia* spp. infections: a review. Expert Rev Anti Infect Ther. 2012;10:1425–37. https://doi.org/10.1586/eri.12.139
33. Sahni A, Fang R, Sahni SK, Walker DH. Pathogenesis of rickettsial diseases: pathogenic and immune mechanisms of an endotheliotropic infection. Annu Rev Pathol. 2019;14:127–52. https://doi.org/10.1146/annurev-pathmechdis-012418-012800
34. Blanton LS, Walker DH, Bouyer DH. *Rickettsia* and *Orientia*. In: Carroll KC, Pfaller MA, Landry ML, McAdam AJ, Patel R, editors. Manual of clinical microbiology. 12th ed. Washington: ASM Press; 2019. p. 1149–1162.
35. Blanton LS. *Rickettsia typhi* in southern California: a growing flea-borne threat. Am J Trop Med Hyg. 2023;110:1–2. https://doi.org/10.4269/ajtmh.23-0742
36. Walker DH, Ismail N. Emerging and re-emerging rickettsioses: endothelial cell infection and early disease events. Nat Rev Microbiol. 2008;6:375–86. https://doi.org/10.1038/nrmicro1866
37. Chikeka I, Dumler JS. Neglected bacterial zoonoses. Clin Microbiol Infect. 2015;21:404–15. https://doi.org/10.1016/j.cmi.2015.04.022
38. Walker DH, Parks FM, Betz TG, Taylor JP, Muehlberger JW. Histopathology and immunohistologic demonstration of the distribution of *Rickettsia typhi* in fatal murine typhus. Am J Clin Pathol. 1989;91:720–4. https://doi.org/10.1093/ajcp/91.6.720
39. Hines MR, von Bahr Greenwood T, Beutel G, Beutel K, Hays JA, Horne A, et al. Consensus-based guidelines for the recognition, diagnosis, and management of hemophagocytic lymphohistiocytosis in critically ill children and adults. Crit Care Med. 2022;50:860–72. https://doi.org/10.1097/CCM.0000000000005361
40. Walter G, Botelho-Nevers E, Socolovschi C, Raoult D, Parola P. Murine typhus in returned travelers: a report of thirty-two cases. Am J Trop Med Hyg. 2012;86:1049–53. https://doi.org/10.4269/ajtmh.2012.11-0794
41. Jacquot R, Gerfaud-Valentin M, Mekki Y, Billaud G, Jamilloux Y, Sève P. Parvovirus B19 infections in adults [in French]. Rev Med Interne. 2022;43:713–26. https://doi.org/10.1016/j.revmed.2022.08.005.
42. Zamora Gonzalez RA, Mayo MS, Jeng AC. Severe flea-borne typhus complicated by hemophagocytic lymphohistiocytosis: a case report and review of literature. IDCases. 2024;36:e01955. https://doi.org/10.1016/j.idcr.2024.e01955
43. Blanton LS, Vohra RF, Bouyer DH, Walker DH. Reemergence of murine typhus in Galveston, Texas, USA, 2013. Emerg Infect Dis. 2015;21:484–6. https://doi.org/10.3201/eid2103.140716
44. Blanton LS, Caravedo Martinez MA, Mendell N, Villasante-Tezanos A, Walker DH, Bouyer D. Increased seroprevalence of typhus group rickettsiosis, Galveston County, Texas, USA. Emerg Infect Dis. 2023;29:212–4. https://doi.org/10.3201/eid2901.221206
45. Vishwanath S. Antigenic relationships among the rickettsiae of the spotted fever and typhus groups. FEMS Microbiol Lett. 1991;65:341–4. https://doi.org/10.1111/j.1574-6968.1991.tb04783.x
46. Vohra RF, Walker DH, Blanton LS. Analysis of health-care charges in murine typhus: need for improved clinical recognition and diagnostics for acute disease. Am J Trop Med Hyg. 2018;98:1594–8. https://doi.org/10.4269/|ajtmh.17-0411

Address for correspondence: Matthew Pickich, University of Texas Medical Branch, 301 University Blvd, Galveston, TX 77555, USA; email: aduarte@utmb.edu or mbpickich@gmail.com

Characteristics of Plausible Source Cases Responsible for Recent *Mycobacterium tuberculosis* Transmission, United States, 2018–2022

Steve Kammerer, Daniel Flanagan, Kala Raz, Tambi Shaw, Jonathan Wortham, Sarah Talarico

Tuberculosis (TB) outbreaks in the United States can cause substantial illness. Using surveillance and genotyping data, we applied a plausible source–case algorithm to identify TB cases reported during 2018–2020 responsible for secondary cases attributed to recent *Mycobacterium tuberculosis* transmission during 2020–2022. We used mixed models and a machine learning workflow to assess sociodemographic, clinical, and social risk factors associated with plausible sources. In mixed models, sputum smear positivity, cavitary disease, race/ethnicity other than non-Hispanic White or non-Hispanic Asian, age <65 years, US birth, and homelessness were associated with plausible sources. An adaptive boosting model achieved an area under the receiver operating characteristic curve of 0.81 on test data. Transmission was heterogeneous; 8.1% of sources linked to 3–15 secondary cases accounted for 24.9% of transmission events. Focusing case management and contact investigations on cases with the characteristics we identified could reduce *M. tuberculosis* transmission and improve TB prevention.

Tuberculosis (TB) is the leading infectious cause of death worldwide (*1*). The World Health Organization estimated that >10 million persons had TB develop during 2023 (*1*). TB incidence in the United States is low at <3 cases/100,000 population (≈9,000 annual cases) reported in recent years (*2*). Most US TB cases reflect reactivation of past *Mycobacterium tuberculosis* infection rather than recent transmission within US borders and most cases are diagnosed among non–US-born persons (*2*,*3*). However, outbreaks resulting from *M. tuberculosis* transmission within the United States continue to occur, disproportionately affect US-born persons, and can cause substantial illness (*4*–*10*). Therefore, targeted interventions to prevent *M. tuberculosis* transmission and TB outbreaks are crucial.

Public health interventions to prevent reactivation of latent TB differ from interventions designed to prevent *M. tuberculosis* transmission (*11*). Whereas preventing reactivation requires diagnosing and treating asymptomatic latent TB among persons with epidemiologic risk factors (e.g., birth outside the United States) (*3*,*12*), preventing *M. tuberculosis* transmission requires intensive case management to promptly initiate treatment to cure TB and identify, fully evaluate, and treat close contacts of TB case-patients (*13*). Clinically distinguishing between TB resulting from reactivation versus recent *M. tuberculosis* transmission often is impossible; thus, estimates of the percentage of cases attributable to recent transmission are needed to inform prioritization of resources and activities for TB prevention (*14*–*20*). With this aim, the Centers for Disease Control and Prevention (CDC) developed and validated a plausible source–case algorithm to estimate the percentage of TB cases attributable to recent transmission within US borders over a 2-year period (*17*,*18*). On the basis of that algorithm, ≈10%–15% of TB cases nationwide were attributed to recent *M. tuberculosis* transmission, but local estimates varied widely (*17*,*21*). During 2020–2021, a total of 1,400 cases were attributed to recent transmission in the 50 US states and the District of Columbia (*21*). Recent literature also suggests heterogeneity in transmission at the individual case level; some analyses have proposed that transmission associated with a few TB cases accounts for a

Author affiliations: Centers for Disease Control and Prevention, Atlanta, Georgia, USA (S. Kammerer, K. Raz, J. Wortham, S. Talarico); Emory University, Atlanta (D. Flanagan); California Department of Public Health, Richmond, California, USA (T. Shaw)

DOI: https://doi.org/10.3201/eid3206.260104

disproportionate share of secondary cases (*15*,*16*,*22*–*25*) and that transmission associated with those cases is more likely to result in outbreaks (*15*,*24*).

Focused interventions to prevent transmission, such as intensive case management and contact investigations for cases most likely to generate secondary cases, could reduce TB illnesses. Nonetheless, few analyses have sought to describe the characteristics of cases presumed to have transmitted *M. tuberculosis* to secondary cases (*17*,*18*). We used national molecular and case surveillance data to characterize the sociodemographic, clinical, and social risk factors associated with plausible TB source cases in the United States.

Materials and Methods

Data Sources

We obtained patient and case characteristics from the National Tuberculosis Surveillance System for incident TB cases reported to CDC during 2018–2022; demographic, clinical, and social risk factors are reported for each case (*21*). We included cases from all 50 US states and the District of Columbia.

For community-level characteristics, we used the CDC/Agency for Toxic Substances and Disease Registry's Social Vulnerability Index (SVI) based on the US Census Bureau's 2016–2020 American Community Survey (*26*). The SVI provides a relative vulnerability ranking for each US county by using 16 social factors grouped into 4 themes (i.e., socioeconomic status [SES], household characteristics, racial and ethnic minority status, and housing type and transportation) and an overall ranking. Rankings are values from 0 to 1, where higher values indicate higher social vulnerability.

We used genotyping data generated from whole-genome sequencing methods that assign a whole-genome multilocus sequence type (wgMLSType). *M. tuberculosis* isolate sequencing has been routinely available for >96% of culture-confirmed TB cases reported since 2018. The wgMLSType is assigned by comparing the sequences of 2,672 genetic loci and designating the same wgMLSType to cases that have matching patterns at ≥99.7% of loci.

We performed whole-genome single-nucleotide polymorphism (wgSNP) comparisons for all isolate pairs identified by the plausible source–case algorithm as a potential source and secondary case during the study period. We used BioNumerics 7.6.3 (Applied Maths, http://www.applied-maths.com) to perform wgSNP comparisons, which provide increased molecular resolution compared with wgMLSType. We excluded any single-nucleotide polymorphisms (SNPs) in a wgSNP comparison if total coverage was <5 reads or if it contained any ambiguous or unreliable bases or gaps. We also excluded all SNPs that were <12 bp from another SNP.

Recent Transmission Estimates

We applied the field-validated plausible source–case algorithm to culture-confirmed, genotyped TB cases reported during 2020–2022 that had nonunique wgMLSTypes. We attributed a case to recent transmission if ≥1 plausible source case of pulmonary or laryngeal TB was diagnosed within the previous 2 years in persons ≥10 years of age who had matching wgMLSType and resided within a 10-mile radius (*18*).

We excluded plausible source cases with isolates that differed by >5 SNPs from the secondary case's isolate to restrict the dataset to case pairs that are most likely to represent recent transmission (*27*). We extracted all remaining plausible source cases reported during 2018–2020; we classified any case not identified as a plausible source case for ≥1 cases attributed to recent transmission as a nonplausible source. Limiting the plausible source–case population to 2018–2020 enabled an equal 2-year follow-up for any subsequent secondary cases when assigning plausible source case status.

Study Population

We used a single binary outcome for analyses, defined as whether a case was identified as a plausible source case during 2018–2020 for ≥1 secondary cases attributed to recent transmission during 2020–2022. Because a secondary case can have multiple plausible sources, we assessed 2 scenarios: inclusion of all plausible sources (all scenario) and selection of a single most likely plausible source (most likely scenario).

We developed a decision tree to determine the most likely plausible source case. For each secondary case, we selected a single most likely source by prioritizing minimum wgSNP distance, then documented epidemiologic link, followed by highest infectiousness index. We resolved ties at random (Figure 1). We applied the most likely scenario to plot the distribution of the number of secondary cases attributed to recent transmission during 2020–2022 associated with each plausible source identified during 2018–2020.

Descriptive Analyses

We compared individual-level demographic, clinical, and social risk factors and community-level SVI measures of plausible versus nonplausible sources under both scenarios. To assess characteristics associated with plausible source cases that transmit to ≥3

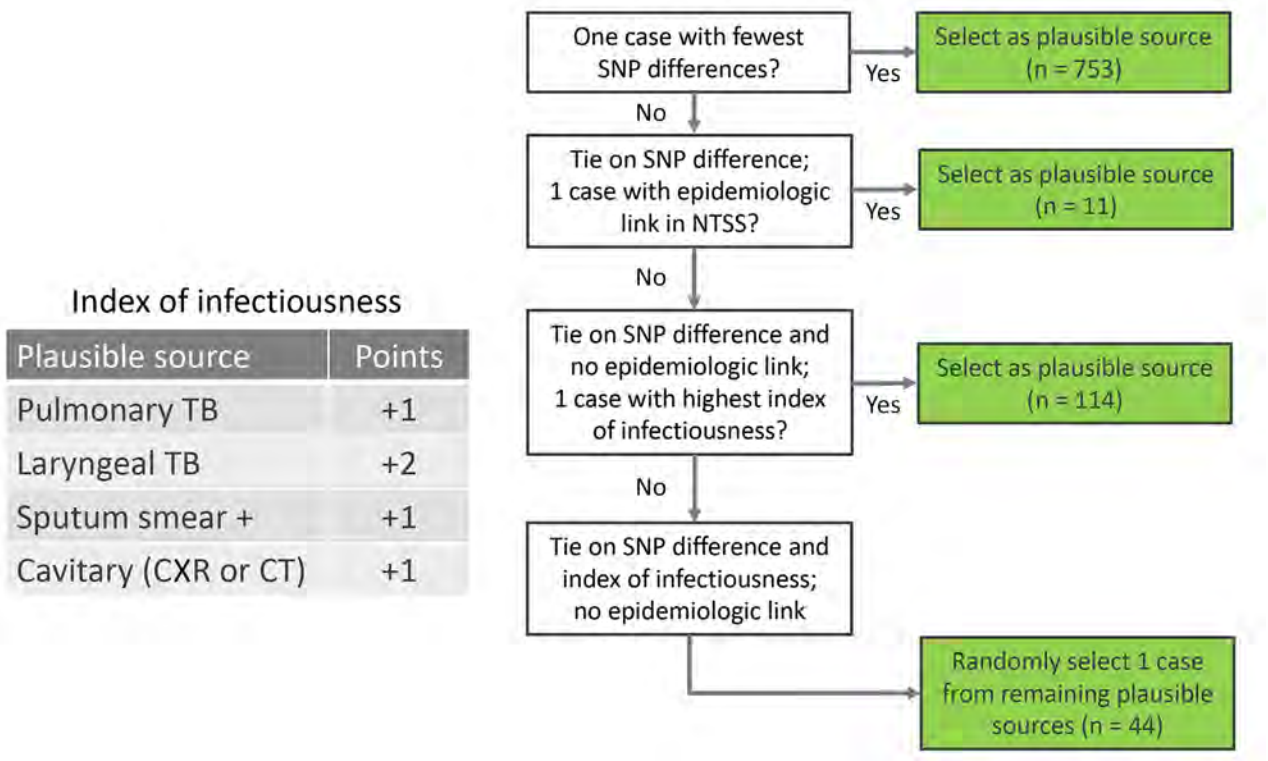

Index of infectiousness

Plausible source	Points
Pulmonary TB	+1
Laryngeal TB	+2
Sputum smear +	+1
Cavitary (CXR or CT)	+1

Figure 1. Determination of the most likely plausible source cases responsible for recent *Mycobacterium tuberculosis* transmission, United States, 2018–2022. Flowchart shows the structured decision process used to identify the most likely plausible source case. The algorithm evaluated SNP differences, epidemiologic links in the NTSS, and an index of infectiousness. If ties remained after applying those criteria, 1 plausible source case was randomly selected from the remaining candidates. CXR, chest radiograph; CT, computed tomography; NTSS, National Tuberculosis Surveillance System; SNP, single-nucleotide polymorphism; TB, tuberculosis.

secondary cases, we performed an additional descriptive analysis by using the most likely scenario and stratified the outcome into 0, 1–2, and ≥3 secondary cases. We used χ^2 test of independence or Fisher exact test for categorical variables and Wilcoxon rank-sum tests for continuous variables. We considered $p<0.05$ statistically significant.

Generalized Linear Mixed Models

We fit a multivariable generalized linear mixed model (GLMM) to determine individual- and community-level characteristics associated with being a plausible source case and developed separate models for the all and most likely scenarios. We incorporated a random intercept for county to accommodate clustering of cases by county and inclusion of county-level SVI measures; we assessed the separate factors in any SVI theme that were significantly associated with the outcome. We performed backward elimination starting with all variables included in the descriptive analysis. We assessed effect modification in the reduced model and evaluated multicollinearity by using variance inflation factors. We sequentially removed covariates if their exclusion decreased the Akaike information criterion, finalized models when no further improvement was observed, and calculated adjusted odds ratios (aORs) and 95% CIs.

Machine Learning Models

We also evaluated machine learning models (MLMs) that predict whether a TB case is estimated to be a plausible source. Using the most likely scenario, we developed a machine learning workflow to assess 10 different methods and included all features (i.e., variables) from the descriptive analysis (*28*) (Appendix, https://wwwnc.cdc.gov/EID/article/32/6/26-0104-App1.pdf).

Sensitivity Analyses

We reran both the GLMM and MLM workflows to evaluate the effects of using the infectiousness index to determine the outcome and smear positivity and cavitary disease as predictors. First, we restricted the data to the subset of secondary cases for which the most likely plausible source was determined using only wgSNP difference or epidemiologic link. Then, we reran the selection hierarchy without the infectiousness index (Appendix).

We used SAS version 9.4 (SAS Institute, Inc., https://www.sas.com) for data management, descriptive analyses, and GLMM development and Python version 3.9.13 (Python Software Foundation, https://www.python.org) for MLM analyses. CDC determined this activity to be routine public health surveillance and not human subjects research. WGS was performed as part of routine public health surveillance and no new sequence data were generated as part of this study. Sequence data included in this analysis are available in the National Center for Biotechnology Information (BioProject no. PRJNA1237251).

Results

Study Population

During 2018–2022, a total of 41,264 TB cases were reported from the 50 US states and the District of Columbia, of which 32,110 (77.8%) were culture-confirmed and genotyped, and 61% (n = 19,577) of culture-confirmed and genotyped cases were reported during 2018–2020. Using the plausible source–case algorithm, we identified 3,762 recent transmission source–secondary case pairs for which 1,922 (51.1%) were supported by wgSNP analysis (Figure 2). The 1,922 case pairs comprised 922 cases attributed to recent transmission during 2020–2022, indicating a mean of 2.1 (range 1–24) plausible source cases per secondary case. We identified 893 (4.6%) unique plausible source cases during 2018–2020 for the all scenario (Table 1; Figure 2; Appendix Table 1). We found secondary cases attributed to recent transmission in 44 states.

For the most likely scenario, we identified 645 (3.3%) unique plausible source cases during 2018–2020 (Table 2; Appendix Table 2). Among the 922 cases attributed to recent transmission, we chose 753 (81.7%) plausible source cases by using wgSNP difference, 114 (12.4%) by using the index of infectiousness, 44 (4.8%) by using random selection, and 11 (1.2%) by using epidemiologic links (Appendix Table 4).

Descriptive Analyses

In the all scenario, plausible sources were more often male sex, US-born, <65 years of age, and other than non-Hispanic White or non-Hispanic Asian race/ethnicity, and they more frequently reported homelessness and substance use. Those plausible sources also more often had smear positivity and cavitary disease. County-level social vulnerability was higher among plausible sources, especially the SES theme (Table 1; Appendix Table 1).

Using the most likely scenario, characteristic distribution differed greatly across the 3 transmission categories (nonplausible source, plausible source for

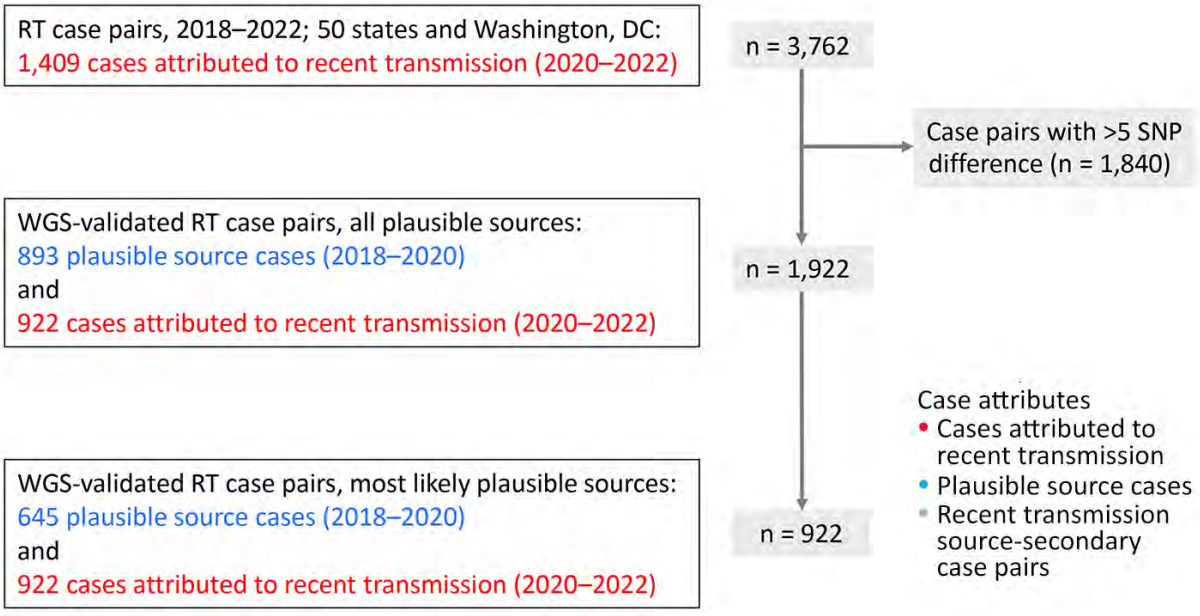

Figure 2. Flow diagram showing selection of recent transmission source–secondary case pairs from 50 states and Washington, DC, included in an analysis of plausible source cases responsible for recent *Mycobacterium tuberculosis* transmission, United States, 2018–2022. Among 3,762 RT case pairs identified, case pairs with >5 SNP differences were excluded (n = 1,840), leaving 1,922 WGS–validated RT case pairs. The analytic dataset included 922 TB cases attributed to RT during 2020–2022 and plausible source cases identified during 2018–2020 (all plausible source cases [n = 893] and most likely plausible source cases [n = 645]). RT, recent transmission; SNP, single-nucleotide polymorphism; TB, tuberculosis; WGS, whole-genome sequencing.

Table 1. Characteristics of all plausible source TB cases during 2018–2020 responsible for recent *Mycobacterium tuberculosis* transmission during 2020–2022, United States*

Characteristic	Nonplausible source	Plausible source	p value†
Total cases, n = 19,577	18,684 (95.4)	893 (4.6)	
Sex			<0.001
M	11,465 (61.4)	631 (70.7)	
F	7,216 (38.6)	262 (29.3)	
Unknown	3 (0)	0	
Age, y			<0.001
<5	185 (1.0)	0	
5–14	191 (1.0)	13 (1.5)	
15–24	1,802 (9.6)	120 (13.4)	
25–44	5,521 (29.5)	338 (37.9)	
45–64	5,503 (29.5)	337 (37.7)	
≥65	5,482 (29.3)	85 (9.5)	
Origin of birth			<0.001
United States	4,829 (25.8)	536 (60.0)	
Non-US country	13,826 (74.0)	356 (39.9)	
Unknown	29 (0.2)	1 (0.1)	
Race and ethnicity‡			<0.001
Hispanic or Latino	5,459 (29.2)	290 (32.5)	
American Indian/Alaska Native	161 (0.9)	47 (5.3)	
Native Hawaiian/Pacific Islander	215 (1.2)	29 (3.2)	
Black	3,377 (18.1)	325 (36.4)	
Asian	7,161 (38.3)	86 (9.6)	
White	2,115 (11.3)	104 (11.6)	
Multiple race	137 (0.7)	6 (0.7)	
Unknown	59 (0.3)	6 (0.7)	
Resident of a correctional facility at TB diagnosis			<0.001
Y	464 (2.5)	49 (5.5)	
N	18,154 (97.2)	834 (93.4)	
Unknown	66 (0.3)	10 (1.1)	
Experiencing homelessness within past 12 mo			<0.001
Y	744 (4.0)	138 (15.4)	
N	17,776 (95.1)	740 (82.9)	
Unknown	164 (0.9)	15 (1.7)	
Excess alcohol use within past 12 mo			<0.001
Y	1,618 (8.7)	184 (20.6)	
N	16,783 (89.8)	687 (76.9)	
Unknown	283 (1.5)	22 (2.5)	
Noninjection drug use within past 12 mo			<0.001
Y	1,213 (6.5)	204 (22.8)	
N	17,022 (91.1)	650 (72.8)	
Unknown	449 (2.4)	39 (4.4)	
Sputum smear			<0.001
Positive	8,788 (47.0)	621 (69.5)	
Negative	7,759 (41.5)	217 (24.3)	
Not done	2,119 (11.3)	55 (6.2)	
Unknown	18 (0.1)	0	
Cavitary disease§			<0.001
Y	6,638 (35.5)	541 (60.6)	
N	9,877 (52.9)	310 (34.7)	
Unknown	2,169 (11.6)	42 (4.7)	
Contact of infectious tuberculosis patient during past 2 y			<0.001
Y	970 (5.2)	122 (13.7)	
Unknown/not reported	17,714 (94.8)	771 (86.3)	
Median Social Vulnerability Index score (IQR) ¶	0.73 (0.49–0.86)	0.83 (0.66–0.89)	<0.001#
Socioeconomic status	0.65 (0.34–0.86)	0.80 (0.58–0.92)	<0.001#
Household characteristics	0.45 (0.23–0.70)	0.56 (0.32–0.74)	<0.001#
Racial and ethnic minority status	0.91 (0.78–0.96)	0.92 (0.82–0.97)	<0.001#
Housing type and transportation	0.78 (0.61–0.90)	0.83 (0.68–0.91)	<0.001#

*Values are no. (%) except as indicated. IQR, interquartile range; TB, tuberculosis.
†χ^2 test or Fisher exact test when <5 cases expected.
‡Except for Hispanic or Latino, all are non-Hispanic.
§Evidence of ≥1 lung cavities with chest radiograph, chest computerized tomography, or both.
¶Overall Social Vulnerability Index includes 16 US Census indicators from the 5-year American Community Survey grouped into 4 themes: socioeconomic status, household characteristics, racial and ethnic minority status, and housing type and transportation. Ranking values range from 0 to 1, and higher values indicate higher vulnerability and are merged to each case using the patient's county of residence.
#Wilcoxon rank sum test.

Table 2. Characteristics of most likely plausible source TB cases during 2018–2020 responsible for recent *Mycobacterium tuberculosis* transmission during 2020–2022, United States*

Characteristic	Nonplausible source	Plausible source	p value†
Total no. (%) cases, n = 19,577	18,932 (96.7)	645 (3.3)	
Sex			<0.001
M	11,640 (61.5)	456 (70.7)	
F	7,289 (38.5)	189 (29.3)	
Unknown	3 (0.0)	0 (0.0)	
Age, y			<0.001
<5	185 (1.0)	0 (0.0)	
5–14	198 (1.0)	6 (0.9)	
15–24	1,828 (9.7)	94 (14.6)	
25–44	5,620 (29.7)	239 (37.1)	
45–64	5,597 (29.6)	243 (37.7)	
≥65	5,504 (29.1)	63 (9.8)	
Origin of birth			<0.001
United States	5,022 (26.5)	343 (53.2)	
Non-US country	13,881 (73.3)	301(46.7)	
Unknown	29 (0.2)	1 (0.2)	
Race and ethnicity‡			<0.001
Hispanic or Latino	5,513 (29.1)	236 (36.6)	
American Indian/Alaska Native	186 (1.0)	22 (3.4)	
Native Hawaiian/Pacific Islander	221 (1.2)	23 (3.6)	
Black	3,486 (18.4)	216 (33.5)	
Asian	7,175 (37.9)	72 (11.2)	
White	2,150 (11.4)	69 (10.7)	
Multiple race	141 (0.7)	2 (0.3)	
Unknown	60 (0.3)	5 (0.8)	
Resident of a correctional facility at time of TB diagnosis			<0.001
Y	483 (2.6)	30 (4.7)	
N	18,381 (97.1)	607 (94.1)	
Unknown	68 (0.4)	8 (1.2)	
Experiencing homelessness within past 12 mo			<0.001
Y	793 (4.2)	89 (13.8)	
N	17,973 (94.9)	543 (84.2)	
Unknown	166 (0.9)	13 (2.0)	
Excess alcohol use within past 12 mo			<0.001
Y	1,683 (8.9)	119 (18.5)	
N	16,961 (89.6)	509 (78.9)	
Unknown	288 (1.5)	17 (2.6)	
Noninjection drug use within past 12 mo			<0.001
Y	1,273 (6.7)	144 (22.3)	
N	17,199 (90.9)	473 (73.3)	
Unknown	460 (2.4)	28 (4.3)	
Sputum smear			<0.001
Positive	8,909 (47.1)	500 (77.5)	
Negative	7,863 (41.5)	113 (17.5)	
Not done	2,142 (11.3)	32 (5.0)	
Unknown	18 (0.1)	0 (0.0)	
Cavitary disease§			<0.001
Y	6,737 (35.6)	442 (68.5)	
N	10,004 (52.8)	183 (28.4)	
Unknown	2,191 (11.6)	20 (3.1)	
Contact of infectious tuberculosis patient during prior 2 y			<0.001
Y	1,030 (5.4)	62 (9.6)	
Unknown/not reported	17,902 (94.6)	583 (90.4)	
Median Social Vulnerability Index score (IQR)¶	0.73 (0.49–0.86)	0.80 (0.65–0.89)	<0.001#
Socioeconomic status	0.65 (0.34–0.87)	0.79 (0.56–0.90)	<0.001#
Household characteristics	0.46 (0.23–0.70)	0.55 (0.32–0.74)	<0.001#
Racial and ethnic minority status	0.91 (0.78–0.97)	0.91 (0.81–0.97)	0.006#
Housing type and transportation	0.78 (0.61–0.90)	0.82 (0.67–0.91)	<0.001#

*Values are no. (%) except as indicated. IQR, interquartile range; TB, tuberculosis.
†χ^2 test or Fisher exact test when <5 cases expected.
‡Except for Hispanic or Latino, all are non-Hispanic.
§Evidence of ≥1 lung cavities with chest radiograph, chest computerized tomography, or both.
¶Overall Social Vulnerability Index includes 16 US Census indicators from the 5-year American Community Survey grouped into 4 themes: socioeconomic status, household characteristics, racial and ethnic minority status, and housing type and transportation. Ranking values range from 0 to 1, and higher values indicate higher vulnerability and are merged to each case using the patient's county of residence.
#Wilcoxon rank sum test.

1–2 cases, and plausible source for ≥3 cases) (Table 3; Appendix Table 3). Descriptively, among plausible source cases estimated to have transmitted to ≥3 (range 3–15) secondary cases, the highest percentages were among persons reporting male sex, 25–44 years of age, US-born, non-Hispanic Black race/ethnicity, experiencing homelessness, noninjection drug use, sputum smear positivity, and cavitary disease. Social vulnerability, including all 4 SVI themes, was also highest for the ≥3 secondary cases category.

GLMMs

Of the 19,577 cases available for analysis, we excluded 311 (1.6%) with missing data for sex, birth country, race/ethnicity, sputum smear, or county. We excluded all cases among children 0–4 years of age from analysis because plausible source cases had to be ≥10 years of age. For the all scenario, we found that the following characteristics were most associated with being a plausible source case: race/ethnicity, specifically Native Hawaiian/Pacific Islander non-Hispanic (aOR 5.34 [95% CI 3.11–9.17]), American Indian/Alaska Native non-Hispanic (aOR 2.12 [95% CI 1.10–4.06]), and Black non-Hispanic (aOR 1.82 [95% CI 1.40–2.36]), compared with White non-Hispanic persons; age <65 years compared with ≥65 years of age, the greatest association of which was 15–24 years of age (aOR 3.01 [95% CI 2.21–4.30]); US-born (aOR 2.41 [95% CI 1.99–2.91]); experiencing homelessness (aOR 1.89 [95% CI 1.49–2.39]); and indicators of infectiousness, specifically positive sputum smear (aOR 1.71 [95% CI 1.42–2.07]) and cavitary disease (aOR 1.69 [95% CI 1.42–2.00]) (Table 4). Noninjection drug use, male sex, and Hispanic ethnicity also were associated with plausible source cases.

Among the SVI themes, only SES was significantly associated with plausible source cases in multivariable generalized linear mixed modeling ($p<0.001$). Thus, we included 2 of the SES component factors in the final model: housing cost burden (aOR 1.20 [95% CI 1.06–1.36]), defined as households spending ≥30% of annual income on housing (*26*); and not having health insurance (aOR 1.13 [95% CI 1.02–1.25]). We calculated SVI aORs on the basis of a 0.20-unit (i.e., 20%) increase for each factor. Multicollinearity was modest for age and race/ethnicity, but no variance inflation factors exceeded 4. We found no statistically significant effect modification in the final model.

The final model for the most likely scenario included the same variables as the all scenario except for SES factors (Table 5). We only retained the not having health insurance (aOR 1.12 [95% CI 1.04–1.21]) factor in that model.

Machine Learning Predictive Models

After random selection of nonplausible source cases, we ran MLMs under the most likely scenario by using 3,456 observations, among which we used 2,686 (77.8%) for training and 770 (22.2%) for testing (Appendix Table 5). We assessed recall and F1 statistic, which is the harmonic mean of weighted-average recall and weighted-average precision computed as prevalence-weighted averages across the classes. We noted recall and F1 statistic were highest for gradient boosting (recall 0.758; F1 0.752), adaptive boosting (recall 0.751; F1 0.750), and random forest (recall 0.755; F1 0.740) methods; we selected those methods for hyperparameter tuning. The tuned adaptive boosting model had the highest area under the receiver operating characteristic curve (AUC; 0.780) (Appendix).

We found no reduction in predictive performance for the tuned adaptive boosting model when applied to the test set (F1 0.761; AUC 0.811) versus model training (F1 0.755; AUC 0.780). Sensitivity was 55.4% (95% CI 48.7%–62.2%), specificity 82.7% (95% CI 79.5%–85.8%), and AUC 0.81 (95% CI 0.78–0.84) with the test set. Individual-level factors dominated feature importance and county-level SVI measures were less predictive (Figure 3; Appendix).

Distribution of Secondary Cases Associated with Plausible Source Cases

The distribution of the number of secondary cases attributed to each plausible source case was right skewed, indicating heterogeneity of TB transmission (Appendix Figure). Most (76.6%, n = 494) plausible source cases transmitted to a single secondary case and comprised 53.6% of all estimated transmission events. Plausible source cases that transmitted to 3–15 secondary cases (8.1%, n = 52) comprised 24.9% of all estimated transmission events.

Sensitivity Analyses

We restricted analyses to source assignments solely on the basis of wgSNP difference or epidemiologic link and we removed the index of infectiousness from the hierarchy. In both instances, associations for smear positivity and cavitary disease were modestly attenuated but remained statistically significant (Appendix Table 6).

Discussion

M. tuberculosis transmission was rare in the United States during 2018–2022; nonetheless, cases attributed to recent transmission were diagnosed in nearly every US state. In mixed models, sputum smear positivity, cavitary disease, race/ethnicity other than

Table 3. Characteristics of most likely plausible TB cases during 2018–2020 responsible for recent *Mycobacterium tuberculosis* transmission to ≥1 secondary TB cases during 2020–2022, United States*

Characteristic	Nonplausible source	Plausible source for ≥1 TB cases		p value†
		1–2 cases	≥3 cases	
Total no. (%) cases, n = 19,577	18,932 (96.7)	593 (3.0)	52 (0.3)	
Sex				<0.001
M	11,640 (61.5)	415 (70.0)	41 (78.9)	
F	7,289 (38.5)	178 (30.0)	11 (21.1)	
Unknown	3 (0.0)	0 (0.0)	0 (0.0)	
Age, y				<0.001
<5	189 (1.0)	0 (0.0)	0 (0.0)	
5–14	198 (1.0)	6 (1.0)	0 (0.0)	
15–24	1,828 (9.7)	87 (14.7)	7 (13.5)	
25–44	5,620 (29.7)	214 (36.1)	25 (48.1)	
45–64	5,597 (29.6)	225 (37.9)	18 (34.6)	
≥65	5,504 (29.1)	61 (10.3)	2 (3.8)	
Origin of birth				<0.001
United States	5,022 (26.5)	306 (51.6)	37 (71.2)	
Non-US country	13,881 (73.3)	286 (48.2)	15 (28.8)	
Unknown	29 (0.2)	1 (0.2)	0 (0.0)	
Race and ethnicity‡				<0.001
Hispanic or Latino	5,513 (29.1)	227 (38.3)	9 (17.3)	
American Indian/Alaska Native	186 (1.0)	15 (2.5)	7 (13.5)	
Native Hawaiian/Pacific Islander	221 (1.2)	22 (3.7)	1 (1.9)	
Black	3,486 (18.4)	188 (31.7)	28 (53.8)	
Asian	7,175 (37.9)	68 (11.5)	4 (7.7)	
White	2,150 (11.4)	66 (11.1)	3 (5.8)	
Multiple race	141 (0.7)	2 (0.3)	0 (0.0)	
Unknown	60 (0.3)	5 (0.8)	0 (0.0)	
Resident of a correctional facility at time of TB diagnosis				<0.001
Y	483 (2.5)	27 (4.5)	3 (5.8)	
N	18,381 (97.1)	559 (94.3)	48 (92.3)	
Unknown	68 (0.4)	7 (1.2)	1 (1.9)	
Experiencing homelessness within past 12 mo				<0.001
Y	793 (4.2)	78 (13.1)	11 (21.1)	
N	17,973 (94.9)	504 (85.0)	39 (75.0)	
Unknown	166 (0.9)	11 (1.9)	2 (3.9)	
Excess alcohol use within past 12 mo				<0.001
Y	1,683 (8.7)	109 (18.4)	10 (19.2)	
N	16,961 (89.6)	471 (79.4)	38 (73.1)	
Unknown	288 (1.5)	13 (2.2)	4 (7.7)	
Noninjection drug use within past 12 mo				<0.001
Y	1,273 (6.7)	124 (20.9)	20 (38.5)	
N	17,199 (90.9)	446 (75.2)	27 (51.9)	
Unknown	460 (2.4)	23 (3.9)	5 (9.6)	
Sputum smear				<0.001
Positive	8,909 (47.1)	455 (76.7)	45 (86.5)	
Negative	7,863 (41.5)	108 (18.2)	5 (9.6)	
Not done	2,142 (11.3)	30 (5.1)	2 (3.9)	
Unknown	18 (0.1)	0 (0.0)	0 (0.0)	
Cavitary disease§				<0.001
Y	6,737 (35.6)	402 (67.8)	40 (76.9)	
N	10,004 (52.8)	173 (29.2)	10 (19.2)	
Unknown	2,191 (11.6)	18 (3.0)	2 (3.9)	
Contact of infectious tuberculosis patient during prior 2 y				<0.001
Y	1,030 (5.4)	55 (9.3)	7 (13.5)	
Unknown/not reported	17,902 (94.6)	538 (90.7)	45 (86.5)	
Median Social Vulnerability Index score (IQR)¶	0.73 (0.49–0.86)	0.80 (0.64–0.89)	0.86 (0.78–0.89)	<0.001
Socioeconomic status	0.65 (0.34–0.86)	0.77 (0.56–0.88)	0.84 (0.70–0.92)	<0.001
Household characteristics	0.46 (0.23–0.70)	0.54 (0.31–0.74)	0.57 (0.32–0.77)	<0.001
Racial and ethnic minority status	0.91 (0.78–0.97)	0.91 (0.81–0.97)	0.93 (0.83–0.97)	0.01
Housing type and transportation	0.78 (0.61–0.90)	0.82 (0.67–0.91)	0.85 (0.68–0.91)	<0.001

*Values are no. (%) except as indicated. IQR, interquartile range; TB, tuberculosis.
†χ^2 test or Fisher exact test when <5 cases expected; indicates differences across the 3 categories.
‡Except for Hispanic or Latino, all are non-Hispanic.
§Evidence of ≥1 lung cavities with chest radiograph, chest computerized tomography, or both.
¶Overall Social Vulnerability Index includes 16 US Census indicators from the 5-year American Community Survey grouped into 4 themes: socioeconomic status, household characteristics, racial and ethnic minority status, and housing type and transportation. Ranking values range from 0 to 1, and higher values indicate higher vulnerability and are merged to each case using the patient's county of residence. p value calculated by Kruskal-Wallis test.

Table 4. Multivariable model results for all plausible source TB cases during 2018–2020 responsible for recent *Mycobacterium tuberculosis* transmission during 2020–2022, United States*

Characteristic	Plausible sources, no. (%)	aOR (95% CI)
Total no. (%) cases, n = 19,266	886 (4.6)†	NA
Sex		
M	625 (70.5)	1.26 (1.07–1.48)
F	261 (29.5)	Referent
Age, y		
10–14	13 (1.5)	2.26 (1.17–4.10)
15–24	120 (13.5)	3.01 (2.21–4.30)
25–44	334 (37.7)	2.70 (2.08–3.51)
45–64	334 (37.7)	2.51 (1.94–3.25)
≥65	85 (9.6)	Referent
Origin of birth		
United States	535 (60.4)	2.41 (1.99–2.91)
Outside United States	351 (39.6)	Referent
Unknown		
Race and ethnicity‡		
Hispanic or Latino	289 (32.6)	1.52 (1.15–2.02)
American Indian/Alaska Native	47 (5.3)	2.12 (1.10–4.06)
Native Hawaiian/Pacific Islander	29 (3.3)	5.34 (3.11–9.17)
Black	325 (36.7)	1.82 (1.40–2.36)
Asian	86 (9.7)	0.63 (0.45–0.90)
White	104 (11.7)	Referent
Multiple race	6 (0.7)	1.03 (0.41–2.61)
Experiencing homelessness within past 12 mo		
Y	137 (15.5)	1.89 (1.49–2.39)
N	735 (83.0)	Referent
Unknown	14 (1.6)	1.22 (0.62–2.39)
Noninjection drug use within past 12 mo		
Y	204 (23.0)	1.38 (1.12–1.69)
N	646 (72.9)	Referent
Unknown	36 (4.1)	1.68 (1.08–2.59)
Sputum smear		
Positive	615 (69.4)	1.71 (1.42–2.07)
Negative	216 (24.4)	Referent
Not done	55 (6.2)	0.98 (0.69–1.39)
Cavitary disease§		
Y	536 (60.5)	1.69 (1.42–2.00)
N	309 (34.9)	Referent
Unknown	41 (4.6)	0.63 (0.44–0.90)
Type of therapy		
Directly observed therapy alone	591 (66.7)	0.72 (0.51–1.02)
Self-administered therapy alone	9 (1.0)	0.35 (0.16–0.73)
Both	230 (26.0)	0.62 (0.43–0.90)
Unknown	56 (6.3)	Referent
Social Vulnerability Index score¶		
SES—housing cost burden	NA	1.20 (1.06–1.36)
SES—no health insurance	NA	1.13 (1.02–1.25)

*Outcome of plausible source versus not a plausible source for all cases of tuberculosis with a genotyped isolate. Excludes cases with missing sex, origin of birth, race/ethnicity, unknown sputum smear status, 0–4 years of age, and county of residence. All plausible source cases identified by the recent transmission algorithm for a given secondary case are included. aOR, adjusted odds ratio; SES, socioeconomic status; TB, tuberculosis.
†Of 19,266 included case-patients.
‡Except for Hispanic or Latino, all are non-Hispanic.
§Evidence of ≥1 lung cavities with chest radiograph, chest computerized tomography, or both.
¶Social Vulnerability Index includes 16 US Census indicators from the 5-year American Community Survey grouped into 4 themes: SES, household characteristics, racial and ethnic minority status, and housing type and transportation. Ranking values range from 0 to 1, and higher values indicate higher vulnerability and are merged to each case using the patient's county of residence. ORs based on a 0.2-unit (20%) change for that indicator.

non-Hispanic White or Asian, age 15–44 years, being US-born, and homelessness were associated with being a plausible source for transmission. We found heterogeneous transmission and 8.1% of plausible source cases identified by the recent transmission algorithm were linked to 3–15 secondary cases and accounted for 24.9% of inferred transmission events. Among plausible source cases identified during 2018–2020 that were linked to ≥3 secondary cases, 86.5% were sputum smear–positive versus 48.1% of all genotyped cases reported during that period; similarly, 76.9% of plausible source cases had cavitary disease versus 36.7% of all genotyped cases. US-born persons only accounted for 27.4% of all genotyped cases, but 71.2% of plausible sources linked to ≥3 secondary cases were among US-born persons.

Our results align with prior investigations of source-case characteristics. A study from the Netherlands defined source cases as the first case diagnosed in a genotype-matched cluster (*29*). That study found fewer secondary cases for female sex and decreasing numbers of cases with increasing source age. In another study conducted among smear-positive TB patients in Barcelona, Spain, researchers used contact investigations to identify secondary cases and found that more secondary cases occurred after cases in younger adults, those with cavitary disease, and persons who injected drugs (*30*). In Peru, sources identified by using wgSNP distance more often were <34 years of age, were male, and had incarceration history or reported alcohol use or smoking (*31*).

Characteristics of plausible source cases in our study were like characteristics of cases estimated to be attributed to recent transmission. One study found that among the largest 10% of recent transmission clusters, cases attributed to recent transmission were more likely to be in persons who were US-born, American Indian/Alaska Native non-Hispanic, Native

Table 5. Multivariable model results for most likely plausible source TB cases during 2018–2020 responsible for recent *Mycobacterium tuberculosis* transmission during 2020–2022, United States

Characteristics	Plausible sources, no. (%)	aOR (95% CI)
Total no. cases, (%); n = 19,126	637 (3.3)	NA
Sex		
M	449 (70.5)	1.26 (1.05–1.52)
F	188 (29.5)	Referent
Age, y		
10–14	6 (0.9)	2.00 (0.83–4.82)
15–24	92 (14.4)	3.03 (2.15–4.27)
25–44	236 (37.1)	2.56 (1.90–3.45)
45–64	240 (37.7)	2.38 (1.78–3.19)
≥65	63 (9.9)	Referent
Origin of birth		
United States	341 (53.5)	1.95 (1.58–2.41)
Outside United States	296 (46.5)	Referent
Race and ethnicity†		
Hispanic or Latino	235 (36.9)	1.72 (1.25–2.35)
American Indian/Alaska Native	22 (3.5)	2.71 (1.47–4.98)
Native Hawaiian/Pacific Islander	23 (3.6)	5.72 (3.30–9.93)
Black	216 (33.9)	1.90 (1.42–2.55)
Asian	72 (11.3)	0.76 (0.52–1.11)
White	69 (10.8)	Referent
Experiencing homelessness within past 12 mo.		
Y	88 (13.8)	1.59 (1.22–2.07)
N	537 (84.3)	Referent
Unknown	12 (1.9)	1.73 (0.88–3.38)
Noninjection drug use within past 12 mo.		
Y	144 (22.6)	1.49 (1.19–1.87)
N	468 (73.5)	Referent
Unknown	25 (3.9)	1.42 (0.87–2.31)
Sputum smear		
Positive	494 (77.5)	2.33 (1.85–2.93)
Negative	112 (17.6)	Referent
Not done	31 (4.9)	1.14 (0.74–1.76)
Cavitary disease‡		
Y	438 (68.8)	2.07 (1.70–2.52)
N	181 (28.4)	Referent
Unknown	18 (2.8)	0.54 (0.33–0.89)
Type of therapy		
Directly observed therapy alone	413 (64.8)	0.62 (0.43–0.90)
Self-administered therapy alone	7 (1.1)	0.38 (0.17–0.88)
Both	173 (27.2)	0.55 (0.37–0.81)
Unknown	44 (6.9)	Referent
Social Vulnerability Index score§		
SES—no health insurance	NA	1.12 (1.04–1.21)

*Outcome of plausible source versus not plausible source for all cases of tuberculosis disease with a genotyped isolate. Excludes cases with missing sex, origin of birth, race/ethnicity, unknown sputum smear status, and children 0–4 years of age. Most likely plausible source identified for each secondary case is included (Figure 1). aOR, adjusted odds ratio; NA, not applicable; SES, socioeconomic status; TB, tuberculosis.
†Except for Hispanic or Latino, all are non-Hispanic.
‡Evidence of 1 or more lung cavities with chest radiograph, chest computerized tomography scan, or both.
§Social Vulnerability Index includes 16 US Census indicators from the 5-year American Community Survey grouped into 4 themes: SES, household characteristics, racial and ethnic minority status, and housing type and transportation. Ranking values range from 0 to 1, and higher values indicate higher vulnerability and are merged to each case using the patient's county of residence. ORs based on a 0.2-unit (20%) change for that indicator.

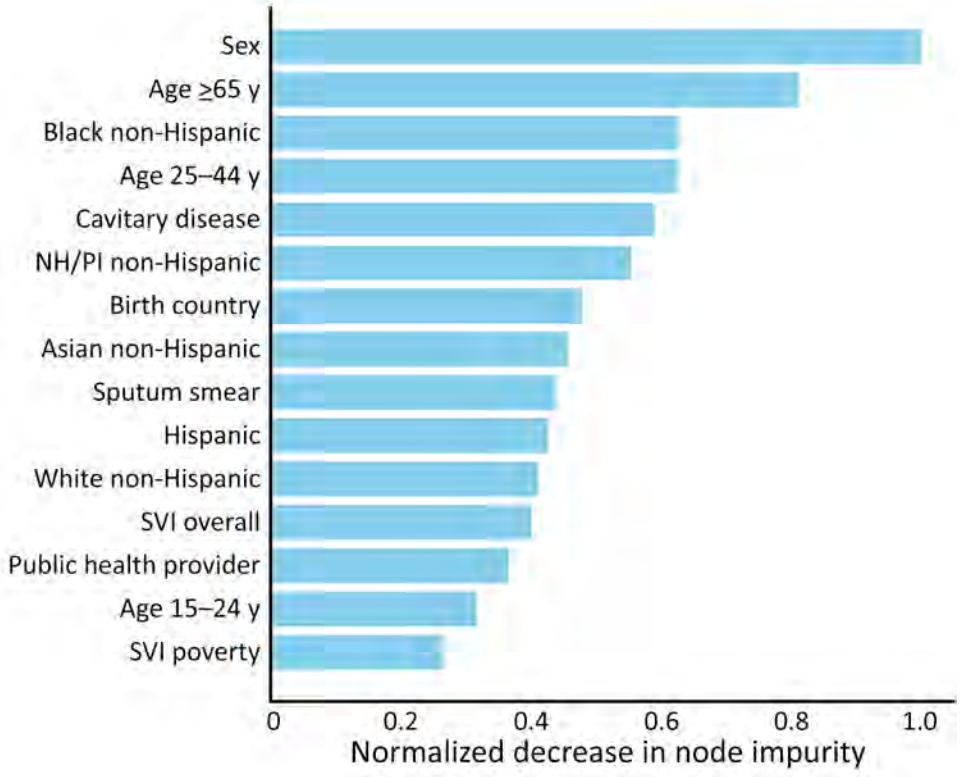

Figure 3. Characteristics from an adaptive boosting model of plausible source cases responsible for recent *Mycobacterium tuberculosis* transmission, United States, 2018–2022. Horizontal bars show the normalized impurity-based importance (mean decrease in node impurity) associated with each predictor; larger values indicate greater importance. NH/PI, Native Hawaiian/Pacific Islander; SVI, Social Vulnerability Index.

Hawaiian/Pacific Islander non-Hispanic, Black non-Hispanic, and Asian non-Hispanic and who reported homelessness (*17*).

In our study, positive sputum smear and cavitary disease, markers of infectiousness and advanced disease (*32*–*34*), were consistently associated with source case status in both GLMM and MLM, including sensitivity analyses where those factors were not used to select between potential source cases. Those associations support the current practice of prioritizing contact investigations for smear-positive and cavitary TB cases (*13*) and suggest that diagnostic delays contribute to transmission. Delays might reflect barriers to care, including homelessness (*4*, *5*,*10*,*35*), or missed diagnoses after seeking healthcare services (*36*). Because TB is uncommon in the United States, clinicians might not routinely consider it in symptomatic patients. Of note, whereas most US TB cases occur among persons born outside the United States, plausible source cases in our study had higher odds of being in US-born persons. Although Asian non-Hispanic persons account for most TB cases (*21*), they were not substantially associated with plausible source status in this study. Missed diagnoses and longer infectious periods among higher-risk groups could explain those findings. Therefore, robust epidemiology and outbreak detection should be used to customize local TB control and prevention efforts focused on at-risk persons.

We found that county-based social determinants of health related to SES (i.e., burdened by housing cost and not having health insurance) were associated with plausible source case attribution in the GLMM (*26*). Those associations could reflect barriers to TB care, including lack of insurance and constrained resources in settings with high housing costs (*37*,*38*). A study that examined data from TB cases reported to the California TB Registry during 2012–2016 found higher TB rates in the lowest SES areas, which defined SES by low education, crowding, poverty, and the California Healthy Places Index (*39*). An ecologic analysis in another study reported that census tracts with lower median incomes, more racial/ethnic minority groups, and more migrants had higher pediatric TB rates; however, overcrowding and unemployment were not associated (*40*). As in those prior studies, our analysis suggests that area-based SES measures could inform TB prevention efforts.

Adaptive boosting ranked male sex and younger age (<65 years) as the main predictors, followed by race/ethnicity, clinical indicators of infectiousness, and birth origin (Figure 3). Ensemble methods outperformed regression-based approaches in this analysis (Appendix Table 5) and have been used to predict TB outcomes, including cluster growth and positive laboratory results (*41*,*42*). The GLMM supports inference through interpretable adjusted

associations, and the MLM offers a complementary perspective focused on prediction. Despite differences in ranking, many of the same predictors were influential across both approaches, including markers of infectiousness, age, race/ethnicity, origin of birth, and several social factors. That convergence supports the robustness of our findings.

Strengths of our analysis included the use of wgSNP comparisons to refute case pairs that were not likely to be the result of recent transmission, assessment of both patient- and community-level predictors for association with being a plausible source case, and analysis of plausible source cases of recent transmission at a national level. The first limitation of this analysis is that some cases could have been misattributed as not sources by the algorithm because the source was reported after the secondary case, the source was outside a 10-mile radius, or the secondary case was not genotyped. Although ≈75% of US cases are culture-confirmed (*21*) and >96% of those are genotyped, TB cases in young children, which would predominantly result from recent transmission, have substantially lower rates of culture confirmation. Furthermore, because we limited running the algorithm to starting in 2020, some of the 2018–2019 cases could have been misattributed as not a source if the resulting secondary case was also reported in 2018–2019. We also might have misattributed cases as not sources if all contacts with latent TB infection underwent successful treatment and did not develop TB disease. Second, the COVID-19 pandemic occurred during the analysis period. The pandemic was associated with changes in healthcare seeking behavior that could have affected TB diagnoses; therefore, generalization of our results to other time periods should be done with caution.

In summary, although *M. tuberculosis* transmission is relatively rare in the United States, targeted control efforts could prevent outbreaks that overwhelm public health programs. We identified both patient-level and, to a lesser extent, community-level characteristics as predictors of being a source of recent transmission. Cases with clinical indicators of increased infectiousness were more likely to be transmission sources, supporting current guidance to prioritize those cases for contact investigation. Demographic characteristics associated with being a source case, such as race and origin of birth, differed from those of overall TB cases, highlighting the need for prompt TB diagnosis in US-born persons with risk factors, particularly homelessness and substance use, for preventing outbreaks. In addition, enhanced efforts to promptly diagnose TB in communities with more uninsured residents and those with high housing costs might also reduce transmission. Findings from this analysis suggest that intensifying public health interventions on TB cases in persons with certain demographic and clinical characteristics could yield a greater than expected reduction in *M. tuberculosis* transmission in the United States.

Acknowledgments

We thank the state and local health departments who collect and report the TB data that were used for these analyses. We specifically thank Noah Schwartz for his helpful comments during manuscript preparation.

CDC's Division of Tuberculosis Elimination, National Center for HIV, Viral Hepatitis, STD, and Tuberculosis Prevention, provided funding support through employee salaries for this publication.

We used the large language model–based tool ChatGPT (OpenAI, https://openai.com) for limited editorial assistance (e.g., wording and formatting suggestions). All analyses, drafts of the manuscript, interpretations, figures, graphs, and final wording decisions were made by the authors.

About the Author

Mr. Kammerer is a health statistician at the Centers for Disease Control and Prevention in Atlanta. His primary research interests include tuberculosis molecular epidemiology and outbreak detection methods.

References

1. World Health Organization. Global tuberculosis report no. 978-92-4-010153-1. Geneva: The Organization; 2024.
2. Williams PM, Pratt RH, Walker WL, Price SF, Stewart RJ, Feng PI. Tuberculosis—United States, 2023. MMWR Morb Mortal Wkly Rep. 2024;73:265–70. https://doi.org/10.15585/mmwr.mm7312a4
3. LoBue PA, Mermin JH. Latent tuberculosis infection: the final frontier of tuberculosis elimination in the USA. Lancet Infect Dis. 2017;17:e327–33. https://doi.org/10.1016/S1473-3099(17)30248-7
4. Raz KM, Talarico S, Althomsons SP, Kammerer JS, Cowan LS, Haddad MB, et al. Molecular surveillance for large outbreaks of tuberculosis in the United States, 2014–2018. Tuberculosis (Edinb). 2022;136:102232. https://doi.org/10.1016/j.tube.2022.102232
5. Haddad MB, Mitruka K, Oeltmann JE, Johns EB, Navin TR. Characteristics of tuberculosis cases that started outbreaks in the United States, 2002–2011. Emerg Infect Dis. 2015;21:508–10. https://doi.org/10.3201/eid2103.141475
6. Stewart RJ, Raz KM, Burns SP, Kammerer JS, Haddad MB, Silk BJ, et al. Tuberculosis outbreaks in state prisons, United States, 2011–2019. Am J Public Health. 2022;112:1170–9. https://doi.org/10.2105/AJPH.2022.306864
7. Stalter RM, Pecha M, Dov L, Miller D, Ghazal Z, Wortham J, et al. Tuberculosis outbreak in a state prison system—

Washington, 2021–2022. MMWR Morb Mortal Wkly Rep. 2023;72:309–12. https://doi.org/10.15585/mmwr.mm7212a3
8. Groenweghe E, Swensson L, Winans KD, Griffin P, Haddad MB, Brostrom RJ, et al. Outbreak of multidrug-resistant tuberculosis—Kansas, 2021–2022. MMWR Morb Mortal Wkly Rep. 2023;72:957–60. https://doi.org/10.15585/mmwr.mm7235a4
9. Labuda SM, McDaniel CJ, Talwar A, Braumuller A, Parker S, McGaha S, et al. Tuberculosis outbreak associated with delayed diagnosis and long infectious periods in rural Arkansas, 2010–2018. Public Health Rep. 2022;137:94–101. https://doi.org/10.1177/0033354921999167
10. Mindra G, Wortham JM, Haddad MB, Powell KM. Tuberculosis outbreaks in the United States, 2009–2015. Public Health Rep. 2017;132:157–63. https://doi.org/10.1177/0033354916688270
11. Churchyard G, Kim P, Shah NS, Rustomjee R, Gandhi N, Mathema B, et al. What we know about tuberculosis transmission: an overview. J Infect Dis. 2017;216:S629–35. https://doi.org/10.1093/infdis/jix362
12. Mangione CM, Barry MJ, Nicholson WK, Cabana M, Chelmow D, Coker TR, et al.; US Preventive Services Task Force. Screening for latent tuberculosis infection in adults: US Preventive Services Task Force recommendation statement. JAMA. 2023;329:1487–94. https://doi.org/10.1001/jama.2023.4899
13. Cole B, Nilsen DM, Will L, Etkind SC, Burgos M, Chorba T. Essential components of a public health tuberculosis prevention, control, and elimination program: recommendations of the Advisory Council for the Elimination of Tuberculosis and the National Tuberculosis Controllers Association. MMWR Recomm Rep. 2020;69:1–27. https://doi.org/10.15585/mmwr.rr6907a1
14. Smith JP, Cohen T, Dowdy D, Shrestha S, Gandhi NR, Hill AN. Quantifying *Mycobacterium tuberculosis* transmission dynamics across global settings: a systematic analysis. Am J Epidemiol. 2023;192:133–45. https://doi.org/10.1093/aje/kwac181
15. Smith JP, Gandhi NR, Silk BJ, Cohen T, Lopman B, Raz K, et al. A cluster-based method to quantify individual heterogeneity in tuberculosis transmission. Epidemiology. 2022;33:217–27. https://doi.org/10.1097/EDE.0000000000001452
16. Shrestha S, Winglee K, Hill AN, Shaw T, Smith JP, Kammerer JS, et al. Model-based analysis of tuberculosis genotype clusters in the United States reveals high degree of heterogeneity in transmission and state-level differences across California, Florida, New York, and Texas. Clin Infect Dis. 2022;75:1433–41. https://doi.org/10.1093/cid/ciac121
17. Yuen CM, Kammerer JS, Marks K, Navin TR, France AM. Recent transmission of tuberculosis—United States, 2011–2014. PLoS One. 2016;11:e0153728. https://doi.org/10.1371/journal.pone.0153728
18. France AM, Grant J, Kammerer JS, Navin TR. A field-validated approach using surveillance and genotyping data to estimate tuberculosis attributable to recent transmission in the United States. Am J Epidemiol. 2015;182:799–807. https://doi.org/10.1093/aje/kwv121
19. Noppert GA, Yang Z, Clarke P, Davidson P, Ye W, Wilson ML. Contextualizing tuberculosis risk in time and space: comparing time-restricted genotypic case clusters and geospatial clusters to evaluate the relative contribution of recent transmission to incidence of TB using nine years of case data from Michigan, USA. Ann Epidemiol. 2019;40:21–27.e3. https://doi.org/10.1016/j.annepidem.2019.10.001
20. Mamiya H, Schwartzman K, Verma A, Jauvin C, Behr M, Buckeridge D. Towards probabilistic decision support in public health practice: predicting recent transmission of tuberculosis from patient attributes. J Biomed Inform. 2015;53:237–42. https://doi.org/10.1016/j.jbi.2014.11.006
21. Centers for Disease Control and Prevention. Reported tuberculosis in the United States, 2021 [cited 2025 Jul 7]. https://www.cdc.gov/tb/statistics/reports/2021/default.htm
22. Ypma RJ, Altes HK, van Soolingen D, Wallinga J, van Ballegooijen WM. A sign of superspreading in tuberculosis: highly skewed distribution of genotypic cluster sizes. Epidemiology. 2013;24:395–400. https://doi.org/10.1097/EDE.0b013e3182878e19
23. Stein RA. Super-spreaders in infectious diseases. Int J Infect Dis. 2011;15:e510–3. https://doi.org/10.1016/j.ijid.2010.06.020
24. Rodriguez CA, Li T, Self JL, Jenkins HE, Horsburgh CR, White LF. Genotyping indicates marked heterogeneity of tuberculosis transmission in the United States, 2009–2018. Epidemiol Infect. 2021;149:e215. https://doi.org/10.1017/S0950268821002041
25. Melsew YA, Gambhir M, Cheng AC, McBryde ES, Denholm JT, Tay EL, et al. The role of super-spreading events in *Mycobacterium tuberculosis* transmission: evidence from contact tracing. BMC Infect Dis. 2019;19:244. https://doi.org/10.1186/s12879-019-3870-1
26. Centers for Disease Control and Prevention; Agency for Toxic Substances and Disease Registry. CDC/ATSDR Social Vulnerability Index 2022 database [cited 2025 Jul 10]. https://www.atsdr.cdc.gov/placeandhealth/svi/data_documentation_download.html
27. Walker TM, Ip CL, Harrell RH, Evans JT, Kapatai G, Dedicoat MJ, et al. Whole-genome sequencing to delineate *Mycobacterium tuberculosis* outbreaks: a retrospective observational study. Lancet Infect Dis. 2013;13:137–46. https://doi.org/10.1016/S1473-3099(12)70277-3
28. Chawla NV, Bowyer KW, Hall LO, Kegelmeyer WP. SMOTE: Synthetic Minority Over-sampling Technique. J Artif Intell Res. 2002;16:321–57. https://doi.org/10.1613/jair.953
29. Borgdorff MW, Nagelkerke NJ, de Haas PE, van Soolingen D. Transmission of *Mycobacterium tuberculosis* depending on the age and sex of source cases. Am J Epidemiol. 2001;154:934–43. https://doi.org/10.1093/aje/154.10.934
30. Rodrigo T, Caylà JA, García de Olalla P, Galdós-Tangüis H, Jansà JM, Miranda P, et al. Characteristics of tuberculosis patients who generate secondary cases. Int J Tuberc Lung Dis. 1997;1:352–7.
31. Trevisi L, Brooks MB, Becerra MC, Calderón RI, Contreras CC, Galea JT, et al. Who transmits tuberculosis to whom: a cross-sectional analysis of a cohort study in Lima, Peru. Am J Respir Crit Care Med. 2024;210:222–33. https://doi.org/10.1164/rccm.202307-1217OC
32. Lau A, Barrie J, Winter C, Elamy AH, Tyrrell G, Long R. Chest radiographic patterns and the transmission of tuberculosis: implications for automated systems. PLoS One. 2016;11:e0154032. https://doi.org/10.1371/journal.pone.0154032
33. Asadi L, Croxen M, Heffernan C, Dhillon M, Paulsen C, Egedahl ML, et al. How much do smear-negative patients really contribute to tuberculosis transmissions? Re-examining an old question with new tools. EClinicalMedicine. 2022;43:101250. https://doi.org/10.1016/j.eclinm.2021.101250

34. Urbanowski ME, Ordonez AA, Ruiz-Bedoya CA, Jain SK, Bishai WR. Cavitary tuberculosis: the gateway of disease transmission. Lancet Infect Dis. 2020;20:e117–28. https://doi.org/10.1016/S1473-3099(20)30148-1
35. Shrestha S, Cilloni L, Asay GRB, Kammerer JS, Raz K, Shaw T, et al. Model-based analysis of impact, costs, and cost-effectiveness of tuberculosis outbreak investigations, United States. Emerg Infect Dis. 2025;31:497–506. https://doi.org/10.3201/eid3103.240633
36. Wallace RM, Kammerer JS, Iademarco MF, Althomsons SP, Winston CA, Navin TR. Increasing proportions of advanced pulmonary tuberculosis reported in the United States: are delays in diagnosis on the rise? Am J Respir Crit Care Med. 2009;180:1016–22. https://doi.org/10.1164/rccm.200901-0059OC
37. Simon AE, Fenelon A, Helms V, Lloyd PC, Rossen LM. HUD housing assistance associated with lower uninsurance rates and unmet medical need. Health Aff (Millwood). 2017;36:1016–23. https://doi.org/10.1377/hlthaff.2016.1152
38. Baker DW, Shapiro MF, Schur CL. Health insurance and access to care for symptomatic conditions. Arch Intern Med. 2000;160:1269–74. https://doi.org/10.1001/archinte.160.9.1269
39. Bakhsh Y, Readhead A, Flood J, Barry P. Association of area-based socioeconomic measures with tuberculosis incidence in California. J Immigr Minor Health. 2023;25:643–52. https://doi.org/10.1007/s10903-022-01424-7
40. Myers WP, Westenhouse JL, Flood J, Riley LW. An ecological study of tuberculosis transmission in California. Am J Public Health. 2006;96:685–90. https://doi.org/10.2105/AJPH.2004.048132
41. Althomsons SP, Winglee K, Heilig CM, Talarico S, Silk B, Wortham J, et al. Using machine learning techniques and national tuberculosis surveillance data to predict excess growth in genotyped tuberculosis clusters. Am J Epidemiol. 2022;191:1936–43. https://doi.org/10.1093/aje/kwac117
42. Smith JP, Milligan K, McCarthy KD, Mchembere W, Okeyo E, Musau SK, et al. Machine learning to predict bacteriologic confirmation of *Mycobacterium tuberculosis* in infants and very young children. PLOS Digit Health. 2023;2:e0000249. https://doi.org/10.1371/journal.pdig.0000249

Address for correspondence: Sarah Talarico, Centers for Disease Control and Prevention, 1600 Clifton Rd NE, Mailstop H24-3, Atlanta, GA 30329-4018, USA; email: mzi4@cdc.gov

Association of Frailty and Frailty Trajectory with Risk for Respiratory Infectious Diseases

Jin Yang,[1] Hao Yan,[1] Huan Chen, Dan Liu, Zhihao Li, Chen Mao

We explored the association between frailty and respiratory infectious diseases (RIDs) through a large cohort of 423,691 participants in the UK Biobank. Participants without baseline RIDs were assessed by physical frailty and frailty index. A total of 16,848 participants had repeated assessments. We divided participants into nonfrail, prefrail, and frail groups and categorized frailty changes as alleviation, maintenance, or aggravation. We estimated risk for RIDs, including influenza, pneumonia, and other acute lower respiratory infections. Compared with nonfrailty, prefrailty and frailty increased risk for RIDs 1.32–2.29 times. Each 0.1-point increase in frailty index per year raised risk for RIDs by 47%; each 1-point increase in physical frailty per year increased risk by 26%. Frailty worsening (e.g., aggravation of prefrailty) amplified risk by 2.31–4.16 times. Partial frailty improvement did not fully eliminate risk. Frailty is a modifiable, dynamic risk factor, underscoring the need for early frailty identification and intervention to reduce RIDs in high-risk populations.

Respiratory infectious diseases (RIDs) seriously affect human health (*1*,*2*). Before COVID-19, pneumonia and influenza were the primary fatal RIDs, particularly among the older adult population (*3*,*4*). Given the substantial burden of respiratory infections on health, identifying factors that contribute to reduced life expectancy related to RIDs is crucial for advancing public health.

Frailty is a clinical syndrome characterized by increased vulnerability caused by decreased physiologic reserves and functions of multiple physiologic systems (*5*,*6*). Two main approaches are used to assess frailty: the frailty phenotype and the deficit accumulation model (*7*,*8*). Growing evidence has demonstrated that frailty increases the risk for various adverse outcomes, including falls, Parkinson's disease, and death (*9*–*11*). Recent reviews have further highlighted frailty as a notable clinical and public health issue in older adults (*12*). Studies also have linked frailty to chronic obstructive pulmonary disease, asthma, and infectious diseases (*13*–*16*). However, previous studies on the relationship between frailty and RIDs have been limited by insufficient sample sizes, and evidence regarding the impact of frailty changes over time remains inconclusive. To address those gaps, we examined the associations of frailty and its long-term changes with risk for RIDs by leveraging data from a large UK cohort.

Author affiliations: School of Public Health, Southern Medical University, Guangzhou, China; National Institute of Health Data Science of China, Southern Medical University, Guangzhou

DOI: https://doi.org/10.3201/eid3206.251235

Methods

We conducted a population-based prospective cohort study by analyzing data from the UK Biobank (https://www.ukbiobank.ac.uk), which recruited ≈500,000 participants 37–73 years of age across England, Wales, and Scotland. Baseline data were collected during 2006–2010 through touchscreen questionnaires capturing self-reported characteristics, verbal interviews for medical history, standardized physical measurements, and biological sample collection. In addition, participant data were linked to electronic health records for longitudinal follow-up.

We assessed frailty by using a physical frailty (PF) phenotype and a frailty index (FI), and categorized persons as nonfrail, prefrail, or frail. We also ascertained incident RIDs from linked health records. From an initial cohort of 502,376 participants, we excluded persons with missing data on frailty variables (n = 1,988), prevalent (n = 56,977), missing follow-up or recruitment information (n = 10), or missing covariates (n = 19,710), resulting in an analytical cohort of 423,691 participants for baseline analysis. In the longitudinal analysis of frailty changes, we included a subset of 16,848 participants who had complete follow-up frailty assessments and did not have interim outcomes (Appendix Figure 1, https://wwwnc.cdc.gov/EID/article/32/6/25-1235-App1.pdf).

[1]These first authors contributed equally to this article.

Assessment of PF and FI

We used the Fried Frailty Phenotype assessment (*7*) to determine PF. In brief, the Fried model assesses 5 criteria: 3 self-reported components (unintended weight loss, fatigue, and low physical activity) and 2 objectively measured components (slow walking speed and reduced grip strength). We divided participants into 3 groups according to the number of Fried model criteria met: nonfrail (0 criteria), prefrail (1–2 criteria), or frail (≥3 criteria).

We used the FI developed by researchers using a population of 500,000 participants from the UK Biobank (*17*). In brief, we calculated FI from a set of 49 self-reported items covering health, diseases and disabilities, and mental well-being, according to standard protocol. For participants with <10 missing responses, we computed FI as the ratio of reported health or functional problems to the total number of possible items, yielding a score of 0–1. Finally, we classified participants as nonfrail (FI ≤0.12), prefrail (FI 0.12–0.24), or frail (FI >0.24). We applied those classifications to both baseline and follow-up assessments of PF and the FI.

Definitions of Outcomes

We defined study outcomes as the first occurrence of RIDs as classified in the International Classification of Diseases, 10th Revision (ICD-10). The primary outcome was a composite of influenza (ICD-10 codes J09–J11), pneumonia (ICD-10 codes J12–J18), and other acute lower respiratory tract infections (OALRTI; ICD-10 codes J20–J22). We also analyzed those conditions individually as secondary outcomes. We determined study outcomes by linking National Health Service (NHS) records, including hospital inpatient data and death registry records. Detailed information about the linkage process is available on UK Biobank.

Covariables

We considered the following potential confounders: age; sex (male or female); ethnicity (White or another race); education level (high, intermediate, or low); Townsend deprivation index (TDI); smoking status (never, former, or current); alcohol consumption status (never, former, or current); cumulative dietary risk factor score (continuous, ranging from 0 to 9 [most healthy to least healthy]); body mass index (BMI, kg/m^2) category (underweight BMI <18.5, normal weight BMI 18.5 to <25, overweight BMI 25 to <30, or obese BMI ≥30); sleep duration (continuous, hours/day); sleeplessness (never, sometimes, or usually); and daytime dozing (never, sometimes, or often). We also examined cofounders related to exposure to pollution, including exposure to particulate matter with an aerodynamic diameter of ≤2.5 μm ($PM_{2.5}$ exposure; continuous, μg/m^3), nitrogen dioxide (continuous, μg/m^3), and nitrogen oxide (continuous, μg/m^3) (Appendix Table 1).

Statistical Analysis

We calculated baseline and follow-up characteristics as mean (SD) or median (IQR) for continuous variables and as no. (%) for categorical variables, which we stratified by frailty status (nonfrail, prefrail, and frail). We used analysis of variance (ANOVA) or Kruskal-Wallis H test to compare differences for continuous variables and χ^2 test to compare categorical variables. The primary outcome was any first-recorded RIDs (composite of influenza, OALRTI, and pneumonia); we further analyzed each of the 3 constituent RIDs as a secondary outcome. We calculated time-to-event from the baseline or first follow-up date until the first RID event, death, or December 31, 2022, whichever occurred first. We used Kaplan-Meier curves to estimate cumulative incidence and compared results by using log-rank tests. We used Cox proportional hazards models to estimate the hazard ratio (HR) and 95% CI for the risk for RIDs and each secondary outcome.

We analyzed frailty both as a categorical variable and as a continuous variable using a 1-unit increment for PF and a 0.1-unit increment for FI score. Fully adjusted models further incorporated restricted cubic splines to evaluate potential nonlinear associations between sustained frailty and risk for RIDs. We considered and adjusted for potential confounders in multivariable models. Model 1 adjusted for age and sex, and model 2 further adjusted for full covariables.

Frailty Trajectories

We derived frailty trajectories by fitting a linear regression model for each participant and using the PF (range 0–5) or FI (range 0–1) score as the dependent variable and follow-up time as the independent variable. We calculated change in FI (ΔFI) or PF (ΔPF) in points per year, which represented a person's frailty trajectory. We defined the association between baseline and follow-up changes in frailty status and RIDs risk. We categorized long-term changes in frailty status as alleviation, maintenance, or aggravation, then included 7 study categories: nonfrailty maintenance, nonfrailty aggravation, prefrailty alleviation, prefrailty maintenance, prefrailty aggravation, frailty alleviation, and frailty maintenance. We used nonfrailty maintenance as the reference group. For ΔFI and ΔPF, values >0 indicated that the degree of frailty increased over time, a value of 0 indicated stable

degree of frailty, and values <0 indicated improvement in degree of frailty. Further, we calculated the population attributable risk for RIDs events to estimate the population-level risk associated with changes in frailty status.

Subgroup Analyses

For analyses, we stratified subgroups by age (<65 vs. ≥65 years) and sex. To address potential reverse causality, we performed a sensitivity analysis by excluding events occurring within the first 2 years of follow-up. Another sensitivity analysis excluded data after 2020 to mitigate the confounding effects of the COVID-19 pandemic. We further evaluated the association between frailty and cause-specific RIDs risk by using Fine-Gray competing risks regression models and treating all-cause mortality as a competing event (Appendix Table 2). We conducted 2-tailed analyses in R version 4.3.1 (The R Project for Statistical Computing, https://www.r-project.org) and considered p<0.05 statistically significant.

Results

Baseline Characteristics

The first assessment cohort included 423,691 persons with a mean age of 56.35 years; 45.5% were male and 54.5% were female (Table 1). In that assessment, we

Table 1. Baseline characteristics of participants in the first and final assessment of physical frailty in a study of association of frailty and frailty trajectory with risk for RIDs*

	First assessment				Final assessment			
Characteristics	Frail, n = 9,075	Prefrail, n = 144,734	Nonfrail, n = 269,882	p value†	Frail, n = 409	Prefrail, n = 8,350	Nonfrail, n = 8,089	p value†
Mean follow-up, y (SD)	12.29 (3.34)	13.02 (2.64)	13.37 (2.25)	<0.001	8.96 (2.33)	9.50 (1.59)	9.69 (1.44)	<0.001
Mean age, y (SD)	57.86 (7.63)	56.96 (8.08)	55.97 (8.09)	<0.001	62.40 (7.52)	62.10 (7.29)	60.36 (7.46)	<0.001
Sex				<0.001				<0.001
M	3,327 (36.7)	62,077 (42.9)	127,389 (47.2)		169 (41.3)	3,950 (47.3)	4,144 (51.2)	
F	5,748 (63.3)	82,657 (57.1)	142,493 (52.8)		240 (58.7)	4,400 (52.7)	3,945 (48.8)	
Ethnicity				<0.001				<0.001
White	7,793 (85.9)	133,415 (92.2)	259,028 (96.0)		389 (95.1)	8,122 (97.3)	7,927 (98.0)	
Another race	1,282 (14.1)	11,319 (7.8)	10,854 (4.0)		20 (4.9)	228 (2.7)	162 (2.0)	
Education				<0.001				<0.001
High	1,398 (15.4)	41,353 (28.6)	99,556 (36.9)		106 (25.9)	3,505 (42.0)	3,868 (47.8)	
Intermediate	4,061 (44.7)	73,466 (50.8)	135,111 (50.1)		219 (53.5)	4,056 (48.6)	3,688 (45.6)	
Low	3,616 (39.8)	29,915 (20.7)	35,215 (13.0)		84 (20.5)	789 (9.4)	533 (6.6)	
Smoking status				<0.001				<0.001
Never	4,229 (46.6)	76,799 (53.1)	154,029 (57.1)		209 (51.1)	4,909 (58.8)	4,944 (61.1)	
Previous	3,047 (33.6)	50,681 (35.0)	91,828 (34.0)		156 (38.1)	2,918 (34.9)	2,676 (33.1)	
Current	1,799 (19.8)	17,254 (11.9)	24,025 (8.9)		44 (10.8)	523 (6.3)	469 (5.8)	
Alcohol status				<0.001				<0.001
Never	1,060 (11.7)	8,211 (5.7)	8,440 (3.1)		30 (7.3)	320 (3.8)	220 (2.7)	
Previous	1,025 (11.3)	6,629 (4.6)	6,649 (2.5)		37 (9.0)	275 (3.3)	184 (2.3)	
Current	6,990 (77.0)	129,894 (89.7)	254,793 (94.4)		342 (83.6)	7,755 (92.9)	7,684 (95.0)	
Mean (SD) Townsend deprivation index	0.74 (3.59)	−0.93 (3.24)	−1.66 (2.88)	<0.001	−0.54 (3.44)	−1.91 (2.75)	−2.27 (2.53)	<0.001
Mean (SD) sleep duration, h/d	6.81 (2.22)	7.07 (1.37)	7.15 (1.08)	<0.001	6.97 (2.19)	7.22 (1.16)	7.21 (0.99)	<0.001
Mean (SD) cumulative dietary risk factor score	5.29 (1.45)	4.99 (1.42)	4.91 (1.38)	<0.001	5.29 (1.38)	4.88 (1.33)	4.87 (1.32)	<0.001
Mean (SD) $PM_{2.5}$, $\mu g/m^3$	10.34 (1.11)	10.07 (1.06)	9.93 (1.04)	<0.001	10.26 (1.13)	10.01 (1.06)	9.92 (1.02)	<0.001
Mean (SD) NO_2, $\mu g/m^3$	29.28 (7.69)	27.33 (7.64)	26.23 (7.56)	<0.001	28.02 (6.97)	26.35 (6.92)	25.71 (6.72)	<0.001
Mean (SD) NO, $\mu g/m^3$	48.91 (16.56)	45.24 (15.86)	43.19 (15.28)	<0.001	47.05 (14.94)	43.78 (14.63)	42.46 (13.87)	<0.001
BMI category‡				<0.001				<0.001
Underweight	62 (0.7)	758 (0.5)	1,184 (0.4)		3 (0.7)	36 (0.4)	46 (0.6)	
Normal weight	1,369 (15.1)	36,742 (25.4)	100,907 (37.4)		68 (16.8)	2,577 (31.1)	3,481 (43.6)	
Overweight	2,728 (30.1)	60,162 (41.6)	118,895 (44.1)		131 (32.4)	3,664 (44.2)	3,369 (42.2)	
Obese	4,916 (54.2)	47,072 (32.5)	48,896 (18.1)		202 (50.0)	2,013 (24.3)	1,096 (13.7)	
RIDs				<0.001				<0.001
N	6,882 (75.8)	125,900 (87.0)	246,801 (91.4)		337 (82.4)	7,695 (92.2)	7,627 (94.3)	
Y	2,193 (24.2)	18,834 (13.0)	23,081 (8.6)		72 (17.6)	655 (7.8)	462 (5.7)	

*Values are no. (%) except as indicated. Data are from UK Biobank (https://www.ukbiobank.ac.uk) during 2006–2010 for the first assessment and during 2012–2013 for the final assessment. BMI, body mass index; $PM_{2.5}$, particulate matter <2.5 μm; NO, nitrogen oxide; NO_2, nitrogen dioxide; RIDs, respiratory infectious diseases.
†Calculated by analysis of variance, Kruskal-Wallis H, or χ^2 test. p<0.05 considered statistically significant.
‡Underweight <18.5 kg/m^2; normal weight, 18.5 kg/m^2 to <25 kg/m^2; overweight, 25 kg/m^2 to <30 kg/m^2; obese, ≥30 kg/m^2.

classified 2.14% as frail and 34.16% prefrail over a mean follow-up period of 13.79 years (Table 1). The final assessment subcohort had a mean follow-up of 9.58 years and included 16,848 persons, 2.43% of whom were classified as frail and 49.56% as prefrail. Persons classified as frail were generally older, were more likely to be female, and had lower education levels. Frail persons also had higher prevalences of smoking, socioeconomic deprivation, adverse sleep patterns, poorer diet quality, and higher air pollution exposure and were more likely to be overweight or obese. Consistent with their risk profiles, frail participants had a markedly higher incidence of RIDs than nonfrail participants.

Overall, baseline patterns for FI were broadly consistent with those observed using PF, and we noted substantial concordance between the 2 measures in both the first and final assessments (Appendix Table 3, 4). The distribution of respiratory infection subtypes was similar across frailty groups, regardless of the assessment tool or time point (Appendix Figure 2). A comparison of participants with and without follow-up data revealed statistically significant but clinically modest differences, suggesting a low risk for meaningful selection bias (Appendix Table 5).

Incident RIDs HRs Associated with Frailty

During a mean follow-up of 13.79 years in the first assessment, a total of 44,108 cases of incident RIDs were recorded. In fully adjusted models, both frailty measures showed a dose-dependent increase in RID risk. For PF, adjusted HR for the prefrail group was 1.32 (95% CI 1.30–1.35) and for the frail group adjusted HR was 2.01 (95% CI 1.92–2.10). For FI, the corresponding HR for the prefrail group was 1.50 (95% CI 1.47–1.53) and for the frail group was 2.29 (95% CI 2.22–2.37) (Table 2).

We observed similar trends in the final assessment cohort. Mean follow-up was 9.58 years, during which 1,189 incident RIDs cases were reported. PF-based HR was 1.17 (95% CI 1.04–1.33) for prefrail group and 2.27 (95% CI 1.75–2.95) for the frail group. FI-based HR was 1.28 (95% CI 1.13–1.45) for the prefrail group and 2.59 (95% CI 2.10–3.19) for the frail group (Table 3). Kaplan-Meier and restricted cubic spline analyses further supported those associations (Appendix Figures 3–6).

Associations of Frailty Trajectory with RIDs

In the analysis of associations between FI trajectories and RIDs, we noted substantially higher risks among the maintained prefrailty (HR 1.39 [95% CI 1.20–1.61]), aggravation of prefrailty (HR 2.63 [1.95–3.55]), alleviation of frailty (HR 1.51 [1.09–2.11]), and maintained frailty (HR 2.55 [1.94–3.35]) subgroups. We also observed similar increases in risk in OALRTI and pneumonia, particularly in the aggravation of prefrailty and maintained frailty groups, where the risk increased by 2.55–2.92 times (Figure 1).

In the analysis of associations between PF trajectories and RIDs, we designated nonfrail as the reference group. For RIDs, we noted substantial increases in risk for the maintained prefrailty (HR 1.45 [95% CI 1.24–1.71]), aggravation of prefrailty (HR 2.31 [1.66–3.20]), and maintained frailty (HR 4.16 [2.65–6.52]) subgroups. We observed similar patterns for OALRTI and pneumonia (Figure 2).

Restricted cubic spline curves showed a statistically significant U-shaped relationship between frailty changes and RIDs risk (overall $p<0.0001$, nonlinearity $p<0.01$). Specifically, persons with deteriorating frailty trajectories (ΔFI or ΔPF >0) exhibited statistically significant and sharp increases in RIDs risk compared with those with stable frailty status (ΔFI or ΔPF = 0) (Figure 3).

Additional Analyses

We noted similar effects in subgroup analyses (Appendix Tables 6–9) as on the main results. Frailty showed a stronger association with the risk for incident RIDs in persons >65 years of age and in female populations. To avoid the possibility of reverse causation and effects of the COVID-19 pandemic on RIDs, we conducted sensitivity analyses that excluded cases with study outcomes ≤2 years of follow-up or cases that occurred after 2020 (Appendix Table 10). We also analyzed the relationship between frailty and deaths caused by RIDs in subgroups and noted slightly lower HR estimates in the competing risk model, but estimates remained robust (Appendix Table 11).

Discussion

In this large prospective cohort study, both baseline frailty and worsening frailty trajectories were associated with higher risk for RIDs. Those findings support frailty as a dynamic marker of vulnerability for identifying populations at elevated risk for RIDs.

Previous studies explored the relationship between frailty and some RIDs, proving that frailty was closely related to RIDs occurrences (*18*,*19*). For example, a recent systematic review and meta-analysis focused on patients ≥60 years of age with pneumonia found that frailty was common (incidence rate of 49%) and greatly increased risk for

death (odds ratio [OR] 3.51) and readmission (*20*). However, that study used a single point in time for frailty assessment, without considering the dynamic changes in frailty status. A prospective cohort study exploring the relationship between influenza and frailty found no association between influenza and frailty phenotype (OR 0.50) (*21*). However, that study had a small (n = 1,135) sample size and included persons ≥50 (median 67.5) years of age from the community, which might have underestimated the long-term association between frailty and influenza risk. That underestimation could result from potential underdetection of influenza cases, particularly milder or asymptomatic cases among frailer persons who might not have sought testing. Another study found that frailty was a predictive factor for poor recovery in patients ≥65 years of age hospitalized with acute respiratory diseases (OR 0.70–0.75) (*22*), but it only used data from the 2011–12, 2012–13, and 2013–14 influenza seasons, which limited the generalizability of the conclusions. In contrast, using a large sample size, long-term follow-up, and multidimensional assessments (PF and FI), our study revealed the independent associations of frailty and its changing trajectory on the risk for RIDs. For participants stratified by FI, prefrail persons had 1.50 times higher risk for RIDs and frail groups had 2.29 times higher risk

Table 2. Hazard ratios of incident RIDs in first assessment of association of frailty and frailty trajectory with risk for RIDs*

		Model 1		Model 2	
Category	Events/no. participants	HR (95% CI)	p value	HR (95% CI)	p value
Grouped by physical frailty					
Nonfrail	23,081/269,882	Referent		Referent	
Prefrail	18,834/144,734	1.51 (1.48–1.54)	<0.001	1.32 (1.30–1.35)	<0.001
Frail	2,193/9,075	2.93 (2.81–3.06)	<0.001	2.01 (1.92–2.10)	<0.001
Per 1-point increase		1.41 (1.39–1.42)	<0.001	1.26 (1.24–1.27)	<0.001
Grouped by frailty index					
Nonfrail	19,181/253,296	Referent		Referent	
Prefrail	19,014/144,591	1.68 (1.65–1.71)	<0.001	1.50 (1.47–1.53)	<0.001
Frail	5,913/25,804	3.02 (2.93–3.11)	<0.001	2.29 (2.22–2.37)	<0.001
Per 0.1-point increase		1.64 (1.62–1.66)	<0.001	1.47 (1.45–1.49)	<0.001
RID subgroups					
Influenza					
Grouped by physical frailty					
Nonfrail	1,209/269,882	Referent		Referent	
Prefrail	931/144,734	1.42 (1.30–1.55)	<0.001	1.30 (1.19–1.42)	<0.001
Frail	132/9,075	3.18 (2.65–3.80)	<0.001	2.44 (2.02–2.95)	<0.001
Per 1-point increase		1.39 (1.33–1.46)	<0.001	1.29 (1.23–1.36)	<0.001
Grouped by frailty index					
Nonfrail	1,054/253,296	Referent		Referent	
Prefrail	924/144,591	1.51 (1.38–1.65)	<0.001	1.41 (1.29–1.54)	<0.001
Frail	291/25,804	2.64 (2.31–3.00)	<0.001	2.19 (1.90–2.51)	<0.001
Per 0.1-point increase		1.52 (1.44–1.59)	<0.001	1.41 (1.34–1.49)	<0.001
OALRTI					
Grouped by physical frailty					
Nonfrail	13,070/269,882	Referent		Referent	
Prefrail	10,308/144,734	1.44 (1.40–1.48)	<0.001	1.27 (1.24–1.30)	<0.001
Frail	1,131/9,075	2.52 (2.37–2.68)	<0.001	1.78 (1.67–1.90)	<0.001
Per 1-point increase		1.34 (1.33–1.36)	<0.001	1.21 (1.19–1.23)	<0.001
Grouped by frailty index					
Nonfrail	10,595/253,296	Referent		Referent	
Prefrail	10,677/144,591	1.70 (1.66–1.75)	<0.001	1.54 (1.49–1.58)	<0.001
Frail	3,237/25,804	2.89 (2.78–3.01)	<0.001	2.26 (2.17–2.36)	<0.001
Per 0.1-point increase		1.62 (1.59–1.64)	<0.001	1.47 (1.44–1.49)	<0.001
Pneumonia					
Grouped by physical frailty					
Nonfrail	11,221/269,882	Referent		Referent	
Prefrail	10,204/144,734	1.66 (1.62–1.71)	<0.001	1.43 (1.39–1.47)	<0.001
Frail	1,370/9,075	3.70 (3.50–3.92)	<0.001	2.39 (2.25–2.53)	<0.001
Per 1-point increase		1.52 (1.50–1.54)	<0.001	1.34 (1.32–1.36)	<0.001
Grouped by frailty index					
Nonfrail	9,413/253,296	Referent		Referent	
Prefrail	9,940/144,591	1.73 (1.68–1.78)	<0.001	1.52 (1.47–1.56)	<0.001
Frail	3,442/25,804	3.39 (3.26–3.53)	<0.001	2.45 (2.35–2.56)	<0.001
Per 0.1-point increase		1.73 (1.70–1.76)	<0.001	1.51 (1.49–1.54)	<0.001

*Data from UK Biobank (https://www.ukbiobank.ac.uk) collected during 2006–2010. Model 1 is adjusted for age and sex; model 2 is adjusted for all covariates. HRs and 95% CIs were estimated using Cox proportional hazards models. A 2-sided p<0.05 was considered statistically significant. FI, frailty index; HR, hazard ratio; OALRTI, other acute lower respiratory tract infection; PF, physical frailty; RID, respiratory infectious disease.

Table 3. Hazard ratios of incident RIDs in final assessment of association of frailty and frailty trajectory with risk for RIDs*

Category	Events/no. participants	Model 1		Model 2	
		HR (95% CI)	p value	HR (95% CI)	p value
Grouped by physical frailty					
Nonfrail	462/8,089	Referent		Referent	
Prefrail	655/8,350	1.28 (1.14–1.45)	<0.001	1.17 (1.04–1.33)	0.011
Frail	72/409	3.04 (2.37–3.90)	<0.001	2.27 (1.75–2.95)	<0.001
Per 1-point increase		1.36 (1.27–1.46)	<0.001	1.25 (1.17–1.35)	<0.001
Grouped by frailty index					
Nonfrail	573/10,424	Referent		Referent	
Prefrail	495/5,794	1.44 (1.27–1.62)	<0.001	1.28 (1.13–1.45)	<0.001
Frail	121/630	3.31 (2.72–4.03)	<0.001	2.59 (2.10–3.19)	<0.001
Per 0.1-point increase		1.66 (1.53–1.80)	<0.001	1.48 (1.36–1.62)	<0.001
RID subgroups					
Influenza					
Grouped by physical frailty					
Nonfrail	9/8,089	Referent		Referent	
Prefrail	20/8,350	2.04 (0.92–4.50)	0.078	1.81 (0.81–4.05)	0.146
Frail	2/409	4.04 (0.87–18.81)	0.075	2.36 (0.45–12.47)	0.312
Per 1-point increase		1.38 (0.96–1.98)	0.079	1.20 (0.79–1.80)	0.382
Grouped by frailty index					
Nonfrail	18/10,424	Referent		Referent	
Prefrail	9/5,794	0.85 (0.38–1.91)	0.696	0.73 (0.32–1.65)	0.443
Frail	4/630	3.35 (1.12–9.98)	<0.05	2.09 (0.63–6.95)	0.228
Per 0.1-point increase		1.82 (1.15–2.90)	<0.05	1.53 (0.94–2.50)	0.087
OALRTI					
Grouped by physical frailty					
Nonfrail	242/8,089	Referent		Referent	
Prefrail	301/8,350	1.12 (0.94–1.33)	0.194	1.03 (0.86–1.22)	0.760
Frail	28/409	2.13 (1.44–3.16)	<0.001	1.64 (1.09–2.48)	<0.05
Per 1-point increase		1.22 (1.10–1.36)	<0.001	1.14 (1.02–1.27)	0.024
Grouped by frailty index					
Nonfrail	278/10,424	Referent		Referent	
Prefrail	233/5,794	1.40 (1.18–1.67)	<0.001	1.28 (1.07–1.53)	0.007
Frail	60/630	3.29 (2.49–4.36)	<0.001	2.77 (2.06–3.73)	<0.001
Per 0.1-point increase		1.63 (1.45–1.83)	<0.001	1.51 (1.32–1.71)	<0.001
Pneumonia					
Grouped by physical frailty					
Nonfrail	247/8,089	Referent		Referent	
Prefrail	408/8,350	1.47 (1.26–1.73)	<0.001	1.34 (1.14–1.58)	<0.001
Frail	53/409	4.12 (3.06–5.55)	<0.001	2.96 (2.16–4.05)	<0.001
Per 1-point increase		1.53 (1.40–1.67)	<0.001	1.39 (1.27–1.52)	<0.001
Grouped by frailty index					
Nonfrail	320/10,424	Referent		Referent	
Prefrail	312/5,794	1.58 (1.35–1.84)	<0.001	1.38 (1.17–1.62)	<0.001
Frail	76/630	3.53 (2.75–4.55)	<0.001	2.67 (2.04–3.50)	<0.001
Per 0.1-point increase		1.73 (1.56–1.92)	<0.001	1.52 (1.35–1.70)	<0.001

*Data from UK Biobank (https://www.ukbiobank.ac.uk) collected during 2012–2013. Model 1 is adjusted for age and sex; model 2 is adjusted for all covariates. HRs and 95% CIs were estimated using Cox proportional hazards models. A 2-sided p<0.05 was considered statistically significant. FI, frailty index; HR, hazard ratio; OALRTI, other acute lower respiratory tract infection; PF, physical frailty; RID, respiratory infectious disease.

compared with the nonfrail group. In the analysis of associations between FI trajectories and RIDs, risks substantially increased in the maintained prefrailty (HR 1.39), aggravation of prefrailty (HR 2.63), alleviation of frailty (HR 1.51), and maintained frailty (HR 2.55) groups. The results grouped according to PF were similar. Our study not only validated the role of frailty as a static risk factor but also quantified the cumulative effect of its dynamic changes on infection.

Previous studies have relied mainly on single point-of-time assessments of degeneration, failing to capture the dynamic evolution of degeneration and its cumulative biologic effects. Persons can gradually fall into a state of frailty, which can lead to adverse health outcomes, including cardiovascular disease, depression, and all-cause deaths (*23*–*25*). However, few studies have examined the relationship between dynamic changes in frailty and RIDs. Our study integrates longitudinal frailty trajectories and demonstrates that the maintenance or aggravation of frailty status can independently predict the long-term risk for RIDs.

Unlike previous research limited to static frailty assessments, our repeated measurements revealed

dynamic frailty patterns. Those findings emphasize that aggravation or maintenance of frailty were key predictors of RIDs risk, and that RIDs risk increased with worsening frailty trajectories. In addition, we found a U-shaped association between the annual rate of frailty progression (ΔFI or ΔPF) and susceptibility to RIDs, indicating that worsening frailty rapidly increases the risk for RIDs. Furthermore, we noted a higher risk for RIDs among participants whose frailty metrics improved.

Frailty is a multidimensional syndrome, in which a person's overall health status might not fully recover to nonfrailty levels, and certain subclinical states (such as chronic inflammation or metabolic disorders) might persist, resulting in a continued high risk for infection. We found that for every 0.1-point increase in FI per year, the risk for RIDs increased by 47%, and for every 1-point increase in PF per year, the risk increased by 26%. When conducting subgroup analyses, we found that for every 0.1-point increase in FI per year, the risk for influenza increased by 41%, OALRTI by 47%, and pneumonia by 51%; for every 1-point increase in PF per year, the risk for influenza increased by 29%, OALRTI by 21%, and pneumonia by 34%. The final assessment of frailty also showed similar outcomes. Those findings emphasize the value of continuous monitoring of frailty, especially in prefrail populations.

Several FI components, such as low physical activity and fatigue, are potential independent risk factors for respiratory infection and illness severity. However, frailty should not be viewed as a simple repetition of conventional epidemiologic risk factors because it reflects cumulative declines in physiologic reserve and multisystem dysregulation (*5*,*9*,*12*). In this study, we quantified vulnerability by using FI, which summarizes multidimensional health deficits; moreover, frailty is considered a distinct clinical syndrome rather than a synonym for underlying conditions or disability (*5*,*7*). Even after adjusting for major confounders including age, sex, education, deprivation, smoking, alcohol use, BMI, diet, sleep characteristics, and air pollution exposure, the association between frailty and RIDs remained evident, suggesting that frailty could capture integrated susceptibility beyond individual risk factors considered separately. At the same time, because some frailty components overlap with established infection-related risk factors, the independent causal

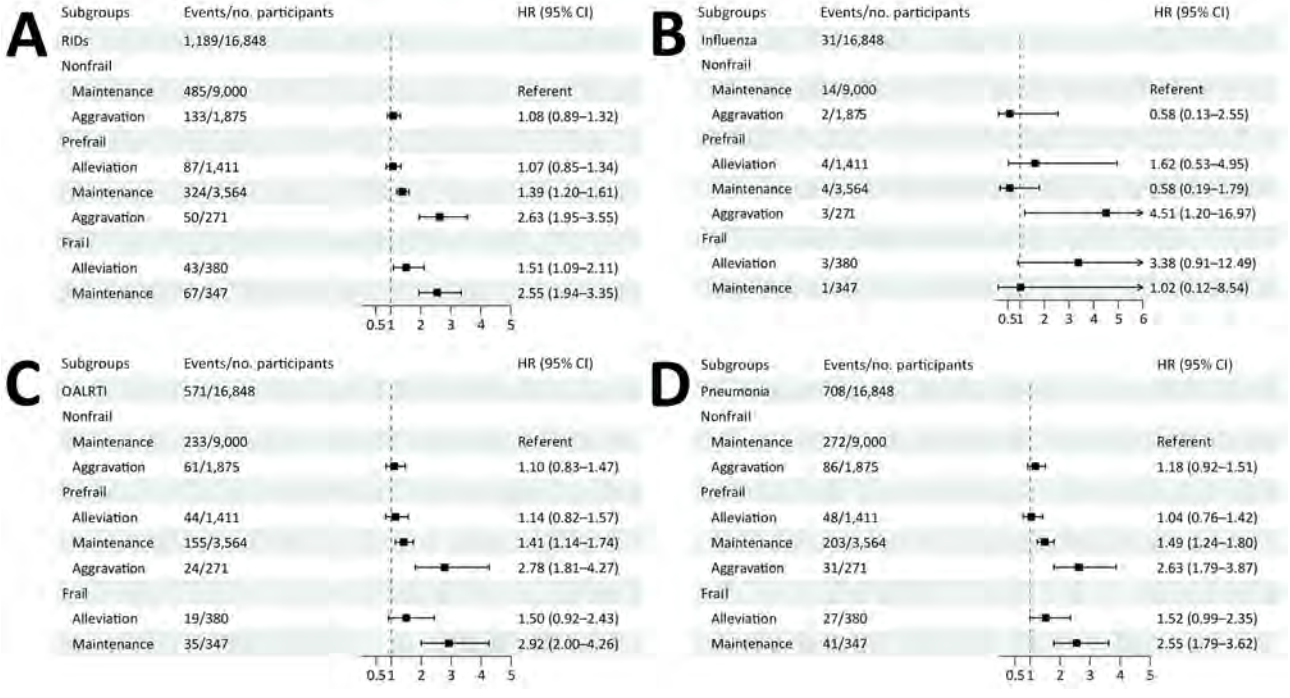

Figure 1. Longitudinal baseline and follow-up associations of frailty index with risk for RIDs. Forest plots show the trajectory of frailty index associated with incident RIDs (A), influenza (B), OALRTI (C), and pneumonia (D). Squares indicate point estimates of HRs; error bars indicate 95% CI; dotted vertical lines indicate null effect. Analyses were adjusted for age, sex, ethnicity, education level, Townsend deprivation index, smoking status, alcohol consumption status, cumulative dietary risk factor score, $PM_{2.5}$ (exposure to particulate matter <2.5 μm), nitrogen dioxide and nitrogen oxide levels, body mass index category, sleep duration, sleeplessness, and daytime dozing. HR, hazard ratio; OALRTI, other acute lower respiratory tract infection; RIDs, respiratory infectious diseases.

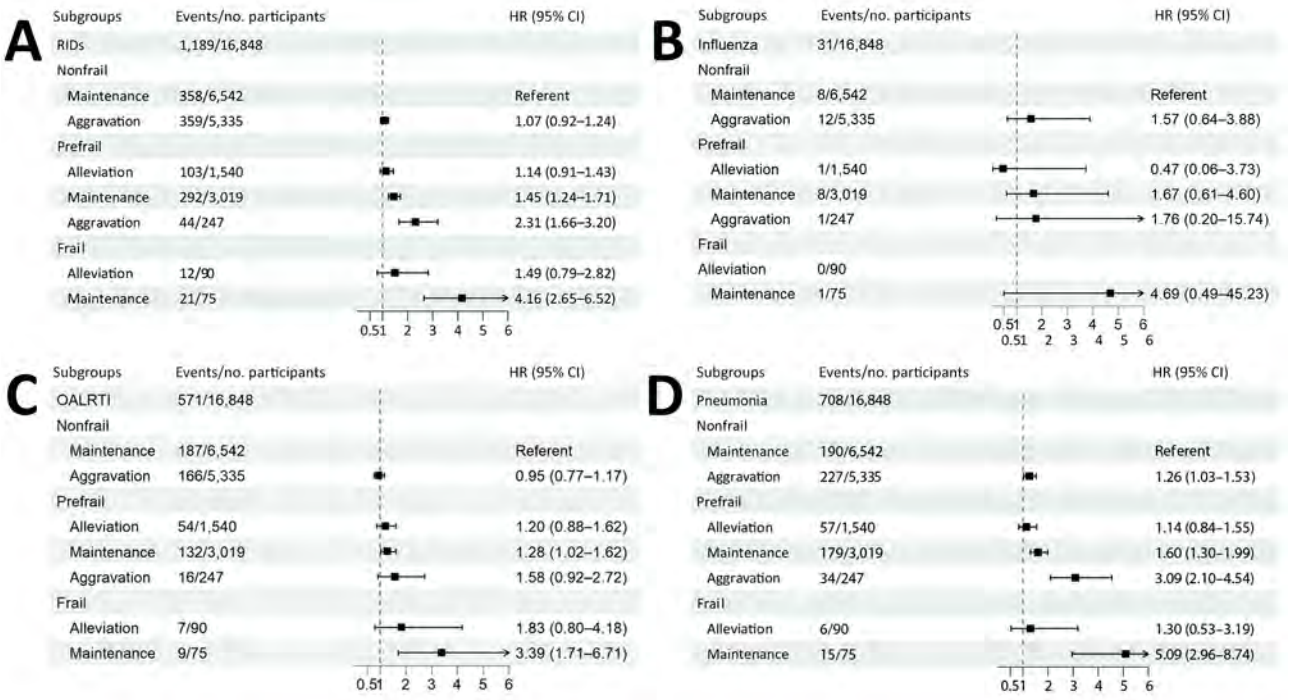

Figure 2. Longitudinal baseline and follow-up associations of physical frailty with risk for RIDs. Forest plots show the trajectory of physical frailty associated with incident RIDs (A), influenza (B), OALRTI (C), and pneumonia (D). Squares indicate point estimates of HRs; error bars indicate 95% CI; dotted vertical lines indicate null effect. Analyses were adjusted for age, sex, ethnicity, education level, Townsend deprivation index, smoking status, alcohol consumption status, cumulative dietary risk factor score, $PM_{2.5}$ (exposure to particulate matter <2.5 μm), nitrogen dioxide and nitrogen oxide levels, body mass index category, sleep duration, sleeplessness, and daytime dozing. HR, hazard ratio; OALRTI, other acute lower respiratory tract infection; RIDs, respiratory infectious diseases.

contribution of frailty itself could not be fully disentangled in this observational study.

Our research also found that participants ≥65 years of age have a higher risk for developing RIDs because of prefrailty and frailty compared with persons <65 years of age. Results of a previous study emphasized that frailty affects the susceptibility to and severity of pneumonia in persons ≥65 years of age (*26*), which is similar to our results.

Mounting evidence suggests that acute influenza infection could have long-lasting health effects, and studies have shown that frailty is associated with poor recovery after hospitalization for influenza (*22*,*27*). Our study also showed that frailty increases the risk of developing influenza by 119%–144% compared with nonfrailty. Those findings further support prioritizing vaccination-focused prevention among persons with frailty, particularly in resource-constrained settings where preventive interventions must be targeted efficiently.

Previous research has shown that frailty is associated with an increased risk for severe COVID-19 outcomes, including hospitalization or death (*28*). Our study extends those findings by showing that frailty was associated with a 1.29–2.20-fold increased risk for death from broader categories of RIDs.

Frailty is associated with an exacerbated inflammatory state, which can impair immune function and increase susceptibility to respiratory infections (*29*). In addition, persons with frailty might be more likely to experience malnutrition, swallowing difficulties, and other underlying conditions (*26*), which could contribute to their susceptibility to RIDs and support the need for nutritional and rehabilitation-based intervention as targets for future study.

Although some factors associated with frailty, such as smoking and alcohol use, can be modified at the patient level, frailty is also shaped by broader social and environmental determinants, including socioeconomic disadvantage and environmental exposures (*9*,*12*). Thus, frailty should not be interpreted as a condition that can be readily prevented through patient-level behavioral advice alone. Accordingly, future prevention efforts should consider broader public health and social policy measures, such as strengthening nutritional support and reducing exposure to harmful environments, and specific measures would depend on local resources and policy conditions.

From a public health perspective, our findings demonstrate that vulnerable populations are at high risk for respiratory infections, and vaccination should be considered for this population. Furthermore, measures such as nutritional support and physical rehabilitation could be potential intervention targets, and those approaches might be better suited for exploration in select high-risk subgroups or demonstration projects. In that sense, our findings are intended not to advocate the immediate broad rollout of all frailty-directed interventions but to provide an epidemiologic basis for risk stratification so that preventive resources, including vaccination and other supportive strategies, can be more rationally prioritized.

The strengths of this study included a prospective design, a large sample size, dual-dimensional frailty assessment using PF and FI, and dynamic change analysis. The first limitation of this study is that unmeasured variables, such as genetic susceptibility or undiagnosed underlying conditions, might have led to residual confounding. Second, the baseline age range of the cohort was 37–73 years, and most participants were White, which limited the generalizability of the results to the entire population. Third, recall bias might have affected some self-reported information, including parts of the PF assessment and all FI items. Fourth, outcomes on the basis of ICD coding might have underestimated mild or unreported RIDs outcomes. Fifth, the UK Biobank did not have records for influenza and pneumonia vaccine administration, making analysis between the role of vaccination in frailty and RIDs impossible. Sixth, our models did not incorporate season-specific effects, and relying on time to first respiratory infection as the primary outcome could underestimate the true frequency and cumulative burden of recurrent respiratory infections. Finally, although we analyzed the frailty trajectory through longitudinal modeling, the evaluation interval might not have captured short-term fluctuations in frailty status. Future research should incorporate more frequent measurements of frailty and explore the mediating biologic mechanisms between frailty and respiratory infections, such as chronic inflammation and immune dysregulation.

In summary, this study provides strong evidence that baseline and dynamic frailty substantially increase the risk for RIDs. Our findings advocate for the inclusion of frailty screening as a preventive strategy for respiratory infections, especially in persons ≥65 years of age.

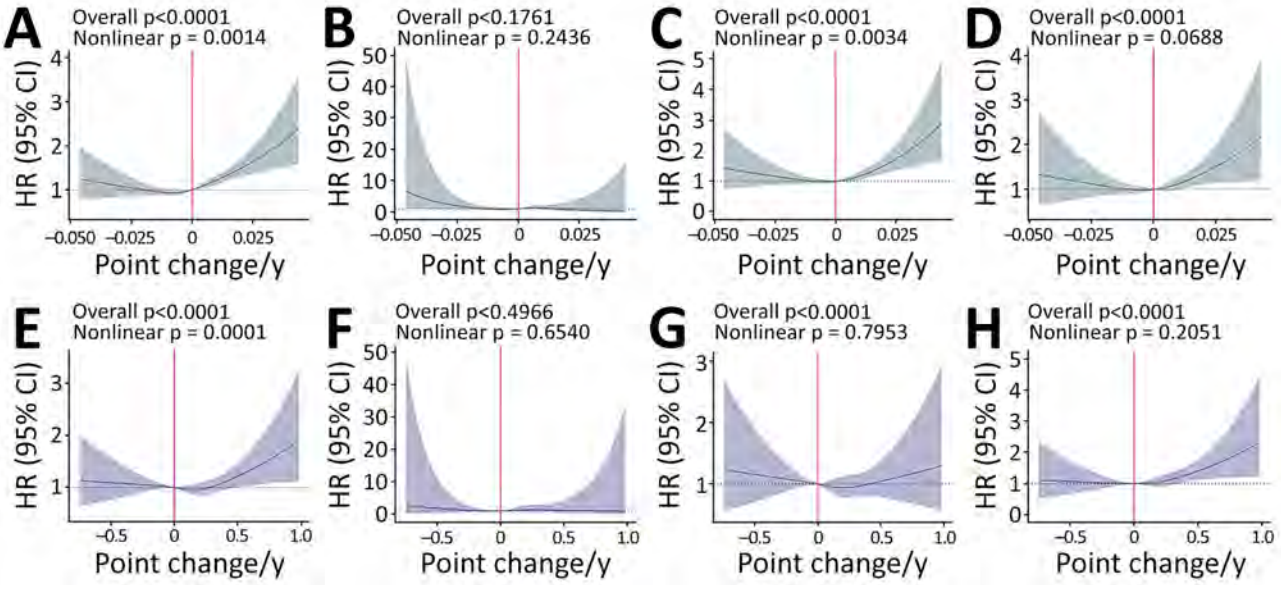

Figure 3. Restricted cubic spline curves from linear regression analysis of frailty changes associated with risk for respiratory infectious diseases. A–D) Dose-response relationships of change in frailty index associated with incident respiratory infectious diseases (A), influenza (B), other acute lower respiratory tract infection (C), and pneumonia (D). E–H) Dose-response relationships of change in physical frailty associated with incident respiratory infectious diseases (E), influenza (F), other acute lower respiratory tract infection (G), and pneumonia (H). Blue lines indicate fitted HR curves; shading indicates 95% CI; horizontal dotted lines indicate HR of 1; vertical lines indicate 0 change. Analyses were adjusted for age, sex, ethnicity, education level, Townsend deprivation index, smoking status, alcohol consumption status, cumulative dietary risk factor score, $PM_{2.5}$ (exposure to particulate matter <2.5 μm), nitrogen dioxide and nitrogen oxide levels, body mass index category, sleep duration, sleeplessness, and daytime dozing. HR, hazard ratio.

Acknowledgments

We thank the UK Biobank participants.

This research was conducted using the UK Biobank resource under application no. 43795. The UK Biobank study was approved by the North West Multi-centre Research Ethics Committee, the England and Wales Patient Information Advisory Group, and the Scottish Community Health Index Advisory Group. All participants provided written informed consent before enrollment in the UK Biobank. This study received approval from the North West Multicenter Research Ethics Committee (approval no. 11/NW/0382). This study was conducted using existing data from UK Biobank, a large-scale biomedical database that does not allow researchers to contact participants directly. Data are available from UK Biobank upon request (https://www.ukbiobank.ac.uk).

This work was supported by the National Natural Science Foundation of China (grant no. 82425052), and the Construction of High-level University of Guangdong (grant no. G624330242).

About the Author

Dr. Yang is currently a postdoctoral fellow in the School of Public Health, Southern Medical University, Guangzhou, China. Her research interests include respiratory infectious disease epidemiology.

References

1. Bourouiba L. Fluid dynamics of respiratory infectious diseases. Annu Rev Biomed Eng. 2021;23:547–77. https://doi.org/10.1146/annurev-bioeng-111820-025044
2. GBD 2021 Lower Respiratory Infections and Antimicrobial Resistance Collaborators. Global, regional, and national incidence and mortality burden of non–COVID-19 lower respiratory infections and aetiologies, 1990–2021: a systematic analysis from the Global Burden of Disease Study 2021. Lancet Infect Dis. 2024;24:974–1002. https://doi.org/10.1016/S1473-3099(24)00176-2
3. Rafeq R, Igneri LA. Infectious pulmonary diseases. Infect Dis Clin North Am. 2024;38:1–17. https://doi.org/10.1016/j.idc.2023.12.006
4. Uyeki TM. Influenza. Ann Intern Med. 2021;174:ITC161–76. https://doi.org/10.7326/AITC202111160
5. Clegg A, Young J, Iliffe S, Rikkert MO, Rockwood K. Frailty in elderly people. Lancet. 2013;381:752–62. https://doi.org/10.1016/S0140-6736(12)62167-9
6. Ofori-Asenso R, Chin KL, Mazidi M, Zomer E, Ilomaki J, Zullo AR, et al. Global incidence of frailty and prefrailty among community-dwelling older adults: a systematic review and meta-analysis. JAMA Netw Open. 2019; 2: e198398. https://doi.org/10.1001/jamanetworkopen.2019.8398
7. Fried LP, Tangen CM, Walston J, Newman AB, Hirsch C, Gottdiener J, et al.; Cardiovascular Health Study Collaborative Research Group. Frailty in older adults: evidence for a phenotype. J Gerontol A Biol Sci Med Sci. 2001; 56:M146–57. https://doi.org/10.1093/gerona/56.3.M146
8. Rockwood K, Stadnyk K, MacKnight C, McDowell I, Hébert R, Hogan DB. A brief clinical instrument to classify frailty in elderly people. Lancet. 1999;353:205–6. https://doi.org/10.1016/S0140-6736(98)04402-X
9. Hoogendijk EO, Afilalo J, Ensrud KE, Kowal P, Onder G, Fried LP. Frailty: implications for clinical practice and public health. Lancet. 2019;394:1365–75. https://doi.org/10.1016/S0140-6736(19)31786-6
10. Ward DD, Ranson JM, Wallace LMK, Llewellyn DJ, Rockwood K. Frailty, lifestyle, genetics and dementia risk. J Neurol Neurosurg Psychiatry. 2022;93:343–50. https://doi.org/10.1136/jnnp-2021-327396
11. Zheng Z, Lv Y, Rong S, Sun T, Chen L. Physical frailty, genetic predisposition, and incident Parkinson disease. JAMA Neurol. 2023;80:455–61. https://doi.org/10.1001/jamaneurol.2023.0183
12. Kim DH, Rockwood K. Frailty in older adults. N Engl J Med. 2024;391:538–48. https://doi.org/10.1056/NEJMra2301292
13. Hanlon P, Nicholl BI, Jani BD, Lee D, McQueenie R, Mair FS. Frailty and pre-frailty in middle-aged and older adults and its association with multimorbidity and mortality: a prospective analysis of 493 737 UK Biobank participants. Lancet Public Health. 2018;3:e323–32. https://doi.org/10.1016/S2468-2667(18)30091-4
14. Wang L, Zhang X, Liu X. Prevalence and clinical impact of frailty in COPD: a systematic review and meta-analysis. BMC Pulm Med. 2023;23:164. https://doi.org/10.1186/s12890-023-02454-z
15. Wang X, Wen J, Gu S, Zhang L, Qi X. Frailty in asthma-COPD overlap: a cross-sectional study of association and risk factors in the NHANES database. BMJ Open Respir Res. 2023;10:e001713. https://doi.org/10.1136/bmjresp-2023-001713
16. Yang Y, Che K, Deng J, Tang X, Jing W, He X, et al. Assessing the impact of frailty on infection risk in older adults: prospective observational cohort study. JMIR Public Health Surveill. 2024;10:e59762. https://doi.org/10.2196/59762
17. Williams DM, Jylhävä J, Pedersen NL, Hägg S. A frailty index for UK Biobank participants. J Gerontol A Biol Sci Med Sci. 2019;74:582–7. https://doi.org/10.1093/gerona/gly094
18. Huang S, Wang Y, Chen L, Chen X. Use of a frailty index based upon routine laboratory data to predict complication and mortality in older community-acquired pneumonia patients. Arch Gerontol Geriatr. 2022;101:104692. https://doi.org/10.1016/j.archger.2022.104692
19. Luo J, Tang W, Sun Y, Jiang C. Impact of frailty on 30-day and 1-year mortality in hospitalised elderly patients with community-acquired pneumonia: a prospective observational study. BMJ Open. 2020;10:e038370. https://doi.org/10.1136/bmjopen-2020-038370
20. Yang Y, Zhong Y. Impact of frailty on pneumonia outcomes in older patients: a systematic review and meta-analysis. Eur Geriatr Med. 2024;15:881–91. https://doi.org/10.1007/s41999-024-00974-3
21. Takahashi P, Wi CI, Ryu E, King K, Hickman J, Pignolo R, et al. Influenza infection is not associated with phenotypical frailty in older patients, a prospective cohort study. Health Sci Rep. 2022;5:e750. https://doi.org/10.1002/hsr2.750
22. Lees C, Godin J, McElhaney JE, McNeil SA, Loeb M, Hatchette TF, et al. Frailty hinders recovery from influenza and acute respiratory illness in older adults. J Infect Dis. 2020;222:428–37. https://doi.org/10.1093/infdis/jiaa092
23. Quach J, Kehler DS, Giacomantonio N, McArthur C, Blanchard C, Firth W, et al. Association of admission frailty and frailty changes during cardiac rehabilitation with

5-year outcomes. Eur J Prev Cardiol. 2023;30:807–19. https://doi.org/10.1093/eurjpc/zwad048
24. Sang N, Liu RC, Zhang MH, Lu ZX, Wu ZG, Zhang MY, et al. Changes in frailty and depressive symptoms among middle-aged and older Chinese people: a nationwide cohort study. BMC Public Health. 2024;24:301. https://doi.org/10.1186/s12889-024-17824-3
25. Shi SM, Olivieri-Mui B, McCarthy EP, Kim DH. Changes in a frailty index and association with mortality. J Am Geriatr Soc. 2021;69:1057–62. https://doi.org/10.1111/jgs.17002
26. Iwai-Saito K, Shobugawa Y, Aida J, Kondo K. Frailty is associated with susceptibility and severity of pneumonia in older adults (a JAGES multilevel cross-sectional study). Sci Rep. 2021;11:7966. https://doi.org/10.1038/s41598-021-86854-3
27. Iwai-Saito K, Sato K, Aida J, Kondo K. Association of frailty with influenza and hospitalization due to influenza among independent older adults: a longitudinal study of Japan Gerontological Evaluation Study (JAGES). BMC Geriatr. 2023;23:249. https://doi.org/10.1186/s12877-023-03979-y
28. Petermann-Rocha F, Hanlon P, Gray SR, Welsh P, Gill JMR, Foster H, et al. Comparison of two different frailty measurements and risk of hospitalisation or death from COVID-19: findings from UK Biobank. BMC Med. 2020;18:355. https://doi.org/10.1186/s12916-020-01822-4
29. Yao X, Li H, Leng SX. Inflammation and immune system alterations in frailty. Clin Geriatr Med. 2011;27:79–87. https://doi.org/10.1016/j.cger.2010.08.002

Address for correspondence: Chen Mao, Department of Epidemiology, School of Public Health, Southern Medical University, 1838 Guangzhou Ave N, Baiyun District, Guangzhou 510515, China; email: maochen9@smu.edu.cn

Antimicrobial-Resistant *Neisseria gonorrhoeae* of Public Health Concern, New South Wales, Australia, 2022–2024

Liz J. Walker,[1] Sebastiaan J. Van Hal,[1] Cecilia Li, Steven J. Nigro, Ellen Donnan, Nathan Ryder, Monica Lahra,[2] Janaki Amin[2]

Antimicrobial-resistant *Neisseria gonorrhoeae* poses a serious public health threat. In Australia, *N. gonorrhoeae* isolates with ceftriaxone MICs ≥0.125 mg/L or azithromycin MICs ≥256 mg/L required follow-up by public health officials. Odds of culture-positive notifications meeting those criteria increased from 2017–2019 (n = 11) to 2022–2024 (n = 94) (odds ratio 8.58 [95% CI 4.81–17.0]). Local acquisition was frequent (78.7%). Isolates with decreased ceftriaxone susceptibility were more common in female and heterosexual patients than were isolates with high-level azithromycin resistance. We identified 9 genomically linked clusters (≤15 single-nucleotide polymorphisms), 3 with sizable clonal expansion. Initial test of cure was negative for 81/94 (86.2%) 2022–2024 cases; of the rest, 9 cases had no follow-up visits, 2 were reinfected, and 2 failed initial treatment. Improving follow-up and reporting of treatment failure would strengthen case management protocols. Culture-based diagnostics remain essential to detect antimicrobial resistance, inform surveillance, and curb the rising resistance trend.

Escalating antimicrobial resistance (AMR) in *Neisseria gonorrhoeae* poses a serious public health threat, undermining treatment and disease control strategies globally. In Australia, national sexually transmitted infection (STI) management guidelines recommend collection of gonococcal culture samples from all infected sites before antimicrobial treatment is initiated (*1*). The current recommended antimicrobial treatment for uncomplicated urogenital and anorectal gonorrhea is dual therapy, comprising ceftriaxone (500 mg intramuscular injection) and oral azithromycin (1 g; 2 g if oropharyngeal infection) (*1*).

New South Wales (NSW), the most populous state in Australia, includes the city of Sydney with its ≈8 million residents. NSW has a robust passive gonococcal surveillance program that routinely performs antimicrobial susceptibility testing (AST) on all cultured gonococcal isolates collected across broad clinical settings, including sexual health clinics, general practices, and hospitals. Cultured isolates that have undergone AST represent ≈27.0% of all gonorrhea notifications in the state and were obtained from a diverse range of persons. In other surveillance programs, collection of gonococcal isolates can be limited by use of quotas, sentinel sites, and designated collection periods each year (*2*–*6*).

NSW's comprehensive surveillance program makes it a key contributor to national monitoring. In 2024, the national proportion of gonococcal isolates with decreased susceptibility (DS) (MIC ≥0.125 mg/L) to ceftriaxone was 0.5% (55/10,702), representing a substantial increase from 2023 (0.2% 22/10,105); of the 2024 isolates, 40% (22/55) were reported from NSW (*7*). Similarly, gonococci with azithromycin high-level resistance (HLR) have shown increasing numbers: 9 notifications in 2022, 27 in 2023, and 46 in 2024; most (26/46 [57%]) of those isolates were from NSW (*7*).

Author affiliations: NSW Health, St. Leonards, New South Wales, Australia (L.J. Walker, C. Li, S.J. Nigro, E. Donnan, N. Ryder, J. Amin); Royal Prince Alfred Hospital, Sydney, New South Wales, Australia (S.J. van Hal); The University of Sydney Central Clinical School, Sydney (S.J. van Hal); The University of Sydney Institute for Infectious Diseases, Sydney (E. Donnan); Prince of Wales Hospital and Community Health Services, Randwick, New South Wales, Australia (M.M. Lahra); University of New South Wales, Sydney (M.M. Lahra); Macquarie University, Sydney (J. Amin)

DOI: https://doi.org/10.3201/eid3206.251399

[1]These first authors contributed equally to this article.

[2]These joint senior authors contributed equally to this article.

The increasing reports of gonococci resistance, particularly in NSW, underscore the need for enhanced knowledge in local epidemiology and transmission networks. We conducted a retrospective observational study integrating AMR data, case investigations, and genomic analyses to provide a comprehensive picture of antimicrobial-resistant gonorrhea of public health concern in NSW. Drawing on intelligence about introduced and locally circulating strains across population groups, this study aimed to provide evidence to support updates to gonorrhea treatment guidelines and strengthen public health response procedures.

Methods

Gonococcal Surveillance Program

In NSW, gonorrhea is a notifiable condition under the Public Health Act 2010; confirmed cases require detection of *N. gonorrhoeae* by nucleic acid amplification test (NAAT), isolation by culture, or both. All cultured isolates are referred to the World Health Organization (WHO) Collaborating Centre for Sexually Transmitted Infections and Antimicrobial Resistance at the NSW Health Pathology Laboratory (Randwick, NSW, Australia) for confirmation of identification and AST. We performed AST using Etest gradient diffusion strips (bioMérieux, https://www.biomerieux.com) to determine MIC values reported in accordance with Clinical and Laboratory Standards Institute breakpoints (*8*) *N. gonorrhoeae* isolates with ceftriaxone DS (MIC ≥0.125 mg/L) or azithromycin HLR (MIC ≥256 mg/L) or both are designated as being of public health concern (PHC) and prompt a public health response (*9*). The managing clinician is responsible for patient recall, treatment, provision of enhanced surveillance data, and contact tracing (*10*). The contact tracing lookback period is 2 months before symptom onset or before date of diagnosis for asymptomatic patients. Clinicians are advised to recall the patient for test of cure (TOC) by NAAT, collecting a swab from each site of infection (genitourinary, rectal, pharyngeal) 2 weeks after treatment completion to detect treatment failure, emerging resistance, or reinfection.

Twelve public and private laboratories support gonorrhea surveillance by providing aggregate annual gonorrhea testing data from NAAT and culture. Those laboratories are estimated to account for 88.0% of all gonorrhea testing in NSW, ensuring comprehensive monitoring of diagnostic activity across the state.

Case Identification and Statistical Analysis

We extracted cases of antimicrobial-resistant gonorrhea of PHC notified during January 1, 2022–December 31, 2024, from the NSW Notifiable Conditions and Information Management System (NCIMS). We also extracted historic notifications for chlamydia, gonorrhea, and syphilis that shared the unique person identifier with an AMR notification. We derived sexual risk group from sex at birth and reported sexual exposures during the exposure period; we classified cases in men who reported sex with men only as men who have sex with men (MSM), cases in men who reported sex with both sexes as bisexual, and cases in men and women who reported sex only with the opposite sex as heterosexual. We categorized country of acquisition of infection in accordance with WHO region (*11*). To examine changes in notification patterns over time, we compared data for 2017–2019 (pre–COVID-19 pandemic) and 2022–2024 (post–COVID-19 pandemic). We compared the characteristics of notifications identified as ceftriaxone DS with notifications of azithromycin HLR. We used Fisher exact and Wilcoxon rank-sum test to test significance of comparisons; we chose a 2-sided α of $p<0.05$ as the threshold for statistical significance. We analyzed epidemiologic data using R version 4.4.1 (The R Project for Statistical Computing, https://www.r-project.org), ggplot version 3.5.1 (https://github.com/tidyverse/ggplot2), and gtsummary version 2.0.2 (https://github.com/ddsjoberg/gtsummary).

Whole-Genome Sequencing

We sent all isolates of PHC for whole-genome sequencing (WGS) using an Illumina platform (https://www.illumina.com) at NSW Health Pathology (Camperdown, NSW, Australia). We used the constructed assemblies to define AMR genes and multilocus sequence types (ST) (*12*). We excluded 1 isolate that did not meet quality metrics. We conducted a network analysis of the mapped single nucleotide matrix against reference isolate FA1090 (GenBank accession no. NC_002964.2) using the R packages tidygraph version 1.3.1 (https://github.com/thomasp85/tidygraph) and ggraph version 2.2.1 (https://github.com/thomasp85/ggraph) to explore associations between isolates using a single-nucleotide polymorphism maximum threshold of 15.

Ethics approval for this investigation was not required because it was undertaken for purposes under the provisions of the Public Health Act 2010 as part of routine public health surveillance and reporting under the governance of Health Protection NSW. No additional data were collected for the purpose of this report, and no personal identifiable data were included. We managed data in accordance with the National Health and Medical Research Council's

Ethical Considerations in Quality Assurance and Evaluation Activities (*13*).

Results

During 2022–2024, gonorrhea notifications increased 36.5%, from 10,288 to 14,045, whereas gonorrhea testing increased 13.1% from 775,161 to 876,447 (Table 1). The percentage of gonorrhea notifications accompanied by positive culture remained relatively stable at 27.0%, with a slight predominance in male (28.1%) versus female (22.6%) patients. Of the 9,941 culture-positive notifications, 94 (0.9%) met the definition of PHC, an overall increase from 0.5% to 1.3%, although the trend was not linear (Table 1). For comparison, in the prepandemic period before the study (2017–2019), such notifications were rare; 11 were reported, 4 of ceftriaxone DS and 7 azithromycin HLR (Table 2). The rise to 1.3% cases of PHC was accompanied by a markedly higher likelihood that culture-positive gonorrhea notifications in 2022–2024 met the definition for an AMR notification of PHC, compared with those from 2017–2019 (odds ratio 8.58, 95% CI 4.81–17.0; p<0.001). No cases of combined resistance (ceftriaxone DS and azithromycin HLR) were notified in the study period.

Case Characteristics

Most (74/94 [78.7%] cases) of the notifications of antimicrobial-resistant gonorrhea of PHC were acquired in Australia (Figure 1). Of those, 40 were notified in 2024. The remaining cases were acquired overseas from countries in the Western Pacific (n = 9), the Americas (n = 6), Europe (n = 3), and Africa (n = 1) WHO regions.

Case Comparison by AMR Profile

We detected notable differences between the ceftriaxone DS and azithromycin HLR groups (Table 3). The ceftriaxone DS group had a greater percentage of female patients (31.5% vs. 2.5%; p<0.001) and persons who reported heterosexual exposures (72.2% vs. 5.0%, p<0.001), compared with the azithromycin HLR group. Most cases acquired their infection in Australia (85.2%); however, overseas acquisition, when reported, occurred exclusively in the Western Pacific region (13.0%). Cases were evenly distributed between sexual health clinics (51.9%) and general practice (40.7%); the remaining 7.4% were diagnosed in hospitals.

In contrast, case-patients with azithromycin HLR were predominantly male (97.5% vs. 68.5% cases with ceftriaxone DS; p<0.001) and reported sexual exposures with men only (MSM) (87.5% vs. 25.9%; p<0.001). Previous STIs were more common in this group (70.0% vs. 35.2%; p<0.002), and of persons with a previous STI, the median was 4 versus 2 infections for ceftriaxone DS (p = 0.11). Infection site distribution also differed between those with azithromycin HLR and ceftriaxone DS (p<0.001). Azithromycin HLR cases were more evenly distributed across infection sites: rectal (37.5%), genitourinary tract (35.0%,) and pharynx (20.0%), whereas the genitourinary tract was most common (81.5%) in the ceftriaxone DS group, followed by pharynx (7.4%), rectal (5.6%), and eye (1.9%) specimens. Source of infection was predominantly within Australia (70.0%); however, overseas acquisition also occurred across multiple WHO regions: Europe (n = 6), the Americas (n = 3), Africa (n = 1), and the Western Pacific (n = 1). Where known, the median number of partners across the lookback period was 5 for the azithromycin HLR group versus 1 for the ceftriaxone DS group (p<0.001). Sexual-health clinics diagnosed 85.0% of cases.

Outcome of initial TOC did not differ between the ceftriaxone DS and azithromycin HLR groups; most returned a NAAT-negative result ≥2 weeks after

Table 1. Tests and notifications of *Neisseria gonorrhoeae*, New South Wales, Australia, 2022–2024*

Characteristic	No. (%)			
	2022	2023	2024	Total
All positive and negative test results†	775,161 (100)	868,741 (112.1)‡	876,447 (113.1)‡	2,520,349 (NA)
All *N. gonorrhoeae* notifications§	10,288 (100.0)	12,453 (100.0)	14,045 (100.0)	36,786 (100.0)
F	2,066 (20.1)	2,651 (21.3)	2,789 (19.9)	7,506 (20.4)
M	8,194 (79.6)	9,759 (78.4)	11,216 (79.9)	29,169 (79.3)
N. gonorrhoeae notifications with positive culture§¶	2,734 (26.6)	3,558 (28.6)	3,649 (26.0)	9,941 (27.0)
F	455 (22.0)	631 (23.8)	609 (21.8)	1,695 (22.6)
M	2,267 (27.7)	2,914 (29.9)	3,028 (27.0)	8,209 (28.1)
N. gonorrhoeae AMR notifications of PHC#	29 (1.1)	17 (0.5)	48 (1.3)	94 (0.9)
F	6 (1.3)	3 (0.5)	9 (1.5)	18 (1.1)
M	23 (1.0)	14 (0.5)	39 (1.3)	76 (0.9)

*AMR, antimicrobial resistance; NA, not applicable; PHC, public health concern.
†Aggregate gonorrhea test results by nucleic acid amplification test and culture from 12 laboratories. Those laboratories account for an estimated 88.0% of all gonorrhea testing in New South Wales.
‡Percentage calculated from baseline tests in 2022.
§Includes persons whose sex was not reported.
¶Percentage calculated from all *N. gonorrhoeae* notifications.
#Percentage calculated from *N. gonorrhoeae* culture notifications.

Table 2. Tests and notifications of *Neisseria gonorrhoeae*, New South Wales, Australia, 2017–2019*

Characteristic	No. (%)			
	2017	2018	2019	Total
All positive and negative test results†	903,272 (100)	934,944 (103.5)‡	969,429 (107.3)‡	2,807,645 (NA)
All *N. gonorrhoeae* notifications§	9,192 (100.0)	10,529 (100.0)	11,671 (100.0)	31,392 (100.0)
F	1,512 (16.4)	1,904 (18.10)	2,397 (20.5)	5,813 (18.5)
M	7,644 (83.2)	8,588 (81.60)	9,232 (79.1)	25,464 (81.1)
N. gonorrhoeae notifications with positive culture§¶	2,812 (30.6)	3,305 (33.3)	3,583 (30.7)	9,700 (31.5)
F	368 (24.3)	515 (27.0)	544 (22.7)	1,427 (24.5)
M	2,427 (31.8)	2,979 (34.7)	3,027 (32.8)	8,433 (33.1)
N. gonorrhoeae AMR notifications of PHC#	3 (0.1)	4 (0.1)	4 (0.1)	11 (0.1)
F	0	1 (0.2)	0	1 (0.1)
M	3 (0.1)	3 (0.1)	4 (0.1)	10 (0.1)

*AMR, antimicrobial resistance; NA, not applicable; PHC, public health concern.
†Aggregate gonorrhea test results by nucleic acid amplification test and culture from 12 laboratories. Those laboratories account for an estimated 88.0% of all gonorrhea testing in New South Wales.
‡Percentage calculated from baseline *N. gonorrhoeae* tests in 2017.
§Includes persons whose sex was not reported.
¶Percentage calculated from all *N. gonorrhoeae* notifications.
#Percentage calculated from *N. gonorrhoeae* culture notifications.

treatment completion (81.5% ceftriaxone DS vs. 92.5% azithromycin HLR; p = 0.14). Both groups reported a small number of patients who returned a NAAT-positive result (2/54 vs. 2/40) (Table 3). In the ceftriaxone DS group, 1 case-patient with a genitourinary infection tested NAAT positive on the initial TOC from the same site but subsequently tested NAAT negative after a repeat round of dual therapy. Both isolates were identical on genomic analysis. Another case-patient with a genitourinary infection underwent multisite screening for the initial TOC and tested NAAT positive on the pharyngeal swab specimen but cleared the infection with repeat dual therapy with increased azithromycin (2 g orally). Unfortunately, no culture nor genomics were performed. In the azithromycin HLR group, 2 patients were believed to be reinfected based on patient history.

Genomic Analysis and Clustering of Isolates

Of the 94 isolates, 93 met the quality mapping criteria. Azithromycin HLR was associated with the A2059G mutation in the 23S rRNA gene in 39/40 (97.5%) cases, whereas ceftriaxone DS was linked to the presence of the *penA*-60.001 allele in 24/53 (45.0%) cases. We noted 17 distinct multilocus ST with evidence of clonal expansion across the 3 years (Figure 2).

We identified 9 clusters on the basis of network analysis using a threshold of ≤15 single-nucleotide polymorphisms (Table 4; Figure 2). We identified 2 large ceftriaxone DS clusters, 1 of sequence type (ST) 7827, consisting of 13 cases (22CRO-1), all locally acquired; 5 case-patients reported recent links to commercial sex work. The cluster was predominantly (92.0%) heterosexual, with 5 female and 8 male case-patients. After that local spread, the clone was infrequently detected after 2022. Subsequent ceftriaxone DS isolates in 2023–2024 were of greater concern because 22/28 cases harbored the *penA*-60.001 allele. Two clusters were detected in 2024. The largest cluster consisted of 5 ST1901 infections in heterosexual cases that were all locally acquired; 2 case-patients reported links to sex work. In contrast, the ST9903 cluster consisted of 3 MSM, 1 of whom acquired the infection in Cambodia. Those cases were diagnosed within a small geographic area.

We detected 2 separate but connected ST11200 clusters, 24AZ-1 (n = 13) and 24AZ-2 (n = 4), in the azithromycin HLR notifications. All cases were

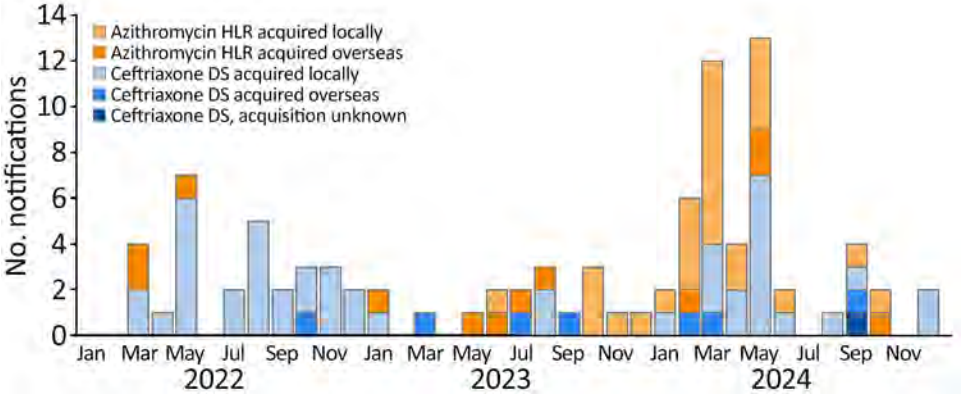

Figure 1. Epidemiologic curve of notifications of antimicrobial-resistant *Neisseria gonorrhoeae* of public health concern, New South Wales, Australia, 2022–2024. Shading indicates type of resistance and acquisition source. DS, decreased susceptibility; HLR, high-level resistance.

locally acquired except for 1 from China. All 17 case-patients were male, 88.2% MSM and 11.7% bisexual. Two reported attendance at sex on premises venues, and 1 had links to sex work. We observed 2 additional clusters, 22AZ-1 ST9363 in 2 MSM cases, both overseas acquired in South America, and 23AZ-1 ST11200 in 2 MSM cases acquired locally.

Genomics linked 46 (49.5%) of 93 notifications. In contrast, epidemiologic links were reported for 5 (5.3%) of 94 notifications. Of note, 2 cases reported an

Table 3. Characteristics of antimicrobial-resistant *Neisseria gonorrhoeae* cases of public health concern, New South Wales, Australia, 2022–2024*

Characteristic	Overall, N = 94	Ceftriaxone DS, n = 54	Azithromycin HLR, n = 40	p value
Patient age at diagnosis, median (IQR)	33 (25–42)	36 (24–43)	30 (27–36)	0.12†
Sex at birth				**<0.001**‡
F	18 (19.1)	17 (31.5)	1 (2.5)	
M	76 (80.9)	37 (68.5)	39 (97.5)	
Sexual risk group				**<0.001**‡
Heterosexual	41 (43.6)	39 (72.2)	2 (5.0)	
MSM	49 (52.1)	14 (25.9)	35 (87.5)	
Bisexual	4 (4.3)	1 (1.9)	3 (7.5)	
Previous STI				**<0.002**‡
Y	47 (50.0)	19 (35.2)	28 (70.0)	
N	47 (50.0)	35 (64.8)	12 (30.0)	
Most recent previous STI occurrence§				0.7‡
Co-infection	18 (38.3)	7 (36.8)	11 (39.3)	
<1 y	22 (46.8)	8 (42.1)	14 (50.0)	
>1 y	7 (14.9)	4 (21.1)	3 (10.7)	
None	47	35	12	
No. previous STIs, median (IQR)	3 (1–5)	2 (1–4)	4 (2–6)	0.11‡
Unknown	47	35	12	
Sex worker or client or SOPV attendance				0.13‡
Yes	15 (16.0)	10 (18.5)	5 (12.5)	
No	38 (40.4)	17 (31.5)	24 (60.0)	
Unknown	41 (43.6)	27 (50.0)	14 (35.0)	
Signs and symptoms				0.095‡
Symptomatic	63 (67.0)	38 (70.4)	25 (62.5)	
Asymptomatic	24 (25.5)	10 (18.5)	14 (35.0)	
Unknown	7 (7.4)	6 (11.1)	1 (2.5)	
Site of infection				**<0.001**‡
Genitourinary tract	58 (61.7)	44 (81.5)	14 (35.0)	
Rectal	18 (19.1)	3 (5.6)	15 (37.5)	
Pharynx	12 (12.8)	4 (7.4)	8 (20.0)	
Eye	1 (1.1)	1 (1.9)	0	
Multiple sites	5 (5.3)	2 (3.7)	3 (7.5)	
Source of infection				**<0.001**‡
Australia	74 (78.7)	46 (85.2)	28 (70.0)	
Africa	1 (1.1)	0	1 (2.5)	
Americas	6 (6.4)	0	6 (15.0)	
Europe	3 (3.2)	0	3 (7.5)	
Western Pacific	9 (9.6)	7 (13.0)	2 (5.0)	
Unknown	1 (1.1)	1 (1.9)	0	
Partners within 2-month lookback				
Total no. partners, median (IQR)	2 (1–5)	1 (1–2)	5 (2–9)	**<0.001**‡
Unknown	26	17	9	
Diagnosing facility				**0.001**‡
General practice	28 (29.8)	22 (40.7)	6 (15.0)	
Sexual health clinic	62 (66.0)	28 (51.9)	34 (85.0)	
Hospital	4 (4.3)	4 (7.4)	0	
Locality				**0.030**‡
Metropolitan	90 (95.7)	54 (100.0)	36 (90.0)	
Regional	4 (4.3)	0	4 (10.0)	
Outcome of initial test of cure				0.14‡
Negative	81 (86.2)	44 (81.5)	37 (92.5)	
Positive	4 (4.3)	2 (3.7)	2 (5.0)	
No follow-up visits	9 (9.6)	8 (14.8)	1 (2.5)	

*Values are no. (%) except as indicated. Ceftriaxone DS is defined as MIC ≥0.125 mg/L; azithromycin HLR is defined as MIC ≥256 mg/L. Bold text indicates statistical significance. DS, decreased susceptibility; HLR, high-level resistance; IQR, interquartile range; MSM, men who have sex with men; SOPV, sex on premises venue; STI, sexually transmitted infection.
†By Wilcoxon rank-sum test.
‡By Fisher exact test.
§Categorizes the most recent STI occurrence.

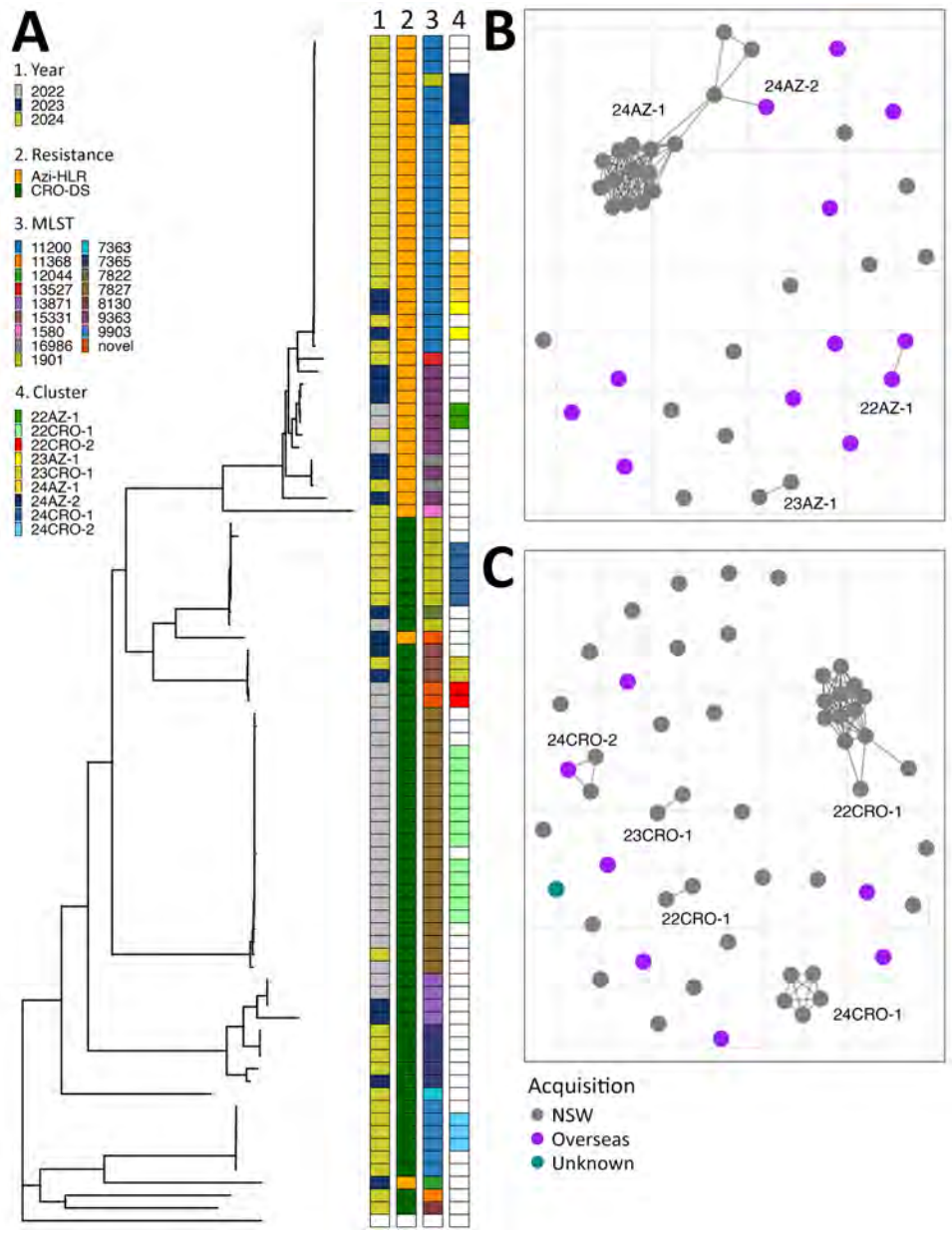

Figure 2. Phylogenetic tree and antimicrobial resistance network analysis from study of antimicrobial-resistant *Neisseria gonorrhoeae* of public health concern, New South Wales, Australia, 2022–2024. A) Phylogenetic tree and isolate data. Ninety-three of the 94 isolates met the quality mapping criteria. B) Network analysis of cases with high-level resistance to azithromycin, with nodes colored according to acquisition source. C) Network analysis of cases with decreased susceptibility to ceftriaxone, with nodes colored according to acquisition source. Azi, azithromycin; CRO, ceftriaxone; DS, decreased susceptibility; HLR, high-level resistance; MLST, multilocus sequence type.

epidemiologic link that was not confirmed by WGS. The discordance between genomic links and self-reported epidemiologic links is not surprising, given the nature of self-reported participation in commercial sex work and attendance at sex on premises venues. Apart from a significantly higher proportion of locally acquired cases within clusters (42 [91.3%] vs. 32 [66.7%] cases; p = 0.047), we determined no statistically significant differences in case characteristics between clustered and nonclustered cases (data not shown).

Discussion

Culture-positive notifications of gonorrhea with ceftriaxone DS or azithromycin HLR were rare before the COVID-19 pandemic and increased notably post-pandemic (2022–2024), highlighting a concerning upward trend. Of greater concern is that ≈80.0% of postpandemic antimicrobial-resistant gonorrhea notifications were locally acquired; clusters arose infrequently from imported cases. That finding suggests that resistant gonococcal strains are actively circulating in communities of sexually active persons in NSW; although clusters in the study were relatively small, there is a risk for future expansion. The risk is perhaps highest among heterosexual populations; the infection can remain asymptomatic in 80.0% of women (*1*), and STI testing rates are lower in heterosexual persons. Lifetime uptake of STI testing is

12.8% in cisgender heterosexual male persons and 15.4% in cisgender heterosexual females versus 38.8% in gay and bisexual and other MSM (GBMSM) and 54.4% in sex workers (*14*). This concept is supported by a previous study in Australia that demonstrated *N. gonorrhoeae* genomic clusters with a higher ratio of women to men were more likely to persist compared with clusters in GBMSM (*15*). Despite higher STI screening rates in GBMSM, the risk for gonorrhea infection and transmission remains high. Uptake of preexposure prophylaxis (PrEP) for HIV prevention among Sydney GBMSM has been substantial (34.9% in 2020 to 53.2% in 2024) (*16*); although evidence of whether PrEP leads to higher STI rates is mixed, data from the NSW GBMSM community suggests STIs were increasing before its introduction (*17*). Instead, the rise in multiple sex partners may be contributing to increased gonorrhea notifications; 26.4% of respondents reported sex with 6–20 men and 16.2% reported sex with ≥20 men in the 6 months before the Sydney GBQ+ Community Survey in 2024 (up from 23.4% in the 6–20 group and 12.5% in the ≥20 group in 2020) (*16*). The observed increase in the percentage of GBMSM reporting multiple sexual partners in the community may have contributed to the expansion of 24AZ-1 cluster, in which cases reported 1–30 contacts.

Although antimicrobial-resistant isolates of PHC in our study remain uncommon (<1.0% of culture-positive *N. gonorrhoeae* notifications), that is likely to change with factors such as increased use of doxycycline postexposure prophylaxis (doxy-PEP). In March 2024, the Australia consensus statement on doxy-PEP to prevent syphilis, chlamydia, and gonorrhea among GBMSM was published, after a collaborative process involving community representatives and experts in clinical care, research, and public health (*18*). The statement acknowledged that doxy-PEP was less likely to be effective for gonorrhea prevention because of high rates of tetracycline resistance in Australia gonococcal isolates (2022–2024, 31.0%–45.0%; in NSW, 20.0%–31.5%) (*7,19,20*). By 2025, data from the Sydney GBQ+ Community Survey reported 12.3% of respondents had used doxy-PEP ≤6 months before the survey for the prevention of bacterial STIs, predominantly syphilis (*21*). Genomic analysis of antimicrobial-resistant gonococcal isolates indicates that mutations associated with tetracycline resistance are often co-selected alongside mutations known to cause resistance to other antimicrobial drugs, which are spread throughout successful clonal lineages (*22*). Therefore, strengthening AMR surveillance and TOC practices and documenting treatment failures are essential.

Although return for TOC was high in our study (86.2%), we found it concerning that 2 treatment failures were identified (both ceftriaxone DS cases: 1 genitourinary and 1 pharyngeal). Standard operating procedures for management of treatment failures are essential to ensure consistent reporting of second-round prescribing practices and appropriate referral of those culture-positive isolates for WGS. Where warranted, complex cases could be escalated to a clinical expert group for specialized advice. Approaches to minimize patients who do not complete follow-up visits could include providing pathology requests, especially in general practice settings at the time of treatment; offering self-collection swab kits; distributing patient information sheets; and ensuring services are provided at no cost to the patient. More broadly, we

Table 4. Summary of antimicrobial-resistant *Neisseria gonorrhoeae* cluster groups, New South Wales, Australia, 2022–2024*

Cluster ID	Size	MLST	*penA* allele type	X23 rRNA	Sex at birth, no. (%)	Sexual risk exposure group, no. (%)	Place of acquisition, no. (%)	SW or client or SOPV, no. (%)	Median no. contacts (range)
22AZ-1	2	9363	2.001	A2059G	2 M (100.0)	2 MSM (100.0)	2 OS (100.0)	0	Unknown
23AZ-1	2	11200	2.001	A2059G	2 M (100.0)	2 MSM (100.0)	2 local (100.0)	0	2.5 (1–4)
24AZ-1	13	11200	2.001	A2059G	13 M (100.0)	12 MSM (92.3), 1 BI (7.7)	13 local (100.0)	2 (15.4)	3.5 (1–30)
24AZ-2	4	11200	2.001	A2059G	4 M (100.0)	3 MSM (75.0), 1 BI (25.0)	3 local (75.0), 2 OS (25.0)	1 (25.0)	9.0 (1–15)
22CRO-1	13	7827	13.001	NA	5 F (38.5), 8 M (61.5)	12 HET (92.3), 1 MSM (7.7)	13 local (100.0)	5 (38.5)	1.0 (1–5)
22CRO-2	2	15331	18.001	NA	2 M (100.0)	2 MSM (100.0)	2 local (100.0)	0	3.0†
23CRO-3	2	15331	18.001	NA	2 M (100.0)	2 MSM (100.0)	2 local (100.0)	0	6.0†
24CRO-1	5	1901	60.001	NA	2 F (40.0), 3 M (60.0)	5 HET (100.0)	5 local (100.0)	2 (40.0)	1.0 (1–2)
24CRO-2	3	9903	60.001	NA	3 M (100.0)	3 MSM (100.0)	2 local (66.6) 1 OS (33.3	0	1.5 (1–2)
Total	46	NA	NA	NA	7 F (15.2) 39 M (84.8)	17 HET (37.0) 27 MSM (58.7), 2 BI (4.3)	42 local (91.3) 4 OS (8.7)	10 (22.7)	2.0 (1–30)

*BI, bisexual; HET, heterosexual; ID, identification; local, Australia acquisition; MLST, multilocus sequence type; MSM, men who have sex with men; NA, not applicable; OS, overseas acquisition; SOPV, sex on premises venue; SW, sex worker.
†Median number of contacts (based on 1 available value).

recommend that national treatment guidelines are regularly reviewed in conjunction with local epidemiology and WGS data.

AMR patterns in gonorrhea observed in NSW reflect global trends. The Western Pacific region is a recognized reservoir of gonococcal resistance; Cambodia reported ceftriaxone DS rates of 31%–38%, Vietnam 27%–28%, and China 8%–9%, including ≈25% in some provinces (*23*–*28*). Patient risk factors contributing to that resistance pattern are sparsely reported from these countries; however, a UK study found all of their local ceftriaxone DS cases were in heterosexuals and ≈90% of overseas acquired cases were associated with travel to the Western Pacific region or adjacent countries (*29*). In contrast, the epidemiology and geographic distribution of azithromycin HLR seems less well defined, with multiple sustained transmission events reported across the Americas and Europe (*30*–*33*).

A limitation of our study was the lack of data on contact tracing outcomes and subsequent transmission. In NSW, contact tracing is the responsibility of the managing clinician, and most clinicians support patients to self-inform their contacts. Provider-initiated contact tracing can be an alternative; however, potential drawbacks are privacy and confidentiality concerns and the potential to damage the patient-provider relationship. Of interest, a public health–led gonorrhea contact tracing intervention in Canada found that the provider-initiated method identified a significantly higher number of female than male cases during the intervention period (*34*). Unfortunately, in our study, many cases reported anonymous contacts, making both methods ineffective to effectively curb transmission. Efforts would be better focused on promoting diagnosis by culture, STI screening, improving sexual health education and awareness of antimicrobial resistance, and ensuring completion of TOC for all antimicrobial-resistant gonorrhea notifications of PHC.

Last, although national guidelines recommend collecting culture samples from all infected sites, not all notifications in NSW had a culture result. Culture success rates are greater for symptomatic infections, which have a higher bacterial load, than for asymptomatic infections, and vary by site of infection (*35*). In addition, factors such as bacterial viability, swab technique, transport medium, and transport time all influence culture success. Although we did not have data on the number of cultures ordered in NSW, we do have data on the *N. gonorrhoeae* culture-positive rate. The culture rate from general practice is lower than from sexual health clinics (19.1% vs. 44.6%) (unpublished data from operational audit). Collectively, those findings suggest that while culture collection practices can be improved, achieving culture positivity for all notifications is not feasible.

In summary, notifications of antimicrobial-resistant gonorrhea of PHC are rapidly rising in Australia and elsewhere. Where possible, culture-based surveillance with robust case management protocols remains the best approach to detect and minimize transmission of resistant gonococcal infection.

Acknowledgments

We thank the staff at Publicly Funded Sexual Health Clinics and Public Health Units in New South Wales, Australia.

About the Authors

L.J. Walker is an epidemiologist at NSW Health. Her research interests include emerging infectious disease, health system strengthening, and reducing health inequalities. Dr. van Hal is a medical microbiologist and infectious-disease physician at the Royal Prince Alfred Hospital in Sydney, Australia. He is responsible for the provision of genomic services for WHO Programmes, Public Health, and hospitals in NSW.

References

1. Australian STI Management Guidelines. Gonorrhoea. 2024 [cited 2025 Dec 3]. https://sti.guidelines.org.au/sexually-transmissible-infections/gonorrhoea
2. Centers for Disease Control and Prevention. Gonococcal Isolate Surveillance Project (GISP) profiles [cited 2025 Dec 3]. https://www.cdc.gov/sti-statistics/gisp-profiles
3. European Centre for Disease Prevention and Control. Gonococcal antimicrobial susceptibility surveillance in the EU/EEA [cited 2025 Dec 3]. https://www.ecdc.europa.eu/sites/default/files/documents/gonococcal-antimicrobial-susceptibility-surveillance-europe.pdf
4. Public Health Agency of Canada. Dashboard on the Enhanced Surveillance of Antimicrobial-resistant Gonorrhea system (ESAG): 2018 to 2023 [cited 2025 Dec 3]. https://health-infobase.canada.ca/esag
5. Sun S, Narayanan P, Vickers A, Pitt R, Doumith MX, David S, et al. GRASP report: data to August 2024 [cited 2025 Dec 3]. https://www.gov.uk/government/publications/gonococcal-resistance-to-antimicrobials-surveillance-programme-grasp-report/grasp-report-data-to-august-2024
6. World Health Organization. Enhanced Gonococcal Antimicrobial Surveillance Programme (EGASP): surveillance report 2023. 2024 [cited 2025 Dec 3]. https://iris.who.int/bitstream/handle/10665/379546/9789240102927-eng.pdf
7. Lahra M, Hurley S, Van Hal S, Hogan T. Australian Gonococcal Surveillance Programme annual report, 2024. Commun Dis Intell. 2025;49. https://doi.org/10.33321/cdi.2025.49.056
8. Clinical and Laboratory Standards Institute (CLSI). Performance standards for antimicrobial susceptibility testing, 36th edition. Supplement M100. Wayne (PA): The Institute; 2026.

9. NSW Health. Antimicrobial resistant gonococcal infections of public health significance. Appendix D: standard operating procedure. 2025 [cited 2025 Dec 3]. www.health.nsw.gov.au/Infectious/controlguideline/Documents/gonorrhoea-appendix-d-sop-amr.pdf
10. Health Protection NSW. Gonococcal notification form for antimicrobial infections of public health significance 2022 [cited 2025 Dec 3]. www.health.nsw.gov.au/Infectious/controlguideline/Documents/gonococcal-notification-form-fillable.pdf
11. World Health Organization. Countries. 2025 [cited 2025 Dec 3]. https://www.who.int/countries
12. van Hal SJ, Sherry N, Coombs G, Mowlaboccus S, Whiley DM, Lahra MM. Emergence of an extensively drug-resistant *Neisseria gonorrhoeae* clone. Lancet Infect Dis. 2024; 24:e547–8. https://doi.org/10.1016/S1473-3099(24)00486-9
13. National Health and Medical Research Council. Ethical considerations in quality assurance and evaluation activities 2024 [cited 2025 Dec 3]. https://www.nhmrc.gov.au/about-us/publications/ethical-considerations-quality-assurance-and-evaluation-activities
14. Ogilvie E, McManus H, Callander D, Guy R, Basheer E, Sullivan E, et al. The Third Australian Study of Health and Relationships: report to the NSW Ministry of Health. 2025 [cited 2025 Dec 3]. https://unsworks.unsw.edu.au/entities/publication/642dd75a-1e94-4032-ad49-765ed5fe7850
15. Taouk ML, Taiaroa G, Duchene S, Low SJ, Higgs CK, Lee DYJ, et al. Longitudinal genomic analysis of *Neisseria gonorrhoeae* transmission dynamics in Australia. Nat Commun. 2024; 15:8076. https://doi.org/10.1038/s41467-024-52343-0
16. MacGibbon J, Chan C, Bavinton B, Mao L, Smith AK, Molyneux A, et al. GBQ+ Community Periodic Survey: Sydney 2024 [cited 2025 Dec 3]. https://doi.org/10.26190/unsworks/30413
17. McManus H, Grulich AE, Amin J, Selvey C, Vickers T, Bavinton B, et al. Comparison of trends in rates of sexually transmitted infections before vs after initiation of HIV preexposure prophylaxis among men who have sex with men. JAMA Netw Open. 2020;3:e2030806. https://doi.org/10.1001/jamanetworkopen.2020.30806
18. Cornelisse VJ, Riley B, Medland NA. Australian consensus statement on doxycycline post-exposure prophylaxis (doxy-PEP) for the prevention of syphilis, chlamydia and gonorrhoea among gay, bisexual and other men who have sex with men. Med J Aust. 2024;220:381–6. https://doi.org/10.5694/mja2.52258
19. Lahra MM, van Hal S, Hogan TR. Australian Gonococcal Surveillance Programme annual report, 2022. Commun Dis Intell. 2023;47:47. https://doi.org/10.33321/cdi.2023.47.45
20. Lahra MM, van Hal S, Hogan TR. Australian Gonococcal Surveillance Programme annual report, 2023. Commun Dis Intell. 2025;49:49. https://doi.org/10.33321/cdi.2025.49.007
21. Broady T, Chan C, MacGibbon J, Smith AK, Mao L, Tremain D, et al. GBQ+ Community Periodic Survey: Sydney 2025 [cited 2025 Dec 3]. https://doi.org/10.26190/unsworks/31367
22. Vanbaelen T, Manoharan-Basil SS, Kenyon C. Doxycycline postexposure prophylaxis could induce cross-resistance to other classes of antimicrobials in *Neisseria gonorrhoeae*: an in silico analysis. Sex Transm Dis. 2023;50:490–3. https://doi.org/10.1097/OLQ.0000000000001810
23. Ouk V, Pham CD, Wi T, van Hal SJ, Lahra MM; EGASP Cambodia Working Group. The Enhanced Gonococcal Surveillance Programme, Cambodia. Lancet Infect Dis. 2023;23:e332–3. https://doi.org/10.1016/S1473-3099(23)00479-6
24. Ouk V, Say HL, Virak M, Deng S, Frankson R, McDonald R, et al. World Health Organization Enhanced Gonococcal Antimicrobial Surveillance Programme, Cambodia, 2023. Emerg Infect Dis. 2024;30:1493–5. https://doi.org/10.3201/eid3007.240354
25. Lan PT, Nguyen HT, Golparian D, Thuy Van NT, Maatouk I, Unemo M, et al. The WHO Enhanced Gonococcal Antimicrobial Surveillance Programme (EGASP) identifies high levels of ceftriaxone resistance across Vietnam, 2023. Lancet Reg Health West Pac. 2024;48:101125. https://doi.org/10.1016/j.lanwpc.2024.101125rn>
26. Adamson PC, Hieu VN, Nhung PH, Whiley DM, Chau TM. Ceftriaxone resistance in *Neisseria gonorrhoeae* associated with the *penA-60.001* allele in Hanoi, Viet Nam. Lancet Infect Dis. 2024;24:e351–2. https://doi.org/10.1016/S1473-3099(24)00230-5
27. Tang Y, Liu X, Chen W, Luo X, Zhuang P, Li R, et al. Antimicrobial resistance profiling and genome analysis of the *penA-60.001 Neisseria gonorrhoeae* clinical isolates in China in 2021. J Infect Dis. 2023;228:792–9. https://doi.org/10.1093/infdis/jiad258
28. Zhu X, Xi Y, Gong X, Chen S. Ceftriaxone-resistant gonorrhea—China, 2022. MMWR Morb Mortal Wkly Rep. 2024;73:255–9. https://doi.org/10.15585/mmwr.mm7312a2
29. Fifer H, Doumith M, Rubinstein L, Mitchell L, Wallis M, Singh S, et al. Ceftriaxone-resistant *Neisseria gonorrhoeae* detected in England, 2015–24: an observational analysis. J Antimicrob Chemother. 2024;79:3332–9. https://doi.org/10.1093/jac/dkae369
30. Fifer H, Cole M, Hughes G, Padfield S, Smolarchuk C, Woodford N, et al. Sustained transmission of high-level azithromycin-resistant *Neisseria gonorrhoeae* in England: an observational study. Lancet Infect Dis. 2018;18:573–81. https://doi.org/10.1016/S1473-3099(18)30122-1
31. Salmerón P, Moreno-Mingorance A, Trejo J, Amado R, Viñado B, Cornejo-Sanchez T, et al. Emergence and dissemination of three mild outbreaks of *Neisseria gonorrhoeae* with high-level resistance to azithromycin in Barcelona, 2016–18. J Antimicrob Chemother. 2021;76:930–5. https://doi.org/10.1093/jac/dkaa536
32. Holderman JL, Thomas JC, Schlanger K, Black JM, Town K, St. Cyr SB, et al. Sustained transmission of *Neisseria gonorrhoeae* with high-level resistance to azithromycin, in Indianapolis, Indiana, 2017–2018. Clin Infect Dis. 2021;73:808–15. https://doi.org/10.1093/cid/ciab132
33. Gianecini RA, Poklepovich T, Golparian D, Cuenca N, Scocozza L, Bergese S, et al. Sustained transmission of *Neisseria gonorrhoeae* strains with high-level azithromycin resistance (MIC ≥ 256 µg/mL) in Argentina, 2018 to 2022. Microbiol Spectr. 2023;11:e0097023. https://doi.org/10.1128/spectrum.00970-23
34. Schleihauf E, Leonard E, Phillips C, Hatchette T, Haldane D, Arnason T, et al. Increase in gonorrhea incidence associated with enhanced partner notification strategy. Sex Transm Dis. 2019;46:706–12. https://doi.org/10.1097/OLQ.0000000000001060
35. Brendefur Corwin LM, Campbell P, Jakobsen K, Müller F, Lai X, Unemo M, et al. Improvement in *Neisseria gonorrhoeae* culture rates by bedside inoculation and incubation at a clinic for sexually transmitted infections. Ann Clin Microbiol Antimicrob. 2023;22:27. https://doi.org/10.1186/s12941-023-00576-0

Address for correspondence: Liz Walker, NSW Health, Health Protection NSW, 1 Reserve Rd, St. Leonards, NSW 2065, Australia; email: liz.walker1@health.nsw.gov.au

Role of Households with Children in Community Spread of Multidrug-Resistant Enterobacterales, St. Louis, Missouri, USA

Barrett Breeze,[1] Ahmed Babiker,[1] Sreenivas Konda, Alaina L. Robinson, Stefan J. Green, Catherine C. Babbs, Federico Cunha, Katherine Y. Shen, India Shepherd Hammond, Stephanie A. Fritz, Latania K. Logan

Community-acquired multidrug-resistant (MDR) Enterobacterales bacteria are an increasing public health concern, yet whether households play a role in community spread remains unclear. We investigated 150 households with children in St. Louis, Missouri, USA, for MDR Enterobacterales. We cultured swab specimens from household members and environmental surfaces for identification and antimicrobial susceptibility testing. We also performed whole-genome sequencing in the 53 (35%) households where >1 MDR Enterobacterales species were recovered. *Enterobacter hormaechei* predominated, followed by *Klebsiella pneumoniae* and *Pantoea* species. Whole-genome sequencing revealed closely related strains shared between persons and environmental surfaces, suggesting potential intra-household transmission. We identified ≥1 horizontal gene transfer event between Enterobacterales genera within a household. On multivariable analysis, households that had children attending daycare, a member with an ADHD diagnosis, and dog ownership were associated with increased odds of household MDR Enterobacterales colonization. Households likely serve as major contributors in acquisition and community spread of MDR Enterobacterales.

Multidrug resistant (MDR) Enterobacterales bacteria have emerged as a serious public health threat. Of major concern is the increasing incidence of extended-spectrum cephalosporin resistance (ESCR) in Enterobacterales. This resistance pattern is commonly associated with the production of extended-spectrum β-lactamases (ESBL), antimicrobial resistance genes (ARGs) carried on mobile genetic elements (MGEs) such as plasmids, which often carry other ARGs. The incidence of infections has increased dramatically during the past decade, reaching nearly 200,000 infections and >9,000 deaths per year in the United States (*1*). Although ESBL Enterobacterales were once largely healthcare-associated pathogens, during the past 2 decades, most ESBL Enterobacterales infections have been caused by clinically and genetically distinct strains that have emerged in the community (*2*).

Adding to the complexity of this group of pathogens, the determinants of resistance yielding the ESCR phenotype might be chromosomal, transferable ARGs on MGEs, or contain both, and are often MDR. Invasive infections caused by community-acquired ESCR Enterobacterales strains are increasingly being reported in young children and persons without major healthcare exposures (*3*,*4*). Of note, those strains are resistant to antimicrobial drugs that are uncommonly used in children; therefore, overuse is unlikely to be driving this resistance.

Factors promoting MDR and ESCR Enterobacterales acquisition and infection in the community are largely unknown. However, in households with an adult known to have acquired ESBL Enterobacterales from healthcare exposures, transmission incidence has been described as upwards of 67% (*5*,*6*). Furthermore, in a multicenter investigation of MDR (primarily ESBL) Enterobacterales in children from Chicago, Illinois, USA, we found that MDR Enterobacterales acquisition reflected geographic clustering and lacked association with the factors driving

Author affiliations: Emory University School of Medicine, Atlanta, Georgia, USA (B. Breeze, C.C. Babbs, F. Cunha, K.Y. Shen, I.S. Hammond, L.K. Logan); Rush University Medical Center, Chicago, Illinois, USA (A. Babiker, S.J. Green); The University of Chicago, Chicago (S. Konda); Washington University School of Medicine, St. Louis, Missouri, USA (A.L. Robinson, S.A. Fritz); Children's Healthcare of Atlanta, Atlanta (L.K. Logan)

DOI: https://doi.org/10.3201/eid3206.251655

[1]These first authors contributed equally to this article.

primary acquisition in adults (e.g., antimicrobial drug and healthcare exposures) (*7*,*8*). We also found that, compared with antimicrobial-sensitive Enterobacterales infections in children, $bla_{\text{CTX-M-9}}$–type ESBL Enterobacterales infections were nearly 5 times more likely to be community-acquired (*8*). To devise strategies to prevent community-acquired MDR Enterobacterales infections, we must first understand key reservoirs for acquisition, including sources of transmission outside of healthcare settings, the role of the natural and built environment in pathogen transmission, and epidemiologic factors associated with community-acquired MDR Enterobacterales acquisition, transmission, and infection.

We believe households are major drivers of MDR Enterobacterales spread in the community and that environmental surfaces are major reservoirs of MDR Enterobacterales in households. That hypothesis is supported by observations that MDR Enterobacterales strains can persist on surfaces in healthcare environments for up to 30 months, likely contributing to healthcare-associated transmission (*9*–*11*). Relevant to those findings, prior studies of household transmission of community-acquired methicillin-resistant *Staphylococcus aureus* (MRSA) in St. Louis, Missouri, USA, have demonstrated that multiple environmental surfaces serve as reservoirs for community-acquired MRSA transmission (*12*–*15*). In addition, households with a higher burden of environmental community-acquired MRSA contamination were 4-fold more likely to enable transmission (*15*). In addition, we believe that critical epidemiologic risk factors for colonization, including the presence of preschool-age children who attend daycare (*16*) and having a pet dog in the household, would be associated with MDR Enterobacterales colonization (*17*).

We used a biorepository of human and household surface samples and associated epidemiologic metadata collected from households of pediatric and adult community participants to understand the clinical and molecular epidemiology of community-acquired MDR Enterobacterales, with a focus on ESCR Enterobacterales. We highlight the household whole-genome sequencing (WGS) data for *Enterobacter* spp., a well-known cause of healthcare-associated infections, which might represent an underrecognized source of community acquisition of antimicrobial drug resistance.

Methods

Study Settings and Population

We used a biorepository and detailed epidemiologic metadata from a well-curated population of 150 otherwise healthy children with community-acquired *S. aureus* infections and their household contacts (n = 489) enrolled in the SHINE study from 2015–2021 in metropolitan St. Louis, Missouri, USA (Clinicaltrials.gov, identification no. NCT02572791). Through the SHINE study, research visits were conducted in participants' homes. Children were defined as 0–18.99 years old. Detailed clinical and epidemiologic data were collected from each participant, including demographics, medical history, topical and systemic antimicrobial drug use, activities outside of the home, personal hygiene practices, and interactions between household contacts. Detailed information regarding household characteristics were also collected, including household environmental cleaning practices, renting versus owning, number of bedrooms, and the presence and characteristics of pets. All data were collected prospectively through the SHINE study and were entered into REDCap, a secure, HIPAA-compliant, web-based data application (*18*). At each study visit, colonization samples were collected from the anterior nares, axillae, and inguinal folds by using BD Eswabs (BD, https://www.bd.com). Rectal or perirectal swab specimens were not collected.

Through the SHINE study, samples were collected from up to 21 household environmental surfaces. A 250-µL aliquot of liquid amies transport media from each swab was enriched and suspended in tryptic soy broth plus 20% glycerol and frozen at −80°C. For this study, we used samples from households collected at SHINE study enrollment (natural history phase). The Washington University Institutional Review Board approved study procedures. Informed consent was obtained for all participating household members.

Bacterial Isolates and Antimicrobial Susceptibility Testing

We chose to use inguinal fold swab specimens on the basis of a higher likelihood of colonization because of proximity to the rectum. We transferred swab suspension samples and environmental surface samples to tryptic soy broth and incubated them overnight at 37°C. We used a 1-µL inoculation loop to streak the enriched broth onto membrane fecal coliform agar to evaluate the presence of Enterobacterales bacteria. In addition, we spread-plated 100 µL of the broth onto CHROMagar ESBL media (CHROMagar, https://www.chromagar.com) (*19*). We incubated plates at 37°C for 16–20 hours, subcultured the resulting colonies on CHROMagar, and incubated them overnight at 37°C. After incubation, we resuspended the colonies in saline and adjusted to a 0.5–0.63 McFarland standard for isolate identification and antimicrobial

susceptibility testing using the automated VITEK 2 system (bioMérieux, https://www.biomerieux.com), according to the manufacturer's instructions.

We used a broad definition for MDR Enterobacterales because isolates were ESCR, with some demonstrating resistance to carbapenems, all of which were resistant to ≥2 antimicrobial classes. We selected the colonies we defined as MDR Enterobacterales for further testing (*20*). We chose a subset of the resistant isolates for WGS if they were from households where Enterobacterales were recovered from >1 surface or person. We extracted DNA by using the QIAGEN DNeasy Blood and Tissue Kit (QIAGEN, https://www.qiagen.com) according to the manufacturer's instructions and shipped the extracted genomic DNA to the Rush University Medical Center Genomics and Microbiome core facility (Chicago, Illinois, USA) for WGS.

WGS

We performed bacterial WGS by using standard shotgun sequencing methods, as described previously (*19*). In brief, we prepared genomic DNA for sequencing by using a NEXTFLEX rapid XP DNA sequencing kit (Revvity, https://www.revvity.com) implemented on a Sciclone G3 NGSx iQ (Revvity) workstation. We normalized DNA inputs to 10 ng and used 10 cycles of amplification. After magnetic bead cleanup (0.8× ratio of beads to template, vol:vol), we sequenced libraries by using an Illumina NovaSeq X (Illumina, https://www.illumina.com) instrument using a 10 billion cluster flowcell lane. Libraries were created by the Rush University Medical Center for Genomics and Microbiome core facility, and sequencing was performed by the DNA Services Core, Carver Biotechnology Center, University of Illinois Urbana-Champaign (Urbana-Champaign, Illinois, USA).

Bioinformatic Analysis

FASTQ files underwent QC screening, and we assembled and analyzed them by using the Bactopia pipeline (*21*). In brief, we only further analyzed FASTQ files if they met the following parameters: estimated genome coverage ≥20×, mean per-read quality score ≥Q12, mean post-trimming read length ≥49 bp, and ≤500 total contigs. We quality filtered Illumina reads by using Trimmomatic (*22*) and assembled de novo by using SPAdes (*23*). We used Prodigal (*24*) to predict gene sequences and annotated them with Prokka (*25*). We assessed antimicrobial resistance content by using AMRFinder Plus (*26*). We defined core genes by using Roary (*27*). We generated a phylogenetic tree on the basis of a core gene alignment by using IQtree (*28*). We generated a maximum-likelihood tree by running 1,000 bootstrap replicates under the generalized time-reversible model of evolution. We inferred the maximum-likelihood phylogeny from the core genome alignment by using IQ-TREE under the Hasegawa–Kishino–Yano nucleotide substitution model with 1,000 ultrafast bootstrap replicates and 1,000 SH-like approximate likelihood ratio test replicates. We visualized and annotated the tree by using iTOL version 4 (*29*). We calculated the core genome pairwise single-nucleotide polymorphism distance for each sample with snp-dists (*30*) and completed pangenome wide comparison of genomes by using Scoary (*31*). We reconstructed, typed, and clustered plasmids by using MOB-suite (*32*). We performed clustering for plasmids with a mash distance ≤0.05 with ≥85% similarity in length. We considered plasmid transfer if a mobilizable or conjugative plasmid within the same primary cluster was detected in a different species within the same household. Sequence data are available in the National Center for Biotechnology Information Sequence Read Archive (https://www.ncbi.nlm.nih.gov/sra; BioProject no. PRJNA1257399).

Statistical Analysis

We used a retrospective case–control study design to assess factors associated with household colonization with MDR Enterobacterales. We presented the descriptives numerical variable by mean ±SD and of categorical variables by counts and percentages (*33*). We conducted bivariate analysis by using a 2-sample t-test and χ^2 test for independence. We conducted multivariate analysis of the binary outcome by using logistic regression. We selected covariates in the final logistic regression by the LASSO method (*34*,*35*) first, and then by clinical importance of the variables because of a large number of covariates associated with households and household members and pets (*12*,*36*).

We performed logistic regression analysis to identify significant household clinical and nonclinical factors associated with household colonization with MDR Enterobacterales. On the basis of the observation numbers, robustness to reporting, prevarication bias, and biologic plausibility regarding Enterobacterales carriage, we selected a covariate with a p≤0.25 in univariate analysis for inclusion in a multivariable model by using a manual forward selection approach in which variables having a p = 0.10 remained in the model. We addressed potential confounding effects by retaining variables whose exclusion from the models changed the effect of the other

covariates by ≥10%. We tested interactions between independent variables and expanded the final multivariable models to include the significant (p<0.10) interaction terms. We checked for any collinearities between independent variables before multivariable analysis and made selections between collinear variables on the basis of an improved model fit as shown by the Akaike information criterion and Bayesian information criterion (*36*,*37*). We expressed bivariate and multivariate associations as odd ratios (ORs) and corresponding 95% CIs. Statistical significance was indicated by p<0.05.

Results

Characteristics of Households in the Study Population

We analyzed 150 households and their characteristics. The mean age of the 639 participants was 20.86 (SD ±6.30); for race, 73% identified as White, 24% as Black, and 3% as mixed race or Asian descent. In addition, ≥1 household member held a college degree (43%), private insurance (77%), or Medicaid insurance (31%). All households had ≥1 child (52% of all participants were children), 71% had ≥1 child in daycare, 51% had ≥1 dog, and the average number of residents per household was 4.31 (SD ±1.34).

We univariately analyzed ≈100 variables from clinical and epidemiologic data. Of those, we summarized 20 risk factors from the univariate analysis results along with their bivariate associations on the basis of the presence and absence of MDR Enterobacterales (Table 1).

Characteristics of Bacterial Isolates at the Household Level

We tested 3,201 samples from 627 humans and 2,574 surfaces in 150 households. Enterobacterales strains phenotypically identified as MDR had been recovered from 53 (35%) of 150 households. Of the 120 MDR Enterobacterales isolated from 53 households, most were *Enterobacter* spp. (71%, n = 85), *Pantoea* spp. (12%, n = 14), and *Klebsiella* spp. (8%, n = 10). The household surfaces most commonly harboring MDR Enterobacterales were the kitchen sink faucet handle (20.7%), sofa (9%), bedsheets (6%), oven door handle (6%), and refrigerator door handle (3%). MDR Enterobacterales were identified in the inguinal folds of 25 (4%) household members.

WGS Analysis of MDR Enterobacterales strains

We chose a subset of isolates for WGS if they were recovered from households where MDR Enterobacterales were found on >1 household surface or household member. Of the 94 samples sequenced, 93 passed pipeline QC metrics. Of those, 76 were Enterobacterales on the basis of genome taxonomy database toolkit taxonomic classification (Table 2). The most common species detected were members of the *Enterobacter cloacae* complex (most were *E. hormaechei* [N = 47]), followed by *K. pneumoniae* (N = 10). All isolates were ESCR; 10 were also resistant to ≥1 carbapenem, none of which were found to contain a transmissible carbapenemase gene.

We conducted a relatedness analysis for all species or sequence types (STs) with ≥4 isolates (*K. pneumoniae* [n = 10], *S. marcescens* [n = 4], and *E. hormaechei* ST50 [n = 5] and ST108 [n = 5]). This analysis revealed clustering of isolates within the same households from multiple surfaces and household members (Appendix Table 1, http://wwwnc.cdc.gov/EID/article/32/6/25-1655-App1.pdf).

We reconstructed, typed, and clustered plasmid sequences to assess whether plasmids with similar identity were found across different species isolated from the same household. A total of 251 plasmids were reconstructed across 69 genomes into 100 unique clusters. Across those clusters, we detected ≥1 potential plasmid transfer event. A plasmid with the same conjugative relaxase type and an identical mash distance to the nearest MOB-suite database reference (GenBank accession no. CP032172) was detected in a *K. pneumoniae* isolate recovered from the inguinal fold of a participant child and *Proteus mirabilis* isolate recovered from the inguinal fold of the child's mother.

Further analysis of the recovered *E. hormaechei* strains revealed a diversity of STs, with 23 unique STs detected (Figure; Appendix Table 2, Figure). Only 2 major STs (defined as ≥5 isolate per ST) were detected: ST50 (n = 5 isolates) and ST108 (n = 5 isolates). The remaining 47 were distributed across minor STs (n < 5 isolates per ST). All isolates had a bla_{ACT} variant *ampC* gene detected. Among the 47 isolates, 15 were detected from a human source (3 from inguinal folds, 12 from bedsheets) and 32 from an environmental source. ST distribution, AMR gene count, and plasmid count was similar among environmental and human isolates (Appendix Table 2). To assess differential gene content between environmental and human isolates, we conducted a pangenome analysis. However, no candidate genes remained statistically significant after Benjamini-Hochberg correction (false discovery rate <0.05). *K. pneumoniae*, the second largest group of strains assessed by WGS, revealed primarily $bla_{SHV\text{-}ESBL}$ and most were also MDR (Table 3).

Analysis of Factors Associated with MDR Enterobacterales

The 53 households with MDR Enterobacterales (cases) were compared to 97 households without MDR Enterobacterales (controls). Although 94 of 150 households identified having ≥1 family member with ≥1 health conditions (Table 1; Appendix Table 3), none of those conditions were found to be associated with MDR Enterobacterales colonization on bivariate analysis; primary conditions reported were often mild or common such as asthma and seasonal allergies. However, households reporting ≥1 antimicrobial drug prescription in the previous 12 months were more common in controls than cases and was inversely associated with MDR Enterobacterales colonization (OR = 0.48, 95% CI 0.24–0.96; p = 0.04). Having smaller homes, fewer rooms, and lower square feet per person were positively associated with MDR Enterobacterales colonization on bivariate analysis.

In the final multivariable logistic regression model (Table 4), factors found to be associated with a lower likelihood of MDR Enterobacterales colonization were households identifying as predominantly White race (adjusted OR [aOR] = 0.18, 95% CI 0.06–0.49;

Table 1. Descriptive statistics by HHs with (cases) and without (controls) MDR Enterobacterales in study of role of HHs with children in community spread of multidrug-resistant Enterobacterales, St. Louis, Missouri, USA*

Variable	Total HHs, n = 150	Controls, n = 97	Cases, n = 53	Odds ratio (95% CI)	p value
Mean HH size (SD)	4.31 (1.34)	4.29 (1.26)	4.36 (1.48)	1.04 (0.81–1.33)	0.76
HH members' mean age, years (SD)	20.86 (6.30)	21.3(5.97)	19.95(6.82)	0.96 (0.91–1.02)	0.19
HH mean home size in square feet (SD)	1,785 (1,021)	1,953(1,027)	1,481 (946)	1.02 (1.01–1.03)	0.01
HH mean number of rooms (SD)	9.85 (3.35)	10.32 (3.58)	9.00 (2.72)	0.88 (0.78–0.98)	0.02
HH mean square feet per person (SD)	441 (262)	478 (259)	374 (255)	0.98 (0.97–0.99)	0.02
HH size >5 membership					
No	130 (87)	87 (90)	43 (81)		
Yes	20 (13)	10 (10)	10 (19)	2.02 (0.77–5.29)	0.15
HH homeownership					
No	56 (37)	30 (31)	26 (49)		
Yes	94 (63)	67 (69)	27 (51)	0.46 (0.23–0.92)	0.03
HHs with ≥1 health conditions					
No	24 (16)	14 (14)	10 (19)		
Yes	126 (84)	83 (86)	43 (81)	0.73 (0.30–1.81)	0.48
HHs with ≥1 ADHD member					
No	94 (75)	66 (80)	28 (65)		
Yes	32 (25)	17 (20)	15 (35)	2.08 (0.91–4.76)	0.08
HHs with ≥1 antimicrobial prescription within 12 mo					
No	85 (57)	49 (51)	36 (68)		
Yes	65 (43)	48 (49)	17 (32)	0.48 (0.24–0.96)	0.04
HHs with ≥1 emergency room visit within 12 mo					
No	10 (6.7)	7 (7.2)	3 (5.7)		
Yes	140 (93)	90 (93)	50 (94)	1.3 (0.34–6.22)	0.72
White households					
No	40 (27)	17 (18)	23 (43)		
Yes	110 (73)	80 (82)	30 (57)	0.28 (0.13–0.58)	<0.01
HHs with ≥1 college degree					
No	86 (57)	53 (55)	33 (62)		
Yes	64 (43)	44 (45)	20 (38)	0.73 (0.36–1.44)	0.37
HH with ≥1 professional degree					
No	102 (68)	62 (64)	40 (75)		
Yes	48 (32)	35 (36)	13 (25)	0.58 (0.26–1.20)	0.15
HHs with ≥1 private insurance member					
No	35 (23)	16 (16)	19 (36)		
Yes	115 (77)	81 (84)	34 (64)	0.35 (0.16–0.77)	0.01
HHs with ≥1 Medicaid recipient					
No	104 (69)	75 (77)	29 (55)		
Yes	46 (31)	22 (23)	24 (45)	2.82 (1.38–5.85)	0.01
HHs with ≥1 child attending daycare					
No	44 (29)	30 (31)	14 (26)		
Yes	106 (71)	67 (69)	39 (74)	1.25 (0.60–2.69)	0.56
HHs with ≥1 dog					
No	74 (49)	51 (53)	23 (43)		
Yes	76 (51)	46 (47)	30 (57)	1.45 (0.74–2.86)	0.28
HHs with ≥1 cat					
No	125 (83)	78 (80)	47 (89)		
Yes	25 (17)	19 (20)	6 (11)	0.52 (0.18–1.34)	0.2

*Values are no. (%) except as indicated. HH, household; MDR, multidrug resistant.

p<0.01) and having ≥1 member of the family with private insurance trended toward significance and was included in the final model (aOR = 0.44, 95% CI 0.16–1.22; p = 0.11). Factors associated with increased risk for household colonization with MDR Enterobacterales included having ≥1 with a diagnosis of ADHD (aOR = 3.47, 95% CI 1.34–9.41; p = 0.01), ≥1 minor attending daycare (aOR = 2.86, 95% CI 1.07–8.38, p = 0.04), and ≥1 dog (aOR = 3.31, 95% CI 1.27–3.31; p = 0.02). Similar differences can be found between aOR and OR (Appendix Table 4).

Discussion

In this study, we focused on understanding the role of the household in acquisition and transmission of MDR Enterobacterales, factors associated with increased or decreased risk for household colonization, the principal genetic determinants, and the relatedness of MDR Enterobacterales strains in community settings. Our research program investigates antimicrobial drug resistance in the community through a One Health lens (*38*).

Table 2. Enterobacterales species detected within households by whole-genome sequence analysis in study of role of households with children in community spread of multidrug-resistant Enterobacterales, St. Louis, Missouri, USA

Species	No. (%), n = 76
Enterobacter hormaechei	47 (61.8)
Enterobacter mori	1 (1.3)
Enterobacter quasihormaechei	1 (1.3)
Enterobacter roggenkampii	1 (1.3)
Klebsiella pneumoniae	10 (13.2)
Klebsiella variicola	1 (1.3)
Serratia marcescens	4 (5.3)
Serratia bockelmannii	3 (3.9)
Pantoea septica	3 (3.9)
Pantoea dispersa	1 (1.3)
Pantoea piersonii	1 (1.3)
Proteus mirabilis	2 (2.6)
Citrobacter braakii	1 (1.3)

Enterobacterales that exhibit higher level resistance are designated as high priority in the 2024 WHO priority report (*39*). Of note, studying colonizing isolates overcomes biases that are intrinsic to surveillance systems reliant on passively collected clinical isolates (*40*), which is critical because colonization frequently

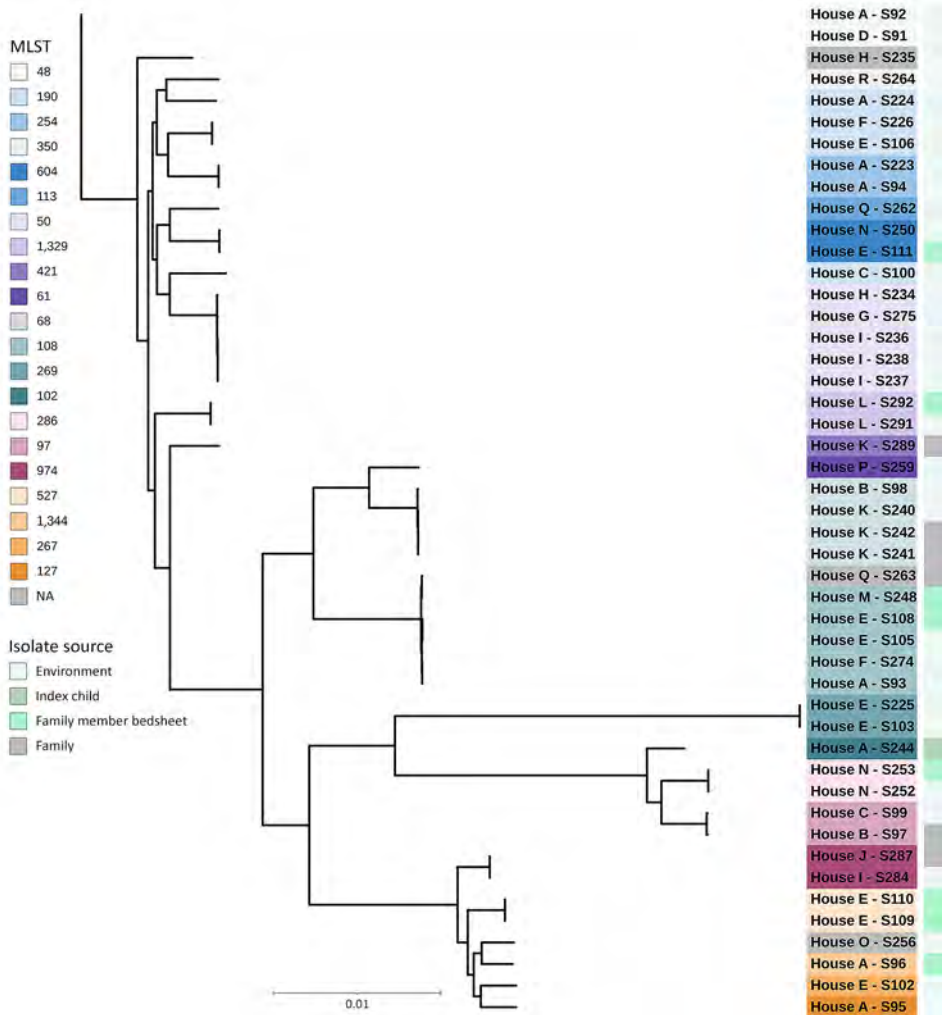

Figure. Phylogenetic tree based on core gene alignment for isolated *Enterobacter hormaechei* species (n = 47) in study of the role of households with children in community spread of multidrug-resistant Enterobacteriaceae, St. Louis, Missouri, USA. Scale bar represents nucleotide substitutions per site. MLST, multilocus sequence type; NA, not available.

precedes infection, and asymptomatic carriers can serve as sources of onward MDR organism transmission. In particular, colonization with MDR and ESCR Enterobacterales in children can last months or years, and silent dissemination of transmissible ARGs in Enterobacterales has been described in healthy pediatric populations (*41*–*43*).

We found that, in households not known to previously harbor MDR Enterobacterales, the prevalence in midwestern US communities was high, 35%. The average household size was 4.31, and 100% of households had ≥1 child. Those findings are consistent with the continued increases of ESCR Enterobacterales in community settings, despite the successes of aggressive infection prevention and control campaigns in healthcare settings (*3*,*4*). We also found the presence of other major transmissible ARGs, such as fluoroquinolone, sulfonamide, fosfomycin, and tetracycline resistance genes, along with the presence of multiple conjugative plasmids among isolates (Table 3; Appendix Table 2). Previous studies that have investigated household transmission of MDR Enterobacterales were predominately among previously hospitalized adult patients with known colonization (*6*).

Table 3. *Klebsiella pneumoniae* characteristics by isolate source in study of role of households with children in community spread of multidrug-resistant Enterobacterales, St. Louis, Missouri, USA*

Characteristic	Total, n = 10	Environmental source, n = 7	Human source, n = 3
MLST			
Unknown	2 (20)	2 (29)	0
1380	1 (10)	1 (14)	0
20	1 (10)	1 (14)	0
29	2 (20)	1 (14)	1 (33)
461	1 (10)	1 (14)	0
466	1 (10)	1 (14)	0
678	2 (20)	0	2 (67)
Median AMR gene count per isolate (IQR)	5 (4.25–5)	5 (3.5–5)	5 (5–5.5)
AMR resistance determinants			
β-lactam AMR determinants	10 (100)	32 (100)	15 (100)
bla$_{SHV}$, unspecified	2 (20)	1 (14)	1 (33)
bla$_{SHV-1}$	1 (10)	1 (14)	0
bla$_{SHV-187}$	1 (10)	1 (14)	0
bla$_{SHV-26}$	1 (10)	1 (14)	0
bla$_{SHV-33}$	1 (10)	1 (14)	0
bla$_{SHV-36}$	2 (20)	2 (29)	0
bla$_{SHV-41}$	2 (20)	0	2 (67)
bla$_{TEM-10}$	2 (20)	1 (14)	1 (33)
Fosfomycin AMR determinants	10 (100)	7 (100)	3 (100)
fosA	6 (60)	3 (43)	3 (100)
fosA10	4 (40)	4 (57)	0
Multiclass AMR determinants			
emrD	10 (100)	7 (100)	3 (100)
Phenicol/quinolone AMR determinants	7 (70)	4 (57)	3 (100)
oqxA	3 (30)	2 (29)	1 (33)
oqxA3	1 (10)	1 (14)	0
oqxA10	3 (30)	1 (14)	2 (67)
oqxB	2 (20)	0	2 (67)
oqxB19	2 (20)	2 (29)	0
oqxB25	3 (30)	2 (29)	1 (33)
Trimethoprim AMR determinants	1 (10)	1 (14)	0
dfrA50	1 (10)	1 (14)	0
Median plasmid count per isolate (IQR)	3.5 (3–4.75)	4 (3.5–5)	3 (2–3)
Plasmids			
Col440I	5 (50)	5 (71)	0
Col440II	3 (30)	3 (43)	0
IncFIB(K)	10 (100)	7 (100)	3 (100)
IncFIB(Mar)	1 (10)	1 (14)	0
IncFIB(pKPHS1)	1 (10)	1 (14)	0
IncFIB(pQil)	1 (10)	1 (14)	0
IncFII	3 (30)	1 (14)	2 (67)
IncFII(K)	8 (80)	6 (86)	2 (67)
IncFII(Yp)	1 (10)	1 (14)	0
IncHI1B	1 (10)	1 (14)	0
IncR	2 (20)	2 (29)	0
IncX5	1 (10)	1 (14)	0
repA	2 (20)	1 (14)	0

*Values are no. (%) except as indicated. AMR, antimicrobial resistance; IQR, interquartile range; MLST, multilocus sequence type.

Table 4. Multivariable logistic regression model for households with resistant Enterobacterales in study of role of households with children in community spread of multidrug-resistant Enterobacterales, St. Louis, Missouri, USA

Variable	Odds ratio (95% CI)	p value
White households	0.18 (0.06–0.49)	<0.01
Households with private insurance	0.44 (0.16–1.22)	0.11
Households with ≥1 ADHD member	3.47 (1.34–9.41)	0.01
Household with ≥1 minors and attending daycare	2.86 (1.07–8.38)	0.04
Households with ≥1 dogs	3.31 (1.27–9.41)	0.02

Although ESBL-producing *K. pneumoniae* and *P. mirabilis* were recovered from households, we did not find a major presence of ESBL-producing *E. coli*. However, we did find the presence of high-risk *E. coli* clones (e.g., ST131, ST69, ST127, ST73) known for their epidemic potential and high potential for acquiring or having ARGs and MGEs.

Of note, the *Enterobacter cloacae* complex group of bacteria are ubiquitous in nature; however, these bacteria are most found in healthcare-associated infections in hospitalized patients or persons with antimicrobial or healthcare exposures. We were surprised to see such a high level of colonization in relatively healthy community households. In addition, most of our isolates within *Enterobacter cloacae* complex were *E. hormaechei*, which is often MDR and known to cause extraintestinal healthcare-associated infections, (e.g., urinary tract, bloodstream, and pneumonia), and can persist in healthcare environments (*44*). We found evidence of clustering of *E. hormaechei* within and between households, suggesting that household and community reservoirs might be a major source of community acquisition and spread of these pathogens.

The first limitation of our study is the relatively small sample size and large number of variables. We could not study the nonlinear and nonmonotonic effects of several count variables, and the suggested multivariate model might not be optimal for the given data. However, the relatively large prevalence of Enterobacterales has shown good statistical classification power of the study population. The multivariate model with 5 covariates showed good predictive power with 81.2% area under the curve. The model classified households with 75% sensitivity and 75% specificity when the threshold was 0.35. Second, because of the relatively small sample size of non-White households, we cannot provide details about the effect modification of race and suspect that race might represent a proxy for differences in socioeconomic status in the region of study. Although we show the link between pets, in particular dog ownership, and the diagnosis of ADHD and their association with household colonization with MDR Enterobacterales, many non-White households, predominantly Black, did not have pets or family members with ADHD diagnosis, limiting the ability for further analysis of those variables. Third, the parent study of the biorepository used for this analysis was initially designed to assess *S. aureus* household colonization, and households were selected on the basis of having a healthy child who had an *S. aureus* skin and soft tissue infection. Therefore, inguinal swab specimens were used to assess for household member colonization for MDR Enterobacterales because rectal or perirectal swab specimens were not collected in the parent study. Although ideally rectal or perirectal swab specimens would have been used, prior surveillance studies have demonstrated that the main reservoir for Enterobacterales is the gastrointestinal tract, and the inguinal folds are the most colonized skin site outside of the perirectal area because of the proximity to the rectum (*45*–*49*). A military study demonstrated that the inguinal folds were the most sensitive anatomic site for detecting MDR gram-negative colonization outside of the perirectum (negative predictive value 98%–100% for ESBL Enterobacterales) (*46*). The inguinal folds in young and diapered children also have a high burden of colonization and secondary infection with bacteria because of incontinence, excess moisture, and friction (*50*). Within our study population, most households (123 of 150) had children 0–5 years of age (*4*,*16*). In addition, our finding of a 4% inguinal fold colonization rate is consistent with prior US-based pediatric studies of intestinal colonization with ESCR (4.4%) and ESBL-producing (3.5%) Enterobacterales in healthy US children collected during well child clinic visits (*42*). Finally, whereas we can demonstrate clustering within households and communities, our retrospective analysis of a single time point cannot establish timing nor directionality of transmission within or between households, surfaces, and its members.

In conclusion, households might serve as a major contributor to the acquisition and spread of MDR Enterobacterales in the community. Factors associated with household colonization with MDR Enterobacterales include having a pet dog or children who attend daycare. Our current and future prospective One Health focused studies continue to investigate community reservoirs of MDR Enterobacterales in humans, animals, the household, and the natural

environment. Our study emphasizes the necessity of investigating community reservoirs and spread of MDR Enterobacterales to learn more about how to mitigate potential sources associated with colonization and infection in the community.

Acknowledgments

We thank the team of curators of the whole-genome MLST databases and National Institutes of Health GenBank database for curating the data and making them publicly available at https://www.ncbi.nlm.nih.gov/bioproject/PRJNA1257399. Sequence data is deposited in the Sequence Read Archive (accession nos. SRR33388617–95).

L.K.L was supported in part by the National Institute of Allergy and Infectious Diseases, National Institutes of Health (grant no. R21AI173471), the Marcus Foundation, and by the Emory University School of Medicine MP3 Initiative Award Program. A.B. was supported in part by an Antibacterial Resistance Leadership Group Early Faculty Seedling Award (award no. UM1AI104681).

About the Author

Mr. Breeze is a lead research specialist in the Department of Pediatrics, Division of Pediatric Infectious Diseases, at Emory University School of Medicine. His research interests include molecular identification of antimicrobial resistance genes in human, animal, and environmental populations and understanding the role of the environment in the spread of antibiotic-resistant bacteria in the community. Dr. Babiker is an assistant professor in the Department of Internal Medicine, Division of Infectious Diseases, at Rush Medical College. His research interests include the clinical and molecular epidemiology antimicrobial resistance organisms, the surveillance of antimicrobial resistance in low- and middle-income settings, and the role of the gastrointestinal microbiome in colonization resistance.

References

1. Centers for Disease Control and Prevention. Antibiotic resistance threats in the United States, 2019. 2019 [cited 2025 Dec 8]. https://www.cdc.gov/antimicrobial-resistance/media/pdfs/2019-ar-threats-report-508.pdf
2. Price LB, Johnson JR, Aziz M, Clabots C, Johnston B, Tchesnokova V, et al. The epidemic of extended-spectrum-β-lactamase-producing *Escherichia coli* ST131 is driven by a single highly pathogenic subclone, H30-Rx. MBio. 2013;4:e00377–13. https://doi.org/10.1128/mBio.00377-13
3. Logan LK, Braykov NP, Weinstein RA, Laxminarayan R; CDC Epicenters Prevention Program. Extended-spectrum β-lactamase-producing and third-generation cephalosporin-resistant *Enterobacteriaceae* in children: trends in the United States, 1999–2011. J Pediatric Infect Dis Soc. 2014;3:320–8. https://doi.org/10.1093/jpids/piu010
4. Lukac PJ, Bonomo RA, Logan LK. Extended-spectrum β-lactamase-producing Enterobacteriaceae in children: old foe, emerging threat. Clin Infect Dis. 2015;60:1389–97. https://doi.org/10.1093/cid/civ020
5. Haverkate MR, Platteel TN, Fluit AC, Cohen Stuart JW, Leverstein-van Hall MA, Thijsen SFT, et al. Quantifying within-household transmission of extended-spectrum β-lactamase-producing bacteria. Clin Microbiol Infect. 2017;23:46.e1–7. https://doi.org/10.1016/j.cmi.2016.08.021
6. Hilty M, Betsch BY, Bögli-Stuber K, Heiniger N, Stadler M, Küffer M, et al. Transmission dynamics of extended-spectrum β-lactamase–producing Enterobacteriaceae in the tertiary care hospital and the household setting. Clin Infect Dis. 2012;55:967–75. https://doi.org/10.1093/cid/cis581
7. Logan LK, Medernach RL, Rispens JR, Marshall SH, Hujer AM, Domitrovic TN, et al. Community origins and regional differences highlight risk of plasmid-mediated fluoroquinolone-resistant Enterobacteriaceae infections in children. Pediatr Infect Dis J. 2019;38:595–9. https://doi.org/10.1097/INF.0000000000002205
8. Logan LK, Medernach RL, Domitrovic TN, Rispens JR, Hujer AM, Qureshi NK, et al. Clinical and molecular epidemiology of CTX-M-9-group-producing Enterobacteriaceae infections in children. Infect Dis Ther. 2019;8:243–54. https://doi.org/10.1007/s40121-019-0237-2
9. Freeman JT, Nimmo J, Gregory E, Tiong A, De Almeida M, McAuliffe GN, et al. Predictors of hospital surface contamination with extended-spectrum β-lactamase-producing *Escherichia coli* and *Klebsiella pneumoniae*: patient and organism factors. Antimicrob Resist Infect Control. 2014;3:5. https://doi.org/10.1186/2047-2994-3-5
10. Kramer A, Schwebke I, Kampf G. How long do nosocomial pathogens persist on inanimate surfaces? A systematic review. BMC Infect Dis. 2006;6:130. https://doi.org/10.1186/1471-2334-6-130
11. Thurlow CJ, Prabaker K, Lin MY, Lolans K, Weinstein RA, Hayden MK; Centers for Disease Control and Prevention Epicenters Program. Anatomic sites of patient colonization and environmental contamination with *Klebsiella pneumoniae* carbapenemase–producing Enterobacteriaceae at long-term acute care hospitals. Infect Control Hosp Epidemiol. 2013;34:56–61. https://doi.org/10.1086/668783
12. Hogan PG, Mork RL, Boyle MG, Muenks CE, Morelli JJ, Thompson RM, et al. Interplay of personal, pet, and environmental colonization in households affected by community-associated methicillin-resistant *Staphylococcus aureus*. J Infect. 2019;78:200–7. https://doi.org/10.1016/j.jinf.2018.11.006
13. Mork RL, Hogan PG, Muenks CE, Boyle MG, Thompson RM, Morelli JJ, et al. Comprehensive modeling reveals proximity, seasonality, and hygiene practices as key determinants of MRSA colonization in exposed households. Pediatr Res. 2018;84:668–76. https://doi.org/10.1038/s41390-018-0113-x
14. Fritz SA, Hogan PG, Singh LN, Thompson RM, Wallace MA, Whitney K, et al. Contamination of environmental surfaces with *Staphylococcus aureus* in households with children infected with methicillin-resistant *S aureus*. JAMA Pediatr. 2014;168:1030–8. https://doi.org/10.1001/jamapediatrics.2014.1218
15. Mork RL, Hogan PG, Muenks CE, et al. Longitudinal, strain-specific *Staphylococcus aureus* introduction and transmission events in households of children with community-associated MRSA skin and soft-tissue infection: a prospective cohort study. Lancet Infect Dis. 2020;20:188–98. https://doi.org/10.1016/S1473-3099(19)30570-5

16. Kaarme J, Riedel H, Schaal W, Yin H, Nevéus T, Melhus Å. Rapid increase in carriage rates of Enterobacteriaceae producing extended-spectrum β-lactamases in healthy preschool children, Sweden. Emerg Infect Dis. 2018;24:1874–81. https://doi.org/10.3201/eid2410.171842
17. van den Bunt G, Fluit AC, Spaninks MP, Timmerman AJ, Geurts Y, Kant A, et al. Faecal carriage, risk factors, acquisition and persistence of ESBL-producing Enterobacteriaceae in dogs and cats and co-carriage with humans belonging to the same household. J Antimicrob Chemother. 2020;75:342–50. https://doi.org/10.1093/jac/dkz462
18. Harris PA, Taylor R, Thielke R, Payne J, Gonzalez N, Conde JG. Research electronic data capture (REDCap)—a metadata-driven methodology and workflow process for providing translational research informatics support. J Biomed Inform. 2009;42:377–81. https://doi.org/10.1016/j.jbi.2008.08.010
19. Perry JD. A decade of development of chromogenic culture media for clinical microbiology in an era of molecular diagnostics. Clin Microbiol Rev. 2017;30:449–79. https://doi.org/10.1128/CMR.00097-16
20. Logan LK, Hujer AM, Marshall SH, Domitrovic TN, Rudin SD, Zheng X, et al. Analysis of β-lactamase resistance determinants in *Enterobacteriaceae* from Chicago children: a multicenter survey. Antimicrob Agents Chemother. 2016;60:3462–9. https://doi.org/10.1128/AAC.00098-16
21. Petit RA III, Read TD. Bactopia: a flexible pipeline for complete analysis of bacterial genomes. mSystems. 2020;5:e00190–20. https://doi.org/10.1128/mSystems.00190-20
22. Bolger AM, Lohse M, Usadel B. Trimmomatic: a flexible trimmer for Illumina sequence data. Bioinformatics. 2014;30:2114–20. https://doi.org/10.1093/bioinformatics/btu170
23. Prjibelski A, Antipov D, Meleshko D, Lapidus A, Korobeynikov A. Using SPAdes de novo assembler. Curr Protoc Bioinformatics. 2020;70:e102. https://doi.org/10.1002/cpbi.102
24. Hyatt D, Chen GL, Locascio PF, Land ML, Larimer FW, Hauser LJ. Prodigal: prokaryotic gene recognition and translation initiation site identification. BMC Bioinformatics. 2010;11:119. https://doi.org/10.1186/1471-2105-11-119
25. Seemann T. Prokka: rapid prokaryotic genome annotation. Bioinformatics. 2014;30:2068–9. https://doi.org/10.1093/bioinformatics/btu153
26. Feldgarden M, Brover V, Haft DH, Prasad AB, Slotta DJ, Tolstoy I, et al. Validating the AMRFinder tool and resistance gene database using antimicrobial resistance genotype–phenotype correlations. Antimicrob Agents Chemother. 2019;63:e00483–19. https://doi.org/10.1128/AAC.00483-19
27. Page AJ, Cummins CA, Hunt M, Wong VK, Reuter S, Holden MT, et al. Roary: rapid large-scale prokaryote pan genome analysis. Bioinformatics. 2015;31:3691–3. https://doi.org/10.1093/bioinformatics/btv421
28. Nguyen LT, Schmidt HA, von Haeseler A, Minh BQ. IQ-TREE: a fast and effective stochastic algorithm for estimating maximum-likelihood phylogenies. Mol Biol Evol. 2015;32:268–74. https://doi.org/10.1093/molbev/msu300
29. Letunic I, Bork P. Interactive tree of life (iTOL) v5: an online tool for phylogenetic tree display and annotation. Nucleic Acids Res. 2021;49(W1):W293–6. https://doi.org/10.1093/nar/gkab301
30. Seemann T. snp-dists: pairwise SNP distance matrix from a FASTA sequence alignment. GitHub [cited 2025 Oct 9]. https://github.com/tseemann/snp-dists
31. Brynildsrud O, Bohlin J, Scheffer L, Eldholm V. Rapid scoring of genes in microbial pan-genome-wide association studies with Scoary. Genome Biol. 2016;17:238. https://doi.org/10.1186/s13059-016-1108-8
32. Robertson J, Nash JHE. MOB-suite: software tools for clustering, reconstruction and typing of plasmids from draft assemblies. Microb Genom. 2018;4:e000206. https://doi.org/10.1099/mgen.0.000206
33. Agresti A. Categorical data analysis. 2nd ed. Hoboken (NJ): John Wiley & Sons; 2002.
34. Tibshirani R. Regression shrinkage and selection via the Lasso. J R Stat Soc Series B Stat Methodol. 1996;58:267–88. https://doi.org/10.1111/j.2517-6161.1996.tb02080.x
35. Tibshirani R. The lasso method for variable selection in the Cox model. Stat Med. 1997;16:385–95. https://doi.org/10.1002/(SICI)1097-0258(19970228)16:4<385::AID-SIM380>3.0.CO;2-3
36. Cavanaugh JE, Neath AA. The Akaike information criterion: background, derivation, properties, application, interpretation, and refinements. Wiley Interdiscip Rev Comput Stat. 2019;11:e1460. https://doi.org/10.1002/wics.1460
37. Neath AA, Cavanaugh JE. The Bayesian information criterion: background, derivation, and applications. Wiley Interdiscip Rev Comput Stat. 2012;4:199–203. https://doi.org/10.1002/wics.199
38. Adisasmito WB, Almuhairi S, Behravesh CB, Bilivogui P, Bukachi SA, Casas N, et al.; One Health High-Level Expert Panel (OHHLEP). One Health: a new definition for a sustainable and healthy future. PLoS Pathog. 2022;18:e1010537. https://doi.org/10.1371/journal.ppat.1010537
39. Sati H, Carrara E, Savoldi A, Hansen P, Garlasco J, Campagnaro E, et al.; WHO Bacterial Priority Pathogens List Advisory Group. The WHO bacterial priority pathogens list 2024: a prioritisation study to guide research, development, and public health strategies against antimicrobial resistance. Lancet Infect Dis. 2025;25:1033–43. https://doi.org/10.1016/S1473-3099(25)00118-5
40. Duffy N, Karlsson M, Reses HE, Campbell D, Daniels J, Stanton RA, et al. Epidemiology of extended-spectrum β-lactamase–producing Enterobacterales in five US sites participating in the emerging infections program, 2017. Infect Control Hosp Epidemiol. 2022;43:1586–94. https://doi.org/10.1017/ice.2021.496
41. Zerr DM, Qin X, Oron AP, Adler AL, Wolter DJ, Berry JE, et al. Pediatric infection and intestinal carriage due to extended-spectrum-cephalosporin-resistant *Enterobacteriaceae*. Antimicrob Agents Chemother. 2014;58:3997–4004. https://doi.org/10.1128/AAC.02558-14
42. Islam S, Selvarangan R, Kanwar N, McHenry R, Chappell JD, Halasa N, et al. Intestinal carriage of third-generation cephalosporin-resistant and extended-spectrum β-lactamase–producing *Enterobacteriaceae* in healthy US children. J Pediatric Infect Dis Soc. 2018;7:234–40. https://doi.org/10.1093/jpids/pix045
43. Logan LK, Coy LR, Pitstick CE, Marshall SH, Medernach RL, Domitrovic TN, et al. The role of the plasmid-mediated fluoroquinolone resistance genes as resistance mechanisms in pediatric infections due to Enterobacterales. Front Cell Infect Microbiol. 2023;13:1249505. https://doi.org/10.3389/fcimb.2023.1249505
44. Yeh TK, Lin HJ, Liu PY, Wang JH, Hsueh PR. Antibiotic resistance in *Enterobacter hormaechei*. Int J Antimicrob Agents. 2022;60:106650. https://doi.org/10.1016/j.ijantimicag.2022.106650
45. Catho G, Huttner BD. Strategies for the eradication of extended-spectrum beta-lactamase or carbapenemase-

producing Enterobacteriaceae intestinal carriage. Expert Rev Anti Infect Ther. 2019;17:557–69. https://doi.org/10.1080/14787210.2019.1645007
46. Weintrob AC, Roediger MP, Barber M, Summers A, Fieberg AM, Dunn J, et al. Natural history of colonization with gram-negative multidrug-resistant organisms among hospitalized patients. Infect Control Hosp Epidemiol. 2010;31:330–7. https://doi.org/10.1086/651304
47. Tschudin-Sutter S, Frei R, Dangel M, Stranden A, Widmer AF. Sites of colonization with extended-spectrum β-lactamases (ESBL)-producing Enterobacteriaceae: the rationale for screening. Infect Control Hosp Epidemiol. 2012;33:1170–1. https://doi.org/10.1086/668027
48. Shimasaki T, Seekatz A, Bassis C, Rhee Y, Yelin RD, Fogg L, et al.; Centers for Disease Control and Prevention Epicenters Program. Increased relative abundance of *Klebsiella pneumoniae* carbapenemase-producing *Klebsiella pneumoniae* within the gut microbiota is associated with risk of bloodstream infection in long-term acute-care hospital patients. Clin Infect Dis. 2019;68:2053–9. https://doi.org/10.1093/cid/ciy796
49. Huttner B, Haustein T, Uçkay I, Renzi G, Stewardson A, Schaerrer D, et al. Decolonization of intestinal carriage of extended-spectrum β-lactamase-producing Enterobacteriaceae with oral colistin and neomycin: a randomized, double-blind, placebo-controlled trial. J Antimicrob Chemother. 2013;68:2375–82. https://doi.org/10.1093/jac/dkt174
50. Janniger CK, Schwartz RA, Szepietowski JC, Reich A. Intertrigo and common secondary skin infections. Am Fam Physician. 2005;72:833–8.

Address for correspondence: Latania Logan, Emory University School of Medicine, 1760 Haygood Dr NE, Ste N448, Atlanta, GA 30322, USA; email: lklogan@emory.edu

In Vitro Antifungal Drug Susceptibility of Feline *Sporothrix schenckii* Complex Isolates, Thailand, 2023–2025

Chompoonek Yurayart, Kanokporn Yingchanakiat, Amonrat Thongbai, Orawan Limsivilai, Sathidpak Nantasanti Assawarachan, Tassanee Jaroensong, Panpicha Sattasathuchana

Feline sporotrichosis is a public health concern because it is a zoonotic illness and has a prolonged treatment time. We report laboratory-confirmed cases of feline *Sporothrix schenckii* complex infection submitted to a laboratory in Thailand during 2023–2025 and evaluate their in vitro antifungal drug susceptibility profiles for amphotericin B, itraconazole, posaconazole, voriconazole, ketoconazole, fluconazole, and flucytosine. A total of 1,178 *S. schenckii* complex isolates were identified. Overall, 368 isolates did not show reduced susceptibility. We observed single-drug reduced susceptibility to amphotericin B (60 isolates), posaconazole (41 isolates), voriconazole (9 isolates), and terbinafine (4 isolates). We observed a reduced susceptibility to itraconazole in 687 isolates: 321 single-drug, 270 co-reduced, and 96 multidrug-reduced isolates. An increasing number of feline sporotrichosis cases and escalating reduced susceptibility to itraconazole underscore the need for continued surveillance and susceptibility testing to support management in complex cases.

Sporothrix schenckii complex is a group of genetically related fungi within the genus *Sporothrix*, which includes *S. schenckii* sensu stricto, *S. brasiliensis*, *S. globosa*, *S. mexicana*, *S. luriei*, and *S. albicans* (*1*). *S. schenckii* are thermal dimorphic pathogens that live and grow in mold form in the environment (*1*,*2*). Humans and animals become infected through the implantation of spores from contaminated materials into subcutaneous tissue through cuts and scratches; the fungus then converts to yeast form within the host tissue (*2*). *S. schenckii* complex causes sporotrichosis in humans and animals; cats are the most susceptible species. The geographic distribution, pathogenicity, clinical manifestations, virulence, and antifungal drug susceptibility differ among species. *S. brasiliensis* is the most virulent and highly prevalent, causing animal sporotrichosis and zoonotic infections in Brazil and other South American countries. *S. globosa* is an emerging human pathogen in China and India, and human infection occurs through environmental transmission (*3*–*5*). *S. schenckii* s.s. has occasionally been reported as causing environmentally acquired infection globally. However, a specific clade of *S. schenckii* s.s. has recently emerged among cats in Thailand, and reports of cat-to-cat and cat-to-human transmission are increasing (*6*–*8*). Cats with sporotrichosis exhibit multiple ulcerative mucosal and cutaneous lesions. Infected cats can shed infectious yeast organisms through saliva, nasal secretions, wound exudates, and scratches or bites to humans, cats, and other species (*9*). Cats serve as a major reservoir and highly efficient transmitter of sporotrichosis (*9*,*10*).

The effective treatment of infected cats with antifungal drugs is essential for controlling feline sporotrichosis. Performing antifungal drug susceptibility testing and analyzing the MIC values of endemic strains are necessary for monitoring antifungal drug susceptibility patterns. Clinical decisions are typically made on the basis of established clinical breakpoints; however, the clinical breakpoints for *Sporothrix* spp. are currently unavailable (*11*). Therefore, characterizing wild-type (WT) or non–wild-type (non-WT) isolates on the basis of the epidemiologic cutoff values (ECVs) is useful for surveillance of emerging antifungal drugs resistance (*12*). WT isolates have no resistance mechanisms and typically exhibit expected antifungal drugs susceptibility profiles, whereas non-WT strains have shown evidence of acquired or mutational

Authors affiliation: Faculty of Veterinary Medicine, Kasetsart University, Bangkok, Thailand

DOI: https://doi.org/10.3201/eid3206.260135

changes, which reduce their susceptibility to antifungal drugs and are associated with higher MICs. Sporotrichosis treatment requires the use of antifungal drugs for several months, which might lead to antifungal drug resistance in clinical cases. Itraconazole is the antifungal drug of choice and the first-line treatment for sporotrichosis (*13*,*14*). Other antifungal drugs, including azoles (i.e., fluconazole, ketoconazole, posaconazole, and voriconazole), polyene (i.e., amphotericin B), pyrimidine analog (i.e., flucytosine), and allylamine (i.e., terbinafine), have also been used as combination therapies for human and feline sporotrichosis and other dimorphic fungal infections to shorten the treatment duration and improve clinical outcomes (*13*,*15*–*17*). Data on antifungal drug susceptibility from feline *S. schenckii* s.s. isolates in Thailand (2018–2021) reported in 2022 and 2023 (*6*,*18*) showed that prolonged treatment and frequent combination therapy might alter susceptibility patterns and lead to more complex resistance. We report laboratory-confirmed cases of feline sporotrichosis in Thailand from 2023–2025; characterize the in vitro antifungal drugs susceptibility profiles of *S. schenckii* complex isolates from cats in Thailand to amphotericin B, itraconazole, posaconazole, voriconazole, terbinafine, ketoconazole, fluconazole, and flucytosine; define the WT population of those isolates from 2023–2025; and determine the cross-reduced susceptibility patterns of itraconazole and other antifungal drugs.

Materials and Methods

Fungal Isolates and Data Collection

All the sample collection and handling procedures were approved by the Institutional Animal Care and Use Committee at Kasetsart University (approval no. ACKU68-VET-085). Clinical samples from cats suspected of feline sporotrichosis, submitted during 2023–2025 from veterinary clinics nationwide to the Department of Microbiology and Immunology, Faculty of Veterinary Medicine, Kasetsart University, Bangkok, were included.

We inoculated wound swab samples collected from cats with ulcerated cutaneous lesions in Sabouraud dextrose agar (SDA) at 30°C and brain–heart infusion agar containing gentamicin (50 mg/L; General Drugs House, https://generaldrugshouse.com) at 35°C for 5–14 days. We identified the causative agent as *S. schenckii* complex on the basis of its thermal dimorphic characteristics: a yeast form on brain–heart infusion agar at 35°C and a mold form as a hyaline septate fungus with a flower-like arrangement of the rosette and sessile conidia on SDA at 30°C. We subcultured and stored the isolates in sterile water for further antifungal drug susceptibility testing. For each cat, we obtained data on the age, sex, breed, body weight, and retrovirus-infected status (feline leukemia virus [FeLV] and feline immunodeficiency virus [FIV]) from hospital database and sample submission.

Antifungal Drug Susceptibility Testing

We tested the *S. schenckii* complex isolates for their susceptibility to 8 antifungal drugs: amphotericin B, itraconazole, posaconazole, voriconazole, ketoconazole, terbinafine, fluconazole, and flucytosine. We performed antifungal drug susceptibility testing by using the broth microdilution method (BMD) according to Clinical and Laboratory Standards Institute (CLSI) for filamentous fungi guidelines (CLSI M38-A3) (*19*,*20*). The final concentrations of all the drugs assigned for testing were 0.06–32 μg/mL for amphotericin B, itraconazole, and posaconazole; 0.12–64 μg/mL for voriconazole; 0.015–8 μg/mL for terbinafine and ketoconazole; and 0.5–256 μg/mL for fluconazole and flucytosine. We sourced the antifungal drugs from MilliporeSigma (Sigma Aldrich, https://www.sigmaaldrich.com). We performed antifungal drug susceptibility testing against the mold form of the *S. schenckii* complex isolates as described previously (*6*). We dissolved the antifungal drugs according to CLSI M38-A3 (*20*) and diluted in Roswell Park Memorial Institute 1640 medium (Invitrogen, https://www.invitrogen.com) buffered to a pH of 7.0 with 0.65 M of 3-(N-morpholino)-propanesulfonic acid (MOPS) buffer (Millipore Sigma) with L-glutamine and without bicarbonate to achieve 2× the final concentration of each drug. We then loaded the solution into 96-well U-shaped microplates. We harvested a conidia suspension from the 3-day-old cultures growing on SDA at 30°C and adjusted the cell density to an absorbance of 0.09–0.11 at 530 nm and diluted at 1:50 in an RPMI 1640 culture medium to obtain the final cell concentration necessary for testing. We incubated the inoculated microplate at 35°C for 72 hours and determined the MIC visually. We included *Candida parapsilosis* ATCC 22019 to verify the accuracy of antifungal drug concentrations and potency in BMD plates but not as a quality control strain for filamentous fungi susceptibility testing.

Antifungal Drug Susceptibility Analysis and Interpretation

To enable the parallel evaluation of the ECVs with those previously reported (*21*), we analyzed the MIC values of the isolates from Thailand. We

calculated the MICs required to inhibit 50% (MIC_{50}), 90% (MIC_{90}), 95% (MIC_{95}), 97.5% ($MIC_{97.5}$), and 99% (MIC_{99}) of the tested isolates. In addition, we determined the statistic mode by the highest frequency of MIC value for each antifungal drug. We identified the non-WT isolates as *S. schenckii* isolates with MIC values higher than the ECVs previously reported for amphotericin B (4 μg/mL), itraconazole (2 μg/mL), posaconazole (2 μg/mL), and voriconazole (64 μg/mL). The ECV for terbinafine has not yet been established; therefore, we defined a study-specific cutoff for terbinafine by statistical cutoff value at $MIC_{97.5}$, according to CLSI M57 guidelines (*22*).

We used JMP Pro version 10 (SAS Institute, https://www.sas.com), GraphPad Prism version 9.0 (GraphPad, https://www.graphpad.com), and Stata version 14.2 (StataCorp, LLC, https://www.stata.com) for statistical analyses. We used Fisher exact test to assess the associations between the retroviral infections and non-WT populations. We also determined the associations between the non-WT isolates among the antifungal drugs. We considered results statistically significant when $p<0.05$.

Table 1. Demographic characteristics of 1,178 cats with sporotrichosis in Thailand, 2023–2025*

Parameter	Cats with sporotrichosis
Total no.	1,178
Age, y	
Median (range)	3.0 (0.1–21.3)
Mean ±SD	4.0 ±3.3
Sex	
Female	428 (36.3)
Male	715 (60.7)
Unknown	35 (3.0)
Breed	
American shorthair	2 (0.2)
Bengal	1 (0.1)
British shorthair	4 (0.3)
Domestic shorthair	1,079 (91.6)
Munchkin	2 (0.2)
Persian	27 (2.3)
Scottish fold	26 (2.2)
Unknown	36 (3.1)
Bodyweight, kg	
Median (range)	3.8 (0.5–9.4)
Mean ±SD	3.83 ± 1.3
Retrovirus infection test, total no.	253
FeLV or FIV negative	182 (71.9)
FeLV or FIV positive	71 (28.1)

*Values are no. (%) except as indicated. FeLV, feline leukemia virus; FIV, feline immunodeficiency virus

Results

We identified 1,178 *S. schenckii* complex isolates over the 3-year sampling period. Of those, in 2023 we recovered 225 isolates, in 2024 we recovered 383 isolates, and in 2025 we recovered 570 isolates. The demographic characteristics of cats with *S. schenckii* complex (Table 1) included mean ±SD age of 4.0 ±3.3 years and mean ±SD bodyweight of 3.83 ±1.3 kg. Most of the cats were male (60.7%) and domestic shorthairs (91.6%). Retroviral testing was performed on 253 cats, of which 28.1% were positive for FeLV or FIV.

We determined the MIC_{50}, MIC_{90}, MIC_{95}, $MIC_{97.5}$, MIC_{99}, and mode MIC values for all tested antifungal drugs (Table 2). Amphotericin B demonstrated MIC values ranging from 4 μg/mL (MIC_{50}) to 16 μg/mL (MIC_{99}). Itraconazole and posaconazole exhibited high MIC values, with MIC_{50} values of 8 μg/mL (itraconazole) and 1 μg/mL (posaconazole), and MIC_{90}–MIC_{99} exceeding 32 μg/mL. Voriconazole exhibited MIC values from 32 μg/mL (MIC_{50}) to ≥64 μg/mL (MIC_{99}), whereas the MIC values for terbinafine ranged from 1 μg/mL (MIC_{50}) to 8 μg/mL (MIC_{99}). The MIC values were between 0.5–4 μg/mL for ketoconazole. Fluconazole and flucytosine had consistently high MIC values, with MIC_{50} to MIC_{99} ≥64 μg/mL. The study-specific cutoff for terbinafine was assigned as 4 μg/mL according to $MIC_{97.5}$.

We observed a predominance of WT isolate susceptibility toward amphotericin B (79.0%), posaconazole (73.9%), voriconazole (97.3%), and terbinafine (98.2%). In contrast, itraconazole revealed a predominance of non-WT isolate susceptibility (58.3%). The distribution of MIC values for amphotericin B,

Table 2. Antifungal drug susceptibility profiles of 8 antifungal drugs against 1,178 *Sporothrix schenckii* complex isolates in Thailand, 2023–2025*

	MICs, μg/mL						
Antifungal drug	Range	Mode	MIC_{50}	MIC_{90}	MIC_{95}	$MIC_{97.5}$	MIC_{99}
Amphotericin B	0.06–>32	4 (WT)	4 (WT)	8 (non-WT)	8 (non-WT)	8 (non-WT)	16 (non-WT)
Itraconazole	0.06–>32	>32 (non-WT)	8 (non-WT)	>32 (non-WT)	>32 (non-WT)	>32 (non-WT)	>32 (non-WT)
Posaconazole	0.06–>32	1 (WT)	1 (WT)	>32 (non-WT)	>32 (non-WT)	>32 (non-WT)	>32 (non-WT)
Voriconazole	0.5–>64	64 (WT)	32 (WT)	64 (WT)	64 (WT)	>64 (non-WT)	>64 (non-WT)
Terbinafine	0.015–>8	1 (WT)	1 (WT)	2 (WT)	4 (WT)	4 (WT)	8 (non-WT)
Ketoconazole	0.015–>8	1	0.5	2	2	2	4
Fluconazole	1–>256	>256	>256	>256	>256	>256	>256
Flucytosine	0.5–>256	64	64	>256	>256	>256	>256

*Mode is the MIC that occurs most frequently. MIC_{50}, MIC_{90}, MIC_{95}, $MIC_{97.5}$, and MIC_{99} values are reported as the minimum concentrations of antifungal drugs required to inhibit 50%, 90%, 95%, 97.5%, and 99% of the growth of *S. schenckii* complex isolates. Susceptibility phenotypes were characterized on the basis of available epidemiologic cutoff values (*21*) and study-specific cutoff value (for terbinafine). Non-WT, non-wild-type; WT, wild-type.

itraconazole, posaconazole, voriconazole, and terbinafine and MICs for antifungal drugs that do not have designated ECVs for *S. schenckii* complex are provided (Table 3).

We did not find an association between retroviral infections and non-WT isolates for amphotericin B (p = 0.2367), itraconazole (p = 0.2569), posaconazole (p = 0.2367), voriconazole (p>0.9999), and terbinafine (p>0.9999). We observed significant associations between non-WT itraconazole isolates and non-WT isolates for amphotericin B (p<0.0001), posaconazole (p<0.0001), and terbinafine (p = 0.0428). The non-WT posaconazole isolates were also significantly associated with the non-WT isolates for amphotericin B (p<0.0001) and terbinafine (p = 0.0005).

We did not observe reduced susceptibility to any of the tested antifungal drugs in 368 isolates (31.2%). We observed single-drug reduced susceptibility to amphotericin B in 60 isolates, to posaconazole in 41 isolates, to voriconazole in 9 isolates, and to terbinafine in 4 isolates. We also observed cross-reduced susceptibility in 8 isolates between amphotericin B and posaconazole, and 1 isolate demonstrated cross-reduced susceptibility between amphotericin B and voriconazole. For itraconazole, 491 isolates showed no reduced susceptibility pattern, whereas 687 isolates exhibited reduced susceptibility. We observed single-drug reduced susceptibility to itraconazole in 321 isolates. We identified co-reduced susceptibility with itraconazole in 270 isolates and observed multidrug reduced susceptibility to itraconazole in 96 isolates (Table 4).

Discussion

We phenotypically identified 1,178 feline *S. schenckii* complex isolates by fungal culture and determined them to have in vitro antifungal drug susceptibilities. Only 31.2% of all the isolates were susceptible to all the tested drugs. Terbinafine, voriconazole, amphotericin B, and posaconazole exhibited high efficacy, whereas itraconazole had limited efficacy. No association was apparent between the retroviral infections and non-WT isolates for amphotericin B, itraconazole, posaconazole, voriconazole, and terbinafine. Various patterns of Various patterns of in vitro reduced susceptibility to antifungal drugs were characterized in this study, including single-drug reduced, co-reduced, and multidrug reduced susceptibility.

Samples were obtained from client-owned cats taken to veterinary clinics and with suspected feline sporotrichosis. Specimens were collected by attending veterinarians for routine diagnostic procedures. During 2023–2025, the number of cats diagnosed with sporotrichosis in Thailand increased steadily: 225 cases in 2023, increasing to 383 cases in 2024 and 570 cases in 2025. Reported cases represent laboratory-confirmed infections. Not all infected cats might have undergone confirmatory testing. As a result, the number of cases reported in this study likely underestimates the true number of feline sporotrichosis infections in Thailand. Although samples were submitted from multiple veterinary clinics across the country, geographic distribution was not analyzed in this study. Further epidemiologic studies are warranted to better

Table 3. MIC distribution and susceptibility phenotypes for 8 antifungal drugs against 1,178 *Sporothrix schenckii* complex isolates in Thailand, 2023–2025*

Antifungal drugs	Susceptibility phenotypes		Distribution of MICs, µg/mL															
	WT	Non-WT	0.015	0.03	0.06	0.12	0.25	0.5	1	2	4	8	16	32	64	128	256	>256
Amphotericin B	931 (79.0)	247 (21.0)	NA	NA	3	6	27	70	48	187	**590**	234	9	2	2‡	NA	NA	NA
Itraconazole	491 (41.7)	687 (58.3)	NA	NA	3	3	38	86	159	202	104	70	40	24	**449**‡	NA	NA	NA
Posaconazole	870 (73.9)	308 (26.2)	NA	NA	1	3	69	165	**388**	244	45	169	12	9	73‡	NA	NA	NA
Voriconazole	936 (97.3)	26 (2.7)	NA	NA		0	0	3	9	18	61	193	171	236	**245**	26‡	NA	NA
Terbinafine§	1,157 (98.2)	21 (1.8)	2	2	11	42	198	330	**333**	168	71	14	7‡	NA	NA	NA	NA	NA
Ketoconazole	ND	ND	4	3	18	71	177	304	**379**	187	31	3	1‡	NA	NA	NA	NA	NA
Fluconazole	ND	ND	NA	NA	NA	NA	NA	0	1	0	1	4	1	2	6	48	131	**984**‡
Flucytosine	ND	ND	NA	NA	NA	NA	NA	4	0	5	29	70	85	209	**246**	197	114	3‡

*Values are no. (%) except as indicated. Bold indicates highest number in each row (mode). Gray shading indicates non-WT. NA, not available because it was not tested; ND, not determined because of the lack of an epidemiologic cutoff value and the drug not being commonly used; non-WT, non-wild-type; WT, wild-type.
†The MIC is compared with the *S. schenckii* epidemiologic cutoff value (*21*).
‡The MICs were greater than the highest tested concentration (>X µg/mL). X was replaced with the actual maximum concentration of each drug (e.g., >32 µg/mL).
§Terbinafine susceptibility phenotypes are characterized by a study-specific cutoff value based on data in the study, that is, the MIC of antifungal drugs required to inhibit 97.5% of the growth of *S. schenckii* complex isolates (4 µg/mL).

Table 4. Distribution of non-WT phenotypes and antifungal drugs with co-reduced susceptibility patterns based on itraconazole susceptibility among feline *Sporothrix schenckii* complex isolates in Thailand, 2023–2025 (n = 1,178)

Itraconazole susceptibility phenotype	No. drugs, non-WT	Itraconazole reduced susceptibility patterns	Frequency	Overall
WT	0	None	491 (41.7)	491 (41.7)
Non-WT	1	Itraconazole	321 (27.2)	321 (27.2)
	2	Itraconazole + posaconazole	165 (14.0)	270 (22.9)
		Itraconazole + amphotericin B	94 (8.0)	
		Itraconazole + voriconazole	7 (0.6)	
		Itraconazole + terbinafine	4 (0.3)	
	3	Itraconazole + posaconazole + amphotericin B	74 (6.3)	88 (7.5)
		Itraconazole + posaconazole + terbinafine	7 (0.6)	
		Itraconazole + posaconazole + voriconazole	5 (0.4)	
		Itraconazole + voriconazole + amphotericin B	2 (0.2)	
	4	Itraconazole + posaconazole + amphotericin B + terbinafine	6 (0.5)	8 (0.7)
		Itraconazole + posaconazole + amphotericin B + voriconazole	2 (0.2)	

*Values are no. (%) except as indicated. Non-WT is defined by previously reported epidemiologic cutoff values (*21*) and study-specific cutoff value (for terbinafine). Non-WT, non-wild-type; WT, wild-type.

define the incidence and prevalence of feline sporotrichosis in Thailand.

In this study, most of the cats were young adult, male, and domestic shorthair cats that were seronegative for FeLV and FIV. Those findings align with previously reported cases of 38 cats with sporotrichosis in Thailand during 2020–2022 (*6*). Young adult male cats exhibit roaming behaviors, which increases their exposure to pathogens. No specific breed has shown a predisposition for *S. schenckii* complex, and all cat breeds can be infected with this pathogen (*6*). The predominance of domestic shorthair cats likely reflects their high ownership in Thailand (*23*). Although retrovirus infections impair immune function by reducing the CD4+/CD8+ lymphocyte ratio (*24*), we found no association between the isolates from cats with seropositive retrovirus and those with non-WT phenotypes. The occurrence of non-WT *S. schenckii* complex isolates might be associated with virulent strains or prior antifungal drug exposure, rather than the underlying immune status of the host.

We used the CLSI M38-A3 BMD method as the reference standard for the surveillance of drug susceptibility in *Sporothrix* spp.; however, its complexity and the need for microbiological expertise limit its use in routine clinical settings. Commercially available antifungal drugs susceptibility testing platforms have limitations. The Vitek 2 (bioMérieux, https://www.biomerieux.com) automated system is widely used for antifungal drug susceptibility testing of *Candida* spp. and *Cryptococcus* spp. (*25*). The Vitek 2 has limited applicability for *Sporothrix* spp. because of the dimorphic nature and slow growth kinetics of the species. Likewise, discordance between Sensititer YeastOne (Thermo Fisher Scientific, https://www.thermofisher.com) and the CLSI reference method has been reported (*26*). The Sensititer YeastOne panel lacks key antifungal drugs, including terbinafine, which is the second-line treatment recommended drug for sporotrichosis (*26*,*27*). Using the CLSI M38-A reference method is essential for establishing an accurate baseline of antifungal drug susceptibility, particularly because of the increasing number of sporotrichosis cases in Thailand. The future development of user-friendly commercial antifungal drug susceptibility testing platforms for *Sporothrix* spp. would support the routine diagnosis and clinical management of sporotrichosis among physicians and veterinarians.

In this study, we applied established ECVs for *S. schenckii* complex to distinguish between the WT and non-WT MIC distributions for amphotericin B, itraconazole, posaconazole, and voriconazole (*21*). A study-specific cutoff at $MIC_{97.5}$ was used to characterize the susceptibility profile of the feline *S. schenckii* complex isolates from Thailand to terbinafine. Most of the testing isolates were obtained from clinical cases that were unresponsive to prior antifungal drug therapy or were specifically submitted for MIC testing to guide veterinarians' clinical decision-making. The high MIC values observed might reflect a subset of reduced susceptibility or clinically challenging strains rather than the baseline susceptibility of feline *S. schenckii* complex isolates from Thailand.

Itraconazole demonstrated a remarkably reduced efficacy compared with previous data from an earlier outbreak in Thailand (*6*,*8*). In this study, most of the isolates were classified as non-WT to itraconazole by MIC_{50} and exhibited reduced susceptibility (MIC_{90} >32 μg/mL), which contrasts with previous findings in which most of the isolates were WT with MIC_{50} at 0.5 μg/mL and non-WT with MIC_{90} at 4 μg/mL (*6*). The reduced susceptibility to itraconazole phenotypes we observed were reflected in the 16-fold increase in MIC_{50} and >8-fold increase in MIC_{90}; a ≥4-fold increase in these values is indicative of acquired reduced susceptibility in non-WT strains (*12*,*28*,*29*).

Our findings align with previously reported MICs from feline and human isolates from Thailand that exhibited reduced susceptibility to itraconazole and identified non-WT isolates (*7*,*10*,*18*). Furthermore, among the itraconazole non-WT isolates, a high rate (31.1%) of cross-reduced susceptibility and multidrug reduced susceptibility was detected, with prominent reduced susceptibility to itraconazole/posaconazole and itraconazole/amphotericin B and the multidrug combination of itraconazole, posaconazole, and amphotericin B. Cross-reduced susceptibility between itraconazole and posaconazole is often documented because both azole drugs share a common molecular target and overlapping binding sites within the ergosterol biosynthesis pathway (*12*). Moreover, the widespread use of itraconazole in feline sporotrichosis in Thailand often involves prolonged or inconsistent dosing because of multiple factors, including drug cost, bioavailability, owner compliance, difficulties in administering medication to cats, zoonotic concerns, and adverse effects. antifungal drug treatment is not subsidized, and financial constraints might affect treatment continuity. In addition, limited access to veterinary care for stray cats and the absence of structured control programs might contribute to ongoing transmission. Those challenges can lead to treatment interruption or incomplete therapy, which might promote reduced susceptibility and multidrug resistance (*12*,*30*–*33*).

A reduction in susceptibility to amphotericin B is a concern. We found that the MIC_{50} had shifted 8-fold (from 0.5 to 4 μg/mL) compared with previous data, in which non-WT strains were not detected (*6*). Amphotericin B is reserved for second-line therapy in severe disseminated sporotrichosis or in cases refractory to itraconazole (*31*,*34*). Most of the clinically challenging isolates in our study remained WT, with borderline susceptibility to amphotericin B. The use of amphotericin B as an empirical choice in those cases without prior antifungal drugs susceptibility testing would therefore have been precarious, because amphotericin B requires a minimum effective concentration of 4–8 μg/mL, which might risk dose-dependent nephrotoxicity (*35*).

Terbinafine is another second-line drug therapy used as a single treatment or in combination with itraconazole. Successful treatment with terbinafine remains controversial; some successful reports have been published in human and dog sporotrichosis cases, whereas the reported success rate in feline sporotrichosis caused by *S. brasiliensis* is low (*36*–*38*). In Thailand, this drug has been used frequently in cats when *S. schenckii* has failed to respond to itraconazole, and terbinafine has previously shown low MICs among *S. schenckii* isolates from Thailand and Malaysia that share closely related genotypes (*6*,*7*,*27*). In our study, terbinafine was the most potent agent in vitro, with consistently low MICs (1.3-fold increase in MIC_{50} and no change in MIC_{90}) compared with those in previous reports (*6*). Cross-drug and multidrug reduced susceptibility to terbinafine, itraconazole, and other drugs were extremely low, especially among the non-WT isolates in our study. Our findings align with those of previous studies suggesting the use of terbinafine as an alternative drug for treating sporotrichosis against itraconazole non-WT isolates, either as a monotherapy or combined with posaconazole, on the basis of in vitro antifungal drug susceptibility testing and an in vivo *Galleria mellonella* model of *S. schenckii* infection (*18*).

This study had a very large and diverse collection of isolates from Thailand for in vitro susceptibility testing. Despite the clinically challenging nature of those isolates, terbinafine MICs remained stable and less variable than those of the other drugs, which indicated that the feline *S. schenckii* complex isolates from Thailand had a suitable susceptibility profile to terbinafine. We found diverse distributions of terbinafine MICs in the populations of *S. schenckii* complex native feline non-genotyped isolates from Thailand. In comparing our mode terbinafine value (mode MIC = 1 μg/mL) to that of a large, diverse population study (mode MIC = 0.5 μg/mL) (*21*), the difference was only 2-fold and not significant for susceptibility testing. Because of the increasing need for terbinafine to treat feline sporotrichosis and the rising rate of zoonotic infections in Thailand, we proposed a study-specific cutoff of 4 μg/mL for terbinafine for *S. schenckii* species complex. That cutoff might help monitor reduced susceptibility and support effective antifungal drug use, particularly because of the reduced susceptibility to itraconazole among strains in Thailand. Furthermore, including strains from Thailand in MIC datasets for ECV determination would broaden global studies on the susceptibility profiles of zoonotic *S. schenckii*.

The first limitation of this study is lack of correlation between the MICs and clinical treatment outcomes and the absence of disease severity analysis for non-WT isolates. Second, molecular identification was not performed to confirm species within the *S. schenckii* complex. Therefore, interpretation of MIC values based on ECVs for *S. schenckii* should be approached with caution. Feline sporotrichosis in Thailand is predominantly caused by *S. schenckii* s.s., supporting the use of those ECVs as a reference in

this study (*6*–*8*), though species-level identification remains limited. A recent study proposed updated ECVs for *Sporothrix* species, which have been approved by the CLSI subcommittee and are expected in a future supplement (A.R. dos Santos, et al. unpub. data, https://www.biorxiv.org/content/10.64898/2025.12.19.695392v1). Those developments emphasize the necessity of species-level identification and standardized criteria for antifungal drug susceptibility testing and the need for standardized protocols to ensure consistent interpretation across studies. Future studies incorporating molecular identification are warranted to validate species-level distribution and improve the accuracy of antifungal drugs susceptibility interpretation. We primarily provided descriptive and surveillance data on in vitro antifungal drug susceptibility patterns and evidence of cross-reduced susceptibility. However, treatment outcomes cannot yet be reliably predicted from susceptibility profiles.

In conclusion, we found an increasing number of confirmed feline sporotrichosis cases in Thailand, with 1,178 cases reported within a 3-year period, together with the occurrence of reduced itraconazole susceptibility. Those results suggest that reliance on empirical therapy alone might be insufficient in refractory cases, as reduced susceptibility patterns can vary across regions and over time. In vitro drug susceptibility testing should be performed for disease surveillance and in selected complex cases.

Acknowledgments

We gratefully thank the veterinarians who submitted samples for fungal culture and antifungal drug susceptibility testing.

About the Author

Dr. Yurayart is a veterinarian and academic who is currently a faculty member at the Faculty of Veterinary Medicine, Kasetsart University, Bangkok, Thailand. She specializes in veterinary microbiology and mycology.

References

1. Oliveira MM, Almeida-Paes R, Gutierrez-Galhardo MC, Zancope-Oliveira RM. Molecular identification of the *Sporothrix schenckii* complex. Rev Iberoam Micol. 2014;31:2–6. https://doi.org/10.1016/j.riam.2013.09.008
2. Chakrabarti A, Bonifaz A, Gutierrez-Galhardo MC, Mochizuki T, Li S. Global epidemiology of sporotrichosis. Med Mycol. 2015;53:3–14. https://doi.org/10.1093/mmy/myu062
3. Etchecopaz A, Toscanini MA, Gisbert A, Mas J, Scarpa M, Iovannitti CA, et al. *Sporothrix brasiliensis*: a review of an emerging South American fungal pathogen, its related disease, presentation and spread in Argentina. J Fungi (Basel). 2021;7:170. https://doi.org/10.3390/jof7030170
4. Cheng S, Zheng S, Zhong M, Gyawali KR, Pan W, Xu M, et al. Current situation of sporotrichosis in China. Future Microbiol. 2024;19:1097–106. https://doi.org/10.1080/17460913.2024.2352283
5. Rudramurthy SM, Shankarnarayan SA, Hemashetter BM, Verma S, Chauhan S, Nath R, et al. Phenotypic and molecular characterisation of *Sporothrix globosa* of diverse origin from India. Braz J Microbiol. 2021;52:91–100. https://doi.org/10.1007/s42770-020-00346-6
6. Yingchanakiat K, Limsivilai O, Sunpongsri S, Niyomtham W, Lugsomya K, Yurayart C. Phenotypic and genotypic characterization and antifungal susceptibility of *Sporothrix schenckii* sensu stricto isolated from a feline sporotrichosis outbreak in Bangkok, Thailand. J Fungi (Basel). 2023;9:590. https://doi.org/10.3390/jof9050590
7. Langsiri N, Banlunara W, Klaychontee O, Worasilchai N, Cognialli R, Queiroz-Telles F, et al. Targeted long-read sequencing analysis and antifungal susceptibility profiles of *Sporothrix schenckii* isolates from Thailand. PLoS Negl Trop Dis. 2025;19:e0013253. https://doi.org/10.1371/journal.pntd.0013253
8. Indoung S, Chanchayanon B, Chaisut M, Buapeth KO, Morteh R, Jantrakajorn S. Feline sporotrichosis caused by *Sporothrix schenckii* sensu stricto in Southern Thailand: phenotypic characterization, molecular identification, and antifungal susceptibility. Med Mycol. 2022;60:myac075. https://doi.org/10.1093/mmy/myac075
9. Gremião ID, Miranda LH, Reis EG, Rodrigues AM, Pereira SA. Zoonotic epidemic of sporotrichosis: cat to human transmission. PLoS Pathog. 2017;13:e1006077. https://doi.org/10.1371/journal.ppat.1006077
10. Jirawattanadon P, Bunyaratavej S, Leeyaphan C, Chongtrakool P, Sitthinamsuwan P, Panjapakkul W, et al. Clinical manifestations, antifungal drug susceptibility, and treatment outcomes for emerging zoonotic cutaneous sporotrichosis, Thailand. Emerg Infect Dis. 2024;30:2583–92. https://doi.org/10.3201/eid3012.240467
11. Bernardes-Engemann AR, Tomki GF, Rabello VBS, Almeida-Silva F, Freitas DFS, Gutierrez-Galhardo MC, et al. Sporotrichosis caused by non-wild type *Sporothrix brasiliensis* strains. Front Cell Infect Microbiol. 2022;12:893501. https://doi.org/10.3389/fcimb.2022.893501
12. Waller SB, Dalla Lana DF, Quatrin PM, Ferreira MRA, Fuentefria AM, Mezzari A. Antifungal resistance on *Sporothrix* species: an overview. Braz J Microbiol. 2021;52:73–80. https://doi.org/10.1007/s42770-020-00307-z
13. Gremião IDF, Miranda LHM, Pereira-Oliveira GR, Menezes RC, Machado ACS, Rodrigues AM, et al. Advances and challenges in the management of feline sporotrichosis. Rev Iberoam Micol. 2022;39:61–7. https://doi.org/10.1016/j.riam.2022.05.002
14. Gremião IDF, Martins da Silva da Rocha E, Montenegro H, Carneiro AJB, Xavier MO, de Farias MR, et al. Guideline for the management of feline sporotrichosis caused by *Sporothrix brasiliensis* and literature revision. Braz J Microbiol. 2021;52:107–24. https://doi.org/10.1007/s42770-020-00365-3
15. Nakasu CCT, Waller SB, Ripoll MK, Ferreira MRA, Conceição FR, Gomes ADR, et al. Feline sporotrichosis: a case series of itraconazole-resistant *Sporothrix brasiliensis* infection. Braz J Microbiol. 2021;52:163–71. https://doi.org/10.1007/s42770-020-00290-5
16. Larsson CE. Sporotrichosis and cryptococcosis. Presented at: World Small Animal Veterinary Association Congress; Mexico City, Mexico; 2005 May 11–14.

17. Easterwood LF, Harkin KR, Rankin AJ. Oral voriconazole therapy in cats with histoplasmosis yielded mild side effects and a favorable outcome. J Am Vet Med Assoc. 2023;261:1–5. https://doi.org/10.2460/javma.23.05.0276
18. Aroonvuthiphong V, Bangphoomi N. Therapeutic alternatives for sporotrichosis induced by wild-type and non-wild-type *Sporothrix schenckii* through in vitro and in vivo assessment of enilconazole, isavuconazole, posaconazole, and terbinafine. Sci Rep. 2025;15:3230. https://doi.org/10.1038/s41598-025-87711-3
19. Indira G. In vitro Antifungal susceptibility testing of 5 antifungal agents against dermatophytic species by CLSI (M38-A) micro dilution method. Clin Microbiol. 2014;3:1–5. https://doi.org/10.4172/2327-5073.1000145
20. Clinical and Laboratory Standards Institute. Reference method for broth dilution antifungal susceptibility testing of filamentous fungi, 3rd ed. M38. Wayne (PA): The Institute; 2017.
21. Espinel-Ingroff A, Abreu DPB, Almeida-Paes R, Brilhante RSN, Chakrabarti A, Chowdhary A, et al. Multicenter, international study of MIC/MEC Distributions for definition of epidemiological cutoff values for *Sporothrix* species identified by molecular methods. Antimicrob Agents Chemother. 2017;61:e01057-17. https://doi.org/10.1128/AAC.01057-17
22. Clinical and Laboratory Standards Institute. Principles and procedures for the development of epidemiological cutoff values for antifungal susceptibility testing. Wayne (PA): The Institute; 2016.
23. Inpankaew T, Sattasathuchana P, Kengradomkij C, Thengchaisri N. Prevalence of toxoplasmosis in semi-domesticated and pet cats within and around Bangkok, Thailand. BMC Vet Res. 2021;17:252. https://doi.org/10.1186/s12917-021-02965-z
24. Hoffmann-Fezer G, Mortelbauer W, Hartmann K, Mysliwietz J, Thefeld S, Beer B, et al. Comparison of T-cell subpopulations in cats naturally infected with feline l eukaemia virus or feline immunodeficiency virus. Res Vet Sci. 1996;61:222–6. https://doi.org/10.1016/S0034-5288(96)90067-3
25. Zhang M, Zhou Z, Wang D, Zhou A, Song G, Chen X, et al. Comparative evaluation of Sensititre YeastOne and VITEK 2 against the clinical and laboratory standards institute M27-E4 reference broth microdilution method for the antifungal susceptibility testing of *Cryptococcus neoformans* and *Cryptococcus gattii*. Med Mycol. 2022;60:myac009. https://doi.org/10.1093/mmy/myac009
26. Alvarado-Ramírez E, Torres-Rodríguez JM. In vitro susceptibility of *Sporothrix schenckii* to six antifungal agents determined using three different methods. Antimicrob Agents Chemother. 2007;51:2420–3. https://doi.org/10.1128/AAC.01176-06
27. Tan XT, Ginsapu SJ. Amran Fb, Sukur SbM, Shukor Sb. Susceptibility of filamentous fungi to voriconazole in Malaysia tested by Sensititre YeastOne and CLSI mirocilution methods. Research Square. 2021; https://doi.org/10.21203/rs.3.rs-199013/v1.
28. Pfaller MA, Diekema DJ. Progress in antifungal susceptibility testing of *Candida* spp. by use of clinical and laboratory standards institute broth microdilution methods, 2010 to 2012. J Clin Microbiol. 2012;50:2846–56. https://doi.org/10.1128/JCM.00937-12
29. Espinel-Ingroff A, Cuenca-Estrella M, Fothergill A, Fuller J, Ghannoum M, Johnson E, et al. Wild-type MIC distributions and epidemiological cutoff values for amphotericin B and *Aspergillus* spp. for the CLSI broth microdilution method (M38-A2 document). Antimicrob Agents Chemother. 2011;55:5150–4. https://doi.org/10.1128/AAC.00686-11
30. Mawby DI, Whittemore JC, Fowler LE, Papich MG. Comparison of absorption characteristics of oral reference and compounded itraconazole formulations in healthy cats. J Am Vet Med Assoc. 2018;252:195–200. https://doi.org/10.2460/javma.252.2.195
31. Lloret A, Hartmann K, Pennisi MG, Ferrer L, Addie D, Belák S, et al. Sporotrichosis in cats: ABCD guidelines on prevention and management. J Feline Med Surg. 2013;15:619–23. https://doi.org/10.1177/1098612X13489225
32. Kelly SL, Lamb DC, Kelly DE, Manning NJ, Loeffler J, Hebart H, et al. Resistance to fluconazole and cross-resistance to amphotericin B in *Candida albicans* from AIDS patients caused by defective sterol delta5,6-desaturation. FEBS Lett. 1997;400:80–2. https://doi.org/10.1016/S0014-5793(96)01360-9
33. Vazquez JA, Arganoza MT, Boikov D, Yoon S, Sobel JD, Akins RA. Stable phenotypic resistance of *Candida* species to amphotericin B conferred by preexposure to subinhibitory levels of azoles. J Clin Microbiol. 1998;36:2690–5. https://doi.org/10.1128/JCM.36.9.2690-2695.1998
34. Kauffman CA, Bustamante B, Chapman SW, Pappas PG; I nfectious Diseases Society of America. Clinical practice guidelines for the management of sporotrichosis: 2007 update by the Infectious Diseases Society of America. Clin Infect Dis. 2007;45:1255–65. https://doi.org/10.1086/522765
35. Gremião I, Schubach T, Pereira S, Rodrigues A, Honse C, Barros M. Treatment of refractory feline sporotrichosis with a combination of intralesional amphotericin B and oral itraconazole. Aust Vet J. 2011;89:346–51. https://doi.org/10.1111/j.1751-0813.2011.00804.x
36. Francesconi G, Francesconi do Valle AC, Passos SL, de Lima Barros MB, de Almeida Paes R, Curi AL, et al. Comparative study of 250 mg/day terbinafine and 100 mg/day itraconazole for the treatment of cutaneous sporotrichosis. Mycopathologia. 2011;171:349–54. https://doi.org/10.1007/s11046-010-9380-8
37. Viana PG, Figueiredo ABF, Gremião IDF, de Miranda LHM, da Silva Antonio IM, Boechat JS, et al. Successful treatment of canine sporotrichosis with terbinafine: case reports and literature review. Mycopathologia. 2018;183:471–8. https://doi.org/10.1007/s11046-017-0225-6
38. Viana PG, Gremião IDF, da Silva Antonio IM, Figueiredo ABF, Correa ML, Boechat JS, et al. Is terbinafine an effective treatment for feline sporotrichosis? Vet Rec. 2024;195:e4435. https://doi.org/10.1002/vetr.4435

Address for correspondence: Panpicha Sattasathuchana, Department of Companion Animal Clinical Sciences, Faculty of Veterinary Medicine, Kasetsart University, Bangkok 10900, Thailand; email: psatta99@gmail.com

Outbreak of *Wickerhamomyces anomalus* (formerly *Candida pelliculosa*) Bloodstream Infections, Venezuela, 2022–2023[1]

Maribel Dolande-Franco,[2] Diego H. Caceres,[2] Juan F. Frey-Carrillo, Antoniellys Pérez-Guzmán, Andres Ceballos-Garzon, Aleiram Chaurio-Briceño, Bram Spruijtenburg, Yusely Roa-Díaz, Eelco F.J. Meijer, Elaine Cristina Francisco, Rodrigo Oliveira, Tatiana Drummond-Suinaga, Jacques F. Meis

During August 2022–December 2023, a total of 110 bloodstream infections caused by *Wickerhamomyces anomalus* (synonym *Candida pelliculosa*) were identified across 8 hospitals in 3 cities in Venezuela. Most cases (82/110 in Caracas) occurred in a single pediatric intensive care unit, predominantly among neonates. Molecular genotyping indicated multiple events of clonal transmission, which was supported by epidemiologic clustering of patients. Antifungal susceptibility testing demonstrated good in vitro activity; most isolates were classified as wild-type. Our findings underscore the need for enhanced fungal diagnostics, infection prevention measures, and national surveillance to mitigate hospital-associated fungal transmission in resource-limited settings.

Wickerhamomyces anomalus (synonyms *Hansenula anomala*, *Candida pelliculosa*, and *Pichia anomala*) has been isolated from soil, grains, fruit juices, and animals (*1*). In agriculture, *W. anomalus* has been used in beer production and for fermentation of cocoa and coffee beans and is responsible for spoilage of bakery products (*2*). *W. anomalus* is also used in the biocontrol of molds, especially those that affect stored postharvest products (*2*). Although use in food and industrial applications is common, clinically, *W. anomalus* is considered a rare emerging pathogen (*3*). Invasive disease by this agent has been reported mainly in low-birthweight infants admitted to neonatal intensive care units (NICUs) (*3*–*9*), occasionally in adult immunocompromised patients (*10*,*11*), and as a cause of keratitis (*12*). The mortality rate for *W. anomalus* fungemia is estimated at 30%, comparable to other yeast pathogens in neonates (*6*). Although antifungal resistance is on the rise for several notorious yeasts like *C. auris* and *C. parapsilosis*, it appears to be rare for *W. anomalus* (*8*,*13*).

Of note, nosocomial clonal outbreaks have been reported mainly in NICUs or pediatric intensive care units (PICUs) (*1*,*14*). When *W. anomalus* fungemia is diagnosed in multiple patients in the same healthcare center, rapid and high-resolution genotyping is required to identify the source and prevent future cases (*15*). In this article, we report a large *W. anomalus* fungemia outbreak spread across several healthcare facilities in Venezuela and apply descriptive

Author affiliations: Instituto Nacional de Higiene "Rafael Rangel," Caracas, Venezuela (M. Dolande-Franco, J.F. Frey-Carrillo, A. Chaurio-Briceño); Immuno-Mycologics, Norman, Oklahoma, USA (D.H. Caceres); Universidad del Rosario, Bogota, Colombia (D.H. Caceres, A. Ceballos-Garzon); Radboudumc-CWZ Center of Expertise for Mycology, Nijmegen, the Netherlands (D.H. Caceres, B. Spruijtenburg, E.F.J. Meijer, J.F. Meis); Hospital Universitario de Caracas, Caracas (A. Pérez-Guzmán, Y. Roa-Díaz, T. Drummond-Suinaga); Canisius-Wilhelmina Hospital/Dicoon, Nijmegen (B. Spruijtenburg, E.F.J. Meijer); Universidade Federal de São Paulo, São Paulo, Brazil (E.C. Francisco); Antimicrobial Resistance Institute of São Paulo, São Paulo (E.C. Francisco); Universidade Federal do Paraná, Curitiba, Brazil (E.C. Francisco, J.F. Meis); Bruker Daltonics GmbH & Co., Bremen, Germany (R. Oliveira); University of Cologne, Cologne, Germany (J.F. Meis)

DOI: https://doi.org/10.3201/eid3206.251978

[1]Preliminary results from this study were presented at the 22nd INFOCUS Conference; November 20–23, 2024; Bogota, Colombia.

[2]These authors share first authorship of this article.

epidemiology, short tandem repeat (STR) analysis, and antifungal susceptibility testing (AFST) to characterize the outbreak.

Material and Methods

We conducted a descriptive, retrospective investigation of bloodstream infections (BSIs) caused by *W. anomalus* in Venezuela during August 2022–December 2023. We defined a confirmed case as a patient with *W. anomalus* isolated from a blood culture in the presence of compatible clinical signs and symptoms of infection. We defined clinical criteria for suspected fungemia on the basis of established risk factors, such as prematurity, low birthweight, prolonged exposure to broad-spectrum antimicrobial agents, presence of a central venous catheter, and receipt of mechanical ventilation. Case notifications were received through the National Mycology Reference Network from 8 hospitals across 3 cities: Caracas (Capital District), Los Teques (Miranda state), and Valencia (Carabobo state). Caracas, in the Capital District, lies near Venezuela's northern coast; Los Teques (Miranda) is ≈18 miles (29 km) southwest of Caracas; and Valencia (Carabobo) is ≈110 miles (177 km) west of Caracas (Figure 1).

We extracted available demographic, clinical, and epidemiologic data from laboratory and hospital records where accessible. Clinical information was not uniformly available and could only be retrieved for a subset of cases. Case counts were plotted by epidemiologic week (EW) and location to describe temporal and spatial clustering. Because of the retrospective nature of the study, real-time intervention throughout the course of the outbreak was not feasible. We did not perform environmental sampling; the investigation was part of a national public health response and was therefore exempt from institutional review board approval.

Isolates

From a total of 110 documented cases of *W. anomalus* BSIs, 99 isolates from unique patients were available for this study. All isolates, initially identified using the automated VITEK 2 system (bioMérieux, https://www.biomerieux.com) (Appendix Table 1, https://wwwnc.cdc.gov/EID/article/32/6/25-1978-App1.pdf), were stored according to standard procedures at −80°C. Isolates were grown on Sabouraud dextrose agar plates (Thermo Fisher Scientific, https://www.thermofisher.com) at 30°C for 1 day before confirmation of identification using matrix-assisted laser desorption ionization-time of flight (MALDI-TOF) mass spectrometry as previously described (*14*).

MALDI-TOF Mass Spectrometry Identification and Data Analysis

We identified isolates using MALDI-TOF mass spectrometry. We performed protein extraction following

Figure 1. Geolocations of reported *Wickerhamomyces anomalus* (formerly *Candida pelliculosa*) bloodstream infection outbreaks, Venezuela, 2022–2023. The map shows the distribution of outbreaks across 8 hospitals in 3 cities: Caracas (Capital District; n = 5 hospitals), Los Teques (Miranda State; n = 1 hospital), and Valencia (Carabobo State; n = 2 hospitals). Caracas, located near Venezuela's northern coast, represents the primary cluster. Los Teques lies ≈29 km southwest of Caracas, and Valencia is located ≈177 km west of Caracas. The geographic dispersion and clustering across multiple healthcare facilities are consistent with regional nosocomial transmission rather than a single point-source event. Insets show location of the 3 states in Venezuela and the location of Venezuela in South America.

the standard procedures recommended by Bruker (https://www.bruker.com). We acquired protein spectra using the MALDI Biotyper Sirius System, and identifications were generated with the MBT Compass HT IVD database (Bruker).

In addition to species-level identification, we further analyzed protein spectral data in MBT Compass Explorer to evaluate spectral relatedness among isolates. This analysis included the generation of similarity matrices and dendrograms using the software's integrated data-processing algorithms.

STR Genotyping

We extracted DNA from all cultured isolates with the MagNA Pure 96 instrument and MagNA Pure DNA and Viral NA Small volume kit (Roche, https://www.roche.com) according to the manufacturer's instruction, as described previously (*16*). We performed multiplex PCR reaction amplifying 6 previously described STR markers using a thermocycler (Analytik Jena, https://www.analytikjena.us) under identical PCR conditions (*14*). We analyzed amplicons on a 3500 XL genetic analyzer (Thermo Fisher Scientific), determined copy numbers using GeneMapper version 5 software (Thermo Fisher Scientific), and inferred phylogenetic relatedness between isolates using BioNumerics version 7.6.1 (bioMérieux, https://www.biomerieux.com) (*14*).

Antifungal Susceptibility Testing

We initially performed AFST using VITEK 2 AST-YS01 cards (bioMérieux) and confirmed results using microbroth dilution Clinical and Laboratory Standards Institute (CLSI) reference standard M27 (*17*) using amphotericin B (Bristol Myers Squib, https://www.bms.com), fluconazole (Merck, https://www.merck.com), itraconazole (Johnson & Johnson, https://www.jnj.com), voriconazole (Pfizer, https://www.pfizer.com), posaconazole (Merck), isavuconazole (Merck), anidulafungin (Merck), and micafungin (Merck). We incubated microtiter plates at 35°C and visually interpreted them after 24 hours. We read MICs as the lowest antifungal concentration with a 50% growth reduction when compared with the growth control, except for amphotericin B with 100% growth reduction. We interpreted MICs according to epidemiologic cutoff values (ECVs) established in CLSI reference standard M57S (*18*), specifically 1 μg/mL for amphotericin B, 8 μg/mL for fluconazole, 1 μg/mL for itraconazole, 0.12 μg/mL for micafungin, 2 μg/mL for posaconazole, and 0.25 μg/mL for voriconazole.

Results

Chronological Narrative of Outbreak

In August 2022, the National Mycology Reference Network in Venezuela received notifications of an unusual increase in yeast bloodstream isolates from the PICU at a public hospital in Caracas (hospital A). This signal was identified through routine laboratory-based surveillance, in a context where clinical and epidemiologic data were not systematically captured or shared with the national network. The first case of BSI caused by *W. anomalus* was identified during EW 32 of 2022. During August 2022–December 2023, a total of 110 confirmed BSI cases were identified from 3 cities: Caracas (n = 88 cases), Los Teques (n = 11 cases), and Valencia (n = 11 cases) (Figure 2). Given the retrospective nature of this investigation, outbreak recognition and characterization occurred after transmission had already been established, and no coordinated real-time public health or infection prevention and control interventions were implemented consistently throughout the course of the outbreak.

In Caracas, 5 hospitals were affected (hospitals A–E); most cases (82 of 88) were concentrated at hospital A. Among Caracas cases, 61 (74%) cases occurred in the NICU/PICU, primarily among neonates (<30 days of age). Although detailed clinical data were only available for a subset of patients, the concentration of cases in high-risk units and the temporal clustering strongly support a nosocomial transmission pattern, consistent with previous reports of *W. anomalus* outbreaks in NICU and PICU settings.

At hospital A, PICU cases occurred in an initial cluster from EW 32 of 2022 through EW 25 of 2023 (43 cases), and 1 case occurred outside the PICU during 2023 EW 3. A second cluster occurred outside the PICU from EW 27 through EW 36 of 2023 (17 cases), followed by 2 additional clusters: 1 in the PICU during EWs 36–43 of 2023 (17 cases), another outside the PICU during EWs 43–45 of 2023 (3 cases), and 1 case at the PICU during EW 51 (Figure 2). The remaining 6 cases from Caracas were distributed among other hospitals: 1 case at hospital B during EW 23 of 2023, 1 case at hospital C during EW 31 of 2023, 1 case at hospital D during EW 32 of 2023, and a cluster of 3 cases at hospital E during EWs 37–41 of 2023 (Figure 2).

In Los Teques, 11 cases were reported from hospital F. The first 2 cases were identified during EW 17 of 2023, followed by 1 sporadic case in EW 24 of 2023 and a subsequent cluster of 8 cases during EWs 37–44 of 2023 (Figure 2). In Valencia, 11 cases were reported during EW 11 of 2023. Ten cases were reported from hospital G, and 1 case was reported from hospital H (Figure 2).

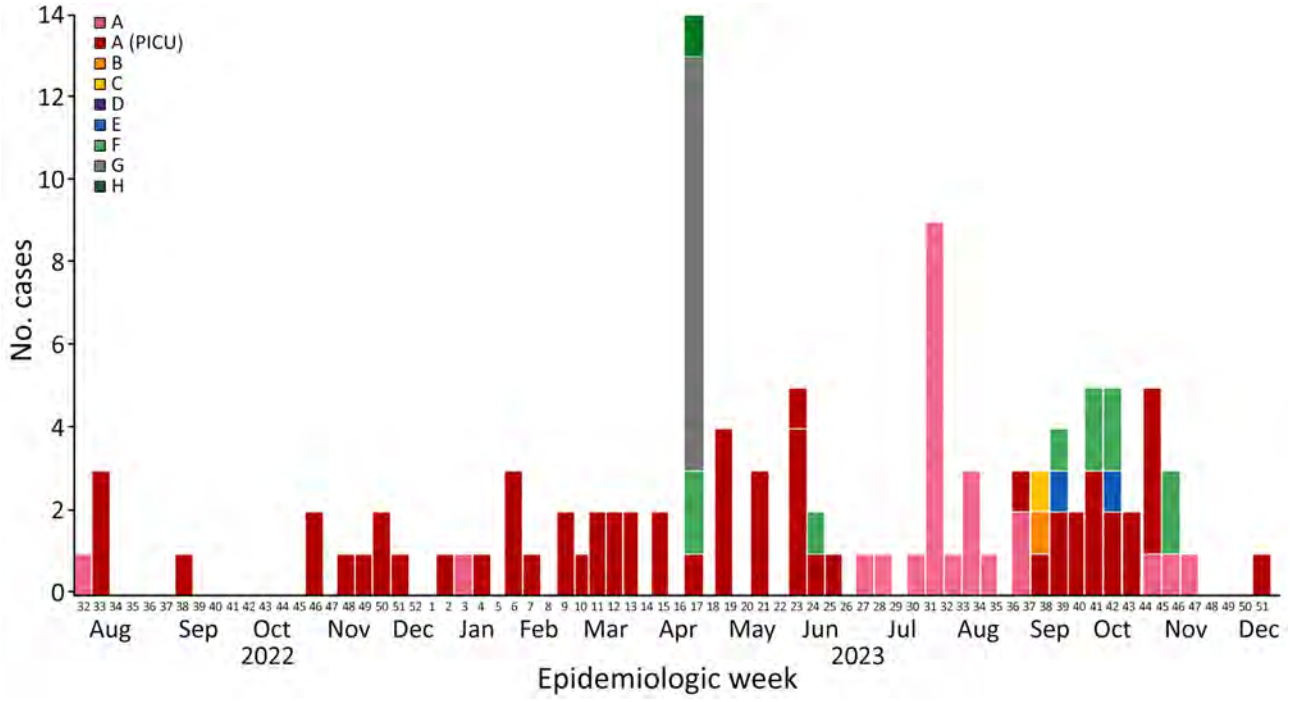

Figure 2. Epidemic curve of outbreak of *Wickerhamomyces anomalus* (formerly *Candida pelliculosa*) bloodstream infections, Venezuela, 2022–2023. Curve is shown for 110 cases by epidemiologic week, with cases color-coded according to the medical center of origin (hospitals A–H). The distribution highlights temporal clustering of cases across multiple institutions, including a sustained cluster in the hospital A PICU and shorter, city-specific clusters in other centers. PICU, pediatric intensive care unit.

Epidemiologic Investigation

The index case was reported in week 32 of 2022 (Figure 2). Beginning in week 46 of 2022, cases were reported at least every 3 weeks; 2 peaks occurred in weeks 17 and 31 of 2023. The first peak occurred predominantly in hospital G in Valencia; those were the only reported cases in that particular week. Hospital A in Caracas reported cases throughout the entire study period. Although cases were initially restricted to the PICU, beginning in week 27 of 2023, the yeast was also found in non–intensive care wards. The investigation suggested nosocomial transmission within NICUs and PICUs. The clustering of cases by hospital unit and time strongly suggests horizontal transmission, most likely occurring through contaminated hands, infusion fluids, or reusable medical equipment. Despite the absence of comprehensive clinical and environmental data, the observed temporal clustering, concentration in specific hospital units, and spread across institutions are consistent with an actual outbreak rather than a pseudo-outbreak, most likely driven by healthcare-associated transmission mechanisms.

Patient Demographics and Clinical Characteristics

Among the 110 patients, 68 (62%) were male and 42 (38%) female. The median age was 11 days (interquartile range 8–22 days). Most patients (99 [90%]) were neonates (0–30 days of age), 6 (5%) were infants (31–365 days of age), 4 (4%) were preschool-aged children (1–5 years), and 1 (1%) was an adult (a 37-year-old man).

Since January 20, 2023, *Candida* and other yeast infections have been included in the list of notifiable epidemiologic events in Venezuela (https://mpps.gob.ve/wp-content/uploads/2023/02/G.O.-42.553-20012023-ENO.pdf). However, at the time this outbreak occurred, surveillance was exclusively laboratory-based, and no standardized instrument existed for reporting epidemiologic or clinical data. Of the 110 cases identified, epidemiologic and clinical information was available for only 15 patients, all of whom were admitted to the PICU of hospital A. Those cases occurred from EW 32 of 2022 through EW 17 of 2023. In 8 of the 15 cases, we did not confirm identification by MALDI-TOF mass spectrometry or sequencing. The predominant risk factors among those 15 patients were PICU admission, prematurity, and the presence of central venous catheters, all of which were reported in all cases. Hematologic abnormalities were frequent; thrombocytopenia was observed in all patients, followed by leukocytosis (10/15), anemia (6/15), and leukopenia (2/15).

Of the 15 patients, 7 initially received fluconazole at 12 mg/kg/day. In 6 of those cases, a change in antifungal treatment was required: 1 patient was

switched to caspofungin (loading dose 70 mg/m²/d, maintenance dose 50 mg/m²/d, administered over 1 h for 14 d) and 5 were switched to deoxycholate amphotericin B (1 mg/kg/d, infused over 3 h). Among the 5 patients treated with deoxycholate amphotericin B, 1 died; however, the antifungal response in this case was favorable, and death was attributed to complications of the underlying disease rather than to fungal infection.

In the remaining 8 patients, deoxycholate amphotericin B was used as the initial antifungal therapy. In 1 of those patients, treatment was subsequently changed from deoxycholate amphotericin B to caspofungin. Of the 8 patients who started therapy with deoxycholate amphotericin B, 1 died because of underlying medical conditions; another patient initially treated with deoxycholate amphotericin B and later switched to caspofungin died from causes directly associated with persistent candidemia.

Microbiological Findings

We performed initial identification of the isolates using the automated VITEK 2 system (bioMérieux), which identified all isolates as *C. pelliculosa* (*W. anomalus*). Because this identification was uncommon, we sent viable isolates (n = 99) to the Department of Medical Microbiology and Immunology, Canisius-Wilhelmina Hospital (CWZ)/Dicoon, Nijmegen, the Netherlands, for confirmation by MALDI-TOF mass spectrometry and molecular analysis.

Overall, the results obtained with the VITEK 2 system (bioMérieux) were consistent with those from MALDI-TOF MS; all isolates were accurately identified as *W. anomalus* (log-score >2.0). Using the VITEK 2 AST-YS01 cards, 4 (4%) of 99 isolates exhibited a MIC ≥32 μg/mL for fluconazole, 18 (18%) exhibited a MIC ≥0.25 μg/mL for voriconazole, and 4 (4%) had a MIC ≥2 μg/mL for amphotericin B. We subsequently tested the 99 *W. anomalus* isolates with CLSI broth microdilution against 8 antifungals, demonstrating major discrepancies with the VITEK 2 system (bioMérieux). All antifungals demonstrated potent in vitro activity; echinocandins showed the lowest MIC_{50} of ≤0.008 μg/mL (Table). For the azoles, isavuconazole had the highest in vitro activity with a MIC_{50} of 0.031 μg/mL. Because breakpoints are absent for *W. anomalus*, available CLSI ECVs were applied, resulting in classification of 1 isolate (L-13) as non–wild-type for fluconazole (MIC 8 μg/mL) and 1 isolate (L-03) as non–wild-type for voriconazole (MIC 0.25 μg/mL), although the MICs of both isolates were at the cutoff value. For amphotericin B, itraconazole, micafungin, and posaconazole, all isolates were classified as wild-type (Appendix Table 2).

Outbreak Investigation

We assessed genetic relatedness between isolates with STR genotyping for all 99 *W. anomalus* isolates, resulting in 22 genotypes with 7 large clusters that consisted of 4–39 isolates (Figure 3). Only 1 large cluster (genotype 6) was confined to a single center; smaller clusters were found in 2–3 centers. Only genotypes 14 and 19 were found in both 2022 and 2023, whereas the other clusters were found exclusively in 2023.

MALDI-TOF mass spectrometry–based dendrogram analysis also separated *W. anomalus* isolates according to geographic origin. Los Teques isolates formed a tight and highly similar cluster, whereas Valencia isolates showed higher heterogeneity, including 1 isolate forming a distinct group and the remaining isolates clustering within a small branch that further resolved into different subclusters. In contrast, isolates from Caracas displayed broader dispersion across multiple subclusters, highlighting greater heterogeneity within this region. Concordance between molecular (STR) and proteomic (MALDI-TOF) approaches supports the robustness of the observed population structure and highlights the predominance of a major Caracas-associated clone (Figure 4).

Discussion

This investigation describes an outbreak of *W. anomalus* BSIs involving 110 patients across 3 cities and 8 hospitals in Venezuela during 2022–2023. A pseudo-outbreak

Table. In vitro antifungal susceptibility testing metrics of 99 *Wickerhamomyces anomalus* isolates in study of outbreak of *W. anomalus* (formerly *Candida pelliculosa*) bloodstream infections, Venezuela, 2022–2023*

Antifungal	Range	Geometric mean	MIC_{50}	MIC_{90}
Amphotericin B	0.063–0.25	0.077	0.063	0.125
Fluconazole	1–8	1.99	2	2
Itraconazole	0.031–0.25	0.068	0.063	0.125
Voriconazole	0.031–0.25	0.064	0.063	0.125
Posaconazole	0.031–0.25	0.059	0.063	0.063
Isavuconazole	0.016–0.125	0.029	0.031	0.063
Anidulafungin	≤0.008–0.031	0.01	≤0.008	0.016
Micafungin	≤0.008–0.063	0.012	≤0.008	0.031

*Values are μg/mL. In vitro antifungal susceptibility testing was conducted using the Clinical and Laboratory Standards Institute M27 broth microdilution (*17*). MIC_{50}, MIC that inhibits 50% of isolates; MIC_{90}, MIC that inhibits 90% of isolates.

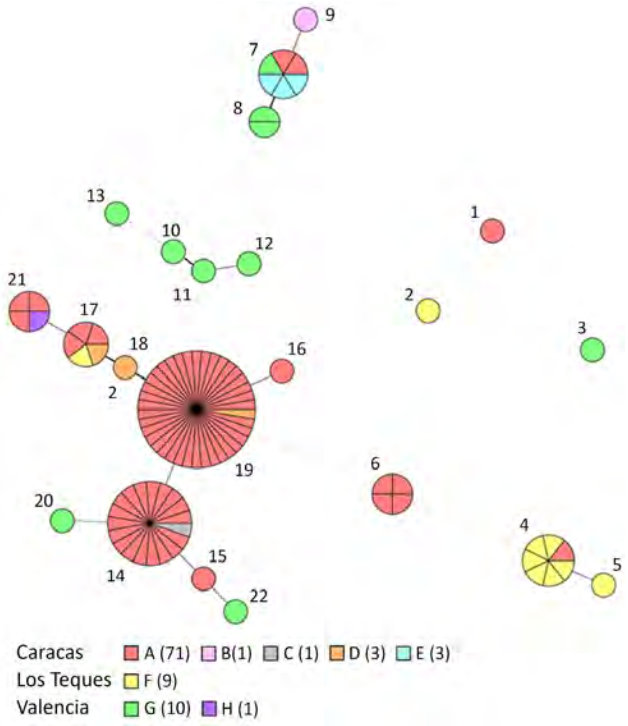

Figure 3. Short tandem repeat genotyping of 99 *Wickerhamomyces anomalus* isolates in study of outbreak of *W. anomalus* (formerly *Candida pelliculosa*) bloodstream infections, Venezuela, 2022–2023. Minimum-spanning tree of 99 *W. anomalus* isolates based on microsatellite markers. Branch lengths indicate similarity between isolates with thick solid lines (variation in 1 allele), thin solid lines (variation in 2 alleles), and thin dotted lines (variation in ≥4 alleles). Isolates are colored according to the city and hospital of origin; parenthetical values in the legend represent the number of isolates.

was ruled out on the basis of several findings. Cases occurred over an extended period with recurrent unit-level clustering, involved multiple hospitals and cities, and affected patients with consistent clinical and laboratory features suggestive of true infection. In addition, the identification of multiple genotypes supports nosocomial transmission rather than a single contamination source, making a pseudo-outbreak unlikely. Previous reports of *W. anomalus* outbreaks describe relatively small clusters, typically ranging from 5 to 20 cases of BSIs, except for a large outbreak from India consisting of 379 cases (*4*). Most reported cases occurred in NICU or pediatric wards in Asia (India, China, Korea, Taiwan, and Pakistan) and Latin America (Brazil) (*1*,*4*–*9*,*11*,*19*–*21*). Despite its reported low virulence, *W. anomalus* can cause severe infections in highly vulnerable patients, particularly preterm neonates and critically ill children exposed to invasive medical procedures (*1*,*4*–*9*,*11*,*19*–*21*).

The marked predominance of neonatal cases and the clustering within PICUs and NICUs in the outbreak we report strongly support a pattern of hospital-associated transmission. Similar outbreaks have previously been linked to contaminated intravenous fluids, parenteral nutrition, reusable medical equipment, or healthcare workers' hands (*1*,*4*,*6*–*9*,*19*,*21*). In this outbreak, the temporal and spatial aggregation of cases with an uncommon yeast within specific hospital units, along with molecular evidence of clonal relatedness as shown by STR genotyping (*15*), further supports nosocomial spread. Nonetheless, whole-genome sequencing is needed to confirm clonal transmission.

Hospital A, where most cases occurred, exhibited multiple epidemic peaks, suggesting persistent or recurrent environmental contamination or inadequate infection prevention and control measures. The development of concurrent clusters in hospitals from different cities also points to systemic weaknesses in infection control practices and limited local laboratory

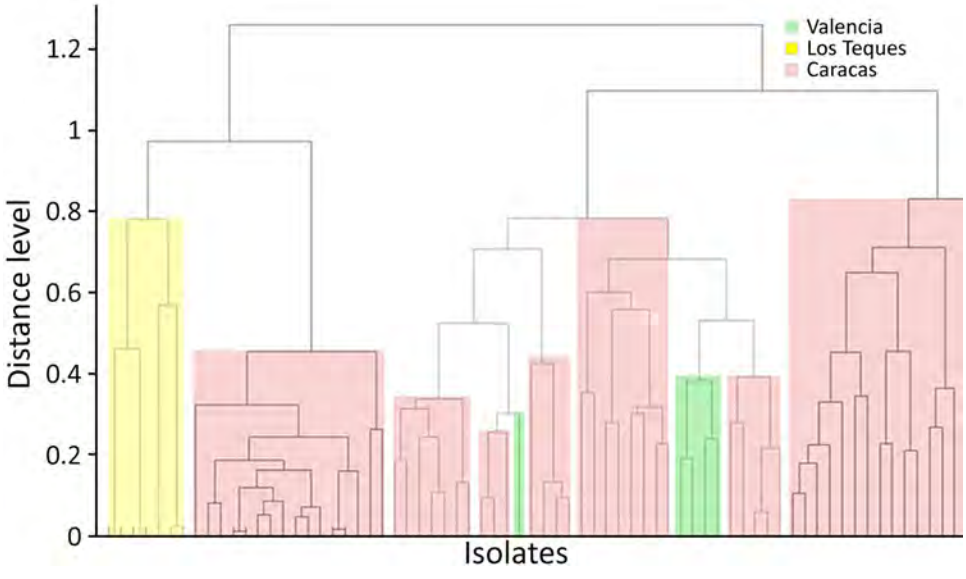

Figure 4. Matrix-assisted laser desorption/ionization time-of-flight mass spectrometry–based dendrogram showing spectral relatedness among *Wickerhamomyces anomalus* isolates in study of outbreak of *W. anomalus* (formerly *Candida pelliculosa*) bloodstream infections, Venezuela, 2022–2023. Clustering reflects geographic origin.

capacity for early fungal detection. Those findings emphasize the urgent need for strengthened hospital hygiene programs, environmental monitoring, and laboratory-based fungal surveillance at the national level.

Antifungal susceptibility testing revealed that nearly all isolates remained susceptible (wild-type) to amphotericin B, echinocandins, and azoles, consistent with previous reports describing *W. anomalus* as generally susceptible to conventional antifungal agents. However, when interpreted with the ECVs established for *C. albicans*, *W. anomalus* has higher MICs for flucytosine, itraconazole, voriconazole, and fluconazole (*1*,*20*,*22*). Therefore, the detection of isolates with elevated MICs to fluconazole and amphotericin B warrants attention. For agents like isavuconazole and anidulafungin, for which formal ECVs are not yet defined, we applied European Committee on Antimicrobial Susceptibility Testing cutoffs (0.25 μg/mL and 0.125 μg/mL), classifying all isolates in this analysis as wild-type (*23*). This overall susceptibility pattern contrasts with recent reports from other regions. A recent study from India reported that 50/70 (72%) *W. anomalus* isolates were non–wild-type for fluconazole, 17% demonstrated cross-resistance with voriconazole, and 1.4% demonstrated cross-resistance with micafungin (*24*). Furthermore, a pan–azole-resistant and pan–echinocandin-resistant *W. anomalus* bloodstream isolate has been recently described in China (*25*). Those findings suggest that while susceptibility remains common, the emergence of resistance, particularly multidrug resistance, poses a potential threat to clinical management, especially in resource-limited settings (*26*).

The MALDI-TOF mass spectrometry dendrogram corroborated those findings and revealed a strong association between clustering patterns and geographic origin, while also indicating potential epidemiologic links beyond individual healthcare institutions. Isolates from Los Teques and Valencia formed compact, highly similar clusters, whereas Caracas isolates were distributed across multiple branches. The detection of genetically and proteomically related isolates across different locations suggests possible shared sources, delayed recognition of transmission events, or gaps in local surveillance capacity. In addition to clustering, MALDI-TOF mass spectrometry successfully identified all isolates at the species level, confirming its reliability for fast and accurate identification of *W. anomalus*. Although MALDI-TOF mass spectrometry enabled rapid and reliable identification in this study, its availability and cost may limit use in resource-constrained settings such as Venezuela. In many hospitals, access remains restricted to reference laboratories, highlighting the need for more accessible and scalable diagnostic alternatives to support timely detection of fungal bloodstream infections.

The main limitation of this investigation was the limited access to clinical data from most cases. Strengthening data integration between clinical and laboratory systems would substantially improve the early detection and management of future fungal outbreaks. This outbreak highlights the capacity of uncommon yeasts, such as *W. anomalus*, to cause large-scale nosocomial infections under conditions of limited infection control and microbiological oversight. Continuous training of healthcare personnel, the adoption of rapid yeast identification tools (e.g., MALDI-TOF mass spectrometry), and the implementation of structured mycological surveillance networks are essential measures to mitigate similar events in the future.

In conclusion, this multicenter outbreak underscores the need for sustained vigilance for opportunistic yeasts in hospital settings, especially in neonatal and pediatric units. Strengthening diagnostic capacity, reinforcing infection prevention and control programs, and integrating fungal BSIs into national surveillance systems are critical to prevent recurrence and improve patient outcomes in Venezuela and similar settings.

This work was partially supported by the Fundação de Amparo à Pesquisa do Estado de São Paulo (FAPESP; project nos. 2021/10599-3, 2024/05974-8, and 2026/04131-2), the Conselho Nacional de Desenvolvimento Científico e Tecnológico (CNPq; project no. 409184/2022-5), and the Canisius-Wilhelmina Hospital (grant CWZ_001421).

D.H.C. is an Immuno-Mycologics (IMMY) employee, serving as the Latin America Account Manager. R.O. is the regional business manager for Latin America at Bruker, Microbiology and Infection Diagnostics. E.F.J.M. has received research grants from Mundipharma and Scynexis, is a member of the scientific advisory board for Pfizer, and has received speaker fees from Gilead Sciences.

About the Author

Dr. Dolande-Franco is a bioanalyst and medical mycologist at the National Reference Laboratory for Mycology in Venezuela. Her work focuses on strengthening diagnostic services, coordinating national surveillance networks for fungal infections, training laboratory professionals, and advancing clinical mycology and public health laboratory capacity nationwide. Dr. Caceres is a microbiologist and epidemiologist with Universidad del Rosario, Bogota, Colombia. His research focuses on outbreak investigations, technology transfer, and diagnostic assay implementation, linking scientific research with regional public health and diagnostic strategies.

References

1. Zhang L, Xiao M, Arastehfar A, Ilkit M, Zou J, Deng Y, et al. Investigation of the emerging nosocomial *Wickerhamomyces anomalus* infections at a Chinese tertiary teaching hospital and a systemic review: clinical manifestations, risk factors, treatment, outcomes, and anti-fungal susceptibility. Front Microbiol. 2021;12:744502. https://doi.org/10.3389/fmicb.2021.744502
2. Kurtzman CP. Wickerhamomyces Kurtzman, Robnett & Basehoar-Powers (2008). In: Kurtzman CP, Fell JW, Boekhout T, editors. The yeasts, 5th edition. London: Elsevier; 2011. p. 899–917.
3. Zhang Z, Cao Y, Li Y, Chen X, Ding C, Liu Y. Risk factors and biofilm formation analyses of hospital-acquired infection of *Candida pelliculosa* in a neonatal intensive care unit. BMC Infect Dis. 2021;21:620. https://doi.org/10.1186/s12879-021-06295-1
4. Chakrabarti A, Singh K, Narang A, Singhi S, Batra R, Rao KL, et al. Outbreak of *Pichia anomala* infection in the pediatric service of a tertiary-care center in Northern India. J Clin Microbiol. 2001;39:1702–6. https://doi.org/10.1128/JCM.39.5.1702-1706.2001
5. Rattani S, Farooqi J, Hussain AS, Jabeen K. Spectrum and antifungal resistance of candidemia in neonates with early- and late-onset sepsis in Pakistan. Pediatr Infect Dis J. 2021;40:814–20. https://doi.org/10.1097/INF.0000000000003161
6. da Silva CM, de Carvalho Parahym AM, Leão MP, de Oliveira NT, de Jesus Machado Amorim R, Neves RP. Fungemia by *Candida pelliculosa* (*Pichia anomala*) in a neonatal intensive care unit: a possible clonal origin. Mycopathologia. 2013;175:175–9. https://doi.org/10.1007/s11046-012-9605-0
7. Lin HC, Lin HY, Su BH, Ho MW, Ho CM, Lee CY, et al. Reporting an outbreak of *Candida pelliculosa* fungemia in a neonatal intensive care unit. J Microbiol Immunol Infect. 2013;46:456–62. https://doi.org/10.1016/j.jmii.2012.07.013
8 Aragão PA, Oshiro IC, Manrique EI, Gomes CC, Matsuo LL, Leone C, et al.; IRIS Study Group. *Pichia anomala* outbreak in a nursery: exogenous source? Pediatr Infect Dis J. 2001;20:843–8. https://doi.org/10.1097/00006454-200109000-00004
9. Jung J, Moon YS, Yoo JA, Lim JH, Jeong J, Jun JB. Investigation of a nosocomial outbreak of fungemia caused by *Candida pelliculosa* (*Pichia anomala*) in a Korean tertiary care center. J Microbiol Immunol Infect. 2018;51:794–801. https://doi.org/10.1016/j.jmii.2017.05.005
10. Ratcliffe L, Davies J, Anson J, Hales S, Beeching NJ, Beadsworth MB. *Candida pelliculosa* meningitis as an opportunistic infection in HIV: the first reported case. Int J STD AIDS. 2011;22:54–6. https://doi.org/10.1258/ijsa.2010.010113
11. Ioannou P, Baliou S, Kofteridis DP. Fungemia by *Wickerhamomyces anomalus*—a narrative review. Pathogens. 2024;13:269. https://doi.org/10.3390/pathogens13030269
12. Park KA, Ahn K, Chung ES, Chung TY. *Pichia anomala* fungal keratitis. Cornea. 2008;27:619–20. https://doi.org/10.1097/ICO.0b013e318166c442
13. Sharma M, Chakrabarti A. Candidiasis and other emerging yeasts. Curr Fungal Infect Rep. 2023;17:15–24. https://doi.org/10.1007/s12281-023-00455-3
14. Spruijtenburg B, Rudramurthy SM, Meijer EFJ, van Haren MHI, Kaur H, Chakrabarti A, et al. Application of novel short tandem repeat typing for *Wickerhamomyces anomalus* reveals simultaneous outbreaks within a single hospital. Microorganisms. 2023;11:1525. https://doi.org/10.3390/microorganisms11061525
15. Spruijtenburg B, Meis JF, Verweij PE, de Groot T, Meijer EFJ. Short tandem repeat genotyping of medically important fungi: a comprehensive review of a powerful tool with extensive future potential. Mycopathologia. 2024;189:72. https://doi.org/10.1007/s11046-024-00877-8
16. Spruijtenburg B, van Haren MHI, Chowdhary A, Meis JF, de Groot T. Development and application of a short tandem repeat multiplex typing assay for *Candida tropicalis*. Microbiol Spectr. 2023;11:e0461822. https://doi.org/10.1128/spectrum.04618-22
17. Clinical and Laboratory Standards Institute. Reference method for broth dilution antifungal susceptibility testing of yeasts, 4th edition. CLSI standard M27. Wayne (PA): The Institute; 2017.
18. Clinical and Laboratory Standards Institute. Epidemiological cutoff values for antifungal susceptibility testing, 4th edition. CLSI standard M57S. Wayne (PA): The Institute; 2022.
19. Pasqualotto AC, Sukiennik TC, Severo LC, de Amorim CS, Colombo AL. An outbreak of *Pichia anomala* fungemia in a Brazilian pediatric intensive care unit. Infect Control Hosp Epidemiol. 2005;26:553–8. https://doi.org/10.1086/502583
20. Francisco EC, Caceres DH, Brunelli JGP, Garcia-Effron G, Arastehfar A, Ribeiro FC, et al. An update on clinically relevant, rare, and emerging *Candida* and Saccharomycotina yeasts that have been recently reclassified from *Candida.* Clin Microbiol Rev. 2025;38:e0006423. https://doi.org/10.1128/cmr.00064-23
21. Yang Y, Wu W, Ding L, Yang L, Su J, Wu B. Two different clones of *Candida pelliculosa* bloodstream infection in a tertiary neonatal intensive care unit. J Infect Dev Ctries. 2021;15:870–6. https://doi.org/10.3855/jidc.12103
22. Turan D, Habip Z, Odabaşı H, Dömbekçi E, Gündoğuş N, Özmen M, et al. Antifungal susceptibilities of rare yeast isolates. J Fungi (Basel). 2025;11:645. https://doi.org/10.3390/jof11090645
23. Astvad KMT, Arikan-Akdagli S, Arendrup MC. A pragmatic approach to susceptibility classification of yeasts without EUCAST clinical breakpoints. J Fungi (Basel). 2022;8:141. https://doi.org/10.3390/jof8020141
24. Verma S, Tilak R, Singh G, Singh S, Kumari A, Rudramurthy SM, et al. Multicentre investigation of *Wickerhamomyces anomalus* fungemia in India: emerging resistance and mechanistic insights. J Antimicrob Chemother. 2026;81:dkaf420. https://doi.org/10.1093/jac/dkaf420
25. Luo Z, Ning Y, Dai R, Ainiwaer A, Li Y, Zhang R, et al. A pan-azole and pan-echinocandin resistant Wickerhamomyces anomalus isolate causing bloodstream infection: ERG11^{Y140F}, ^{K151R} with copy number variation and FKS1^{F665S} mutation. Int J Med Microbiol. 2025;321:151689. https://doi.org/10.1016/j.ijmm.2025.151689
26. Luo Z, Ning Y, Xiao M, Guo D, Xu H, Liu Y, et al. High azole non-wild type rates and nosocomial microsatellite typing aggregation of *Wickerhamomyces anomalus* in China according to a 12-year multicenter surveillance study. J Antimicrob Chemother. 2025;80:1964–71. https://doi.org/10.1093/jac/dkaf156

Address for correspondence: Diego H. Caceres, Immuno-Mycologics, 2701 Corporate Centre Dr, Norman, OK 73069, USA; email: diegocaceres84@gmail.com

Wickerhamomyces anomalus Fungemia during Healthcare-Associated Outbreak, Pereira, Colombia, 2025

Karen M. Ordoñez,[1] Diego H. Caceres,[1] Andres Ceballos-Garzon, Natalia Salazar-Giraldo, Bram Spruijtenburg, Lina M. Velasquez-Orozco, Eelco F.J. Meijer, Gabriel Vinazco, Elaine Cristina Francisco, Rodrigo Oliveira, Patricia Escandon, Jacques F. Meis

During March–July 2025, ten cases of *Wickerhamomyces anomalus* bloodstream infection were identified in Pereira, Colombia, mainly affecting pediatric patients; 9 cases occurred in children (8 neonates and a 5-year-old girl) and 1 case was in an adult. Most neonates were preterm and had multiple underlying conditions, such as congenital anomalies, respiratory complications, and adverse perinatal conditions, often compounded by limited prenatal care and maternal infections. All patients required intensive medical interventions, including central and peripheral venous catheters, mechanical ventilation, parenteral nutrition, and, in some cases, surgical procedures. Broad-spectrum antibacterial therapy was widely used, and antifungal treatment, primarily caspofungin, was initiated in half of cases. Antifungal susceptibility testing demonstrated low MICs for all agents. Short tandem repeat genotyping of 6 isolates indicated clonal transmission, supporting a healthcare-associated outbreak. Despite prolonged hospitalizations and severe clinical conditions, all patients survived, highlighting the importance of prompt diagnosis, strict infection control, and appropriate antifungal management.

Wickerhamomyces anomalus (synonym *Candida pelliculosa*, *Pichia anomala*, and *Hansenula anomala*) is an uncommon opportunistic yeast increasingly recognized as a cause of healthcare-associated infections, particularly in neonatal and pediatric intensive care units, and is associated with contaminated medical devices and inadequate infection control practices (*1*–*11*). Although the yeast is part of the environmental and sometimes human microbiota, under certain conditions it can cause invasive disease, especially in immunocompromised or critically ill patients (*10*). *W. anomalus* was overrepresented in bloodstream infections (BSIs) among persons who use intravenous drugs and is increasingly recognized as an emerging opportunistic pathogen (*12*).

In recent years, several healthcare-associated outbreaks caused by this yeast have been documented. In 2025, a cluster of *W. anomalus* BSIs was identified in Pereira, Colombia. The affected population consisted predominantly of neonatal and pediatric patients with severe underlying conditions and multiple invasive exposures. We describe the clinical, microbiological, and epidemiologic characteristics of the outbreak, as well as the infection control measures that were implemented and microbiological findings supporting clonal transmission.

Material and Methods

The outbreak investigation was conducted in accordance with the national guidelines and protocols of

Author affiliations: E.S.E. Hospital Universitario San Jorge de Pereira, Secretaría de Salud de Risaralda, Pereira, Colombia (K.M. Ordoñez, N. Salazar-Giraldo, L.M. Velasquez-Orozco, G. Vinazco); Immuno-Mycologics, Norman, Oklahoma, USA (D.H. Caceres); Universidad del Rosario, Bogota, Colombia (D.H. Caceres, A. Ceballos-Garzon); Radboudumc-CWZ Center of Expertise for Mycology, Nijmegen, the Netherlands (D.H. Caceres, B. Spruijtenburg, E.F.J. Meijer, J.F. Meis); Canisius-Wilhelmina Hospital (CWZ)/Dicoon, Nijmegen (B. Spruijtenburg, E.F.J. Meijer); Universidade Federal de São Paulo, São Paulo, Brazil (E.C. Francisco); Antimicrobial Resistance Institute of São Paulo, São Paulo (E.C. Francisco); Universidade Federal do Paraná, Curitiba, Brazil (E.C. Francisco, J.F. Meis); Bruker Daltonics GmbH & Co. KG, Bremen, Germany (R. Oliveira); Instituto Nacional de Salud, Bogotá (P. Escandon); University of Cologne, Cologne, Germany (J.F. Meis)

DOI: https://doi.org/10.3201/eid3206.251980

[1]These authors share first authorship for this article.

the Healthcare-Associated Infections Program of the Instituto Nacional de Salud of Colombia. Epidemiologic investigation, case identification, implementation of infection prevention and control measures, and data collection followed protocols established by the national surveillance system for healthcare-associated infections. This study was conducted as part of a public health outbreak investigation; therefore, institutional review board approval and informed consent were not required.

We collected clinical, epidemiologic, and microbiological data from patients from hospital records and laboratory databases as part of the outbreak investigation and control activities. We defined age groups as follows: neonates (0–30 days of age), infants (31–364 days of age), preschool-aged children (1–5 years of age), school-aged children (6–12 years of age), adolescents (13–17 years of age), and adults (≥18 years of age). We extracted data on patient demographics, underlying conditions, exposure to invasive procedures, antimicrobial therapy, and clinical outcomes using a standardized case report form designed for outbreak investigations. We accessed institutional infection prevention records to document infection control measures implemented during the outbreak. We performed descriptive statistical analyses with categorical variables summarized as frequencies and percentages and continuous variables summarized as medians and ranges. All procedures were conducted in accordance with institutional guidelines for outbreak investigation and response.

We processed blood cultures using aerobic and anaerobic BACT/ALERT bottles and incubated them in the BACT/ALERT VIRTUO (bioMérieux, https://www.biomerieux.com) system. We initially identified yeast isolates using the VITEK 2 system with the YST identification card (bioMérieux) and confirmed identification by using matrix-assisted laser desorption/ionization time-of-flight mass spectrometry and molecular sequencing.

We performed antifungal susceptibility testing (AFST) with the VITEK 2 YST AST card (bioMérieux), followed by confirmatory testing with a broth microdilution testing according to the Clinical and Laboratory Standards Institute (CLSI) reference standard M27 (*13*). We prepared fluconazole, voriconazole, anidulafungin, and amphotericin B stock solutions in dimethyl sulfoxide and made subsequent dilutions RPMI 1640 medium. In microdilution plates, we combined 2-fold serial dilutions of antifungals with a yeast inoculum standardized to 1–5 × 10^3 CFU/mL in a final volume of 200 µL/well. After 24 hours of incubation at 35°C, we determined MICs visually. We defined the MIC endpoints as the lowest drug concentration that produced ≥50% growth inhibition for the azoles (fluconazole, voriconazole) and anidulafungin and 100% growth inhibition for amphotericin B, compared with the drug-free control well. We ensured quality control using *C. parapsilosis* ATCC 22019 and *C. krusei* ATCC 6258.

For short tandem repeat (SRT) genotyping, we extracted DNA from all cultured isolates with the MagNA Pure 96 instrument and MagNA Pure DNA and Viral NA Small volume kit (Roche, https://www.roche.com) according to the manufacturer's instructions, as described previously (*14*). We performed multiplex PCR reaction amplifying 6 previously described STR markers with a thermocycler (Analytik Jena, https://www.analytik-jena.us) under identical PCR conditions (*14*). We analyzed amplicons on a 3500 XL genetic analyzer (Thermo Fisher Scientific, https://www.thermofisher.com), determined copy numbers using GeneMapper version 5 software (Thermo Fisher Scientific), and inferred phylogenetic relatedness between isolates using BioNumerics version 7.6.1 (bioMérieux) (*14*).

Results

Description of Cases

A total of 10 cases of BSI caused by *W. anomalus* were identified in 1 healthcare institution in Pereira, Risaralda Department, Colombia, during March–July 2025, epidemiologic weeks (EWs) 10–30 (Figure 1). Of the 10 case-patients, 6 were female and 4 were male. Nine cases occurred in pediatric patients, 8 neonates (<30 days of age) and 1 infant (a 5-year-old girl); 1 case was reported in a 65-year-old woman.

Of the 10 patients, 7 were admitted to the neonatal intensive care unit (NICU), 1 was admitted to the intermediate neonatal care unit, and 2 (the infant and the adult patient) were admitted through the emergency department. Two of the 10 case-patients were referred from other healthcare institutions.

The median time from hospital admission to onset of symptoms was 17 (range 6–47) days. Peripheral blood cultures were collected on the same day clinical signs and symptoms first appeared. The median interval from blood culture collection to the report of a positive result was 5 (range 2–14) days. The median time from hospital admission to microbiological confirmation of infection was 27 (range 11–50) days.

Initial identification of the isolates was performed using the automated VITEK 2 system, which identified the organisms as *Candida pelliculosa* (currently classified as *W. anomalus*). Because of the uncommon nature of this identification, all isolates were reported to the

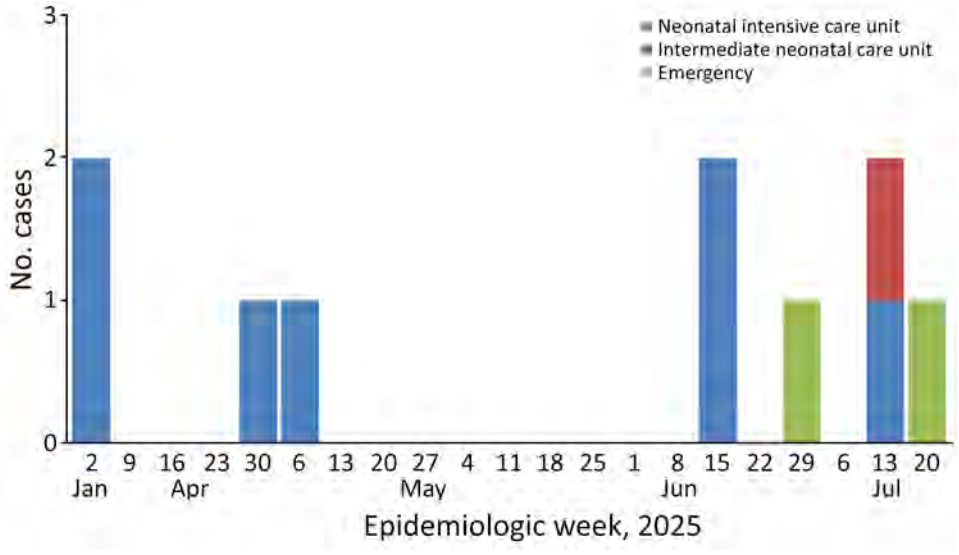

Figure 1. Epidemic curve of bloodstream infections caused by *Wickerhamomyces anomalus* during healthcare-associated outbreak, Pereira, Colombia, March–July 2025.

central laboratory of the State Department of Health of Risaralda, then referred to the National Institute of Health, according to the national guidelines for submission of compulsory notification of mycosis (https://www.ins.gov.co/BibliotecaDigital/criterios-para-el-envio-de-aislamientos-bacterianos-y-levaduras-genero-candida-spp-recuperados-en-iaas-para-confirmacion-de-mecanismos-de-resistencia-2024.pdf). Isolates were also referred for confirmatory testing using matrix-assisted laser desorption/ionization time-of-flight mass spectrometry (Bruker, https://www.bruker.com) and molecular analysis, as well as antifungal susceptibility testing. Those procedures were conducted by the Grupo de Microbiologia at the Instituto Nacional de Salud (Bogotá, Colombia); the Studies in Translational Microbiology and Emerging Diseases Research Group, School of Medicine and Health Sciences, Universidad del Rosario (Bogotá, Colombia); the Division of Infectious Diseases, Escola Paulista de Medicina–Universidade Federal de São Paulo (São Paulo, Brazil); and the Department of Medical Microbiology and Immunology, Canisius-Wilhelmina Hospital/Dicoon (Nijmegen, the Netherlands).

AFST results obtained with the VITEK 2 YST AST card (bioMérieux) were concordant with the reference broth microdilution method performed according to CLSI (*13*). Both methods confirmed that *W. anomalus* isolates exhibited low MIC values for all antifungal agents tested. The reference CLSI method yielded the following results: the MIC range (and mode) for fluconazole was 2–4 μg/mL (4 μg/mL), for itraconazole was 0.06–0.25 μg/mL (0.12 μg/mL), and for amphotericin B was 0.25–1 μg/mL (0.5 μg/mL). All isolates had an anidulafungin MIC of ≤0.03 μg/mL. Given the absence of both clinical breakpoints and epidemiologic cutoff values for *W. anomalus* from CLSI, no formal interpretation (e.g., susceptible, resistant, or non–wild-type) can be assigned to those results.

Of 10 available isolates, 6 (cases 5–10) were subjected to genotypic analysis (Table 1). To assess

Table 1. Summary of comorbidities and intrinsic risk factors of patients with *Wickerhamomyces anomalus* fungemia during healthcare-associated outbreak, Pereira, Colombia, 2025

Case	Underlying conditions	Intrinsic risk factors
1	Esophageal atresia	Age 15 d. Cesarean delivery, transverse fetal position, neonatal hypotonia. Referred from another hospital
2	Trisomy 21	Age 10 d. Poor neonatal adaptation, Cesarean delivery
3	Fetal growth restriction, polyhydramnios	Age 18 d. Prematurity (37.5 wks), suspected tracheoesophageal fistula
4	Neonatal hypoxia, respiratory distress	Age 30 d. No prenatal care, meconium-stained fluid, maternal infection. Referred from another hospital
5	Respiratory distress syndrome	Age 14 d. Prematurity (32 wks), rupture of membranes, gastrointestinal bleeding
6	Hyaline membrane disease, suspected congenital pneumonia	Age 30 d. Extreme prematurity (28.5 wks), high septic risk
7	Suspected neonatal sepsis	Age 5 y. Fever, leukocytosis, abdominal discomfort
8	Respiratory failure, apnea	Age 30 d. Prematurity (31.5 wks), twin pregnancy, growth restriction
9	Upper gastrointestinal bleeding (adult case)	Age 63 y. Prior hospitalization, incomplete diagnostic workup
10	Prematurity (34.1 weeks)	Age 30 d. Twin pregnancy, no prenatal care

genetic diversity and potential transmission patterns, we performed STR genotyping and compared our results to control outbreak isolates from Venezuela and Brazil. The STR profiles indicated clonal transmission, because all 6 isolates exhibited an identical genotype suggesting a common source or closely linked transmission chain (Figure 2).

Summary of Underlying Conditions and Intrinsic Risk Factors

The analyzed cases primarily involved neonates with multiple underlying conditions and intrinsic risk factors for candidemia. Congenital anomalies were common, including esophageal atresia, more occasionally tracheosophageal fistula, and suspected trisomy 21. Prematurity was reported in 3 patients; gestational age ranged from 28.5 to 37.5 weeks. Prematurity was frequently accompanied by severe respiratory complications, such as respiratory distress syndrome, hyaline membrane disease, apnea, and requirement for intubation and mechanical ventilation. Additional perinatal complications included fetal growth restriction and twin pregnancies, which both contributed to increased neonatal vulnerability (Table 1).

Maternal factors also played a role. Absence of prenatal care, untreated vaginal infections, premature rupture of membranes, and meconium-stained amniotic fluid were recurrent findings. Those conditions were associated with neonatal hypoxia, hypotonia, low Apgar scores, and episodes of hypoglycemia. Several neonates were at high risk for sepsis, frequently linked to maternal fever, leukocytosis, and suspected congenital pneumonia. An isolated case of upper gastrointestinal bleeding was documented in an adult patient, unrelated to the neonatal population (Table 1). Overall, the main predisposing factors identified were prematurity, congenital malformations, respiratory complications, and adverse maternal conditions, underscoring the importance of comprehensive perinatal management and close clinical monitoring from birth.

Common Exposure Factors

Across the analyzed cases, several invasive procedures and therapeutic interventions were consistently identified. The most frequent exposure factors included epicutaneous and central venous catheters, as well as umbilical arterial and venous lines, which were often maintained for extended periods. Endotracheal mechanical ventilation was common, particularly among neonates with respiratory distress. Parenteral nutrition was widely administered (n = 9), reflecting the presence of gastrointestinal complications and the need for postoperative nutritional support (Table 2). Multiple surgical procedures were performed, including laparotomy; intestinal resection and anastomosis; correction of

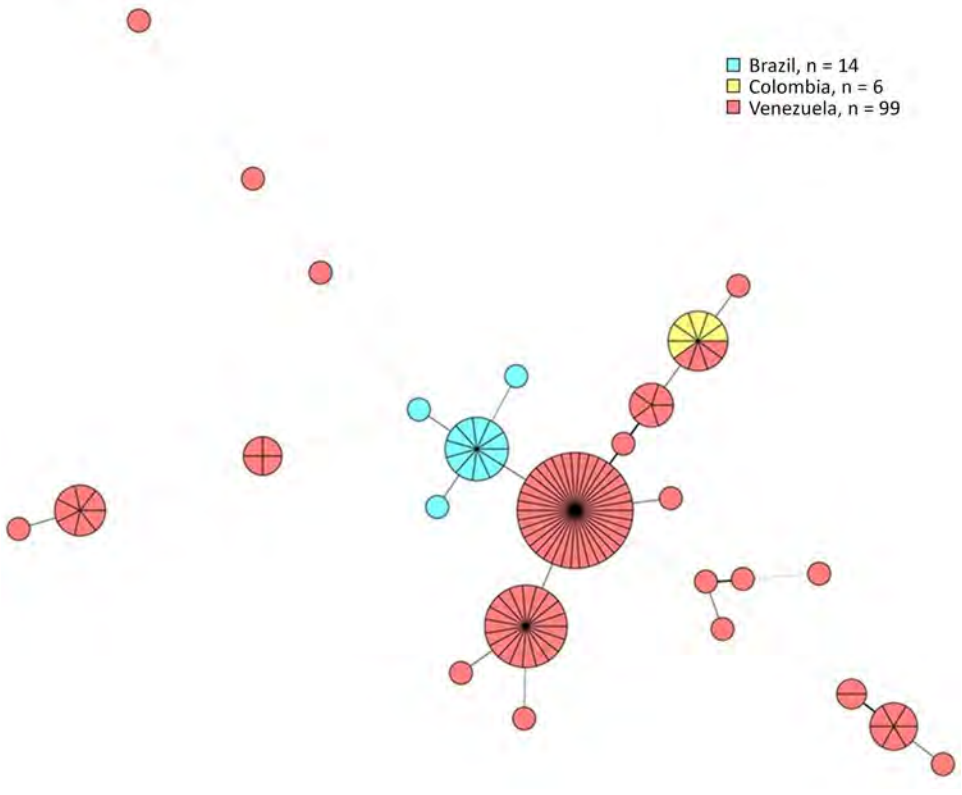

Figure 2. Minimum-spanning tree of *Wickerhamomyces anomalus* genotypes based on short tandem repeat genotyping in study of *W. anomalus* fungemia during healthcare-associated outbreak, Pereira, Colombia, 2025. Isolates from Colombia are compared with control isolates from Venezuela and Brazil (*1*,*15*).

Table 2. Common exposure factors identified in cases of *Wickerhamomyces anomalus* fungemia during healthcare-associated outbreak, Pereira, Colombia, 2025

Exposure factor	Frequency, no. (%) n = 10	Clinical context
Epicutaneous catheter	8 cases (80)	Long-term intravenous therapy, parenteral nutrition
Peripheral catheter	9 cases (90)	Initial intravenous access, supportive therapy
Central venous catheter	3 cases (30)	Advanced monitoring, multiple drug infusions
Umbilical venous/arterial catheter	1 case (10)	Neonatal stabilization
Endotracheal tube	8 cases (80)	Airway management, mechanical ventilation
Nasofibrolaryngoscopy	1 case (10)	Diagnostic airway evaluation
Thoracostomy tube	1 case (10)	Pleural drainage postsurgery
Femoral catheter	1 case (10)	Complex surgical/postoperative care
Jugular catheter	1 case (10)	Additional vascular access
Parenteral nutrition	9 cases (90)	Nutritional support in gastrointestinal surgery or prematurity
Major abdominal surgery	6 cases (60)	Laparotomy, intestinal resection, anastomosis
Antimicrobial therapy	10 cases (100)	Empiric and targeted treatment for infection risk

malrotation and duodenal atresia; colostomy or ileostomy; and peritoneal lavage, frequently accompanied by abdominal drainage or the use of negative pressure therapy devices. Endoscopic procedures such as esophagogastroduodenoscopy were also reported (Table 2). Overall, these findings highlight the high frequency of invasive device use, complex surgical interventions, parenteral nutrition, and broad antimicrobial exposure, factors that collectively predispose patients to nosocomial infection and associated complications.

Invasive Devices and Surgical Interventions

Invasive device use was a predominant feature among all analyzed cases, reflecting the complexity of care required for critically ill neonatal and pediatric patients. Peripheral and epicutaneous catheters were the most frequently used devices; peripheral catheters were documented in 9 (90%) cases and epicutaneous catheters were documented in 8 (80%) cases, primarily for prolonged intravenous therapy and parenteral nutrition. Endotracheal tubes were also placed in 8 (80%) cases and were most commonly associated with mechanical ventilation during surgical procedures or respiratory distress management. Central venous catheters were inserted in 3 (30%) patients, requiring advanced hemodynamic monitoring or administration of multiple drugs, whereas umbilical venous and arterial catheters were used in 1 neonate (10%) during early stabilization. Other less frequently reported devices included femoral and jugular catheters and thoracostomy tubes (each reported 1 case [10%]), generally related to complex postoperative care (Table 2; Figure 3).

Device exposure was often simultaneous and prolonged; epicutaneous or peripheral catheters used in combination with endotracheal tubes were the most prevalent. The cumulative exposure to multiple invasive devices, coupled with extended parenteral nutrition and sequential broad-spectrum antimicrobial therapy, highlights the increased vulnerability of this population to healthcare-associated infections. Extensive surgical interventions were also documented, particularly in neonates with congenital or gastrointestinal anomalies. In 1 complex case, multiple abdominal surgeries were required to manage congenital malformations and postoperative complications, culminating in esophageal reconstruction with gastric interposition. The timeline of interventions and identified risk factors illustrates the temporal overlap of hospitalizations, clinical procedures, and key events such as central venous catheter manipulation and antifungal therapy initiation, which together highlight potential periods of common exposure and support the hypothesis of healthcare-associated transmission (Figure 3).

Summary of Antimicrobial Therapy Use

According to hospital protocol, antibiotic therapy in neonates was initiated upon the diagnosis of sepsis; all neonates received antibiotics per protocol. In adults, antibiotic therapy was initiated only in patients with documented bacterial coinfection. Antimicrobial exposure was extensive across all cases; multiple sequential and combination regimens. β-lactams were the most frequently used class in all cases. Among those, ampicillin was administered in 6 cases (60%), oxacillin was administered in 4 cases (40%), and cefepime was administered in 4 cases (40%). Cefotaxime and ampicillin/sulbactam were each used in 2 cases (20%), whereas piperacillin/tazobactam, meropenem, and ertapenem were documented in 3 cases (30%) (Table 3). Aminoglycosides were highly prevalent; gentamicin was used in 7 cases (70%) and amikacin was used in 6 cases (60%). Vancomycin was administered in 6 cases (60%), primarily for gram-positive coverage. Metronidazole was included in 6 cases (60%) for anaerobic coverage in abdominal surgical scenarios (Table 3).

Antifungal therapy (caspofungin) was initiated in all cases; in 1 case, fluconazole was documented after

a switch from caspofungin after 7 days of treatment, and fluconazole was administered for an additional 6 days. The average duration of caspofungin therapy was 14 days (range 7–22 days) (Table 3).

Overall, antimicrobial regimens were characterized by frequent changes and combination therapy. Those factors reflect the complexity of infections and surgical interventions in critically ill neonates and pediatric patients.

Containment and Infection Control Measures

After the detection of fungal BSIs, a series of infection control interventions were implemented and reinforced. Environmental disinfection with sodium dichloroisocyanurate was intensified, progressively increasing the chlorine concentration in NICUs and PICUs to 4,000 ppm. Cleaning and disinfection routines were performed >2×/day; deep terminal cleaning was conducted weekly. For patients who had invasive devices, bathing using chlorhexidine (2%) was standardized to 3×/week and later increased to daily practice. Hygiene audits and staff training sessions were conducted weekly to reinforce hand hygiene and aseptic techniques. Environmental surveillance, including surface cultures from critical areas such as parenteral nutrition preparation rooms and air circulation systems, was performed biweekly to assess microbial contamination and guide interventions. Following the hospital infection control manual, surveillance cultures were obtained from all 8 neonatal incubators. Specimens were collected from internal surfaces where infants were placed and from the drainage systems that remove the water generated by incubators. In addition, environmental cultures were obtained from operating rooms (6 samples). All cultures yielded negative results.

Outcomes

All patients had negative follow-up blood cultures at 72 hours after initiation of antifungal therapy. The median length of hospital stay was 44 days, and all patients were discharged alive.

Discussion

This outbreak of 10 bloodstream infections caused by *W. anomalus* highlights the vulnerability of critically ill neonates and pediatric patients to emerging opportunistic fungal pathogens. Although several outbreaks have been reported over the years (Table 4), few studies have used robust molecular genotyping for confirmation. We used a recently developed panel of 6 highly polymorphic microsatellite markers, validated with whole-genome sequencing single-nucleotide polymorphism calling, to detect a fungemia

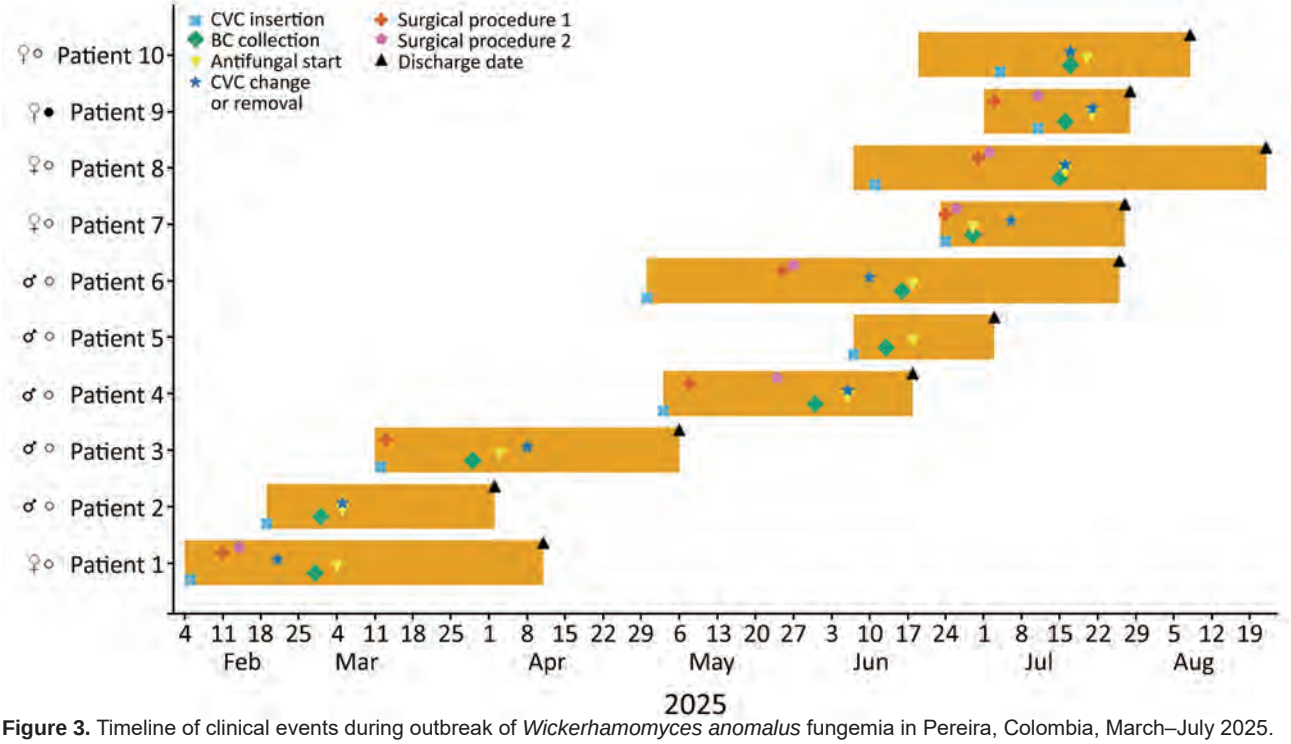

Figure 3. Timeline of clinical events during outbreak of *Wickerhamomyces anomalus* fungemia in Pereira, Colombia, March–July 2025. Each bar represents the hospitalization period of each affected patient; symbols indicate key clinical events. Male patients are indicated with ♂, female patients with ♀, pediatric patients with white circle, adult patient with a filled circle. BC, blood culture; CVC, central venous catheter.

outbreak of *W. anomalus* in a single hospital in Colombia and compared results with previously published outbreaks in Venezuela and Brazil (*1*,*20*). All Colombia isolates displayed an identical genotype, and the STR assay is known to have a high discriminatory power, strongly suggesting clonal transmission, which is supported by the epidemiologic data. Nonetheless, WGS is needed for confirmation of the nosocomial transmission (*20*). Curiously, the Colombia isolates clustered with the Venezuela isolates; some even displayed identical genotypes. That clustering indicates transmission between those countries, which could be encouraged by patient transfer. Alternatively, a population of *W. anomalus* could have spread within the environments of Colombia and Venezuela recently, after which the patients acquired the yeast from there.

The predominance of cases in neonates, particularly preterm infants with multiple underlying conditions, underscores the interplay of intrinsic risk factors, such as prematurity, congenital anomalies, and severe respiratory compromise, with extrinsic exposures, such as invasive devices, parenteral nutrition, and extensive surgical interventions (*2*,*3*,*7*). Maternal factors, including limited prenatal care and perinatal complications, further contributed to neonatal susceptibility. The median intervals from hospital admission to symptom onset (17 days) and to microbiological confirmation (27 days) emphasize the diagnostic challenges associated with rare yeasts. Antifungal susceptibility testing revealed that timely initiation of targeted therapy, primarily with echinocandins, can be critical in managing such infections. However, prophylactic strategies and empiric antifungal therapy remain complex decisions in high-risk neonatal populations.

The clinical interpretation of the MIC values is challenging because of the absence of species-specific

Table 3. Summary of antimicrobial drugs used for patients with *Wickerhamomyces anomalus* fungemia during healthcare-associated outbreak, Pereira, Colombia, 2025

Antimicrobial drug	Average duration	No. (%) cases
Ampicillin and gentamicin	2–8 d	7 (70)
Amikacin	1–10 d	6 (60)
Vancomycin	2–26 d	6 (60)
Metronidazole	2–15 d	6 (60)
Oxacillin	2–8 d	4 (40)
Cefepime	3–36 d	4 (40)
Piperacillin/tazobactam	2–3 d	3 (30)
Meropenem	4–5 d	3 (30)
Ertapenem	4 d	2 (20)
Cefotaxime	6 d	2 (20)
Ampicillin/sulbactam	5 d	2 (20)
Caspofungin	14 d	10 (100)
Fluconazole*	6 d	1 (10)

*Switched from caspofungin.

Table 4. Summary of reported *Wickerhamomyces anomalus* (synonyms *Candida pelliculosa*, *Pichia anomala*, and *Hansenula anomala*) outbreaks worldwide*

Reference	Year	Country	Key findings
(*10*)	2021	China	Case–control study; broad-spectrum antibiotics and prolonged hospital stay increased risk; biofilm formation associated. No deaths.
(*15*)	2009–2021	China	307 isolates; high resistance to fluconazole (48.5%) and voriconazole (34.5%) (broth microdilution, CLSI methods M27 [*13*]); 118 genotypes; nosocomial outbreaks identified.
(*14*)	2018–2019	India	New STR scheme (6 markers); 90 isolates; 38 genotypes; 4 simultaneous outbreaks within a single hospital.
(*11*)	2015	South Korea	11 patients; multiple risk factors; effective outbreak control after environmental interventions. No deaths.
(*16*)	2014–2016	China	13 cases; 38% mortality; risk factors include ventral venous catheter, antibiotics, TPN; high azole MICs (CLSI and EUCAST).
(*5*)	2013	Brazil	Neonatal outbreak; possible clonal origin; uncommon pathogen.
(*6*)	2013	China	Neonatal outbreak; 6 cases, 1 death; single predominant clone; control achieved with prophylaxis and hygiene measures.
(*9*)	2012–2013	China	14 neonates infected; 2 distinct clones; good clinical outcomes; 2 NICU outbreaks. High in vitro susceptibility to multiple antifungals (susceptibility testing method not described). No deaths.
(*1*)	2002–2004	Brazil	Outbreak affecting 17 children with 41% mortality, linked to central venous catheters; caused by a single strain.
(*17*)	2001	Croatia	*H. anomala* infection in 8 ICU adults. Case-control analysis (32 patients) identified blood alkalosis duration as the only significant risk factor. Source was not identified.
(*7*)	1998	Brazil	Four infants with *P. anomala* infection, one of whom also had *Candida parapsilosis* infection. *P. anomala* acquisition was likely exogenous.
(*18*)	1997	Brazil	24 cases outbreak, in an oncological hospital in Rio de Janeiro. Leukemia was reported in 65% of cases, demonstrating the opportunistic behavior of *H. anomala*.
(*8*)	1996–1998	India	379 children/neonates affected; transmission through healthcare workers' hands; control achieved through strict hygiene.
(*19*)	1986	United Kingdom	52 colonized neonates, 8 developed infections: 5 fungaemia, 2 fungaemia with ventriculitis, 1 ventriculitis. Seven were very low birthweight (<1,500 g). All were successfully treated with 5-flucytosine and amphotericin B.

*CLSI, Clinical Laboratory Standards Institute; EUCAST, European Committee on Antimicrobial Susceptibility Testing; NICU, neonatal intensive care unit; STR, short tandem repeat; TPN, total parenteral nutrition.

clinical breakpoints for *W. anomalus* from the CLSI, the methodology used in this study. To provide context for our findings, we referenced the epidemiologic cutoff values (ECOFFs) established by EUCAST (*21*). According to EUCAST ECOFFs (fluconazole ≥32 μg/mL, anidulafungin ≥0.12 μg/mL, amphotericin B ≥2 μg/mL), all isolates in our cohort would be classified as wild-type, exhibiting no acquired resistance mechanisms. Crucially, however, ECOFFs are method-specific, and applying EUCAST criteria to CLSI-derived data is for informational purposes only and does not constitute a formal interpretation. Consequently, although the low MICs suggest that the circulating clone is likely drug-susceptible, the definitive correlation of those in vitro results remains uncertain. The *W. anomalus* isolates analyzed in this study demonstrated markedly higher susceptibility to all antifungal agents tested. That finding contrasts with several reports from Asia, in which isolates frequently exhibited elevated MICs, particularly to azoles such as fluconazole and voriconazole. Recent studies from China and India have documented substantial high non–wild-type rates and high azole MICs, suggesting regional variability in antifungal susceptibility patterns. India reported that 50/70 (72%) *W. anomalus* isolates were non–wild-type for fluconazole, 17% demonstrated cross-resistance with voriconazole, and 1.4% demonstrated cross-resistance with micafungin (*22*). A larger, similar study from China found 149/307 (48.5%) non–wild-type to fluconazole and 106/307 (34.5%) voriconazole (*15*).

A pan–azole-resistant and pan–echinocandin-resistant *W. anomalus* bloodstream isolate was recently reported in China (*23*). Although most isolates remain susceptible, the emergence of multidrug resistance represents a growing threat to clinical management, particularly in resource-limited settings (*23*).

This outbreak was closely associated with exposure to multiple invasive devices, prolonged hospitalization, parenteral nutrition, and broad-spectrum antimicrobial use, reflecting a classic pattern of healthcare-associated infections in intensive care settings (*2*,*3*,*7*). Infection control interventions, such as enhanced environmental cleaning, standardized chlorhexidine bathing, and staff education on aseptic techniques, were instrumental in containing the outbreak, illustrating the importance of rapid, multifaceted infection prevention strategies in high-risk units. A search for the environmental origin of the outbreak was conducted, but *W. anomalus* was not detected after testing numerous inanimate surfaces. Although the source was not uncovered, implementing strict infection control measures after the outbreak was recognized was successful in curbing ongoing cases of fungemia.

Despite the severity of underlying conditions and the complexity of care, all patients survived, suggesting that early recognition, appropriate microbiological work-up, adherence to strict infection control protocols, and timely initiation of antifungal therapy are pivotal in favorable outcomes. This series reinforces the need for vigilance regarding uncommon yeasts in neonatal and pediatric intensive care units, particularly in regions where surveillance is limited.

The first limitation of this study is that the small number of cases and absence of a comparison group limited our ability to assess independent risk factors or establish causal associations. Despite extensive environmental sampling, the source of the outbreak could not be identified. Interpretation of antifungal susceptibility results was constrained by the lack of species-specific breakpoints for *W. anomalus*. In addition, the single-center, retrospective design might limit generalizability and introduce incomplete data capture.

In conclusion, *W. anomalus* BSI represents a rare but clinically significant nosocomial infection, predominantly affecting preterm and critically ill neonates with multiple underlying conditions and extensive exposure to invasive procedures. Comprehensive perinatal management, strict aseptic care, and robust infection control measures are essential to prevent outbreaks and optimize patient outcomes. Ongoing surveillance and reporting are critical to improving understanding of epidemiology, risk factors, and effective management of this emerging pathogen.

Funding was provided by Fundação de Amparo à Pesquisa do Estado de São Paulo–FAPESP (project number: 2021/10599-3, and Conselho Nacional de Desenvolvimento Científico e Tecnológico (project no. 409184/2022-5).

D.H.C. is an Immuno-Mycologics employee, serving as the Latin America Account Manager. R.O. is the Regional Business Manager for Latin America at Bruker, Microbiology & Infection Diagnostics. E.F.J.M. has received research grants from Mundipharma and Scynexis, is a member of the scientific advisory board for Pfizer, and has received speaker fees from Gilead Sciences.

About the Author

Dr. Ordoñez is an infectious diseases physician with E.S.E. Hospital Universitario San Jorge de Pereira, Secretaría de Salud de Risaralda, Pereira, Colombia. Her work focuses on patient care, antimicrobial stewardship, and the integration of clinical practice with diagnostic and

public health strategies. Dr. Caceres is a microbiologist and epidemiologist with Universidad del Rosario, Bogota, Colombia. His research focuses on outbreak investigations, technology transfer, and diagnostic assay implementation, linking scientific research with regional public health and diagnostic strategies.

References

1. Pasqualotto AC, Sukiennik TC, Severo LC, de Amorim CS, Colombo AL. An outbreak of *Pichia anomala* fungemia in a Brazilian pediatric intensive care unit. Infect Control Hosp Epidemiol. 2005;26:553–8. https://doi.org/10.1086/502583
2. Francisco EC, Caceres DH, Brunelli JGP, Garcia-Effron G, Arastehfar A, Ribeiro FC, et al. An update on clinically relevant, rare, and emerging *Candida* and Saccharomycotina yeasts that have been recently reclassified from *Candida.* Clin Microbiol Rev. 2025;38:e0006423. https://doi.org/10.1128/cmr.00064-23
3. Ioannou P, Baliou S, Kofteridis DP. Fungemia by *Wickerhamomyces anomalus*—a narrative review. Pathogens. 2024;13:269. https://doi.org/10.3390/pathogens13030269
4. Rattani S, Farooqi J, Hussain AS, Jabeen K. Spectrum and antifungal resistance of Candidemia in neonates with early- and late-onset sepsis in Pakistan. Pediatr Infect Dis J. 2021;40:814–20. https://doi.org/10.1097/INF.0000000000003161
5. da Silva CM, de Carvalho Parahym AM, Leão MP, de Oliveira NT, de Jesus Machado Amorim R, Neves RP. Fungemia by *Candida pelliculosa* (*Pichia anomala*) in a neonatal intensive care unit: a possible clonal origin. Mycopathologia. 2013;175:175–9. https://doi.org/10.1007/s11046-012-9605-0
6. Lin HC, Lin HY, Su BH, Ho MW, Ho CM, Lee CY, et al. Reporting an outbreak of *Candida pelliculosa* fungemia in a neonatal intensive care unit. J Microbiol Immunol Infect. 2013;46:456–62. https://doi.org/10.1016/j.jmii.2012.07.013
7. Aragão PA, Oshiro IC, Manrique EI, Gomes CC, Matsuo LL, Leone C, et al.; IRIS Study Group. *Pichia anomala* outbreak in a nursery: exogenous source? Pediatr Infect Dis J. 2001; 20:843–8. https://doi.org/10.1097/00006454-200109000-00004
8. Chakrabarti A, Singh K, Narang A, Singhi S, Batra R, Rao KL, et al. Outbreak of *Pichia anomala* infection in the pediatric service of a tertiary-care center in Northern India. J Clin Microbiol. 2001;39:1702–6. https://doi.org/10.1128/JCM.39.5.1702-1706.2001
9. Yang Y, Wu W, Ding L, Yang L, Su J, Wu B. Two different clones of *Candida pelliculosa* bloodstream infection in a tertiary neonatal intensive care unit. J Infect Dev Ctries. 2021;15:870–6. https://doi.org/10.3855/jidc.12103
10. Zhang L, Xiao M, Arastehfar A, Ilkit M, Zou J, Deng Y, et al. Investigation of the emerging nosocomial *Wickerhamomyces anomalus* infections at a Chinese tertiary teaching hospital and a systemic review: clinical manifestations, risk factors, treatment, outcomes, and anti-fungal susceptibility. Front Microbiol. 2021;12:744502. https://doi.org/10.3389/fmicb.2021.744502
11. Jung J, Moon YS, Yoo JA, Lim JH, Jeong J, Jun JB. Investigation of a nosocomial outbreak of fungemia caused by *Candida pelliculosa* (*Pichia anomala*) in a Korean tertiary care center. J Microbiol Immunol Infect. 2018;51:794–801. https://doi.org/10.1016/j.jmii.2017.05.005
12. Paccoud O, Lortholary O, Imbert S, Letscher-Bru V, Boukris-Sitbon K, Obadia T, et al.; French Mycoses Study Group. Yeast fungaemia among injection drug users in France (2012–2022): a cross-sectional observational study. Lancet Reg Health Eur. 2025;55:101365. https://doi.org/10.1016/j.lanepe.2025.101365
13. Clinical and Laboratory Standards Institute. Reference method for broth dilution antifungal susceptibility testing of yeasts, 4th ed. CLSI standard M27. Wayne (PA): The Institute; 2017.
14. Spruijtenburg B, Rudramurthy SM, Meijer EFJ, van Haren MHI, Kaur H, Chakrabarti A, et al. Application of novel short tandem repeat typing for *Wickerhamomyces anomalus* reveals simultaneous outbreaks within a single hospital. Microorganisms. 2023;11:1525. https://doi.org/10.3390/microorganisms11061525
15. Luo Z, Ning Y, Xiao M, Guo D, Xu H, Liu Y, et al. High azole non-wild type rates and nosocomial microsatellite typing aggregation of *Wickerhamomyces anomalus* in China according to a 12-year multicenter surveillance study. J Antimicrob Chemother. 2025;80:1964–71. https://doi.org/10.1093/jac/dkaf156
16. Zhang Z, Cao Y, Li Y, Chen X, Ding C, Liu Y. Risk factors and biofilm formation analyses of hospital-acquired infection of *Candida pelliculosa* in a neonatal intensive care unit. BMC Infect Dis. 2021;21:620. https://doi.org/10.1186/s12879-021-06295-1
17. Kalenic S, Jandrlic M, Vegar V, Zuech N, Sekulic A, Mlinaric-Missoni E. *Hansenula anomala* outbreak at a surgical intensive care unit: a search for risk factors. Eur J Epidemiol. 2001;17:491–6. https://doi.org/10.1023/A:1013739802940
18. Thuler LC, Faivichenco S, Velasco E, Martins CA, Nascimento CR, Castilho IA. Fungaemia caused by *Hansenula anomala*—an outbreak in a cancer hospital. Mycoses. 1997;40:193–6. https://doi.org/10.1111/j.1439-0507.1997.tb00213.x
19. Murphy N, Buchanan CR, Damjanovic V, Whitaker R, Hart CA, Cooke RW. Infection and colonisation of neonates by *Hansenula anomala*. Lancet. 1986;1:291–3. https://doi.org/10.1016/S0140-6736(86)90827-5
20. Franco MD, Caceres DH, Carrillo JFF, Pérez-Guzmán A, Ceballos-Garzon A, Briceño AC, et al. Outbreak of *Wickerhamomyces anomalus* (formerly *Candida pelliculosa*) bloodstream infections, Venezuela, 2022–2023. Emerg Infect Dis. 2026;32:933–40.
21. Pfaller MA, Castanheira M, Diekema DJ, Messer SA, Jones RN. Triazole and echinocandin MIC distributions with epidemiological cutoff values for differentiation of wild-type strains from non-wild-type strains of six uncommon species of *Candida*. J Clin Microbiol. 2011;49:3800–4. https://doi.org/10.1128/JCM.05047-11
22. Verma S, Tilak R, Singh G, Singh S, Kumari A, Rudramurthy SM, et al. Multicentre investigation of *Wickerhamomyces anomalus* fungemia in India: emerging resistance and mechanistic insights. J Antimicrob Chemother. 2026;81:dkaf420. https://doi.org/10.1093/jac/dkaf420
23. Luo Z, Ning Y, Dai R, Ainiwaer A, Li Y, Zhang R, et al. A pan-azole and pan-echinocandin resistant *Wickerhamomyces anomalus* isolate causing bloodstream infection: ERG11^{Y140F}, ^{K151R} with copy number variation and FKS1^{F665S} mutation. Int J Med Microbiol. 2025;321:151689. https://doi.org/10.1016/j.ijmm.2025.151689

Address for correspondence: Diego H. Caceres, Immuno-Mycologics, 2701 Corporate Centre Dr, Norman, OK 73069, USA; email: diegocaceres84@gmail.com

Identification of Novel Recombinant Human Adenovirus Genotype B117 from Pediatric Cases, China

Jinjin Wang,[1] Ling Jing,[1] Yali Duan, Xiaolei Guan, Yue Cui, Junhong Ai, Ran Wang, Xiangpeng Chen, Yuhai Bi, Xiaomei Liu, Baoping Xu,[2] Yun Zhu,[2] Zhengde Xie[2]

During molecular surveillance of human adenoviruses (HAdVs) in children hospitalized with acute lower respiratory tract infections in Beijing, China, during 2014–2024, the most prevalent genotypes were HAdV-B114 (53.85%) and HAdV-B7 (27.18%). A novel recombinant genotype, HAdV-B117, was identified in 2 children <5 years of age with severe community-acquired pneumonia and serious complications. Genomic analysis revealed that HAdV-B117 arose from HAdV-B114 (P7H3F3) with the fiber gene from HAdV-B7. We observed amino acid substitutions and deletions in the pivotal regions of 3 major capsid proteins, and some were predicted to alter the protein structure. In vitro, the replication kinetics of HAdV-B117 were similar to those of HAdV-B3 and HAdV-B7. Clinical manifestations resembled severe pneumonia caused by HAdV-B3 or HAdV-B7. Both children recovered after treatment. The emergence of HAdV-B117 highlights the need for continuous genomic surveillance of HAdVs to detect novel recombinants with potential public health effects.

Human adenoviruses (HAdVs) are nonenveloped, double-stranded DNA viruses of the genus *Mastadenovirus*, Adenoviridae family (*1*). To date, 116 genotypes have been recognized within 7 species (A–G) (http://hadvwg.gmu.edu). Currently, the nomenclature protocol primarily follows the system proposed by the international HAdV Working Group (*2*), which defines genotypes on the basis of the nucleotide sequences of the penton base, hexon, and fiber genes. HAdV-B (HAdV-3, -7, -55), HAdV-C (HAdV-1, -2, -5, -6), and HAdV-E (HAdV-4) are considered major causative agents of acute respiratory tract infections in children (*3*). Within species B, HAdV-B3 and HAdV-B7 are the most frequently reported etiologic agents worldwide and are associated with severe pneumonia and occasional fatalities in pediatrics (*4*,*5*). Homologous recombination, particularly within the 3 major capsid protein genes, largely contributes to HAdV-B diversity, yielding recombinant genotypes with high virulence and broad tissue tropism (*6*), some of which have caused severe outbreaks (e.g., HAdV-B55, HAdV-B66) (*7*–*10*).

Densely populated and highly mobile metropolises are hotspots for HAdV transmission. However, in China, the disease effects of HAdVs, including HAdV-B, remain unclear because of the absence of a specialized surveillance system (*11*). We conducted a molecular epidemiologic investigation of HAdVs in Beijing, China, during 2014–2024. By applying whole-genome sequencing (WGS) to HAdV isolates from children hospitalized with acute lower respiratory tract infections (LRTIs) and analyzing genomic data, a novel intertypic recombinant HAdV-B genotype was identified from 2 children <5 years of age with severe community-acquired pneumonia (CAP). According to the evaluation of the international HAdV Working Group, the virus was designated HAdV-117 (P7H3F7). The identification of the novel recombinant HAdV-B117 underscores the need for ongoing genomic surveillance to monitor emerging HAdV threats.

Materials and Methods

Patients and Clinical Data Collection

Children <18 years of age hospitalized with acute RLTI at Beijing Children's Hospital, Capital Medical

Author affiliations: Beijing Children's Hospital, Capital Medical University, Beijing, China (J. Wang, Y. Duan, X. Guan, Y. Cui, J. Ai, R. Wang, X. Chen, X. Liu, B. Xu, Y. Zhu, Z. Xie); Chinese Academy of Medical Sciences & Peking Union Medical College, Beijing (L. Jing); Chinese Academy of Sciences, Beijing (Y. Bi).

DOI: https://doi.org/10.3201/eid3206.250940

[1]These first authors contributed equally to this article.

[2]These senior authors contributed equally to this article.

University, Beijing, China, during 2014–2024 were enrolled. Children with a disease course >7 days or whose parents or guardians did not consent were excluded. We collected clinical data from the clinical electronic medical record system.

Specimen Collection and HAdV Detection

Respiratory specimens, including sputum, throat and nasopharyngeal swab specimens, bronchoalveolar lavage fluid, and nasopharyngeal aspirates, were collected within 24 hours of admission and transported at 4°C to our laboratory. We tested all samples by using the Multiplex Respiratory Viral Panel (Diasorin, https://us.diasorin.com) for the presence of viral nucleic acids, including HAdV and other common respiratory viruses.

Virus Isolation and WGS

We inoculated HAdV-positive samples into Hep-2 or A549 cell lines for virus isolation and purified the novel genotype HAdV through 3 rounds of plaque purification in A549 cells. We sent the purified nucleic acids of the HAdV strains to Annoroad Gene Technology Co., Ltd (Beijing, China, https://www.annoroad.com) for WGS by using the Illumina sequencing platform (Illumina, https://www.illumina.com). We used reference-based assembly to construct consensus sequences. We determined the reference genomes by the traditional HAdV typing method as previously described (*12*). We used the HAdV-B3 prototype strain (the GB strain, GenBank accession no. AY599834) as the reference genome of the novel genotype HAdV. If ≥2 distinct genomic sequences >34 kb were obtained from the same strain, we considered the possibility of co-infection. We annotated complete genome sequences by using Prokka version 1.11 (https://github.com/tseemann/prokka) and submitted them to GenBank.

HAdV Typing

We extracted the penton base, hexon, and fiber gene sequences from the HAdV whole-genome sequences obtained and aligned them with sequences in GenBank by using BLAST (https://blast.ncbi.nlm.nih.gov) for preliminary typing. We retrieved the reference sequences for the 3 genes of HAdV from GenBank, excluding those with high consistency in region, time, and sequence. We performed multiple sequence alignment by using MAFFT (https://www.ebi.ac.uk/Tools/msa/mafft). We constructed phylogenetic trees by using MEGA version 7.0.26 (https://www.megasoftware.net/older_versions) with the neighbor-joining method and Kimura 2-parameter model, with a bootstrap test of 1,000 replicates to further determine the type.

Phylogenetic Analysis

We selected whole-genome sequences of prototype or representative strains of all genotypes within the same species as the candidate novel genotype from GenBank. On the basis of their annotations, we extracted the penton base, hexon, fiber, and early gene (*E1–E4*) gene sequences for phylogenetic analysis. We constructed the phylogenetic trees by using the maximum-likelihood method with 1,000 bootstrap replicates in MEGA version 7.0.26 after multiple sequence alignments. We considered the model with the lowest Bayesian information criterion score optimal.

Recombination Analysis

We conducted recombination analysis of the whole-genome sequences of the novel genotype by using RDP4 (https://www.h3abionet.org/categories/blog-post/tools-services/recombination-detection-program) with 7 methods (RDP, GENECONV, BootScan, MaxChi, Chimaera, SiScan, and 3Seq). We corrected the probability of each putative recombination event by using the Bonferroni procedure and set the significance threshold at $p<0.05$. We considered credible only recombination events supported by ≥3 methods. We validated the identified recombination events by using SimPlot version 3.5.1 (https://sray.med.som.jhmi.edu/SCRoftware/SimPlot) using window size 1,000, step size 200, gap stripping turned on, and Kimura 2-parameter distance correction.

Genetic Variation Analysis

We used BioEdit version 7.2.05 (http://www.mbio.ncsu.edu/BioEdit) to perform genetic variation analysis. We constructed homology models of proteins by using Python version 3.10.7 (https://www.python.org) and Swiss-Model ExPASy (https://swissmodel.expasy.org).

Ethics Considerations

This study was approved by the Institutional Ethics and Review Committees of the Beijing Children's Hospital, Capital Medical University (ethics approval nos. [2023]-E-171-Y, 2019-k-357), and conducted in accordance with Helsinki Declaration (revised in 2013). Written informed consent was obtained from all parents or legal guardians of children included.

Results

Detection Rate of HAdV

A total of 3,875 children with acute RLTI were enrolled in this study; 310 (8%) tested positive for HAdV. Viral isolation and genotyping were successfully achieved for 195 of the HAdV-positive specimens. The identified viruses included species B (HAdV-3, -7, -14, -21, -55, -66, and -114) and C (HAdV-1, -6, -89, and -108). The most common genotype was HAdV-114 (105 isolates, 53.85%), followed by HAdV-7 (53 isolates, 27.18%), HAdV-1 (12 isolates, 6.15%), and HAdV-108 (11 isolates, 5.64%). We identified a novel HAdV-B genotype (2 isolates, 1.03%).

Clinical Manifestations of Patients with the Novel HAdV-B Genotype

The clinical characteristics of 2 cases infected with the novel HAdV-B genotype are provided (Appendix Table 1, http://wwwnc.cdc.gov/EID/article/32/6/25-0940-App1.pdf). Both patients were diagnosed with severe CAP. The first patient, a 4-year-old boy living in Beijing, China, with allergic rhinitis, was admitted to the general ward on December 19, 2019, and had high fever (40°C, reference range 36°C–37.2°C), cough, and sputum secretion. The leukocyte count was unremarkable, and C-reactive protein and erythrocyte sedimentation rate were mildly elevated. Chest radiograph and computed tomography (CT) both suggested pneumonia. Adenovirus nucleic acid was detected in throat swab specimens, plasma, and bronchoalveolar lavage fluid, and the adenovirus antigen test of respiratory secretions was positive. The patient's complications included liver dysfunction and sinus bradycardia. Atelectasis was observed >1 month later. The patient received intravenous immunoglobulin, methylprednisolone, bronchoalveolar lavage, and antimicrobial drug therapy. The second patient was a 3-year-old girl from Hebei, China, with a patent foramen ovale. She was admitted to the respiratory ward on December 26, 2019, with a high fever (40.7°C), cough, sputum secretion, and slight tachypnea. The leukocyte count was unremarkable, and C-reactive protein, erythrocyte sedimentation rate, procalcitonin, and ferritin were increased. Chest radiograph and CT also suggested pneumonia. Adenovirus was detected in throat swab specimens, plasma, and nasopharyngeal swab specimens. Complications such as liver function damage, myocardial damage, and coagulopathy developed, and the patient received intravenous immunoglobulin, methylprednisolone, bronchoalveolar lavage, and antiviral therapy. Both patients fully recovered after treatments.

Novel HAdV Genotype Identification

We isolated 2 HAdV strains (BJ-2024-563/2019 and BJ-2024-565/2019). BLAST alignment and phylogenetic analysis of penton base, hexon, and fiber genes revealed no matches with the 116 known HAdV genotypes. WGS of each strain yielded a single contiguous sequence of >34 kb, which we annotated and deposited in GenBank (accession nos. PV092676 [BJ-2024-563/2019] and PV092675 [BJ-2024-565/2019]). Both genomes are 35,299 bp with 50.83% guanine and cytosine content, indicating classification within species HAdV-B (49%–51% guanine and cytosine content).

Phylogenetic Analysis of the Whole Genome and 3 Major Capsid Protein Genes

The whole-genome sequences of the 2 novel strains shared 99.7% nucleotide (nt) identity and 99.6% amino acid (aa) identity, with a genetic distance of 0.001. The penton base, hexon, and fiber gene sequences of the 2 strains exhibited 98.8%–99.9% nt identity and 97.5%–100% aa identity, with genetic distances ranging from 0.000–0.007. We retrieved reference sequences for the whole genome and penton base, hexon, and fiber genes of other genotypes of species HAdV-B from GenBank (Appendix Table 2).

Phylogenetic analysis of the whole-genome sequences confirmed that the 2 novel strains belonged to the species HAdV-B and clustered together with a bootstrap value of 100%, forming a new evolutionary branch distinct from other known HAdV-B genotypes (Figure 1, panel A). Analysis of the penton base gene showed clustering with HAdV-B114 (88% bootstrap support) within the HAdV-7 evolutionary branch, including HAdV-B7 and HAdV-B66 (Figure 1, panel B). For the hexon gene, the strains grouped with HAdV-B114 (66% bootstrap support) within the HAdV-3 evolutionary branch, including HAdV-B3 and HAdV-B68 (Figure 1, panel C). The fiber gene phylogenetic analysis revealed clustering with HAdV-B7 (99% bootstrap support) within the HAdV-7 evolutionary branch, alongside HAdV-B77 and HAdV-B78 (Figure 1, panel D). The nt and aa identity analyses revealed that the whole genome, penton base, and hexon genes of the novel strains had high similarity with those of HAdV-B114, whereas the fiber gene aligned closely with HAdV-B7 (Table). Given that HAdV-B114 is a known recombinant genotype (P7H3F3) (*13*) and adhering to the current HAdV naming convention on the basis of the 3 major capsid protein genes (*2*), the 2 strains were proposed as a novel recombinant genotype, HAdV-B117, designated P7H3F7.

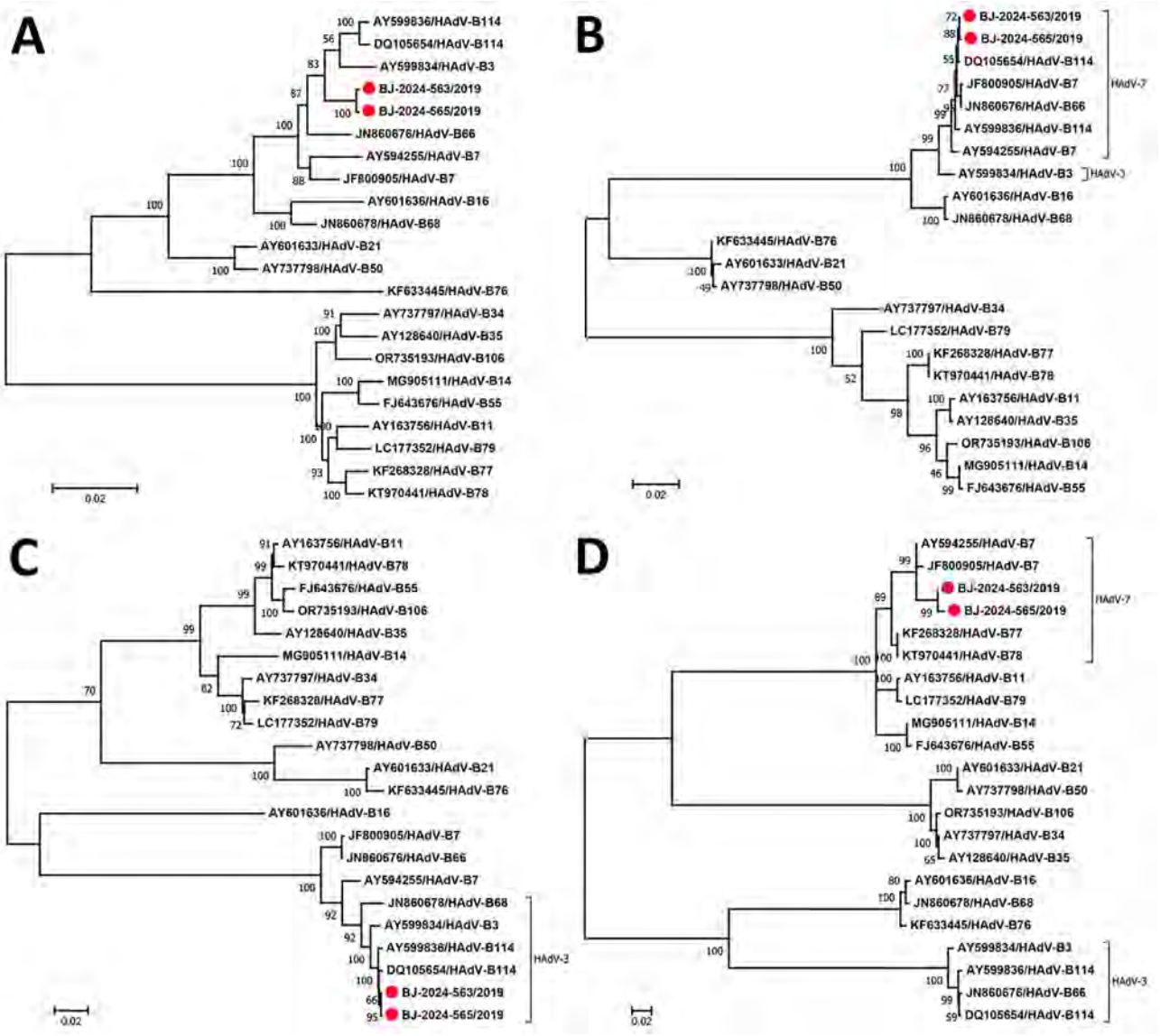

Figure 1. Phylogenetic analysis of the whole genome and 3 major capsid protein genes of 2 novel strains and other species HAdV-B genotypes from a study of novel recombinant human adenovirus genotype B117 from 2 pediatric cases, China. A) The phylogenetic tree of the whole genome, constructed by the general time reversible model. B) The phylogenetic tree of the penton base gene, constructed by the Kimura 2-parameter model. C, D) Phylogenetic trees of hexon (C) and fiber (D) genes, constructed by the Hasegawa-Kishino-Yano model. All trees were constructed by the maximum-likelihood method by using 1,000 replicates. Red dots indicate the 2 novel strains obtained in this study. Scale bars indicate nucleotide substitutions per site. HAdV, human adenovirus.

Phylogenetic Analysis of Early Genes

The early gene (*E1*–*E4*) sequences of the 2 strains exhibited 99.7%–99.8% nt identity and 99.4%–99.8% aa identity, with genetic distances of 0.000–0.001. Phylogenetic trees consistently showed clustering with HAdV-B114, supported by bootstrap values of 89%–100% (Appendix Figure 1). Identity analyses confirmed that the *E1*–*E4* genes were most similar to those of HAdV-B114 (Table). Specifically, the phylogenetic tree of *E1* genes revealed that the 2 sequences clustered together with HAdV-B114, -66, -7, and -3. HAdV-B16/21/50/68, HAdV-B14/34/55/79/106, and HAdV-B35/77/78 each formed a distinct cluster (Appendix Figure 1, panel A). Phylogenetic analysis of *E2* genes revealed that the 2 sequences clustered together with HAdV-B114. HAdV-B14/55/79/106 and HAdV-B11/34/35/77/78 clustered separately (Appendix Figure 1, panel B). The phylogenetic tree on the basis of *E3* genes revealed that the 2 sequences clustered together with HAdV-B114 and -3. The remaining genotypes grouped into 5 clusters: HAdV-B16/21/50, HAdV-B7/66/68, HAdV-B14/55, HAdV-B77/78, and

Table. Nucleotide and amino acid identity between BJ-2024-563/2019 HAdV-B isolate and counterparts from other HAdV-B genotypes from study of novel recombinant human adenovirus genotype B117 from 2 pediatric cases, China*

	Nucleotide/amino acid identity, %							
Genotype	Whole genome	Penton base	Hexon	Fiber	E1	E2	E3	E4
HAdV-3	96.8/95	98.5/99	97.4/97.3	64.3/57.3	96.9/94.2	98.2/96.4	94.7/92.1	98.5/97.5
HAdV-7	97.2–97.7/ 95.4–95.8	99.3–99.6/ 99.4–99.6	95.4–97.2/ 96.2–97.8	97.2–97.9/ 96.6–97.8	97.7–98.4/ 95.3–96	85.8–98.2/ 83.1–96.5	95.8–97.2/ 92.4–94.1	97.9–99.1/ 95.1–97.9
HAdV-11	82.9/73.1	79.5/83.5	78.5/85.3	92.5/91.3	80.6/57.4	55.9/49.2	76.6/63.6	95.5/90.1
HAdV-14	82.6/72.4	80.4/83.6	78/84.7	91.6/89.8	79.8/55.7	73.3/61.5	76.3/62.8	95.5/89.8
HAdV-16	93.6/91.2	93.7/94.4	79.9/86.5	59/52.8	96.8/93.4	96.6/93.1	95.3/92.6	72.3/65.8
HAdV-21	92.4/88.7	83.7/85.6	80.6/85.5	65.5/58.7	93.8/89.7	65/63.3	87.7/85.2	95.2/93.1
HAdV-34	82.2/72	79.9/83.5	77.4/84.2	66.4/60.2	77.8/54.5	79.9/66.2	69.7/58.2	93/88.3
HAdV-35	82.1/72.1	79.5/83.3	78/84.7	66.2/59.9	78/55.1	55.8/49.1	45.9/37.7	83.9/80.7
HAdV-50	92.4/88.7	83.4/85.4	81.5/86	65.4/58.4	96.1/92.3	83/75.8	96/93.2	98.2/96.3
HAdV-55	82.6/72.5	80.3/83.3	78.7/85	91.2/88.8	68.9/48.3	55.6/48.8	76.2/62.6	95.3/89.8
HAdV-66	96.1/94.4	99.6/99.8	95.5/96.3	65/58.5	95.4/94.1	85.8/83.3	88.5/86.3	95.6/94.8
HAdV-68	94.9/92.2	93.7/94.2	96/97.2	59/52.5	93.8/89.8	85.6/82.7	88.1/85.3	90.4/81.9
HAdV-76	85.2/76.1	83.8/85.8	79.8/85.1	58.7/53.3	83.7/65.8	79.4/70.6	75.8/65.4	79/60.8
HAdV-77	82.7/72.9	80/83.8	77.7/84.2	94.6/92.5	77.9/54.9	74.1/62.2	69.7/57.9	93.1/88.6
HAdV-78	83.1/73.3	80/83.8	78.3/84.9	94.6/92.5	78.2/55.5	74/62.3	76.7/63.4	93.2/89.1
HAdV-79	82.9/73	80/83.8	77.4/84.1	92.4/91.3	80.6/57.7	74/62.2	69.7/57.9	93.1/88
HAdV-106	82.3/72.3	80/83.5	78.4/85	66.3/59.9	78.2/55.2	55.8/49	69.7/58.2	84.2/80.9
HAdV-114	98–98.2/ 97.1–97.4	99.6–99.8/ 99.4–99.8	98.1–98.2/ 97.6–97.7	64.8–65/ 58.2–58.5	98.1–99.7/ 97.5–99.4	88.1–99.7/ 87–99.3	96.4–96.6/ 94.6–94.8	99.3–99.5/ 98.7–99

*There are high nucleotide and amino acid identities of the whole genome, penton base, hexon, fiber and E1–E4 sequences of the 2 novel strains obtained in this study, and according to nucleotide and amino acid identity analyses, the results were coincident. For this reason, BJ-2024-563/2019 was chosen as the representative to show the results. HAdV, human adenovirus.

HAdV-B11/34/35/79/106 (Appendix Figure 1, panel C). The phylogenetic analysis of *E4* genes revealed that the 2 sequences clustered with HAdV-B114, -7, and -66. HAdV-B21/50, HAdV-B14/55, HAdV-B11/34/35/77/78/79/106, and HAdV-B16/68 clustered together separately (Appendix Figure 1, panel D). Those findings indicate that the early gene regions of HAdV-B also harbored recombination hotspots.

Recombination Analysis

Recombination analysis by using RDP4 predicted 3 recombination events for the BJ-2024-563/2019 strain and 2 for the BJ-2024-565/2019 strain (Appendix Table 3). Simplot confirmed 2 events, establishing both strains as recombinants of HAdV-B7 and HAdV-B114. The genomic backbone corresponded to the Guangzhou02 strain (HAdV-B114; GenBank accession no. DQ105654) isolated from Guangzhou, China, in 2004. Because of the high sequence identity to the Gomen strain (HAdV-B7 prototype strain; GenBank accession no. AY594255), the fiber gene of the BJ-2024–563/2019 strain likely originated from a prototype-like strain of HAdV-B7, whereas the fiber gene of the BJ-2024–565/2019 strain was more closely related to the 0901HZ/ShX/CHN/2009 strain isolated in Shaanxi, China in 2009 (HAdV-B7; GenBank accession no. JF800905) (Figures 2, 3). Those results corroborated the phylogenetic findings and supported the designation of the 2 strains as a novel recombinant genotype, HAdV-B117 (P7H3F7).

Variation Analysis in aa

Compared with the parental Guangzhou02 strain, both novel strains had 3 aa substitutions in the penton base protein: V128I, G163D, and A482T, but none in the RGD Loop region (Appendix Figure 2, panel A). Homology modeling revealed no major structural differences at these substitution sites between the Guangzhou02 strain and the novel strains. Within HAdV-B, the RGD Loop region was the most variable region of Penton base protein (Appendix Figure 2, panel A).

For hexon protein, both novel strains had 9 aa substitutions (R18Q, A99T, N155G, R156E, E197D, V239M, A289D, A454D, and H563Y), 8 aa deletions (T194, E195, G196, T265, G290, T446, D452, and D453),

Figure 2. Genetic organization of novel HAdV-B117 isolate from a study of novel recombinant HAdV-B117 from 2 pediatric cases, China. HAdV, human adenovirus.

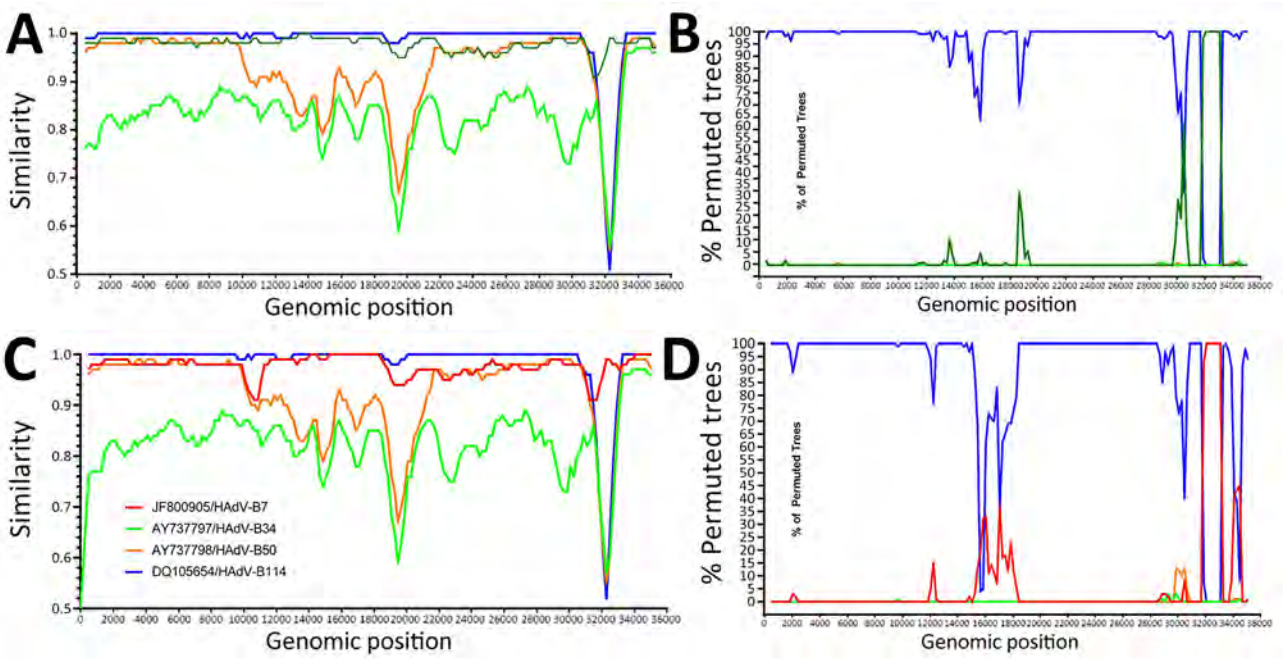

Figure 3. Recombination analysis between 2 novel strains and other species HAdV-B genotypes from a study of novel recombinant human adenovirus genotype B117 from 2 pediatric cases, China. A, B) SimPlot (A) and BootScan (B) analysis of the whole genome of the BJ-2024-563/2019 strain. C, D) SimPlot (C) and BootScan (D) analysis of the whole genome of the BJ-2024-565/2019 strain. HAdV, human adenovirus.

and 1 aa insertion (321D) relative to the Guangzhou02 strain. In addition, the BJ-2024-563/2019 strain had 4 unique substitutions (D157E, N158R, T193E, and E198N), whereas the BJ-2024-565/2019 strain had 3 (T193A, E198K, and V288A) (Appendix Figure 2, panel B). Homology models of both strains were built and superimposed with that of the Guangzhou02 strain to visualize the structural variations (Appendix Figure 2, panels C, D). The root mean square deviation for the 2 superimposed structures were both 0.029. Disparities were observed at the deletion sites in the Loop1 and Loop2 regions. However, the functional implications of those alterations warrant further study.

For the fiber protein, both novel strains exhibited identical 7 aa substitutions (T2A, V5A, D9T, T22N, S23L, Y353S, and R356T) compared with their parental strains, 2 of which (Y353S and R356T) were in the Knob region (Appendix Figure 2, panel E). Homology modeling indicated no major structural differences at those sites. Within HAdV-B, Fiber protein exhibited high variability across all regions (Appendix Figure 2, panel E).

Discussion

This molecular epidemiologic investigation revealed that HAdV-B114 and HAdV-B7 were the most common genotypes of HAdVs in children hospitalized with acute LRTI in Beijing, China, during 2014–2024. However, previous studies have reported that HAdV-B3 and HAdV-B7 were the predominant genotypes among children with respiratory tract infections in northern China (*14*,*15*). Recently, a study found that a multitude of complete genome sequences from China labeled as HAdV-B3 from the past 2 decades should be considered as HAdV-B114 (P7H3F3) (*16*), suggesting major HAdV-B114 circulation in China over the past 2 decades. Those findings revealed that HAdV-B114 might have replaced HAdV-B3 as a dominant HAdV genotype for respiratory tract infections among children in northern China.

In this study, a novel HAdV genotype, HAdV-B117 (P7H3F7), was isolated from 2 children hospitalized with severe CAP. WGS, phylogenetic, and recombination analyses confirmed that HAdV-B117 was a novel intertypic recombinant of species HAdV-B. Its genomic backbone was derived from HAdV-B114 (P7H3F3), with the fiber gene acquired from HAdV-B7 (P7H7F7).

The 2 patients, a boy and a girl both <5 years of age, aligned with the typical age profile of HAdV susceptibility (*17*,*18*). One resided in Beijing and was admitted to the general ward on December 19, 2019; the other came from Hebei Province and entered the respiratory ward on December 26, 2019. Our findings indicate that HAdV-B117 was detected in 2 different areas in China, suggesting the potential for

a new epidemic in the future. Both patients' symptoms included high fever, cough, and sputum secretion, which were hallmarks of HAdV respiratory infections, and both patients were diagnosed with severe CAP accompanied with serious complications. The clinical manifestations resembled severe HAdV-B3 or HAdV-B7 pneumonia cases previously reported and indicate a potentially severe phenotype of HAdV-B117 infection. Increased vigilance and enhanced surveillance for HAdV-B117 are warranted. The inflammatory markers of 1 child who had a patent foramen ovale were extremely elevated, and bacterial co-infection could not be ruled out. Both children eventually recovered.

Recombination is a hallmark of HAdV evolution and a primary driver of new genotype emergence (*19*,*20*). HAdV-53–116 genotypes were intertypic recombinants (http://hadvwg.gmu.edu). HAdV-B117 also exemplified that process, integrating the fiber gene of HAdV-B7 into HAdV-B114 backbone. Because the fiber protein mediates viral attachment to host cells and the fiber gene of HAdV-B117 was from HAdV-B7, HAdV-B117 might share tropism and infectivity traits with HAdV-B7 and become a critical pathogen of acute respiratory infections.

Although HAdV-B117 was isolated from 2 patients with CAP in different regions of China, the prevalence and potential effect on public health of HAdV-B117 are not clear and need further monitoring. The hexon protein is the main antigenic protein of HAdV and induces the host immune response (*21*). The hexon gene of HAdV-B117 came from HAdV-B114 and the hexon gene of HAdV-B114 was from HAdV-B3. Comparative analysis revealed that the hexon protein of HAdV-B117 was highly similar to its parental strain (HAdV-B114), with nearly identical aa sequences. Therefore, HAdV-B114 and HAdV-B117 might exhibit similar antigenic characteristics as HAdV-B3, suggesting that exposure to HAdV-B3/114 might provide protective cross-immunity against HAdV-B117, which requires further experimental validation. However, previous studies have reported that receptor-binding regions in the knob region of the fiber protein could also elicit neutralizing antibodies (*22*,*23*). The fiber gene of HAdV-B117 originated from HAdV-B7 and was different from that of HAdV-B3/114, so the cross-immunity generated by HAdV-B3/114 might not be sufficient to block its transmission. Furthermore, previous studies demonstrated low levels of herd immunity against HAdV-B3 and HAdV-B7 in children from China (*24*,*25*), indicating that HAdV-B117 might cause potential epidemics in this population. Of note, mutations were also observed in the loop 1 and loop 2 regions of the hexon protein and the knob region of the fiber protein of HAdV-B117. Homology modeling revealed that aa deletions in the loop 1 and loop 2 regions of the hexon protein might alter protein structure, potentially impairing neutralizing antibody production and binding and enabling immune evasion, which merits further investigation. In addition, the replication dynamics of HAdV-B117 resembled those of currently prevalent HAdV-B genotypes, including HAdV-B3, HAdV-B7, HAdV-B14, and HAdV-B55 (data not shown), which were associated with severe infections and outbreaks (*26*,*27*). Those findings indicate that HAdV-B117 has the potential to cause epidemic outbreaks of respiratory disease and further monitoring is needed.

HAdV-B7 was generally considered to have higher replication, virulence, and infectivity than HAdV-B3 (*4*,*28*). Whole-genome comparative analysis revealed that the primary differences between HAdV-B3 and HAdV-B7 were in the fiber protein (*29*,*30*). A previous study (*31*) found that the higher binding affinities of fiber protein's knob region to cellular receptors resulted in greater infectivity and virulence of HAdV-B7 and HAdV-B55 than those of HAdV-B3, thereby increasing their pathogenicity. HAdV-B117 acquired the fiber gene from HAdV-B7 through recombination; therefore, further monitoring of the virulence, infectivity, and pathogenicity of HAdV-B117 is needed.

In conclusion, this study identified a novel recombinant genotype within species HAdV-B, HAdV-B117 (P7H3F7), isolated from 2 pediatric cases of severe respiratory illness. In vitro, the replication kinetics of HAdV-B117 were similar to those of HAdV-B3 and HAdV-B7. Future research on its biological characteristics and epidemiology is needed. The emergence of this novel recombinant highlights the need for continuous genomic surveillance of HAdV.

Acknowledgments

The authors thank the researchers who have conducted and individuals who have participated in this and related studies.

All data generated or analyzed during this study are included in this published article (and its supplemental files). The sequences generated in this study were submitted to GenBank (accession nos. PV092675 and PV092676). The raw data were deposited in the National Centre for Biotechnology Information Sequence Read Archive (https://www.ncbi.nlm.nih.gov/sra; BioProject accession no. PRJNA1344832).

This work was supported by National Key Research and Development Program of China (award no. 2023YFC2306001), National Natural Science Foundation of China (award no. 32470141), Beijing Municipal Administration of Hospitals Incubating Program (award no. PX2024043), Beijing Research Centre for Respiratory Infectious Diseases Project (award no. BJRID2025-008), the Chinese Academy of Medical Sciences Innovation Fund for Medical Sciences (award no. 2022-I2M-CoV19-006), Funding for Reform and Development of Beijing Municipal Health Commission, and CAMS Innovation Fund for Medical Sciences (award no. 2019-I2M-5-026).

About the Author

Ms. Wang is a doctoral candidate at the Laboratory of Infection and Virology of Beijing Children's Hospital, Capital Medical University, specializing in pediatrics. Her research interests include the clinical, molecular epidemiology, and genetic characteristics of human adenoviruses, aiming to provided reference for the monitoring, prevention and control of human adenoviruses, and the research and development of vaccines and drugs.

References

1. Davison AJ, Benkő M, Harrach B. Genetic content and evolution of adenoviruses. J Gen Virol. 2003;84:2895–908. https://doi.org/10.1099/vir.0.19497-0
2. Seto D, Chodosh J, Brister JR, Jones MS; Members of the Adenovirus Research Community. Using the whole-genome sequence to characterize and name human adenoviruses. J Virol. 2011;85:5701–2. https://doi.org/10.1128/JVI.00354-11
3. Khanal S, Ghimire P, Dhamoon AS. The repertoire of adenovirus in human disease: the innocuous to the deadly. Biomedicines. 2018;6:30. https://doi.org/10.3390/biomedicines6010030
4. Liu W, Qiu S, Zhang L, Wu H, Tian X, Li X, et al. Analysis of severe human adenovirus infection outbreak in Guangdong Province, southern China in 2019. Virol Sin. 2022;37:331–40. https://doi.org/10.1016/j.virs.2022.01.010
5. Marcone DN, Culasso ACA, Reyes N, Kajon A, Viale D, Campos RH, et al. Genotypes and phylogenetic analysis of adenovirus in children with respiratory infection in Buenos Aires, Argentina (2000–2018). PLoS One. 2021;16:e0248191. https://doi.org/10.1371/journal.pone.0248191
6. Robinson CM, Singh G, Lee JY, Dehghan S, Rajaiya J, Liu EB, et al. Molecular evolution of human adenoviruses. Sci Rep. 2013;3:1812. https://doi.org/10.1038/srep01812
7. Zhu Z, Zhang Y, Xu S, Yu P, Tian X, Wang L, et al. Outbreak of acute respiratory disease in China caused by B2 species of adenovirus type 11. J Clin Microbiol. 2009;47:697–703. https://doi.org/10.1128/JCM.01769-08
8. Walsh MP, Seto J, Jones MS, Chodosh J, Xu W, Seto D. Computational analysis identifies human adenovirus type 55 as a reemergent acute respiratory disease pathogen. J Clin Microbiol. 2010;48:991–3. https://doi.org/10.1128/JCM.01694-09
9. Niel C, Moraes MT, Mistchenko AS, Leite JP, Gomes SA. Restriction site mapping of four genome types of adenovirus types 3 and 7 isolated in South America. J Med Virol. 1991;33:123–7. https://doi.org/10.1002/jmv.1890330211
10. Murtagh P, Cerqueiro C, Halac A, Avila M, Kajon A. Adenovirus type 7h respiratory infections: a report of 29 cases of acute lower respiratory disease. Acta Paediatr. 1993;82:557–61. https://doi.org/10.1111/j.1651-2227.1993.tb12753.x
11. Mao N, Zhu Z, Rivailler P, Yang J, Li Q, Han G, et al. Multiple divergent human mastadenovirus C co-circulating in mainland of China. Infect Genet Evol. 2019;76:104035. https://doi.org/10.1016/j.meegid.2019.104035
12. Wang JJ, Duan YL, Ai J, Zhu Y, Wang R, Chen XP, et al. Epidemiological characteristics of acute lower respiratory tract infection with human adenovirus among children in China from 2017 to 2020. [in Chinese]. Chi J Prev Med. 2024;25:283–8. https://doi.org/10.16506/j.1009-6639.2024.03.005
13. Kolb AW, Chau VQ, Miller DL, Yannuzzi NA, Brandt CR. Phylogenetic and recombination analysis of clinical vitreous humor-derived adenovirus isolates reveals discordance between serotype and phylogeny. Invest Ophthalmol Vis Sci. 2024;65:12. https://doi.org/10.1167/iovs.65.2.12
14. Wang F, De R, Han Z, Xu Y, Zhu R, Sun Y, et al. High-frequency recombination of human adenovirus in children with acute respiratory tract infections in Beijing, China. Viruses. 2024;16:828. https://doi.org/10.3390/v16060828
15. Huang Y, Wang C, Ma F, Guo Q, Yao L, Chen A, et al. Human adenoviruses in paediatric patients with respiratory tract infections in Beijing, China. Virol J. 2021;18:191. https://doi.org/10.1186/s12985-021-01661-6
16. Ganzenmueller T, Wolf M, Wolfram L, Gkioule C, Steinbrück L, Heim A. An epidemic of respiratory and ocular infections caused by the reemergence of a recombinant human adenovirus, the novel type HAdV-B114 (P7H3F3). J Med Virol. 2025;97:e70464. https://doi.org/10.1002/jmv.70464
17. Wang S, Zou X, Fu J, Deng F, Yu H, Fan H, et al. Genotypes and phylogenetic analysis of human adenovirus in hospitalized pneumonia and influenza-like illness patients in Jiangsu Province, China (2013–2021). Infect Drug Resist. 2024;17:2199–211. https://doi.org/10.2147/IDR.S456961
18. Calzado-Dacasin C, Foronda JL, Arguelles VL, Daga CM, Quimpo MT, Lupisan S, et al. Serotype identification of human adenoviruses associated with influenza-like illnesses in the Philippines from 2006–2012 by microneutralization and molecular techniques. Int J Infect Dis. 2022;117:326–33. https://doi.org/10.1016/j.ijid.2022.02.008
19. Walsh MP, Chintakuntlawar A, Robinson CM, Madisch I, Harrach B, Hudson NR, et al. Evidence of molecular evolution driven by recombination events influencing tropism in a novel human adenovirus that causes epidemic keratoconjunctivitis. PLoS One. 2009;4:e5635. https://doi.org/10.1371/journal.pone.0005635
20. MacNeil KM, Dodge MJ, Evans AM, Tessier TM, Weinberg JB, Mymryk JS. Adenoviruses in medicine: innocuous pathogen, predator, or partner. Trends Mol Med. 2023;29:4–19. https://doi.org/10.1016/j.molmed.2022.10.001
21. Tian X, Su X, Li H, Li X, Zhou Z, Liu W, et al. Construction and characterization of human adenovirus serotype 3 packaged by serotype 7 hexon. Virus Res. 2011;160:214–20. https://doi.org/10.1016/j.virusres.2011.06.017
22. Liebermann H, Mentel R, Döhner L, Modrow S, Seidel W. Inhibition of cell adhesion to the virus by synthetic peptides of fiber knob of human adenovirus serotypes 2 and 3 and virus neutralization by anti-peptide antibodies. Virus

Res. 1996;45:111–22. https://doi.org/10.1016/S0168-1702(96)01369-X
23. Liu Z, Xian Y, Lan J, Zhou Z, Li X, Zhou R, et al. Human adenovirus species B knob proteins as immunogens for inducing cross-neutralizing antibody responses. MSphere. 2025;10:e0064424. https://doi.org/10.1128/msphere.00644-24
24. Tian X, Fan Y, Wang C, Liu Z, Liu W, Xu Y, et al. Seroprevalence of neutralizing antibodies against six human adenovirus types indicates the low level of herd immunity in young children from Guangzhou, China. Virol Sin. 2021;36:373–81. https://doi.org/10.1007/s12250-020-00307-1
25. Hong L, Li J, Zeng W, Li Y, Yu C, Zhao S, et al. The seroprevalence of adenoviruses since 2000. Emerg Microbes Infect. 2025;14:2475831. https://doi.org/10.1080/22221751.2025.2475831
26. Lin GL, Lu CY, Chen JM, Lee PI, Ho SY, Weng KC, et al. Molecular epidemiology and clinical features of adenovirus infection in Taiwanese children, 2014. J Microbiol Immunol Infect. 2019;52:215–24. https://doi.org/10.1016/j.jmii.2018.07.005
27. Liu MC, Xu Q, Li TT, Wang T, Jiang BG, Lv CL, et al. Prevalence of human infection with respiratory adenovirus in China: a systematic review and meta-analysis. PLoS Negl Trop Dis. 2023;17:e0011151. https://doi.org/10.1371/journal.pntd.0011151
28. Fu Y, Tang Z, Ye Z, Mo S, Tian X, Ni K, et al. Human adenovirus type 7 infection causes a more severe disease than type 3. BMC Infect Dis. 2019;19:36. https://doi.org/10.1186/s12879-018-3651-2
29. Marttila M, Persson D, Gustafsson D, Liszewski MK, Atkinson JP, Wadell G, et al. CD46 is a cellular receptor for all species B adenoviruses except types 3 and 7. J Virol. 2005;79:14429–36. https://doi.org/10.1128/JVI.79.22.14429-14436.2005
30. Hograindleur MA, Effantin G, Fenel D, Mas C, Lieber A, Schoehn G, et al. Binding mechanism elucidation of the acute respiratory disease causing agent adenovirus of serotype 7 to desmoglein-2. Viruses. 2020;12:1075. https://doi.org/10.3390/v12101075
31. Zhang Q, Zhou Z, Fan Y, Liu T, Guo Y, Li X, et al. Higher affinities of fibers with cell receptors increase the infection capacity and virulence of human adenovirus type 7 and type 55 compared to type 3. Microbiol Spectr. 2024;12:e0109023. https://doi.org/10.1128/spectrum.01090-23

Address for correspondence: Zhengde Xie, Beijing Children's Hospital, No. 56 Nanlishi Road, Xicheng District, Beijing 100045, China; email: xiezhengde@bch.com.cn

Suspected Sexual Transmission of Dermatophilosis among Men Who Have Sex with Men, Lyon and Paris, France, 2025–2026

Matthieu Degreze, François Durupt, Marine Ibranosyan, Anne-Lise Maucotel, Audrey Lapendry, Laurie Gouillon, Matthieu Godinot, Maxime Bonjour

We report a genomically linked cluster of 9 *Dermatophilus congolensis* cutaneous infections diagnosed within 2 months among men who have sex with men in Lyon and Paris, France, 2025–2026. Genomic similarity and shared sexual exposures strongly suggest interhuman sexual transmission of this zoonotic bacterium.

Dermatophilus congolensis is a gram-positive, facultatively anaerobic actinomycete responsible for dermatophilosis, an exudative dermatitis of animals (*1*). The disease predominantly affects cattle, sheep, and horses, mainly in tropical and subtropical climates. It typically manifests as benign, crusting superficial skin lesions but occasionally progresses to extensive disease, sometimes resulting in significant mortality in cattle herds (*2*,*3*). The pathogenesis relies on 2 factors, skin microabrasions and moisture, which activate motile zoospores to penetrate the epidermis (*1*).

Human infections are rare and considered accidental zoonoses. Those infections are classically described in farmers, hunters, veterinarians, or animal riders following direct contact with infected animals (*4*–*10*). The clinical manifestation typically involves nonpruritic, pustular, and crusty lesions. *D. congolensis* is susceptible to β-lactams, macrolides, and tetracyclines. Systematic susceptibility testing is rarely performed in clinical practice. Reported treatments include penicillins, although lesions are often self-limiting. To date, human-to-human transmission has not been documented, and urban cases without reported animal exposure have rarely been described (*11*). We describe a temporally clustered series of human dermatophilosis cases occurring in France among urban men who have sex with men (MSM) without livestock exposure, raising the hypothesis of an alternative mode of transmission.

Author affiliations: Hospices Civils de Lyon, Lyon, Auvergne-Rhône-Alpes, France (M. Degreze, F. Durupt, M. Ibranosyan, A.-L. Maucotel, A. Lapendry, L. Gouillon, M. Godinot, M. Bonjour); Laboratoire de Biométrie et Biologie Évolutive, UMR CNRS 5558, Villeurbanne, France (M. Bonjour)

DOI: https://doi.org/10.3201/eid3206.260401

The Study

During December 2025–February 2026, a total of 9 men sought care at the sexually transmitted infections (STI) clinics of the University Hospital in Lyon, France, for skin infections that were determined to be caused by *D. congolensis*. All patients were MSM living in urban areas; they were 22–63 years of age (median 50, interquartile range [IQR] 34–59.5 years). None reported occupational exposure to livestock or direct contact with farm animals or horses, although some did report regular or occasional contact with domestic pets (cats or dogs). None reported recent travel to tropical regions.

All patients exhibited nonspecific erythematous papules, occasionally pustular or squamous, mainly located in the genital region (penis, scrotum, pubic area; n = 8), trunk (n = 5), perioral region (beard area; n = 4), lower limbs (n = 4), and, less frequently, anal margin (n = 1) (Table; Figure 1). Lesions predominantly involved areas exposed during sexual contact, without mucosal involvement. Pruritus was variably present. No systemic symptoms were reported except for patient 7, who experienced fever and vomiting 2 days before medical consultation. Given the clinical manifestations and epidemiologic context, differential diagnoses included staphylococcal folliculitis, sexually transmitted dermatophytosis (*Trichophyton mentagrophytes* genotype VII), *Klebsiella aerogenes* folliculitis, secondary syphilis, mpox, and molluscum contagiosum.

Table. Characteristics of 9 patients with cutaneous *Dermatophilus congolensis* infection in cluster of suspected sexual transmission of dermatophilosis among men who have sex with men, Lyon and Paris, France, 2025–2026*

Pt. no.	Age, y	Underlying conditions	Lesion locations	Cutaneous co-infection or superinfection	Sauna attendance (location)	Symptom onset date	STI clinic consultation date	ENA accession nos.
1	63	HIV PrEP use, STI history (CT, HSV)	Neck, beard, trunk, pubic region	Pubic pthiriasis	2–3 times/wk, 2 wks before symptoms (Lyon)	2025 Dec 23	2025 Dec 31	ERS29280943
2	50	HIV PrEP use, STI history (HPV)	Beard	None	2025 Dec 18 (Lyon)	1 week after sauna attendance	2026 Jan 19	ERS29280944
3	26	HIV PrEP use, STI history (CT, NG)	Beard, umbilicus, scrotum, inguinal folds	*Staphylococcus aureus* (beard)	2026 Jan 28 (Lyon); 2026 Feb 1 (Paris)	2026 Feb 1	2026 Feb 6	ERS29314550
4	51	HIV PrEP use, STI history (CT, NG, Tp)	Legs, groin, back, scrotum	None	2026 Feb 3 (Lyon)	2026 Feb 7	2026 Feb 10	ERS29314551
5	60	HIV PrEP use, STI history (Tp)	Penis, pubic region	None	2026 Jan 29–30 (Paris); 2026 Feb 3 (Paris)	2026 Feb 6	2026 Feb 10	ERS29380148
6	59	HIV+ (CD4: 643/mm^3), STI history (CT, NG, Tp, HSV)	Upper thighs, umbilicus, groin	None	2026 Feb 3 (Lyon)	2026 Feb 11	2026 Feb 18	ERS29380149
7	42	STI history (NG, Tp), cannabis and cocaine use	Scalp, beard, scrotum, abdomen, limbs, anal margin	*S. aureus*	Regular attendance, 1×/wk (Lyon)	2026 Feb 10	2026 Feb 19	ERS29380150
8	45	HIV PrEP use, STI history (CT)	Penis, scrotum, pubic region, upper left thigh	*Staphylococcus lugdunensis*	2026 Feb 5 (Lyon)	2026 Feb 11	2026 Feb 20	ERS29380440
9	22	HIV PrEP use	Scrotum, inguinal folds	*S. aureus*	None	2026 Feb 6	2026 Feb 20	Not sequenced

*CT, *Chlamydia trachomatis*; ENA, European Nucleotide Archive; HSV, herpes simplex virus; HPV, human papillomavirus; NG, *Neisseria gonorrheae*; PrEP, preexposure prophylaxis; Pt., patient; STI, sexual transmitted infection; Tp, *Treponema pallidum* subspecies *pallidum*; +, positive.

For all patients, we cultured lesion swab samples from involved areas on nonselective media: blood agar plates (aerobic atmosphere) and chocolate agar plates (with 5% CO_2). After 40 hours, cultures yielded β-hemolytic, rhizoid, adherent, rough, shiny, and yellowish colonies on both culture media (Figure 2, panels A, B), and occasionally along with colonies from the skin microbiota. Gram staining revealed identical filamentous, branching gram-positive bacilli with transverse and longitudinal septations producing a characteristic tram-track appearance (Figure 2, panel C). Bacterial identification by matrix-assisted laser desorption/ionization time-of-flight mass spectrometry identified *D. congolensis* with a high confidence score in all cases. In 4 patients, bacterial cultures also yielded pyogenic pathogens: *Staphylococcus aureus* (patients 3, 7 and 9) or *S. lugdunensis* (patient 8). Whole-genome sequencing (NextSeq550; Illumina, https://www.illumina.com) and pairwise alignment of *D. congolensis* isolates from patients 1–8 revealed 1–5 single-nucleotide polymorphisms, covering >94% of the genome, supporting close relatedness and recent direct or indirect transmission from a common source. Reads are available for consultation on the European Nucleotide Archive database (Table). Concomitant STIs were diagnosed in 2 patients (pubic pthiriasis in patient 1 and syphilitic reinfection in patient 7).

Epidemiologic interviews revealed that 7 of the 9 patients reported recent sexual encounters at a gay sauna in Lyon within days or weeks before symptom onset (Table). Patient 5 reported multiple sexual partners in various saunas in Paris during the same period, including 1 that patient 3 visited 2 days earlier. Patient 9 did not report any sauna attendance. On the basis of reported exposures, incubation period ranged from 3 to 14 days; survival modeling with interval censoring estimated a median of 6.7 (95% CI 4.3–10.1) days. However, multiple potential contacts limited precision (Table).

Amoxicillin MIC determined for 1 isolate using Etest (bioMérieux, https://www.biomerieux.com) was 0.064 mg/L, supporting high susceptibility to β-lactams. All patients received oral amoxicillin (1 g 3×/d) or pristinamycin (1 g 3×/d) for 7 days, sometimes combined with topical antiseptic care, with rapid improvement. No patient relapsed; median follow-up was 10 (IQR 5–52) days after treatment. However, on follow-up, patient 1 showed with a new

Figure 1. Dermatophilosis lesions in patients in cluster of suspected sexual transmission of dermatophilosis among men who have sex with men, Lyon and Paris, France, 2025–2026. A) Papular lesions of the neck and torso in patient 1. B) Folliculitis of the beard in patient 2. C) Papules of the groin and scrotum in patient 3. D) Papulopustular lesions of the buttocks during second occurrence in patient 1.

D. congolensis infection on the buttocks, occurring 8 weeks after the first occurrence (Figure 1, panel D). His ongoing visits to the same sauna after recovery and the different infection site suggest reinfection rather than relapse.

Compared with previous reports of dermatophilosis, the predominantly papular and noncrusted manifestation observed here might differ from the classical description, raising the possibility of a distinct clinical phenotype. Moreover, lesions mainly

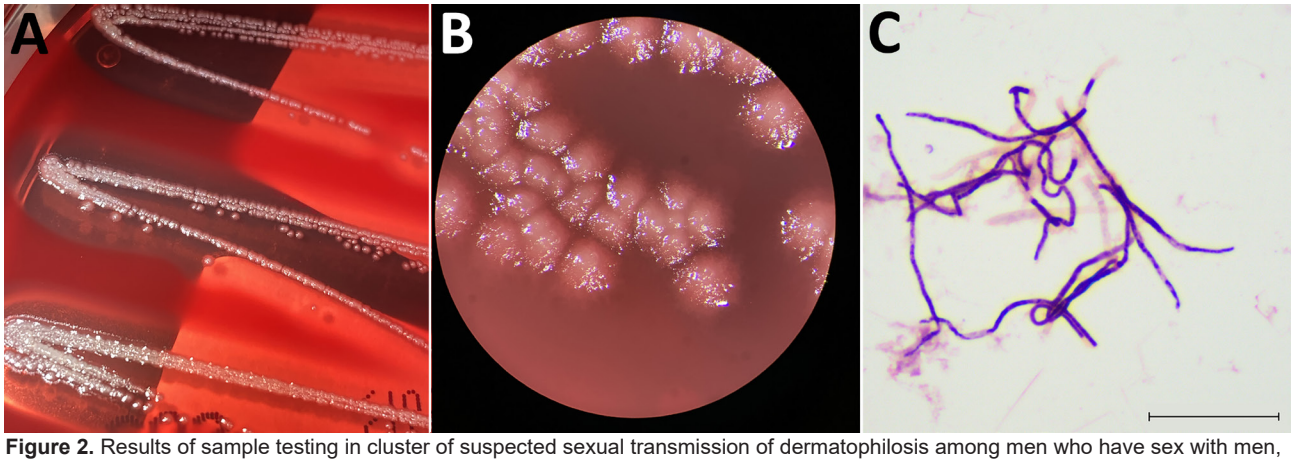

Figure 2. Results of sample testing in cluster of suspected sexual transmission of dermatophilosis among men who have sex with men, Lyon and Paris, France, 2025–2026. A, B) *Dermatophilus congolensis* colonies obtained on blood agar after 40 hours of incubation, seen with the naked eye (A) and by stereomicroscope (B). C) Microscopic examination of *D. congolensis* isolated from patient 1 skin sample. Gram staining; scale bar indicates 25 μm.

affected areas exposed during sexual intercourse (face and genitals), mirroring patterns seen in sexually transmitted dermatophytosis or *K. aerogenes* folliculitis (*12*–*14*). Whereas no mucosal lesions were observed in this cluster, rare literature reports indicate that *D. congolensis* can infect human mucosa, justifying detailed clinical examination (*6*,*11*). In some occurrences, *S. aureus* and *S. lugdunensis* were also isolated from lesion sampling and might have modified clinical manifestations. Their involvement complicates the interpretation of *D. congolensis* pathogenicity in the given occurrences. Secondary infection of *Dermatophilus*-induced lesions by such pathogens is the most probable explanation, although co-transmission remains possible.

Although no direct sexual contact between patients could be formally established, the temporal clustering, overlapping sexual exposures, shared multiple STI history, lesion distribution, and close genomic relatedness of isolates strongly support transmission occurring within shared exposure networks, likely involving close physical or sexual contact. The presence of viable bacteria within lesions is consistent with the hypothesis of contact-driven transmission, although the exact transmission route remains uncertain. Environmental or indirect transmission within shared venues remains possible; no environmental sampling or carriage screening was performed at the time of the study to clarify transmission pathways.

Conclusions

We describe a large occurrence of human dermatophilosis cases in an urban population of sexually active MSM without reported livestock exposure. The combination of close genomic relatedness between the 8 sequenced isolates and shared sexual exposures suggest interhuman transmission within sexual networks. Systematic microbiologic evaluation of atypical cutaneous lesions is essential for identifying similar cases and clarifying transmission of emerging cutaneous STIs among MSM. Evolving sexual practices in the HIV preexposure prophylaxis era (*15*) could lead to emergence of new transmissible dermatoses (*12*–*14*). Microbiologists should ensure that *D. congolensis* is included in reference spectral libraries, be able to recognize its colonies in the context of skin infection, and report its identification to clinicians.

Acknowledgments

We are sincerely grateful to Didier Pin for his expertise on *D. congolensis* infections in animals and to Aubin Souche for genomic analysis and comparison.

About the Author

Dr. Degreze is a medical biology resident at the University Hospital in Lyon. Specializing in infectious agents, his research at the Center for Infectiology Research (CIRI) focuses on antistaphylococcal bacteriophages and the mechanisms of phage resistance. Alongside his research, he acts as a clinical microbiologist dedicated to the diagnosis of bacterial infections.

References

1. Zaria LT. *Dermatophilus congolensis* infection (Dermatophilosis) in animals and man! An update. Comp Immunol Microbiol Infect Dis. 1993;16:179–222. https://doi.org/10.1016/0147-9571(93)90148-X
2. Faccin M, Wiener DJ, Rech RR, Santoro D, Rodrigues Hoffmann A. Common superficial and deep cutaneous bacterial infections in domestic animals: a review. Vet Pathol. 2023;60:796–811. https://doi.org/10.1177/03009858231176558
3. Naves M, Vallée F, Barré N. Observations on a dermatophilosis outbreak in Brahman cattle in Guadeloupe. Description, epidemiological and economical aspects [in French]. Rev Elev Med Vet Pays Trop. 1993;46:297–302. https://doi.org/10.19182/remvt.9382
4. Burd EM, Juzych LA, Rudrik JT, Habib F. Pustular dermatitis caused by *Dermatophilus congolensis*. J Clin Microbiol. 2007;45:1655–8. https://doi.org/10.1128/JCM.00327-07
5. Amor A, Enríquez A, Corcuera MT, Toro C, Herrero D, Baquero M. Is infection by *Dermatophilus congolensis* underdiagnosed? J Clin Microbiol. 2011;49:449–51. https://doi.org/10.1128/JCM.01117-10
6. Bunker ML, Chewning L, Wang SE, Gordon MA. *Dermatophilus congolensis* and "hairy" leukoplakia. Am J Clin Pathol. 1988;89:683–7. https://doi.org/10.1093/ajcp/89.5.683
7. Aubin GG, Guillouzouic A, Chamoux C, Lepelletier D, Barbarot S, Corvec S. Two family members with skin infection due to *Dermatophilus congolensis*: a case report and literature review. Eur J Dermatol. 2016;26:621–2. | https://doi.org/10.1684/ejd.2016.2850
8. de Lorenzi C, Quenan S, Fontao L. *Dermatophilus congolensis* dermatitis in a traveller from Thailand. J Travel Med. 2021;28:taab017. https://doi.org/10.1093/jtm/taab017
9. Alejo-Cancho I, Bosch J, Vergara A, Mascaro JM, Marco F, Vila J. Dermatitis by *Dermatophilus congolensis*. Clin Microbiol Infect. 2015;21:e73–4. https://doi.org/10.1016/j.cmi.2015.06.013
10. Towersey L, Martins EC, Londero AT, Hay RJ, Soares Filho PJ, Takiya CM, et al. *Dermatophilus congolensis* human infection. J Am Acad Dermatol. 1993;29:351–4. https://doi.org/10.1016/0190-9622(93)70194-X
11. Ramanathan VS, Jahng AW, Shlopov B, Pham BV. *Dermatophilus congolensis* infection of the esophagus. Gastroenterology Res. 2010;3:173–4. https://doi.org/10.4021/gr216w
12. Jabet A, Dellière S, Seang S, Chermak A, Schneider L, Chiarabini T, et al. Sexually transmitted *Trichophyton mentagrophytes* genotype VII infection among men who have sex with men. Emerg Infect Dis. 2023;29:1411–4. https://doi.org/10.3201/eid2907.230025
13. Bérot V, Monsel G, Dauendorffer JN, Aubry A, Nebbad B, Schneider P, et al.; Groupe Infectiologie Dermatologique

et Infections Sexuellement Transmissibles (GrIDIST) de la Société Française de Dermatologie. *Klebsiella aerogenes*–related facial folliculitis in men having sex with men: a hypothetical new STI? J Eur Acad Dermatol Venereol. 2025;39:e10–2. https://doi.org/10.1111/jdv.20008

14. Yin N, Krygier J, Mairesse C, Libois A, Quoilin S, Martiny D. *Klebsiella aerogenes* ST117 causing folliculitis in men having sex with men, Belgium, February 2025. Euro Surveill. 2025;30:2500304. https://doi.org/10.2807/1560-7917.ES.2025.30.20.2500304
15. Milam J, Jain S, Dubé MP, Daar ES, Sun X, Corado K, et al.; CCTG Team. Sexual risk compensation in a pre-exposure prophylaxis demonstration study among individuals at risk of HIV. J Acquir Immune Defic Syndr. 2019;80:e9–13. https://doi.org/10.1097/QAI.0000000000001885

Address for correspondence: Matthieu Degreze, Service de bactériologie, Institut des Agents Infectieux, Laboratoire de Biologie Médicale Multisites, Hospices Civils de Lyon, 103 Grande Rue de la Croix-Rousse, 69004 Lyon, France; email: matthieu.degreze@chu-lyon.fr

Suspected Sexual Transmission of Dermatophilosis among Men Who Have Sex with Men, Barcelona, Spain, 2025–2026

Vicente Descalzo,[1] Albert Moreno-Mingorance,[1] Patricia Álvarez-López, Paula Salmerón, Jorge N. García-Pérez, Ferran P. Pericás-Cladera, Jordi Arcarons, Guillem Puigsech-Boixeda, Ilaria Furlan, Ester del Barrio-Tofiño, Sol M. San José, Nieves Larrosa, Vicenç Falcó, Mayli Lung, Maider Arando,[2] Juan José González-López[2]

Dermatophilosis is considered a zoonotic infection. We report 9 cases among men who have sex with men in Barcelona, Spain, during December 2025–March 2026. Whole-genome sequencing revealed highly related isolates forming a distinct lineage within the genus *Dermatophilus*. Epidemiologic and clinical features of the cases support human-to-human transmission via sexual contact.

Dermatophilosis is a skin infection caused by *Dermatophilus congolensis*, a gram-positive actimoycete that primarily affects animals in tropical and subtropical regions (*1*). Human infections are rare and typically associated with zoonotic exposure to livestock or wildlife; manifestations include pitted keratolysis, folliculitis, and pustules (*2*–*6*). Human-to-human transmission has not been documented. Here, we report 9 cases of dermatophilosis diagnosed in Barcelona, Spain, and assess the possibility of autochthonous human-to-human transmission via sexual contact.

The Study

The cases involved 2 patients who attended primary healthcare centers in December 2025 and March 2026 and 7 patients who attended a reference clinic for sexually transmitted infections (STIs) during January–March 2026 (Table). All patients were cisgender men who reported having sex with men (MSM). The median age was 47 years (interquartile range 30.5–57.5 years). Four patients were HIV-positive and 3 were receiving HIV preexposure prophylaxis therapy. Four patients had concomitant STIs, and 3 reported engaging in chemsex (drug use in a sexual context).

None of the patients reported contact with livestock or wildlife, and none had traveled to tropical regions in the month before symptom onset. Four patients reported recent travel to other cities in Europe where they engaged in sexual activity. All patients reported visiting venues for sexual encounters within the week preceding symptom onset, including 8 who had visited a sauna. Two patients were regular sexual partners, and 2 others reported partners with similar symptoms who were treated in other centers without microbiological confirmation.

Median symptom duration at consultation was 6 days (interquartile range 4.5–15 days). Lesions manifested as an itchy folliculitis-like rash characterized by papules, vesicles, pustules, scabs, nodules, or scaly lesions (Figure 1). Multiple anatomic sites were affected, most commonly the genitals, thighs, groin, and beard area.

Five patients were treated with cefadroxil (500 mg 2×/d for 7 d) resulting in complete resolution of lesions in all but 1 case, who had a residual nodular lesion.

Author affiliations: Vall d'Hebron University Hospital, Barcelona, Spain (V. Descalzo, P. Álvarez-López, P. Salmerón, J.N. García-Pérez, F.P. Pericás-Cladera, J. Arcarons, G. Puigsech-Boixeda, I. Furlan, E. del Barrio-Tofiño, S.M. San José, N. Larrosa, V. Falcó, M. Lung, M. Arando, J.J. González-López); Universitat Autònoma de Barcelona, Barcelona (V. Descalzo, N. Larrosa, V. Falcó, M. Lung, M. Arando, J.J. González-López); Vall d'Hebron Research Institute, Barcelona (A. Moreno-Mingorance, P. Salmerón, F.P. Pericás-Cladera, G. Puigsech-Boixeda, E. del Barrio-Tofiño, S.M. San José, N. Larrosa, V. Falcó, M. Lung, J.J. González-López); CIBER of Infectious Diseases (CIBERINFEC), Madrid, Spain (A. Moreno-Mingorance, G. Puigsech-Boixeda, N. Larrosa, M. Lung, J.J. González-López)

DOI: https://doi.org/10.3201/eid3206.260476

[1]These first authors contributed equally to this article.

[2]These senior authors contributed equally to this article.

One patient was successfully treated with cloxacillin (500 mg/6 h for 7 d). Two patients showed cleared lesions after treatment for concomitant STIs (benzathine penicillin G for syphilis and ceftriaxone and doxycycline for gonorrhea and lymphogranuloma venereum). One patient initially received topical mupirocin with partial response but achieved complete resolution after doxycycline therapy (100 mg 2×/d for 7 d). None of the patients required hospitalization or experienced any complications. As of April 2026, no recurrences had been observed.

Skin lesion samples cultured on Columbia 5% sheep blood agar produced small yellowish β-hemolytic colonies. Gram staining revealed gram-positive coccoid forms occasionally arranged in irregular filaments with transverse septa. Identification by matrix-assisted laser desorption/ionization time-of-flight mass spectrometry confirmed *D. congolensis*.

All isolates showed identical antimicrobial susceptibility profiles and were susceptible to amoxicillin/clavulanate (MIC ≤2/1 mg/L), ceftriaxone (MIC ≤4 mg/L), cefepime (MIC ≤1 mg/L), imipenem (MIC ≤2 mg/L), linezolid (MIC 1 mg/L), amikacin (MIC 4 mg/L), moxifloxacin (MIC ≤0.25 mg/L), doxycycline (MIC ≤0.12 mg/L), minocycline (MIC ≤1 mg/L), clarithromycin (MIC ≤0.06 mg/L), and trimethoprim/sulfamethoxazole (MIC ≤0.25/4.75 mg/L). All isolates were resistant to tobramycin (MIC 16 mg/L) and showed intermediate susceptibility to ciprofloxacin (MIC 2 mg/L). We interpreted susceptibility on the basis of CLSI 2023 breakpoints for other aerobic actinomycetes (*7*) because no organism-specific breakpoints are available for *D. congolensis*. MIC for mupirocin was >1,024 mg/L for all isolates; no clinical breakpoints are available.

Table. Epidemiologic and clinical characteristics of dermatophilosis cases in men who have sex with men, Barcelona, Spain, December 2025–March 2026*

Pt no.	Age, y	HIV	Travel in previous month	Chemsex	Visited sex venue in week before symptom onset	Sexual partner with symptoms	STI co-infection	Symptom duration, d	Infection site	Lesion types	Treatment
1	61	N	London, UK	N	Y, sauna	Y	Early latent syphilis	15	Thorax	Vesicles, Pustules	Benzathine penicillin
2	27	N, on PrEP	Toulouse, France	N	Y, sauna	Y	N	5	Beard, penis, scrotum, thigh	Papules, vesicles, pustules	Mupirocin, doxycycline
3	47	Y, on ART; CD4 495 cells/mm^3	N	Y, CM	Y, sex club	N	Early latent syphilis	10	Buttock, scrotum, groin	Scaly papules	Cefadroxil
4	49	N, on PrEP	Vienna, Austria; Budapest, Hungary	N	Y, sauna	Y, pt. no. 5	N	6	Beard, penis, groin	Pustules, nodules	Cefadroxil
5	54	N, on PrEP	Vienna, Austria; Budapest, Hungary	N	Y, sauna	Y, pt. no. 4	N	3	Thigh, armpit	Vesicles, pustules	Cefadroxil
6	32	N	No	N	Y, sauna	N	NG, LGV, HSV-2	45	Thigh	Nodules, scaly lesions	Ceftriaxone, doxycycline
7	66	Y, on ART; CD4 217 cells/mm^3	N	Y, CM, GHB, 4-MMC	Y, sauna	N	No	15	Beard	Scaly papules, scabs	Cefadroxil
8	29	Y, on ART; CD4 860 cells/mm^3	N	N	Y, sauna	N	NG, CT	4	Scrotum	Pustules, scabs	Cefadroxil
9	37	Y, on ART; CD4 475 cells/mm^3	N	Y, CM, GHB	Y, sauna	N	N	5	Perianal, groin, thigh	Scaly papules, pustules, scabs	Cloxacillin

*4-MMC, mephedrone; ART, antiretroviral therapy; chemsex, drug use in a sexual context; CM, methamphetamine; CT, *Chlamydia trachomatis*; GHB, gamma-hydroxybutyric acid; HSV-2, herpes simplex virus type 2; LGV, lymphogranuloma venereum; NG, *Neisseria gonorrhoeae*; PrEP: preexposure prophylaxis; STI, sexually transmitted infection; pt., patient.

Figure 1. Dermatophilosis lesions in patients in cluster of suspected sexual transmission among men who have sex with men, Barcelona, Spain, December 2025–March 2026. A) Papule-pustules on the beard area; B) papulovesicular lesions on the penis and scrotum; C) pustular rash in the armpit; D) vesicle-pustules on the thigh; E) erythematous scaling papules on the beard area; F) erythematous scaling papules in the perianal region.

We performed whole-genome sequencing (WGS) on isolates from patients 1–7. WGS demonstrated extremely close genetic relatedness among isolates; pairwise single-nucleotide polymorphism (SNP) distances were 0–4 SNPs. We also performed phylogenetic comparisons between the isolates from this study and publicly available *D. congolensis* genomes, including 40 genomes from cattle in Saint Kitts and Nevis (*8*) and reference strain *D. congolensis* DSM 44180 from the Democratic Republic of the Congo, all from the National Center for Biotechnology Information Sequence Read Archive (https://www.ncbi.nlm.nih.gov/sra). Those comparisons showed that the study isolates formed a distinct cluster clearly separated from previously described strains; minimum SNP distance was 20,410 to the closest reference genome (Figure 2).

Genomic comparison with reference strain *D. congolensis* DSM 44180 yielded an average nucleotide identity of 94.55%, below the species delineation threshold of 95%–96% (*9*). Digital DNA–DNA hybridization values among study isolates were 99.9%–100%, whereas values compared with the reference strain were 58.7%, below the 70% threshold for species delineation (*9*). Those findings suggest that the isolates are genetically distinct from currently described *D. congolensis* strains and are consistent with a potentially novel *Dermatophilus* taxon, although further taxonomic characterization would be required to formally define a new species.

Conclusions

We report human cases of dermatophilosis for which no animal exposure was identified and which are

suspected to have been sexually acquired. All cases occurred in MSM with high exposure to STIs, several patients reported partners with similar symptoms, and lesions were commonly located in sites exposed during sexual contact. Those features were similarly described for other considered zoonotic pathogens that emerged as sexually transmissible, such as mpox virus (*10*) and *Trichophyton mentagrophytes* (*11*). As has already been observed, MSM are particularly vulnerable to such emerging infections, probably because of the complexity of their sexual networks (*12*).

Attendance at sexual venues might have been a factor in transmission in this cluster. In particular, 8 patients developed lesions shortly after visiting a sauna, where humid conditions could favor the release and environmental persistence of infective *Dermatophilus* zoospores (*13*,*14*). Indirect transmission might occur via contaminated surfaces; fomite-mediated outbreaks have been described in animals (*15*). However, based on the anatomic distribution of lesions, direct skin-to-skin contact during sexual activity likely represents the main route of transmission.

All cases in this series were mild and resolved easily without complications. Most patients responded well to short courses of commonly used antibiotics, including β-lactams or doxycycline. That finding is consistent with previous reports of human dermatophilosis as a mostly benign condition (*2*–*6*). Although dermatophilosis might resolve spontaneously over several weeks, accelerated recovery through antibiotic therapy could help reduce transmission within the community. Antimicrobial susceptibility testing showed a broad susceptibility profile to several antibiotic classes, suggesting that standard oral treatments remain effective. In the case of mupirocin, the finding of a high MIC suggests that this topical antibiotic might not be the most suitable treatment option.

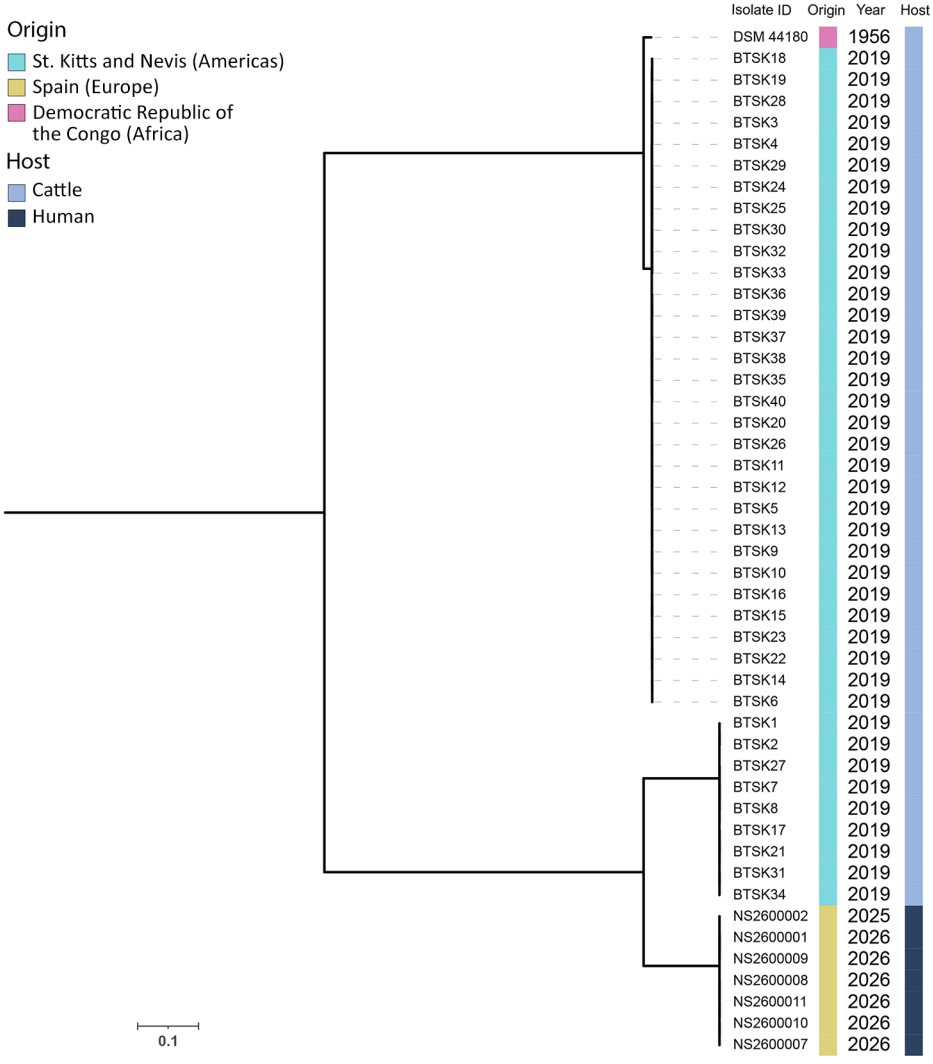

Figure 2. Phylogenetic analysis of *Dermatophilus* isolates in cluster of suspected sexual transmission of dermatophilosis among men who have sex with men, Barcelona, Spain, December 2025–March 2026. Maximum-likelihood phylogenetic tree shows *Dermatophilus* isolates from patient nos. 1–7 obtained in this study (bottom of tree) compared with 40 genomes from cattle in Saint Kitts and Nevis (*8*), and reference strain *D. congolensis* DSM 44180 (all from the National Center for Biotechnology Information Sequence Read Archive, https://www.ncbi.nlm.nih.gov/sra). Scale bar indicates nucleotide substitutions per site.

Genomic findings support recent *Dermatophilus* transmission among humans. The WGS of isolates showed a close genetic relationship, consistent with a recent common ancestor and short transmission chains. The isolates formed a well-supported phylogenetic cluster distinct from publicly available *D. congolensis* genomes, suggesting the circulation of a single lineage rather than multiple independent introductions and representing a novel taxon within the genus *Dermatophilus*. This previously undescribed taxon circulating in humans could potentially contribute to the epidemiologic pattern observed, although further studies are needed to clarify its ecologic niche, host range, and transmission dynamics.

In summary, this cluster of genetically closely related cases of dermatophilosis within sexual networks suggests that this condition might be emerging as a sexually transmissible infection, although environmental transmission cannot be excluded. Because clinical manifestations can be nonspecific and laboratory identification is uncommon in STI clinics, cases could remain unrecognized. Clinicians should therefore suspect dermatophilosis in MSM who have a folliculitis-like pustular rash involving genital or adjacent areas and should consider oral antibiotic treatment and comprehensive STI screening. Cross-border surveillance could help determine whether similar cases are occurring elsewhere.

This work was carried out within the frame of the Doctoral Program in Medicine at the Universitat Autonoma de Barcelona. The study was approved by the Ethics Committee of Vall d'Hebron Hospital, reference no. PR(AG)080/2026. The study was conducted in accordance with the principles laid out in the Declaration of Helsinki and in accordance with the principles of Good Clinical Practice. Informed consent was obtained from participants prior to the inclusion of their data in the analysis, including authorization for the publication of clinical images.

WGS data generated in this study has been deposited in the National Center for Biotechnology Information Sequence Read Archive under BioProject accession no. PRJNA1433182. All *D. congolensis* sequences used in this study, including accession numbers and associated metadata, are described in the Appendix (https://wwwnc.cdc.gov/EID/article/32/6/26-0476-App1.xlsx).

This study was partially supported by the "Centro de Investigación Biomédica en Red" (CIBER de Enfermedades Infecciosas; grant no. CB21/13/00054).

About the Author

Dr. Descalzo is an internal medicine specialist working in the STI/HIV unit Drassanes-Hospital Vall d'Hebron in Barcelona, Spain. His primary research interest is in emerging sexually transmissible infections.

References

1. Zaria LT. *Dermatophilus congolensis* infection (Dermatophilosis) in animals and man! An update. Comp Immunol Microbiol Infect Dis. 1993;16:179–222. https://doi.org/10.1016/0147-9571(93)90148-X
2. Dean DJ, Gordon MA, Severinghaus CW, Kroll E, Reilly JR. Streptothricosis: a new zoonotic disease. NY State J Med. 1961;61:1285–7.
3. Towersey L, Martins EC, Londero AT, Hay RJ, Soares Filho PJ, Takiya CM, et al. *Dermatophilus congolensis* human infection. J Am Acad Dermatol. 1993;29:351–4. https://doi.org/10.1016/0190-9622(93)70194-X
4. Burd EM, Juzych LA, Rudrik JT, Habib F. Pustular dermatitis caused by *Dermatophilus congolensis*. J Clin Microbiol. 2007;45:1655–8. https://doi.org/10.1128/JCM.00327-07
5. Alejo-Cancho I, Bosch J, Vergara A, Mascaro JM, Marco F, Vila J. Dermatitis by *Dermatophilus congolensis*. Clin Microbiol Infect. 2015;21:e73–4. https://doi.org/10.1016/j.cmi.2015.06.013
6. Aubin GG, Guillouzouic A, Chamoux C, Lepelletier D, Barbarot S, Corvec S. Two family members with skin infection due to *Dermatophilus congolensis*: a case report and literature review. Eur J Dermatol. 2016;26:621–2. https://doi.org/10.1684/ejd.2016.2850
7. Clinical and Laboratory Standards Institute. Performance standards for susceptibility testing of mycobacteria, *Nocardia* spp., and other aerobic actinomycetes (document M24S). Wayne (PA): The Institute; 2023.
8. Branford I, Boyen F, Johnson S, Zayas S, Chapwanya A, Butaye P, et al. Identification and antimicrobial resistance of *Dermatophilus congolensis* from cattle in Saint Kitts and Nevis. Vet Sci. 2021;8:135. https://doi.org/10.3390/vetsci8070135
9. Riesco R, Trujillo ME. Update on the proposed minimal standards for the use of genome data for the taxonomy of prokaryotes. Int J Syst Evol Microbiol. 2024;74:006300. https://doi.org/10.1099/ijsem.0.006300
10. Tarín-Vicente EJ, Alemany A, Agud-Dios M, Ubals M, Suñer C, Antón A, et al. Clinical presentation and virological assessment of confirmed human monkeypox virus cases in Spain: a prospective observational cohort study. Lancet. 2022;400:661–9. https://doi.org/10.1016/S0140-6736(22)01436-2
11. Descalzo V, Martín MT, Álvarez-López P, García-Pérez JN, Alcázar-Fuoli L, López-Pérez L, et al. *Trichophyton mentagrophytes* genotype VII and sexually transmitted tinea: an observational study in Spain. Mycoses. 2025;68:e70049. https://doi.org/10.1111/myc.70049
12. Spicknall IH, Gift TL, Bernstein KT, Aral SO. Sexual networks and infection transmission networks among men who have sex with men as causes of disparity and targets of prevention. Sex Transm Infect. 2017;93:307–8. https://doi.org/10.1136/sextrans-2016-052676
13. Abu-Samra MT. The epizootiology of *Dermatophilus congolensis* infection. Rev Elev Med Vet Pays Trop. 1980;33:23–32.
14. Martinez D, Prior P. Survival of *Dermatophilus congolensis* in tropical clay soils submitted to different water potentials.

Vet Microbiol. 1991;29:135–45. https://doi.org/10.1016/0378-1135(91)90121-U

15. García Sánchez A, Zurita SG, Gil Molino M, Martin Cano FE, Barraso Gil C, Hermoso de Mendoza Salcedo J. Outbreak of dermatophilosis in horses possibly transmitted by sharing riding equipment. Braz J Vet Med. 2024;46:e002124. https://doi.org/10.29374/2527-2179.bjvm002124

Address for correspondence: Maider Arando, STI/HIV Unit Drassanes–Vall d'Hebron, Hospital Universitari Vall d'Hebron, 17 Sant Oleguer, 08001 Barcelona, Spain; email: maider.arando@vallhebron.cat; or Mayli Lung, Clinical Microbiology Department, Hospital Universitari Vall d'Hebron, Pg Vall d'Hebron 119-129, 08035 Barcelona, Spain; email: mayli.lung@vallhebron.cat

Placental Vascular Pathology Associated with Congenital Lymphocytic Choriomeningitis Virus Infection, Philadelphia, Pennsylvania, USA

Abin Abraham, Rebecca L. Linn, Dustin D. Flannery, Scott M. Gordon

Congenital lymphocytic choriomeningitis virus (LCMV) infection is associated with major neurologic malformations and fetal demise. We report 2 cases of probable congenital LCMV infection and chorioretinitis, cerebral ventriculomegaly, and placental histopathology in Philadelphia, Pennsylvania, USA. Clinicians who suspect congenital LCMV infection should screen for chorioretinitis, LCMV antibodies, and evidence of placental pathology.

Lymphocytic choriomeningitis virus (LCMV) is an underappreciated congenital pathogen carried by rodents (*1*). Congenital LCMV infection is associated with pathognomonic chorioretinitis and a variety of neurologic malformations (*2*). A case of fetal hydrops caused by congenital LCMV also has been reported (*3*). In a large maternal seroprevalence study, we found that 2.5% of a random sample of 1,000 women who gave birth in Philadelphia, Pennsylvania, USA, were LCMV IgG–positive (*4*). Those data support that pregnant women are at risk for LCMV exposure in a major urban area and that LCMV acquired during pregnancy can cause devastating short- and long-term outcomes for newborns.

The placenta nourishes the fetus in the womb and protects it from pathogens (*5*). Select pathogens can inflame and disrupt the structure and function of the placenta (*6*). The effects of congenital LCMV infection on the placenta remain unknown. Here, we provide evidence of inflammatory and vascular placental pathology in 2 cases of probable congenital LCMV infection in Philadelphia, diagnosed by clinical history, clinical findings, and neonatal and maternal serologic studies.

Author affiliations: Children's Hospital of Philadelphia, Philadelphia, Pennsylvania, USA (A. Abraham, R.L. Linn, D.D. Flannery, S.M. Gordon); University of Pennsylvania Perelman School of Medicine, Philadelphia (R.L. Linn, D.D. Flannery, S.M. Gordon)

DOI: https://doi.org/10.3201/eid3206.260165

The Cases

The first case occurred in a 22-year-old G2P1 (2 pregnancies, 1 delivery) woman examined for multidisciplinary evaluation after severe fetal cerebral ventriculomegaly was identified on routine ultrasound growth scan at 36 weeks' gestation (Figure 1, panel A). Umbilical artery, middle cerebral artery, and ductus venosus Doppler indices were within normal limits for gestational age. The anatomy scan at 26 weeks' gestation revealed echogenic bowel but no other abnormalities. The pregnancy was complicated by gestational diabetes. Maternal prenatal laboratory testing demonstrated immunity to rubella virus, as well as prior exposure (IgG-positive) to cytomegalovirus (CMV) and *Toxoplasma*. The woman reported 2 pet dogs at home but denied exposure to rodents during pregnancy. She recalled subjective fever and chills at 16 weeks' gestation.

A male infant was born by repeat cesarean delivery at 38 weeks 4 days' gestation. Birthweight was at the 71st percentile and head circumference at the 97th percentile for age. Postnatal magnetic resonance imaging (MRI) confirmed cerebral ventriculomegaly, and ophthalmologic evaluation demonstrated chorioretinitis (Figure 1, panels B, C), prompting evaluation for congenital infection. Newborn laboratory evaluation showed *Toxoplasma* IgG-positive and IgM-negative and rubella virus IgM-negative on serology; PCR of urine was

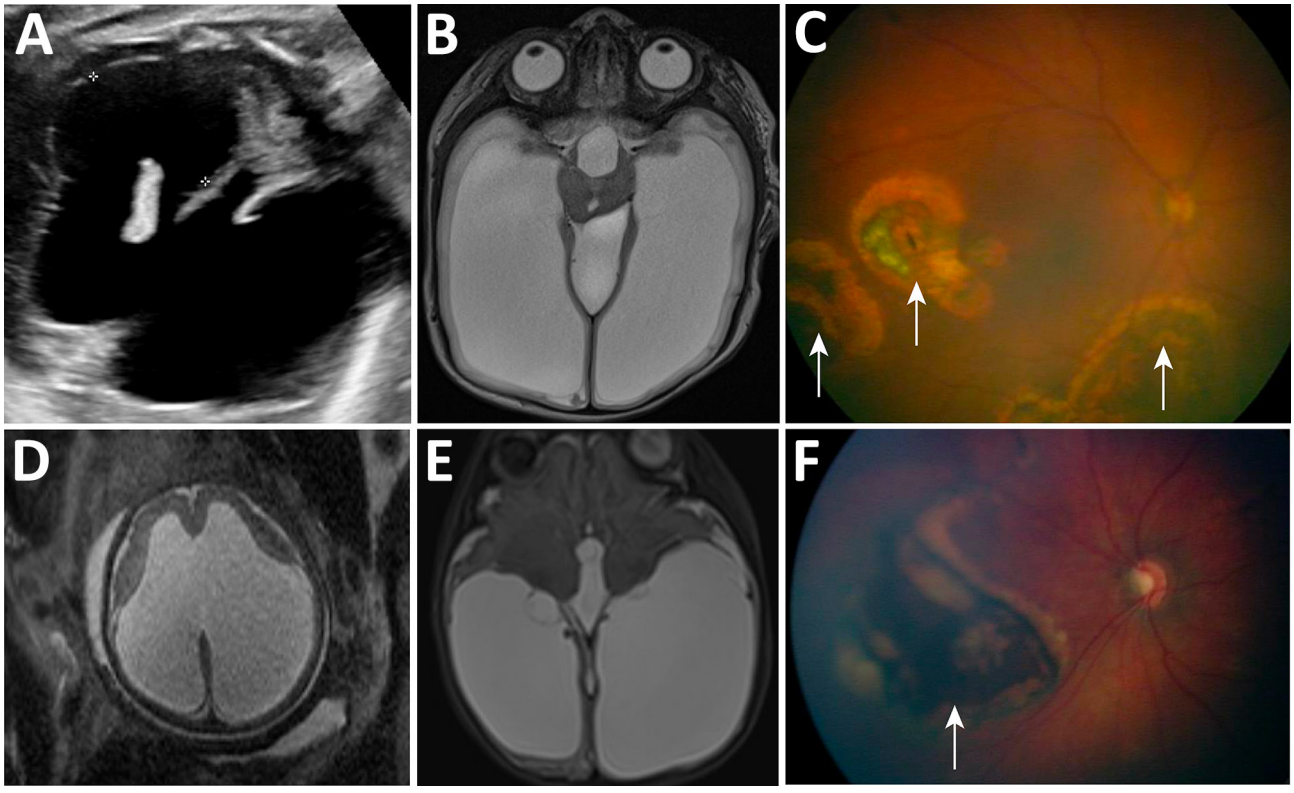

Figure 1. Imaging findings for ventriculomegaly and chorioretinitis associated with congenital lymphocytic choriomeningitis virus infection, Philadelphia, Pennsylvania, USA. A–C) Case 1; D–F) case 2. A) Routine ultrasonography at 36 weeks' gestation, demonstrating severe cerebral ventriculomegaly in the fetus (black space between markers on the anatomic right and the unmarked black space on the anatomic left). B) Postnatal (38 weeks 4 days' gestation) brain magnetic resonance imaging of newborn confirmed severe cerebral ventriculomegaly (large, white, fluid-filled spaces bilaterally and in the center of the image). C) Fundoscopic examination of newborn, revealing multiple areas of chorioretinitis (arrows). D) Routine ultrasonography at 36 weeks' gestation, demonstrating severe cerebral ventriculomegaly in the fetus. E) Postnatal (38 weeks 5 days' gestation) brain magnetic resonance imaging of newborn confirmed severe cerebral ventriculomegaly. F) Fundoscopic examination of newborn, revealing a large area of chorioretinitis (arrow).

CMV-negative, and PCR of serum was herpes simplex virus (HSV)–negative. The infant's LCMV IgG titer was 1:2,560 and LCMV IgM was negative (<1:10). Maternal LCMV serologic testing was not performed.

Placental weight was at the 50th percentile for gestational age. Gross pathology showed 2 subchorionic intervillous thrombi and a peripheral intraparenchymal thrombus (Figure 2, panels A, B). Pathologic examination demonstrated high-grade

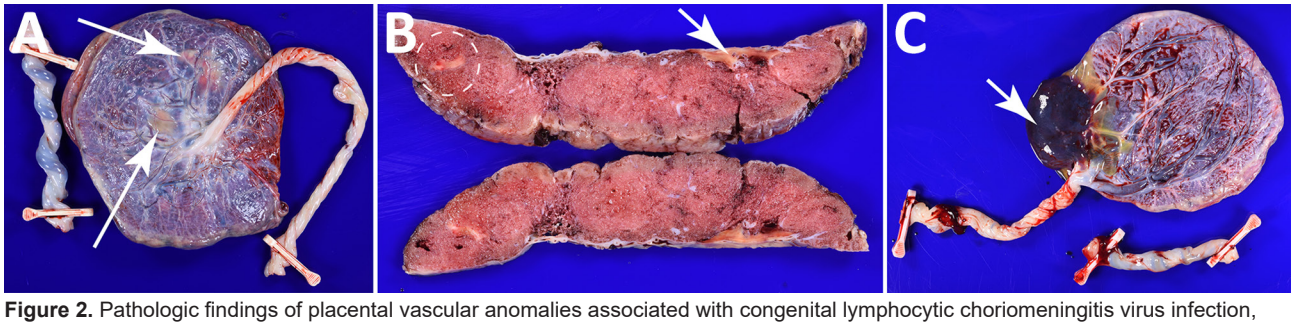

Figure 2. Pathologic findings of placental vascular anomalies associated with congenital lymphocytic choriomeningitis virus infection, Philadelphia, Pennsylvania, USA. A, B) Placenta from case 1; C) placenta from case 2. A) Gross pathology of the fetal surface showing yellow-white subchorionic intervillous thrombi (arrows). B) Cross sections of the placenta showing a subchorionic intervillous thrombus (arrow) and a peripheral intraparenchymal thrombus (white dashed circle). C) Gross pathology of the fetal surface of placenta with marginal insertion of three vessel umbilical cord and acute subamniotic hemorrhage (arrow). No additional gross lesions were identified after serial sectioning.

fetal vascular malperfusion. We noted multiple foci of avascular villi, similar to that reported in congenital CMV infection (*7*), and some villi had stromal hemosiderin deposition (Figure 3, panels A, B). The maternal-fetal interface showed chronic deciduitis with plasma cell infiltration (not shown) and focal, low-grade chronic villitis in the placental parenchyma (Figure 3, panel B). We noted evidence of low-grade maternal vascular perfusion, and mural hypertrophy of membrane arterioles, mild accelerated villous maturation with patchy increase in syncytial knots (*8*,*9*), mildly increased perivillous fibrin deposition, and variable villous agglutination.

The second case occurred in a 27-year-old G5P4 woman examined for multidisciplinary evaluation at 38 weeks' gestation. Routine ultrasound growth scan revealed severe fetal cerebral ventriculomegaly (Figure 1, panel D). Doppler velocimetry studies were within reference limits for gestational age. As in case 1, this mother had an unremarkable prenatal anatomy scan at 20 weeks' gestation. Routine prenatal laboratory tests were unremarkable, and no additional testing for CMV, HSV, or *Toxoplasma* was performed. By maternal report, at 24 weeks' gestation, she had severe meningitis diagnosed during a 2-week hospital admission. A causative agent was not identified, and the mother reported

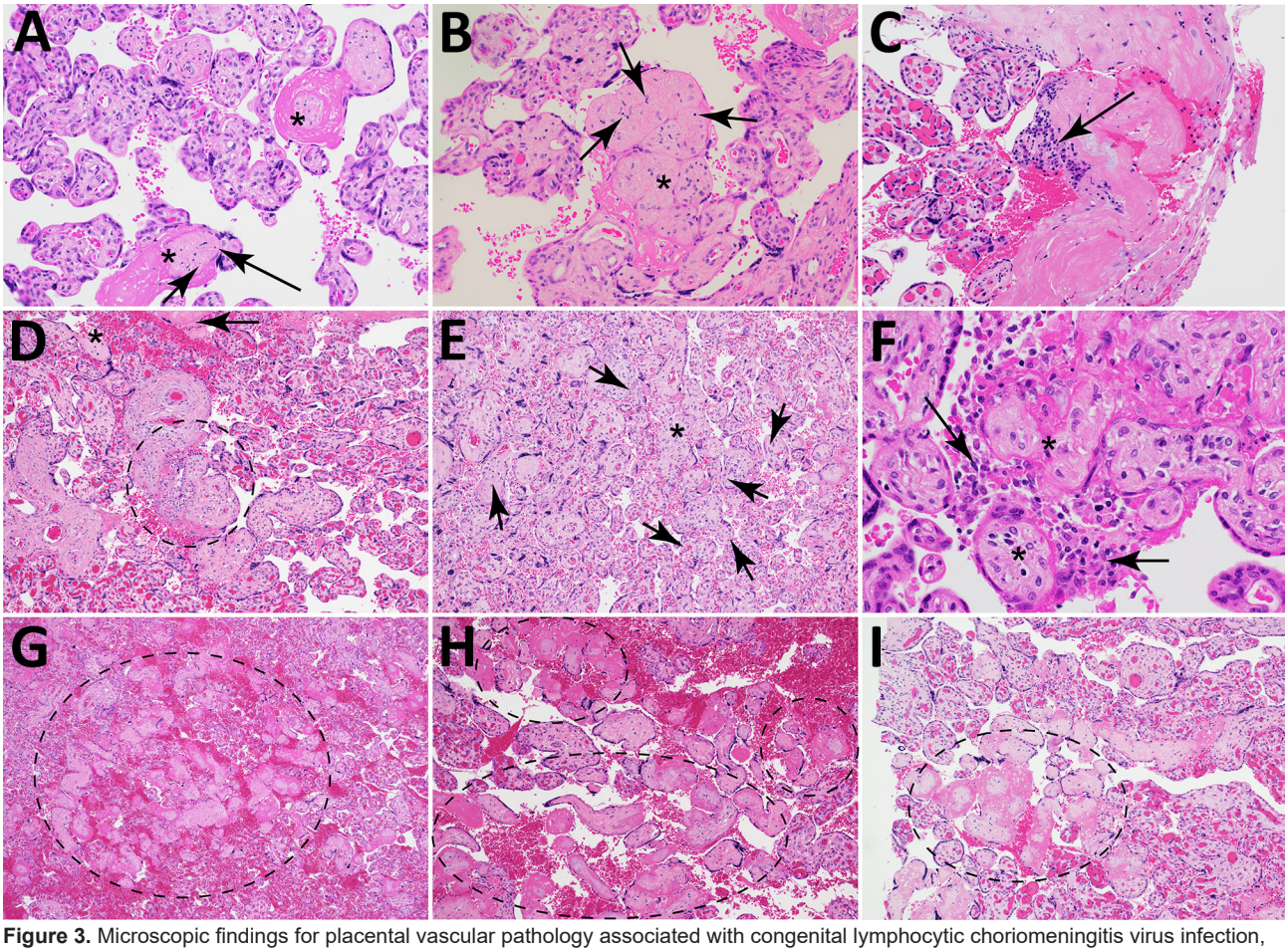

Figure 3. Microscopic findings for placental vascular pathology associated with congenital lymphocytic choriomeningitis virus infection, Philadelphia, Pennsylvania, USA. Hematoxylin and eosin–stained cross-sections of placenta from case 1 (A, B) and case 2 (C–I). A) Avascular villi surrounded by pink perivillous fibrin (asterisks) with scattered foci of rust-colored hemosiderin deposition (arrows) within the hyalinized stroma. Original magnification ×200. B) Cluster of avascular villi in the center of the image (asterisk) with scattered intravillous lymphocytes (arrows), compatible with chronic villitis. Original magnification ×200. C) Plasma cells (arrow) within the basal plate, consistent with chronic deciduitis. Original magnification ×200. D) Chronic villitis and perivillitis involving stem villi vessels (circle), with an associated avascular villus (asterisk) and fibrin deposition (arrow). Original magnification ×100. E) Chronic villitis (asterisk) with villous stromal vascular karyorrhexis; arrows point to examples of extravasated, fragmented erythrocytes and nuclear debris. Original magnification ×100. F) Histiocytic intervillositis (arrows) adjacent to avascular villi (asterisks) with perivillous fibrin deposition. Original magnification ×400. G–I) Avascular villi with associated perivillous fibrin deposition (dashed ellipses). G) Original magnification ×40; H, I) original magnification ×100.

recovering fully from the illness. The pregnancy was otherwise uncomplicated.

A female infant was born at 38 weeks 5 days' gestation by primary cesarean delivery because of fetal hydrocephalus and macrocephaly. Birthweight was at the 16th percentile and head circumference at the 54th percentile for age. Postnatal neuroimaging demonstrated severe ventriculomegaly, and postnatal ophthalmologic examination demonstrated chorioretinitis (Figure 1, panels E, F). Therefore, we evaluated the newborn for congenital infections; serum test results were negative for *Toxoplasmosis* IgM and IgG and rubella IgM, and PCR on urine was CMV-negative. The newborn's serum LCMV IgG was 1:2,560; LCMV IgM was negative (<1:10).

Upon further questioning, the mother revealed exposure to a rodent infestation in the home during pregnancy. The mother's serum LCMV IgG was 1:10,240 and was IgM-positive at 1:10. The maternal exposure to rodent excreta, plus meningitis, serologic data, and timing of the fetal ventriculomegaly, suggest a diagnosis of congenital LCMV infection acquired during the second trimester.

Placental weight was less than the 10th percentile for gestational age. Gross pathology showed an acute subamniotic hemorrhage (Figure 2, panel C). The placenta in case 2 exhibited inflammatory changes of the maternal–fetal interface, including mild chronic deciduitis with plasma cell infiltrates (Figure 3, panel C), chronic chorionitis (not shown), multifocal low-grade chronic villitis, and perivillitis involving terminal and stem villi (Figure 3, panels D, E). The placenta from case 2 also exhibited focal histiocytic intervillositis (Figure 3, panel F), defined by inappropriate accumulation of macrophages into the intervillous space and associated with fetal growth restriction or demise (*10*,*11*). We noted multiple foci of avascular villi and villous stromal vascular karyorrhexis, often associated with perivillous fibrin deposition (Figure 3, panels E–I). Those pathologic changes are compatible with high-grade fetal vascular malperfusion (*12*). Given the proximity of the microanatomic abnormalities and inflammation, the placental pathology might reflect progression of the inflammatory changes observed.

The clinical, radiographic, ophthalmologic, and serologic data in the 2 cases we describe support probable congenital LCMV infection, acquired during the 2nd trimester of pregnancy, with profound long-term consequences. Both children underwent ventriculoperitoneal shunt placement for hydrocephalus and endured several episodes of shunt malfunctions requiring shunt revisions. The child in case 1 had hemiplegia, obstructive sleep apnea, and motor and cognitive delays diagnosed. The child in case 2 had spastic quadriplegic cerebral palsy, epilepsy, and motor and cognitive delays diagnosed. Both children remain dependent on multiple subspecialists, an array of medical technologies, and aggressive physical, occupational, and speech therapy regimens.

Conclusions

Whole-exome sequencing was unrevealing for either case in this report. In an era of increasingly accessible but costly and time-intensive genetic testing, obstetric and neonatal providers should consider congenital LCMV in the differential diagnosis of congenital neurologic malformations. Definitive diagnosis of any congenital infection remains challenging, however. Diagnosis is often made retrospectively, long after acute maternal infection. Mothers can exhibit minimal systemic symptoms (as in case 1) or severe clinical illness (as in case 2). Because few readily available tools are available to identify LCMV within the placenta, clinicians have relied on a constellation of clinical, imaging, and serologic findings in the mother and infant to diagnose congenital LCMV infection (*13*).

To establish causality between LCMV and congenital findings in the future, detecting LCMV within the placenta of suspected cases will be essential. In the meantime, we propose that infants with suspected congenital infection undergo ophthalmologic screening for chorioretinitis and serologic testing for LCMV antibodies. We also recommend maternal serologic testing to support the diagnosis and provide insight into the timing of infection. Preventing congenital LCMV requires minimizing prenatal exposures and halting vertical transmission during pregnancy. Future mechanistic investigations into LCMV-associated fetoplacental injury are urgently needed. Then, we can develop new therapies to preserve healthy placental function and normal fetal neurodevelopment in the setting of congenital LCMV.

This work was supported by the Children's Hospital of Philadelphia and the National Institute of Allergy and Infectious Diseases (grant no. K08AI151265 to S.M.G.)

About the Author

Dr. Abraham is a neonatology fellow at Children's Hospital of Philadelphia, Philadelphia, Pennsylvania, USA. His research interests are studying congenital infections to improve perinatal health using computational biology.

References

1. Olivieri NR, Othman L, Flannery DD, Gordon SM. Transmission, seroprevalence, and maternal-fetal impact of lymphocytic choriomeningitis virus. Pediatr Res. 2024;95:456–63. https://doi.org/10.1038/s41390-023-02859-w
2. Bonthius DJ, Wright R, Tseng B, Barton L, Marco E, Karacay B, et al. Congenital lymphocytic choriomeningitis virus infection: spectrum of disease. Ann Neurol. 2007;62:347–55. https://doi.org/10.1002/ana.21161
3. Meritet JF, Krivine A, Lewin F, Poissonnier MH, Poizat R, Loget P, et al. A case of congenital lymphocytic choriomeningitis virus (LCMV) infection revealed by hydrops fetalis. Prenat Diagn. 2009;29:626–7. https://doi.org/10.1002/pd.2240
4. Flannery DD, Cossaboom CM, Flietstra TD, Barboza AZ, Burris HH, Puopolo KM, et al. Lymphocytic choriomeningitis virus seroprevalence among urban pregnant women and newborns, Philadelphia, Pennsylvania, USA, 2021. Emerg Infect Dis. 2026;32:324–31. https://doi.org/10.3201/eid3203.250910
5. Megli CJ, Coyne CB. Infections at the maternal-fetal interface: an overview of pathogenesis and defence. Nat Rev Microbiol. 2022;20:67–82. https://doi.org/10.1038/s41579-021-00610-y
6. Pereira L. Congenital viral infection: traversing the uterine-placental interface. Annu Rev Virol. 2018; 5:273–99. https://doi.org/10.1146/annurev-virology-092917-043236
7. Heerema-McKenney A. Defense and infection of the human placenta. APMIS. 2018;126:570–88. https://doi.org/10.1111/apm.12847
8. Fogarty NM, Ferguson-Smith AC, Burton GJ. Syncytial knots (Tenney-Parker changes) in the human placenta: evidence of loss of transcriptional activity and oxidative damage. Am J Pathol. 2013;183:144–52. https://doi.org/10.1016/j.ajpath.2013.03.016
9. Burton GJ, Jones CJ. Syncytial knots, sprouts, apoptosis, and trophoblast deportation from the human placenta. Taiwan J Obstet Gynecol. 2009;48:28–37. https://doi.org/10.1016/S1028-4559(09)60032-2
10. Brady CA, Williams C, Sharps MC, Shelleh A, Batra G, Heazell AEP, et al. Chronic histiocytic intervillositis: a breakdown in immune tolerance comparable to allograft rejection? Am J Reprod Immunol. 2021;85:e13373. https://doi.org/10.1111/aji.13373
11. Moar L, Simela C, Nanda S, Marnerides A, Al-Adnani M, Nelson-Piercy C, et al. Chronic histiocytic intervillositis (CHI): current treatments and perinatal outcomes, a systematic review and a meta-analysis. Front Endocrinol (Lausanne). 2022;13:945543. https://doi.org/10.3389/fendo.2022.945543
12. Redline RW, Ravishankar S, Bagby CM, Saab ST, Zarei S. Four major patterns of placental injury: a stepwise guide for understanding and implementing the 2016 Amsterdam consensus. Mod Pathol. 2021;34:1074–92. https://doi.org/10.1038/s41379-021-00747-4
13. Pencole L, Sibiude J, Weingertner AS, Mandelbrot L, Vauloup-Fellous C, Picone O. Congenital lymphocytic choriomeningitis virus: a review. Prenat Diagn. 2022;42:1059–69. https://doi.org/10.1002/pd.6192

Address for correspondence: Scott M. Gordon, Children's Hospital of Philadelphia, Abramson Pediatric Research Center, 3615 Civic Center Blvd, 11th Fl, Office 1107C, Philadelphia, PA 19104, USA; email: gordons1@chop.edu

Concurrent Detection of Swine-Origin Influenza A(H1N1) Virus in Pigs and Farmer, Switzerland

Jonas Steiner,[1] Mike Mwanga,[1] Larise Oberholster, Matthias Licheri, Manon F. Licheri, Heiko Nathues,[2] Ronald Dijkman,[2] Jenna N. Kelly[2]

We report zoonotic transmission of Eurasian avian-like swine influenza A(H1N1) virus from pigs to a farmer. The pigs and farmer experienced influenza-like illness. Whole-genome sequencing revealed >99.9% viral sequence identity between hosts. Our findings highlight the risk posed by enzootic swine influenza A virus and the need for genomic and epidemiologic surveillance.

Since the 2009 swine influenza pandemic, sporadic human infections with swine influenza A viruses (swIAVs) continue to occur, including rare instances of onward human-to-human transmission, highlighting the ongoing pandemic risk (*1*–*4*). Pigs are key reservoirs and mixing vessels for influenza A virus (IAV) evolution; transmission between humans and pigs is frequent and bidirectional (*5*,*6*). Active epidemiologic and genomic surveillance at the swine–human interface is therefore essential for early detection and risk assessment of emerging strains.

In Switzerland, pig production is less intensive; herds remain relatively isolated from neighboring countries because of strict regulations and minimal import of live pigs (*7*,*8*). Infrequent use of swIAV vaccines allows for natural viral evolution without vaccine-driven selective pressures (*9*); country-specific transmission chains may exist within pig herds in Switzerland. The ongoing national surveillance program for swIAV relies primarily on partial hemagglutinin (HA) and neuraminidase (NA) gene sequences, limiting its ability to identify emerging swIAV lineages in pig herds (*10*).

To investigate the epidemiology and genetic diversity of swIAV in pig herds, we established a whole-genome sequencing (WGS)–based swIAV surveillance program. We obtained samples from symptomatic and randomly selected pig herds; pig caretakers with respiratory illness voluntarily provided self-collected nasal swab specimens. Here, we report a zoonotic transmission event involving Eurasian avian-like (EA) swine influenza A(H1N1) virus detected concurrently in a farmer and his pig herd through WGS surveillance.

The Study

On November 27, 2023, a respiratory disease outbreak was reported in a herd of ≈180 fattening pigs, 4 weeks after the introduction of 90 growing pigs from another herd from within Switzerland. Upon clinical examination, ≈80% of pigs showed apathy and fever (≤40.3°C) and sporadic respiratory signs. The farmer, who was 40–50 years of age with no reported underlying conditions, experienced a mild influenza-like illness 2 weeks earlier and reported similar symptoms in 2 household members. The farmer was not vaccinated against seasonal influenza and reported no contact with other pig herds.

We collected nasal swab samples from pigs and the farmer through our WGS-based surveillance program and the national swIAV surveillance system. Within the WGS surveillance framework, we screened 5 pig samples (A0001–A0005) and 1 farmer sample (H0001) for IAV using a pan-IAV matrix gene–specific quantitative reverse transcription PCR assay on extracted viral RNA (Appendix Table 1, https://wwwnc.cdc.gov/EID/article/32/6/

Author affiliations: University of Bern Multidisciplinary Center for Infectious Diseases, Bern, Switzerland (J. Steiner, M. Mwanga, L. Oberholster, M. Licheri, M.F. Licheri, H. Nathues, R. Dijkman, J.N. Kelly); University of Bern Vetsuisse Faculty, Bern (J. Steiner, M. Mwanga, H. Nathues, J.N. Kelly); University of Bern Faculty of Medicine, Bern (M. Mwanga, L. Oberholster, M. Licheri, M.F. Licheri, R. Dijkman); Institute of Virology and Immunology, Bern and Mittelhäusern, Switzerland (M. Mwanga, J.N. Kelly)

DOI: https://doi.org/10.3201/eid3206.251487

[1]These first authors contributed equally to this article.

[2]These senior authors contributed equally to this article.

Table 1. Sample and sequencing data collected in study of influenza A(H1N1) virus in pigs and farmer, Switzerland, November 2023*

Sample	Host	Life stage*	Crossing point value	Total no. reads	No. (%) viral reads
A0001	Pig	Fattening pig	24.60	454,678	448,020 (98.5)
A0002	Pig	Fattening pig	25.76	276,888	271,662 (98.1)
A0003	Pig	Fattening pig	23.79	571,358	563,098 (98.5)
A0004	Pig	Fattening pig	25.10	358,462	353,591 (98.6)
A0005	Pig	Fattening pig	26.07	1,173,972	1,161,694 (98.9)
H0001	Human	Adult	32.47	10,779	8,174 (74.6)

*Life stage for pigs is »22 wk; for human adult, 40–50 y.

25-1487-App1.pdf) (*11*). All samples tested positive; viral loads were higher in pigs (crossing point [Cp] value 24–26) than in the farmer sample (Cp 32) (Table 1). After confirming variant H1N1 (H1N1v) infection in the farmer, we notified veterinary and public health authorities and reported the case through the World Health Organization National Focal Point in accordance. Nine days after case confirmation, nasal swabs from all 3 household contacts tested negative for IAV at the Swiss National Reference Centre for Influenza (NRCI) (Figure 1) (A.R. Gonçalves Cabecinhas, pers. comm., email, 2024 Dec 2).

We performed WGS as described previously (*12*), achieving high read depth (≥1,000´) overall; 1 segment showed lower coverage (≥100´), sufficient for complete genome assembly (Table 1; Appendix

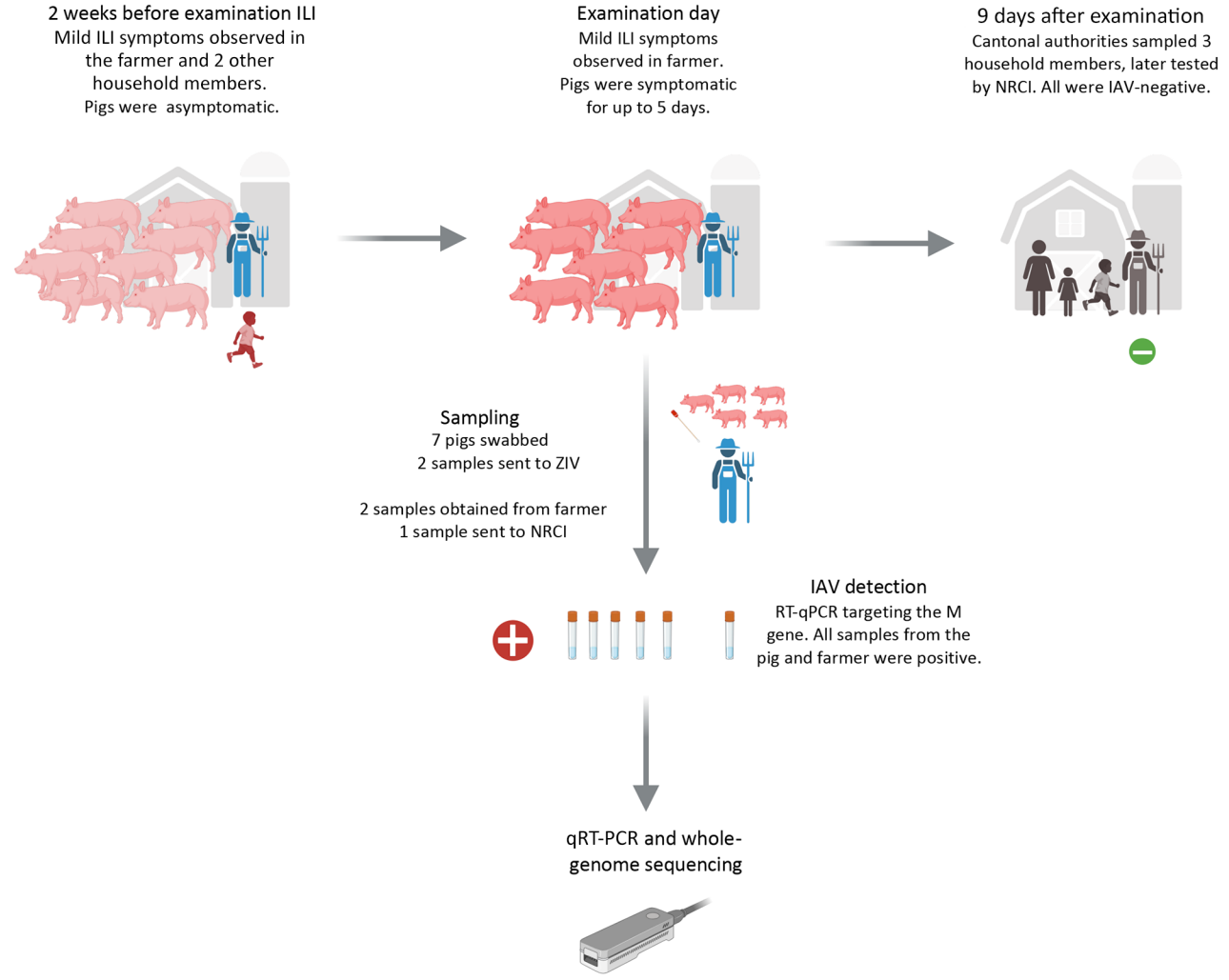

Figure 1. Timeline of events from study of swine-origin influenza A(H1N1) virus in pigs and farmer, Switzerland, November 2023. Image depicts the chronology of symptoms in pigs and humans, sampling dates, and household investigations, along with corresponding qRT-PCR results. Figure created in BioRender (Mwanga M, 2025, https://BioRender.com/te6k5rt). IAV, influenza A virus; ILI, influenza-like illness; NRCI, National Reference Centre for Influenza, Switzerland; M, matrix; qRT-PCR, quantitative reverse transcription PCR; ZIV, Institute of Virology, Vetsuisse Faculty, University of Zurich; –, negative; +, positive.

Table 1, Figure 1). We subtyped all viruses from human and pig samples as swine H1N1 (swH1N1); nucleotide identity was >99.9% across all genomic segments. Phylogenetic analysis with publicly available swH1N1 sequences from Switzerland and Europe showed that all study viruses were assigned

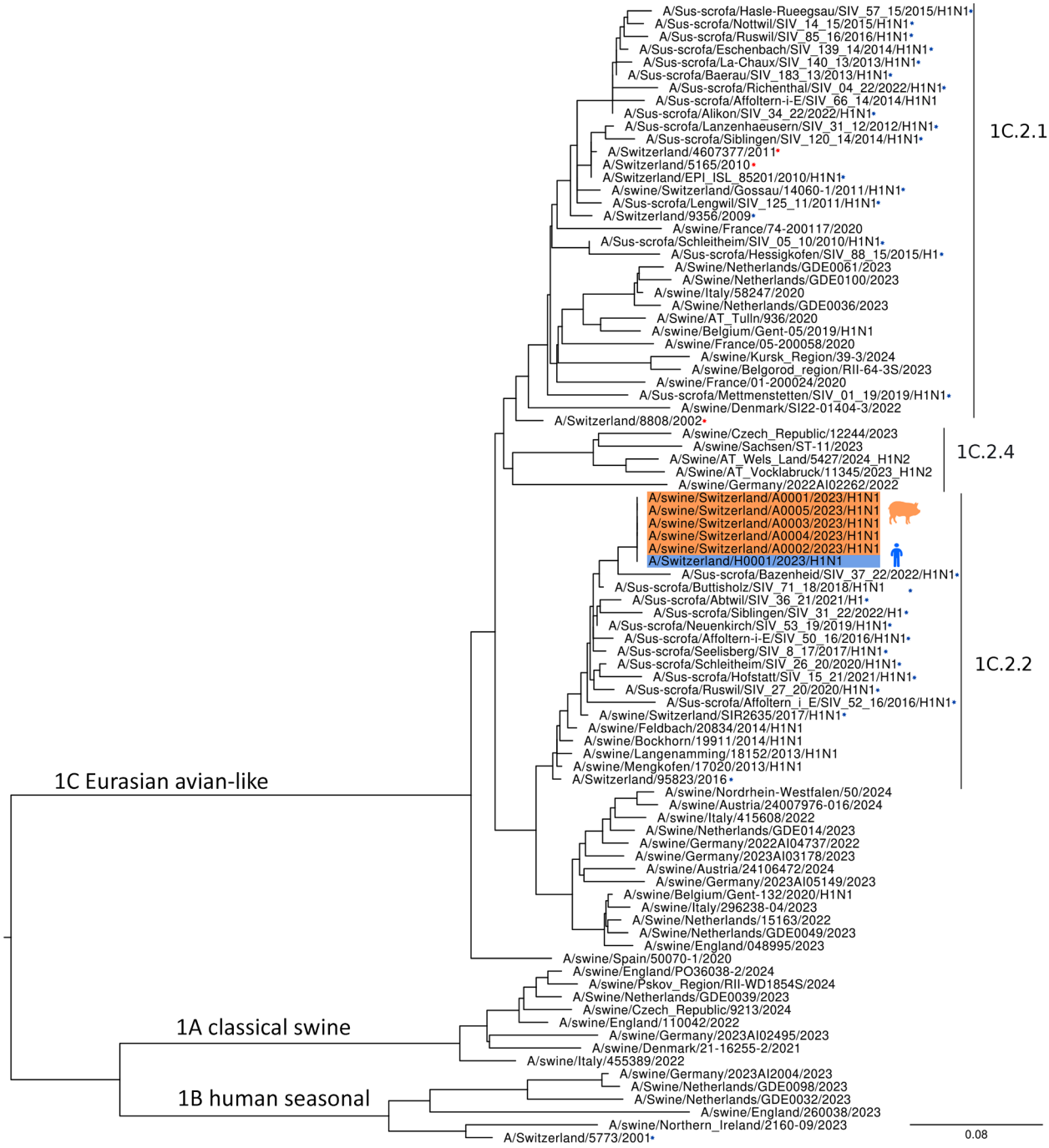

Figure 2. Maximum-likelihood phylogenetic tree from study of swine-origin influenza A(H1N1) virus in pigs and farmer, Switzerland, November 2023. We mapped hemagglutinin (HA) gene codon sequences, showing lineage classification of the study swine H1N1 virus based on lineage reference sequences and HA-H1 sequences from viruses identified in Switzerland and other Europe countries (2020–2023). The tree shows classification based on the 3 major swine H1N1 lineages: 1A, 1B, and 1C. Orange shading indicates swine H1N1 HA sequences from pig samples; blue indicates sequence from the farmer. Other swine H1N1 HA sequences from Switzerland are marked with asterisks: blue for those identified in pig samples and red for those identified in human samples. Study sequences cluster within the Eurasian avian-like lineage clade 1C.2.2. Pig sequences from previous years are grouped in clades 1C.2.1. and 1C.2.2. Scale bar indicates substitutions per site.

Table 2. Comparison of amino acid sequences in the hemagglutinin antigenic region of swine H1N1, human seasonal H1N1, and seasonal vaccine strains in study of influenza A(H1N1) virus in pigs and farmer, Switzerland, November 2023*

Isolate	HA-H1 residue positions												
Antigenic site Sa	124	125	153	154	155	156	157	159	160	161	162	163	164
Vaccine A/Wisconsin/67/2022	P	N	K	K	G	K	S	P	K	I	N	Q	T
Vaccine A/Victoria/4897/2022/H1N1	P	N	K	K	G	K	S	P	K	I	N	Q	T
Study A/Switzerland/H0001/2023/H1N1	P	N	K	K	G	N	A	P	K	I	R	K	S
Human seasonal H1N1	P	N	K	K	G	K	S	P	K	I	N	Q	T
Antigenic site Sb	184	185	186	187	188	189	190	191	192	193	194	195	
Vaccine A/Wisconsin/67/2022	T	I	T	D	Q	E	S	L	Y	Q	N	A	
Vaccine A/Victoria/4897/2022/H1N1	T	I	T	D	Q	E	S	L	Y	Q	N	A	
Study A/Switzerland/H0001/2023/H1N1	T	D	S	D	Q	Q	T	L	Y	Q	N	N	
Human seasonal H1N1	T	I	T	D	Q	E	S	L	Y	Q	N	A	
Antigenic site Ca1	166	167	168	169	170	203	204	205	235	236	237		
Vaccine A/Wisconsin/67/2022	I	N	D	K	G	T	S	R	E	P	G		
Vaccine A/Victoria/4897/2022/H1N1	I	N	D	K	G	T	S	R	E	P	G		
Study A/Switzerland/H0001/2023/H1N1	T	N	N	K	G	S	S	K	D	Q	G		
Human seasonal H1N1	I	N	D	Q	G	T	S	R	E	P	G		
Antigenic site Ca2	137	138	139	140	141	142	221	222					
Vaccine A/Wisconsin/67/2022	S	H	A	G	A	R	R	D					
Vaccine A/Victoria/4897/2022/H1N1	S	H	A	G	A	R	R	D					
Study A/Switzerland/H0001/2023/H1N1	S	H	S	G	T	K	R	E					
Human seasonal H1N1	P	H	A	G	A	K	R	D					
Antigenic site Cb	70	71	72	73	74	75							
Vaccine A/Wisconsin/67/2022	L	S	T	A	R	S							
Vaccine A/Victoria/4897/2022/H1N1	L	S	T	A	R	S							
Study A/Switzerland/H0001/2023/H1N1	L	L	T	A	D	S							
Human seasonal H1N1	L	S	T	A	R	S							

*Comparison of amino acid sequences in the antigenic region among the human 2023–24 seasonal vaccine strains, the swine H1N1 (swH1N1) virus identified in this study, and a representative human seasonal H1N1 virus. Numbering is based on the recommended HA-H1 numbering scheme using the HA Subtype Numbering Conversion tool (https://www.bv-brc.org/app/HASubtypeNumberingConversion). Orange shading denotes mutations distinguishing the vaccine strain from the study swine H1N1 virus. Gray shading indicates mutations distinguishing the vaccine strain from the representative human seasonal virus. A, alanine; D, aspartic acid; E, glutamic acid; G, glycine; H, histidine; HA, hemagglutinin; I, isoleucine; K, lysine; L, leucine; N, asparagine; P, proline; Q, glutamine; R, arginine; S, serine; T, threonine; Y, tyrosine.

to the EA swH1N1 lineage, clade 1C.2.2, forming a monophyletic cluster for all genomic segments (Figure 2; Appendix Figure 2). Similar to other EA swH1N1 viruses, the Switzerland sequences harbored several amino acid substitutions associated with host specificity and antiviral resistance (Appendix Table 2).

We assessed low-frequency diversity by variant calling across all genomic segments. We detected 26 minor single-nucleotide variants (SNVs) at 6%–50% frequency, resulting in 17 nonsynonymous mutations. We detected 4 human-specific SNVs, including C1771T (H0001), which resulted in a premature stop codon in the polymerase acidic (PA) gene (Q591*). We identified 4 SNVs shared between human and pig samples, including G515A, which resulted in the HA-G172E mutation associated with antigenic drift and potential immune escape (Appendix Table 3, Figure 3) (*13*). We detected 1 SNV (PB2–1447), leading to a T483A mutation, in all samples. The presence of shared SNVs supports epidemiologic linkage between the farmer and pigs.

Finally, we compared HA antigenic residues of study viruses to the 2023–24 human seasonal vaccine strain and a contemporaneous (2023) human H1N1 sequence (Table 2). We identified multiple substitutions in the swH1N1 sequences across defined antigenic sites Sa/Sb, Ca1, Ca2, and Cb; the contemporaneous human seasonal virus differed from the vaccine strain by 2 antigenic residues. Overall, swH1N1 sequences from pigs and the farmer showed greater divergence at HA antigenic sites relative to the vaccine strain than the contemporaneous human seasonal virus, consistent with their evolutionary divergence from human H1N1 viruses.

Conclusions

This study reports the concurrent detection of EA swH1N1 virus in a farmer and his pigs in Switzerland. Evidence for zoonotic transmission is >99.9% genomic identity between viruses from the farmer and pigs, shared SNVs between hosts, and epidemiologic data consistent with transmission at the swine–human interface. We identified several human-specific SNVs, but their functional significance remains unknown. We observed 1 SNV, PA C1771T (Q591*), at the consensus level in 1 pig sample; however, we cannot infer transmission direction or functional significance on the basis of the available data. The lower viral load we observed in the farmer sample may reflect previous immunity, timing of sampling, host-specific constraints, or the effects of the detected SNVs. We detected no onward transmission to household contacts; we could not exclude the possibility of secondary transmission because of the timing of sample collection.

Genomic analysis revealed that the swH1N1 viruses identified in this study clustered with previously detected Switzerland sequences belonging to the EA lineage, clade 1C.2.2 (*10*). Despite limited availability of complete swH1N1 genome sequences from Switzerland, our findings are consistent with the presence of a relatively homogeneous swIAV population in pigs, likely shaped by the closed herd system and low annual importation of live pigs. Similarly, in Norway, the circulation of a single lineage under a closed system highlighted the effect of production structure on viral evolution (*14*). In contrast, greater swIAV genetic diversity has been reported in other countries in Europe (*15*).

HA sequences of study swH1N1 viruses harbored multiple amino acid substitutions across defined antigenic regions, whereas contemporary human H1N1 strains differed from vaccine strains by only 1 or 2 residues. The detection of 1 SNV associated with HA antigenic drift highlighted hidden evolution; that finding suggests potentially limited cross-protection from human vaccines for exposed workers, underscoring the need for targeted vaccination strategies for high-risk occupational groups. Our investigation was restricted to 1 outbreak and a limited number of samples; we used no serologic data and only partial comparative sequences from Switzerland, which limited our assessment of evolutionary viral dynamics. Despite those constraints, the clinical, epidemiologic, and genomic evidence supports zoonotic transmission.

Concurrent detection of swIAV in pigs and humans is rare globally. The detection of EA swH1N1 in pigs and a farmer in our study demonstrates zoonotic spillover and highlights the value of One Health surveillance. The viruses were genetically homogenous, yet antigenically distinct from contemporary human vaccine strains, emphasizing the need for active WGS surveillance and genomic characterization at the swine–human interface, as well as continued monitoring and targeted preventive strategies for pig-exposed workers.

Acknowledgments

We thank the Swiss Pig Health Service (Schweinegesundheitsdienst) within SUISAG and the collaborating veterinary practices for referring the case to us, as well as members of the Experimental Virology group and NGS sequencing unit at the Institute for Infectious Diseases, the Swine Clinic of the University of Bern, and the Institute of Virology and Immunology for their support. We thank Ana Rita Goncalves Cabecinhas for kindly sharing the results of samples processed at the Swiss National Reference Centre for Influenza.

This study was supported by the Multidisciplinary Center for Infectious Diseases, University of Bern, and the Swiss National Science Foundation (grant no. IZCOZ0_220329).

We used ChatGPT version 5.2 to assist with structuring the manuscript and adjusting the formatting of the text and the references.

About the Author

Dr. Steiner is a veterinarian and PhD student at the Clinic for Swine, Department of Clinical Veterinary Medicine, Vetsuisse Faculty, University of Bern, and the Multidisciplinary Center for Infectious Diseases, University of Bern. His work focuses on the epidemiology of influenza A viruses in pig herds and their caretakers.

References

1. Andersen KM, Vestergaard LS, Nissen JN, George SJ, Ryt-Hansen P, Hjulsager CK, et al. Severe human case of zoonotic infection with swine-origin influenza A virus, Denmark, 2021. Emerg Infect Dis. 2022;28:2561–4. https://doi.org/10.3201/eid2812.220935
2. Dürrwald R, Wedde M, Biere B, Oh DY, Heßler-Klee M, Geidel C, et al. Zoonotic infection with swine A/H1$_{av}$N1 influenza virus in a child, Germany, June 2020. Euro Surveill. 2020;25:2001638. https://doi.org/10.2807/1560-7917.ES.2020.25.42.2001638
3. Parys A, Vandoorn E, King J, Graaf A, Pohlmann A, Beer M, et al. Human infection with Eurasian avian-like swine influenza A(H1N1) virus, the Netherlands, September 2019. Emerg Infect Dis. 2021;27:939–43. https://doi.org/10.3201/eid2703.201863
4. Jhung MA, Epperson S, Biggerstaff M, Allen D, Balish A, Barnes N, et al. Outbreak of variant influenza A(H3N2) virus in the United States. Clin Infect Dis. 2013;57:1703–12. https://doi.org/10.1093/cid/cit649
5. Vincent Baker AL, Van Reeth K. Influenza viruses. In: Burrough ER, Karriker LA, Schwartz KJ, Zhang J, editors. Diseases of swine. 12th ed. Hoboken (NJ): John Wiley & Sons; 2026. p. 645–64.
6. Gray GC, McCarthy T, Capuano AW, Setterquist SF, Olsen CW, Alavanja MC, et al. Swine workers and swine influenza virus infections. Emerg Infect Dis. 2007;13:1871–8. https://doi.org/10.3201/eid1312.061323
7. Federal Office for Customs and Border Security. Swiss-Impex—public import/export database. 2025 [cited 2025 Jan 27]. https://www.gate.ezv.admin.ch/swissimpex/index.xhtml
8. Federal Food Safety and Veterinary Office. Pig husbandry [cited 2025 Jan 31]. https://www.blv.admin.ch/blv/de/home/tiere/tierschutz/nutztierhaltung/schweine.html
9. Li C, Culhane MR, Schroeder DC, Cheeran MCJ, Galina Pantoja L, Jansen ML, et al. Quantifying the impact of vaccination on transmission and diversity of influenza A variants in pigs. J Virol. 2024;98:e0124524. https://doi.org/10.1128/jvi.01245-24
10. Lechmann J, Szelecsenyi A, Bruhn S, Harisberger M, Wyler M, Bachofen C, et al. The Swiss national program for the surveillance of influenza A viruses in pigs and humans: genetic variability and zoonotic transmissions

from 2010–2022. Schweiz Arch Tierheilkd. 2025;167:600–16. https://doi.org/10.17236/sat00466
11. Nagy A, Černíková L, Kunteová K, Dirbáková Z, Thomas SS, Slomka MJ, et al. A universal RT-qPCR assay for "One Health" detection of influenza A viruses. PLoS One. 2021;16:e0244669. https://doi.org/10.1371/journal.pone.0244669
12. Licheri M, Mwanga M, Licheri MF, Graaf-Rau A, Sägesser C, Bittel P, et al. Optimized high-throughput whole-genome sequencing workflow for surveillance of influenza A virus. Genome Med. 2025;17:103. https://doi.org/10.1186/s13073-025-01512-x
13. Yoshida R, Igarashi M, Ozaki H, Kishida N, Tomabechi D, Kida H, et al. Cross-protective potential of a novel monoclonal antibody directed against antigenic site B of the hemagglutinin of influenza A viruses. PLoS Pathog. 2009;5:e1000350. https://doi.org/10.1371/journal.ppat.1000350
14. Forberg H, Hauge AG, Gjerset B, Hungnes O, Kilander A. Swine influenza in Norway: a distinct lineage of influenza A(H1N1)pdm09 virus. Influenza Other Respir Viruses. 2013;7(Suppl 4):21–6. https://doi.org/10.1111/irv.12194
15. Richard G, Ryt-Hansen P, Byrne A, European Swine Influenza Network. European Swine Influenza Network report #2 on swine influenza A viruses evolution and diversity of in Europe from October 2022–September 2024. 2025 [cited 2026 May 7]. https://doi.org/10.5281/zenodo.15673794

Address for correspondence: Jenna N. Kelly, Institute of Virology and Immunology (IVI), Länggassstrasse 122, CH-3012 Bern, Switzerland; email: jenna.kelly@unibe.ch

Therapeutic Challenges in Case of *Trichophyton indotineae* Dermatophytosis, Singapore, 2025

Tiara Joy Foo, Matthew Chung Yi Koh, Ka Lip Chew, Lester Juay, Sean Jiawei Wu

Trichophyton indotineae is an emerging dermatophyte frequently associated with terbinafine resistance. We report a case of recalcitrant *T. indotineae* infection in Singapore with limited response despite prolonged azole therapy, which only resolved after combination therapy with anidulafungin and itraconazole. This case highlights therapeutic challenges and need for improved diagnostics in *T. indotineae* infections.

Dermatophytosis is a globally prevalent superficial fungal infection predominantly caused by *Trichophyton* species. *T. indotineae* has emerged globally and is frequently associated with terbinafine resistance, although susceptibility is not universal (*1*). Treatment options are limited and often require prolonged systemic therapy. We describe a case of recalcitrant dermatophytosis in Singapore and its management challenges; clinical resolution occurred only after combined treatment with anidulafungin and itraconazole. Informed consent was obtained from the patient for publication.

The Study

A 68-year-old man with hypertension sought care at National University Hospital, Singapore, for a 3-year history of recurrent pruritic groin plaques. Tinea cruris had been diagnosed initially by his general practitioner, and he received multiple courses of topical (clotrimazole and miconazole) and oral (griseofulvin, terbinafine, and itraconazole capsules) antifungal drugs; improvement was transient despite adherence. He reported intermittent use of over-the-counter topical corticosteroid-containing creams. Over the course of 3 years, lesions extended to the abdomen and gluteal region.

Initial examination showed extensive, sharply marginated, annular plaques with raised, scaly borders and central clearing over the lower abdomen, inguinal folds, gluteal region, and inner thigh (Figure, panel A); we noted no nail or scalp involvement. He was afebrile with no lymphadenopathy or systemic findings. His hemoglobin A1c, renal, and liver function test results were unremarkable. A fourth-generation HIV assay was negative. He was not on immunosuppressive therapy.

Skin scrapings were obtained for fungal culture. Matrix-assisted laser desorption/ionization time-of-flight mass spectrometry using the VITEK MS System Knowledge Base version 3.2 (bioMérieux, https://www.biomerieux.com) identified the isolate as *T. interdigitale*, likely because of the absence of *T. indotineae* in the reference database. Sanger sequencing of the internal transcribed spacer 1 region identified *T. indotineae*, which was thereafter established by whole-genome sequencing as well. At the time of management, clinical susceptibility testing was unavailable.

The patient was started on itraconazole oral capsules at 200 mg/day. Itraconazole levels checked 1 week into treatment were below the assay's limit of detection (<0.50 mg/L) despite adherence. Although target serum concentrations for dermatophytes are not well established, this finding raised concerns about inadequate bioavailability. The itraconazole dose was increased to 200 mg 2×/day. However, despite 6 weeks of therapy, the rash progressed. Adjunctive topical clotrimazole was applied to localized areas 2×/day, and strict hygiene measures were advised. We did not recheck itraconazole levels because further dose escalation was deemed unfeasible. After 6 months, itraconazole was stopped because of limited response.

Voriconazole was started after shared decision-making but discontinued after 3 days because of neuropsychiatric side effects. Combination therapy of intravenous anidulafungin (100 mg/d) and oral itraconazole (capsules 200 mg 2×/d) was selected empirically because of prolonged disease, partial

Author affiliation: National University Hospital, Singapore

DOI: https://doi.org/10.3201/eid3206.251606

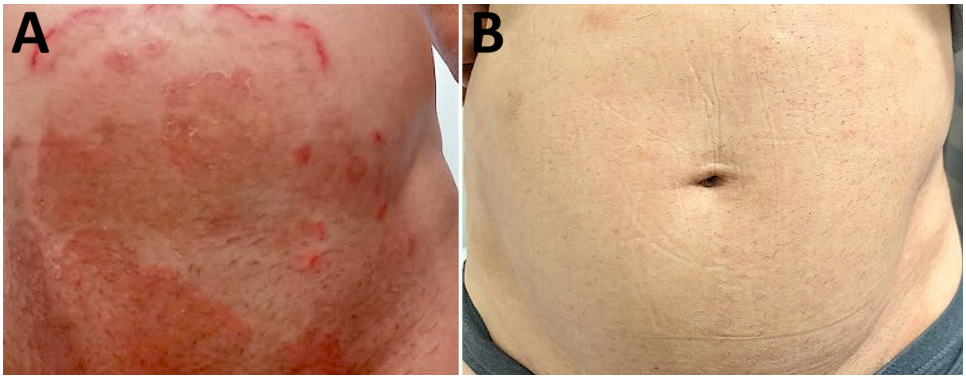

Figure. Skin lesions in case of *Trichophyton indotineae* dermatophytosis, Singapore, 2025. A) Before treatment; B) after 6 weeks of anidulafungin and itraconazole.

response to azoles, and limited therapeutic options, not on the basis of in vitro synergy data. Off-label echinocandin use was undertaken after informed consent. This regimen finally resulted in marked flattening of plaques within 2 weeks. Treatment continued for 6 weeks through outpatient parenteral antimicrobial therapy; mild postinflammatory hyperpigmentation was noted at completion (Figure, panel B). The patient experienced no adverse effects, and liver function test results remained unremarkable. Follow-up fungal culture demonstrated no dermatophyte growth. The patient was in sustained remission at 6 months after therapy.

T. indotineae is an emerging cause of refractory dermatophytosis and causes considerable illness (*1*). The fungus is transmitted through direct contact or fomites, and manifests as pruritic, scaly, annular plaques. Terbinafine resistance is commonly linked to squalene epoxidase gene mutations (*1*,*2*), leading to elevated terbinafine MICs and clinical failure. Because clinical breakpoints are not established, MICs are often interpreted using European Committee on Antimicrobial Susceptibility Testing dermatophyte methodology and wild-type upper limits or epidemiological cutoff value–based approaches (*3*). A study from France proposed terbinafine MIC ≥0.2 mg/L as a threshold associated with resistance (*4*). In a series from the United Kingdom, 75% of isolates exhibited elevated terbinafine MICs (≥0.5 mg/L) (*5*). However, clinical failure has been reported even with low terbinafine MICs (0.015 mg/L), indicating imperfect MIC-outcome correlation (*6*).

Itraconazole remains a therapeutic mainstay but might require prolonged high-dose courses, which increases risk for side effects (*7*). Fluconazole and griseofulvin show poorer activity, having higher MICs against *T. indotineae* (*8*–*10*).

A study from Singapore (*11*), this patient's country of residence, examined whole-genome sequencing of 33 isolates and found nearly 80% of *T. indotineae* isolates were terbinafine-resistant. Azole MICs were generally below European Committee on Antimicrobial Susceptibility Testing wild-type upper limits. No phenotypic azole resistance was observed, and no azole resistance–associated *cyp51A/cyp51B* alterations or gene amplification were detected. Well-known azole resistance mechanisms, including erg11 gene amplification, have been described elsewhere (*12*). This patient's isolate had a MIC of 0.03 mg/L for itraconazole and 0.5 mg/L for voriconazole, determined later in a research setting using Sensititer YeastOne YO10 plates (Thermo Fisher Scientific, https://www.thermofisher.com) and not available at the time of management. Despite low MICs, clinical failure occurred. MIC for terbinafine was 8 mg/L and determined using Clinical Laboratory Standards Institute M38 methodology (*13*). Echinocandin susceptibility testing was not performed.

Comparable antifungal susceptibility data have been observed across Canada (*14*) and Asia (*15*); terbinafine resistance has been demonstrated to be widespread and MICs for azoles are elevated. The isolates in Canada retained low minimum effective concentrations (MEC) to anidulafungin (MEC_{90} ≤0.015 mg/L) and micafungin (MEC_{90} ≤0.015 mg/L) (*10*). In Asia, elevated MICs for azoles were again reported (itraconazole MIC 0.5 mg/L, voriconazole MIC 1 mg/L) (*14*). Echinocandins consistently demonstrated low MECs (MEC_{90} ≤0.004 mg/L for caspofungin, micafungin, anidulafungin). Although MICs and MECs are not directly comparable, those data suggest echinocandins consistently demonstrate strong in vitro activity against *T. indotineae*. However, clinical efficacy of echinocandins remains uncertain; data are limited to in vitro studies (*9*).

Beyond susceptibility data, the previous Singapore study (*11*) also provided epidemiologic insights. Most affected patients were migrant workers, and phylogenetic analysis suggested multiple independent introductions rather than clonal spread. Our patient reported no international travel, raising

concern for local acquisition and possible reduced susceptibility that might be emerging beyond that shown in current laboratory data. Enhanced surveillance and access to species-level diagnostics are needed to define transmission patterns and guide public health measures.

In addition, recalcitrant cases should prompt consideration of alternative systemic therapies. Echinocandins have not been routinely used for superficial dermatophytosis and might have limited penetration into keratinized skin (*15*). Prolonged intravenous echinocandin therapy is costly and logistically challenging and carries risk for line-related complications and hepatic enzyme elevation. However, unlike terbinafine and azoles, which target ergosterol synthesis, echinocandins inhibit 1,3-β-D-glucan synthesis, avoiding cross-resistance.

Conclusions

Given the strong rationale supported by those pharmacological differences and in vitro data, as well as the limited alternative options, combination therapy including an echinocandin was attempted for this patient after multiple standard regimens had failed. Evidence supporting echinocandins for dermatophytosis remains sparse, and this approach should not be interpreted as a standard recommendation. Rather, clinicians should suspect *T. indotineae* when tinea infections fail to respond to first-line therapy and pursue culture with species-level identification where available. Still, this case highlights the potential role of echinocandins for recalcitrant tinea, given the global surge in terbinafine-resistant dermatophytosis and the paucity of effective oral treatment options (*1*,*2*,*7*,*15*).

In summary, although itraconazole remains a first-line treatment for *T. indotineae*, prolonged courses are typically required. Echinocandins might have a role in selected treatment-refractory cases. Further studies are needed to define dosing strategies, tissue penetration, and long-term outcomes to establish the role of echinocandins as antifungal resistance continues to rise. This case highlights therapeutic challenges in Singapore and underscores antifungal stewardship: confirming species-level identification when available, optimizing adherence and conventional therapy, and reserving intravenous agents for truly refractory cases.

Sequence read data for the isolate from this study are deposited in the National Center for Biotechnology Information Sequence Read Archive (https://www.ncbi.nlm.nih.gov/sra) under BioProject PRJNA1028951 and BioSample SAMN46240067.

T.J.F. and M.C.Y.K. contributed to the conception and original draft of the manuscript. C.K.L., L.J., and S.J.W.W. contributed to the conception and critical review of the manuscript.

About the Author

Dr. Foo is an infectious diseases fellow at the National University Hospital in Singapore. Her primary research interests are fungal infections and antimicrobial resistance. Dr. Wu is an infectious diseases specialist at the National University Hospital in Singapore. His primary research interests are infection prevention and control and emerging infectious diseases.

References

1. Lockhart SR, Chowdhary A, Gold JAW. The rapid emergence of antifungal-resistant human-pathogenic fungi. Nat Rev Microbiol. 2023;21:818–32. https://doi.org/10.1038/s41579-023-00960-9
2. Jabet A, Normand A-C, Brun S, Dannaoui E, Bachmeyer C, Piarroux R, et al. *Trichophyton indotineae*, from epidemiology to therapeutic. J Mycol Med. 2023;33:101383. https://doi.org/10.1016/j.mycmed.2023.101383
3. Arendrup MC, Jørgensen KM, Guinea J, Lagrou K, Chryssanthou E, Hayette MP, et al. Multicentre validation of a EUCAST method for the antifungal susceptibility testing of microconidia-forming dermatophytes. J Antimicrob Chemother. 2020;75:1807–19. https://doi.org/10.1093/jac/dkaa111
4. Moreno-Sabater A, Normand AC, Bidaud AL, Cremer G, Foulet F, Brun S, et al. Terbinafine resistance in dermatophytes: a French multicenter prospective study. J Fungi (Basel). 2022;8:220. https://doi.org/10.3390/jof8030220
5. Abdolrasouli A, Barton RC, Borman AM. Spread of antifungal-resistant *Trichophyton indotineae*, United Kingdom, 2017–2024. Emerg Infect Dis. 2025;31:192–4. https://doi.org/10.3201/eid3101.240923
6. Blanchard G, Amarov B, Fratti M, Salamin K, Bontems O, Chang YT, et al. Reliable and rapid identification of terbinafine resistance in dermatophytic nail and skin infections. J Eur Acad Dermatol Venereol. 2023;37:2080–9. https://doi.org/10.1111/jdv.19253
7. Khurana A, Sharath S, Sardana K, Chowdhary A. Clinico-mycological and therapeutic updates on cutaneous dermatophytic infections in the era of *Trichophyton indotineae*. J Am Acad Dermatol. 2024;91:315–23. https://doi.org/10.1016/j.jaad.2024.03.024
8. Burmester A, Hipler U-C, Uhrlaß S, Nenoff P, Singal A, Verma SB, et al. Indian *Trichophyton mentagrophytes* squalene epoxidase *erg1* double mutants show high proportion of combined fluconazole and terbinafine resistance. Mycoses. 2020;63:1175–80. https://doi.org/10.1111/myc.13150
9. Su H, Jiang W, Verweij PE, Li L, Zhu J, Han J, et al. The *in vitro* activity of echinocandins against clinical *Trichophyton rubrum* isolates and review of the susceptibility of *T. rubrum* to echinocandins worldwide. Infect Drug Resist. 2023;16:5395–403. https://doi.org/10.2147/IDR.S423735
10. Sonego B, Corio A, Mazzoletti V, Zerbato V, Benini A, di Meo N, et al. *Trichophyton indotineae*, an emerging drug-resistant dermatophyte: a review of the treatment

options. J Clin Med. 2024;13:3558. https://doi.org/10.3390/jcm13123558
11. Teo JWP, Cheng JWS, Wee JS, Chan D, Chew KL. Genomic insights into the dermatophyte *Trichophyton indotineae* in Singapore: resistance and transmission dynamics. Med Mycol. 2025;63:myaf062. https://doi.org/10.1093/mmy/myaf062
12. Gupta AK, Venkataraman M, Hall DC, Cooper EA, Summerbell RC. The emergence of *Trichophyton indotineae*: implications for clinical practice. Int J Dermatol. 2023;62:857–61. https://doi.org/10.1111/ijd.16362
13. Clinical and Laboratory Standards Institute. Reference method for broth dilution antifungal susceptibility testing of filamentous fungi. CLSI standard M38. 3rd ed. Wayne (PA): The Institute; 2017.
14. McTaggart LR, Cronin K, Ruscica S, Patel SN, Kus JV. Emergence of terbinafine-resistant *Trichophyton indotineae* in Ontario, Canada, 2014–2023. J Clin Microbiol. 2025;63:e0153524. https://doi.org/10.1128/jcm.01535-24
15. Xie W, Kong X, Zheng H, Mei H, Ge N, Liu W, et al. *In vitro* susceptibility profiles of 16 antifungal drugs against *Trichophyton indotineae*. Microbiol Spectr. 2025;13:e0061825. https://doi.org/10.1128/spectrum.00618-25

Address for correspondence: Sean Jiawei Wu, Department of Infectious Diseases, National University Hospital, 5 Lower Kent Ridge Rd, 119074, Singapore; email: sean_jw_wu@nuhs.edu.sg

Emergence of Ceftriaxone-Resistant *Neisseria gonorrhoeae penA*-60–Carrying Strains, Thailand, 2025

Rossaphorn Kittiyaowamarn, Pongsathorn Sangprasert,[1] Natnaree Girdthep,[1] Sirintra Pharanut,[1] Tawan Nongpian,[1] Thanakorn Arunngamwong,[1] Ruechakorn Kunkhajornphan,[1] Ismael Maatouk,[1] Magnus Unemo[1]

We report 5 gonorrhea cases caused by ceftriaxone-resistant *penA*–60-carrying *Neisseria gonorrhoeae* bacteria during January–April 2025 in Thailand, successfully cured by ceftriaxone therapy. Most patients had prior over-the-counter antimicrobial drug exposure. Ceftriaxone-resistant gonococcal strains are spreading in Thailand, and strengthened gonorrhea and resistance surveillance and effective antimicrobial stewardship programs are needed.

Antimicrobial-resistant *Neisseria gonorrhoeae* is a major global public health concern and has been designated as an urgent threat by the US Centers for Disease Control and Prevention (*1*). Ceftriaxone is the only remaining option for effective therapy of gonorrhea in most countries (*2*,*3*). In 2018, a gonococcal strain with resistance to ceftriaxone and high-level resistance to azithromycin was reported in England, and this extensively drug-resistant strain infected a patient in Thailand (*4*). Occasional ceftriaxone-resistant gonococcal strains with links to Thailand subsequently have been detected in several countries in Europe (*3*,*5*). However, the National Gonococcal Antimicrobial Resistance program in Thailand, implemented in 2003, did not identify any ceftriaxone-resistant strains until 2023, when 2 ceftriaxone-resistant isolates caused by the mosaic *penA*-60 allele were confirmed (*6*). In response, a previously described *penA*-60–specific PCR (*7*) was implemented for further investigation of ceftriaxone-resistant isolates. No ceftriaxone-resistant gonococcal isolates were found in 2024 in Thailand; however, during January–April 2025, national surveillance identified 5 ceftriaxone-resistant gonococcal isolates.

The National Gonococcal Antimicrobial Resistance program has been included in Thailand's national surveillance since 2003, whereas the World Health Organization Enhanced Gonococcal Antimicrobial Surveillance Program (EGASP) was established in sentinel clinics in 2015 (*8*,*9*). Gonococcal isolates and patient data from the national surveillance system are collected from the Bangrak Sexually Transmitted Infections (STIs) Center in Bangkok and from 6 regional Offices of Disease Prevention and Control that cover the main regions of Thailand (Figure 1). Gonococcal isolates are obtained from symptomatic and asymptomatic male and female patients attending STI clinics across Thailand. The 5 EGASP sites (2 in Bangkok, 1 in Chiang Mai, and 2 in Pattaya) strengthen surveillance among men with urethritis and men who have sex with men (*8*,*9*). The local laboratories send all isolates with resistance to ceftriaxone, cefixime, or azithromycin to the Bangrak STIs Center for further confirmation of *N. gonorrhoeae* bacteria and antimicrobial MIC testing. We determined MICs of ceftriaxone, cefixime, azithromycin, gentamicin, and tetracycline by using Etest (bioMérieux, https://www.biomerieux.com) according to the manufacturer's instructions. We further examined ceftriaxone-resistant isolates through a *penA*-60–specific real-time reverse transcription PCR

Author affiliations: Bangrak STIs Center, Department of Disease Control, Ministry of Public Health, Bangkok, Thailand (R. Kittiyaowamarn, P. Sangprasert, N. Girdthep, S. Pharanut, T. Nongpian); Bhattamakun Hospital, Chonburi, Thailand (T. Arunngamwong); Patong Hospital, Phuket, Thailand (R. Kunkhajornphan); World Health Organization, Geneva, Switzerland (I. Maatouk); Örebro University, Örebro, Sweden (M. Unemo); University College London Institute for Global Health, London, UK (M. Unemo)

DOI: https://doi.org/10.3201/eid3206.251860

[1]These authors contributed equally to this article.

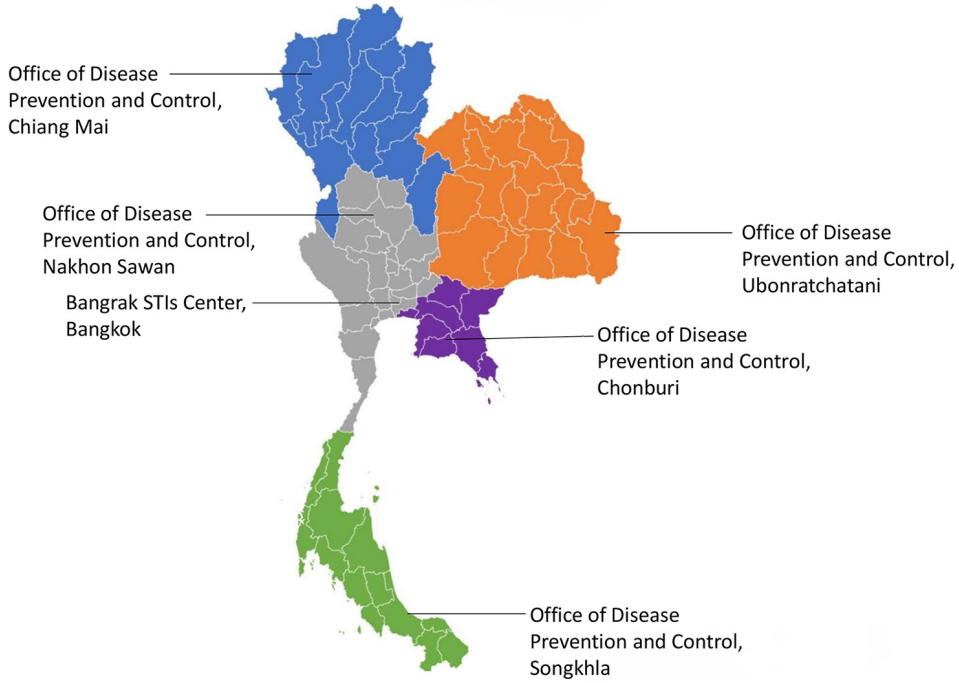

Figure 1. Locations of Bangrak STIs Center (Bangkok) and 6 regional Offices of Disease Prevention and Control that collect gonococcal isolates in national surveillance system (National Gonococcal Antimicrobial Resistance program and World Health Organization Enhanced Gonococcal Antimicrobial Surveillance Program), Thailand. STIs, sexually transmitted diseases.

(7) by using a CFX96 Real-Time PCR system (Bio-Rad Laboratories, https://www.bio-rad.com).

The Study

During January–April 2025, we identified 5 ceftriaxone-resistant gonococcal isolates among 272 isolates collected through the National Gonococcal Antimicrobial Resistance program in Thailand. The 5 isolates had been obtained from 5 male patients, 16–55 years of age, who sought care for dysuria at STI clinics in Thailand's eastern region (4 patients in Pattaya, Chonburi Province) and southern region (1 patient in Phuket Province) of Thailand. Our case investigations were conducted by authorized public health officers according to the Communicable Disease Act in Thailand. Case identification information was confidential.

The patients were from Thailand (n = 3), Russia (n = 1), and China (n = 1) (Table 1). All 5 patients were men who have sex with women, and 4 of them

Table 1. Characteristics of case-patients with gonorrhea caused by ceftriaxone-resistant *Neisseria gonorrhoeae* isolates, Thailand, January–April 2025*

Case no.	Date	Nationality/ notified province (city)	Age, y	Occupation	Previous antimicrobial drug exposure	Symptoms	Travel history in past month	Prior sexually transmitted infection	No. partners in past 3 months
1	2025 Jan	Thai/ Chonburi (Pattaya)	35	Waiter	Yes (azithromycin 1 g twice)	Urethral discharge, dysuria	No	No	1 regular partner, 2 casual partners (FSWs)
2	2025 Feb	Thai/ Chonburi (Pattaya)	16	Waiter	Yes (azithromycin 1 g twice)	Urethral discharge, dysuria	No	No	1 regular partner living in different location, 1 one-night-stand partner
3	2025 Mar	Russian/ Phuket	55	–	–	Urethral discharge, dysuria	–	–	–
4	2025 Mar	Thai/ Chonburi (Pattaya)	23	Government official	Yes (quinolone and then azithromycin 1 g)	Urethral discharge, dysuria	No	Gonorrhea 10 y ago	1 casual partner (FSW)
5	2025 Apr	Chinese/ Chonburi (Pattaya)	25	–	Yes (unknown antibiotic)	Urethral discharge, dysuria	–	–	1 casual partner

*FSW, female sex worker; –, no data available.

reported recent sexual contact with a casual partner, including a 1-night-stand partner and a female sex worker. Four patients reported self-treatment with oral antimicrobial drugs (mostly azithromycin 1 g) obtained from pharmacies in Pattaya Province before any visit to an STI clinic; however, because of persisting symptoms, they all subsequently visited an STI clinic. Gram-stained microscopic examination of urethral discharge from all 5 patients revealed gram-negative intracellular diplococci, and culture on modified Thayer-Martin medium confirmed the presence of gonococci. On the basis of European Committee on Antimicrobial Susceptibility Testing resistance breakpoints (*10*), we determined that all 5 gonococcal isolates were resistant to ceftriaxone (MIC >0.125 μg/mL) and cefixime (MIC >0.125 μg/mL), and 3 isolates showed high-level resistance to azithromycin (Table 1). Three of the 5 isolates also were nonsusceptible to ceftriaxone based on the Clinical Laboratory and Standards Institute clinical breakpoint (MIC ≥0.5 μg/mL) (*11*) (Table 2; Figure 2). All 5 isolates contained the *penA*-60 allele, which is associated with ceftriaxone resistance in *N. gonorrhoeae* bacteria (*2*–*7*,*12*,*13*).

On the same day results of the gram-stained microscopic examination of urethral discharge were available, all 5 patients were treated with intramuscular ceftriaxone (1 g) (n = 1) or intramuscular ceftriaxone (1 g) plus oral azithromycin (1 g) or a 7-day regimen of oral doxycycline (n = 4) in accordance with current gonorrhea management guidelines in Thailand (*14*). All 3 Thailand patients returned for test-of-cure 1–2 weeks after treatment; results of culture and the Xpert CT/NG assay (Cepheid, https://www.cepheid.com) from urethral and oropharyngeal sites were negative, and all 5 patients were asymptomatic. The 2 patients of foreign nationality did not return for test-of-cure. Only the first Thailand case-patient, who had a regular female partner, could bring his sexual partner to the STI clinic for examination and treatment. An Xpert CT/NG assay of pooled cervical and oropharyngeal specimens detected *N. gonorrhoeae* bacteria, whereas cervical and oropharyngeal cultures were negative. The woman was treated with intramuscular ceftriaxone (1 g) but did not return for test-of-cure.

Conclusions

Increasing clinicians' awareness of ceftriaxone-resistance is essential. Ceftriaxone is the last remaining gonorrhea treatment option and has acquired high levels of resistance in several countries in Asia, especially Cambodia, China, and Vietnam

Table 2. Diagnostic testing, treatment, and antimicrobial susceptibility of ceftriaxone-resistant *Neisseria gonorrhoeae* isolates, Thailand, January–April 2025*

Case no.	Syphilis rapid test	HIV testing	NAAT testing†	Treatment	MIC, μg/mL (R/S)‡	TOC, culture and NAAT†	Sexual partner testing
1	Negative	Negative	Pooled specimen from urine and OP site: positive	IM ceftriaxone 1 g + oral azithromycin 1 g	CRO 0.25 (R); CFM 1 (R); AZM 256 (R)	OP and urethral specimens: negative	Regular female partner (NG detected in pooled cervical and oropharyngeal specimens by Xpert CT/NG assay, but cervical and oropharyngeal cultures negative)
2	Negative	Negative	Not tested	IM ceftriaxone 1 g + oral doxycycline (200 mg/day for 7 d)	CRO 0.5 (R); CFM 2 (R); AZM 256 (R)	OP and urethral specimens: negative	One-night-stand partner (contact tracing not possible)
3	Not tested	Not tested	Pooled specimen from urine and OP site: positive	IM ceftriaxone 1 g	CRO 0.25 (R); CFM 2 (R); AZM 256 (R)	Not conducted	No partner reported
4	Negative	Negative	Not tested	IM ceftriaxone 1 g + oral doxycycline (200 mg/d for 7 d)	CRO 0.5 (R); CFM 1 (R); AZM 1 (S)	OP and urethral specimens: negative	FSW (contact tracing not possible)
5	Not tested	Not tested	Not tested	IM ceftriaxone 1 g + oral doxycycline (200 mg/d for 7 d)	CRO 0.5 (R); CFM 2 (R); AZM 0.125 (S)	Not conducted	Casual female partner (contact tracing not possible)

*AZM, azithromycin; CFM, cefixime; CRO, ceftriaxone; IM, intramuscular; NAAT, nucleic acid amplification test; NG, *Neisseria gonorrhoeae*; OP, oropharyngeal; R, resistant; S, susceptible; TOC, test-of-cure.
†NAAT testing using Xpert CT/NG assay (Cepheid, https://www.cepheid.com).
‡Based on European Committee on Antimicrobial Susceptibility testing breakpoints (*10*).

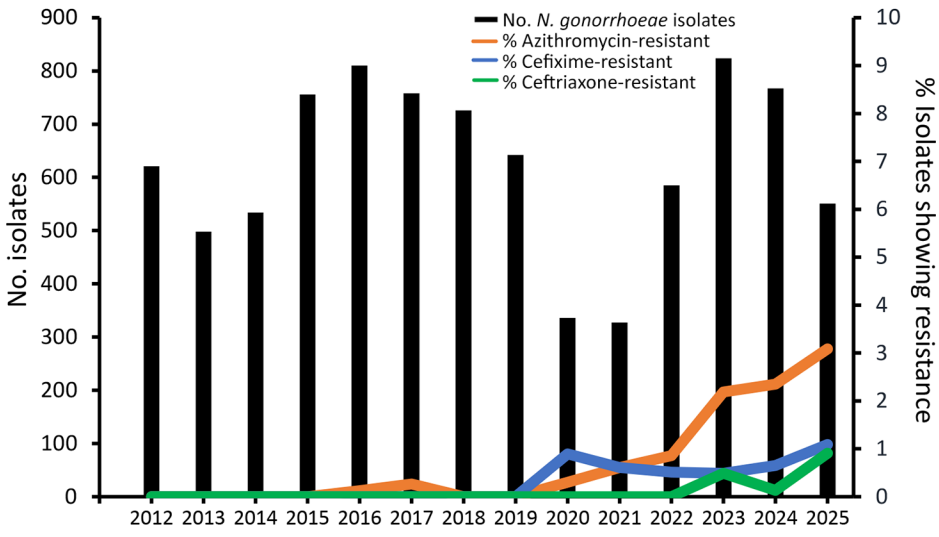

Figure 2. Number of *Neisseria gonorrhoeae* bacteria isolates examined and percentages of isolates with resistance to azithromycin, cefixime, and ceftriaxone in national surveillance system (National Gonococcal Antimicrobial Resistance program and World Health Organization Enhanced Gonococcal Antimicrobial Surveillance Program), by year, Thailand, January 2012–August 15, 2025. Isolates were identified by using Etest (bioMérieux, https://www.biomerieux.com).

(*2*,*3*,*9*,*12*,*13*). Data from the National Gonococcal Antimicrobial Resistance program and EGASP in Thailand for 2015–2023 have shown that antimicrobial-resistant *N. gonorrhoeae* also is an emerging major concern in Thailand, particularly resistance to oral antimicrobial drugs such as ciprofloxacin (which exhibits >90% resistance), azithromycin, and (since 2020) cefixime, all of which are commonly available without a prescription at pharmacies in Thailand. However, before 2025, only 2 ceftriaxone-resistant gonococcal isolates had been confirmed in national surveillance of gonococcal antimicrobial resistance (*6*,*8*,*9*).

We report 5 ceftriaxone-resistant isolates detected during January–April 2025 in Thailand. Most of the patients with ceftriaxone-resistant gonorrhea were initially self-treating with antimicrobial drugs instead of seeking care at STI clinics, and their sexual encounters involved 1-night stand partners and female sex workers, behaviors that are associated with further rapid transmission of the ceftriaxone-resistant gonococcal strains and substantial health risks and can complicate sexual contact tracing efforts. In Thailand, STIs have also become 1 of the top 5 conditions for which persons seek treatment at pharmacies (*15*), and the resulting widespread use of oral antimicrobial drugs probably has contributed to the increase in gonococcal antimicrobial resistance. Of note, we detected 3 additional ceftriaxone-resistant isolates during October–December 2025, which are undergoing further investigation.

One limitation of our study is the lack of whole-genome sequencing of all the ceftriaxone-resistant isolates. However, we plan to conduct whole-genome sequencing in 2026.

The emergence of ceftriaxone-resistant gonorrhea cases in Thailand poses a serious public health challenge, and treatment of all gonorrhea cases with ceftriaxone, consistent with the updated gonorrhea management guidelines in Thailand, is critical (*14*). The increasing practice of self-treatment by purchase of antimicrobial drugs without a prescription at pharmacies (*15*), often resulting in inappropriate and failing treatment and further driving antimicrobial resistance, is a major concern.

The spread of ceftriaxone-resistant gonococcal strains in Thailand and other countries in Asia (*2*,*3*,*9*,*12*,*13*) underscores the urgent need to promote safer sex practices and ensure access to professional medical care (diagnostics, treatment, and follow-up of patients and sexual contacts). In a promising development, novel drugs such as zoliflodacin and gepotidacin have been approved by the US Food and Drug Administration (*2*,*3*). However, encouraging responsible antimicrobial use and stewardship remains critical to protect health. Among the cases we describe, the 2 foreign male patients with ceftriaxone-resistant gonorrhea, who were subsequently lost to follow-up, underscore major gaps in continuity of care and highlight the urgent need to strengthen global gonococcal antimicrobial resistance surveillance and enhance coordinated international efforts to address gonococcal antimicrobial resistance.

Acknowledgments

We are very grateful to all the patients, nurses, doctors and laboratory staff involved in the National Gonococcal Antimicrobial Resistance program and the World Health Organization Enhanced Gonococcal Antimicrobial Surveillance Program in Thailand.

About the Author

Dr. Rossaphorn chief of the Bangrak Sexually Transmitted Infections Center, Department of Disease Control, Ministry of Public Health, Thailand. Her primary research interests include sexually transmitted infections.

References

1. US Centers for Disease Control and Prevention. Antibiotic resistance threats in the United States, 2013. 2013 [cited 2025 Nov 2]. https://stacks.cdc.gov/view/cdc/20705
2. Unemo M, Lahra MM, Cole MJ, Marcano Zamora D, Jacobsson S, Galarza P, et al. WHO global gonococcal antimicrobial surveillance programmes, 2019–22: a retrospective observational study. Lancet Microbe. 2025; 6:101181. https://doi.org/10.1016/j.lanmic.2025.101181
3. Jensen JS, Unemo M. Antimicrobial treatment and resistance in sexually transmitted bacterial infections. Nat Rev Microbiol. 2024;22:435–50. https://doi.org/10.1038/s41579-024-01023-3
4. Eyre DW, Sanderson ND, Lord E, Regisford-Reimmer N, Chau K, Barker L, et al. Gonorrhoea treatment failure caused by a *Neisseria gonorrhoeae* strain with combined ceftriaxone and high-level azithromycin resistance, England, February 2018. Euro Surveill. 2018;23:1800323. https://doi.org/10.2807/1560-7917.ES.2018.23.27.1800323
5. Fifer H, Doumith M, Rubinstein L, Mitchell L, Wallis M, Singh S, et al. Ceftriaxone-resistant *Neisseria gonorrhoeae* detected in England, 2015–24: an observational analysis. J Antimicrob Chemother. 2024;79:3332–9. https://doi.org/10.1093/jac/dkae369
6. Sangprasert P, Golparian D, Paopang P, Girdthep N, Lawung R, Gopinath D, et al. Complete reference genomes of two ceftriaxone-resistant *Neisseria gonorrhoeae* strains identified in routine surveillance in Bangkok, Thailand, using Nanopore Q20+ chemistry, VolTRAX V2b, and Illumina sequencing. Microbiol Resour Announc. 2024;13:e0123123. https://doi.org/10.1128/mra.01231-23
7. Whiley DM, Mhango L, Jennison AV, Nimmo G, Lahra MM. Direct detection of *penA* gene associated with ceftriaxone-resistant *Neisseria gonorrhoeae* FC428 strain by using PCR. Emerg Infect Dis. 2018;24:1573–5. https://doi.org/10.3201/eid2408.180295
8. Kittiyaowamarn R, Girdthep N, Cherdtrakulkiat T, Sangprasert P, Tongtoyai J, Weston E, et al. *Neisseria gonorrhoeae* antimicrobial susceptibility trends in Bangkok, Thailand, 2015–21: Enhanced Gonococcal Antimicrobial Surveillance Programme (EGASP). JAC Antimicrob Resist. 2023;5:dlad139. https://doi.org/10.1093/jacamr/dlad139
9. Maatouk I, Vumbugwa P, Cherdtrakulkiat T, Heng LS, Hoffman I, Palaypayon N, et al.; WHO EGASP Study Group. Antimicrobial resistance in *Neisseria gonorrhoeae* in nine sentinel countries within the World Health Organization Enhanced Gonococcal Antimicrobial Surveillance Programme (EGASP), 2023: a retrospective observational study. Lancet Reg Health West Pac. 2025;61:101663. https://doi.org/10.1016/j.lanwpc.2025.101663
10. European Committee on Antimicrobial Susceptibility Testing. Breakpoint tables for interpretation of MICs and zone diameters. Version 15.0. 2025 [cited 2025 Nov 2]. https://www.eucast.org/fileadmin/eucast/pdf/breakpoints/v_15.0_Breakpoint_Tables.pdf
11. Clinical and Laboratory Standards Institute. Performance standards for antimicrobial susceptibility testing. Thirty-third edition (M100–ED33). Wayne (PA): The Institute; 2023. p. 132–4.
12. Lan PT, Phan Nguyen TT, Anh VT, Golparian D, Thuy Van NT, Maatouk I, et al.; WHO EGASP-Viet Nam WGS study group. The World Health Organization (WHO) Enhanced Gonococcal Antimicrobial Surveillance Programme (EGASP) reports continuously high levels of ceftriaxone resistance across Viet Nam, 2024. Lancet Reg Health West Pac. 2025;63:101709. https://doi.org/10.1016/j.lanwpc.2025.101709
13. Ouk V, Heng LS, Virak M, Deng S, Lahra MM, Frankson R, et al.; EGASP Cambodia Working Group. High prevalence of ceftriaxone-resistant and XDR *Neisseria gonorrhoeae* in several cities of Cambodia, 2022–23: WHO Enhanced Gonococcal Antimicrobial Surveillance Programme (EGASP). JAC Antimicrob Resist. 2024;6:dlae053. https://doi.org/10.1093/jacamr/dlae053
14. Ministry of Public Health, Thailand. STI management guidelines 2024 [in Thai]. 2024 [cited 2025 Nov 2]. https://stisqsa.ddc.moph.go.th/app-assets/manual/2567/%E0%B9%81%E0%B8%99%E0%B8%A7%E0%B8%97%E0%B8%B2%E0%B8%87%E0%B8%81%E0%B8%B2%E0%B8%A3%E0%B8%94%E0%B8%B9%E0%B9%81%E0%B8%A5%E0%B8%A3%E0%B8%B1%E0%B8%81%E0%B8%A9%E0%B8%B2%E0%B9%82%E0%B8%A3%E0%B8%84%E0%B8%95%E0%B8%B4%E0%B8%94%E0%B8%95%E0%B9%88%E0%B8%AD%E0%B8%97%E0%B8%B2%E0%B8%87%E0%B9%80%E0%B8%9E%E0%B8%A8%E0%B8%AA%E0%B8%B1%E0%B8%A1%E0%B8%9E%E0%B8%B1%E0%B8%99%E0%B8%98%E0%B9%8C_2567.pdf
15. Siltrakool B, Berrou I, Griffiths D, Alghamdi S. Antibiotics' use in Thailand: community pharmacists' knowledge, attitudes and practices. Antibiotics (Basel). 2021;10:137. https://doi.org/10.3390/antibiotics10020137

Address for correspondence: Rossaphorn Kittiyaowamarn, Bangrak STIs Center, Division of AIDS and STIs, Department of Disease Control, Ministry of Public Health, 9 South Sathon Rd, Yan Nawa, Sathon, Bangkok 10120, Thailand; email: rossaphorn@gmail.com

etymologia

Bacteria
[bak-tēr'-ē-ə]

Hellen C.O. Santos-Dutra, Caroline C.P. da Costa,
Diogo Nery Maciel, Rodrigo S. Santos, Mônica S. Barbosa

A bacterium is a unicellular prokaryotic microorganism, and bacteria is the plural form that refers to these organisms as a group, historically classified within the former Monera kingdom. The term bacteria derives from Greek baktērion (βακτήριον), meaning small staff or cane, describing rod-like forms observed in early microscopic studies. Christian Gottfried Ehrenberg introduced the term bacterium in 1838, before modern bacteriology, and bacteria later became the plural form. Once viewed as microscopic plants, bacteria were later recognized as a distinct group of prokaryotic life and are now essential in ecologic processes, biotechnology, and public health, as beneficial or pathogenic agents.

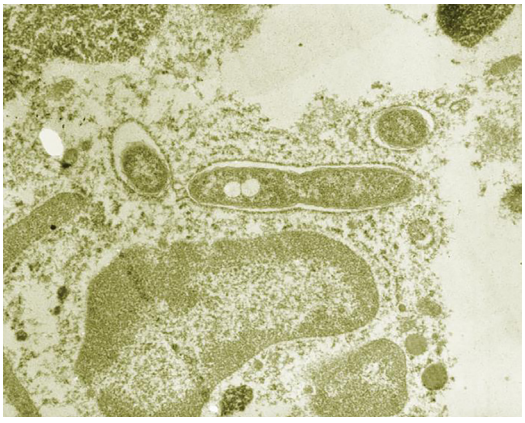

Ultrastructural morphology of numerous *Legionella pneumophila* bacteria in tissue section. Image from https://phil.cdc.gov

Sources

1. Grote M. Microbes before microbiology: Christian Gottfried Ehrenberg and Berlin's infusoria. Endeavour. 2022;46:100815. https://doi.org/10.1016/j.endeavour.2022.100815
2. Osorio C. About the origin of the term bacteria: a semantic paradox [in Spanish]. Rev Chilena Infectol. 2017;34:265–9. https://doi.org/10.4067/S0716-10182017000300011
3. Santos-Beneit F. What is the role of microbial biotechnology and genetic engineering in medicine? MicrobiologyOpen. 2024;13:e1406. https://doi.org/10.1002/mbo3.1406
4. Shishkin-Skarð Y. When and how did the names bacteria and eubacteria originate: resurrected facts. Microbiol Res. 2024;283:127676. https://doi.org/10.1016/j.micres.2024.127676
5. Soni J, Sinha S, Pandey R. Understanding bacterial pathogenicity: a closer look at the journey of harmful microbes. Front Microbiol. 2024;15:1370818. https://doi.org/10.3389/fmicb.2024.1370818

Address for correspondence: Mônica Santiago Barbosa, Biosciences and Biotechnology, Setor Leste Universitário, Federal University of Goiás, Rua 235 S/N, Goiânia 74605-220, Brazil; email: santiago@ufg.br

Authors affiliation: Federal University of Goiás, Goiânia, Goiás, Brazil

DOI: https://doi.org/10.3201/eid3206.251514

Repeated Extraneous Introductions of Cholera, Thailand, 2007–2025

Kazuhisa Okada, Amonrattana Roobthaisong, Warawan Wongboot, Pawinee Doung-ngern, Wichan Bhunyakitikorn, Pilailuk A. Okada, Thanee Wongchai, Witaya Swaddiwudhipong, Tetsuya Iida, Shigeyuki Hamada

Genomic analyses identified 4 seventh pandemic *Vibrio cholerae* El Tor clades in Thailand (2007–2025). Closely related to other South Asian strains, the clades reveal that repeated cross-border introductions, rather than local persistence, drive outbreaks. Our findings highlight the importance of genomic surveillance for monitoring transmission and informing regional control strategies.

Cholera, caused by *Vibrio cholerae* O1, is a potentially life-threatening diarrheal disease and remains a major global public health threat (*1*). In recent years, large-scale outbreaks have occurred in several countries in Africa and the Middle East, including Sudan and Yemen, where conflict, population displacement, and limited access to clean water have contributed to increased transmission (*2*,*3*). South Asia, particularly the Bengal Delta, serves as a hub for genetically diverse pandemic strains and contributes to their global dissemination (*4*,*5*). Outbreak occurrence and severity are influenced by environmental and socio-economic factors, and *V. cholerae* can persist in aquatic environments, although long-term local persistence varies by region (*6*–*9*).

Cholera has resurged periodically in Thailand, notably from 2007, when a large-scale outbreak affected 50 provinces, peaking in northeastern regions between September and November. Analyses during 2007–2010 using pulsed field gel electrophoresis and multilocus variable-number tandem repeat analysis indicated that those outbreaks were driven by repeated introductions of *V. cholerae* O1, particularly in border areas (*10*). Independent evidence further suggested regional transmission or shared infection sources among Thailand, Laos, and Vietnam. Previous studies have revealed high clonal diversity among Thailand isolates collected during 1999–2002 (*11*), whereas isolates of the El Tor serotype Ogawa strain from 2007 displayed a distinct ribotype, consistent with the introduction of a new clone in northeastern Thailand. Despite those insights, understanding of the genomic relationships between historical and more recent Thailand isolates and global pandemic strains remains incomplete.

Author affiliations: The University of Osaka Thailand–Japan Research Collaboration Center on Emerging and Re-emerging Infections, Mueang, Thailand (K. Okada, A. Roobthaisong); The University of Osaka Research Institute for Microbial Diseases, Suita, Japan (K. Okada, T. Iida, S. Hamada); Ministry of Public Health, Mueang (W. Wongboot, P. Doung-ngern, W. Bhunyakitikorn, P.A. Okada); Maesot General Hospital, Maesot, Thailand (T. Wongchai, W. Swaddiwudhipong)

DOI: http://doi.org/10.3201/eid3206.251747

The Study

We analyzed 498 *Vibrio cholerae* O1 isolates from Thailand collected from 2007 through April 2025 and selected 157 representative isolates for whole-genome sequencing: 85 from 2007–2012, 52 from 2015–2016, and 20 from 2023–2025 (including 72 newly sequenced in this study). We chose our isolate pool to reflect the genetic diversity observed in the multilocus variable-number tandem-repeat analysis and to ensure variation in the collection site and isolation period (Appendix 1 Tables 1, 2, https://wwwnc.cdc.gov/EID/article/32/6/25-1747-App1.xlsx). Cholera case numbers and their geographic distribution in Thailand, obtained from reports by the Division of Epidemiology (Appendix 2 Figure 1, https://wwwnc.cdc.gov/EID/article/32/6/25-1747-App2.pdf), showed a marked nationwide decline in outbreak size and frequency. From 2017 to early 2025, the annual number of cases in Thailand remained <20 (mean 7.2), and no large-scale, nationwide outbreaks occurred during that period. We included in our analyses isolates from smaller clusters near the northwestern border and sporadic cases from samples collected in late 2024 and early 2025.

We conducted a series of analyses to investigate the evolutionary dynamics of *V. cholerae* O1 isolates

in Thailand during 2007–2025, clarifying their origins, transmission patterns, and the relationships between isolates from Thailand and those from outside the country. We sequenced genomic DNA from the isolates using an Illumina MiSeq platform (https://www.illumina.com) and mapped to the *V. cholerae* N16961 reference genome. For global comparison, we curated *V. cholerae* O1 genomes from the National Center for Biotechnology Information Sequence Read Archive (https://www.ncbi.nlm.nih.gov/sra) and GenBank on the basis of published studies (Appendix 1 Table 3), ensuring balanced geographic and temporal representation. We quality-filtered data from the Sequence Read Archive using fastp software (https://github.com/opengene/fastp; -q parameter), retaining only high-quality sequences. We then identified core genome single-nucleotide polymorphisms (SNPs) using Snippy (https://github.com/tseemann/snippy), excluding regions associated with prophages (identified using PHAST [https://github.com/CshlSiepelLab/phast]), repeats (identified using NUCmer [https://github.com/nf-core/modules/tree/master/modules/nf-core/nucmer]), and recombination (identified using Gubbins [https://github.com/nickjcroucher/gubbins]). We masked these regions using VCFtools (https://github.com/vcftools/vcftools) before phylogenetic analysis. We reconstructed maximum-likelihood phylogenetic trees using RAxML software (https://cme.h-its.org/exelixis/web/software/raxml) and analyzed temporal signals using root-to-tip regression. We estimated divergence times using Bayesian molecular clock analysis. Pairwise SNP comparisons identified the 5 closest non-Thailand isolates for each outbreak cluster (Table). We used CholeraeFinder (Center for Genomic Epidemiology, https://www.genomicepidemiology.org) to detect virulence genes and mobile genetic elements. We also used Mantel tests as a complementary metric to assess broad congruence but drew the primary conclusions from the phylogenetic topologies to account for evolutionary structure.

Comparative genomic analysis of 157 Thailand isolates and global genomes identified 2 lineages: the seventh pandemic El Tor (7PET; 150 isolates) and the El Tor sister group (ST75; 7 isolates) (Figure 1). The 7PET clade comprised 4 distinct groups (TH1–TH4), corresponding to 3 outbreak periods (Figure

Table. Single-nucleotide polymorphism differences between Thailand outbreak clusters and the most closely related non-Thailand strains from study of repeated extraneous introductions of cholera, Thailand, 2007–2025*

Lineage (cluster)	SNP range within cluster	Closest non-Thailand strains	Origin, country/year	SNPs from Thailand isolate
TH1 (a)	0–7	MAB004	Bangladesh/2005	7
		MAB006	Bangladesh/2005	8
		4488	India/2006	13
		THSTI_J4770	India/2004	13
		BGD005	Bangladesh/2007	13
TH1 (b)	0–7	MAB004	Bangladesh/2005	9
		MAB006	Bangladesh/2005	12
		4488	India/2006	17
		THSTI_J4770	India/2004	17
		BGD005	Bangladesh/2007	17
TH2 (c)	0–21	THSTI_K9398	India/2005	12
		MAB001	Bangladesh/2004	13
		CNRVC060089	India/2006	13
		CNRVC060333	India/Nepal/2006	13
		MBN17	India/2004	14
TH3 (d)	0–14	PCS-0023	Bangladesh/2010	6
		IDH-07956	India/2015	7
		BGD133	Bangladesh/2015	8
		HCIS-055B	Bangladesh/2013	10
		BGD128	Bangladesh/2015	10
TH4 (e)	0–5	DMAVC-8	Bangladesh/2022	5
		DMAVC-18	Bangladesh/2022	5
		DMAVC-17	Bangladesh/2022	7
		DMAVC-19	Bangladesh/2022	7
		DMAVC-4	Bangladesh/2022	8

*To identify the closest non-Thailand relatives, we calculated pairwise SNP distances for all 150 Thailand seventh pandemic isolates against the global dataset using snp-dists (https://github.com/tseemann/snp-dists). To capture the full genetic diversity, we compared each Thailand genome independently rather than using a single representative per cluster. For each cluster, we selected the 5 non-Thailand strains with the smallest SNP distances. SNP ranges within clusters reflect internal diversity, whereas differences from non-Thailand strains indicate potential geographic origins. SNP, single-nucleotide polymorphism.

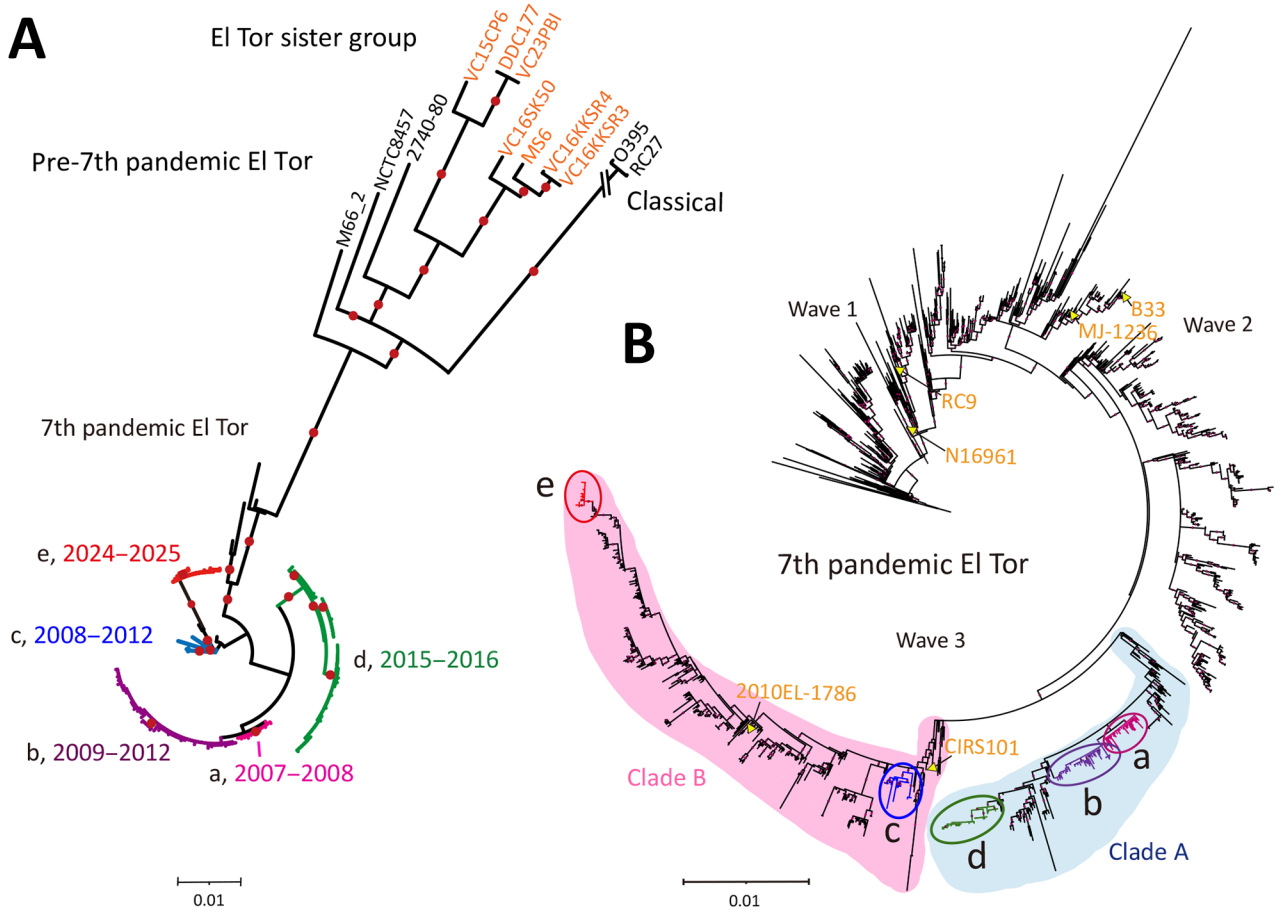

Figure 1. Maximum-likelihood phylogenetic trees of Vibrio cholerae O1 isolates reconstructed for study of repeated extraneous introductions of cholera, Thailand, 2007–2025. A) Phylogenetic relationships of 157 Thailand isolates and 11 representative O1 reference strains. Seven Thailand isolates (orange) belong to the El Tor Sister group lineage. The 7th pandemic El Tor lineage is divided into 5 distinct clusters (a–e), color-coded by isolation period: red-purple (cluster a, 2007–2008), blue-purple (cluster b, 2009–2010), blue (cluster c, 2011–2012), green (cluster d, 2015–2016), and red (cluster e, 2024–2025). B) Detailed phylogeny of the 7th pandemic El Tor lineage incorporating 150 Thailand isolates and 1,425 global genomes. Yellow labels explicitly identify the global reference strains (e.g., N16961, CIRS101) used in the analysis to provide genomic context for the Thailand clades. Light blue shaded region highlights clade A; light pink shaded region highlights clade B. Both were selected for molecular clock analysis. Outbreak-associated Thailand clades (TH1–TH4) are nested within these broader genomic groups. Both trees were reconstructed using maximum-likelihood estimation based on high-quality core genome single-nucleotide polymorphisms and visualized using Interactive Tree of Life (https://itol.embl.de). Dots on the branches indicate bootstrap values >80%.

2). Period I (2007–2012) included TH1 (clusters a and b, Ogawa, CTX-3) and TH2 (cluster c, Inaba, CTX-3), with characteristic deletions in *Vibrio* seventh pandemic island [VSP] II. Period II (2015–2016) included TH3 (cluster d, Ogawa), characterized by CTX-3, VPI-1ΔVC0819, Δ*hlyA*, and variable presence of PLE1, which varied by the geographic region of cholera cases. Period III (2024–2025) was dominated by TH4 (cluster e, Ogawa), carrying CTX-3b (*ctxB7*), OmpU G325D, and deletions in VSP-II. Although deletions in canonical pathogenicity islands (e.g., VSP-II, VPI) could theoretically influence fitness, we observed no obvious association with clinical severity in the study dataset.

We conducted temporal analysis (Appendix 2 Figure 2) and Bayesian molecular clock modeling (8,137 recombination-filtered SNPs) to estimate the temporal dynamics and evolutionary divergence of *V. cholerae* clades circulating in Thailand and worldwide (Figure 3). The clades exhibited clear evolutionary patterns over time, and the statistical analysis was well supported (effective sample size >200), indicating that the estimated divergence times were reliable. Thailand clades were closely related to other South Asia clades: TH1 corresponded to BD-2 (MAB004 and MAB006), TH2 to BD-1 (MAB001), TH3 to BD-2 (HCIS-055B, BGD133, and IDH-7956), and TH4 to BD-1.2 (DMAVC-4, -8, -17, -18, and -19). In Bangla-

desh, BD-1 and BD-2 have been the 2 most prominent clades during the past 2 decades, with BD-1.2 emerging more recently and responsible for a massive 2022 cholera outbreak (*12*).

Conclusions

This study confirmed that Thailand experienced multiple independent waves of cholera during 2007–2025, primarily associated with repeated introductions of *V. cholerae* O1 strains from South Asia. Outbreak clades in Thailand during period I (2007–2012) were most closely related to the prominent BD-1 and BD-2 clades in Bangladesh. During period II (2015–2016), 3 distinct waves emerged in both the northwestern and southern regions of Thailand, and the southern isolates exhibited multilocus variable-number tandem-repeat analysis profiles identical to strains predominant in Mandalay, Myanmar, 6 months earlier (*13*), suggesting direct cross-border introductions. By period III (2024–2025), most cholera cases in Thailand were imported, primarily from Myanmar, which reported >2,000 cases in 2024 (*1*). Of note, CTX-3b isolates in Thailand were first detected in period III and belonged to the recently emerged BD-1.2 clade, responsible for a massive 2022 cholera outbreak in Bangladesh. Although our phylogenetic data highlight repeated introductions as the primary driver of outbreaks, the potential role of long-term environmental persistence cannot be ruled out owing to a lack of systematic environmental genomic data.

Our analysis also revealed non-7PET (El Tor sister, sequence type [ST] 75) isolates: 6 of the 7 we detected lacked cholera toxin genes and 1 was the toxigenic strain MS6 previously described in a border area in 2008 (*14*). During 2010–2020, ST75, rather than ST69, the major seventh pandemic lineage, emerged as the dominant clonal group in China and South Africa (*15*).

Although the geographic spread and origins of ST75 in Thailand remain unclear, our findings demonstrate the importance of continuous genomic surveillance for elucidating cholera transmission dynamics and informing outbreak response strategies. To translate our data into public health action, implementing routine genomic sequencing at border checkpoints and establishing a real-time data sharing framework

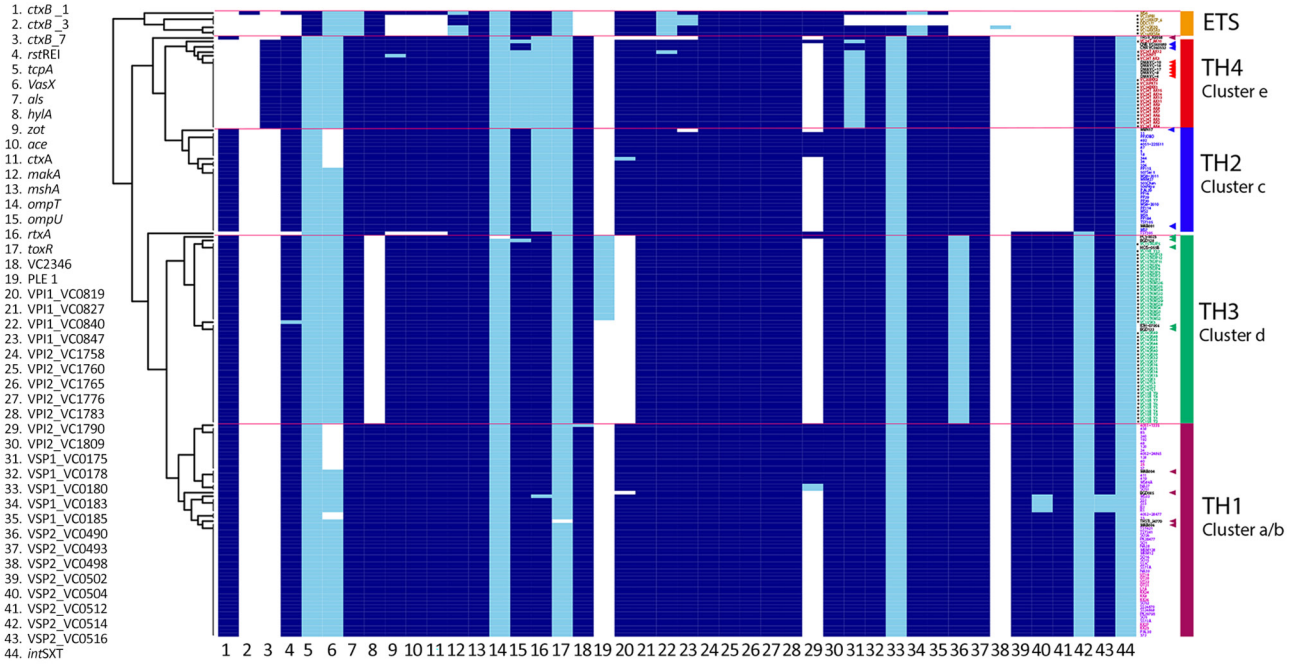

Figure 2. Phylogenetic relationships, genomic features, and outbreak cluster associations of Vibrio cholerae isolates from study of repeated extraneous introductions of cholera, Thailand, 2007–2025. Black dots indicate newly sequenced Thailand isolates in this study (n = 72) to distinguish them from reference strains. Virulence genes, integrative conjugative elements, and mobile genetic elements identified using CholeraeFinder (Center for Genomic Epidemiology, https://www.genomicepidemiology.org) in BLASTN mode (minimum coverage and identity 90%) (Appendix 2, Table 1). The blue cells in the heatmap represent the presence of genes, light blue cells indicate mutated genes, and blank cells signify the absence of genes. Phylogenetic relationships analyzed using a RAxML tree (https://cme.h-its.org/exelixis/web/software/raxml); genomic features are numerically coded (gene present = 1, gene absent = 0, mutated gene = 0.5). Thailand clades (TH1, TH2, TH3, and TH4) defined based on phylogenetic clustering and characteristic genomic features: TH1 (clusters a and b), TH2 (cluster c), TH3 (cluster d), and TH4 (cluster e). Arrowheads highlight the 5 closest non-Thailand isolates associated with each outbreak cluster, identified by pairwise single-nucleotide polymorphism comparisons. ETS, El Tor sister V. cholerae isolates.

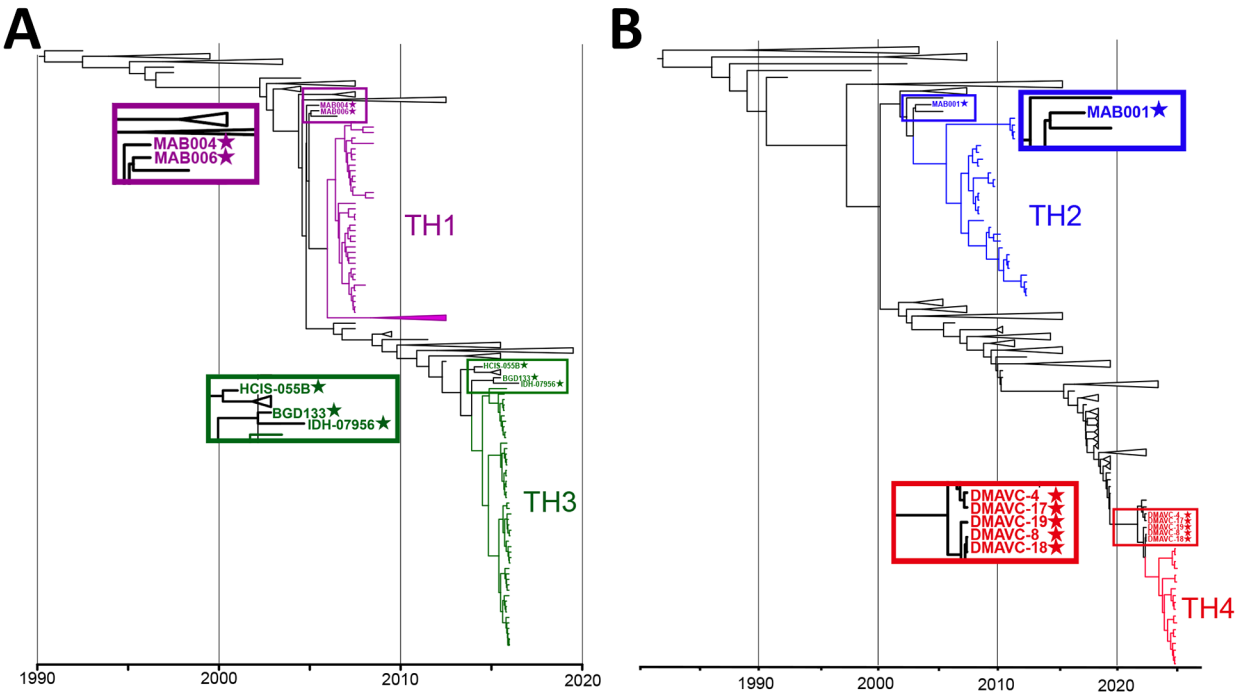

Figure 3. Temporal signal and divergence dating of Thailand Vibrio cholerae O1 isolates during the seventh pandemic from study of repeated extraneous introductions of cholera, Thailand, 2007–2025. Maximum clade credibility trees for clade A (panel A) and clade B (panel B) were reconstructed using a relaxed molecular clock (log-normal distribution) and a coalescent exponential population model. For clade A (n = 254; DRR189295 excluded), sampling years covered 1992–2019; for clade B (n = 417; ERR2265665 and DRR189283 excluded), sampling years covered 1992–2025. Both clades demonstrated strong temporal signals, confirmed by root-to-tip regression analysis (R2 > 0.91) (Appendix 2, Figure 2). and showed strong statistical support with effective sample size values >200. Temporal estimates suggest interregional transmission during the pandemic and highlight the preservation of specific genetic traits within Thailand populations, supporting the inferred lineage connections. Different colors indicate distinct clades, and stars indicate strains with characteristic genomic features.

with regional partners, particularly with Myanmar, Bangladesh, and India, is essential for the early detection and mitigation of future cholera waves in the South Asia region.

This research was supported by the Japan Initiative for Global Research Network on Infectious Diseases from the Ministry of Education, Culture, Sports, Science, and Technology, the Japan Agency for Medical Research and Development (grant no. 24wm0125010h0005), and the Department of Medical Sciences and Department of Disease Control, Ministry of Public Health, Thailand.

We used ChatGPT (OpenAI, https://chatgpt.com) for language refinement. All content was reviewed and verified by the authors.

About the Author

Dr. Okada is an associate professor at The University of Osaka whose research interests focus on the prevention and control of diarrheal diseases caused by *Vibrio cholerae* and other enteropathogens of significant public health concern.

References

1. World Health Organization. Global situation report for cholera, 2024. Wkly Epidemiol Rec. 2025;100:347–64 [cited 2025 Oct 1]. https://www.who.int/publications/i/item/who-wer10036-347-364
2. Hassan IN, Ahmed S, Ahmad E, Khan A, Ashraf H. Impact of conflict on cholera epidemiology in Sudan. Lancet. 2025;406:441–2. https://doi.org/10.1016/S0140-6736(25)01369-8
3. Weill FX, Domman D, Njamkepo E, Almesbahi AA, Naji M, Nasher SS, et al. Genomic insights into the 2016–2017 cholera epidemic in Yemen. Nature. 2019;565:230–3. https://doi.org/10.1038/s41586-018-0818-3
4. Qin C, Lypaczewski P, Sayeed MA, Cuénod A, Brinkley L, Creasy-Marrazzo A, et al. *Vibrio cholerae* lineage and pangenome diversity vary geographically across Bangladesh over 1 year. Microb Genom. 2025;11:001437. https://doi.org/10.1099/mgen.0.001437
5. Mutreja A, Kim DW, Thomson NR, Connor TR, Lee JH, Kariuki S, et al. Evidence for several waves of global transmission in the seventh cholera pandemic. Nature. 2011;477:462–5. https://doi.org/10.1038/nature10392
6. Shackleton D, Economou T, Memon FA, Chen A, Dutta S, Kanungo S, et al. Seasonality of cholera in Kolkata and the influence of climate. BMC Infect Dis. 2023;23:572. https://doi.org/10.1186/s12879-023-08532-1
7. Leckebusch GC, Abdussalam AF. Climate and socioeconomic influences on interannual variability of cholera in Nigeria.

Health Place. 2015;34:107–17. https://doi.org/10.1016/j.healthplace.2015.04.006
8. Colwell RR. Global climate and infectious disease: the cholera paradigm. Science. 1996;274:2025–31. https://doi.org/10.1126/science.274.5295.2025
9. Mavian C, Paisie TK, Alam MT, Browne C, Beau De Rochars VM, Nembrini S, et al. Toxigenic *Vibrio cholerae* evolution and establishment of reservoirs in aquatic ecosystems. Proc Natl Acad Sci U S A. 2020;117:7897–904. https://doi.org/10.1073/pnas.1918763117
10. Okada K, Roobthaisong A, Nakagawa I, Hamada S, Chantaroj S. Genotypic and PFGE/MLVA analyses of *Vibrio cholerae* O1: geographical spread and temporal changes during the 2007–2010 cholera outbreaks in Thailand. PLoS One. 2012;7:e30863. https://doi.org/10.1371/journal.pone.0030863
11. Tapchaisri P, Na-Ubol M, Jaipaew J, Srimanote P, Chongsa-Nguan M, Yamasaki S, et al. Virulence genes of clinical *Vibrio cholerae* O1 isolates in Thailand and their ribotypes. J Infect. 2007;55:557–65. https://doi.org/10.1016/j.jinf.2007.08.001
12. Monir MM, Islam MT, Mazumder R, Mondal D, Nahar KS, Sultana M, et al. Genomic attributes of *Vibrio cholerae* O1 responsible for 2022 massive cholera outbreak in Bangladesh. Nat Commun. 2023;14:1154. https://doi.org/10.1038/s41467-023-36687-7
13. Roobthaisong A, Okada K, Htun N, Aung WW, Wongboot W, Kamjumphol W, et al. Molecular epidemiology of cholera outbreaks during the rainy season in Mandalay, Myanmar. Am J Trop Med Hyg. 2017;97:1323–8. https://doi.org/10.4269/ajtmh.17-0296
14. Okada K, Roobthaisong A, Swaddiwudhipong W, Hamada S, Chantaroj S. *Vibrio cholerae* O1 isolate with novel genetic background, Thailand–Myanmar. Emerg Infect Dis. 2013;19:1015–7. https://doi.org/10.3201/eid1906.120345
15. Ke Z, Pang B, Yang J, Gao Y, Zhang X, Xu H, et al. Emergence and prevalence of *Vibrio cholerae* O1 sequence type 75 clonal complex, Fujian Province, China, 2009–2023. Emerg Infect Dis. 2025;31:1428–31. https://doi.org/10.3201/eid3107.241838

Address for correspondence: Kazuhisa Okada, The University of Osaka Thailand–Japan Research Collaboration Center on Emerging and Re-emerging Infections, Bldg 10, Department of Medical Sciences, Ministry of Public Health, Tiwanon Rd, Muang, Nonthaburi 11000, Thailand; email: kazuhisa@biken.osaka-u.ac.jp

Yellow Fever Virus Surveillance in *Callithrix* spp. Marmosets during Epizootic Outbreak, Brazil, 2024–2025

Márcio Junio Lima Siconelli, Jéssica Caroline de Almeida Dias, Eduardo Ferreira Machado, Mariana Sequetin Cunha, Natália Coelho Couto de Azevedo Fernandes, Juliana Mariotti Guerra, Luana Bonon, Alline Borges Salomão, Karin Werther, Karina Paes Bürger, Adolorata Aparecida Bianco Carvalho, Daniel Marques, Benedito Antonio Lopes da Fonseca

In 2023, a new yellow fever virus (YFV) lineage was introduced in São Paulo state, Brazil. During July 2024–June 2025, nine *Callithrix penicillata* marmosets tested YFV–positive, showing high viral loads and characteristic organ lesions. Those results highlight the need to include these animals in multispecies surveillance strategies for early YFV detection.

Yellow fever virus (YFV; *Orthoflavivirus flavi*), is an arbovirus of the Flaviviridae family transmitted by *Aedes* spp. mosquitoes in the urban cycle and *Haemagogus*/*Sabethes* spp. mosquitoes in the sylvatic cycle (*1*,*2*). Nonhuman primates (NHPs) are key sentinel animals for early YFV detection and a core component of the Brazilian Yellow Fever Surveillance Program (*3*). However, YFV pathogenicity varies among species, and the role of Brazil's diverse NHP populations in continued YFV circulation remains poorly understood (*4*). *Alouatta* spp. howler monkeys are the most susceptible to YFV infection (*5*–*7*). Infected NHPs develop clinical and pathologic manifestations similar to those in humans (*4*,*8*,*9*), who exhibit high viral loads and pronounced liver damage, including areas of necrosis and apoptosis, Councilman–Rocha Lima (CRL) bodies, steatosis, and inflammatory infiltrates (*10*,*11*).

During 2016–2018, Brazil experienced its worst wild yellow fever outbreak in 70 years, in which most human and NHP cases occurred in the southeastern region (*1*,*2*). In that outbreak, most infected NHPs were *Callithrix* spp. marmosets, revealing 2 infection patterns: one with a high viral load and characteristic histopathologic hepatic lesions and another with low viral loads, absence of clinical disease, and minimal or absent hepatic lesions (*4*,*12*).

In 2023, a new YFV lineage emerged in eastern São Paulo state (*13*), then spread throughout most of the state. The first confirmed NHP deaths attributed to YFV in the region of Ribeirão Preto city occurred in late December 2024. During the following months, the outbreak intensified, and more confirmed NHP infections and 1 human case occurred in the surrounding municipalities (Figure 1). We investigated clinical and laboratory findings of YFV infection among NHPs during that epizootic outbreak.

Author affiliations: Unidade de Vigilância de Zoonoses da Divisão de Vigilância Ambiental em Saúde, Secretaria Municipal da Saúde, Ribeirão Preto, Brazil (M.J.L. Siconelli); Faculdade de Medicina de Ribeirão Preto, Universidade de São Paulo, Ribeirão Preto (M.J.L. Siconelli, J.C. de Almeida Dias, B.A. Lopes da Fonseca); Centro de Patologia, Instituto Adolfo Lutz de São Paulo, Secretaria Estadual da Saúde de São Paulo, São Paulo, Brazil (E.F. Machado, N.C.C.A. Fernandes); Centro de Virologia, Instituto Adolfo Lutz de São Paulo, Secretaria Estadual da Saúde de São Paulo, São Paulo (M.S. Cunha); Universidade de São Paulo Departamento de Patologia da Faculdade de Medicina Veterinária e Zootecnia, São Paulo (J.M. Guerra); Programa de Residência em Área Profissional da Saúde, Medicina Veterinária e Saúde, do Departamento de Patologia, Reprodução e Saúde Única da Faculdade de Ciências Agrárias e Veterinárias, Universidade Estadual Paulista, Jaboticabal, Brazil (L. Bonon, A.B. Salomão, K. Werther, K.P. Bürger, A.A.B. Carvalho); Grupo de Vigilância Epidemiológica, Centro de Vigilância Epidemiológica "Prof. Alexandre Vranjac," Secretaria Estadual da Saúde de São Paulo, São Paulo (D. Marques)

DOI: https://doi.org/10.3201/eid3206.251388

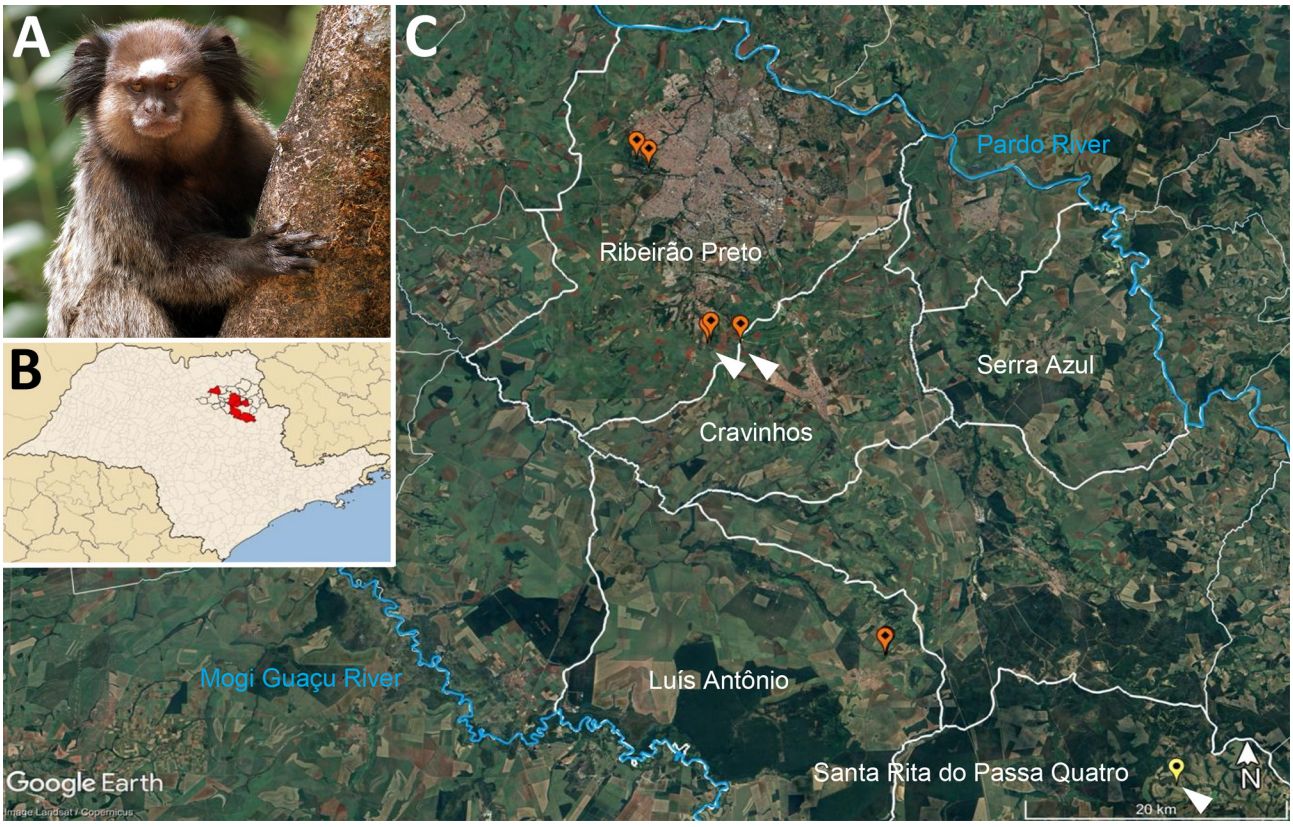

Figure 1. Location and example species for yellow fever virus (YFV) surveillance in *Callithrix* spp. marmosets during epizootic outbreak, Brazil, 2024–2025. A) *C. penicillata* marmoset. Source: Miguelrangeljr, CC BY-SA 3.0, via Wikimedia Commons, https://creativecommons.org/licenses/by-sa/3.0. B) São Paulo state map with dark lines highlighting the municipalities of the regional Epidemiologic Surveillance Group; red indicates areas affected by yellow fever. Map created by Raphael Lorenzeto de Abreu on WikiMedia (https://commons.wikimedia.org/w/index.php), modified by the authors and used according to permissions. C) Partial aerial view of the Ribeirão Preto region. White outlines represent borders of municipalities where YFV was detected during July 2024–June 2025. Orange dots indicate locations where YFV-positive *C. penicillata* marmosets were found; yellow dot indicates confirmed human yellow fever case; white arrowheads indicate areas without *Alouatta* spp. howler monkeys. Map from Google Earth, 2025 (https://earth.google.com).

The Study

During July 2024–June 2025, the regional Epidemiologic Surveillance Group reported 233 NHP deaths, of which 79% (184/233) were *Callithrix penicillata* black-tufted marmosets, 18% (42/233) *Alouatta caraya* black howler monkeys, 2.15% (5/233) *Sapajus nigritus* black capuchin monkeys, and 0.85% (2/233) *Callicebus nigrifrons* black fronted titi monkeys. Among the 233 NHPs, we necropsied and collected biologic samples from 154 (66.1%), 88.9% (n = 137) of which were Callitrichid marmosets.

We confirmed YFV infection in a total of 54 NHPs: 22 by laboratory testing on organ samples collected during necropsy and 32 by epidemiologic criteria. We could not obtain samples from the 32 NHPs identified by epidemiologic criteria because the carcasses were in an advanced state of decomposition. However, we included those animals because they were found in the same epidemiologic context and area in which YFV was detected in other animals.

Among 22 NHPs with laboratory-confirmed YFV infection, most were *A. caraya* monkeys (50%; 11/22), followed by *C. penicillata* (40.9%; 9/22) marmosets and *C. nigrifrons* (9.1%; 2/22) monkeys. As expected, samples from *Alouatta* and *Callicebus* spp. NHPs had low cycle threshold (Ct) values and typical organ lesions, including extensive hepatocellular necrosis, CRL bodies, hepatic steatosis, varying degrees of inflammatory infiltrates, and YFV antigens detectable by immunohistochemistry (IHC) (Figure 2). The YFV-positive marmosets exhibited a consistent pattern: low Ct values (Ct 11.14–20.08), typical histopathologic lesions, and detectable YFV antigens. One marmoset, stored frozen for a month before necropsy, showed a higher Ct value of 28.9.

All 9 *C. penicillata* marmosets were YFV-positive by IHC (Figure 3); 2 (22%) showed advanced autolysis, which precluded evaluation of histopathologic features, but we did detect CRL bodies in 1 of those 2 marmosets. Histopathologic findings in the other 7

animals showed all had hepatic necrosis, 3 (42%) with multifocal panlobular distribution and 4 (57%) with widespread panlobular involvement. Necrosis severity ranged from moderate in 2 (29%) to marked in the other 5 (71%) animals. All 7 animals had CRL bodies, and 3 (43%) had inflammatory infiltrates, consisting of mixed cellular contents in 1 (33.3%) and mononuclear cells in the other 2 (66.7%); we observed multifocal distribution and moderate severity in 2 (66.7%) cases and discrete distribution in 1 (33.3%). We identified hemorrhage in 4 (57%) of those animals, characterized by diffuse distribution in most (75%; 3/4); 3 (75%) exhibited moderate severity and 1 (25%) marked severity. We observed steatosis in 6 (86%) animals and panlobular macrovesicular and microvesicular patterns of moderate severity in 2 (34%) and marked severity in 4 (66%).

During the 2016–2018 outbreak, 7 *Callithrix* spp. marmosets were YFV-positive, 5 of which were from Ribeirão Preto and neighboring cities, but none had hepatic lesions or YFV antigens detected (*14*). In 2020, an urban *C. penicillata* marmoset from midwestern Brazil showed the same pattern, YFV-positive by quantitative reverse transcription PCR but no liver lesions nor YFV antigen detection (*15*).

The IHC and molecular findings of this study, representing the data from the 2024–2025 epizootic

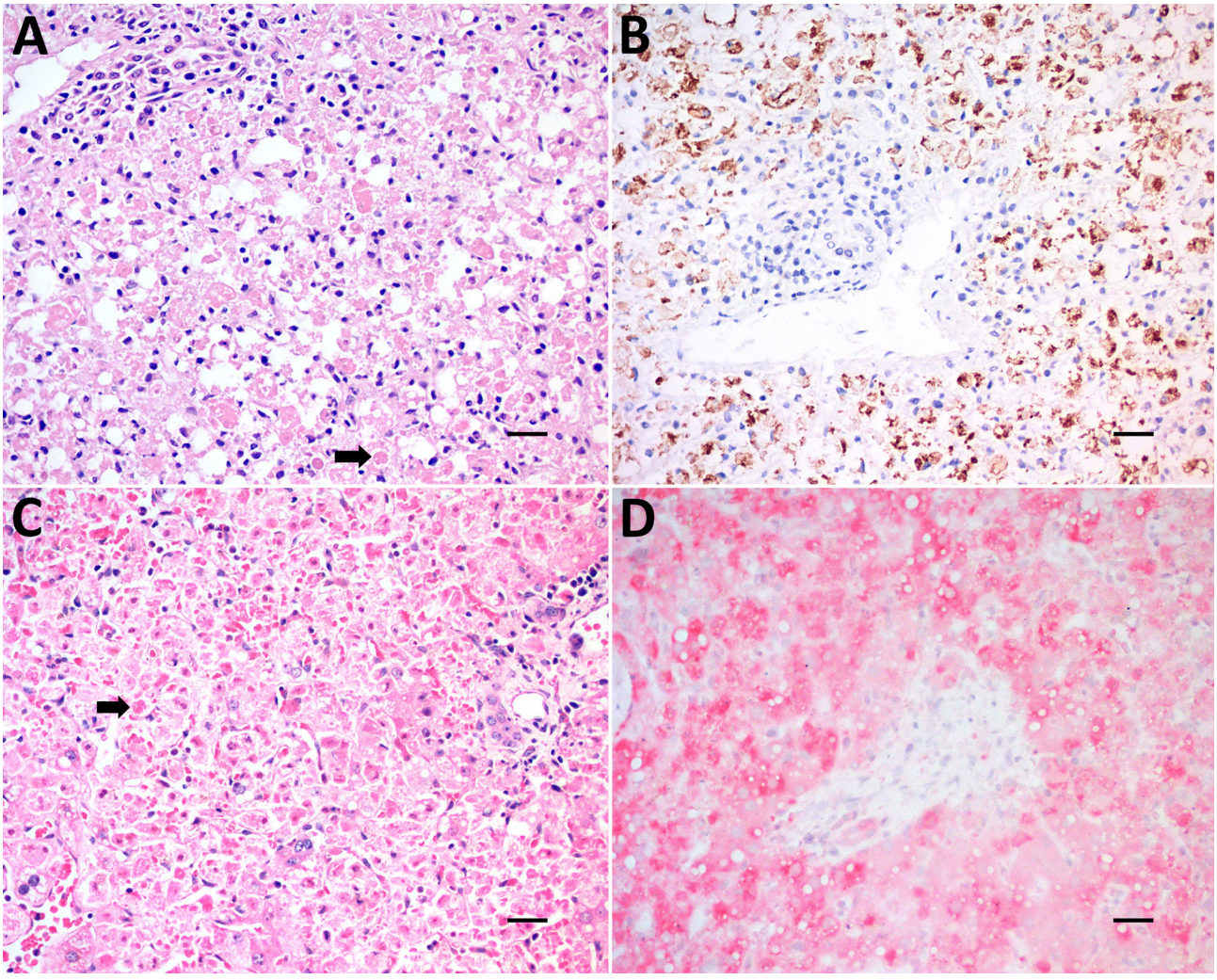

Figure 2. Laboratory analysis of liver samples from nonhuman primates collected for yellow fever virus (YFV) surveillance in *Callithrix* spp. marmosets during epizootic outbreak, Brazil, 2024–2025. A, B) Samples from *Callicebus nigrifrons* black fronted titi monkeys; C, D) samples from *Alouatta caraya* black howler monkeys. A) Hematoxylin and eosin stain of liver showing acute and severe hepatic damage characterized by diffusely individual cellular apoptosis and necrosis with Councilman–Rocha Lima bodies (arrow). B) Immunohistochemistry stain of hepatocytes; brown stain indicates cells positive for YFV antigen. C) Immunohistochemistry stain showing acute and severe hepatic damage characterized by individual cellular apoptosis and necrosis with Councilman–Rocha Lima bodies (arrow); brown indicates hepatocytes positive by YFV antigen. D) Immunohistochemistry stain of hepatocytes positive for YFV antigen (red). Scale bars indicate 20 μm.

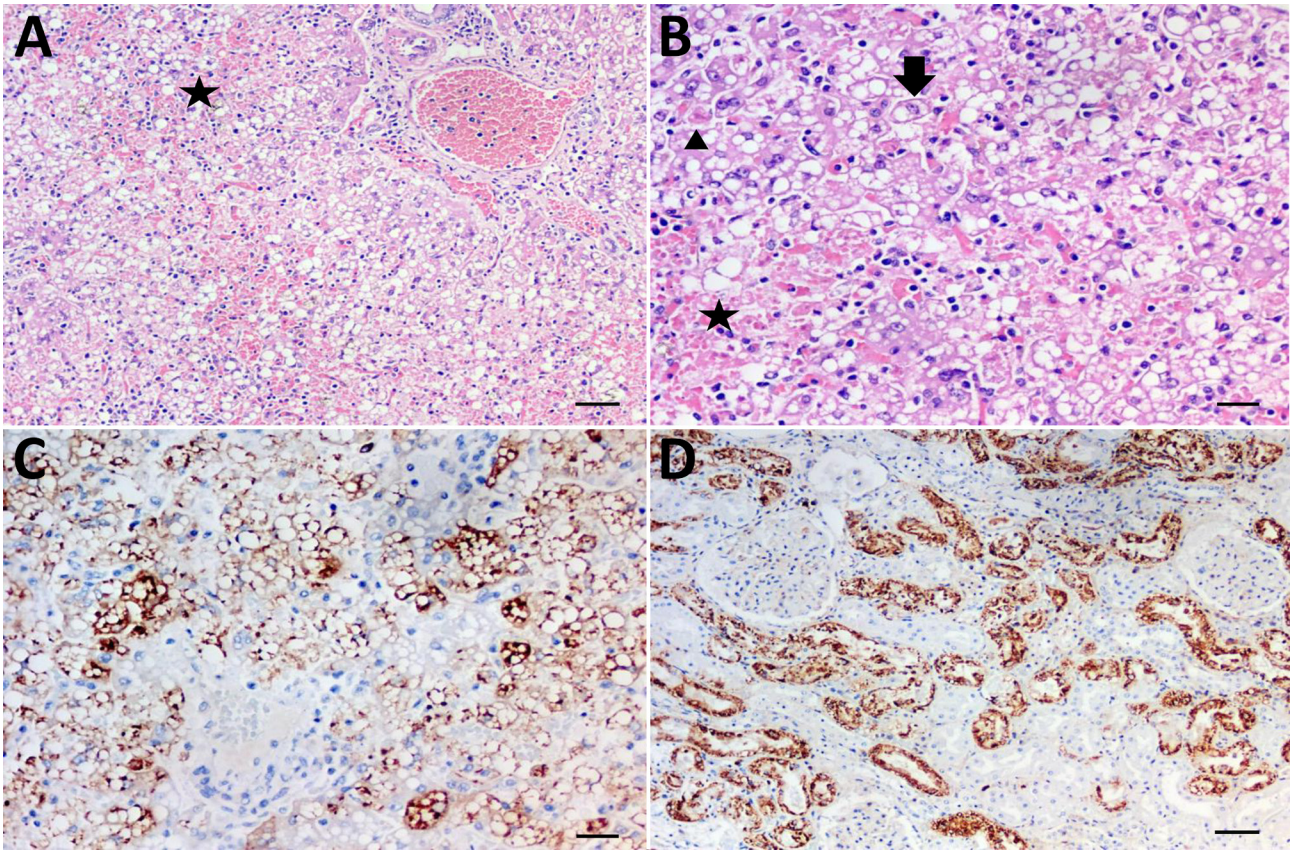

Figure 3. Laboratory analysis of organ samples collected from *Callithrix penicillata* marmosets with severe hepatic lesions due to yellow fever during epizootic yellow fever outbreak, Brazil, 2024–2025. A) Hematoxylin and eosin stain of liver showing acute and severe hepatic damage characterized by diffuse macrovesicular steatosis and focal hemorrhage (star). Original magnification ×10. B) Hematoxylin and eosin stain of liver showing acute and severe hepatic damage with macrovesicular steatosis (black arrowhead), focal hemorrhage (star), and a Councilman–Rocha Lima body (elongated arrow). Original magnification ×20. C) Immunohistochemisty stain showing hepatocytes positive for yellow fever virus antigen (brown staining). Original magnification ×20. D) Immunohistochemistry stain of renal tubular epithelial cells; brown stained cells are positive for yellow fever virus antigen. Original magnification ×10.

outbreak in São Paulo state demonstrate a consistent pattern of severe acute hepatitis in neotropical primates infected with YFV. All 22 confirmed NHP cases revealed characteristic hepatic lesions, with hepatocellular necrosis in all evaluated specimens, predominantly showing diffuse and multifocal to coalescing patterns. Those findings corroborate previous reports describing panlobular necrosis as a hallmark of fatal YFV infection in primates (*4*).

We identified CRL bodies, characteristic of YFV lesions, in 80% (18/22) of cases, and noted a much higher frequency in *A. caraya* and *C. nigrifrons* monkeys and *C. penicillata* marmosets. Even in specimens with marked autolysis (typically observed 1–3 days after death) CRL bodies remained detectable in 3 NHPs, reinforcing the strong association of CRL bodies with YFV infections, even under suboptimal tissue preservation conditions. Inflammatory infiltrates were predominantly mixed (polymorphonuclear and mononuclear) or mononuclear, with panlobular or periportal and portal distribution. We observed macrovesicular, microvesicular, or mixed steatosis with diffuse or multifocal distribution and consistent panlobular zonation. Severity was marked to moderate in 72.2% (13/18) of affected animals.

The high prevalence and severity of lesions combined with limited inflammatory response, despite extensive necrosis and steatosis, might indicate a YFV-induced metabolic dysfunction and support YFV as the main mechanism of liver injury. The histopathologic data we present need further investigation because they point to a possible association with the new YFV lineage circulating in southern Brazil. A relevant finding that supports that hypothesis is IHC confirmation of active YFV infection in 100% of cases, including all analyzed *C. penicillata* marmoset specimens. That contrasts with prior observations during 2017–2018, when *Callithrix* spp. marmosets often

exhibited lower viral loads and milder hepatic lesions (*4*,*14*,*15*). In the NHPs evaluated here, marmosets had severe liver damage comparable to that seen in howler monkeys, with extensive necrosis and unequivocal IHC positivity. The severe lesions observed in *Callithrix* spp. marmosets underscore this primate's relevance in NHP-based YFV surveillance, particularly in areas where *Alouatta* spp. monkey populations have been greatly reduced.

Conclusions

Our results confirm the classic histopathologic profile of YFV infection in neotropical primates, with striking severity in *C. penicillata* marmosets during an outbreak in an area with reduced *Alouatta* spp. monkey populations. The combination of hepatocellular necrosis, CRL bodies, steatosis, and 100% IHC positivity provides robust evidence for YFV pathogenicity across multiple primate species and reinforces the need for continuous surveillance in NHPs, placing *Callithrix* genus NHPs under the public health spotlight in this and in future epidemics. Its ability to adapt to urbanized environments, its proximity to humans, and the high *Ae. aegypti* mosquito population raise concerns for yellow fever reurbanization.

Our findings underscore the need for establishing a new NHP surveillance system based on *Callithrix* spp. marmosets in areas where *Alouatta* spp. monkey populations have been reduced or extinguished. Therefore, local zoonotic surveillance services in high-risk areas must be strengthened to detect early YFV circulation in the face of current NHP deaths, especially in view of a possible change in the yellow fever epidemiologic pattern.

This article was preprinted at https://www.medrxiv.org/content/10.1101/2025.09.07.25335112v2.

Acknowledgments

We thank all the municipal zoonotic surveillance services of XXXIII Health Region of São Paulo state, particularly the municipalities of Ribeirão Preto, Cravinhos, and Luís Antônio, for their prompt response and for providing the necessary samples for official diagnostic confirmation.

Animal samples were collected by the zoonotic surveillance unit of each municipality as part of national yellow fever surveillance program and sent to the Molecular Virology Laboratory of Ribeirão Preto Medical School, University of São Paulo, for initial detection of YFV and to Adolfo Lutz Institute to confirm the diagnosis. Because yellow fever is a disease with a high impact to the public health system, every detection of YFV needs to be confirmed by a national reference laboratory that, in São Paulo state, is the Adolfo Lutz Institute. All animals were found dead. This study did not require ethics committee approval according to Brazilian normative resolution no. 30, of February 2, 2016, of the National Animal Experimentation Control Council–CONCEA.

This work was funded, in part, by a grant of the FESIMA (São Paulo State Health Secretariat)–Ofício CAF no. 003/2016 and SEI process no. 024.00036429/2025-14.

Author contributions: M.J.L.S. conceptualized, devised methodology, conducted investigations, curated data, co-wrote the first draft and reviewed and edited subsequent drafts, and was responsible for project administration and acquiring funding; J.C.A.D. conducted investigations and processed samples; E.F.M. curated data, co-wrote the first draft, and reviewed and edited subsequent drafts; M.S.C., N.C.C.A.F., and J.M.G. conducted investigations, processed samples, and reviewed and edited manuscript drafts; L.B. and A.B.S. participated in investigations and sample collection; K.W., K.P.B., A.A.B.C., and D.M. reviewed and edited manuscript drafts. B.A.L.F. supervised, conceptualized, devised methodology, and provided resources for the study, reviewed, and edited manuscript drafts, served as project administrator, and acquired funding. All authors read, reviewed, and approved the final version of the manuscript.

About the Author

Dr. Siconelli is veterinarian specialized in zoonotic diseases at Unidade de Vigilância de Zoonoses da Divisão de Vigilância Ambiental em Saúde, Brazil. His research interests focus on surveillance programs with emphasis on arboviruses, particularly yellow fever virus and West Nile virus.

References

1. Silva NIO, Sacchetto L, de Rezende IM, Trindade GS, LaBeaud AD, de Thoisy B, et al. Recent sylvatic yellow fever virus transmission in Brazil: the news from an old disease. Virol J. 2020;17:9. https://doi.org/10.1186/s12985-019-1277-7
2. Possas C, Lourenço-de-Oliveira R, Tauil PL, Pinheiro FP, Pissinatti A, Cunha RVD, et al. Yellow fever outbreak in Brazil: the puzzle of rapid viral spread and challenges for immunisation. Mem Inst Oswaldo Cruz. 2018;113:e180278. https://doi.org/10.1590/0074-02760180278
3. Brazil Ministry of Health. Guide to epizootic surveillance in non-human primates and entomology applied to yellow fever surveillance, 2nd ed. Brasília (Brazil): The Ministry; 2017.
4. de Azevedo Fernandes NCC, Guerra JM, Díaz-Delgado J, Cunha MS, Saad LD, Iglezias SD, et al. Differential yellow fever susceptibility in New World nonhuman primates, comparison with humans, and implications for surveillance. Emerg Infect Dis. 2021;27:47–56. https://doi.org/10.3201/eid2701.191220

5. de Almeida MA, dos Santos E, da Cruz Cardoso J, da Fonseca DF, Noll CA, Silveira VR, et al. Yellow fever outbreak affecting *Alouatta* populations in southern Brazil (Rio Grande do Sul State), 2008–2009. Am J Primatol. 2012;74:68–76. https://doi.org/10.1002/ajp.21010
6. Moreno ES, Agostini I, Holzmann I, Di Bitetti MS, Oklander LI, Kowalewski MM, et al. Yellow fever impact on brown howler monkeys (*Alouatta guariba clamitans*) in Argentina: a metamodelling approach based on population viability analysis and epidemiological dynamics. Mem Inst Oswaldo Cruz. 2015;110:865–76. https://doi.org/10.1590/0074-02760150075
7. Bicca-Marques JC, Freitas DS. The role of monkeys, mosquitoes, and humans in the occurrence of a yellow fever outbreak in a fragmented landscape in south Brazil: protecting howler monkeys is a matter of public health. Trop Conserv Sci. 2010;3:78–89. https://doi.org/10.1177/194008291000300107
8. Fernandes NCCA, Cunha MS, Guerra JM, Réssio RA, Cirqueira CDS, Iglezias SD, et al. Outbreak of yellow fever among nonhuman primates, Espírito Santo, Brazil, 2017. Emerg Infect Dis. 2017;23:2038–41. https://doi.org/10.3201/eid2312.170685
9. Moreno ES, Spinola R, Tengan CH, Brasil RA, Siciliano MM, Coimbra TL, et al. Yellow fever epizootics in non-human primates, São Paulo State, Brazil, 2008–2009. Rev Inst Med Trop São Paulo. 2013;55:45–50. https://doi.org/10.1590/S0036-46652013000100008
10. Vieira WT, Gayotto LC, de Lima CP, de Brito T. Histopathology of the human liver in yellow fever with special emphasis on the diagnostic role of the Councilman body. Histopathology. 1983;7:195–208. https://doi.org/10.1111/j.1365-2559.1983.tb02235.x
11. Quaresma JA, Barros VL, Pagliari C, Fernandes ER, Guedes F, Takakura CF, et al. Revisiting the liver in human yellow fever: virus-induced apoptosis in hepatocytes associated with TGF-β, TNF-α and NK cells activity. Virology. 2006;345:22–30. https://doi.org/10.1016/j.virol.2005.09.058
12. Santos DOD, de Oliveira AR, de Lucena FP, de Mattos SA, de Carvalho TP, Costa FB, et al. Histopathologic patterns and susceptibility of neotropical primates naturally infected with yellow fever virus. Vet Pathol. 2020;57:681–6. https://doi.org/10.1177/0300985820941271
13. Fernandes NCCA, Cunha MS, Suarez PEN, Machado EF, Garcia JM, De Carvalho ACSR, et al. Phylogenetic analysis reveals a new introduction of yellow fever virus in São Paulo State, Brazil, 2023. Acta Trop. 2024;251:107110. https://doi.org/10.1016/j.actatropica.2023.107110
14. Cunha MS, da Costa AC, de Azevedo Fernandes NCC, Guerra JM, Dos Santos FCP, Nogueira JS, et al. Epizootics due to yellow fever virus in São Paulo State, Brazil: viral dissemination to new areas (2016–2017). Sci Rep. 2019;9:5474. https://doi.org/10.1038/s41598-019-41950-3
15. Sousa DER, Wilson TM, Macêdo IL, Romano APM, Ramos DG, Passos PHO, et al. Case report: urbanized non-human primates as sentinels for human zoonotic diseases: a case of acute fatal toxoplasmosis in a free-ranging marmoset in coinfection with yellow fever virus. Front Public Health. 2023;11:1236384. https://doi.org/10.3389/fpubh.2023.1236384

Address for correspondence: Benedito Antonio Lopes da Fonseca, Faculdade de Medicina de Ribeirão Preto, Universidade de São Paulo, Avenida Bandeirantes 3900, Ribeirão Preto 14040-030, Brazil; email: baldfons@fmrp.usp.br

Adverse Outcomes of Travel-Related Cosmetic Procedures among US Residents, 2014–2024

Kiara McNamara, Adam Rowh, Rhett Stoney, Kiran M. Perkins

We describe infections and other adverse outcomes among US residents who traveled for cosmetic procedures within the United States or abroad during 2014–2024. Outbreaks of adverse events related to such procedures often involve multiple states and geographically separated patients, making outbreak detection and investigation challenging.

Reports of adverse outcomes among persons who travel across domestic and international borders for planned medical care are reported globally (*1*–*4*). Cosmetic procedures remain a prominent category of planned medical care for which patients travel (*1*,*3*,*5*). The number of persons who travel for cosmetic procedures is unknown but is predicted to increase as demand for low-cost procedures rises and services that enable destination-based medical care expand (*3*,*6*). Additional motivators to travel for cosmetic procedures might include shorter wait times, preference for culturally similar providers, perceived quality of care, desired cultural appearances, and convenience of combining procedures with leisure travel. We reviewed Centers for Disease Control and Prevention (CDC) consultations with local and state jurisdictions to describe risks associated with traveling for cosmetic procedures among US residents.

The Study

CDC's Division of Healthcare Quality Promotion (DHQP) (National Center for Emerging and Zoonotic Infectious Diseases) supports health departments investigating reports of patient harm resulting from breaches in healthcare infection prevention and control (IPC) through consultation. We defined consultation as a verbal or written request to CDC from health departments for investigation and technical assistance. We reviewed DHQP consultation records for the period of January 1, 2014–December 31, 2024, using specific search terms (Appendix, https://wwwnc.cdc.gov/EID/article/32/6/25-1883-App1.pdf) to identify investigations in which US residents traveled for cosmetic procedures. We included consultations in which US residents traveled (i.e., within or outside the United States) for cosmetic procedures that involved an adverse outcome. We excluded consultations involving US residents who traveled for nonmedical purposes; received incidental, noncosmetic medical care; or underwent reconstructive or bariatric surgery.

We abstracted information regarding the number of patients, country or state where the procedure occurred, type of procedure performed, reporting jurisdiction(s), infection type, pathogen(s), healthcare setting, postsurgical interventions, treatment of complications, clinical outcomes, and findings from IPC assessments where available. Two authors (K.M. and A.R.) reviewed included consultations and 10% of excluded consultations for agreement and jointly abstracted the above variables to ensure consistency.

Of 2,162 total consultations, 34 consultations involved patients who traveled for medical care. Of those, 21 consultations involved ≈145 patients who traveled for cosmetic procedures and were included. US residents traveled to international (n = 17) and domestic destinations (n = 4) and underwent liposuction (n = 12), abdominoplasty (n = 9), and other cosmetic procedures (Table 1). Sixteen consultations included >1 cosmetic procedure. The number of patients per consultation ranged from 1 to 38 patients, although 12 consultations involved only 1 patient. Seven (range 2–20) consultations involved patients from multiple states who underwent cosmetic procedures in

Author affiliation: Centers for Disease Control and Prevention, Atlanta, Georgia, USA

DOI: https://doi.org/10.3201/eid3206.251883

Table 1. Characteristics of consultations related to travel by US residents for elective cosmetic medical procedures reported to the Centers for Disease Control and Prevention, 2014–2024

Characteristics	No. consultations, N = 21
Location of procedure	
International	17
United States	4
Setting*	
Surgery center or surgery clinic	14
Med-spa	1
Unknown	6
Type of cosmetic procedure†	
Liposuction with or without fat transfer	12
Abdominoplasty	9
Gluteal augmentation	7
Breast augmentation	6
Other cosmetic surgery‡	4
Unspecified cosmetic medical procedure	4
Pathogen, n = 20§	
Nontuberculous mycobacteria	12
Suspected nontuberculous mycobacteria¶	1
Methicillin-resistant *Staphylococcus aureus*	1
Fusarium solani complex	1
Carbapenem-resistant *Pseudomonas aeruginosa*	1
Unknown	4
Type of infection, n = 20§	
Surgical site infection	16
Central nervous system infection	1
Sepsis	1
Unknown site	2
Postsurgical procedural intervention, n = 20#	
Surgical or procedural treatment**	7
Other	5
Antibiotic treatment	7
Outcomes	
Hospitalization	4
Death	4
Unknown	14

*Categorization of setting types was based on descriptions relayed by public health jurisdictions and partners and may have variable interpretations in international and domestic locations.
†Types of cosmetic medical procedures were not mutually exclusive.
‡Other types of procedures were upper and lower blepharoplasty, facial fat grafting, lip filler, zygoma reduction-plasty, "thread lift," dimpleplasty, removal of gluteal implants, panniculectomy, and rhytidectomy.
§One consultation was excluded from the denominator of this section because investigation indicated patient outcomes were due to fat emboli and unrelated to an infectious etiology.
¶Suspected nontuberculous mycobacterium were defined as growth on acid-fast bacillus culture without mycobacterial species identification.
#Surgical or procedural interventions were not mutually exclusive.
**Surgical or procedural treatments include incision and drainage, surgical debridement, and therapeutic surgical revisions.

international (n = 5) and domestic locations (n = 2) and were associated with the same provider, procedure location, or type of procedure during a specific time (Table 2).

Postsurgical infections were described in 20 consultations, of which 12 identified suspected or confirmed nontuberculous mycobacteria (NTM). Suspected NTMs were defined as growth on acid-fast bacillus culture without mycobacterial species identification. Surgery centers or surgery clinics (n = 14) were the most frequently reported healthcare setting. Four consultations reported patient deaths (*7*). IPC findings available from 1 domestic and 1 international consultation highlighted gaps in environmental cleaning practices, use of personal protective equipment, hand hygiene, and reprocessing of surgical equipment.

Conclusions

We identified adverse outcomes among US residents who traveled outside their state of residence for cosmetic procedures within the United States or abroad. This analysis highlights potential for lapses in infection control to contribute to transmission both internationally and domestically and the challenges of detecting and investigating outbreaks in which patients travel. Our findings reinforce the importance of risk mitigation strategies, including effective communication of potential risks to patients, to prevent serious complications of medical procedures or surgeries. CDC provides guidance and information for healthcare personnel and patients who are considering medical tourism abroad (*3*,*8*). US residents might also benefit from those

risk mitigation strategies when choosing a domestic destination for cosmetic procedures.

Identifying adverse outcomes among persons who travel for cosmetic procedures is challenging and relies on clinical vigilance and reporting to public health authorities. Approximately one third of consultations reported large outbreak investigations involving multiple patients and states, which often requires extensive case-finding methods and information networks to connect information about geographically dispersed patients (*2*,*7*,*9*). One CDC Data (https://www.cdc.gov/data-modernization/php/one-cdc-data-platform/index.html) is a unified data platform that enables communication among public health professionals. Improved surveillance, continued partnership among clinicians and public health agencies, and strong patient engagement can encourage early identification of adverse outcomes and inform targeted prevention efforts for those settings (*10*,*11*). CDC is working with partners to explore opportunities to improve surveillance of adverse outcomes linked to medical tourism.

Table 2. Examples of select consultations and adverse outcomes related to travel for elective cosmetic procedures reported to Centers for Disease Control and Prevention, 2014–2024*

Location of procedures, y	Pathogen(s)	No. patients	Procedure(s)	Description	Outcome(s)
Dominican Republic, 2017	NTM	52	Liposuction with and without fat transfer; breast augmentation; abdominoplasty	Multiple strains of NTMs identified, suggesting widespread infection prevention and control lapses across multiple clinics and surgical providers. Extensive case-finding methods used, including call for cases through Epidemic Information Exchange, state-based health alert systems, Infectious Disease Society of America's Emerging Infections Network, and American Society of Plastic Surgeons' email distribution list (*14*)	≥11 patients received >1 antibiotic; ≥14 patients required therapeutic surgical procedures; 1 death reported
Florida, USA, 2017	NTM	3	Gluteal augmentation	3 patients from 2 states developed surgical site infections attributed to NTM after cosmetic procedures Procedures completed sequentially on same day by same surgeon in rented operating room	Outcomes not documented
Dominican Republic, 2018	Methicillin-resistant *Staphylococcus aureus*	3	Abdominoplasty; gluteal augmentation; liposuction	3 patients from same state of residence developed surgical site infections after cosmetic procedures performed at 3 surgical centers abroad by 3 surgeons. 1 clinic associated with prior healthcare-associated outbreak of NTM Wound cultures from 1 patient identified methicillin-resistant *Staphylococcus aureus* No other pathogens reported	Outcomes not documented
Florida, USA, 2022–2023	NTM	19	Gluteal augmentation; liposuction with and without fat transfer; abdominoplasty	Postsurgical infections were identified among 19 patients; of those, 15 patients from 9 states underwent cosmetic procedures at the same clinic and met the investigation's definition of a confirmed case (*2*). *Mycobacterium abscessus* was identified from wound cultures from all confirmed cases. Case-finding methods included a national call for cases through CDC Epidemic Information Exchange. Surgery center where procedures were performed was closed, and therefore, infection control practices could not be evaluated. Evaluation of infection control practices at another clinic where the same staff worked identified gaps in personal protective equipment use, medical device reprocessing, and environmental cleaning and disinfection	≥6 case-patients required intravenous antibiotics; ≥1 patient hospitalized; ≥4 case-patients required additional interventions, including computed tomography–guided percutaneous abscess drainage, needle aspiration, incision and drainage, wound debridement, and surgical skin excision with drainage

*Consultations were defined as a verbal or written request to CDC from health departments for investigation and technical assistance in response to reports of patient harm resulting from breaches in healthcare infection prevention and control. CDC, Centers for Disease Control and Prevention; NTM, nontuberculous mycobacterium.

More than half of consultations were attributed to NTM, accounting for all domestic consultations and most international consultations. The invasive nature of cosmetic procedures and potential exposure to nonsterile ice and water, which have been associated with NTM outbreaks in healthcare settings, might contribute to the large proportion of travel-related cosmetic consultations involving NTMs (*1*,*10*,*12*). Clinicians might be more likely to report difficult-to-treat and rare infections such as NTM than other infection types. Although NTMs are not nationally notifiable, public health experts recommend investigating even a single case of healthcare-associated extrapulmonary NTM (*13*). Observing IPC practices and evaluating clinical use of nonsterile water or ice before, during, and after cosmetic procedures is a high-yield action for those investigations.

Regulation for facilities where cosmetic procedures are performed can vary, creating challenges to ascertain IPC standards and ensure patient safety. US state regulations can differ by locality, and not all facilities are federally regulated by the Centers for Medicare and Medicaid Services, potentially contributing to varying IPC and water management practices. The existence of international IPC regulations can be unclear, given the complexities of different regulatory frameworks by country. As a result, IPC standards in other countries might be unknown or uncertain. When adverse outcomes related to medical tourism have been identified in the United States, CDC has connected with country public health authorities, such as ministries of health, to alert international partners and help address IPC concerns, decreasing future risk to patients (*7*,*9*). Persistent IPC gaps contribute to a higher risk for infection, and addressing those gaps should be prioritized to ensure safety of cosmetic procedures.

The first limitation of our review is that we used a convenience sample from health departments that requested CDC consultation, and findings do not represent all travel-related healthcare outbreaks. Full investigation details, including specific IPC issues potentially contributing to transmission, were not systematically provided to CDC and, therefore, might be missing or incomplete in CDC records. Outbreaks were likely underdetected and underreported because facilities might not track patient outcomes and reporting standards vary by jurisdiction. Last, we did not include consultations involving cosmetic procedures occurring within a patient's state of residence, which could pose similar infectious risks.

Outbreaks among persons who travel for cosmetic procedures, regardless of destination, might be difficult to detect and can lead to complex investigations associated with special challenges. Patients should consider the potential risks when traveling for cosmetic procedures. Clinicians should consider risk for infection, particularly NTM, among this population, and have a low threshold for notifying health departments. In addition to notifying the state or local health department, CDC requests notification of complications related to medical tourism by emailing medicaltourism@cdc.gov.

Acknowledgments

We thank the local and state health departments who investigated outbreaks of infections or other adverse outcomes after cosmetic procedures among persons who traveled for their time, effort, and initiative. We would also like to acknowledge the vigilant clinicians who recognized and reported patient infections to public health.

About the Author

Ms. McNamara is a doctoral-prepared nurse practitioner who works as a nurse epidemiologist at the Centers for Disease Control and Prevention in the Division of Healthcare Quality Promotion, National Center for Emerging and Zoonotic Infectious Diseases. Her primary research interests include infection prevention and control and response to outbreaks in healthcare settings.

References

1. Stoney RJ, Kozarsky PE, Walker AT, Gaines JL. Population-based surveillance of medical tourism among US residents from 11 states and territories: findings from the Behavioral Risk Factor Surveillance System. Infect Control Hosp Epidemiol. 2022;43:870–5. https://doi.org/10.1017/ice.2021.245
2. Saunders KE, Reyes JM, Cyril L, Mitchell M, Colter S, Erskine J, et al. Notes from the field: nontuberculous mycobacteria infections after cosmetic surgery procedures in Florida—nine States, 2022–2023. MMWR Morb Mortal Wkly Rep. 2024;73:66–7. https://doi.org/10.15585/mmwr.mm7303a4
3. Centers for Disease Control and Prevention. CDC Yellow Book: Health Information for International Travel. Oxford: Oxford University Press; 2025.
4. Beaudoin AL, Torso L, Richards K, Said M, Van Beneden C, Longenberger A, et al. Invasive group A *Streptococcus* infections associated with liposuction surgery at outpatient facilities not subject to state or federal regulation. JAMA Intern Med. 2014;174:1136–42. https://doi.org/10.1001/jamainternmed.2014.1875
5. Piyaphanee W, Stoney RJ, Asgeirsson H, Appiah GD, Díaz-Menéndez M, Barnett ED, et al. Healthcare seeking during travel: an analysis by the GeoSentinel surveillance network of travel medicine providers. J Travel Med. 2023;30:taad002. https://doi.org/10.1093/jtm/taad002
6. Chen LH, Wilson ME. The globalization of healthcare: implications of medical tourism for the infectious disease

clinician. Clin Infect Dis. 2013;57:1752–9. https://doi.org/10.1093/cid/cit540
7. Hudson M, Matos JA, Alvarez B, Safstrom J, Torres F, Premjee S, et al. Deaths of U.S. citizens undergoing cosmetic surgery—Dominican Republic, 2009–2022. MMWR Morb Mortal Wkly Rep. 2024;73:62–5. https://doi.org/10.15585/mmwr.mm7303a3
8. Centers for Disease Control and Prevention. Medical tourism. Travel to another country for medical care [cited 2025 Sep 19]. https://wwwnc.cdc.gov/travel/page/medical-tourism
9. Smith DJ, Misas E, Gold JAW, Evert N, Dang T, Prot E, et al. Fungal meningitis in U.S. patients who received epidural anesthesia in Matamoros, Mexico. Clin Infect Dis. 2026;82:e477–84.
10. McNamara KX, Perz JF, Perkins KM. Association of healthcare and aesthetic procedures with infections caused by nontuberculous mycobacteria, France, 2012–2020. Emerg Infect Dis. 2022;28:1303. https://doi.org/10.3201/eid2806.220520
11. Winthrop KL, Henkle E, Walker A, Cassidy M, Hedberg K, Schafer S. On the reportability of nontuberculous mycobacterial disease to public health authorities. Ann Am Thorac Soc. 2017;14:314–7. https://doi.org/10.1513/AnnalsATS.201610-802PS
12. Perkins KM, Reddy SC, Fagan R, Arduino MJ, Perz JF. Investigation of healthcare infection risks from water-related organisms: summary of CDC consultations, 2014–2017. Infect Control Hosp Epidemiol. 2019;40:621–6. https://doi.org/10.1017/ice.2019.60
13. The Council for Outbreak Response. Healthcare-associated infections and antimicrobia-resistant pathogens. Nontuberculous mycobacteria: recommended practices for healthcare outbreak response [cited 2025 Sep 19]. https://corha.org/assets/documents/CORHA-Proposed-NTM-Thresholds-and-Definition08-19.pdf
14. Gaines J, Poy J, Musser KA, Benowitz I, Leung V, Carothers B, et al. Notes from the field: nontuberculous mycobacteria infections in U.S. medical tourists associated with plastic surgery—Dominican Republic, 2017. MMWR Morb Mortal Wkly Rep. 2018;67:369–70. https://doi.org/10.15585/mmwr.mm6712a5

Address for correspondence: Kiara McNamara, Centers for Disease Control and Prevention, 1600 Clifton Rd NE, Mailstop 16-3, Atlanta, GA, 30329-4018, USA; email: rhv0@cdc.gov or kiara.x.mcnamara@gmail.com

Disseminated Coccidioidomycosis and Coccidioidal Meningitis Hospitalization, Texas, USA, 2016–2023[1]

Chun Ho Szeto,[2] Alfredo Chavez-Morales,[2] John Garza, Fariba Donovan

We analyzed inpatient data from Texas, USA, to characterize hospitalizations for disseminated coccidioidomycosis and coccidioidal meningitis from 2016–2023. Geographic mapping revealed a substantial disease effect in both western Texas and metropolitan areas. Our findings suggest the need for enhanced surveillance and increased healthcare provider awareness regarding coccidioidomycosis in Texas.

Coccidioidomycosis is a fungal infection caused by *Coccidioides* spp. Approximately 1% of all coccidioidomycosis progress to extrapulmonary disseminated coccidioidomycosis (DCM), with involvement of the central nervous system leading to coccidioidal meningitis (CM), the most severe and potentially fatal form of the disease (*1*,*2*).

Coccidioidomycosis is endemic to the southwestern United States, including Texas, where it is not currently a reportable disease (*3*,*4*). During 2016–2021, ≈3,200 coccidioidomycosis-related hospital discharges were recorded in Texas (*5*). Although previous reports have described DCM and CM cases at individual medical centers, state level data for Texas are lacking (*5*,*6*). Our study describes the epidemiology, clinical characteristics, and outcomes of DCM and CM hospitalizations in Texas.

The Study

We obtained data from Texas Inpatient Public Use Data files (TIPUDF) for January 1, 2016–December 31, 2023, from the Texas Department of State Health Services Center for Health Statistics (https://www.dshs.texas.gov/center-health-statistics). Because the study used publicly available and deidentified data, it was exempt from institutional review board approval. TIPUDF includes claims for medical services from all state-licensed, nonfederal hospitals in Texas, capturing ≈97% of hospital discharges. Each record represents a hospital encounter, containing the final discharge and all related claims information for a deidentified patient.

We identified the main cohort of DCM on the basis of the presence of codes from the International Classification of Diseases, 10th Revision (ICD-10), related to DCM (B38.7) or CM (B38.4) in all available patient records, including principal and other diagnosis fields (Figure 1). We restricted the analytic sample according to the patients' US state of residence in record and included only patients with a residence in Texas. This inclusion enabled us to characterize coccidioidomycosis within the Texas population and inform state-specific public health surveillance.

We divided the cohort into CM and non-CM DCM groups. We identified underlying conditions by using ICD-10 codes (Appendix Tables 1, 2, http://wwwnc.cdc.gov/EID/article/32/6/25-1469-App1.pdf). We identified hospitalizations with intensive care unit (ICU) admissions on the basis of hospital charges coded for an ICU or coronary care unit. We adjusted hospital charges, including facility fee, professional services, pharmacy, laboratory, and all other hospital-billed services, to 2023 Q4 dollars by using the Consumer Price Index for All Urban Consumers obtained from the US Bureau of Labor Statistics (https://www.bls.gov/news.release/archives/cpi_01112024.htm). We based geographic distribution analyses and

Author affiliations: Texas Tech University Health Science Center Permian Basin, Odessa, Texas, USA (C.H. Szeto, A. Chavez-Morales, J. Garza); University of Arizona College of Medicine–Tucson, Tucson, Arizona, USA (F. Donovan); BIO5 Institute, University of Arizona, Tucson (F. Donovan)

DOI: https://doi.org/10.3201/eid3206.251469

[1]Preliminary results from this study were presented at IDWeek 2025; October 19–22, 2025; Atlanta, Georgia, USA.

[2]These authors contributed equally to this article.

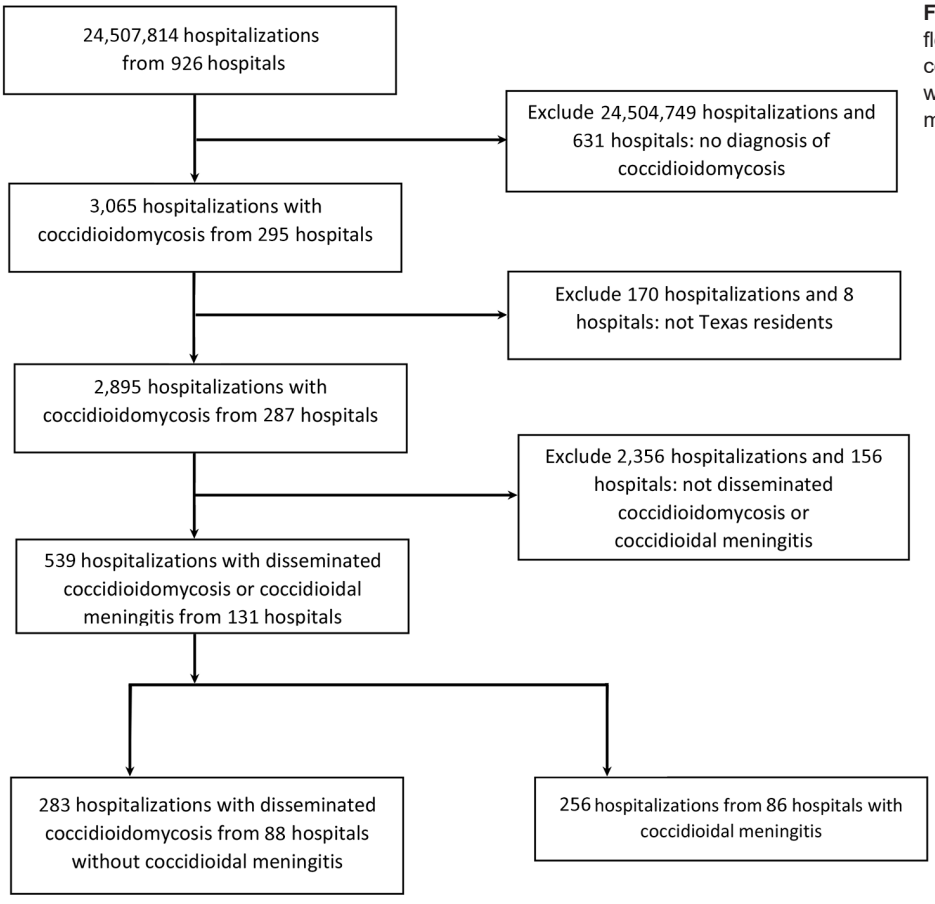

Figure 1. Cohort derivation flowchart for study of disseminated coccidioidomycosis hospitalization, with or without coccidioidal meningitis, Texas, USA, 2016–2023.

mapping on patient county of residence. We used the Fisher exact test for comparison of categorical variables and Student t-test for comparison of continuous variables and considered 2-sided $p<0.05$ statistically significant. We conducted all analyses by using R version 4.4.1 (The R Project for Statistical Computing, https://www.r-project.org). This study is reported in accordance with the RECORD guidelines for observational studies (https://www.record-statement.org) by using routinely collected health data.

For 2016–2023, we identified 539 DCM associated hospitalizations in Texas, USA (Appendix Table 3). Of those, 47.5% (n = 256) involved CM, and 52.5% (n = 283) were DCM without CM. Men represented 59.2% and women 40.8% of hospitalizations. The most affected age group was 18–44 years of age (43.4%), followed by 45–64 years (36.0%). Hispanic patients represented 51.9% of the hospitalizations, followed by Black patients (20.0%).

Pulmonary coccidioidomycosis was documented in 12.6% of DCM hospitalizations. The most common underlying conditions were malnutrition (27.8%), diabetes mellitus (27.3%), and nicotine dependence (23.6%). HIV infection was noted in 15.2% and renal disease in 20.8% of hospitalizations. ICU admission was required in 50.1% of hospitalizations. The mean length of stay was 14.6 days, and the mean adjusted hospitalization charges were $190,933 per stay. In-hospital mortality occurred in 5.9% of hospitalizations, and 4.6% of patients were discharged to hospice.

The highest rate of DCM hospitalizations occurred in the Odessa–San Angelo region (15.18 hospitalizations/100,000 population), followed by El Paso (6.98 hospitalizations/100,000 population) and Corpus Christi–Laredo (3.34 hospitalizations/100,000 population) (Table). County-level mapping revealed clustering in west-central, south, and east Texas; several counties reported >40 hospitalizations (Figure 2). Hospitalizations for CM and non-CM DCM showed similar patterns in age, gender, and outcomes, but CM hospitalizations showed lower rates of diabetes mellitus, malnutrition, and renal disease.

Conclusions

Our study characterizes the geographic distribution and clinical effect of DCM and CM hospitalizations in Texas. Approximately 46% of hospitalizations involved residents of traditionally endemic regions

Table. Geographic distribution of disseminated coccidiomycosis and coccidioidal meningitis associated hospitalizations in Texas, 2016–2023

Public health region*	No. hospitalizations in the region/population in the region†	Crude hospitalization rate per 100,000 population (95% CI)
Odessa-San Angelo (9)	93/612,773	15.18 (12.25–18.59)
El Paso (10)	62/888,720	6.98 (5.35–8.94)
Corpus Christi-Laredo (11)	75/2,246,397	3.34 (2.63–4.19)
San Antonio (8)	63/3,026,095	2.08 (1.60–2.66)
Amarillo–Lubbock (1)	18/900,807	2.00 (1.18–3.16)
Tyler (4)	16/1,149,993	1.39 (0.80–2.26)
Austin-Temple (7)	46/3,661,292	1.26 (0.92–1.68)
Dallas-Fort Worth (3)	88/8,044,641	1.09 (0.88–1.35)
Houston (6)	67/7,297,022	0.92 (0.71–1.17)
Abilene-Wichita Falls (2)	5/549,130	0.91 (0.30–2.12)
Beaumont (5)	4/768,635	0.52 (0.14–1.33)

*Defined by Texas Department of State Health Services (https://www.dshs.texas.gov/center-health-statistics/texas-county-numbers-public-health-regions). Numbers in parentheses represent region assignment.
†Defined by the US Census in 2020, data provided by Texas Demographic Center (https://demographics.texas.gov/Projections/2024)

(*5*,*7*). The Odessa–San Angelo region, despite its small population, had the highest rate of DCM and CM hospitalizations, likely reflecting its suitable *Coccidioides* habitat and oil and gas industry activities involving soil disturbance (*7*) (https://www.eia.gov/petroleum/drilling). We observed high absolute numbers of hospitalizations among residents of metropolitan areas, such as Dallas–Fort Worth and Houston, which are not recognized as endemic regions. That observation might reflect the large metropolitan population bases but could also indicate endemic region expansion in Texas related to increased temperatures and altered precipitation patterns (*5*). Travel to endemic regions, both in-state or out-of-state, might also contribute to the observed distribution. However, our dataset lacks travel history information, preventing distinction between locally acquired and travel-related infections.

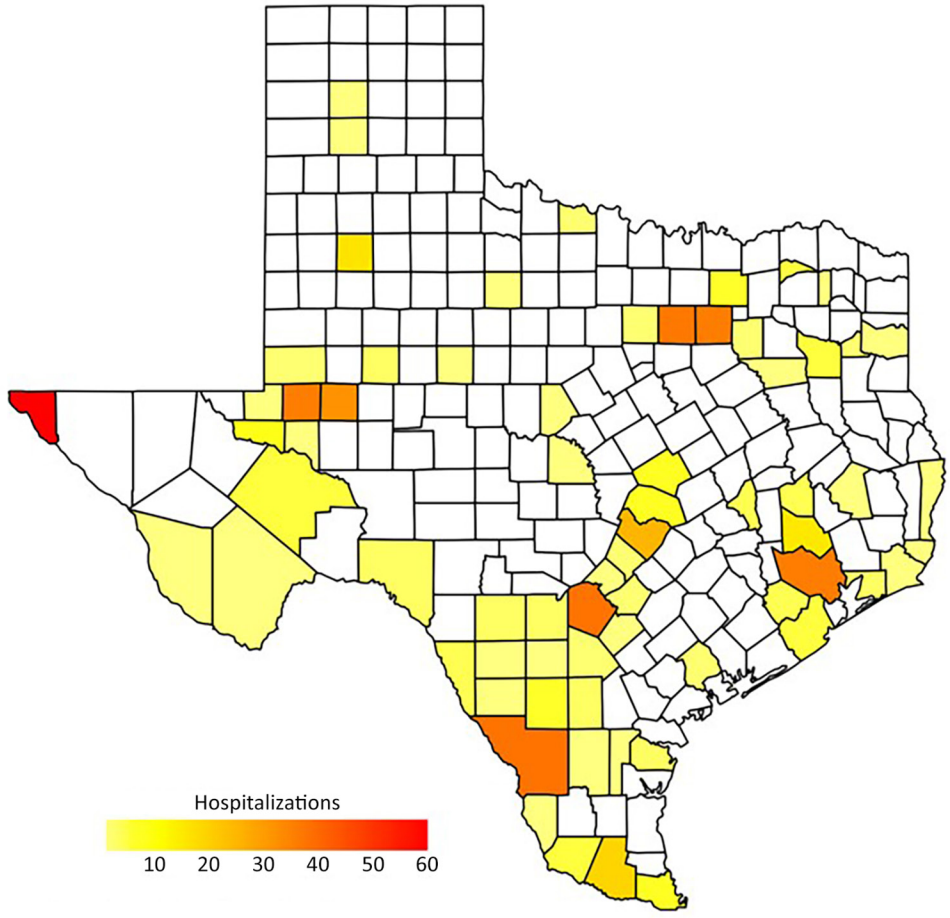

Figure 2. Geographic distribution of hospital visits for disseminated coccidioidomycosis, with and without coccidioidal meningitis, on the county level, Texas, USA, 2016–2023. All counties of Texas with reported cases (n = 96) were included in the study.

The predominance of working-age men in our study is consistent with other publications (*8*,*9*) and likely reflects occupational exposure in construction, agriculture, and oil and gas extraction (*10*,*11*). We also observed a high number of DCM hospitalizations among Hispanic patients (51.9%) in Texas, likely because they comprise 69.4% of the population in endemic west Texas counties (https://demographics.texas.gov/Projections/2024). Black patients, who comprise only 3.9% of the west Texas endemic region population, were disproportionately affected (20.0%) relative to their regional presence, consistent with previous studies documenting higher risk for DCM in African American populations (*8*) (https://demographics.texas.gov/Projections/2024). CM hospitalizations showed lower rates of diabetes, malnutrition, and renal disease compared with non-CM DCM, although the underlying mechanisms remain unclear.

Our study reveals the mortality, length of stay, and charges of hospitalizations among the DCM hospitalizations in Texas. DCM hospitalizations in Texas carry a large financial weight; >50% of patients are hospitalized for ≈2 weeks, and ≈50% required ICU admission. Comparing those outcomes with previously reported national data is limited by methodological and temporal differences. CM-associated mean hospitalization charges were 3.8-fold higher than the national cost estimate reported previously because of our use of unadjusted charges versus cost-to-charge ratio conversions, rather than true differences in resource utilization (*9*). Comparisons of clinical outcomes are further confounded by differing study periods and COVID-19 pandemic-related healthcare disruptions.

The first limitation of our study is that the sensitivity and specificity of ICD-10 codes for DCM and CM have not been evaluated. Coding errors might result in underestimation of cases. Recent validation work revealed 38.9% of cases coded as unspecified coccidioidomycosis represented disseminated disease (*12*). Second, TIPUDF suppression rules mask gender for patients with a diagnosis code determined to be of a sensitive nature, such as polysubstance use and HIV. That rule affected ≈21.0% (n = 115) study records, which might influence our results. Third, TIPUDF does not distinguish recurrent admissions of individual patients, resulting in duplicated data and overrepresentation of cases with severe disease requiring multiple visits. Fourth, readmission rates for DCM can reach 59%, particularly for CM (*13*). Therefore, our hospitalization-level mortality estimate of 10.5% likely underestimates true patient-level mortality. Finally, lack of mandatory reporting and limited provider awareness might contribute to underdiagnosis (*14*).

Our findings highlight the clinical and economic effects of DCM and CM hospitalizations in Texas and suggest possible expansion of endemic regions. Further economic analysis is warranted to elucidate the financial hardships of coccidioidomycosis on Texas residents. Enhanced surveillance, provider awareness, and targeted public health interventions are needed to address the evolving epidemiology of coccidioidomycosis in Texas.

Acknowledgments

We thank Sai Siva Mungara for her full support of this study and the project evaluating coccidioidomycosis in Odessa, Texas, USA.

All data used for this study are publicly available from the Texas Department of State Health Services.

About the Author

Dr. Szeto is an internal medicine resident physician at Texas Tech University Health Sciences Center at Permian Basin. His interests include fungal pulmonology, advanced lung diseases, and critical care.

References

1. Smith CE, Beard RR. Varieties of coccidioidal infection in relation to the epidemiology and control of the diseases. Am J Public Health Nations Health. 1946;36:1394–402. https://doi.org/10.2105/AJPH.36.12.1394
2. Ampel NM. New perspectives on coccidioidomycosis. Proc Am Thorac Soc. 2010;7:181–5. https://doi.org/10.1513/pats.200907-080AL
3. Crum NF. Coccidioidomycosis: a contemporary review. Infect Dis Ther. 2022;11:713–42. https://doi.org/10.1007/s40121-022-00606-y
4. Centers for Disease Control and Prevention. Reportable fungal diseases by state. [cited 2026 Feb 15]. https://www.cdc.gov/fungal/php/case-reporting
5. Mayfield H, Davila V, Penedo E. Coccidioidomycosis-related hospital visits, Texas, USA, 2016–2021. Emerg Infect Dis. 2024;30:882–9. https://doi.org/10.3201/eid3005.231624
6. Pena-Ruiz MA, Meza AD, Mulla ZD. Coccidioidomycosis infection in a predominantly Hispanic population. Ann N Y Acad Sci. 2007;1111:122–8. https://doi.org/10.1196/annals.1406.038
7. Dobos RR, Benedict K, Jackson BR, McCotter OZ. Using soil survey data to model potential Coccidioides soil habitat and inform valley fever epidemiology. PLoS One. 2021;16:e0247263. https://doi.org/10.1371/journal.pone.0247263
8. Seitz AE, Prevots DR, Holland SM. Hospitalizations associated with disseminated coccidioidomycosis, Arizona and California, USA. Emerg Infect Dis. 2012;18:1476–9. https://doi.org/10.3201/eid1809.120151
9. Coleman CI, Donovan F, Miriyapalli L, Shan R, Lovelace B. Burden of hospitalization for coccidioidal meningitis: an analysis of the national inpatient sample, 2019–2021. Open

Forum Infect Dis. 2024;11:ofae706. https://doi.org/10.1093/ofid/ofae706
10. Peterson C, Chu V, Lovelace J, Almekdash MH, Lacy M. Coccidioidomycosis cases at a regional referral center, west Texas, USA, 2013–2019. Emerg Infect Dis. 2022;28:848–51. https://doi.org/10.3201/eid2804.211912
11. Rosenstein NE, Emery KW, Werner SB, Kao A, Johnson R, Rogers D, et al. Risk factors for severe pulmonary and disseminated coccidioidomycosis: Kern County, California, 1995–1996. Clin Infect Dis. 2001;32:708–15. https://doi.org/10.1086/319203
12. Coleman CI, Danese S, Ulloa J, Bresnik M, Lovelace B, Donovan F. Misuse of the unspecified coccidioidomycosis diagnosis code: an audit of electronic health records. Med Mycol. 2025;63:myaf091. https://doi.org/10.1093/mmy/myaf091
13. Sivasubramanian G, Kadakia S, Kim JM, Pervaiz S, Yan Y, Libke R. Challenges in the long-term management of patients with coccidioidal meningitis: a retrospective analysis of treatment and outcomes. Open Forum Infect Dis. 2023;10:ofad243. https://doi.org/10.1093/ofid/ofad243
14. Donovan FM, Wightman P, Zong Y, Gabe L, Majeed A, Ynosencio T, et al. Delays in coccidioidomycosis diagnosis and associated healthcare utilization, Tucson, Arizona, USA. Emerg Infect Dis. 2019;25:1745–7. https://doi.org/10.3201/eid2509.190023

Address for correspondence: Chun Ho Szeto, Department of Internal Medicine, Texas Tech University Health Science Center Permian Basin, 701 West 5th Street, Suite 3106, Odessa, TX 79763, USA; email: chun-ho.szeto@ttuhsc.edu

Caballeronia Bacteremia in Children with Cancer, United States

Heather L. Glasgow, Sara M. Federico, Raul C. Ribiero, Elisabeth E. Adderson

Caballeronia spp. are gram-negative bacteria belonging to the Burkholderiaceae family, commonly found in the environment and in association with plants and animals. However, the bacteria are an uncommon cause of human infection. We describe *Caballeronia* bacteremia in 2 children with cancer in Tennessee, USA.

Burkholderiaceae is a large and heterogeneous bacterial group, ubiquitous in the environment and animal microbiomes, including plant and animal endophytes, nitrogen-fixing symbionts, and plant and animal pathogens (*1*–*3*). Analysis of 16S rRNA and conserved sequence insertion/deletions split the group into 7 distinct clades, including the new genus *Caballeronia*, represented by type species *C. glathei* (*1*–*4*). Named after Mexican microbiologist Jesús Caballero-Mellado, *Caballeronia* are gram-negative nonsporulating oval or rod-shaped cells that occur singly, in pairs, or in short chains. They can grow on tryptone soy and occasionally on MacConkey agar. Whereas members of the *Burkholderia* genus are established human pathogens, *Caballeronia* spp. are not (*2*,*3*). Two strains of *C. concitans* isolated from lung tissue and blood and 1 of *C. turbans* isolated from pleural fluid have been characterized phenotypically, but the clinical details of those or other infections have not been previously reported (*1*,*5*). We describe *Caballeronia* bacteremia in 2 children with cancer in Tennessee, USA.

Author affiliations: St. Jude Children's Research Hospital, Memphis, Tennessee, USA (H.L. Glasgow, S.M. Federico, R.C. Ribiero, E.E. Adderson); St. Jude Children's Research Hospital Graduate School of Biomedical Sciences, Memphis (S.M. Federico, R.C. Ribiero, E.E. Adderson); University of Tennessee Health Science Center, Memphis (S.M. Federico, R.C. Ribiero, E.E. Adderson)

DOI: https://doi.org/10.3201/eid3206.260342

The Cases

Case 1 was in a 3-year-old boy with neuroblastoma who was admitted to St. Jude Children's Research Hospital (Memphis, TN, USA) with a fever of 39.7°C, chills, tachycardia, and hypotension. At the time of hospitalization, he had completed chemotherapy, had undergone resection of his primary tumor and autologous hematopoietic stem-cell transplant, and was receiving radiation therapy to his abdomen. A double-lumen tunneled central venous catheter (CVC) had been placed 15 months earlier. He had a history of catheter-associated bloodstream infections caused by *Escherichia coli* and *Staphylococcus aureus* bacteremia, both successfully treated with antibacterial drugs.

His physical examination was remarkable for pallor, an ill appearance, tachycardia (heart rate 192 beat/min), hypotension (blood pressure 63/51 mm Hg), and a delayed capillary refill of 4–5 seconds. Physical examination showed no focal findings. His leukocyte count was 2.67 × 10^3 cells/mm^3 (reference range 5.60–17.00 × 10^3 cells/mm^3), and absolute neutrophil count (ANC) was 1,730/mm^3 (reference range 1,500–8,500/mm^3). Findings from a complete metabolic panel were unremarkable. Blood cultures were obtained, and intravenous fluids, ceftriaxone, and vancomycin were administered. The patient's vital signs promptly normalized, and his fever resolved.

Elongated gram-negative bacilli were identified in blood cultures obtained from 1 lumen of the central line after 35.11 incubation and a peripheral vein at 36.17 hours of incubation. Eplex BCID-GN multiplex PCR (Roche, https://www.roche.com) and Accelerate Pheno BC Kit (Accelerate Diagnostics, https://acceleratediagnostics.com) did not identify any organisms. Subcultures grew on blood and chocolate agar but not on MacConkey agar,

raising concern for a potential biothreat agent. The Gram stain morphology was consistent with *Burkholderia* spp. but not *Brucella*, *Francisella*, or *Yersinia* spp. Rapid biochemical testing showed the isolate was weakly catalase positive, urea negative, and oxidase positive. A zone of inhibition around a polymyxin B disk ruled out *Burkholderia mallei* and *B. pseudomallei*. Matrix-assisted laser desorption/ionization time-of-flight (MALDI-TOF) mass spectrometry by VITEK MS (bioMérieux, https://www.biomerieux.com) produced no identification. VITEK 2 (bioMérieux) automated biochemical identification cards produced an initial identification of *Burkholderia gladioli* with a confidence score of 89%, which was below the acceptable threshold. Repeat testing from chocolate agar produced no identification but from blood agar produced an identification of *Acinetobacter lwoffii* (confidence score 99%). However, reference laboratory testing (Mayo Clinic Laboratories, Rochester, MN, USA) identified *Caballeronia glathei* by MALDI-TOF mass spectrometry. The identification was confirmed by bacterial whole genome sequencing, as previously described (*6*), and species identification with SpeciesFinder-2.0 (Center for Genomic Epidemiology, https://cge.food.dtu.dk/services/SpeciesFinder). The isolate failed to grow on antimicrobial susceptibility test media.

Additional blood cultures obtained on the second and fourth hospital days were sterile, as was a culture of the patient's urine. The CVC was retained because the differential time-to-positivity suggested it was not a source of infection. Vancomycin was discontinued after 48 hours, and the patient completed a 10-day course of ceftriaxone.

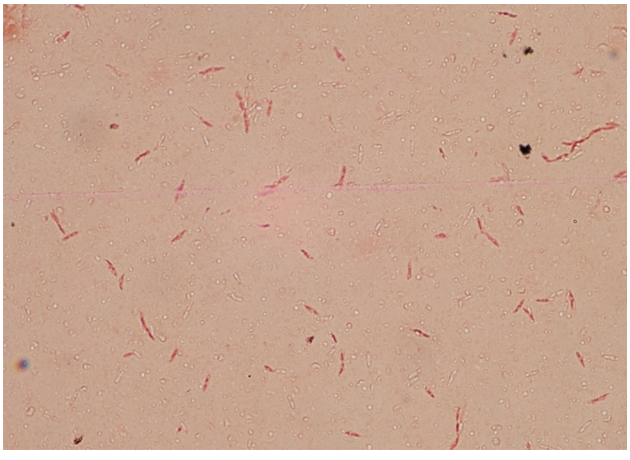

Figure. Gram stain of isolate from case 2 in report of 2 cases of *Caballeronia* bacteremia in children with cancer, United States. Staining shows a gram-negative bacillus in pairs and chains with tapered ends and possible endospores. Original magnification ×100.

Case 2 was in a 6-year-old boy with blastic plasmacytoid dendritic cell neoplasm who was admitted to St. Jude Children's Research Hospital with a history of a fever of 38.2°C at home and loose stools. He was receiving an individualized chemotherapy protocol and had no prior complications from that therapy. A double-lumen CVC had been placed 5 months previously. On evaluation, he was afebrile and well-looking. He received a dose of ceftriaxone and was discharged but was recalled and admitted to hospital the following day when growth was detected in blood cultures (both lumens, at 19.10 and 26.42 hours of incubation). No concurrent blood cultures from a peripheral vein were obtained.

Physical examination at admission was unremarkable, and he had no complaints. His leukocyte count was 1.2 × 10^3 cells/mm^3 (reference range 4.40–10.60 × 10^3 cells/mm^3) and ANC was 1,281/mm^3 (reference range 1,500–7,600/mm^3). Findings of a complete metabolic panel were unremarkable. Additional blood cultures were obtained and cefepime was administered. Later that day, fever recurred (38.1°C), hypotension (blood pressure 82/45 mm Hg) and neutropenia (ANC 334/mm^3) were noted, and meropenem and trimethoprim/sulfamethoxazole (TMP/SMX) were substituted for cefepime. The patient's vital signs promptly normalized.

A blood culture broth smear revealed gram-negative bacilli with tapered ends and possible endospores (Figure). Microbiologic characteristics were as described for case 1, with no growth on MacConkey agar. Rapid biochemical testing was negative for oxidase, weakly positive for catalase, and urea positive. After biothreat was ruled out, the reference laboratory testing identified the organism as *Caballeronia* spp. (undetermined species) by 16S ribosomal RNA gene sequencing. The isolate was susceptible to all tested antimicrobial agents, including piperacillin/tazobactam (MIC ≤8/4 μg/mL), aztreonam (MIC ≤4 μg/mL), ceftazidime (MIC ≤4 μg/mL), cefepime (MIC ≤2 μg/mL), meropenem (MIC 1 μg/mL), ciprofloxacin (MIC 0.5 μg/mL), levofloxacin (MIC ≤0.5 μg/mL), tobramycin (MIC ≤1 μg/mL), gentamicin (MIC ≤1 μg/mL), amikacin (MIC ≤1 μg/mL), and TMP/SMX (MIC ≤0.5/9.5 μg/mL).

Subsequent blood cultures were positive for the same organism on the patient's second hospital day (1 lumen only); cultures were sterile thereafter. The CVC was retained because of the patient's prompt clinical response and the rapid sterilization of blood cultures. He completed a 10-day course of meropenem and TMP/SMX. Bacterial identification and

antimicrobial susceptibility test results were not available until antimicrobial therapy was completed.

Conclusions

A clear source of these patients' infections was not found. Physical examination did not reveal a focus of infection that could have resulted in bacteremia. Differential time-to-positivity suggested the second patient had a catheter-related bloodstream infection; contamination of medical devices by Burkholderiaceae has been reported (*7*). Given that the human gastrointestinal microbiome includes *Caballeronia*, infection might have been related to gastrointestinal barrier dysfunction and translocation of bacteria, a route suggested by diarrhea in case 2. Consistent with that hypothesis, some patients with COVID-19 and gastrointestinal symptoms were reported to have elevated markers of gut permeability and plasma microbiomes that contain *Caballeronia* spp. and other gut flora (R. Prasad et al., unpub. data, https://doi.org/10.1101/2021.04.06.438634). Because the 2 cases occurred years apart, healthcare-associated transmission was not suspected.

As in the cases we describe, identification of *Caballeronia* spp. is unlikely to be made with current standard methods available in most clinical laboratories, and misidentification as other *Burkholderia* or *Acinetobacter* spp. could occur. *Caballeronia* spp. are absent from current VITEK MS (bioMérieux) or MALDI Biotyper (Bruker Daltonics) Food and Drug Administration–cleared databases; however, they can be identified by MALDI-TOF mass spectrometry with a custom database (*8*).

The optimal treatment for infections caused by *Caballeronia* spp. is unknown. Administration of broad-spectrum antimicrobial drugs led to clinical and microbiological resolution of the patients' infections; in case 2, in vitro susceptibility to all antimicrobial drugs tested was confirmed. Of note, both patients' ANC results were within reference ranges or transiently low; the absence of severe neutropenia might have contributed to a successful outcome. This report of 2 *Caballeronia* bacteremia cases serves as a reminder that emerging pathogens continue to pose clinical challenges in severely immunocompromised patients.

Acknowledgments

The authors thank Carolyn Hewitt for providing images and Jessica Brazelton for isolate sequencing.

About the Author

Dr. Glasgow is director of Bacteriology, Mycology, and Infectious Diseases Serology at St. Jude Children's Research Hospital, Memphis. Her research interests are in developing and evaluating new microbiologic diagnostics.

References

1. Dobritsa AP, Linardopoulou EV, Samadpour M. Transfer of 13 species of the genus *Burkholderia* to the genus *Caballeronia* and reclassification of *Burkholderia jirisanensis* as *Paraburkholderia jirisanensis* comb. nov. Int J Syst Evol Microbiol. 2017;67:3846–53. https://doi.org/10.1099/ijsem.0.002202
2. Dobritsa AP, Samadpour M. Transfer of eleven species of the genus *Burkholderia* to the genus *Paraburkholderia* and proposal of *Caballeronia* gen. nov. to accommodate twelve species of the genera *Burkholderia* and *Paraburkholderia*. Int J Syst Evol Microbiol. 2016;66:2836–46. https://doi.org/10.1099/ijsem.0.001065
3. Vandamme P, De Brandt E, Houf K, Salles JF, Dirk van Elsas J, Spilker T, et al. *Burkholderia humi* sp. nov., *Burkholderia choica* sp. nov., *Burkholderia telluris* sp. nov., *Burkholderia terrestris* sp. nov. and *Burkholderia udeis* sp. nov.: *Burkholderia glathei*-like bacteria from soil and rhizosphere soil. Int J Syst Evol Microbiol. 2013;63:4707–18. https://doi.org/10.1099/ijs.0.048900-0
4. Mullins AJ, Mahenthiralingam E. The hidden genomic diversity, specialized metabolite capacity, and revised taxonomy of *Burkholderia* sensu lato. Front Microbiol. 2021;12:726847. https://doi.org/10.3389/fmicb.2021.726847
5. Peeters C, Meier-Kolthoff JP, Verheyde B, De Brandt E, Cooper VS, Vandamme P. Phylogenomic study of *Burkholderia glathei*-like organisms, proposal of 13 novel *Burkholderia* species and emended descriptions of *Burkholderia sordidicola*, *Burkholderia zhejiangensis*, and *Burkholderia grimmiae*. Front Microbiol. 2016;7:877. https://doi.org/10.3389/fmicb.2016.00877
6. Hakim H, Glasgow HL, Brazelton JN, Gilliam CH, Richards L, Hayden RT. A prospective bacterial whole-genome-sequencing-based surveillance programme for comprehensive early detection of healthcare-associated infection transmission in paediatric oncology patients. J Hosp Infect. 2024;143:53–63. https://doi.org/10.1016/j.jhin.2023.10.015
7. Li B, Hu Y, Wang Y, Zhang C, Wang Z, Peng X, et al. Periodic detection and disinfection maintenance of dental unit waterlines in dental simulation head model laboratories. Sci Rep. 2025;15:5234. https://doi.org/10.1038/s41598-025-89010-3
8. Fergusson CH, Coloma JMF, Valentine MC, Haeckl FPJ, Linington RG. Custom matrix-assisted laser desorption ionization-time of flight mass spectrometric database for identification of environmental isolates of the genus *Burkholderia* and related genera. Appl Environ Microbiol. 2020;86:e00354-20. https://doi.org/10.1128/AEM.00354-20

Address for correspondence: Elisabeth Adderson, St. Jude Children's Research Hospital, Rm E5008, 262 Danny Thomas Pl, Memphis, TN 38105, USA; email: elisabeth.adderson@stjude.org

Phenotypic and Genomic Characterization of Antimicrobial-Resistant *Neisseria gonorrhoeae* of Public Health Concern

Johan H. Melendez

The increasing rates of antimicrobial resistance (AMR) in *Neisseria gonorrhoeae* globally pose a major threat to the management of gonorrhea (*1*). In the United States and many other developed countries, ceftriaxone, a third-generation cephalosporin, is the recommended therapy for the treatment of uncomplicated gonorrhea (*2*,*3*). In Australia, dual treatment with ceftriaxone and azithromycin is currently recommended (*4*). To mitigate the threat of AMR on public health, surveillance of AMR in *N. gonorrhoeae* is critical for monitoring antimicrobial susceptibility trends, assessing emergence of AMR, and guiding treatment recommendations (*5*).

In this issue, Walker et al. (*4*) describe the results of an integrated phenotypic, epidemiologic, and genomic analysis of *N. gonorrhoeae* isolates collected in New South Wales (NSW), Australia, as part of a comprehensive surveillance program during January 2022–December 2024. The isolates were subjected to antimicrobial susceptibility testing and classified as *N. gonorrhoeae* of public health concern because they displayed either decreased susceptibility (DS) to ceftriaxone (MIC ≥0.125 mg/L) or high-level resistance (HLR) to azithromycin (MIC ≥256 mg/L). In NSW, detection of an *N. gonorrhoeae* isolate of public health concern prompts a public health response, including collection of samples from each site of infection for test-of-cure (TOC) and enhanced surveillance protocols for identifying treatment failures, informing of emerging resistance trends, and enhancing AMR surveillance. That type of systematic monitoring for treatment failures helps enhance AMR surveillance practices and is a key component of the World Health Organization global action plan to control the spread and impact of AMR in *N. gonorrhoeae* (*5*).

In the analysis by Walker et al., of the 54 patients with ceftriaxone DS *N. gonorrhoeae*, 46 (85.2%) returned for TOC; of those, 2 (4.3%) returned a positive TOC result by nucleic acid amplification test (NAAT) for *N. gonorrhoeae* ≥2 weeks after treatment, which is suggestive of treatment failure. The high return rate for follow-up TOC reported in this study is notable, considering that other studies have reported lower return rates of 41%–64% (*6*–*9*). In addition, the prospective evaluation and identification of isolates of public health concern helped to identify treatment failures which might otherwise have remained undiagnosed, suggesting that the targeted public health response approach might be a suitable intervention to identify persons requiring retreatment and prevent onward transmission of ceftriaxone DS *N. gonorrhoeae*.

Despite increasing rates of ceftriaxone-resistant *N. gonorrhoeae* globally (*10*), reporting and confirmation of treatment failure cases remain low; possible causes are inconsistent treatment regimens, limited access to culture diagnostics, and heterogenous definitions of treatment failures (*11*). Furthermore, ceftriaxone resistance, for which MIC breakpoints have not been clearly or uniformly defined globally, might not always result in treatment failure (*11*), which suggests that current ceftriaxone resistance breakpoints might need to be reexamined (*12*). Of note, the Clinical and Laboratory Standards Institute guidelines recommend classifying *N. gonorrhoeae* isolates with ceftriaxone MIC ≤0.125 mg/L as susceptible and those with MIC ≥0.5 mg/L as resistant (*13*). In the study by Walker et al., of the patients with ceftriaxone DS (MIC ≥0.125 mg/L) who underwent TOC, 44/46 (95.7%) returned a negative NAAT result. That finding suggests that dual therapy with ceftriaxone and azithromycin was effective in eradicating almost all

Author affiliation: Division of Infectious Diseases, Department of Medicine, Johns Hopkins University School of Medicine, Baltimore, Maryland, USA

DOI: https://doi.org/10.3201/eid3206.260310

infections caused by ceftriaxone DS *N. gonorrhoeae* but does not conclusively demonstrate the clinical significance of the ≥0.125 mg/L breakpoint for defining ceftriaxone DS or resistance.

The increasing rates of ceftriaxone-resistant *N. gonorrhoeae* globally have been driven by surges of *N. gonorrhoeae* harboring the mosaic *penA*-60 allele in the Asia Pacific region (*10*). In the study by Walker et al., 45% of ceftriaxone DS *N. gonorrhoeae* isolates harbored the *penA*-60 allele; that finding is consistent with global reports that the *penA*-60 allele is the most common genetic variation associated with ceftriaxone DS and resistance (*10*,*14*). Network analysis revealed 5 different ceftriaxone DS clusters, including a large cluster of 13 isolates, which suggested local transmission of ceftriaxone DS *N. gonorrhoeae*. The study also provided evidence of overseas acquisition of ceftriaxone DS *N. gonorrhoeae* and local transmission of those overseas-acquired infections, highlighting the possibility of further emergence of ceftriaxone resistance in Australia through importation of resistant strains.

Walker et al. also reported on cases of *N. gonorrhoeae* with azithromycin HLR, which were primarily from nonheterosexual patients (95%), and patients with a history of sexually transmitted infections (70%); cases were approximately evenly distributed across the anatomic sites (urogenital tract, rectum, and pharynx). Of note, whereas genomic analysis identified 2 separate but connected clusters (17/40 cases) of *N. gonorrhoeae* with HLR, many (19 [47.5%]) cases lacked genetic relatedness, suggesting that different strains of *N. gonorrhoeae* with azithromycin HLR are circulating in NSW, Australia. That finding, together with the post–COVID-19 (2022–2024) increase of gonorrhea cases in NSW caused by azithromycin HLR *N. gonorrhoeae*, is consistent with the evolving global epidemiology of *N. gonorrhoeae* with azithromycin HLR (*15*). Of note, *N. gonorrhoeae* multilocus sequence type (MLST) ST9363, which was the second most common MLST (22.5%, 9/40) of cases with HLR reported by Walker et al, is the most widely disseminated ST globally in *N. gonorrhoeae* with HLR to azithromycin (*15*). Although azithromycin HLR was not associated with treatment failures in that study, the increasing rates of *N. gonorrhoeae* with this phenotype is an example of the rapid and constant evolution of AMR in *N. gonorrhoeae*.

The public health approach described by Walker et al. involving phenotypic, genotypic, and epidemiologic analysis of *N. gonorrhoeae* of public health concern is a practical and effective tool to identify treatment failures, prevent further emergence of ceftriaxone resistance, and ultimately help to preserve the clinical utility of ceftriaxone. Additional public health approaches, including monitoring of treatment failures in pharyngeal gonorrhea, which can be caused by ceftriaxone-susceptible *N. gonorrhoeae*, are necessary to prevent onward transmission of antimicrobial-resistant gonorrhea. Culture-based characterization of AMR in *N. gonorrhoeae* needs to be expanded to establish ceftriaxone resistance breakpoints. Finally, clinical trials are warranted not only to determine the efficacy of ceftriaxone in the era of increasing ceftriaxone resistance but also to better define the relationship between AMR in *N. gonorrhoeae* and treatment failures.

About the Author

Dr. Melendez is an assistant professor of medicine in the Division of Infectious Diseases at The Johns Hopkins School of Medicine. His main research interests are focused on the development and translation of novel approaches for characterization of bacterial pathogens, with an emphasis on antimicrobial-resistant *Neisseria gonorrhoeae*.

References

1. Unemo M, Seifert HS, Hook EW III, Hawkes S, Ndowa F, Dillon JR. Gonorrhoea. Nat Rev Dis Primers. 2019;5:79–101. https://doi.org/10.1038/s41572-019-0128-6
2. St Cyr S, Barbee L, Workowski KA, Bachmann LH, Pham C, Schlanger K, et al. Update to CDC's treatment guidelines for gonococcal infection, 2020. MMWR Morb Mortal Wkly Rep. 2020;69:1911–6. https://doi.org/10.15585/mmwr.mm6950a6
3. World Health Organization. 2024 Updated recommendations for the treatment of *Neisseria gonorrhoeae*, *Chlamydia trachomatis*, and *Treponema pallidum* (syphilis) and new recommendations on syphilis testing and partner services. 2024 [cited 2026 Feb 12]. https://www.who.int/publications/i/item/9789240090767.
4. Walker LJ, Van Hal S, Li C, Nigro SJ, Donnan E, Ryder N, et al. Antimicrobial-resistant Neisseria gonorrhoeae of public health concern, New South Wales, Australia, 2022–2024. Emerg Infect Dis. 2026;6:905–13. https://doi.org/10.3201/eid3206.251399
5. World Health Organization. Global action plan to control the spread and impact of antimicrobial resistance in *Neisseria gonorrhoeae*. 2012 [cited 2026 Feb 12]. http://www.who.int/reproductivehealth/publications/rtis/9789241503501
6. Schlanger K, Mauk K, Learner ER, Schillinger JA, Nishiyama M, Kohn R, et al. Test of cure return rate and test positivity, strengthening the US response to resistant gonorrhea, United States, 2018–2019. Sex Transm Dis. 2021; 48:S167–73. https://doi.org/10.1097/OLQ.0000000000001539
7. Jenks JD, Hester L, Ryan E, Stancil C, Hauser Q, Zitta JP, et al. Test-of-cure after treatment of pharyngeal gonorrhea in Durham, North Carolina, 2021–2022. Sex Transm Dis. 2022;49:677–81. https://doi.org/10.1097/OLQ.0000000000001679
8. Quilter LAS, Horowitz R, Hall K, Bardier C, Bell J, Bergstrom AA, et al. Routine pharyngeal gonorrhea test of cure: is it an effective cephalosporin-resistant gonorrhea

control strategy? Sex Transm Dis. 2025;52:407–14. https://doi.org/10.1097/OLQ.0000000000002157
9. Blanco P, Meheust C, Gibaud-Papin S, Pasquier E, Corvec S, Bernier C. Culture yield and test of cure utility in pharyngeal *Neisseria gonorrhoeae* infections. Sex Transm Infect. 2025;102:59–60.
10. Xiu L, Zhang L, Peng J. Surge in ceftriaxone-resistant *Neisseria gonorrhoeae* FC428-like strains, Asia-Pacific region, 2015–2022. Emerg Infect Dis. 2024;30:1683–6. https://doi.org/10.3201/eid3008.240139
11. Fagan L, Alexander S, Fifer H. The invisible tide of *Neisseria gonorrhoeae* treatment failures: a review and commentary. Clin Infect Dis. 2026;81:S223–30. https://doi.org/10.1093/cid/ciaf532
12. Miari VF, Mosoff JM, Chico RM. Minimum inhibitory concentrations of extended-spectrum cephalosporins: a systematic review and meta-analysis of *Neisseria gonorrhoeae* treatment failures. Sex Transm Dis. 2025;52:279–84. https://doi.org/10.1097/OLQ.0000000000002116
13. Clinical Laboratory Standards Institute (CLSI). Performance standards for antimicrobial susceptibility testing; thirty-sixth informational supplement (M100-S36). Wayne (PA): The Institute; 2026.
14. Fifer H, Doumith M, Rubinstein L, Mitchell L, Wallis M, Singh S, et al. Ceftriaxone-resistant *Neisseria gonorrhoeae* detected in England, 2015–24: an observational analysis. J Antimicrob Chemother. 2024;79:3332–9. https://doi.org/10.1093/jac/dkae369
15. Melendez JH, Edwards VL, Muniz Tirado A, Hardick J, Mehta A, Aluvathingal J, et al. Local emergence and global evolution of *Neisseria gonorrhoeae* with high-level resistance to azithromycin. Antimicrob Agents Chemother. 2024;68:e0092724. https://doi.org/10.1128/aac.00927-24

Address for correspondence: Johan H. Melendez, Johns Hopkins School of Medicine, Mason F. Lord Building, 5200 Eastern Ave, Rm 675, Baltimore, MD 21224, USA; email: jmelend3@jhmi.edu

Who is this person and what did he accomplish?

Here is a clue: He devised high-powered microscopes that extended our perception beyond the naked eye to the microbial world.

Who is he?

1. Robert Hooke
2. Jan Swammerdam
3. Thomas Molyneux
4. Antony van Leeuwenhoek
5. Nicolaas Hartsoeker

Decide first, then see next page for the answer.

Antony van Leeuwenhoek, Pioneer of the Microscopic World

Robert Gaynes

This is a painting of Antony van Leeuwenhoek (1632–1723), who is sometimes credited with inventing the microscope; he did not. However, he did markedly enhance it, devising a high-powered microscope that opened up the microscopic world. Others have seen deeper into this tiny domain, but van Leeuwenhoek was the first to witness it. He extended our perception beyond what could be seen with the naked eye to directly observe an entirely new universe.

Antony van Leeuwenhoek was born in 1632 in a small village in Holland named Delft. That was also the same town and year that Dutch painter Jan Vermeer entered the world. Their lives would take different paths but intermingle (*1*).

At age 16, van Leeuwenhoek went to Amsterdam and learned the drapery business. After about 6 years in Amsterdam, van Leeuwenhoek returned to Delft, where he began a reasonably successful drapery business. In 1660, he was appointed to a local government post that he held for 39 years. That position led van Leeuwenhoek to be appointed as official receiver of the estate of the painter Jan Vermeer when he died at age 43. Art historians have hypothesized that van Leeuwenhoek may have been the subject in 2 of Vermeer's paintings—*The Geographer* and *The Astronomer*.

The salary from his local government post, along with an inheritance after his mother's death in 1664, enabled van Leeuwenhoek to pursue interests outside his drapery business. Notably, van Leeuwenhoek began crafting lenses that he placed between 2 metal plates. With this handheld microscope, van Leeuwenhoek began to examine all sorts of objects. So-called microscopes up to that point were essentially magnifying glasses, capable of enlarging 20 times. van Leeuwenhoek created single-lens microscopes that could magnify 270 times and some as much as 500 times, a magnification far greater than that of any previous microscope. His skill at producing high-quality lenses for microscopes eventually caught the attention of the secretary of the British Royal Society, Henry Oldenburg, who was impressed. For the next 50 years, until his death, van Leeuwenhoek sent hundreds of letters describing his investigations to the Royal Society.

Figure. Antony van Leeuwenhoek (1632–1723). Painting by Jan Verkolje (1680–1686). Public domain image. Source: Wikimedia Commons.

van Leeuwenhoek's observations on single-celled organisms began in 1674 when he started looking through his microscope at pond water. In a letter to Oldenburg, he described what he saw:

> . . . there were many small green globules. Among these there were, besides, very many little animalcules, some were roundish, while others, a bit bigger, consisted of an oval (*2*).

Author affiliation: Emory University School of Medicine, Atlanta, Georgia, USA

DOI: https://doi.org/10.3201/eid3206.260531

van Leeuwenhoek described single-cell protozoa that probably included *Giardia*, judging from his sketches, making him the first man to ever see creatures that small. Some questioned such a claim. In 1680, the Royal Society sent a team to Delft and fully corroborated van Leeuwenhoek's observations. Modern-day scientists have confirmed van Leeuwenhoek's findings, even using some of his surviving microscopes (*3*).

In September 1683, van Leeuwenhoek reported to the Royal Society what he had seen in plaque from a healthy person's mouth:

> With great wonder, that, in the said matter there were many very little living animalcules very prettily a-moving. The biggest sort had the shape of [a rod]: these had a very strong and swift motion and shot through the water like a pike does through water. These were most always few in number. The second sort had the shape of [a small rod]. These often spun round like a top, and every now and then took a [spiral] course and were far more in number (*3*).

These words are the first known descriptions of bacteria. For 40 more years, he continued his correspondence with the Royal Society that published his letters, making him well known in Europe.

van Leeuwenhoek's simple microscopes produced wondrous images but were exceedingly difficult to use. The instrument was ≈3 inches (7.5 cm) long, consisting of 2 metal plates, a lens placed in a hole made in the plates, and, on one side, a small metal pointer on which the specimen was held. The user would look through the opposite side of the device with a light source behind the specimen. The focal length of the lens was so short that the user needed to place an eye so close to the lens that the eyeball was nearly touching it. van Leeuwenhoek also kept his methods of producing the lenses secret, never teaching them to anyone. He had a businessman's mind and wanted to keep trade secrets on his microscope's lens formation and use. As he wrote to the Royal Society:

> My method for seeing the very smallest animalcules and minute eels, I do not impart to others; nor how to see very many animalcules at one time. That I keep for myself alone (*3*).

Whereas a new world of microorganisms had been revealed, van Leeuwenhoek did not make any connection between the microorganisms and disease. The bacteria that van Leeuwenhoek observed were in humans who were not ill. No one else in the scientific and medical communities of the time made any connection to microorganisms as pathogens either. Until the seat of disease was reassessed from a change in the balance of humors to our modern medical pathophysiologic approach, the existence of such microorganisms was only a curiosity of nature (*4*).

Despite van Leeuwenhoek's technical advance, the cumbersome instruments he created were difficult to use. van Leeuwenhoek's secrecy in fashioning lenses added to the limited use of microscopes for more than a century. Simple microscopes would eventually yield to compound microscopes when technical problems such as chromatic aberration were solved in the 19th Century. However, the limited interest in microscopy in the 17th and 18th Centuries cannot diminish van Leeuwenhoek's pioneering contributions that fundamentally changed the way we think of the living world.

References

1. Mitchell L. Delft neighbors: Vermeer and van Leeuwenhoek. Emerg Infect Dis. 2026;32.1033–1035
2. Dobell C. Antony van Leeuwenhoek and his little animals. New York: Harcourt, Brace and Company; 1932.
3. Ford BJ. Specimens from the dawn of microscopy. Biologist. 1981;28:180–1.
4. Gaynes R. Germ theory: medical pioneers in infectious diseases. Washington: John Wiley & Sons; 2023.

Address for correspondence: Robert Gaynes, Emory University School of Medicine, James B. Williams Medical Education Building, 100 Woodruff Cir, Atlanta, GA 30322, USA; email: rgaynes@emory.edu

Neisseria gonorrhoeae Sequence Type 16676 in Disseminated Infections, Minnesota, USA, 2025

Daniel Evans, Allison LaPointe, Christine Peel, Khalid Bo-Subait, Elizabeth Dufort, Jenell Stewart, John Kaiyalethe, Bradley Craft, Matthew Plumb, Bonnie Weber, Laura Bohnker-Voels, Kelly Pung, Alyssa Mondelli, Jacob Garfin, Sarah Namugenyi, Paula Snippes-Vagnone, M. Elizabeth Gyllstrom, Kathryn Como-Sabetti, Ruth Lynfield

Author affiliations: Health Protection Bureau, Minnesota Department of Health, St. Paul, Minnesota, USA (D. Evans, A. LaPointe, C. Peel, K. Bo-Subait, E. Dufort, J. Kaiyalethe, B. Craft, M. Plumb, B. Weber, L. Bohnker-Voels, K. Pung, A. Mondelli, J. Garfin, S. Namugenyi, P. Snippes-Vagnone, M.E. Gyllstrom, K. Como-Sabetti, R. Lynfield); University of Minnesota, Minneapolis, Minnesota, USA (J. Stewart); Hennepin Healthcare, Minneapolis (J. Stewart)

DOI: https://doi.org/10.3201/eid3206.260126

We summarize an outbreak investigation of *Neisseria gonorrhoeae* sequence type 16676 associated with disseminated gonococcal infections in Minnesota, USA, in 2025. This strain emerged rapidly, carried a plasmid with a tetracycline resistance gene, and encoded a *porB1a* allele. Prospective genomic surveillance enabled detection and epidemiologic investigation of this outbreak.

The sexually transmitted pathogen *Neisseria gonorrhoeae* can circulate from mucosal tissue at sites of exposure to other locations in the body, causing disseminated gonococcal infection (DGI) (*1*). In 2024, the Minnesota (USA) Department of Health initiated whole-genome sequencing (WGS) analysis of isolates from all DGI cases in the state (*2*). This article expands upon our previous study from 2024 (*2*).

In 2025, cases of DGI in Minnesota continued to occur at an elevated incidence rate compared with the 2020–2023 baseline. Minnesota state reporting rules require *N. gonorrhoeae* specimens from normally sterile sites to be submitted to the state public health laboratory. Analysis of those cases and linked specimens is considered enhanced surveillance and therefore deemed exempt from Institutional Review Board approval.

We performed WGS using the Illumina MiSeq, NextSeq, or MiSeq i100 platforms (https://www.illumina.com) and performed molecular epidemiologic analyses as previously described (*2*). Our genomic investigation showed that a new multilocus sequence type (ST), ST16676, emerged during the summer of 2025 (*3*,*4*). During June–September 2025, we sequenced 14 isolates from DGI cases whose genomes were assigned to ST16676. All 14 genomes encoded a *porB1a* allele, the tetracycline resistance gene *tet(M)*, the extended spectrum β-lactamase gene bla_{TEM}, a Type XIV nonmosaic *penA* allele, and a gonococcal genetic island sequence (Figure 1; Appendix Table, Figure 1, https://wwwnc.cdc.gov/EID/article/32/6/26-0126-App1.pdf) (*3*–*6*). Those genomes did not match any documented *N. gonorrhoeae* sequence type by antimicrobial resistance profiles (*5*). Long-read sequencing (Oxford Nanopore Technologies, https://nanoporetech.com) of 4 ST16676 isolates consistently resolved the acquired *tet(M)* and bla_{TEM} genes on separate plasmid sequences of 42kb and 5.6kb and the *porB1a* allele on the bacterial chromosome.

In October 2025, we performed a global comparison of those genomes to others in the National Center for Biotechnology Information Pathogen Detection database (https://www.ncbi.nlm.nih.gov/pathogens). That comparison grouped the genomes into a cluster (PDS000214546.4) with 12 other genomes (Appendix Figure 2). Analysis of those 26 genomes using the Dryad version 3.0 pipeline showed that the Minnesota DGI genomes ranged in genetic similarity to each other by 0–62 (median 6) single-nucleotide polymorphisms (SNPs) and to the other 12 genomes by 215–320 (median 248) SNPs (Figure 2) (Dryad, https://github.com/wslh-bio/dryad). An iterative time-scaled phylodynamic analysis of those genomes showed that 28 of 32 iterations converged at early May 2025, weeks before the first case-patient sought care, as an estimated time of a most recent common ancestor for all 14 Minnesota genomes (Appendix) (*7*).

Epidemiologists completed investigations of ST16676 DGI cases on the basis of findings from genomic surveillance. Of the 13 ST16676-infected case-patients interviewed, 12 (92.3%) resided within the Minneapolis-St. Paul-Bloomington metropolitan area; 11 (84.6%) were male and 2 (15.5%) female, and 9 (69.2%) were 15–44 years of age. Seven (53.8%) case-patients reported anonymous sexual encounters with multiple partners, 3 (23.1%) of whom reported substance use while doing so. Two (15.4%) reported having used doxycycline postexposure prophylaxis. Nine (69.2%) case-patients reported previous sexually transmitted infections; 4 (44.4%) reported gonorrhea and 5 (55.5%) reported HIV. Epidemiologic investigation confirmed a direct link between 2 cases whose isolates' genomes were genetically identical at 0 SNPs. The 14th case-patient, who refused interviews, had an isolate that was identical at 0 SNPs

to the 2 directly linked isolates, lived in an adjacent state, and received care for the infection in Minnesota.

Antimicrobial susceptibility test results were available in medical records of 10 (71.4%) of the 14 ST16676-infected patients. Consistent with results from *N. gonorrhoeae* sequence type by antimicrobial resistance and AMRFinderPlus analyses (*5*,*6*), all 10 isolates showed phenotypic resistance to tetracycline and ciprofloxacin and phenotypic susceptibility to ceftriaxone.

Prospective WGS detected the emergence of a tetracycline-resistant strain of *N. gonorrhoeae* that replaced the predominant DGI-associated strain from the previous year. The sudden emergence of a DGI-associated strain that carries both a *porB1a* allele (*8*) and a tetracycline resistance gene on a mobilizable plasmid poses epidemiologic concern, given the use of doxycycline postexposure prophylaxis to reduce potential illness and subsequent transmission risk

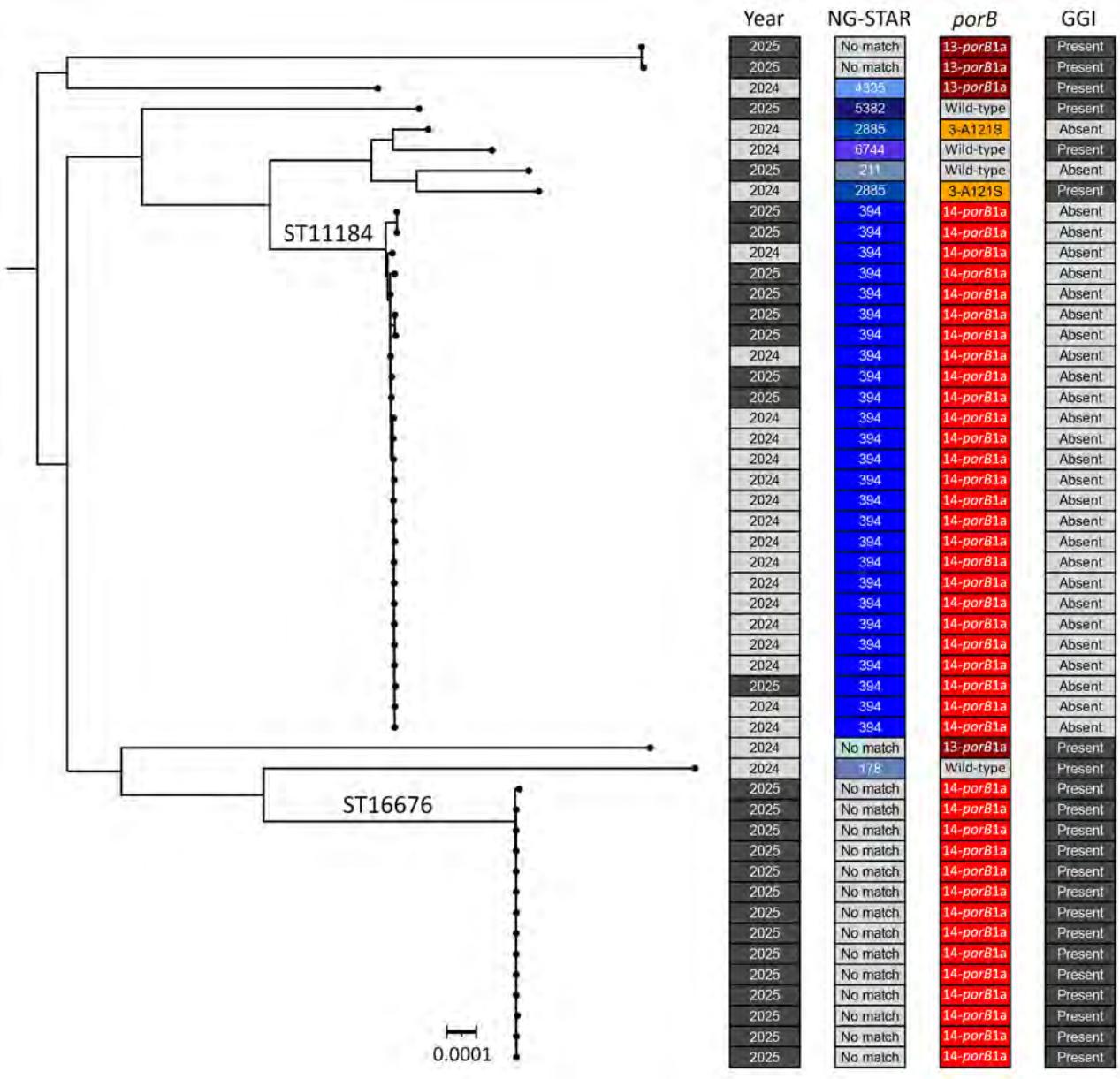

Figure 1. Midpoint-rooted phylogenetic tree constructed from an alignment of 1,626 core genes shared by 50 genomes of *Neisseria gonorrhoeae* isolates from study of outbreak of *N. gonorrhoeae* ST16676 among disseminated infections, Minnesota, USA, 2025. Annotations denote calendar year of specimen collection, *N. gonorrhoeae* sequence type by antimicrobial resistance (determined by using NG-STAR, https://ngstar.canada.ca), *porB* allele type, and presence of a GGI. Clades of genomes assigned to ST16676 and ST11184 are labeled on the tree. Scale bar represents substitutions per site. Figure was constructed using ITOL software (https://itol.embl.de). GGI, gonococcal genetic island; ST, sequence type.

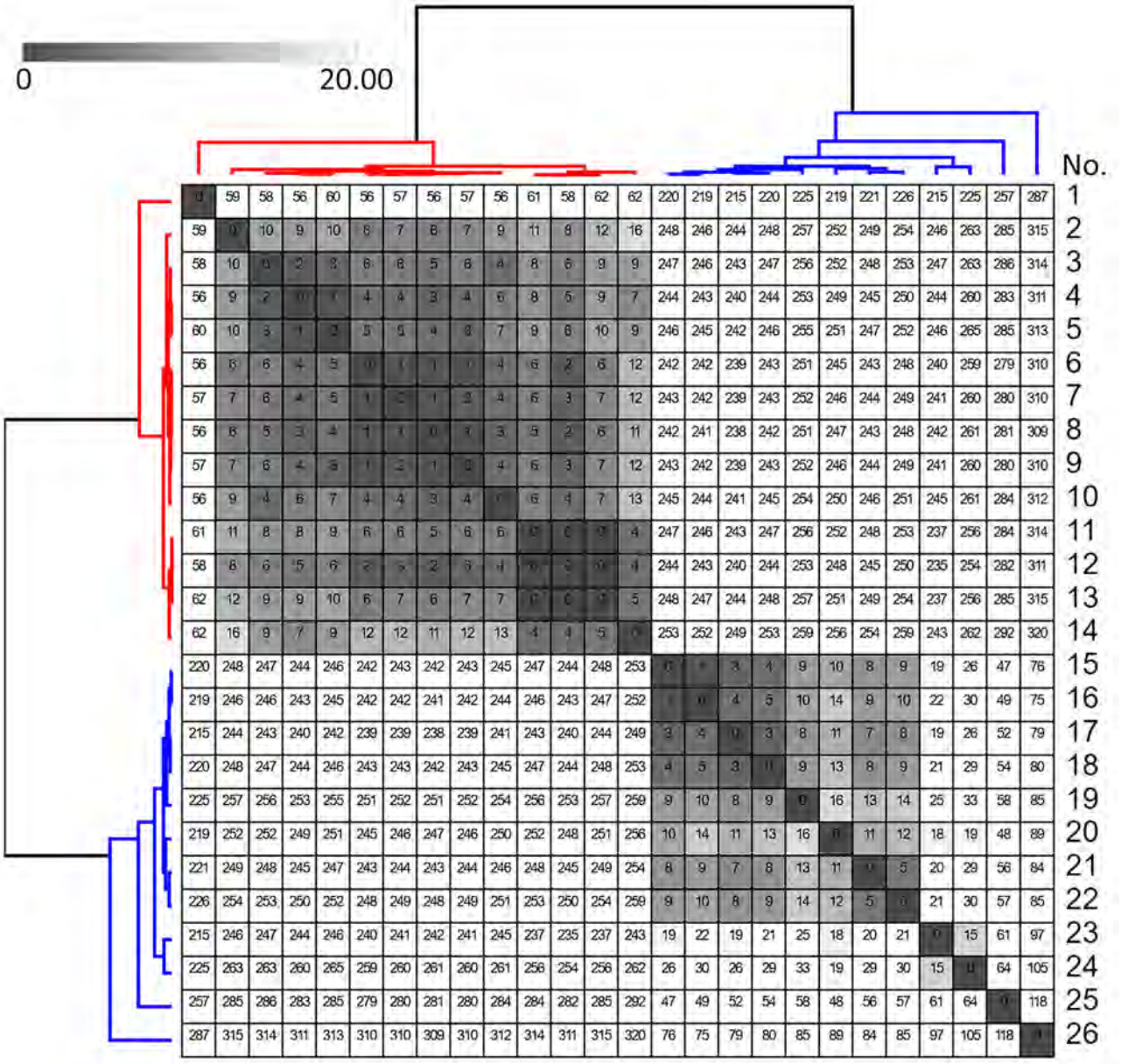

Figure 2. Reference-based pairwise single-nucleotide polymorphism (SNP) matrix of 26 *Neisseria gonorrhoeae* sequence type 16676 infections from study of outbreak of *N. gonorrhoeae* sequence type 16676 among disseminated infections, Minnesota, USA, 2025. Genomes numbered 1–14 (red) are from Minnesota disseminated gonococcal infection isolates in 2025. Genomes numbered 15–26 (blue) represent the other genomes grouped in the same National Center for Biotechnology Information Pathogen Detection cluster (PDS000214546.4.) in October 2025. SNP calls were clustered and displayed using Morpheus software (https://software.broadinstitute.org/morpheus). SNP calls <20 are highlighted in grayscale. Genome number 7 was used as an internal reference for calling SNPs with the Dryad version 3.0 pipeline (*7*).

of gonorrhea (*9*). In addition, the presence of 2 antimicrobial resistance genes on separately mobilizable plasmids highlights the importance of monitoring horizontal gene transfer in genomic surveillance of *N. gonorrhoeae*.

Our findings highlight the importance of DGI surveillance and the value of genomic surveillance for sexually transmitted infections. Prompt case investigations spurred by genomic analysis enabled epidemiologists to identify a direct link between DGI cases and notify a neighboring state health agency of transmission. Phylodynamic approaches also yielded insights into rates at which DGI-associated strains can emerge by estimating a timeline of weeks to months between the estimated time of a most recent common ancestor of a strain and the time at which infected case-patients sought care at healthcare facilities. Continuing prospective genomic surveillance, including performing large-scale studies

of the evolution of DGI-causing *N. gonorrhoeae* strains, will help the field more thoroughly understand and intervene against this public health threat.

This article was preprinted at https://doi.org/10.64898/2026.01.09.26343522.

Acknowledgments

We thank Amber Poppe for her support of this epidemiological investigation. We also thank Marcie Babcock, Jeffrey Dennis, Hannah Friedlander, Brian Kendrick, Dakota Schneider, and Jennifer Zipprich for their support of STI surveillance in Minnesota. We acknowledge John C. Cartee and Sandeep J. Joseph for conducting nationwide genomic surveillance that contextualized the results of our local investigations. We also thank the National Center for Biotechnology Information Pathogen Detection team, as well as all healthcare providers in Minnesota and Wisconsin who provided clinical care to patients with disseminated gonococcal infection and reported cases to the Minnesota Department of Health.

Sequencing reads and genome assemblies for the *N. gonorrhoeae* genomes sequenced for this study are publicly available at the National Center for Biotechnology Information (BioProject no. PRJNA1204341).

Funding for this investigation was provided through the following Centers for Disease Control and Prevention–funded grants: Strengthening STD Prevention and Control for Health Departments Award (grant no. NH25PS005172), Emerging Infections Program (grant no. NU50CK000648), Epidemiology and Laboratory Capacity (grant nos. NU51CK000361 and NU50CK000508), and Pathogen Genomics Centers of Excellence (grant no. NU50CK000628). The findings do not necessarily reflect the official opinions of the agencies that funded this work.

About the Author

Mr. Evans is a genomic epidemiologist with the Minnesota Department of Health. His work focuses on developing, implementing, and optimizing the use of microbial genomics for pathogen surveillance and outbreak intervention.

References

1. Weston EJ, Heidenga BL, Farley MM, Tunali A, D'Angelo MT, Moore A, et al. Surveillance for disseminated gonococcal infections, active bacterial core surveillance (ABCs)—United States, 2015–2019. Clin Infect Dis. 2022;75:953–8. https://doi.org/10.1093/cid/ciac052
2. Evans D, Friedlander H, Bo-Subait K, Dennis J, Kaiyalethe J, Craft B, et al. Genomic investigation of disseminated gonococcal infections, Minnesota, USA, 2024. Emerg Infect Dis. 2025;31:2003–7. https://doi.org/10.3201/eid3110.250785
3. Jolley KA, Bray JE, Maiden MCJ. Open-access bacterial population genomics: BIGSdb software, the PubMLST.org website and their applications. Wellcome Open Res. 2018;3:124. https://doi.org/10.12688/wellcomeopenres.14826.1
4. Maiden MC, Bygraves JA, Feil E, Morelli G, Russell JE, Urwin R, et al. Multilocus sequence typing: a portable approach to the identification of clones within populations of pathogenic microorganisms. Proc Natl Acad Sci U S A. 1998;95:3140–5. https://doi.org/10.1073/pnas.95.6.3140
5. Demczuk W, Sidhu S, Unemo M, Whiley DM, Allen VG, Dillon JR, et al. *Neisseria gonorrhoeae* sequence typing for antimicrobial resistance, a novel antimicrobial resistance multilocus typing scheme for tracking global dissemination of N. gonorrhoeae strains. J Clin Microbiol. 2017;55:1454–68. https://doi.org/10.1128/JCM.00100-17
6. Feldgarden M, Brover V, Gonzalez-Escalona N, Frye JG, Haendiges J, Haft DH, et al. AMRFinderPlus and the Reference Gene Catalog facilitate examination of the genomic links among antimicrobial resistance, stress response, and virulence. Sci Rep. 2021;11:12728. https://doi.org/10.1038/s41598-021-91456-0
7. Sagulenko P, Puller V, Neher RA. TreeTime: maximum-likelihood phylodynamic analysis. Virus Evol. 2018;4:vex042. https://doi.org/10.1093/ve/vex042
8. Welch G, Reed GW, Rice PA, Ram S. A meta-analysis to quantify the risk of disseminated gonococcal infection with porin B serotype. Open Forum Infect Dis. 2024;11:ofae389.
9. Berçot B, Assoumou L, Caméléna F, Voitichouk C, Mérimèche M, Ouattara M, et al. Antimicrobial-resistant *Neisseria gonorrhoeae* infections in men using doxycycline post-exposure prophylaxis: a substudy of the ANRS 174 DOXYVAC Trial. Clin Infect Dis. 2025 Nov 10 [Epub ahead of print].

Address for correspondence: Daniel Evans, Minnesota Department of Health—Public Health Laboratory, 601 Robert St N, St. Paul, MN 55101, USA; email: dan.r.evans@state.mn.us

Cutibacterium avidum Bacteria in Post-Mastectomy Breast with Prior Silicone Injections, Singapore

Surya Subramanian, Isaac Chung De Wei, Chua Hui Wen, Allen Wei-Jiat Wong

Author affiliations: Sengkang General Hospital, Singapore (S. Subramanian, C.H. Wen, A.W.-J. Wong); Ministry of Health Holdings, Singapore (I. Chung De Wei); Duke-National University of Singapore (NUS) Medical School, Singapore (A.W-J. Wong)

DOI: http://doi.org/10.3201/eid3206.251717

We isolated *Cutibacterium avidum* bacteria from remanant siliconomas noted during left mastectomy with reconstruction and right breast reduction in a 48-year-old woman with prior history of silicon injections. Chronic siliconomas can support anaerobic colonization, posing infection risks relevant to reconstructive and oncologic timelines.

We report a case of *Cutibacterium avidum* bacteria isolated from breast tissue in a 48-year-old woman with a diagnosis of left breast triple-negative carcinoma and a prior history of breast augmentation by free silicone injections to bilateral breasts. Twenty years before, the patient received multiple series of non–Food and Drug Association-approved silicone injections administered to bilateral breast tissue in all anatomic planes at an unidentified center in a foreign country. She underwent left endoscopic nipple-sparing mastectomy with pedicled transverse rectus abdominis myocutaneous flap reconstruction and contralateral reduction mammoplasty with free nipple graft. Prior research from our institution details those reconstructive techniques (*1*,*2*). Intraoperatively, we discovered multiple loculated lesions of varied size and consistency during dissection, confirming a diagnosis of siliconomas (Figure). Because of the extensive presence of lesions in both breasts, we sent tissue from the siliconomas for histopathology and conducted culture analysis, including Gram stain, aerobic, anaerobic, acid-fast bacilli, and fungal cultures, which confirmed the unusual presence of *C. avidum* bacteria. We then consulted an infectious disease specialist and, thereafter, placed the patient on a regimen of oral clindamycin 300 mg twice daily for 10 days as per standard sensitivity reports. While on that antibiotic regimen, the patient recovered without any complications.

Cutibacterium species (particularly *C. acnes*) are well recognized in breast implant infections and capsular contracture; however, our case demonstrated the colonization of this bacterial species in free silicon injection. *C. avidum* following reduction mammoplasty has been reported (*3*), and more recently has been reported in cosmetic breast implant augmentation, where the bacterium displayed true pathogenic behavior rather than acting as simply a contaminant (*4*). Other reports investigating infections relevant to aesthetic surgery have emphasized the pathogen's association with foreign material and surgical manipulation, underscoring that *C. avidum* cannot be dismissed as a benign commensal (*5*,*6*).

Chronic siliconomas emerge as a result of a long-standing foreign-body environment. Our case suggests that siliconomas might harbor anaerobic pathogens similar to those harbored by implants or prostheses. Our findings are novel in that they suggest an extension of the clinical spectrum of *C. avidum* bacteria to silicone-injected breasts, a scenario distinct from conventional implant-based infections. Infection is an independent risk factor for flap failure (*7*,*8*), and contributes to delayed healing, flap

Figure. Intraoperative image from a case report of *Cutibacterium avidum* in post-mastectomy breast with prior silicone injections, Singapore. Image taken during an ongoing right breast reduction, depicting multiple loculations of foreign body embedded in the breast tissue.

compromise, and partial or total necrosis. Even low-grade infection can increase the risk for flap failure through inflammatory microthrombosis and impaired perfusion. Expedited healing is important in patients undergoing breast reconstruction to facilitate adjuvant chemotherapy or radiotherapy and improve overall survival (*9*). Therefore, *C. avidum* bacteria isolated from an operative field with established pathogenic potential in implant-associated infections should be regarded with appropriate diligence and treated irrespective of the clinical symptoms.

We highlight this case to alert surgeons that *C. avidum* bacteria is clinically relevant in patients with silicone injections or foreign material in breast tissue, especially as they maneuver through the course of concomitant reconstructive procedures. Awareness may influence interpretation of intraoperative cultures, antimicrobial selection, and management of late or indolent infections in this unique subgroup. In the setting of a free flap reconstruction, it is prudent to treat *C. avidum* formally with a course of antimicrobial drugs rather than risk an infection-related flap death.

About the Author

Dr. Subramanian is a plastic, reconstructive, and aesthetic surgeon, currently pursuing an advanced microsurgery fellowship at Sengkang General Hospital, Singapore. Her fields of interest include breast, lower limb, and lymphatic reconstruction, plastic surgery education, and research.

References

1. Wong AWJ, Kuo WL, Cheong DCF, Tsai HP, Kao SW, Chen CF, et al. Six steps for a successful aesthetic free flap reconstruction after minimally invasive mastectomy: a retrospective case-control study. Int J Surg. 2024;110:645–53. https://doi.org/10.1097/JS9.0000000000000871
2. Tan TJK, Wong AWJ, Chua HW. Traction-assisted chest elevation (TRACE)—a novel technique for improving intraoperative ergonomics in endoscopic mastectomy. J Surg Case Rep. 2025;2025:rjaf321. https://doi.org/10.1093/jscr/rjaf321
3. Panagea S, Corkill JE, Hershman MJ, Parry CM. Breast abscess caused by *Propionibacterium avidum* following breast reduction surgery: case report and review of the literature. J Infect. 2005;51:e253–5. https://doi.org/10.1016/j.jinf.2005.04.005
4. Isabel R, Monica M. *Cutibacterium avidum*: a rare but expected agent of breast implant infection. IDCases. 2019;17:e00546. https://doi.org/10.1016/j.idcr.2019.e00546
5. Ray A, Zaremba S, Baldwin L. *Cutibacterium avidum*: a unique skin flora infection without foreign body in mastopexy. Am J Cosmet Surg. 2024;41:30–3.
6. Isabel Cristina RS, Diego P-R. *Cutibacterium avidum*: a virulent pathogen in esthetic surgery infection, a case series. Anaerobe. 2025;92:102944. https://doi.org/10.1016/j.anaerobe.2025.102944
7. Ouyang SB, Wu ZH, Zhang YP, Lu XL. Comprehensive analysis of risk factors for flap necrosis in free flap reconstruction of postoperative tissue defects in oral and maxillofacial tumors. Sci Rep. 2024;14:18676. https://doi.org/10.1038/s41598-024-69159-z
8. Las DE, de Jong T, Zuidam JM, Verweij NM, Hovius SE, Mureau MA. Identification of independent risk factors for flap failure: a retrospective analysis of 1530 free flaps for breast, head and neck and extremity reconstruction. J Plast Reconstr Aesthet Surg. 2016;69:894–906. https://doi.org/10.1016/j.bjps.2016.02.001
9. Lanthaler M, Spechtler K, Krapf J, Egle D, Sieb M, Tasch C, et al. Does the breast reconstruction method have an impact on time delay to adjuvant chemotherapy – a comparison between autologous and expander/implant breast reconstruction. JPRAS Open. 2022;33:131–8. https://doi.org/10.1016/j.jpra.2022.06.001

Address for correspondence: Allen Wei-Jiat Wong, Sengkang General Hospital, Sengkang East Way, Singapore 544886; email: allen.wong.wei.jiat@gmail.com

Increase in *bla*$_{NDM}$ among Carbapenemase-Producing, Carbapenem-Resistant Enterobacterales, United States, 2016–2023

Uzma Afroz Ansari, Davina Campbell, Joshua M. Brandenburg, Nadezhda Duffy, Julian E. Grass, Alice Y. Guh, Joseph D. Lutgring, Christopher A. Elkins, Maria Karlsson, Amy S. Gargis, HAIC MuGSI Working Group[1]

Author affiliations: Centers for Disease Control and Prevention, Atlanta, Georgia, USA (U.A. Ansari, D. Campbell, J.M. Brandenburg, N. Duffy, J.E. Grass, A.Y. Guh, J.D. Lutgring, C.A. Elkins, M. Karlsson, A.S. Gargis); Chenega Government Missions Solutions, Chesapeake, Virginia, USA (M. Karlsson)

DOI: http://doi.org/10.3201/eid3206.251404

We report an increase of *bla*$_{NDM}$ among carbapenemase-producing, carbapenem-resistant Enterobacterales collected in the United States through the Emerging Infections Program's Multi-site Gram-negative Surveillance Initiative. Among 1,288 isolates identified, the percentage harboring *bla*$_{NDM}$ increased from 5.4% in 2016 to 39.8% in 2023.

Carbapenem-resistant Enterobacterales (CRE) are an urgent public health threat. In 2022, an estimated 13,387 CRE infections occurred among hospitalized patients in the United States (*1*). Different mechanisms may contribute to carbapenem resistance, but carbapenemase-producing CRE (CP-CRE) are of particular concern. Carbapenemase genes confer broad resistance to β-lactam antimicrobial drugs and are often located on mobile genetic elements, enabling them to spread between bacterial species. Metallo-β-lactamases (MBLs), including New Delhi metallo-β-lactamase (NDM)–producing CRE, are especially problematic because few antimicrobial drugs have activity against them (*2*). We report an increase in *bla*$_{NDM}$ among CP-CRE collected through the Centers for Disease Control and Prevention's Emerging Infections Program (EIP) Multi-site Gram-negative Surveillance Initiative.

The EIP Multi-site Gram-negative Surveillance Initiative conducts active, population- and laboratory-based surveillance of CRE (*3*–*5*). During 2016–2023, a total of 10 EIP sites participated in surveillance for carbapenem-resistant *Enterobacter cloacae* complex, *Escherichia coli*, and *Klebsiella* species (*K. pneumoniae*, *K. oxytoca*, and *K. aerogenes*) in isolates from a usually sterile site or from urine. Each site submitted a convenience sample of isolates to the Centers for Disease Control and Prevention for testing, including in-house reference broth microdilution incorporating an MBL screen, species identification, and real-time PCR for carbapenemase genes (*3*). We tested all isolates for *bla*$_{KPC}$, *bla*$_{NDM}$, and *bla*$_{OXA-48-like}$ genes; we also tested isolates with a positive MBL screen for *bla*$_{VIM}$ and *bla*$_{IMP}$ (*4*). We defined CP-CRE as isolates positive for a carbapenemase gene by real-time PCR and resistant to ertapenem, imipenem, or meropenem as determined by broth microdilution and Clinical and Laboratory Standards Institute breakpoints (Appendix Table, https://wwwnc.cdc.gov/EID/article/32/6/25-1404-App1.pdf) (*6*). Using the Pearson χ^2 test, we compared the percentages of *bla*$_{NDM}$

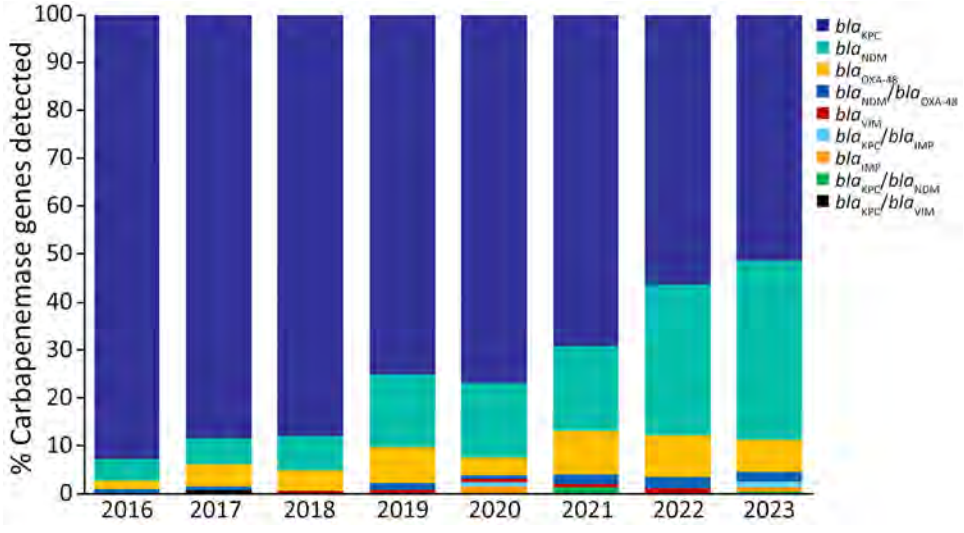

Figure. Percentage of carbapenemase genes detected by real-time PCR among 1,288 CP-CRE chosen for a study analyzing an increase in *bla*$_{NDM}$ among carbapenemase-producing, carbapenem-resistant Enterobacterales, United States, 2016–2023. IMP, imipenemase; KPC, *Klebsiella pneumoniae* carbapenemase; OXA-48, oxacillinase; NDM, New Delhi metallo-β-lactamase; VIM, Verona integron-encoded metallo-β-lactamase.

[1]HAIC MuGSI Working Group members are listed at the end of this article.

Table. Frequency of *bla*$_{NDM}$ by species from study investigating increase in *bla*$_{NDM}$ among CP-CRE, United States, 2016–2023*

Year	Total no. CP-CRE isolates	No. (%) isolates			
		All *bla*$_{NDM}$†	*Escherichia coli*	*Klebsiella* spp.	*Enterobacter cloacae* complex
2016	111	6 (5.4)	2 (1.8)	4 (3.6)	0
2017	149	9 (6.0)	5 (3.4)	4 (2.7)	0
2018	166	12 (7.2)	6 (3.6)	5 (3.0)	1 (0.6)
2019	145	24 (16.6)	13 (9.0)	9 (6.2)	2 (1.4)
2020	134	22 (16.4)	13 (9.7)	6 (4.5)	3 (2.2)
2021	153	32 (20.9)	17 (11.1)	10 (6.5)	5 (3.3)
2022	181	61 (33.7)	27 (14.9)	23 (12.7)	11 (6.1)
2023	249	99 (39.8)	57 (22.9)	29 (11.6)	13 (5.2)
Total	1288	265 (20.6)	140 (10.9)	90 (7.0)	35 (2.7)

*Data are updated for accuracy and may differ from online reports (accessed 2025 Aug 19) (*5*). CP-CRE, carbapenemase-producing, carbapenem-resistant Enterobacterales.
†Includes isolates carrying *bla*$_{NDM}$ (n = 245), dual mechanism *bla*$_{NDM}$+*bla*$_{OXA-48}$ (n = 17), and *bla*$_{NDM}$+*bla*$_{KPC}$ (n = 3).

among CP-CRE collected in 2016 and 2023. Annual reports with epidemiologic, clinical, and laboratory data are available online (*5*).

Among 1,288 CP-CRE identified, *bla*$_{KPC}$ was the most common carbapenemase gene detected among all confirmed CP-CRE during 2016–2023 (72.7%, 937 isolates), followed by *bla*$_{NDM}$ (20.6%, 265 isolates), *bla*$_{OXA-48-like}$ (7.5%, 96 isolates), *bla*$_{IMP}$ (0.6%, 8 isolates), and *bla*$_{VIM}$ (0.5%, 7 isolates) (Figure); 25 (1.9%) isolates harbored >1 carbapenemase gene (Appendix Table). The percentage of *bla*$_{NDM}$ isolates increased from 5.4% in 2016 (n = 6) to 39.8% in 2023 (n = 99) (p<0.00001). Conversely, *bla*$_{KPC}$ decreased from 92.8% in 2016 (n = 103) to 53.0% in 2023 (n = 132) (p<0.00001) (Figure). Again comparing 2016 and 2023, we observed an increase in *bla*$_{NDM}$ among *E. coli* (1.8% to 22.8%), *Klebsiella* spp. (3.6% to 11.6%), and *E. cloacae* complex (0.6% to 5.2%) (Table). NDM-producing Enterobacterales were more resistant to β-lactam combination agents than were *K. pneumoniae* carbapenemase–producing Enterobacterales (Appendix Table).

We report a notable shift in the type of carbapenemase genes among a convenience sample of 1,288 CP-CRE collected in the United States during 2016–2023. Although *bla*$_{KPC}$ remained the most common carbapenemase gene, we observed a decrease in the proportion of *bla*$_{KPC}$ coupled with an increase in *bla*$_{NDM.}$ This shift was most striking among *E. coli*, with *bla*$_{NDM}$ representing 73% of all carbapenemase-producing *E. coli* in 2023; in contrast, we observed *bla*$_{NDM}$ among only 14.3% of carbapenemase-producing *E. coli* in 2016.

The increase of *bla*$_{NDM}$ is alarming given that NDM-producing CRE are more resistant than other CRE isolates (*7*). Furthermore, newer β-lactam combination agents, including ceftazidime-avibactam, meropenem-vaborbactam, and imipenem-relebactam, are ineffective against MBL enzymes, and treatment options are limited (*2*,*8*). Aztreonam/avibactam and cefiderocol have demonstrated in vitro efficacy, but resistance has also been reported (*7*).

Our study is limited because it is based on a convenience sample of isolates from population-based surveillance and might be affected by sampling bias. We collected isolates from 10 EIP sites and national trends may not be extrapolated based on these data. This study is not able to determine whether there are changes in the incidence of NDM-producing CRE, however, our findings align with recent reports of rising NDM-positive CRE in New York City and among the Antimicrobial Resistance Laboratory Network (*9*,*10*). Whole-genome sequencing analysis is needed to determine gene variants and whether increases are driven by specific sequence types.

In conclusion, we report a concerning increase in *bla*$_{NDM}$ among a convenience sample of CP-CRE collected across 10 EIP sites in the United States. Further investigation is needed to assess if this is a nationwide trend, to analyze epidemiologic data comparing characteristics of patients infected with *bla*$_{NDM}$-CRE and those with *bla*$_{KPC}$, and to examine whole-genome sequencing data to determine if the observed increase is related to clonal expansion. Our findings should alert clinicians to the increase in *bla*$_{NDM}$ and encourage mechanism testing in clinical laboratories.

Acknowledgments

We acknowledge contributions of the Healthcare-Associated Infections–Community Interface Activity Multi-site Gram-negative Surveillance Initiative Working Group (Brittany Von Bank, Christopher Czaja, Ginette Dobbins, Jennifer Driscoll, Angela Dusko, Ghinwa Dumyati, Kristina Flores, Annastasia Gross, Heather Hertzel, Karlie Hoetzer, Marisa Hoffman, Jesse Jacob, Ruth Lynfield, Shannon O'Brien, Sean O'Malley, Patricia Ryan, Paula Snippes, Gillian Smith, Tara Suhs, Rebecca Tsay, Christopher Wilson, Lucy Wilson, Medora Witwer) and the Clinical and Environmental Microbiology Branch's Panel Pour Team (National Center for Emerging and Zoonotic Infectious Diseases, Division of Healthcare Quality Promotion).

This activity was reviewed by CDC, deemed not research, and was conducted consistent with applicable federal law and CDC policy (e.g., 45 C.F.R. part 46.102(l)(2), 21 C.F.R. part 56; 42 U.S.C. §241(d); 5 U.S.C. §552a; 44 U.S.C. §3501 et seq.). Similarly, the protocol was reviewed by all participating EIP sites and either was deemed nonresearch or received institutional review board approval with a waiver of informed consent. The findings and conclusions in this report are those of the authors and do not necessarily represent the official position of CDC or the Agency for Toxic Substances and Disease Registry.

About the Author

Ms. Ansari is a biologist in the Division of Healthcare Quality Promotion, National Center for Emerging and Zoonotic Infectious Diseases, Centers for Disease Control and Prevention. Her work focuses on antimicrobial resistance of healthcare-associated pathogens.

References

1. Wolford H, McCarthy NL, Baggs J, Hatfield KM, Maillis A, Olubajo B, et al. Antimicrobial-resistant infections in hospitalized patients. JAMA Netw Open. 2025;8:e2462059. https://doi.org/10.1001/jamanetworkopen.2024.62059
2. Lutgring JD, Balbuena R, Reese N, Gilbert SE, Ansari U, Bhatnagar A, et al. Antibiotic susceptibility of NDM-producing *Enterobacterales* collected in the United States in 2017 and 2018. Antimicrob Agents Chemother. 2020;64:e00499–20. https://doi.org/10.1128/AAC.00499-20
3. Karlsson M, Lutgring JD, Ansari U, Lawsin A, Albrecht V, McAllister G, et al. Molecular characterization of carbapenem-resistant Enterobacterales collected in the United States. Microb Drug Resist. 2022;28:389–97. https://doi.org/10.1089/mdr.2021.0106
4. Grome HN, Grass JE, Duffy N, Bulens SN, Ansari U, Campbell D, et al. Carbapenem-resistant and extended-spectrum β-lactamase-producing Enterobacterales in children, United States, 2016-2020. Emerg Infect Dis. 2024;30:1104–14. https://doi.org/10.3201/eid3006.231734
5. Centers for Disease Control and Prevention (CDC). Multi-site Gram-negative Surveillance Initiative (MuGSI). Updated February 1, 2024 [cited 2025 Jul 24]. https://www.cdc.gov/healthcare-associated-infections/php/haic-eip/mugsi.html#cdc_research_or_data_summary_resources-resources
6. Clinical and Laboratory Standards Institute. Performance standards for antimicrobial susceptibility testing; 31st informational supplement. Document M100–S35. Wayne (PA): The Institute; 2025.
7. Sabour S, Huang JY, Bhatnagar A, Gilbert SE, Karlsson M, Lonsway D, et al. Detection and characterization of targeted carbapenem-resistant health care-associated threats: findings from the Antibiotic Resistance Laboratory Network, 2017 to 2019. Antimicrob Agents Chemother. 2021;65:e0110521. https://doi.org/10.1128/AAC.01105-21
8. Tamma PD, Heil EL, Justo JA, Mathers AJ, Satlin MJ, Bonomo RA. Infectious Diseases Society of America 2024 guidance on the treatment of antimicrobial-resistant gram-negative infections. Clin Infect Dis. 2024;ciae403. https://doi.org/10.1093/cid/ciae403
9. Devinney K, Burton N, Alroy KA, Crawley A, Da Costa-Carter CA, Kratz MM, et al. Notes from the field: increase in New Delhi metallo-β-lactamase-producing carbapenem-resistant Enterobacterales—New York City, 2019–2024. MMWR Morb Mortal Wkly Rep. 2025;74:401–3. https://doi.org/10.15585/mmwr.mm7423a2
10. Rankin DA, Stahl A, Sabour S, Khan MA, Armstrong T, Huang JY, et al. Changes in carbapenemase-producing carbapenem-resistant Enterobacterales, 2019 to 2023. Ann Intern Med. 2025;178:1818–21. https://doi.org/10.7326/ANNALS-25-02404

Address for correspondence: Uzma Afroz Ansari, Centers for Disease Control and Prevention, 1600 Clifton Rd NE, Mailstop H17-4, Atlanta, GA 30329-4018, USA; email: glv9@cdc.gov

Correction: Vol. 32, No. 5

A description of the mortality rate among cranes was unclear in Highly Pathogenic Avian Influenza A(H5N1) Clade 2.3.4.4b Virus and Mass Mortality in Eurasian Cranes, Germany, 2025 (A. Günther). The article has been corrected online (https://wwwnc.cdc.gov/eid/article/32/5/26-0170_article).

Dangerous Miracle: The Astonishing Rise and Looming Disaster of Antibiotics

Liam Shaw; Simon & Shuster, New York, New York, USA, 2023; ISBN-13: 9781668023631; Pages: 352; Price: US$30.00

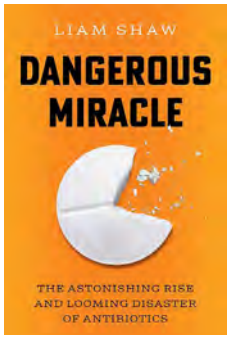

It is easy to forget that the first antibiotic was discovered merely 100 years ago, yet its impact on medicine has been profound. In Dangerous Miracle: The Astonishing Rise and Looming Disaster of Antibiotics, University of Bristol evolutionary biologist Liam Shaw traces the rapid arc from discovery of the first antibacterial agents to the present-day crisis of ever-worsening antimicrobial resistance. Written for a general audience, the book weaves a highly readable journey through the science behind antibiotic development while situating their rise and decline within broader historical, political, and economic contexts.

Dangerous Miracle begins with the development of Prontosil, the first clinically useful sulfonamide, tracing its origins to the European dye industry. This account illustrates how advances in industrial chemistry unexpectedly intersected with medical therapeutics, ushering in the antimicrobial era. Shaw then turns to penicillin, describing Alexander Fleming's observation of mold-mediated inhibition of *Staphylococcus aureus* and the herculean efforts required to translate this discovery into a widely available drug. He emphasizes that penicillin's success depended on extensive multinational collaboration, particularly during World War II, when large-scale production became a strategic priority.

The author deftly chronicles the labor-intensive process of antibiotic discovery, including systematic screening of soil organisms for antimicrobial activity. He adds drama by highlighting disputes over scientific achievements and providing recognition for underappreciated contributors, such as Albert Schatz's discovery of streptomycin. The discussion of streptomycin and isoniazid is enhanced by a personal narrative involving the author's grandfather's protracted bout with tuberculosis, which contextualizes the dramatic change these drugs brought to the treatment of a previously fatal disease.

The later portions of the book shift toward the structural and economic forces shaping contemporary antimicrobial development. Shaw argues that antibiotics are exploited in a manner similar to fossil fuels. Factors such as the consolidation of pharmaceutical research within large multinational companies and robust patent protection laws have contributed to a decline in antibiotic innovation. He situates those trends alongside the problems created by the emergence of first methicillin-resistant *Staphylococcus aureus* and then carbapenem-resistant Enterobacterales, framing resistance as both a microbiologic and systems-level problem.

In the final chapters, Dangerous Miracle examines the economic paradox of antibiotics: expensive to develop yet intended for short courses and judicious use, often constrained by antimicrobial stewardship programs. Limited space is devoted to potential solutions, but Shaw does advocate for several policy responses, including subscription-based reimbursement models that decouple profitability from sales volume and international public–private partnerships designed to support antimicrobial research and development. Although such proposals are discussed at a high level, the book offers limited evaluation of their feasibility or early outcomes.

Overall, Dangerous Miracle provides a balanced, chronological overview of the history of antibiotic discovery and the challenges posed by antimicrobial resistance. Its strengths lie in historical narrative and accessibility, rather than detailed policy analysis. This book will be of interest to clinicians, microbiologists, and public health experts seeking an overarching account of how one of medicine's greatest successes has evolved into one of its most pressing global threats, and it serves as a call to action to reexamine how we invest in and regulate antimicrobials.

John P. Mills

Author affiliation: Rutgers Robert Wood Johnson Medical School, New Brunswick, New Jersey, USA

DOI: https://doi.org/10.3201/eid3206.260224

Address for correspondence: John P. Mills, Rutgers Robert Wood Johnson Medical School, Division of Allergy, Immunology, and Infectious Diseases, 125 Paterson St, New Brunswick, NJ 08901, USA; email: jpm@rwjms.rutgers.edu

Myriad, Microscopic and Marvelous: The World of Antoni van Leeuwenhoek

Geertje Dekkers; Translated by Andy Brown; Reaktion Books Ltd., London, United Kingdom, 2025; ISBN-13: 9781836390978; Pages 240; Price: US$30.00 (hardcover and ebook)

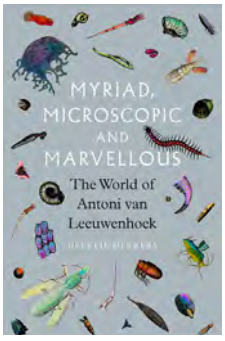

In Myriad, Microscopic and Marvellous: The World of Antoni van Leeuwenhoek, Dutch historian and journalist Geertje Dekkers invites readers to examine the life of the "father of microbiology," Antoni (sometimes spelled Antony or Antonie) van Leeuwenhoek (1632–1723), and the rudimentary practices by which he observed, theorized, and reported on plants, "little animals" (now known to be microorganisms), spermatozoa, and other specimens in the 17th and 18th Centuries. Although Dekkers contextualizes some of van Leeuwenhoek's work with contemporary knowledge, the book primarily describes his atypical entry into scientific research, his motivations for conducting research, and his interactions with the broader scientific community. The author grounds readers in thorough historical background, citing several research letters written by van Leeuwenhoek (among other sources), but provides space for readers to speculate on what van Leeuwenhoek observed, how he felt, and how his environment shaped his work. In doing so, Dekkers situates readers in a largely unfamiliar world, one in which the concepts and vocabulary to describe unicellular organisms had not yet emerged.

Van Leeuwenhoek spent most of his life in Delft, Dutch Republic, where he worked first as a textile merchant and later as a municipal civil servant. Despite lacking academic training, he began conducting microscopy research, driven by personal curiosity and the work of other scientists. Although unrecognizable by modern standards, the microscopes van Leeuwenhoek made were superior to those made by others, capable of greater magnification and clarity because of their single-lens construction. That advantage enabled him to make more accurate and detailed observations of his specimens, which were the underpinning of his scientific legacy. In 1673, van Leeuwenhoek's early work was sent to the Royal Society of England and published in the society's official journal, Philosophical Transactions. He continued publishing research in the journal until his death in 1723, including the first descriptions of microorganisms, although he did not know what they were. Dekkers emphasizes that van Leeuwenhoek "had no notion of the composition of the creatures, how they lived, and the impact they had on their environments… They were interesting to look at, but that was all." He was elected a fellow to the Society in 1680.

The book elicits the comparison of the scientific process from van Leeuwenhoek's era to today. Van Leeuwenhoek, an untrained person driven by often misguided theories, used homemade contraptions to look at (at the time) incomprehensibly small creatures with limited reproducibility. Yet his research was widely recognized, and his observations revolutionized the field of biology. Could someone like van Leeuwenhoek succeed today? Historical successes such as van Leeuwenhoek's raise questions about whether a self-driven, self-taught citizen scientist could achieve such revolutionary success in today's research landscape.

Ultimately, readers can expect to gain a better understanding of both van Leeuwenhoek's legacy and the nature of scientific inquiry itself. Dekkers draws readers into van Leeuwenhoek's world in an engaging and accessible biographical narrative, featuring 58 illustrations drawn by van Leeuwenhoek and others. Readers need no technical knowledge to understand its content, but those with research experience may have greater appreciation for the unstructured environment in which he worked.

Jonathan H. Sogin

Author affiliation: Cornell University, Ithaca, New York, USA

DOI: https://doi.org/10.3201/eid3206.260353

Address for correspondence: Jonathan H. Sogin, Cornell University, Department of Food Science, 411 Tower Rd, #360, Ithaca, NY 14853, USA; email: jhs397@cornell.edu

Johannes [Jan] Vermeer (1632–1675), *The Geographer*, 1668–1669 (detail). Oil on canvas. 53 cm × 46.5 cm (20.9 in × 18.3 in). Städel Museum, Frankfurt am Main, Germany. https://www.johannesvermeer.org.

Delft Neighbors—Vermeer and van Leeuwenhoek

Lesli Mitchell

Jan Vermeer's *The Geographer*, featured on the cover of this issue, is widely considered to be a pendant of *The Astronomer*, thematically similar and intended to be displayed together. EID featured *The Astronomer* on the cover of its January 2004 issue, with an accompanying essay by the journal's esteemed Founding Managing Editor, Polyxeni Potter. An extensive background in art history coupled with her insightful writing have contributed to EID's current reputation for its signature artwork.

In her essay, Potter noted that Vermeer is often linked to Antonie van Leeuwenhoek (sometimes spelled Antoni or Anthony), whose portrait was featured in EID's January 2024 cover essay by Byron Breedlove. Van Leeuwenhoek was a Dutch inventor who discovered through his microscope the cellular nature of spermatozoa and bacteria and was skilled in navigation, astronomy, and mathematics. There is also speculation that he was the model for the subject of both paintings.

This irresistible notion that Vermeer and van Leeuwenhoek were connected in some way continues

Author affiliation: Centers for Disease Control and Prevention, Atlanta, Georgia, USA

DOI: https://doi.org/10.3201/eid3206.AC3206

today and, considering their backgrounds, it is hard to believe they would *not* have known each other. Born only a few days apart in Delft in October 1632 and baptized in the same church, they lived within a few minutes' walk of each other. Delft was not so large a town that its most famous artists and scientists would be unknown to each other. The two men had friends in common, including Constantijn Huygens, an influential diplomat, artist, and poet who possessed a keen interest in microscopy and the natural sciences. From the windows of City Hall, where van Leeuwenhoek worked as a city official, one could see the front of Mechelen Inn, the tavern Vermeer owned.

Fortunate to live and work during a period referred to as the Dutch Golden Age, Vermeer and van Leeuwenhoek embraced the mindset of that time—one of scientific exploration and discovery. Their interests in optics and light are reflected in their work. Vermeer's *The Geographer* is a carefully composed allegorical image of scientific progress. It includes a host of objects that emphasize not only the focus on scientific exploration but also specific Dutch contributions. The map on the wall is so precisely detailed that it can be identified: it is one of the Pascaarten, printed by Willem Janszoon Blaeu in Amsterdam in the early 17th Century. The globe is also an acknowledgment of Dutch scientific achievement: it's a model of one made in 1600 by Flemish engraver and cartographer Jodocus Hondius the Elder in Amsterdam. He sold the globe together with its celestial counterpart, featured in Vermeer's *The Astronomer*. The pair of globes forms a cosmological whole, unifying heaven and earth. The geographer's globe is also turned to show the Indian Ocean, the route used by ships of the Dutch East India Company. The youth and energy of the scholar in both paintings convey the excitement of the times. The geographer seems to be on the brink of an insight, holding a divider while referencing a scholarly text, his face illuminated by the light through the window.

Like Vermeer, van Leeuwenhoek was fascinated by light, and his interest in optics led to his experiments in lenses to improve clarity and magnification. van Leeuwenhoek learned glass-blowing techniques and used them to make numerous lenses that could magnify 500 times, enabling him to visualize bacteria. He did not share the techniques he used, and what was a mystery then is still a mystery today, but his lenses were far superior to others made during that time. Versions of a microscope appeared as early as 1595, but van Leeuwenhoek refined it in devising a high-powered microscope that magnified 200–500 times, far greater than any previous microscope. Through his high-powered microscope, he made a host of discoveries: "animalcules" (tiny animals) swimming in a drop of pond water, blood cells, bacteria, free-living and parasitic microscopic protists,

Figure. Cornelis de Man, *Anatomic lesson of Cornelis van's-Gravensande*, 1681. Oil on canvas. 173.0 × 212.0 cm (68.1 in × 83.5 in). Collection of the Museum Prinsenhof Delft, Delft, the Netherlands. Gift of the Reinier de Graaf Groep; photograph by Tom Haartsen.

sperm cells, microscopic nematodes and rotifers, and more. His discoveries opened a new world of microscopic life to scientists.

Recognizing how these visionary men of Delft contributed to the Dutch Golden Age, it's tempting to connect them, and many scholars have done so, suggesting that they knew each other and even influenced each other's work. The speculation that van Leeuwenhoek was the model for the young man in both *The Astronomer* and *The Geographer* is difficult to prove, however; the scholar in Vermeer's paintings bears little resemblance to the portrait of van Leeuwenhoek painted by Jan Verkolje in 1686 (see page 1019). van Leeuwenhoek is also one of the figures in the 1681 painting *Anatomic lesson of Cornelis van's-Gravensande* by Cornelis de Man (Figure). He sat for the group portrait for the surgeon's guild at the age of 49 and is featured near the top left of the painting. The resemblance is clear in those two paintings, but it is arguable whether they resemble the young man featured in Vermeer's works.

In fact, the only solid evidence linking both men is a legal one: van Leeuwenhoek was appointed as executor of Vermeer's estate after the artist's early death at the age of 43. That fact suggests a connection, but the appointment does not mean that the men knew each other personally; curator duties were part of van Leeuwenhoek's job with the magistrate's court, and the Vermeer case was the fifth of about 10 known cases. If the two men did have a relationship or friendship, it is hard to see in van Leeuwenhoek's treatment of Vermeer's widow, Catharina Bolnes, in the dispensation of the estate. As art historian Gary Schwartz notes, "The curator of an estate has permissible options that can benefit the heirs to a bankrupt estate. Van Leeuwenhoek did not employ them." Despite Vermeer being bankrupt at the end of his life, his widow hoped to keep *The Art of Painting* within the family as a memento. van Leeuwenhoek noticed the omission of the painting in the home's inventory and made sure it was auctioned off to pay Vermeer's creditors.

As James Galbraith notes in his blog at the Corning Museum of Glass, "Until someone in Delft discovers a letter in their attic from Vermeer to van Leeuwenhoek or a similarly revealing document comes to light, we will never know with certainty whether or not the two men knew each other." Even so, a relationship between the two men need not be romanticized to appreciate their influence in the city of Delft and the lasting contributions they made to art and science. The tantalizing question of their connection, even to this day, is a testament to their legacy and to the enduring esteem both men have in the public imagination. This issue's theme on bacterial infections and their treatment includes more information on van Leeuwenhoek, including a book review of *Myriad, Microscopic and Marvelous: The World of Antoni van Leeuwenhoek*. The articles in this issue highlight that we not only see microorganisms more clearly now but also understand their role in disease and how to treat them when they are human pathogens.

Acknowledgments

The author thanks the peer reviewers for their comments on the manuscript, which contributed to the final article.

Bibliography

1. Breedlove B, Partin C. From observing little animalcules to detecting fastidious bacteria. Emerg Infect Dis. 2024 Jan [cited 2026 May 8]. https://wwwnc.cdc.gov/eid/article/30/1/ac-3001_article
2. Ford BJ. The Leeuwenhoek legacy. London: Biopress and Farrand Press; 1991.
3. Galbraith J. The uncertain friendship of van Leeuwenhoek and Vermeer. Corning Museum of Glass. 2016 Nov 17 [cited 2026 Apr 4]. https://blog.cmog.org/2016/uncertain-friendship-van-leeuwenhoek-and-vermeer
4. Google Vermeer Project. The Geographer. Google Arts & Culture [cited 2026 Apr 4]. https://artsandculture.google.com/story/4gXxBhB2iA5cIA
5. Gunderman R. The 17th-century cloth merchant who discovered the vast realm of tiny microbes—an appreciation of Antonie van Leeuwenhoek [cited 2026 Apr 26]. https://theconversation.com/the-17th-century-cloth-merchant-who-discovered-the-vast-realm-of-tiny-microbes-an-appreciation-of-antonie-van-leeuwenhoek-158177
6. Janson J. Anthony van Leeuwenhoek and Johannes Vermeer [cited 2026 Apr 25]. https://www.essentialvermeer.com/dutch-painters/dutch_art/Van Leeuwenhoek.html
7. Potter P. Johannes [Jan] Vermeer (1632–1675). The Astronomer (1668). Emerg Infect Dis. 2004 Jan [cited 2026 Mar 15]. https://wwwnc.cdc.gov/eid/article/10/1/ac-1001_article
8. Lens on Leeuwenhoek. Sat for Cornelis de Man's Anatomy Lesson of Dr.'s Gravezande [cited 2026 May 8]. https://lensonleeuwenhoek.net/content/sat-cornelis-de-mans-anatomy-lesson-dr-s-gravezande
9. Sogin JH. Myriad, microscopic and marvelous: the world of Antoni van Leeuwenhoek. Emerg Infect Dis. 2026; 32:1016–1018.
10. Lens on Leeuwenhoek. The Vermeer Connection [cited 2026 Apr 4]. https://lensonleeuwenhoek.net/content/vermeer-connection
11. University of California Berkeley. UC Museum of Paleontology. Antony van Leeuwenhoek [cited 2026 Apr 26]. https://ucmp.berkeley.edu/history/leeuwenhoek.html
12. Volpe C. Vermeer's Geographer [cited 2026 Apr 4]. https://streamlinepublishing.com/inside-art/vermeers-geographer
13. Wood G. Two Dutch visionaries. The American Scholar. 2015 Mar 4 [cited 2026 Apr 25]. https://theamericanscholar.org/two-dutch-visionaries

Address for correspondence: Lesli Mitchell, Centers for Disease Control and Prevention, 1600 Clifton Rd NE, Mailstop H16-2, Atlanta, GA 30329-4018, USA; email: aul6@cdc.gov

EMERGING INFECTIOUS DISEASES®

Upcoming Issue

- HTLV-1 Mother-to-Child Transmission—Emerging Risk With Breastfeeding Support in HIV-Infected Women
- Trichinellosis Outbreak Linked to Undercooked Bear Jerky, North Carolina, 2024
- Outbreak of Legionnaires' Disease Linked to Newly Installed Residential Water Heaters, the Netherlands, 2023
- Predictive Approach to Understanding *Angiostrongylus cantonensis* Distribution in the Canary Islands
- Prognostic Value of PCR Cycle Threshold in Crimean-Congo Hemorrhagic Fever, Iraq, 2022–2023
- National Surveillance of Enterovirus D68 Upsurge, France, 2024
- Qualitative Risk Assessment of Infectious Agents Associated With Canine Importation Into Canada
- Skin-Dwelling Filariae in Gabon—Molecular Epidemiology of Scapular Skin Snips and Risk Factors for *Mansonella streptocerca*
- Clinical Predictors of Fatal Outcomes in Human Leptospirosis, Thailand, 2015–2024
- Adeno-Associated Virus Type 2 and Human Adenovirus Species F Type 41 Co-infection Associated with Acute Severe Hepatitis in Children, California, USA
- On the Discovery of Cinchona as an Antimalarial (c.1630, Viceroyalty of Peru)
- Cluster of Human Tanapox Cases in Wildlife Reserve, South Africa, 2024
- Vascularized Iris Mass as Sentinel Manifestation of Syphilis in Patient with HIV Infection, Spain, 2025
- Complete Mitochondrial Genomes and Prevalence of *Angiostrongylus cantonensis* Detected From Oral Swabs of *Rattus rattus* Collected in Manombo Special Reserve, Southeastern Madagascar
- Autochthonous Neurocysticercosis Manifesting as Multiple Brain Lesions Mimicking Metastatic Disease
- Nipah Virus Shedding in Urine from Fruit Bats, Sri Lanka, 2018–2019
- Household Transmission of Enterovirus D68 in Washington and Oregon, USA, 2022–2024
- Recurrent Facial Folliculitis Caused by *Klebsiella aerogenes* ST117 in Men Who Have Sex With Men
- Trends in Congenital Syphilis Cases by Maternal Country of Birth, Spain, 2016–2024
- *Phormia regina* Fly as Vector for *Ignatzschineria* spp. Bacteremia in Persons Experiencing Homelessness, Canada, 2025
- Cat Scratch Disease Associated with Acute Hearing Loss
- Human Pulmonary Dirofilariasis in the Context of Pulmonary Adenocarcinoma, North Queensland, Australia, 2023
- Detection and Early Genomic Insights into Chikungunya Virus in Bolivia, 2025
- Clustered Outbreak of Acute External Ophthalmomyiasis Caused by *Oestrus Ovis* in Algeria, 2025
- Molecular Confirmation of Autochthonous *Taenia saginata* in Timor-Leste
- Neurological Alveolar Echinococcosis in a Postpartum Western Lowland Gorilla (*Gorilla gorilla gorilla*), the Netherlands, 2024
- *Dracunculus* sp. PantanalBr Infection of Florida Panthers and Bobcat, Florida, USA
- *Ancylostoma ceylanicum* Hookworm in Rural Papua New Guinea, 2020
- Chikungunya Outbreak, Cuba, July 2025
- Emergence of the West African HTLV-1aC Subgroup, Brazilian Amazon
- Inconsistent Strategies to Mitigate the Impact of *Batrachochytrium salamandrivorans* in Europe

Complete list of articles in the July issue at http://www.cdc.gov/eid/#issue-333

Earning CME Credit

To obtain credit, you should first read the journal article. After reading the article, you should be able to answer the following, related, multiple-choice questions. To complete the questions (with a minimum 75% passing score) and earn continuing medical education (CME) credit, please go to http://www.medscape.org/journal/eid. Credit cannot be obtained for tests completed on paper, although you may use the worksheet below to keep a record of your answers.

You must be a registered user on http://www.medscape.org. If you are not registered on http://www.medscape.org, please click on the "Register" link on the right hand side of the website.

Only one answer is correct for each question. Once you successfully answer all post-test questions, you will be able to view and/or print your certificate. For questions regarding this activity, contact the accredited provider, CME@medscape.net. For technical assistance, contact CME@medscape.net. American Medical Association's Physician's Recognition Award (AMA PRA) credits are accepted in the US as evidence of participation in CME activities. For further information on this award, please go to https://www.ama-assn.org. The AMA has determined that physicians not licensed in the US who participate in this CME activity are eligible for AMA PRA Category 1 Credits™. Through agreements that the AMA has made with agencies in some countries, AMA PRA credit may be acceptable as evidence of participation in CME activities. If you are not licensed in the US, please complete the questions online, print the AMA PRA CME credit certificate, and present it to your national medical association for review.

Article Title

Cerebrospinal Fluid Findings among Patients with Anaplasmosis and Central Nervous Involvement, Minnesota and Wisconsin, USA

CME Questions

1. Which of the following statements regarding anaplasmosis is most accurate?

A. The incidence rate in the US has been increasing
B. Symptoms are generally limited to headache and mental status changes
C. Most patients demonstrate leukocytosis
D. Most patients demonstrate thrombocytosis

2. What was the most common presentation of central nervous system infection in the current study?

A. Meningitis
B. Meningoencephalitis
C. Encephalitis
D. No CNS infection

3. What was the most common finding on CSF analysis of patients with anaplasmosis in the current study?

A. Reduced glucose
B. Elevated protein
C. Neutrophilic pleocytosis
D. Lymphocytic pleocytosis

4. Which of the following statements regarding outcomes of anaplasmosis in the current study is most accurate?

A. No patients required ICU admission
B. The severity of CNS symptoms correlated with the degree of CSF pleocytosis
C. Doxycycline was ineffective for the majority of patients
D. The benefits of doxycycline appeared directed toward improvements in systemic inflammation vs. direct activity in the CNS

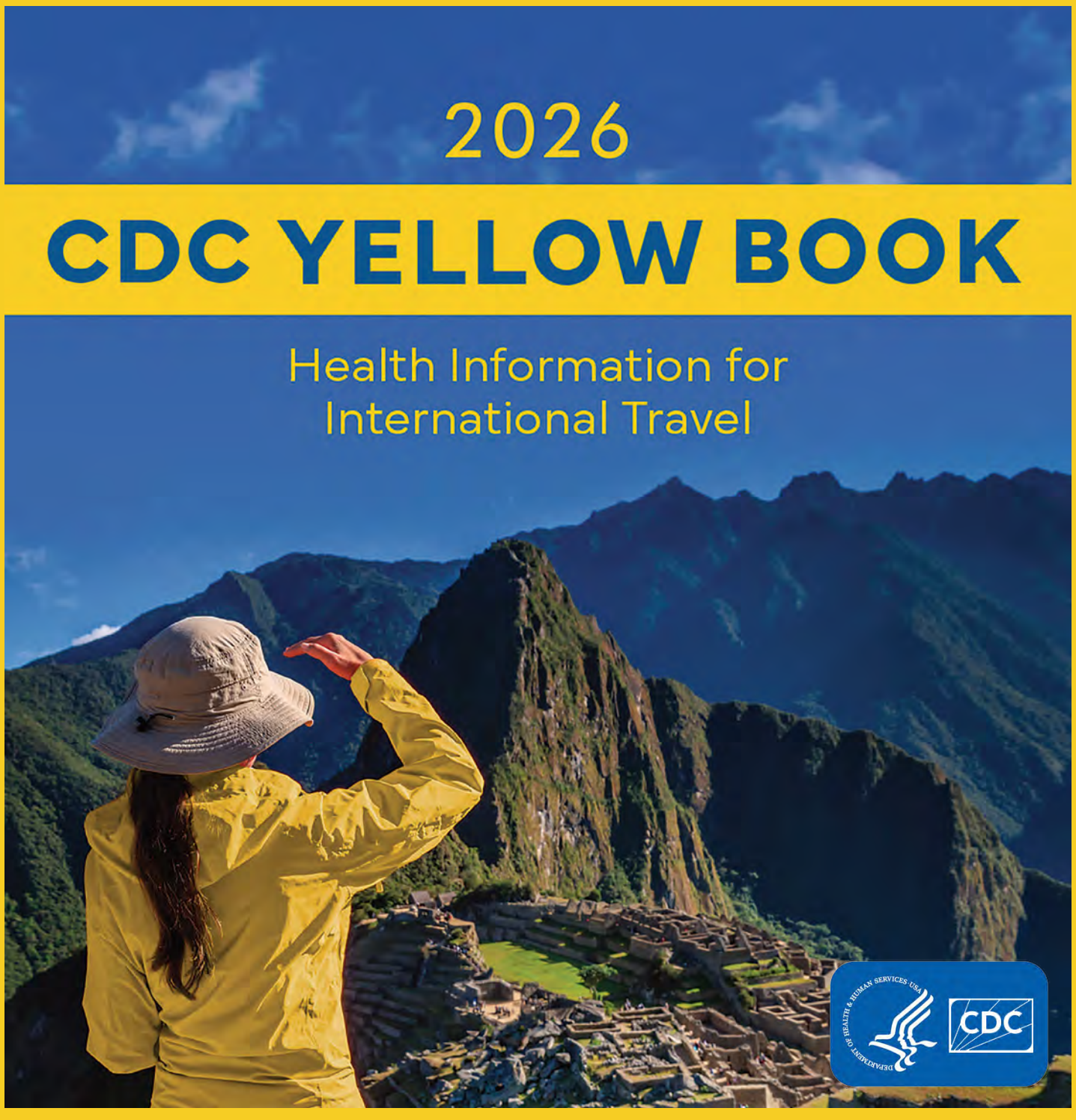

Launch of CDC Yellow Book 2026– A Trusted Travel Medicine Resource

CDC is pleased to announce the launch of the **CDC Yellow Book 2026**. The CDC Yellow Book is a resource containing the U.S. government's travel medicine recommendations and has been trusted by the travel medicine community for over 50 years. Healthcare professionals can use the print and digital versions to find the most up-to-date travel medicine information to better serve their patients' healthcare needs.

The CDC Yellow Book is available online now at www.cdc.gov/yellowbook and in print starting in June 2025 through Oxford University Press and other major online booksellers.